SIMULATION OF GROUND-WATER FLOW IN THE SAN ANDRES-GLORIETA AQUIFER IN THE ACOMA EMBAYMENT AND EASTERN ZUNI UPLIFT, WEST-CENTRAL NEW MEXICO

By Peter F. Frenzel

U.S. GEOLOGICAL SURVEY
Water-Resources Investigations Report 91-4099

Prepared in cooperation with the
NEW MEXICO STATE ENGINEER OFFICE,
PUEBLO OF ACOMA,
PUEBLO OF LAGUNA,
and the
U.S. BUREAU OF INDIAN AFFAIRS

Albuquerque, New Mexico
1992

U.S. DEPARTMENT OF THE INTERIOR

MANUEL LUJAN, JR., Secretary

U.S. GEOLOGICAL SURVEY

Dallas L. Peck, Director

For additional information
write to:

District Chief
U.S. Geological Survey
Pinetree Corporate Centre
4501 Indian School Road NE, Suite 200
Albuquerque, New Mexico 87110

Copies of this report can
be purchased from:

U.S. Geological Survey
Books and Open-File Reports
Federal Center
Box 25425
Denver, Colorado 80225

CONTENTS

CONTENTS--Continued

CONTENTS--Concluded

FIGURES

FIGURES--Continued

FIGURES--Continued

FIGURES--Continued

FIGURES--Concluded

TABLES

TABLES--Concluded

CONVERSION FACTORS AND VERTICAL DATUM

Multiply	By	To obtain
inch	25.4	millimeter
foot	0.3048	meter
mile	1.609	kilometer
acre-foot per acre	0.003048	cubic hectometer per hectare
per foot	3.281	per meter
acre	0.4047	hectare
square mile	2.590	square kilometer
cubic foot	0.02832	cubic meter
acre-foot	0.001233	cubic hectometer
million gallons	3,785	cubic meter
foot per mile	0.1894	meter per kilometer
foot squared per second	0.09290	meter squared per second
foot squared per day	0.09290	meter squared per day
gallon per day per foot squared	0.04075	meter per day
cubic foot per second	0.02832	cubic meter per second
gallon per minute	0.06309	liter per second
gallon per day	0.003785	cubic meter per day

The traditional unit acre-foot was used in this report for which conversion factors are: 1 cubic foot per second is approximately equal to 724 acre-feet per year or 362 acre-feet per half year.

Temperature in degrees Celsius (°C) can be converted to degrees Fahrenheit (°F) by the equation:

$$°F = 9/5\ (°C) + 32$$

Sea level: In this report "sea level" refers to the National Geodetic Vertical Datum of 1929--a geodetic datum derived from a general adjustment of the first-order level nets of the United States and Canada, formerly called Sea Level Datum of 1929.

SIMULATION OF GROUND-WATER FLOW IN THE SAN ANDRES-GLORIETA AQUIFER IN THE ACOMA EMBAYMENT AND EASTERN ZUNI UPLIFT, WEST-CENTRAL NEW MEXICO

By Peter F. Frenzel

ABSTRACT

The San Andres-Glorieta aquifer and overlying valley fill were studied in cooperation with the New Mexico State Engineer Office, the Pueblo of Acoma, the Pueblo of Laguna, and the U.S. Bureau of Indian Affairs. The purpose of the study was to determine the effects of current and projected water development on flow in the Rio San Jose and on hydraulic heads in the San Andres-Glorieta aquifer.

A digital flow model containing 2 layers, 76 rows, and 43 columns was constructed. This model simulated ground-water flow in the San Andres-Glorieta aquifer in an area from the Continental Divide on the west to the Rio Grande rift on the east and from Hospah, New Mexico, on the north to the Rio Salado on the south. In addition to simulating ground-water flow in the valley fill near The Malpais, Grants, and Bluewater, the model also simulated flow to and from Bluewater Lake, Bluewater and Cottonwood Creeks, and the Rio San Jose. Ojo del Gallo (rooster spring) and Horace Springs were simulated as streams.

Historical ground-water withdrawals and recharge were simulated for the period of fall 1899 to fall 1985. Measured hydraulic heads and streamflows were considered to have been matched reasonably well by the simulated values. Simulated drawdowns caused by historical ground-water development were about 8 feet at a location east of the San Rafael fault.

Projections were made from 1985 to 2020 in which the current (1986) level of ground-water development was simulated; in addition, 10,000 acre-feet per year of withdrawal from the San Andres-Glorieta aquifer near the west side of the Pueblo of Acoma was simulated. Model results indicate that drawdowns would be about 200 feet after 35 years east of San Rafael fault and about 20 feet at locations west of the fault. However, the accuracy of the drawdowns is uncertain because of (1) the assumed degree of hydraulic disconnection at San Rafael fault being critical to the simulation of cross-fault drawdowns, (2) the possible effects of leakage from confining beds, (3) the southward extent of the aquifer being unknown, and (4) the uncertainty of the artesian storage coefficient. The projected withdrawal of 10,000 acre-feet per year did not result in significant springflow or streamflow depletion, most of the withdrawal being derived from ground-water storage.

Steady-state springflows at Horace Springs were about 5.6 cubic feet per second, whereas simulated historical springflows were between 5.1 and 5.6 cubic feet per second. Projected springflows at Horace Springs were not greatly affected by projected ground-water development. Simulated decreases in flow of the Rio San Jose at Horace Springs were variable but averaged about 6 cubic feet per second. The reappearance of spring discharge at Ojo del Gallo during the early 1980's was simulated as a result of abnormally high streamflows and little ground-water irrigation, but when more normal streamflow and ground-water usage were projected, simulated springflows at Ojo del Gallo ceased.

INTRODUCTION

The Pueblo of Acoma and the Pueblo of Laguna are in a semiarid area of west-central New Mexico (fig. 1). The inhabited part of this area, which generally is in the valleys along the Rio San Jose and its tributaries, receives about 8 inches of precipitation annually. Because of these limited water resources, it is necessary to ensure that development occurs in an informed and orderly manner in the context of State and Federal water law. The San Andres-Glorieta aquifer yields large quantities of water for irrigation and other uses in an area northwest of the pueblo lands, but because it is more deeply buried beneath the pueblos, this aquifer had been largely unexplored before this study. In order to obtain the information needed to make informed decisions about the development of the San Andres-Glorieta aquifer, this study was conducted by the U.S. Geological Survey in cooperation with the New Mexico State Engineer Office, the Pueblos of Acoma and Laguna, and the U.S. Bureau of Indian Affairs.

The study area (fig. 1) is in parts of Cibola, Bernalillo, McKinley, Sandoval, Socorro, and Valencia Counties in New Mexico. Most of the area lies between the Continental Divide on the west, the Rio Puerco on the east, the village of Hospah in the San Juan Basin on the north, and the Rio Salado on the south. The topography generally is composed of mesas (gently dipping cuestas) that stand several hundred to a thousand feet above broad valleys. These mesas are dissected by steep canyons. The highest point is Mount Taylor (altitude 11,301 feet) in the San Mateo Mountains, which consists of a volcanic mass atop sedimentary rocks in the north-central part of the study area. The Zuni Mountains occupy the southwestern rim of the Zuni uplift (fig. 2) in the western part of the area. The largest population center consists of the city of Grants and the nearby village of Milan. The study area has a long history of irrigated agriculture using surface water. Surface water and ground water are closely interrelated, and competition for water has increased during the past century as flow from springs has been utilized, dams have been built, and water wells have been drilled.

This study was designed to: (1) determine the quantity and quality of water that can be developed from the San Andres-Glorieta aquifer near and beneath Acoma and Laguna Pueblo lands; (2) provide hydrologic information to evaluate the potential for developing ground-water supplies that are adequate for irrigation and other possible uses; and (3) provide hydrologic information that can be used to establish the effect of previous and new development on water rights.

The study included the following activities: (1) review of previous studies and existing ground-water, surface-water, water-use, topographic, weather, and geologic data; (2) collection of additional water-level, water-quality, and streamflow data; (3) drilling of test wells and aquifer testing and interpretation; (4) exploration of geologic structure by surface-geophysical methods; and (5) interpretation and assimilation of the data acquired from these activities into a digital ground-water flow model that simulates stream/aquifer interactions. The first four activities resulted in a description of the geohydrologic system (Baldwin and Anderholm, in press). Included in that report are the data collected and the interpretation of those data.

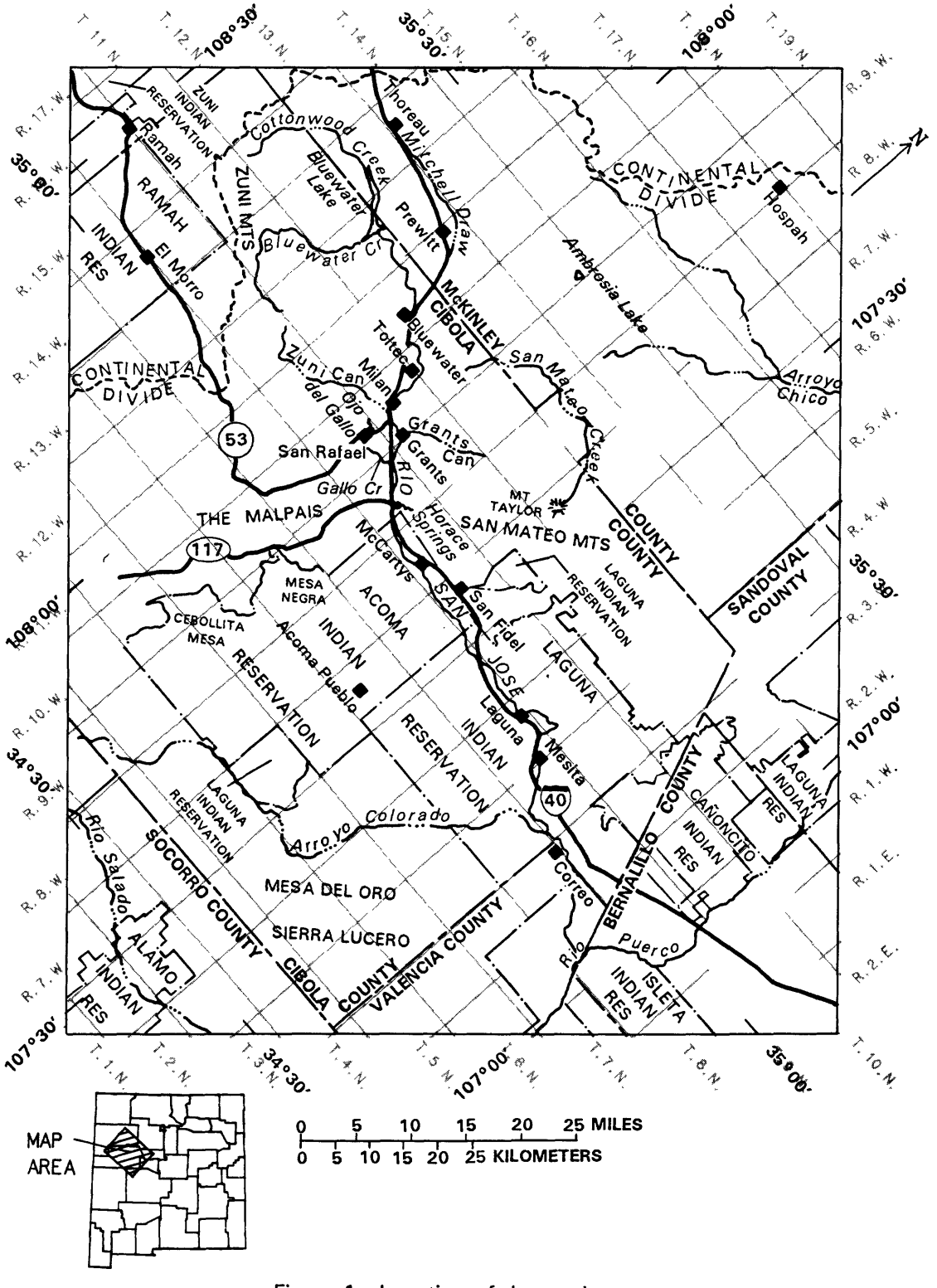

Figure 1.--Location of the study area.

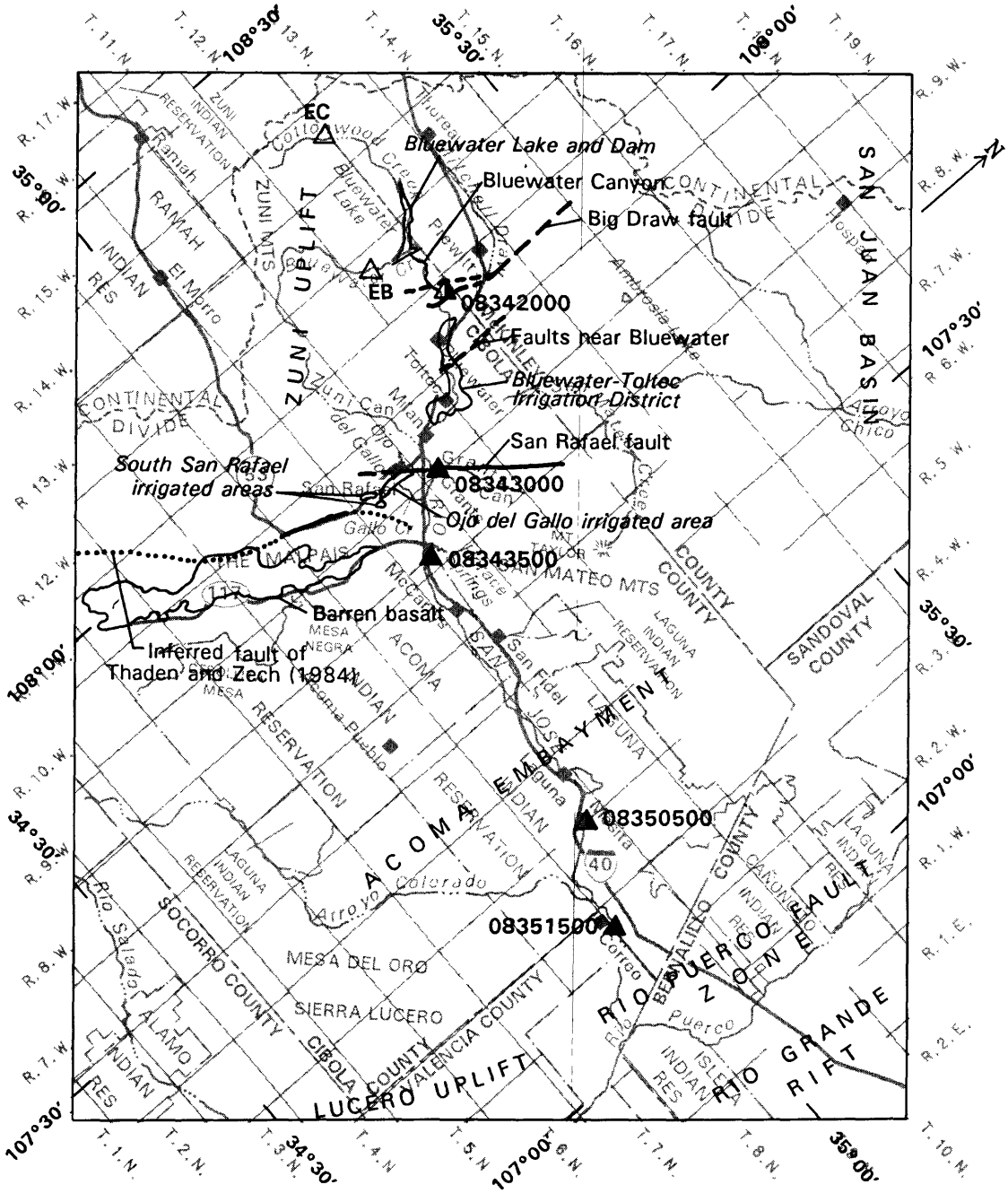

EXPLANATION

FAULT--Dashed where approximately located; dotted where inferred

08351500 ▲ CONTINUOUS-RECORD STREAMFLOW-GAGING STATION AND NUMBER

08350500 ⚠ DISCONTINUED STREAMFLOW-GAGING STATION

EB △ LOCATION OF ESTIMATED STREAMFLOW--
EC on Cottonwood Creek, EB on Bluewater Creek

Figure 2.--Location of steamflow-gaging stations and selected features of study area.

Purpose and Scope

This report resulted from the assimilation of the hydrologic data into a ground-water flow model. The ground-water flow model was used to test the internal consistency of the conceptual model and to provide a mechanism for estimating the effects of previous and new development on water levels, springflow, and streamflow.

The purpose of this report is to describe (1) the conceptual model of the geohydrologic flow system and selected elements of surface water and water use, (2) the representation of the geohydrologic flow system in a digital model, (3) the results of simulating previous and new development, and (4) the potential use of the model as an aid in improving our understanding of the geohydrologic system and as a management tool. The brief description of the ground-water flow system relies heavily on the work of previous studies and includes additional assumptions and quantitative estimates such as water used for irrigation. Representation of this complex conceptual model in a digital model of ground-water flow requires additional simplification to represent the heterogeneous aquifer media and the complex boundary conditions. The hydraulic heads and model inflows and outflows are used to describe the effect of both previous and new development. The method of sensitivity testing is used to demonstrate how the model can be used to improve our understanding of the geohydrologic system and to discuss the potential use of the model as a management tool.

The area modeled was from Thoreau to the Pueblo of Acoma and the surrounding locale (fig. 1). The model simulated steady-state and transient conditions, using the steady-state simulation to establish a starting point for the transient condition. The transient simulation included water withdrawals from fall 1899 through summer 1985. Projections were made from 1985 to 2020. The purpose of the digital-model simulation was to estimate the effects of previous and new development of the San Andres-Glorieta aquifer on hydraulic heads in the aquifer and on streamflow in Bluewater Creek and the Rio San Jose.

Previous Investigations

Numerous reports describing the hydrology of parts of the study area have been published. Geohydrology has been investigated in the Grants-Bluewater area (Gordon, 1961), in southwestern McKinley County (Cooper and John, 1968), in Cibola County outside of the Grants-Bluewater area (J.A. Baldwin, Hydrologist, U.S. Geological Survey, written commun., 1988), and in most of the study area (Baldwin and Anderholm, in press). Early water-use history and discharge estimates for Ojo del Gallo (rooster spring) were presented by Hodges (1938). Methods of estimating irrigation ground-water withdrawals were described in a series of U.S. Geological Survey Water-Supply Papers (1949-57). Numerous consultants' reports contain aquifer-characteristic and water-use data for the Grants-Bluewater area. Examples are Hydro-Search, Inc. (1978a,b, and 1981), Geohydrology Associates, Inc. (1981, 1984), Aqua Science, Inc. (1982), Hydro-Engineering (1983), and Dames and Moore (1986).

Well- and Spring-Numbering System

The system of numbering wells and springs in this report, used by the Geological Survey and the New Mexico State Engineer Office, is based on the common subdivision of public lands into sections. The number, in addition to designating the well or spring, locates its position to the nearest 10-acre tract in the land network (fig. 3). The first number denotes the township north of the New Mexico Base Line, the second denotes the range west of the New Mexico Principal Meridian, and the third denotes the section in which the well or spring is located. The fourth number locates the well or spring within the section to the nearest 10 acres by the system of quartering shown. If two or more wells or springs occur in the same 10-acre tract, the wells are distinguished by letters (a, b, etc.) following the location number. The use of zeros in the fourth segment of the location number indicates that the well or spring could not be located to the nearest 10-acre area. Well number 10.09.26.300 would indicate that the well could not be located more accurately than the southwest quarter of section 26, a 160-acre area. Parts of Cibola County have not been subdivided by township, range, and section. Location numbers for such areas were determined by extending section lines from adjacent areas.

Acknowledgments

Professor R.R. Lansford of New Mexico State University supplied some of the irrigated acreage records. Jane Wells of the U.S. Bureau of Indian Affairs located railroad records in court depositions. Charles Wohlenberg of the New Mexico State Engineer Office and personnel in the U.S. Bureau of Indian Affairs provided ground-water-withdrawal data. J.D. Dewey, U.S. Geological Survey, estimated excess precipitation, which was used to estimate recharge in the Zuni uplift area. Several ground-water consultants helped to locate some of the ground-water-withdrawal data. Several area residents, especially Joseph Nielson, discussed the history of the area with the author. Many landowners allowed access to their land for data collection, and the courtesy of these area residents is particularly appreciated.

CONCEPTUAL MODEL OF THE GEOHYDROLOGIC SYSTEM

Although ground water within the study area occurs in rocks that range in age from Precambrian to Quaternary, the aquifer of interest to this study consists of the San Andres Limestone and the Glorieta Sandstone, both of Permian age. This section of the report describes the: (1) occurrence of ground water in the San Andres-Glorieta aquifer, underlying units, and overlying units; (2) characteristics of the aquifer; (3) characteristics of the principal confining unit; (4) direction of ground-water flow and hydrologic boundaries of the San Andres-Glorieta aquifer and overlying valley fill; (5) predevelopment ground-water flow; and (6) history of water development including estimates of ground-water withdrawals and artificial recharge. The hydrology of the study area is described in Baldwin and Anderholm (in press). Much of the following summarizes their findings and describes estimated hydrologic characteristics not found in that report.

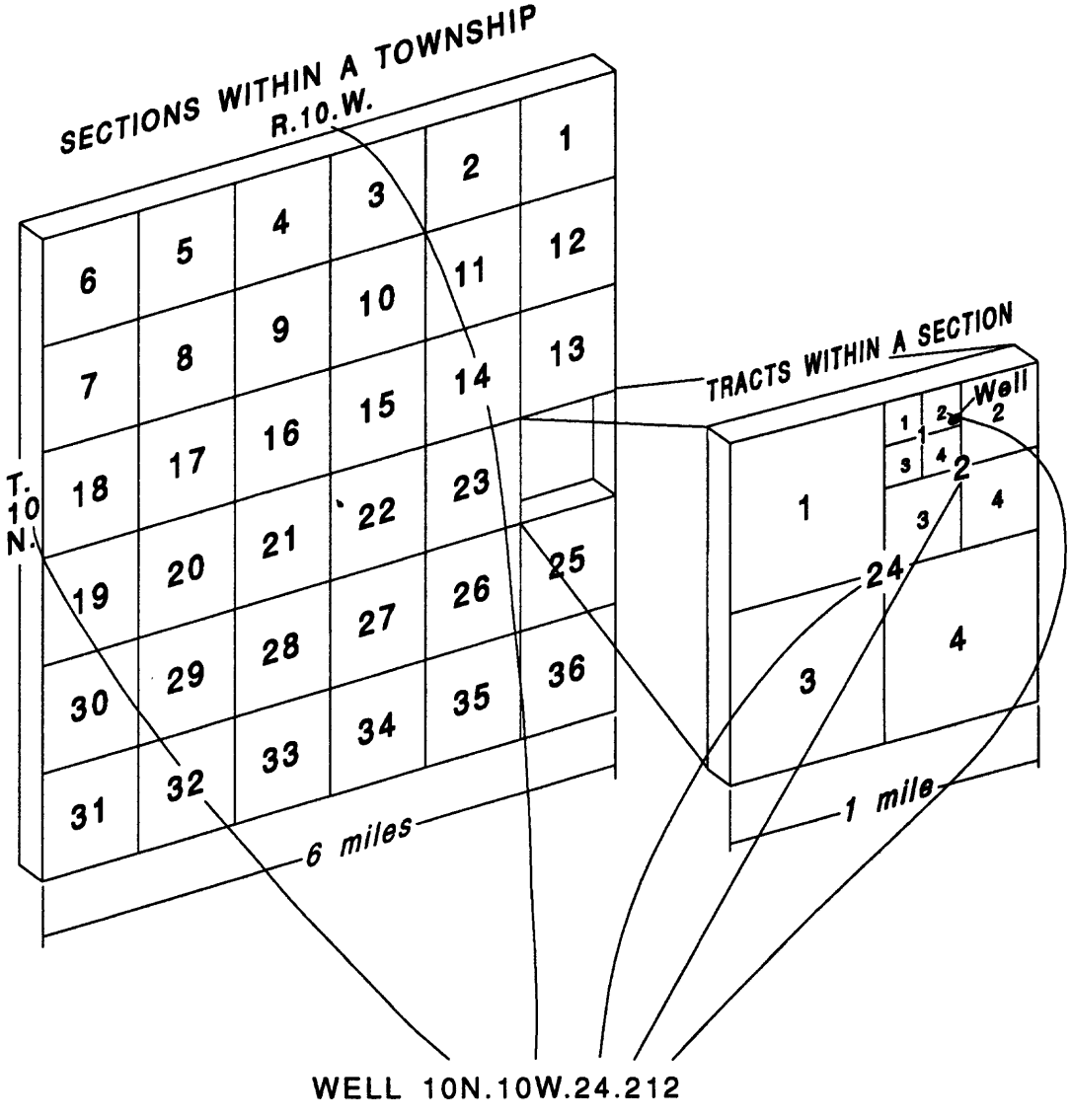

Figure 3.--System of numbering wells and springs in New Mexico.

Many of the estimates of hydrologic characteristics in this section were made for the sole purpose of preparing input for the digital ground-water flow model described later in this report. Some of these estimates were made on the basis of sparse data, in some cases using unconventional methods, and therefore are quite tentative. As methods are developed, or as data become available to make the necessary estimates using more conventional methods, these estimates will be superseded and the model described in this report will become obsolete. In some cases, no quantitative estimates were possible and thus only guidelines or constraints will be discussed. All digital-model-dependent values will be discussed in the section describing the digital model.

General Geology and Ground-Water Occurrence

The aquifer system is comprised of the San Andres-Glorieta aquifer, underlying units, and the valley fill (Baldwin and Anderholm, in press, pl. 1). The San Andres-Glorieta aquifer extends throughout the study area except where it has been removed by erosion in the middle of the Zuni uplift and at the eastern margin at the Lucero uplift (fig. 4). The San Andres Limestone may be cavernous in a strip extending southeastward from Bluewater, possibly covering one-third of the study area. The San Andres Limestone overlies the Glorieta Sandstone and they are in good hydraulic connection.

EXPLANATION

AREA WHERE SAN ANDRES LIMESTONE AND GLORIETA SANDSTONE ARE ABSENT

OUTCROP OR SUBCROP AREA OF SAN ANDRES LIMESTONE AND GLORIETA SANDSTONE

250 — LINE OF EQUAL THICKNESS OF CHINLE FORMATION--Dashed where inferred. Contour interval 500 feet, supplemental 250-foot contour

FAULT--Dashed where approximately located; dotted where inferred

B B' LINE OF SECTION--Sections shown in figure 6

120+ WELL--Number shows thickness of Chinle Formation, in feet. + indicates eroded top of formation

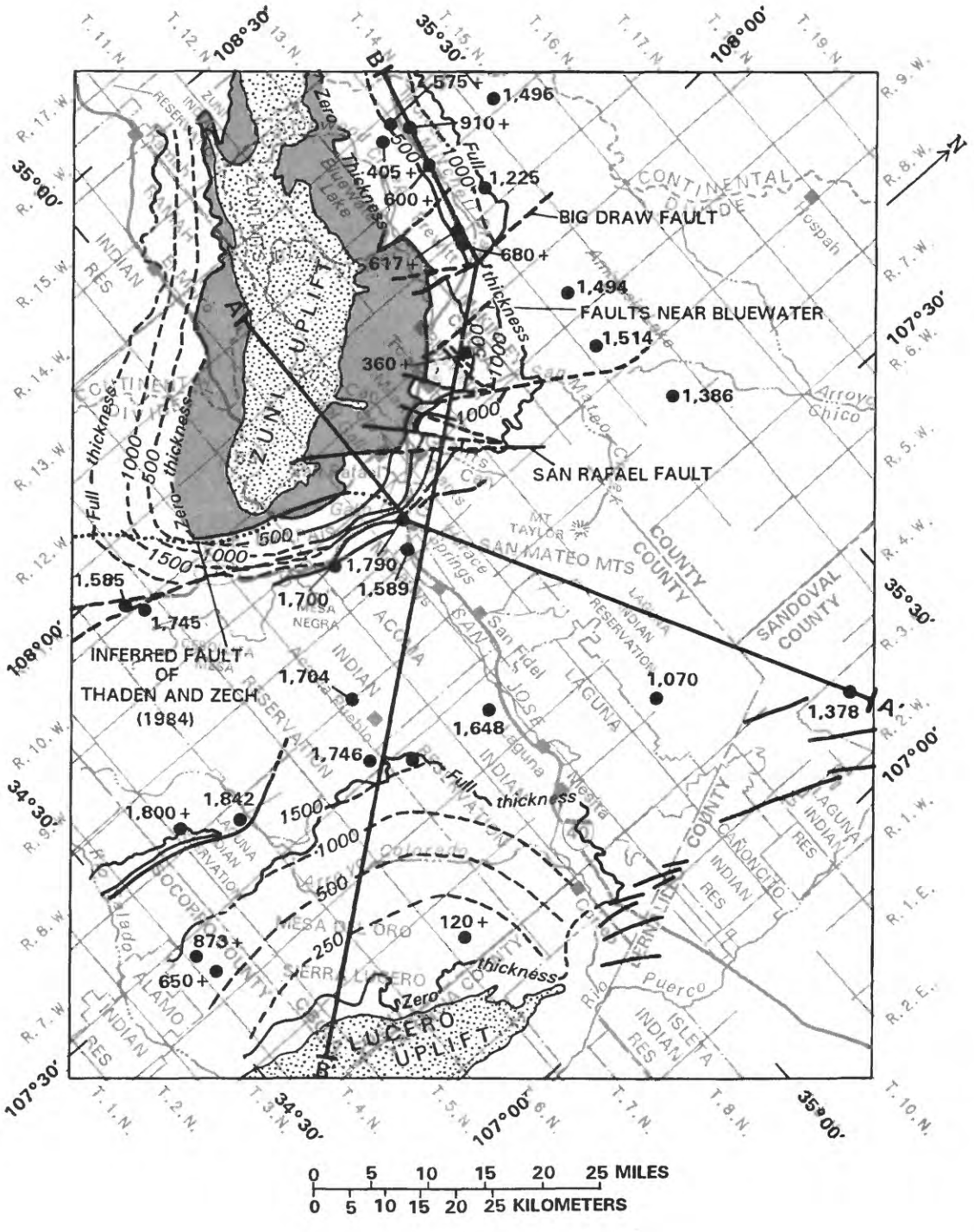

Figure 4.--Extent of the San Andres-Glorieta aquifer and thickness of the Chinle Formation in the study area (modified from Baldwin and Anderholm, in press).

Valley fill overlies and is hydraulically connected to the San Andres-Glorieta aquifer (fig. 5) in places near the Zuni uplift. Valley fill directly overlies the San Andres-Glorieta aquifer near the outcrop area around the Zuni uplift (parts of area II in fig. 5 where alluvium or basalt is shown). Adjacent to this area, an eroded wedge of Chinle Formation (area III in fig. 5) intervenes between the San Andres-Glorieta aquifer and the overlying valley fill. In The Malpais, this wedge of Chinle intervenes between the San Andres-Glorieta and most of the basaltic valley fill, and the area of direct hydraulic connection may be limited to an area west of an inferred fault (fig. 2) of Thaden and Zech (1984). (The Malpais is a large valley, mainly covered by basalt, that is approximately bounded by the Continental Divide and State Highways 117, 53, and Interstate 40. The term "malpais" locally means basaltic badlands.) In the Grants-Bluewater area, the zone of direct hydraulic connection may be only a few square miles; however, the existence of a good hydraulic connection is well established (Gordon, 1961, p. 44). The bottom of the valley fill follows an ancient valley mainly eroded into the Chinle Formation. The topography of the ancient valley is unknown but may be rough with remnants of Chinle Formation between places where the valley was eroded to the underlying San Andres-Glorieta aquifer. Therefore, the exact location of the area of direct hydraulic connection between the valley fill and San Andres-Glorieta aquifer is not precisely known. Along the Rio San Jose between Horace Springs and Mesita (fig. 1), a narrow strip of valley fill is separated from the San Andres-Glorieta aquifer by rocks of Jurassic and Cretaceous age in addition to the full thickness of the Chinle Formation and is not shown in figure 5.

Overlying the San Andres-Glorieta aquifer are the Triassic Chinle Formation, Jurassic and Cretaceous rocks, and Quaternary valley fill. The Chinle overlies the San Andres-Glorieta aquifer over most of the study area and comprises a 1,500-foot-thick confining bed of shale and siltstone. Near the Zuni uplift and Sierra Lucero, the Chinle thins to zero thickness at the outcrop of the San Andres (fig. 4). Where the Chinle is full thickness, it is overlain by Jurassic and Cretaceous rocks. Because of the great thickness and small permeability of the Chinle, the ground-water flow system in the Jurassic and Cretaceous rocks does not greatly affect that of the San Andres-Glorieta aquifer. The valley-fill deposits of Quaternary alluvium and basalt flows lie along stream channels throughout the study area.

Underlying the San Andres-Glorieta aquifer are the Permian Yeso and Abo Formations. In much of the study area these Permian rocks are underlain by rocks of Pennsylvanian age (fig. 6A). The Glorieta Sandstone directly overlies the Yeso Formation and, because the contact is gradational (Gordon, 1961, p. 23), the Glorieta and upper part of the Yeso are probably hydraulically connected. Because the Yeso contains some beds that may be confining, it is not considered to be an aquifer. The Yeso Formation directly overlies the Abo Formation. Because of the fine-grained texture of the Abo, it is probably much less permeable than the Yeso. Horizontal ground-water flow in the Yeso and Abo may be small and probably enters as downward leakage from the overlying San Andres-Glorieta aquifer. The Yeso and Abo are relatively impermeable compared to the San Andres-Glorieta aquifer and therefore may be considered to be leaky confining beds. The Abo overlies Precambrian rocks near the Zuni uplift; elsewhere, the Abo overlies Pennsylvanian rocks (fig. 6A). Precambrian rocks underlying the Pennsylvanian rocks are relatively impermeable and form the lower boundary of the flow system.

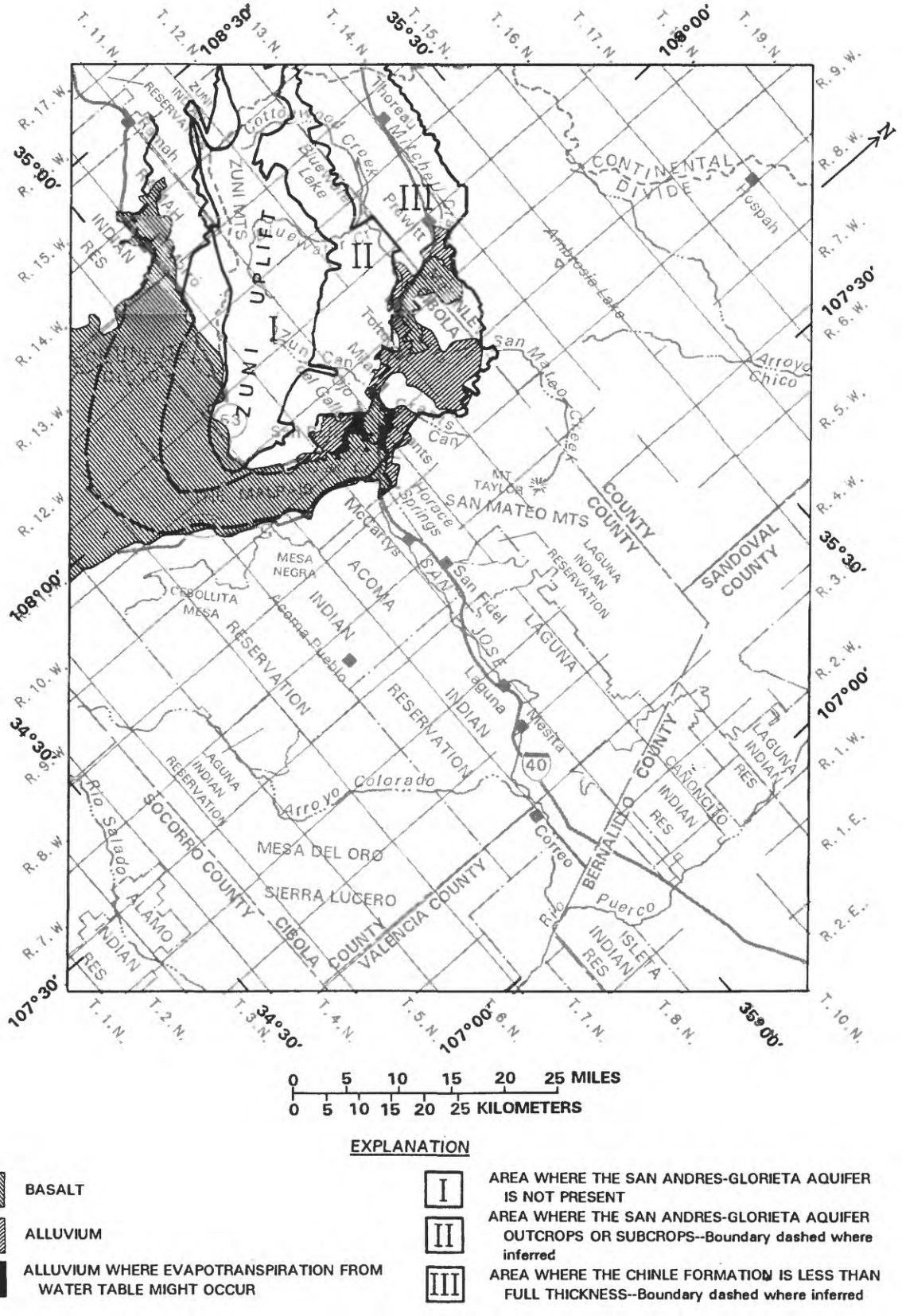

Figure 5.--Valley fill hydraulically connected to the San Andres-Glorieta aquifer near the Zuni uplift.

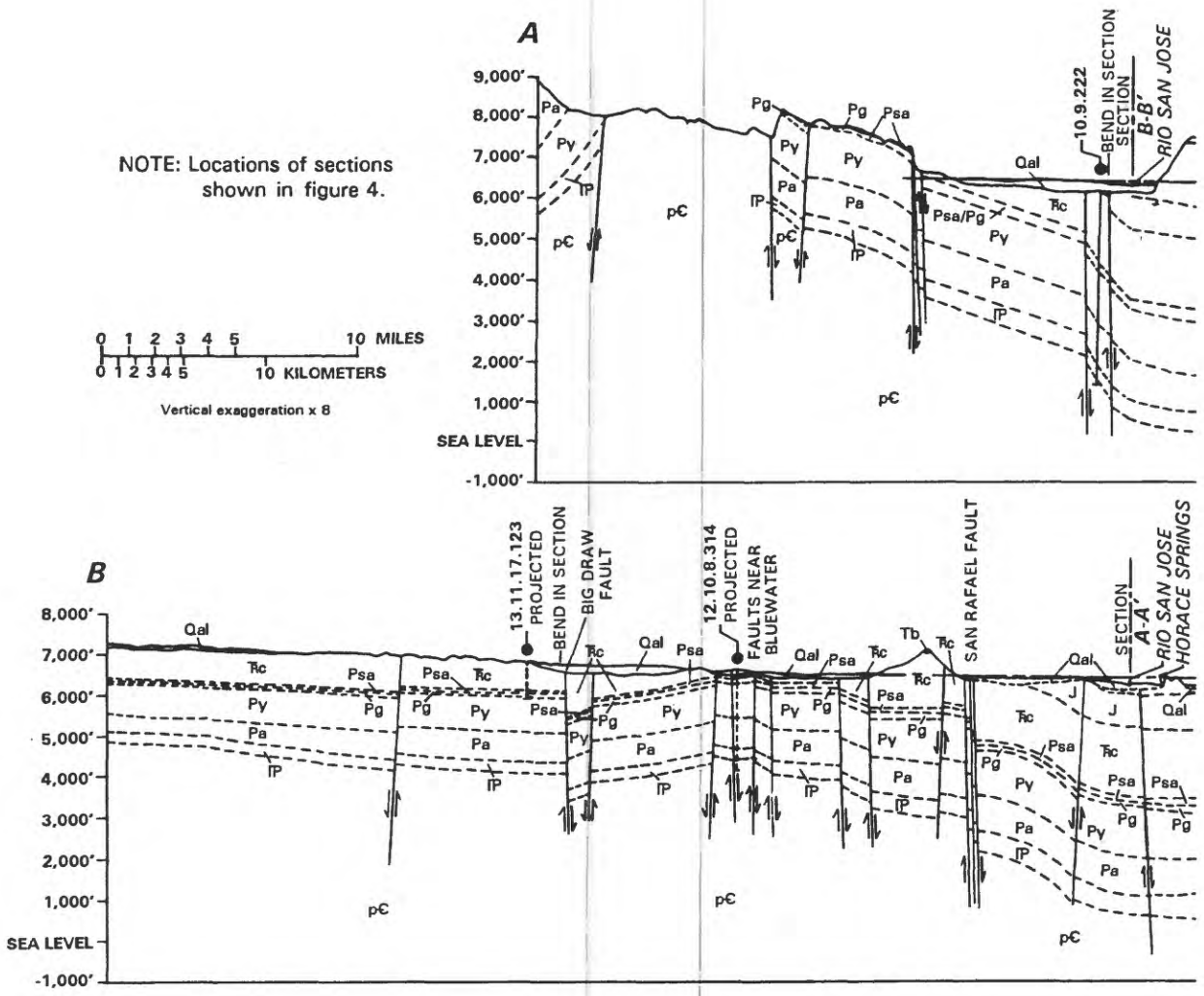

EXPLANATION

Qal	ALLUVIUM
QTb	QUATERNARY AND TERTIARY BASALT
Tb	TERTIARY BASALT
K	CRETACEOUS SEDIMENTARY ROCKS, UNDIVIDED
J	JURASSIC SEDIMENTARY ROCKS, UNDIVIDED
Trc	TRIASSIC CHINLE FORMATION--As much as 1,900 feet of red, brown, and green shale, siltstone, and poorly sorted sandstone; some thin beds of limestone in upper part. Includes the Wingate Sandstone where present
Psa	PERMIAN SAN ANDRES LIMESTONE--As much as 700 feet of limestone, dolomite, sandstone, and gypsum
Pg	PERMIAN GLORIETA SANDSTONE--As much as 300 feet of white to buff, very fine to medium-grained, well-sorted sandstone; some gypsum and siltstone

Figure 6.--Geologic sections through the study area (modified from Baldwin and Anderholm, in press, pl.1).

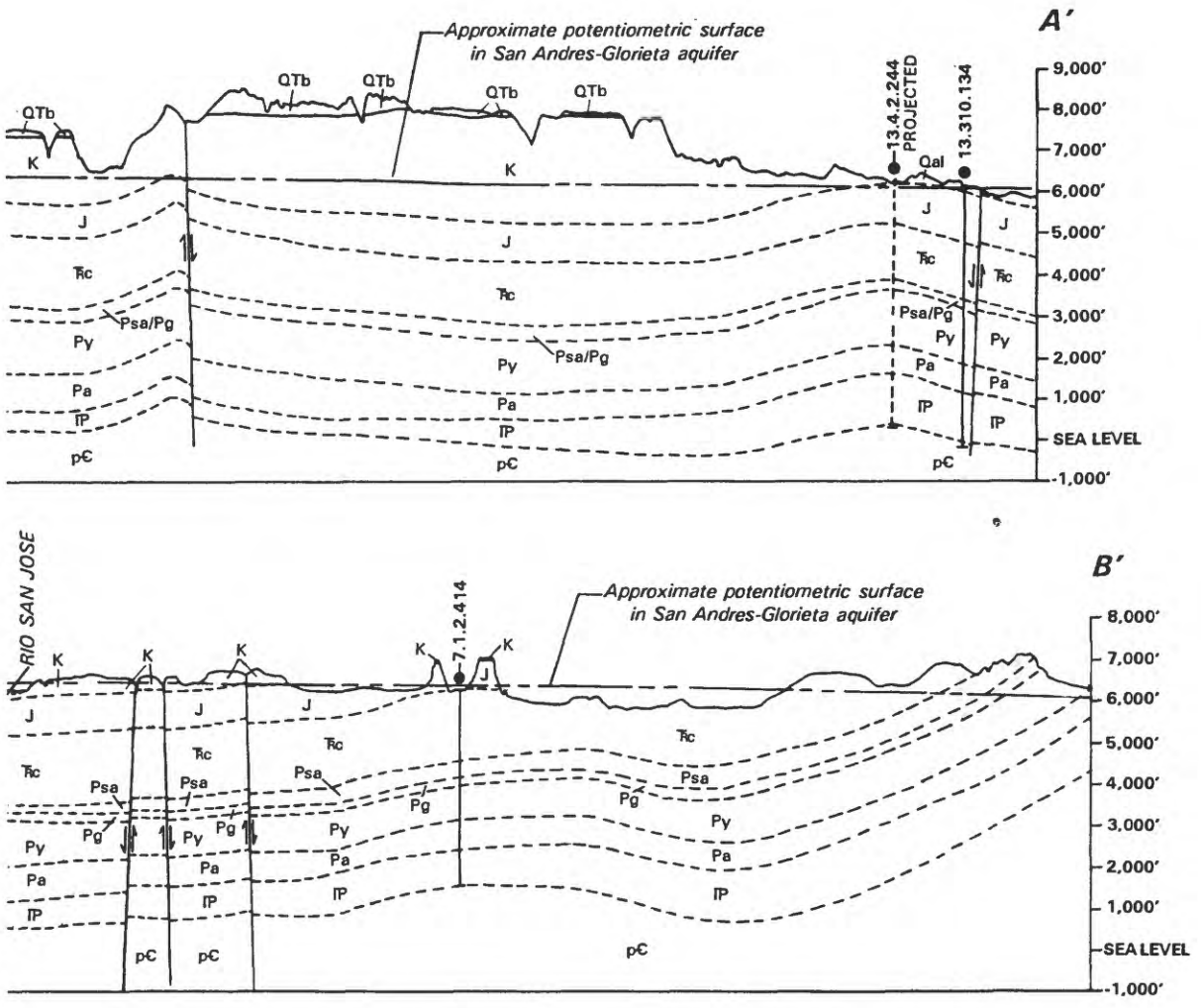

Py — PERMIAN YESO FORMATION--As much as 1,400 feet of siltstone, sandstone, and shale; several thin beds of limestone in the lower middle part

Pa — PERMIAN ABO FORMATION--As much as 1,600 feet of red siltstone, sandstone, and shale

IP — PENNSYLVANIAN SEDIMENTARY ROCKS, UNDIVIDED

pC — PRECAMBRIAN ROCKS, UNDIVIDED

CONTACT BETWEEN GEOLOGIC UNITS--Dashed where approximately located

FAULT

7.1.2.414 — WELL AND WELL NUMBER

Aquifer Characteristics

The storage and transport of water in the San Andres-Glorieta aquifer are influenced by geology. In areas where the San Andres Limestone is cavernous, the San Andres is the principal part of the aquifer and aquifer characteristics are typical of cavernous limestone. In areas where the San Andres Limestone is either missing or not cavernous, the Glorieta Sandstone is the principal part of the aquifer and aquifer characteristics are typical of Permian sandstone. Between these extremes probably lie transition zones having intermediate values of transmissivity and storage coefficient.

Transmissivity and Hydraulic Conductivity

Transmissivity values for the San Andres-Glorieta aquifer range from 10 to 200,000 feet squared per day. Seven transmissivity zones (fig. 7) were identified by Baldwin and Anderholm (in press). Zone I includes areas where the San Andres Limestone is either missing or not cavernous and the transmissivity is mainly in the Glorieta Sandstone. Zones III and V include areas where the San Andres Limestone is cavernous and includes most of the transmissivity of the San Andres-Glorieta aquifer. Zone II is intermediate between zones I and III. Much of the transmissivity of the aquifer system in zones VI and VII may be in rocks of the Glorieta Sandstone. Cavernous limestone has not been found in zones VI and VII and the San Andres Limestone is largely gypsum. Zone IV is intermediate between the surrounding zones, and the transmissivity assigned to zone IV is based on only one aquifer test. North of zone IV, the transmissivity of the San Andres-Glorieta aquifer probably diminishes because the aquifer thins to zero thickness along an east-west line (Baars, 1962, figs. 17 and 18) that crosses the northern corner of the study area. No aquifer-test data are available for that area. Around the Zuni uplift, between the area where the San Andres-Glorieta aquifer is absent and zones I-IV, the San Andres Limestone forms the caprock on the mountainside and the San Andres-Glorieta is not completely saturated. The transmissivity in that area certainly varies with saturation; however, the degree of saturation is unknown.

EXPLANATION

AREA WHERE SAN ANDRES LIMESTONE AND GLORIETA SANDSTONE ARE ABSENT

OUTCROP OR SUBCROP AREA OF SAN ANDRES LIMESTONE AND GLORIETA SANDSTONE

TRANSMISSIVITY ZONE BOUNDARY--Roman numeral is zone designation; number is transmissivity, in feet squared per day

FAULT--Dashed where approximately located; dotted where inferred

OIL-TEST HOLE OR WELL WHERE CAVERNOUS OR HIGHLY FRACTURED ZONES WERE PENETRATED IN THE SAN ANDRES LIMESTONE AND/OR GLORIETA SANDSTONE--Number is transmissivity, in feet squared per day

WELL--Number is transmissivity, in feet squared per day

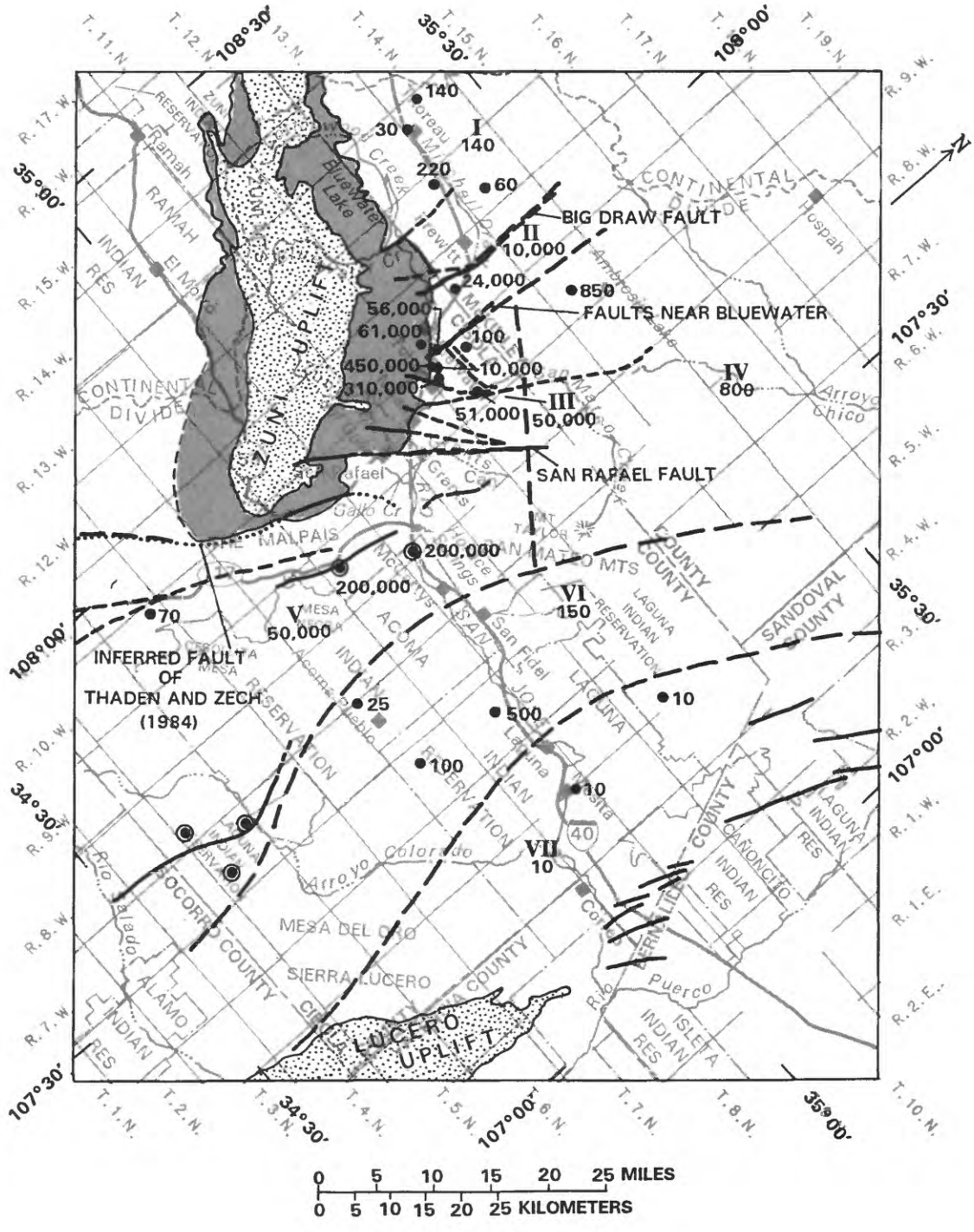

Figure 7.--Generalized transmissivity zones for the San Andres-Glorieta aquifer (modified from Baldwin and Anderholm, in press).

Transmissivity values for older Permian and Pennsylvanian rocks, which have not been tested, may be about the same as values for the Glorieta Sandstone. On the basis of possible rock properties, carbonates may transmit most of the water, and values of transmissivity for a 1,000-foot-thick section could range from 0.5 to 1,000 feet squared per day (Baldwin and Anderholm, in press).

A wide range of hydraulic-conductivity values for the alluvial deposits has been reported in studies near the Anaconda (T. 12 N., R. 11 W., sec. 24) and Homestake (T. 12 N., R. 10 W., sec. 26) uranium mills. Near the Anaconda mill, hydraulic-conductivity values of 75 and 150 feet per day were calculated by dividing transmissivity values derived from aquifer tests by the lengths of tested intervals (Dames and Moore, 1981, table 1, and p. D-1 and E-1). Near the Homestake mill, reported values of hydraulic conductivity at 55 sites range from 0.16 to 770 feet per day (Hydro-Engineering, 1983, table 2.5-1). Of these values, the first quartile is between 11 and 12 feet per day, the median is 31 feet per day, and the third quartile is 59 feet per day.

The range in hydraulic conductivity for basalt may be much larger than that for alluvial deposits depending on the nature of the basalt, which may range from impervious to cavernous. A large range ("less than 1" to "1,000 or greater" feet per day) was simulated by Dames and Moore (1986, pl. B-9) where the larger values of hydraulic conductivity appear to approximately coincide with basalt flows.

Storage Coefficient and Specific Yield

For confined conditions, the storage characteristic of interest is the storage coefficient, which is the product of specific storage and saturated thickness. Within the study area, confined conditions occur in the Glorieta Sandstone or the San Andres Limestone. The specific storage of the San Andres-Glorieta aquifer probably approaches the average of about 1×10^{-6} per foot reported by Lohman (1972, p. 8) although the San Andres Limestone and evaporites may not contribute greatly to the storage of the aquifer. Using this value for average specific storage results in a storage coefficient of 4×10^{-4} for a 400-foot-thick section. Reported values of storage coefficient range from 5.3×10^{-5} to 1.4×10^{-2} (Dames and Moore, 1981, table 1). A narrower range of 4.2×10^{-4} to 1.1×10^{-3} was reported by Gordon (1961, table 8). The divergence occurs because the usual aquifer-test assumptions of homogeneity, radial flow, and infinite extent are not valid for the cavernous San Andres Limestone and because areas tested in the Grants-Bluewater area could include a combination of artesian and water-table conditions.

For unconfined conditions, the storage characteristic of interest is the specific yield. Within the study area, unconfined conditions occur in the Glorieta Sandstone, the San Andres Limestone, basalt, and alluvium. Lohman (1972, p. 8) gave a range of specific yield for unconfined aquifers of 0.1 to 0.3. The specific yield of rocks such as the Glorieta Sandstone probably is on the small end of Lohman's range because they are indurated. The large-scale porosity of the San Andres may be small (Gordon, 1961, p. 56), leading to the conclusion that the specific yield could be small. Similarly, the specific yield of fractured basalt may be small. The specific yield of alluvium is probably in the range of 0.1 to 0.3 reported by Lohman.

Bottom Altitude and Saturated Thickness of the Valley Fill

The bottom altitude of valley fill follows ancestral valleys and is unknown in much of the area especially in The Malpais. The bottom altitude of valley fill (fig. 8; and table 9 in Supplemental Information) was estimated by contouring formation data from wells in the Grants-Bluewater area and by projecting an ancient stream-channel slope of approximately 30 feet per mile. Higher bedrock altitudes at some well sites than at others probably are caused by remnants of the Chinle Formation in the ancient valley. These possible remnants were not accounted for in the generalized contours shown in figure 8. The saturated thickness of the valley fill (table 10 in Supplemental Information) was estimated as the water-table altitude (Baldwin and Anderholm, in press, fig. 17) minus the estimated bottom altitude of valley fill. This saturated thickness is greatest between Grants and Horace Springs where the valley fill is almost fully saturated. Although the water-table altitude and saturated thickness in the southern part of The Malpais are unknown, some saturated thickness probably exists because the valley fill is underlain by the shale and siltstone of the Chinle Formation, which are probably much less permeable than the valley fill. It was assumed that the saturated thickness was 10 feet in the middle and southern parts of The Malpais. These estimates of bottom altitude and saturated thickness of the valley fill are not reliable but were made because they were required for the preparation of input for the digital model.

Characteristics of the Chinle Confining Unit

Throughout most of the study area, the San Andres-Glorieta aquifer is confined above by the Chinle Formation, which is as much as 1,800 feet thick and mainly consists of siltstones and mudstones (Baldwin and Anderholm, in press). Although leakage from the Chinle could be substantial in reducing long-term drawdowns in the San Andres-Glorieta aquifer, Jobin (1962, p. 32) reported that the mudstone and siltstone of the Chinle constitute "* * * perhaps the most effective aquaclude in the Colorado Plateau."

The hydraulic connection between the San Andres Limestone and the valley-fill deposits through the Chinle formation probably is greatest where less than the full thickness of the Chinle Formation (fig. 4) intervenes between the San Andres-Glorieta aquifer and valley fill. The Chinle is less than full thickness in the western part of the study area near the Zuni uplift and in the eastern part of the study area northwest of the Lucero uplift (fig. 4). Valley fill overlies a reduced thickness of Chinle Formation in The Malpais area and in the Rio San Jose valley near Bluewater and Toltec (fig. 5).

The vertical hydraulic conductivity of the Chinle Formation is unknown, and although various methods exist to test it, all are subject to question. Laboratory values of vertical hydraulic conductivity of three samples, collected from depths of 105 to 280 feet at locations near the Homestake mill north of Milan, were 3.5×10^{-10}, 5.8×10^{-10}, and 1.3×10^{-9} foot per second ($3. \times 10^{-5}$, $5. \times 10^{-5}$, and 1.1×10^{-4} foot per day) (Hydro-Engineering, 1983, table 3.4-1). These small samples may not be representative of the full thickness and area of the Chinle. Similarly, aquifer tests probably would not test the thickness and area of the Chinle adequately because decades or centuries may be required to substantially change the hydraulic-head gradient within a confining bed of the thickness and lithology of the Chinle. Furthermore, it may not be possible in such a test to definitely determine which confining beds or other formations are being tested.

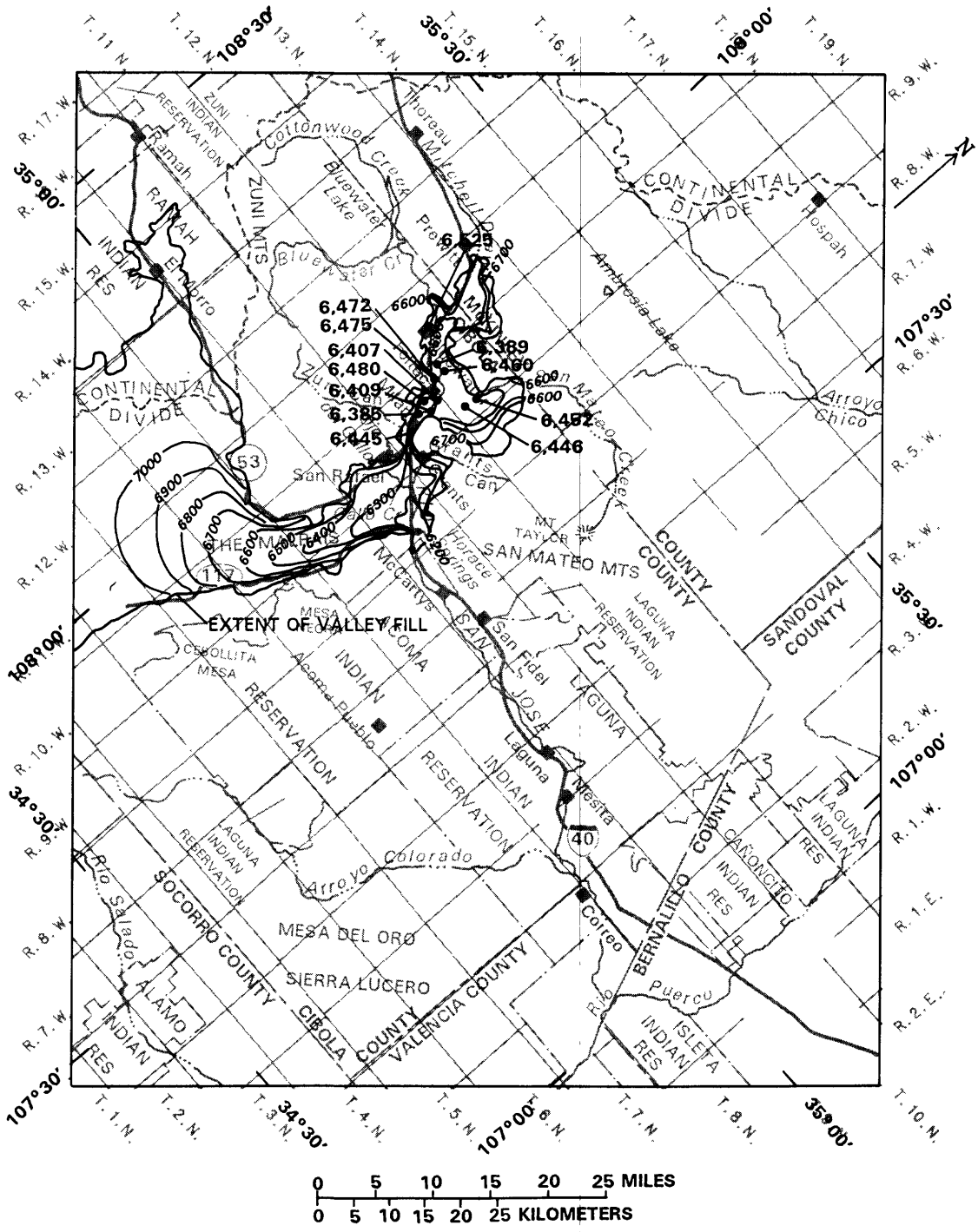

EXPLANATION

7000 STRUCTURE CONTOUR--Shows altitude of base of valley fill. Estimated by projection of buried stream-channel slope. Contour interval 100 feet. Datum is sea level

• 6,445 WELL--Number is altitude of base of valley fill. Datum is sea level

Figure 8.--Estimated altitude of base of valley fill.

Hydraulic-conductivity values for siltstone and shale may range from approximately 10^{-13} to 10^{-9} foot per second (10^{-8} to 10^{-4} foot per day) (Freeze and Cherry, 1979, p. 29). Fractured shale can be on the more permeable end of this range. However, pressures within the Chinle probably would close most open fractures and faults. During test-hole drilling the Chinle rock tended to squeeze into the drill holes (Baldwin and Anderholm, in press). The tendency for fractures to close may be greater at depth than at or near the land surface. The depth of the bottom of the Chinle is generally more than the full thickness and may be as much as 5,000 feet in the northeastern part of the study area (fig. 6A).

A substantial portion of water pumped from artesian wells may come from storage in overlying and underlying confining beds. The following table shows estimates of the percentage of water pumped from wells that might come from confining beds with various assumed values of hydraulic conductivity. These estimates were made with the method of Hantush (1960) assuming an aquifer of infinite areal extent, with a storage coefficient of 4×10^{-4}, bounded on both sides by 1,500-foot-thick confining beds with specific storage of 10^{-6} per foot of thickness. Dashes (--) are shown where the equation does not apply. The years since start of discharge are the same as those used in the digital-model projection described in this report. The hydraulic-conductivity values shown approximately span those values that might be expected to represent a shale confining bed:

Years since start of discharge	Hydraulic conductivity of the confining beds (feet per second)				
	10^{-9}	10^{-10}	10^{-11}	10^{-12}	10^{-13}
	Percentage of discharge derived from confining beds				
1	54	25	9	3	1
4	72	41	17	6	2
9	--	53	24	9	3
14	--	59	29	11	4
24	--	66	35	14	5
35	--	70	40	16	6

For a hydraulic conductivity less than 10^{-11}, the percentage of water derived from the confining beds would not be significant within a reasonable time of projection because of the extreme uncertainty of other features of any projection such as ground-water-withdrawal scenarios. However, if the hydraulic conductivity were 10^{-9} foot per second, near the maximum for shale, substantial leakage would occur within the first year. The effects of leakage from confining beds would be most noticeable in wells the most distant from the outcrop. However, the effect on drawdowns seems to take more time to develop than the effect on the source of water.

Drawdowns in an aquifer with leaky confining beds are less than in an aquifer with impermeable confining beds, all other things being equal. The comparative effects of leaky confining beds can be elucidated by analytical models. The Theis solution estimates drawdown assuming no leakage from confining beds, and the Hantush (1960) solution estimates drawdown assuming finite values of storage and vertical conductivity in confining beds. Both assume an aquifer of infinite radial extent from the discharging well. Both are "classical" ground-water theory and can be found in ground-water textbooks such as Lohman (1972) or Freeze and Cherry (1979). Lohman (1972, table 5) lists tabulated values of an integral necessary for the Theis solution, and Hantush (1960, table 1) lists tabulated values necessary for the Hantush solution. The following table shows the comparison of drawdown calculated using both solutions. The assumed values of variables relate to this study. The column marked percent (%) calculated under the leakage assumption shows the percentage of drawdown calculated under the no-leakage assumption. Dashes (--) indicate where the leakage equation does not apply. Other symbols in the table are the same as symbols used in the equations:

$$\text{Theis (no leakage) equation} \qquad s = \frac{Q}{4\pi T} W(u) \tag{1}$$

$$\text{Hantush (leakage) equation} \qquad s = \frac{Q}{4\pi T} H(u,\beta) \tag{2}$$

Where s = drawdown (feet),
Q = discharge of the well (assumed to be 13.8 cubic feet per second),
T = transmissivity (assumed to be 0.579 square foot per second),
$W(u)$ = a dimensionless function of u, and
$H(u,\beta)$ = a dimensionless function of u and β.

The functions $W(u)$ and $H(u,\beta)$ are taken from published tables on the basis of values of u and β:

$$u = \frac{r^2 S}{4Tt} \tag{3}$$

$$\beta = \frac{2r}{4}\sqrt{\frac{K'/b'}{T}\,\frac{S'}{S}}$$

Where r = the radial distance from the discharging well (variable in the following table),
S = the storage coefficient of the aquifer (assumed to be 4×10^{-4}, dimensionless),
t = the time in seconds since discharge began (variable in the following table),
K' = the vertical hydraulic conductivity, in feet per second, of overlying and underlying confining beds (variable in the following table),
b' = the thickness of the overlying and underlying confining beds (assumed to be 1,500 feet each), and
S' = the storage coefficient of the overlying and underlying confining beds (assumed to be 1.5×10^{-3} each, dimensionless).

Estimates of drawdown at a radius of
10,000 feet (1.9 miles) from withdrawal well

	Time (t) since beginning of withdrawal					
Years	1	4	9	14	24	35
Seconds	3.16×10^{7}	1.26×10^{8}	2.84×10^{8}	4.42×10^{8}	7.57×10^{8}	1.10×10^{9}
u (dimensionless)	5.47×10^{-4}	1.37×10^{-4}	6.08×10^{-5}	3.91×10^{-5}	2.28×10^{-5}	1.57×10^{-5}
W(u) (dimensionless)	6.9	8.3	9.1	9.6	10.1	10.5
Drawdown (feet), assuming no leakage	13	16	17	18	19	20

		Drawdown (feet) assuming leakage and various values of K' and t															
K' (feet per second)	B	H(u,B)	s	%	H(u,B)	s	%	H(u,B)	s	%	H(u,B)	s	%	H(u,B)	s	%	H(u,B)	s	%
10^{-9}	1.04×10^{-2}	6.2	12	92	7.2	14	88	--	--	--	--	--	--	--	--	--	--	--	--
10^{-10}	3.29×10^{-3}	6.7	13	100	8.0	15	94	8.5	16	94	8.8	17	94	9.1	17	89	9.5	18	90
10^{-11}	1.04×10^{-3}	6.8	13	100	8.1	15	94	8.9	17	100	9.2	17	94	9.7	18	95	10	19	95

Estimates of drawdown at a radius of
100,000 feet (19 miles) from withdrawal well

	Time (t) since beginning of withdrawal					
Years	1	4	9	14	24	35
Seconds	3.16×10^{7}	1.26×10^{8}	2.84×10^{8}	4.42×10^{8}	7.57×10^{8}	1.10×10^{9}
u (dimensionless)	5.47	1.37	6.08×10^{-1}	3.91×10^{-1}	2.28×10^{-1}	1.57×10^{-1}
W(u) dimensionless	2.4	3.7	4.5	5.0	5.5	5.9
Drawdown (feet), assuming no leakage	4.6	7.0	8.5	9.5	10	11

		Drawdown (feet) assuming leakage and various values of K' and t															
K' (feet per second)	B	H(u,B)	s	%	H(u,B)	s	%	H(u,B)	s	%	H(u,B)	s	%	H(u,B)	s	%	H(u,B)	s	%
10^{-9}	1.04×10^{-1}	1.8	3.4	74	2.5	4.7	67	--	--	--	--	--	--	--	--	--	--	--	--
10^{-10}	3.29×10^{-2}	2.1	4.0	87	3.3	6.3	90	3.9	7.4	87	4.2	8.0	84	4.7	8.9	89	4.9	9.3	85
10^{-11}	1.04×10^{-2}	2.3	4.4	96	3.6	6.8	97	4.3	8.2	96	4.6	8.7	92	5.1	9.7	97	5.4	10	91
10^{-12}	3.29×10^{-3}	2.4	4.6	100	3.7	7.0	100	4.5	8.5	100	4.9	9.3	98	5.4	10	100	5.8	11	100
10^{-13}	1.04×10^{-3}	2.4	4.6	100	3.7	7.0	100	4.5	8.5	100	4.9	9.3	98	5.5	10	100	5.9	11	100

Estimates of drawdown at a radius of
1,000,000 feet (190 miles) from withdrawal well

	Time since beginning of withdrawal					
Years	1	4	9	14	24	35
Seconds	3.16×10^{7}	1.26×10^{8}	2.84×10^{8}	4.42×10^{8}	7.57×10^{8}	1.10×10^{9}
u (dimensionless)	5.47×10^{-2}	1.37×10^{-2}	6.08×10^{-3}	3.91×10^{-3}	2.28×10^{-3}	1.57×10^{-3}
W(u) (dimensionless)	0.00068	0.13	0.45	0.72	1.11	1.41
Drawdown (feet), assuming no leakage	0.0013	0.25	0.85	1.37	2.11	2.67

		Drawdown (feet) assuming leakage and various values of K' and t																		
K' (feet per second)	B	H(u,B)	s	%	H(u,B)	s	%	H(u,B)	s	%	H(u,B)	s	%	H(u,B)	s	%	H (u,B)	s	%
10^{-9}	1.04	0.00011	0.0002	16	0.025	0.05	20	--	--	--	--	--	--	--	--	--	--	--	--
10^{-10}	3.29×10^{-1}	0.00046	0.00087	67	0.12	0.23	92	0.23	0.44	52	0.36	0.68	50	0.48	0.91	43	0.72	1.4	51
10^{-11}	1.04×10^{-1}	0.00063	0.0012	92	0.13	0.25	100	0.36	0.68	80	0.55	1.0	76	0.66	1.3	59	1.1	2.1	80
10^{-12}	3.29×10^{-2}	0.00073	0.0014	108	0.13	0.25	100	0.42	0.80	94	0.65	1.2	90	0.79	1.5	71	1.3	2.5	94
10^{-13}	1.04×10^{-2}	0.00075	0.0014	108	0.15	0.28	112	0.44	0.83	98	0.69	1.3	96	0.82	1.6	74	1.4	2.7	101

Drawdowns estimated using the leakage assumption for the radius of 10,000 feet are more than 80 percent of drawdowns estimated using the no-leakage assumption. A possible exception would be the estimates that were not made assuming a K′ of 10^{-9} feet per second, where the leakage equation does not apply. Although drawdowns were not estimated using the leakage assumption for K′ less than 10^{-11} feet per second because the table of the function $H(u,\beta)$ was not extensive enough to facilitate these estimates, the percentage of drawdowns estimated using the no-leakage assumption would be greater than the percentage for K′ equal to 10^{-11} feet per second. Drawdowns estimated for the radius of 100,000 feet are more than 80 percent of drawdowns estimated assuming no leakage except, again, for drawdowns estimated assuming K′ of 10^{-9} feet per second.

Some error in these estimates is caused by an imperfect interpolation between published values of the function $H(u,\beta)$, and possibly by rounding errors in the estimated drawdowns. For example, where the mantissa of β is equal to 3.29, the published values of $H(u,\beta)$ are for mantissas of β 2 and 5, and an interpolation was necessary. Linear interpolation was used. These errors do not seriously affect the generalization that drawdowns estimated using the leakage assumption are more than 80 percent of no-leakage drawdowns, except for K′ of 10^{-9} feet per second.

The Hantush and Theis equations assume an aquifer of infinite radial extent from the pumping well. This is a serious shortcoming when transmissivity (0.579 square foot per second, or 50,000 feet squared per day) representative of cavernous limestone is used. To demonstrate how serious this shortcoming might be, measurable drawdowns were estimated for the radius of 1,000,000 feet (190 miles). The extent of the aquifer in the north, south, and east directions is much less than 190 miles from the hypothetical discharging well, and although the extent of the aquifer to the west is more than 190 miles, it is obstructed by the Zuni uplift and other structural features in that direction. The extent of cavernous limestone is not infinite. If the hydrologic boundaries could be simulated with the use of image-well theory, the drawdowns estimated with these equations would certainly be more than shown above. Image-well theory is not used here because the boundaries of the aquifer as seen in the following sections of this report are complex, and proceeding further on this subject would not be beneficial.

Where long-term, wide-area effects of leakage through a confining bed can be identified, digital-model simulation may yield the best estimate of the effects of confining beds. Also, the cumulative effects of a large variety of boundaries can best be simulated by a distributive-type model such as is the subject of this report. Leakage will appear as a delayed yield from storage and may lead to an unreasonably large storage coefficient in a model that does not account for leakage from confining beds.

Direction of Ground-Water Flow and Hydrologic Boundaries

In homogeneous, isotropic porous media, ground water flows at right angles to the equipotential lines. Potentiometric contours for the San Andres-Glorieta aquifer (fig. 9) can be interpreted as describing two flow systems separated by the unnamed fault (Thaden and Zech, 1984) extending southward from the southeast end of the Zuni uplift. An eastern flow system lies north and east of the uplift where ground water generally flows away from the uplift and toward the east. A western flow system lies southwest of the uplift where ground water generally flows southwestward. This report describes only the eastern flow system, which is the primary flow system in the study area. The interpretation presented below may be oversimplified. Flow is assumed to be generally perpendicular to equipotential lines, as is the case for a homogeneous, isotropic aquifer. However, because the San Andres-Glorieta aquifer is neither homogeneous nor isotropic, the principal flow direction may not be at right angles to the equipotential lines.

EXPLANATION

AREA WHERE SAN ANDRES LIMESTONE AND GLORIETA SANDSTONE ARE ABSENT

OUTCROP OR SUBCROP AREA OF SAN ANDRES LIMESTONE AND GLORIETA SANDSTONE

6100 POTENTIOMETRIC CONTOUR--Shows altitude at which water level would have stood in tightly cased wells. Dashed where approximate. Contour interval 100 feet, supplemental 50-foot contour. Datum is sea level.

FAULT--Indicates fault zone where offset may impede ground-water flow in San Andres-Glorieta aquifer. Dashed where approximately located, dotted where inferred

WELL USED TO CONSTRUCT POTENTIOMETRIC-SURFACE CONTOURS

SPRING

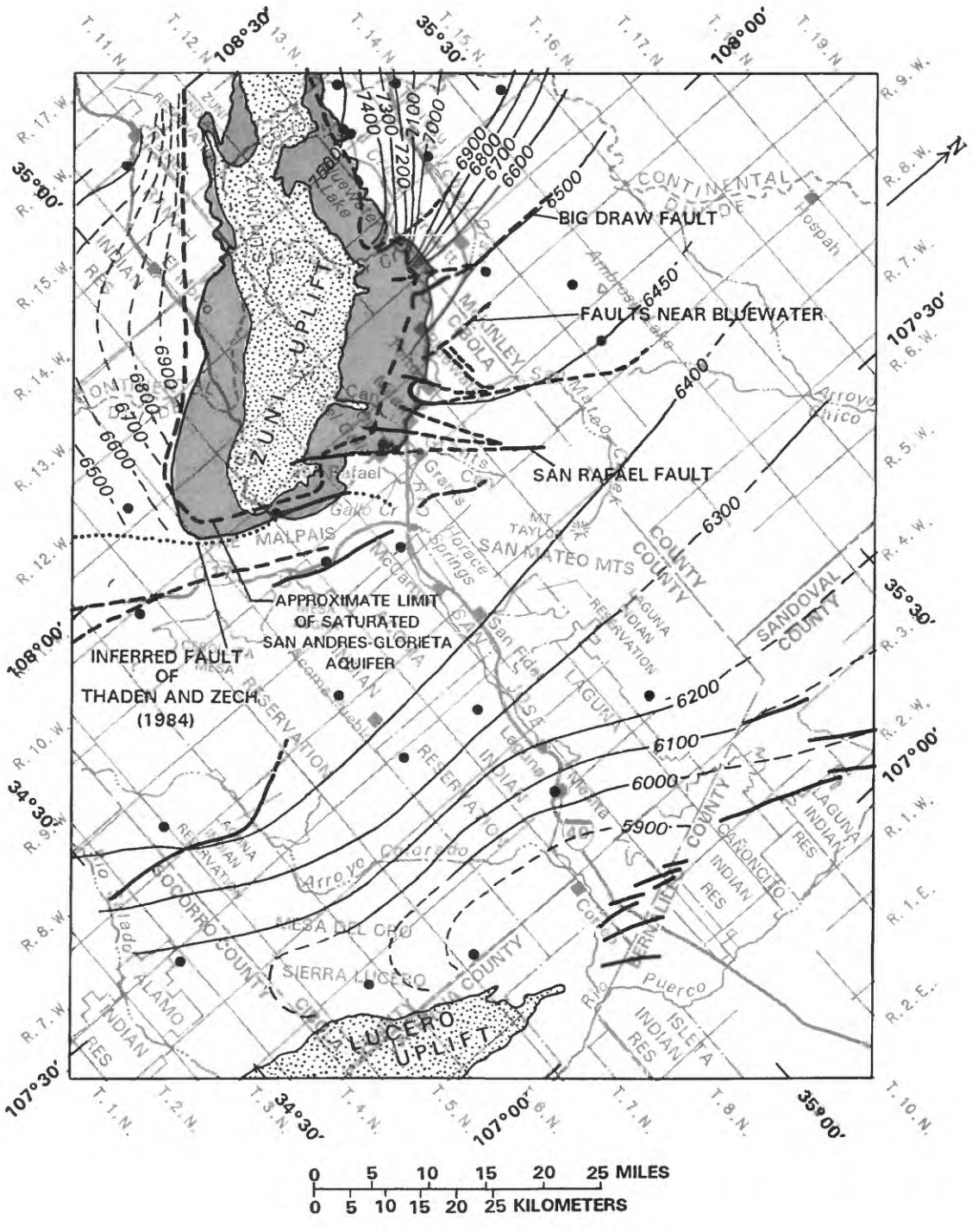

Figure 9.--Potentiometric-surface contours for the San Andres-Glorieta aquifer based on the highest hydraulic heads of record (modified from Baldwin and Anderholm, in press).

Concentrations of dissolved constituents (Baldwin and Anderholm, in press) in the San Andres-Glorieta aquifer tend to support the concept of a general eastward direction of flow. Generally, the longer water is in contact with aquifer material, the more dissolved material it contains. The less mineralized water is in the western part of the study area and the more mineralized water is in the eastern part. This pattern generally is observed in water samples from wells in T. 8 N. and T. 9 N. However, the geochemistry of the area is complex and water samples from wells further south do not follow this simple pattern. Ground-water flow may be mainly southward from the vicinity of T. 9 N., R. 9 W. to the vicinity of T. 5 N., R. 8 W. This flow probably follows the path of least resistance through the more transmissive zones of the aquifer toward the south and then eastward toward the Rio Grande rift in the southeast corner of the study area. However, the southward flow may go beyond the boundary of the study area before turning southeastward or eastward toward the rift. The general eastward flow may not be dominant throughout the study area.

The direction of ground-water flow in the valley fill along Bluewater Creek and the Rio San Jose generally is parallel to the streams. In the north end of The Malpais, ground water flows northeastward. The direction of flow in the remainder of The Malpais may also be northeastward on the basis of water levels in adjacent bedrock wells. However, ground water in the southern part of The Malpais may converge toward the area (fig. 5), near the south side of the Zuni uplift, where the valley fill directly overlies the San Andres-Glorieta aquifer.

Effects of Faulting on Ground-Water Flow and Hydraulic Head

Faults affect the flow of water in the San Andres-Glorieta aquifer. The unnamed fault (figs. 2 and 4) inferred by Thaden and Zech (1984) to extend southward from the southeast end of the Zuni uplift seems to block eastward flow in the San Andres-Glorieta aquifer south of the uplift where the inferred offset is large. This blockage possibly causes the 100-foot drop in the potentiometric surface over a distance of 9 miles between wells in T. 7 N., R. 12 W. and T. 6 N., R. 10 W. (fig. 9). However, the degree of hydraulic connection across the fault near its north end where ground water may flow from west to east is unknown. The Big Draw fault (figs. 2, 4, and 6) near Prewitt probably blocks ground-water flow from west to east where offset is large north of Prewitt, although hydraulic-head measurements that might indicate such a blockage are not available. To the south along Big Draw fault, near the mouth of Bluewater Canyon, where Bluewater Creek crosses the southern extensions of Big Draw fault, the offset of the fault is less than the thickness of the San Andres-Glorieta aquifer, and ground-water flow probably is not blocked by the fault. The San Rafael fault (figs. 2, 4, and 6) near Grants probably blocks west-to-east flow from a point near Ojo del Gallo northeastward to a point near the Cibola-McKinley County line. Southwest from Ojo del Gallo, the offset of the San Rafael fault may not exceed the thickness of the San Andres-Glorieta aquifer. At Ojo del Gallo, the San Rafael fault forces the water table to rise above the land surface, causing the spring (fig. 10), which is a major ground-water discharge point.

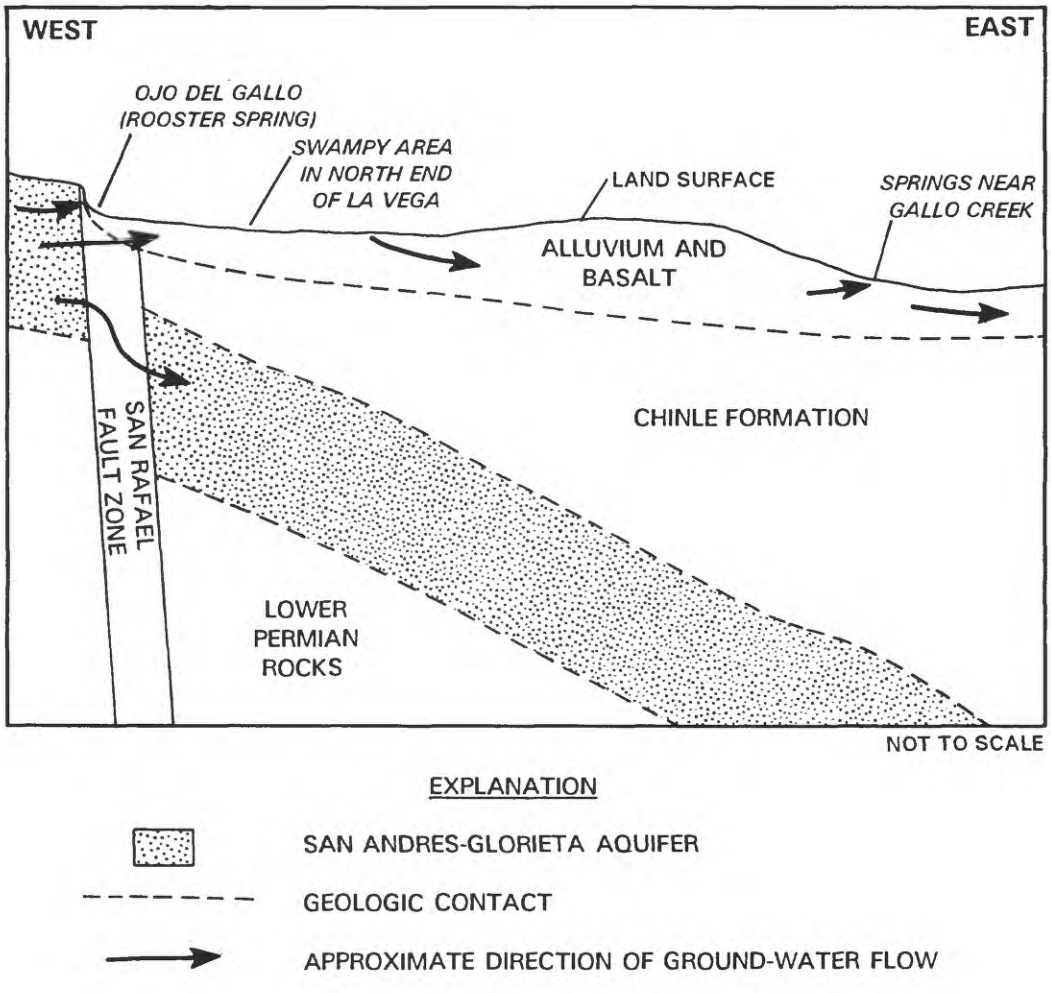

Figure 10.--Ground-water flow through a section from Ojo del Gallo to the Rio San Jose near the end of Gallo Creek.

Changes in the gradient of the potentiometric surface may result from hydraulic restrictions or blockages at faults. Figure 11 shows the potentiometric surface along a line from north of Bluewater to Acoma. Hydraulic heads generally group into one of three intervals in which head changes are small; these steps are separated by short distances over which most of the head changes occur. The first change in hydraulic head on the left side of figure 11 is near a swarm of faults near Bluewater (figs. 2 and 4) and may result from a hydraulic restriction associated with the faults. The next large change in hydraulic head occurs near the San Rafael fault and may result from a hydraulic restriction associated with that fault. To avoid the effects of drawdown as much as possible, the hydraulic heads in figure 11 were taken from a detailed map (not shown) of the highest heads of record at each well site represented in the U.S. Geological Survey Ground-Water Site-Inventory computer file. The values shown in figure 11 were selected to be representative of hydraulic heads on the upgradient and downgradient sides of faults. Most of the heads shown in figure 11 were measured in the mid-1980's except for that at well 10.10.10.433, which was 6 feet higher in 1956 than in 1986. The highest hydraulic heads of record at sites in the area designated in figure 11 as "Bluewater step" tend to be about 6,550 feet. The highest hydraulic heads of record at sites in the area designated as "Toltec step" range from about 6,470 to 6,455 feet. The highest hydraulic heads of record at sites near San Rafael within or near the east side of the San Rafael fault tend to be about 6,430 feet except for sites on the flank of the Zuni uplift, which are higher. From there southeastward, extending 20 miles south of the last well shown in figure 11, the hydraulic head is about 6,420 feet, indicating very little blockage of ground-water flow or very little flow through the area designated as "Acoma embayment step."

Faults could also affect the flow of ground water by providing a preferred path for vertical leakage. Geochemical data indicate that such leakage may occur at some locations in the Grants-Bluewater area (Baldwin and Anderholm, in press). These leakage rates are assumed to be small.

Recharge from Precipitation

An unknown amount of recharge results from precipitation on the San Andres-Glorieta aquifer outcrop around the flanks of the Zuni uplift (fig. 4), on the basalt and alluvium near the mountain front (fig. 5), and on the San Andres-Glorieta aquifer outcrop on the Lucero uplift (fig. 4). Recharge rates were estimated for each of these areas.

With some exceptions, estimated excess precipitation on the San Andres-Glorieta aquifer outcrop of the Zuni uplift was assumed to infiltrate the aquifer either immediately, or if it becomes runoff, to infiltrate the aquifer before the stream leaves the outcrop of the aquifer. Surface water from most of the watersheds around the Zuni uplift (except Bluewater Creek, Cottonwood Creek, and Zuni Canyon) normally does not reach the Rio San Jose, but usually infiltrates into the ground. Also, some of the canyons on the east end of the Zuni uplift debouch onto the valley-fill aquifer in The Malpais where the water either evaporates or recharges the valley fill. The proportion of excess precipitation that recharges the valley fill near the east end of the Zuni uplift is unknown.

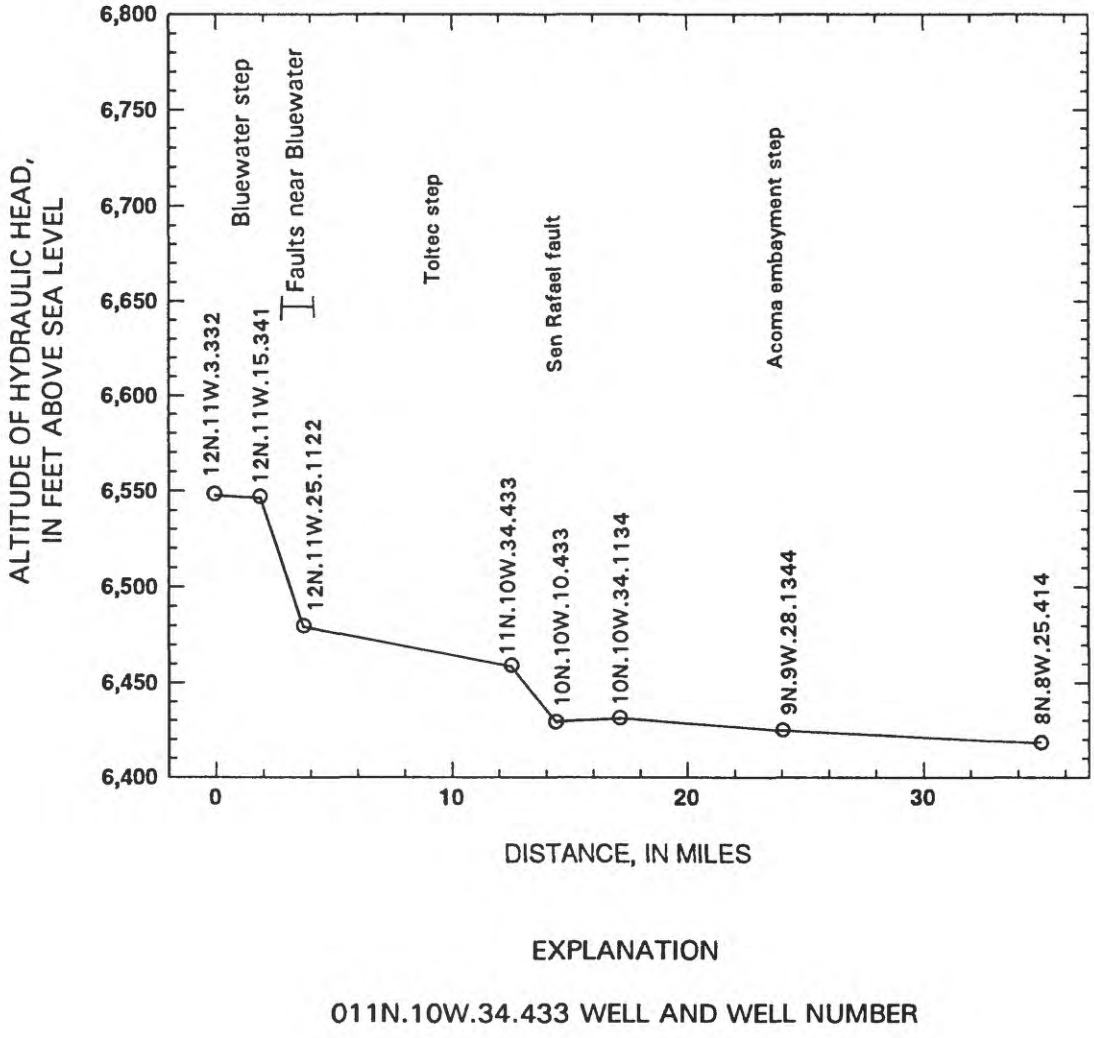

Figure 11.--Relation between hydraulic head and faults between Bluewater and the Pueblo of Acoma.

The rate of recharge in the mountains of the Zuni uplift was estimated from climatic and land-cover data in a two-step process. First, initial estimates of excess precipitation, that part of precipitation not used by evapotranspiration, were calculated by a method developed for the San Juan Mountains of Colorado (Hearne and Dewey, 1988, p. 14-29). The details of these calculations are in the Supplemental Information section of this report. However, these initial estimates seem to be too large for the Zuni uplift. Where underlying rocks are relatively impervious, excess precipitation is discharged as surface flow. Surface flow in streams discharging mainly from relatively impervious basins upstream from Bluewater Lake has been estimated for water years 1959-72 (Risser, 1982, table 4). Surface-water discharge for these 14 years totaled 58,000 acre-feet (rounded) (6 cubic feet per second), which is about 30 percent of the initial estimate of 194,000 acre-feet (rounded) (19 cubic feet per second) calculated by the San Juan method for the same years and basins. Therefore, in the second step, excess precipitation on the Zuni uplift was estimated to be about 30 percent of the initial estimate calculated by the San Juan method. For basins overlying permeable rocks in the Zuni uplift, excess precipitation was assumed to recharge ground water. For the water years 1932-85, the San Juan method calculated an average initial estimate of 17 cubic feet per second for basins overlying permeable rocks. For the Zuni uplift, recharge from precipitation was estimated to be 30 percent of these initial estimates or about 5 cubic feet per second.

Because of variations in altitude and land cover, recharge was expected to vary greatly over the area of the Zuni uplift; however, the average flux was about 0.1 cubic foot per second per mile of mountain front. Estimated excess precipitation was used as a guide to the spatial variation of estimated recharge. The mountain front was arbitrarily divided into five zones (fig. 12) within which no spatial variation was assumed. The estimated recharge for each zone (0.3 times the excess precipitation) was divided by the length of the zone to derive a flux in cubic feet per second per mile. The average fluxes are as follows:

Zone	Average recharge rate, in cubic feet per second	Length of zone, in miles	Flux, in cubic feet per second per mile (rounded)
1	1.6	16	0.10
2	.49	5	.1
3	1.3	12	.11
4	.46	5	.09
5	1.2	15	.08

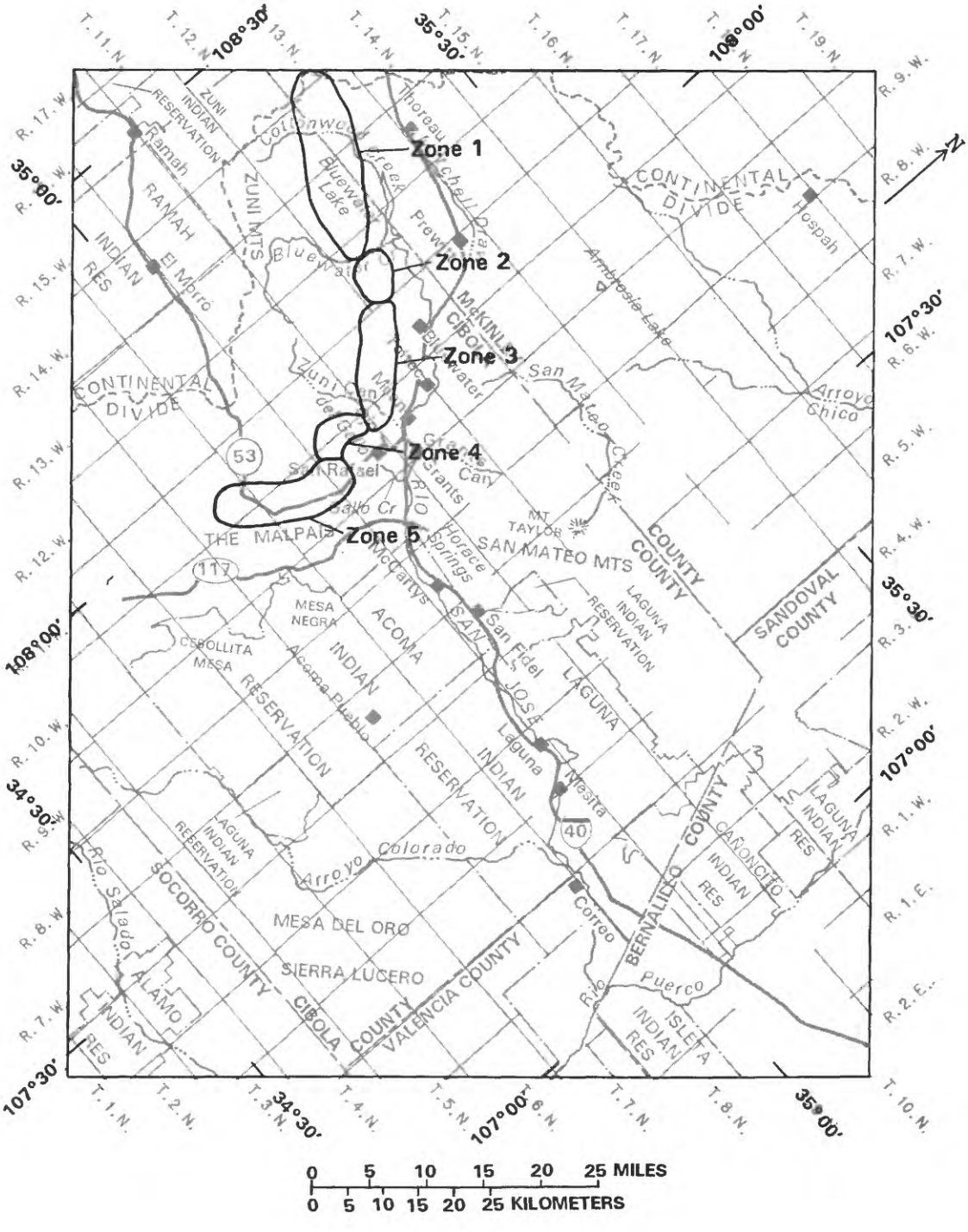

Figure 12.--Recharge zones on the mountains of the Zuni uplift.

Because precipitation varies greatly from year to year in the Zuni uplift, the excess precipitation method was used to estimate the variation of recharge with time. Recharge rates for the Zuni uplift, estimated on a 6-month basis, are shown in figure 13 for each zone (graphs A-E) and for the total of the five zones (graph F). Although the average flux in cubic feet per second per mile is about the same for each of zones 1-5, the 6-month rates are not exactly proportional to each other because they were estimated as functions of several variables including precipitation, temperature, and water stored in the snowpack.

Estimated excess precipitation for the parts of the Bluewater Creek and Cottonwood Creek basins that are on outcrops of rocks less permeable than the San Andres-Glorieta aquifer was assumed to discharge as surface water. Because much of the Zuni Canyon basin is on rocks underlying and less permeable than the Glorieta Sandstone, most of the discharge of Zuni Canyon was assumed to go into surface flow of the Rio San Jose rather than into recharge of the San Andres-Glorieta aquifer.

Recharge of the valley fill by infiltration of precipitation probably is not great because excess precipitation is not great. Estimated excess precipitation for most of The Malpais area that has vegetative cover was zero for most years. However, there is an area of barren, very broken basalt (fig. 2) for which excess precipitation is unknown. Because of the lack of soil and plant cover in this area evapotranspiration would consist mainly of evaporation from rock surfaces, a mechanism that is not accounted for by the San Juan method of estimating excess precipitation. No method is known to estimate evaporation from these extremely rough and broken basalt surfaces. This evaporation could constitute a large percentage of precipitation. Recharge might range from near zero to some value less than precipitation. Over the 60-square-mile area of the barren basalt field, recharge would be about 4.4 cubic feet per second for each inch of precipitation not evaporated. Precipitation at the nearest station, Grants, is about 10 inches per year. If it were assumed that precipitation averages 10 inches per year and evaporation between 1 and 9 inches per year, average recharge would be in the range of 4 to 40 cubic feet per second.

Time-varying recharge on the barren basalt field was estimated as a portion of precipitation at Grants. For times when precipitation data at Grants were not available (1973, and before 1953), the average of annual precipitation at San Fidel, Laguna, and Crownpoint (Risser, 1982, table 2) was substituted. (Crownpoint is about 20 miles north of Thoreau and is outside the study area.) When these annual values were used, all recharge was assumed to occur during late summer because inspection of Grants precipitation data shows most precipitation during late summer.

Recharge on a smaller barren basalt field in the western part of The Malpais was not estimated. There, west of the unnamed fault of Thaden and Zech (1984), recharge probably goes directly into the western flow system of the underlying San Andres-Glorieta aquifer.

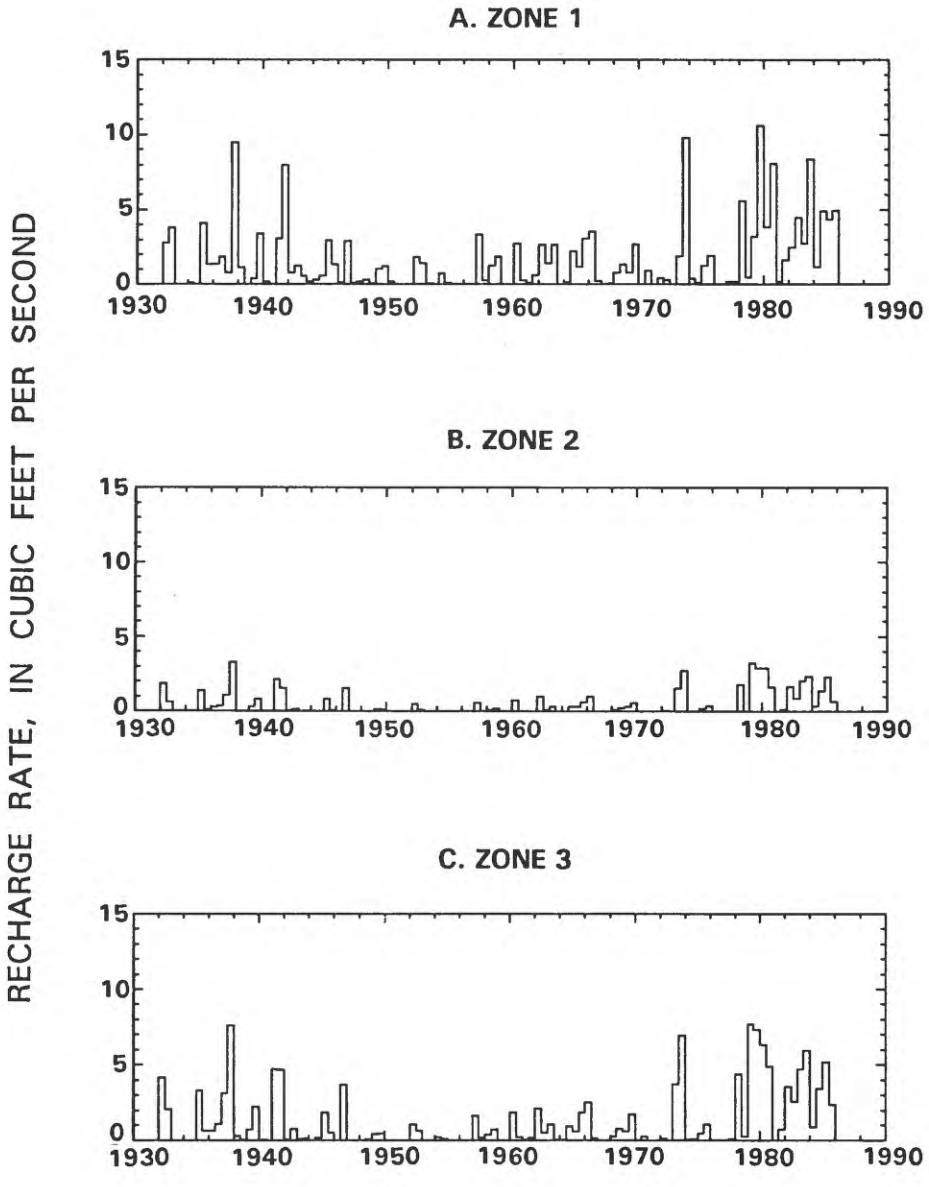

Figure 13.--Estimated 6-month recharge rates for the Zuni uplift during 1932-85.

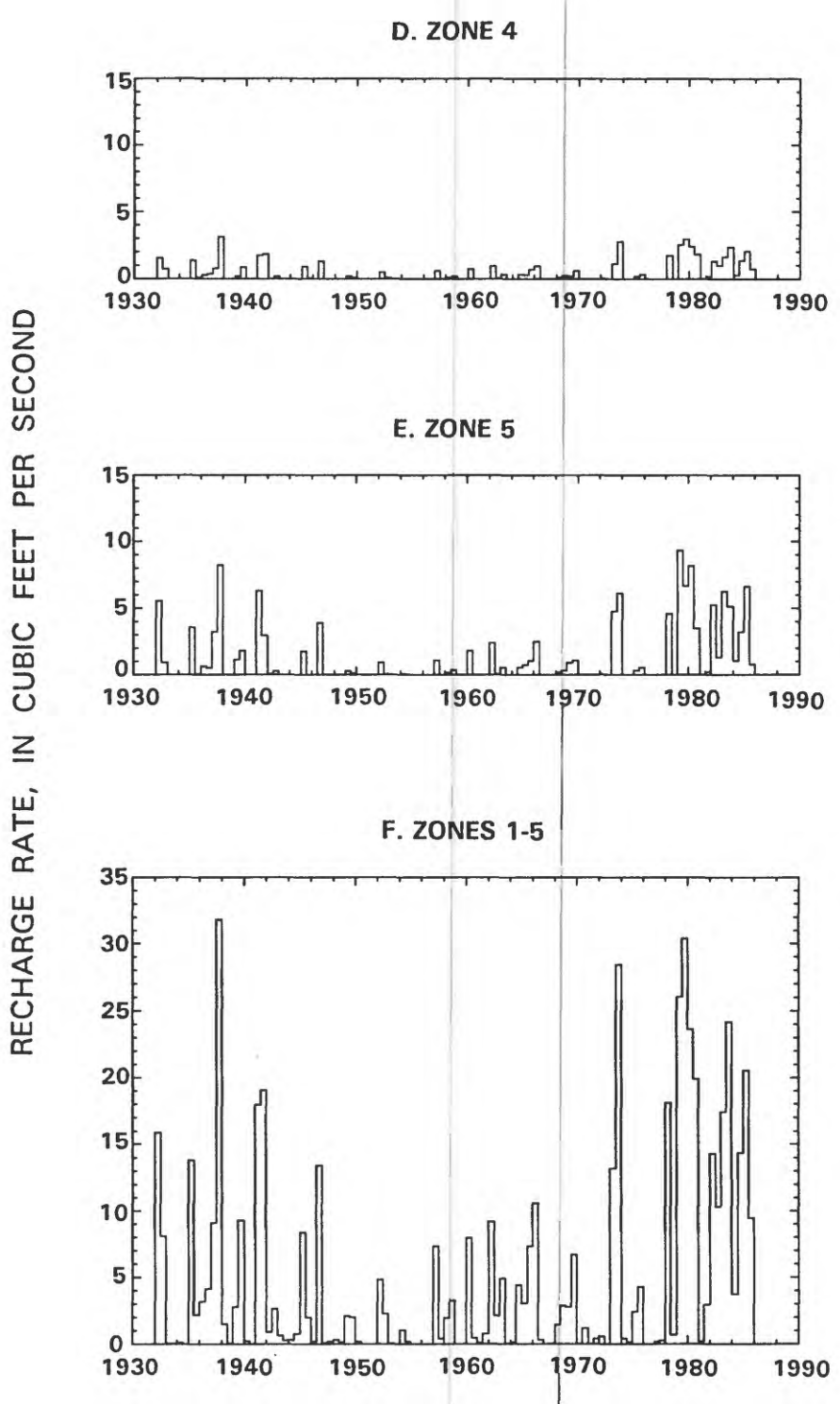

Figure 13.--Concluded.

The rate of recharge from precipitation on Lucero uplift is unknown but is probably very small. Interpretation of water-quality data indicates that Sierra Lucero is a recharge area and that ground-water flows westward from Sierra Lucero (Baldwin and Anderholm, in press). However, precipitation on the Lucero uplift is about half that on the mountains of the Zuni uplift and the land surface generally is covered by the types of soil and plant cover for which the San Juan method calculated no excess precipitation on the Zuni uplift. By this analogy, the recharge rate on the Lucero uplift also was estimated to be approximately zero. Recharge probably is small relative to other ground-water flows. Although recharge may occur in the Lucero uplift, interpretation of the direction of ground-water flow indicates that the area is regionally a discharge area. Interpolation of hydraulic heads between the potentiometric surface (figs. 6B and 9) and the land surface at springs east of Sierra Lucero (altitude about 5,600-5,800 feet) indicates that the San Andres-Glorieta aquifer may be unsaturated. Water recharged on the Lucero uplift may mix with water in the San Andres-Glorieta aquifer, affecting the water quality locally. This local flow system is superimposed on the regional flow system that discharges to the east.

Discharge by Evapotranspiration from Shallow Ground Water

Natural evapotranspiration (evapotranspiration not caused by human activities) from ground water occurs where the water table is near land surface in La Vega (the meadow) downstream from Ojo del Gallo, along Gallo Creek, and along the Rio San Jose between Grants and Horace Springs (fig. 5). Spring-related tufa deposits occur in the north end of La Vega over an area of about 2 square miles (William D. White, Hydrologist, U.S. Bureau of Indian Affairs, written commun., 1985) in and near the swampy area downstream from Ojo del Gallo. These deposits indicate substantial evapotranspiration. Evapotranspiration in this area probably increases and decreases along with the discharge of Ojo del Gallo, which varies in direct response to water levels in the San Andres-Glorieta aquifer. The water table and evapotranspiration probably declined as spring discharge from Ojo del Gallo declined in the 1940's. Downstream from Grants, the "alkali" deposits indicate substantial evapotranspiration. (The term "alkali" commonly refers to a white precipitate that remains on the ground where water evaporates. The chemical constituents generally are unknown and therefore this usage does not infer the presence of alkali metals.) Evapotranspiration occurs along the Rio San Jose in Grants downstream from the valley-fill spring at 11.10.26.43 when that spring rises to near the land surface. When water levels in the San Andres-Glorieta aquifer decline, water levels near the spring at 11.10.26.43 and nearby evapotranspiration probably also decline. However, farther downstream on the Rio San Jose toward Horace Springs, where water levels in the valley fill are less sensitive to variations in the hydraulic head in the San Andres-Glorieta aquifer, natural evapotranspiration probably is more constant.

The rate of discharge by natural evapotranspiration is unknown and will be estimated by the digital model on the basis of assumed properties. However, an estimate is useful for evaluating the plausibility of model-derived evapotranspiration values. Average annual lake evaporation is about 45 inches per year (U.S. Department of Agriculture, 1972). Evapotranspiration of shallow ground water may approach lake evaporation when the water table is at or above land surface, and might diminish to near zero when the water table is about 10 feet deep (Emery, 1970, fig. 3).

On the basis of visible evidence of evapotranspiration and altitudes, water levels may be within about 10 feet of the land surface over about 7 square miles in La Vega, along Gallo Creek, and along the Rio San Jose in and downstream from Grants. Visible evidence of evapotranspiration is such things as pools of water and "alkali." From such areas of visibly evident evapotranspiration, the area of shallow water table was expanded to include adjacent, nearly flat areas shown on topographic maps. However, evapotranspiration of 45 inches per year over 7 square miles (23 cubic feet per second) would not occur because the water table is not at land surface over most of that area. Therefore, the maximum rate of evapotranspiration would be less than 23 cubic feet per second. If evapotranspiration of 45 inches per year were to occur over the area of tuff deposits, the rate would be about 7 cubic feet per second. If it were assumed that, in addition, evapotranspiration averages 10 inches per year from the remaining 5 square miles, evapotranspiration would total about 10 cubic feet per second. Annual discharge to evapotranspiration from the water table was assumed to average about 5 to 15 cubic feet per second.

Stream-Aquifer Interactions and Ground-Water Flow Between the San Andres-Glorieta and Valley-Fill Aquifers

Flow between the San Andres-Glorieta aquifer and the valley-fill aquifer is often driven by surface-water interactions. The surface-water boundary is critical to estimating the effect of previous and new water development on streamflow, which was part of the purpose of this model study. The valley-fill aquifer often lies between the San Andres-Glorieta aquifer and the surface-water boundary.

The Rio San Jose and its tributaries comprise the main drainage system in the area. Bluewater Creek and its main tributary, Cottonwood Creek, discharge streamflow from the Zuni uplift (fig. 2). Bluewater Dam on Bluewater Creek downstream from the mouth of Cottonwood Creek has regulated discharge since 1928. Mitchell Draw, tributary to Bluewater Creek, generally does not flow. Between Mitchell Draw and San Mateo Creek, Bluewater Creek becomes the Rio San Jose. San Mateo Creek is tributary to the Rio San Jose, but it generally does not flow at its lower end where the channel is indistinct. Streams in Zuni and Grants Canyons are tributary to the Rio San Jose but only flow occasionally. Bluewater Creek is perennial through Bluewater Canyon but the Rio San Jose at Grants is ephemeral upstream from the sewer-plant discharge.

Ojo del Gallo discharges from the San Andres Limestone into a swampy area in the north end of La Vega, which drains into a small swale referred to as Gallo Creek in this report. Gallo Creek is tributary to the Rio San Jose between Grants and Horace Springs. Most of The Malpais area has no surface drainage. Horace Springs emerges in the Rio San Jose where the valley fill of alluvium and basalt narrows. The Rio San Jose discharges into the Rio Puerco, which discharges into the Rio Grande.

Ground-water flow between aquifers is shown schematically along Bluewater Creek and the Rio San Jose between Bluewater Lake and Horace Springs in figure 14. Water flows from Bluewater Lake into the San Andres Limestone, some of which emerges in Bluewater Canyon within the first 2 miles downstream from the lake. Through most of Bluewater Canyon, Bluewater Creek flows near the contact between the San Andres-Glorieta aquifer and older Permian rocks and may gain or lose water. Downstream from the canyon, water lost from Bluewater Creek flows through the alluvium and into the San Andres Limestone. Farther downstream, near Milan, water leaks upward into the valley fill. Ground water emerges at the land surface along the Rio San Jose in Grants, and from there to McCartys (fig. 1). East of the San Rafael fault, which cuts through the middle of Grants where the San Andres-Glorieta aquifer underlies a great thickness of Chinle confining bed, upward leakage into the valley fill probably is very small.

At Ojo del Gallo, about 2 miles south of Grants along the San Rafael fault, the water table in the San Andres-Glorieta aquifer intersects land surface (fig. 10) except when water levels in the San Andres-Glorieta are drawn down due to ground-water withdrawals in the area from Bluewater to Milan. The water table in the San Andres-Glorieta aquifer is almost flat upstream from Ojo Del Gallo and discharges from Ojo del Gallo are very sensitive to small changes in hydraulic head in the upstream aquifer. Near the spring, water flows horizontally from the San Andres Limestone into the valley fill across the fault (fig. 10). Discharge from Ojo del Gallo enters a swampy area of La Vega where much of the water may be lost to natural evapotranspiration and some of the water recharges the valley fill. Water that recharges the valley fill in the swampy part of La Vega possibly returns to the surface in springs and seeps along Gallo Creek (fig. 10) or farther downstream along the Rio San Jose.

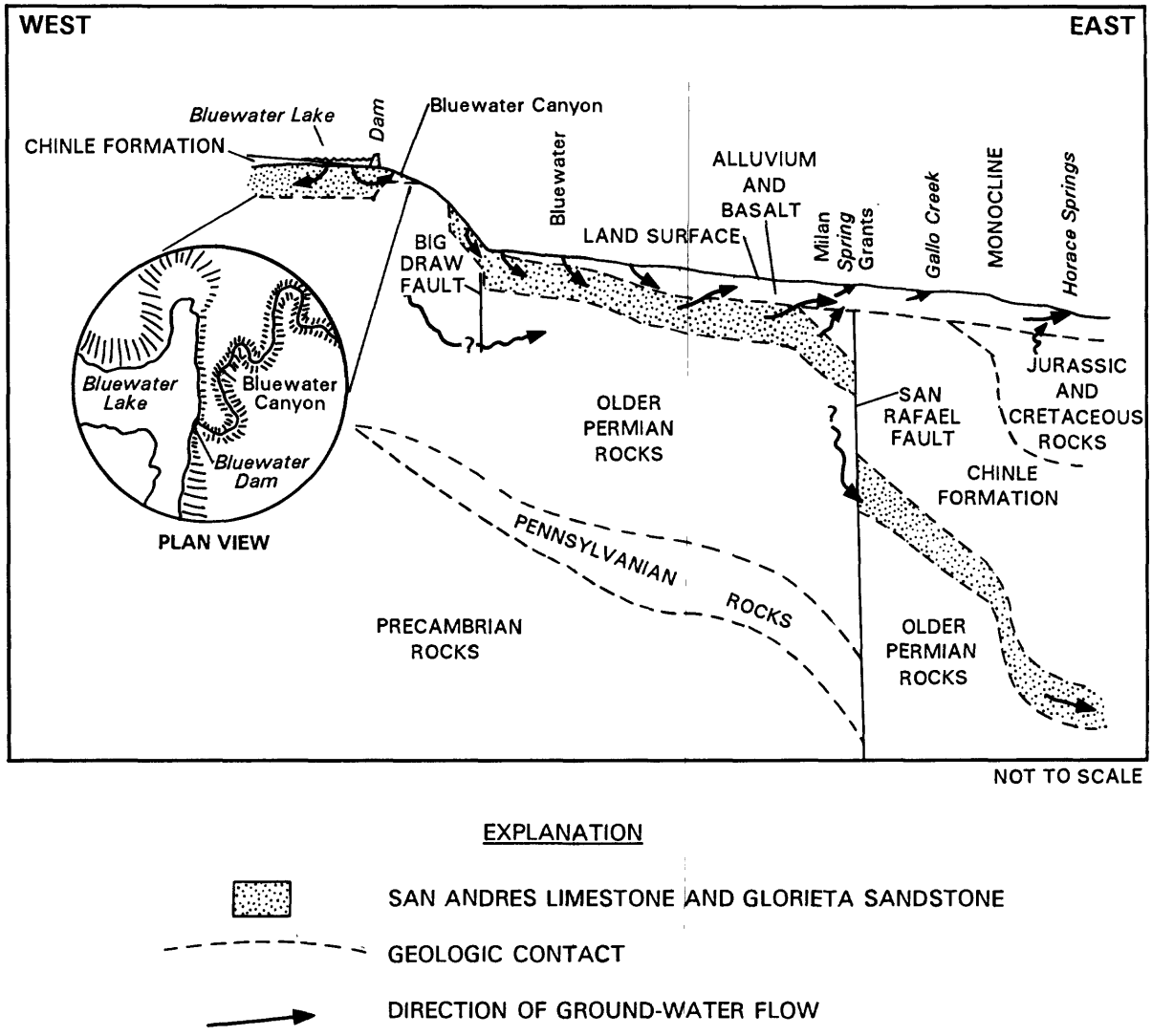

Figure 14.--Direction of ground-water flow along Bluewater Creek and the Rio San Jose from Bluewater Lake to Horace Springs.

Measured and estimated streamflows

Streamflows on Bluewater Creek and the Rio San Jose have been measured for many years. However, many streamflows were estimated in this report because they were required to simulate the stream-aquifer boundary. These estimates were based on streamflow measurements on Bluewater Creek near the mouth of Bluewater Canyon (gaging station 08342000, fig. 2), on precipitation, and on physical dimensions and characteristics of the stream-aquifer system.

Streamflow on Bluewater Creek near the mouth of Bluewater Canyon was measured intermittently before Bluewater Dam was installed in 1927. The yearly mean discharges in cubic feet per second (U.S. Geological Survey, 1960, p. 465) for 5 years of record before Bluewater Dam was installed are as follows:

Water year	Mean annual discharge, in cubic feet per second
1913	8.40
1914	15.1
1915	34.8
1917	9.94
1918	6.54

The mean of these annual values is about 15 cubic feet per second, and the median is about 10 (9.94) cubic feet per second.

After Bluewater Dam was installed, the mean discharge for 45 years of record from 1928 to 1972 was about 8.24 cubic feet per second (Risser, 1982, table 4). Natural streamflow would have been greater. Streamflow adjusted for evaporation losses from Bluewater Lake and change in lake contents averaged about 10 cubic feet per second (Risser, 1982, table 4). In addition, Bluewater Lake probably causes some ground-water recharge that would not otherwise occur, and some streamflow capture may occur in the perennial reaches of Bluewater Creek because of drawdowns in the San Andres-Glorieta aquifer. Because of the lack of long-term streamflow measurements before the dam was installed, capture and ground-water recharge caused by the lake were not estimated. Part of the purpose of the model study was to derive such estimates. Assuming that capture and recharge caused by the lake together have averaged about 1 cubic foot per second, natural flow in Bluewater Creek at the mouth of Bluewater Canyon would have averaged 11 cubic feet per second, which was an assumption used for this study.

Because the stream is regulated, streamflow at the mouth of Bluewater Canyon (gaging station 08342000, fig. 2) cannot be simulated by a routing procedure but rather must be independently derived (measured or estimated) and then specified as model input. Streamflow has not been measured since 1972, and no records of regulated discharges are available, so it was necessary to estimate streamflow. Measured and estimated streamflows at gaging station 08342000 are shown in figure 15A. The values shown in figure 15A are average streamflows for half water years for 1928-73 when streamflows were measured. For 1900-28, the estimated annual average of 11 cubic feet per second was assumed. For the period after 1985, the projected value was the average of measured values for 1928-73.

The estimates shown in figure 15A for 1973-85 were made in a multistep process. (1) Natural annual streamflows were estimated from precipitation. (2) Estimates were adjusted to account for net evaporation from Bluewater Lake and changes in lake contents. (3) Annual flows were divided into half-year flows on the basis of the average winter/summer proportion of flows during the time (1928-72) when flows had been measured (in this report winter is October through March, and summer is April through September). Although most natural inflow to Bluewater Lake occurs during the winter half of the water year, most regulated outflow occurs during the summer half for irrigation. During 1928-72 about 14 percent (rounded) of the total flow passing gage 08342000 at the mouth of Bluewater Canyon was during the winter half of the year and 86 percent was during the summer half of the year.

Estimates of natural streamflow were based on estimated excess precipitation calculated by the method developed for the San Juan Mountains of Colorado (Hearne and Dewey, 1988, p. 14-29). The details of these calculations are in the Supplemental Information section of this report. Excess precipitation was regressed against Risser's (1982, table 4) estimates of natural streamflow for 1959-72 (not accounting for recharge caused by Bluewater Lake and stream capture). The regression equation was:

$$Y = 0.3548\ EP - 748.6 \qquad (4)$$

where Y = natural streamflow, in acre-feet; and
EP = excess precipitation, in acre-feet.

From this equation natural streamflow was estimated for 1973-85, and regulated streamflow was estimated as natural streamflow minus estimated evaporation from Bluewater Lake, then adjusted for change in lake contents. These values are shown in table 11 (in Supplemental Information). Net evaporation from Bluewater Lake (table 11) was estimated by the method described in Risser (1982, p. 17-19), which accounts for lake area and precipitation on the lake. Precipitation data for McGaffey was adjusted for altitude, then used for the estimate of net evaporation. (McGaffey is in the mountains about 15 miles southwest of Thoreau.) Records of lake stage and contents are available in U.S. Geological Survey annual data reports. These streamflow estimates (last column of table 11) are very poor. They were made only to provide input required by the digital model and probably are not appropriate for any other purpose.

A. BLUEWATER CREEK AT MOUTH OF BLUEWATER CANYON

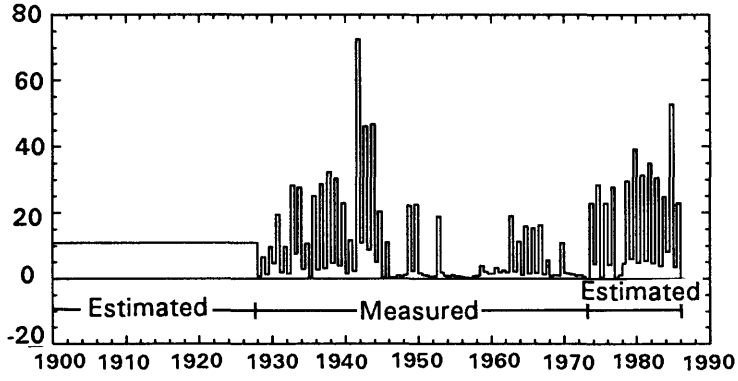

STREAMFLOW, IN CUBIC FEET PER SECOND

B. COTTONWOOD CREEK AT SAN ANDRES-GLORIETA OUTCROP

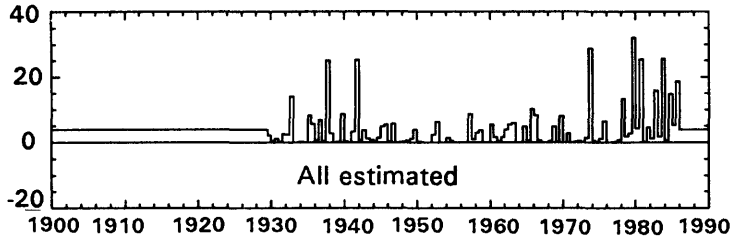

C. BLUEWATER CREEK AT SAN ANDRES-GLORIETA OUTCROP

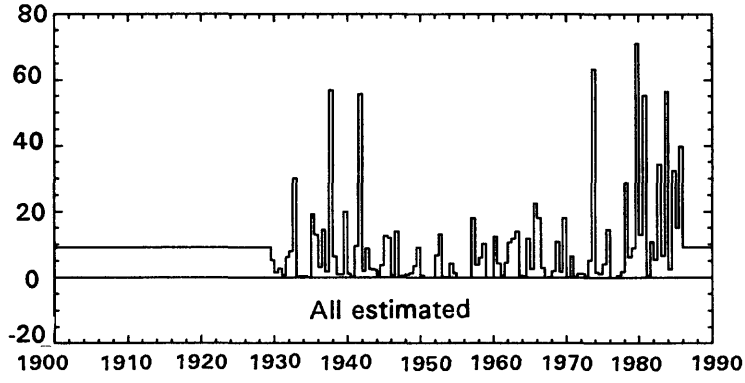

Figure 15.--Measured and estimated streamflows on Cottonwood and Bluewater Creeks.

Streamflows were estimated for Bluewater and Cottonwood Creeks upstream from Bluewater Lake where these streams cross the outcrop of the San Andres-Glorieta aquifer. These locations are shown in figure 2 as sites EB (Bluewater) and EC (Cottonwood). Although these streams are considered to be perennial, they may not flow every year especially during droughts that sometimes last for several years. In order for the digital model to simulate dry-stream or low-flow conditions during droughts, it was necessary to estimate streamflows at points EB and EC. The estimated flows, shown in figure 15B and 15C, were derived on the bases of estimated excess precipitation for the upstream watersheds and estimated average natural streamflow (11 cubic feet per second) at the mouth of Bluewater Canyon (gaging station 08342000). Bluewater and Cottonwood Creeks are the main contributors to streamflow at the mouth of Bluewater Canyon and, for this estimate, were assumed to be the sole contributors. It was also assumed that 2 cubic feet per second would be lost to ground water in the intervening reaches for a total average of 13 cubic feet per second. This average flow was divided between the two watersheds on the basis of estimated excess precipitation; 70 percent (9.1 cubic feet per second) was attributed to the Bluewater Creek watershed and 30 percent (3.9 cubic feet per second) was attributed to the Cottonwood Creek watershed. Finally the half-water-year flow rates shown in figure 15A were estimated as the excess precipitation times 3.9 cubic feet per second divided by the average excess precipitation (5.2 cubic feet per second). Similarly, the flow rates shown in figure 15B were estimated as the excess precipitation times 9.1 cubic feet per second divided by the average excess precipitation (11.6 cubic feet per second). These estimates are extremely poor. They were made only to provide a rationale for distinguishing between wet- and dry-stream conditions in the model input, and for this purpose are not critical. These estimates, however, should not be used for any other purpose.

The next gaging station downstream from the mouth of Bluewater Canyon is the Rio San Jose at Grants (gaging station 08343000). Because most of the flows at the mouth of Bluewater Canyon either are used for irrigation or are lost to ground water, streamflow at Grants is related mainly to local storm activity, which was not accounted for in the ground-water model. Measured streamflow at Grants was not used in this analysis.

Gallo Creek was probably perennial in the past but has not flowed for many years because flow at Ojo del Gallo has only recently (1980's) resumed after having been dry for about 30 years. The reported discharge of Ojo del Gallo has been as much as 7 cubic feet per second (Hodges, 1938, p. 339) and may have been greater previously. Hodges (1938, p. 340) estimated flow in Gallo Creek to be 4 cubic feet per second but considered that it would have been more if flow had not been obstructed by manmade diversions. Because irrigation diversions of springflow at Ojo del Gallo began in the late 1800's, no streamflow estimates on and downstream from Gallo Creek reflect natural conditions on Gallo Creek. The discharge of Gallo Creek probably has always been smaller than that of Ojo del Gallo because of losses to natural evapotranspiration and ground-water recharge in the intervening swamp.

Streamflows on the Rio San Jose downstream from Horace Springs (fig. 2, gaging station 08343500) have been measured since 1936 and have averaged 6.81 cubic feet per second (U.S. Geological Survey, 1985). Because Bluewater Creek, the main tributary of the Rio San Jose, has been controlled by Bluewater Dam during the period of measurement, most of the measured flow at this station has emerged from Horace Springs except for local storm flows and effluent from the Grants sewage-treatment plant, which has increased gradually to about 2 cubic feet per second in the late 1970's and 1980's. Risser (1982, fig. 11) estimated natural streamflow downstream from Horace Springs to have been about 12,000 to 14,000 acre-feet per year (about 17-19 cubic feet per second), with a possible error of 25 percent in addition to unquantifiable errors (Risser, 1982, p. 34). A gain of 2.5 to 3 cubic feet per second occurs between Horace Springs and McCartys (Risser, 1982, p. 32). Part of this gain comes from the Jurassic and Cretaceous bedrock that underlies the valley fill in that reach, judging on the basis of hydraulic heads in the Jurassic system (Frenzel and Lyford, 1982, figs. 17 and 18; D.W. Risser and F.P. Lyford, Hydrologists, written commun., 1984, pl. 1). However, this streamflow gain probably comes mainly from the same source as Horace Springs because it comes from the same cavernous basalt flow as Horace Springs and the underlying bedrock is probably much less permeable than the basalt.

For the next 20 miles downstream from McCartys, the Rio San Jose is separated from the San Andres-Glorieta aquifer by the full thickness (1,500 feet) of Chinle Formation confining bed and as much as 1,000 feet of Jurassic and Cretaceous aquifers and confining beds. Farther downstream, where the Jurassic and Cretaceous rocks are not present, the Rio San Jose is separated from the San Andres-Glorieta aquifer by nearly the full thickness of Chinle Formation confining bed. Leakage through the Chinle is discussed elsewhere in this report.

Streambed conditions

The digital model requires that a conductance be specified for each model block where a stream is represented. The conductance may be estimated by any reasonable procedure but is normally estimated as the area of the streambed in the model block times the vertical hydraulic conductivity of the streambed divided by the thickness of the streambed (McDonald and Harbaugh, 1988, chap. 6, p. 5). These properties were not measured. The following discussion gives physical conditions upon which assumed streambed properties were based.

Cottonwood Creek flows northward out of the middle of the Zuni uplift over successively younger rocks. Most of the Cottonwood Creek watershed is underlain by rocks older and less permeable than the San Andres-Glorieta aquifer. Where Cottonwood Creek crosses the outcrop of the San Andres-Glorieta aquifer, it may gain or lose flow. After Cottonwood Creek crosses the outcrop of the San Andres-Glorieta aquifer, it is underlain by the Chinle Formation confining bed, which increases to an estimated 200 feet in thickness where Cottonwood Creek enters the west end of Bluewater Lake. The Chinle Formation under Bluewater Lake thins to the east and the lake is underlain by San Andres Limestone at the east end. The thickness of the Chinle Formation underlying Cottonwood Creek and Bluewater Lake was estimated by projecting the dip slope of the San Andres Limestone that crops out on the south side of the lake. Cottonwood Creek upstream from Bluewater Lake was assumed by casual observation to be about 20 feet wide.

The Bluewater Creek watershed also is underlain by rocks older and less permeable than the San Andres-Glorieta aquifer, and Bluewater Creek flows northward out of the Zuni uplift over successively younger rocks. Bluewater Creek flows on the San Andres-Glorieta aquifer for about 2 miles before entering the southeast corner of Bluewater Lake and does not flow over the Chinle Formation. Bluewater Creek upstream from Bluewater Lake was assumed to be about 50 feet wide where it flows over the San Andres-Glorieta aquifer.

Bluewater Lake submerges parts of Cottonwood and Bluewater Creeks. (This part of Cottonwood Creek also is called Azul (Blue) Creek.) The width of Bluewater Lake was assumed to vary linearly between a minimum of 20 feet at streambed level when empty to a maximum of as much as 3,100 feet determined by the 7,400-foot contour when the lake is full. (The uncontrolled spillway altitude is 7,403 feet.)

The 2-mile-long east side of Bluewater Lake is formed by a shear wall of San Andres Limestone that occurs along a fault upthrown on the east side. (This fault probably does not offset the aquifer completely.) Bluewater Dam, a concrete-arch structure, is located where Bluewater Canyon breaches the wall, and the dam is anchored in the limestone. About 0.25 mile from the dam, the canyon abruptly turns and meanders northward for about a mile subparallel to the side of the lake (fig. 14, inset) so that the limestone separating the lake from the canyon is 0.2 to 0.5 mile wide. Water seeps through the limestone to the stream in the canyon, and when the lake level is high, the seepage face occurs on the canyon wall. On April 4, 1986, streamflow increased from an estimated 0.1 to 0.3 cubic foot per second at the dam to 3.8 cubic feet per second at a point about 2.0 miles downstream from the dam (about 1 mile northeast of the dam on a straight line), which was downstream from the visible seeps. At that time, the lake level was 7,395 feet (U.S. Geological Survey, 1987). Bluewater Canyon meanders eastward for about 6 miles and ends abruptly as it crosses a fault that is downthrown on the east. This fault on the downstream end of Bluewater Canyon may be a southern extension of Big Draw fault, but may not offset the aquifer where Bluewater Creek crosses. In the canyon, Bluewater Creek flows near or below the bottom of the San Andres-Glorieta aquifer and, although it gains flow in the first mile or two below the lake, it may gain or lose flow in most of the canyon reach. The width of Bluewater Creek in Bluewater Canyon is about 40 feet during low-flow conditions. However, near Bluewater Lake, the width may be as much as 200 feet, depending on lake level, if the seepage from the lake is included in the width of the stream. The streambed is composed largely of gravel and boulders and probably does not greatly inhibit the flow of water into or out of the aquifer.

From the mouth of Bluewater Canyon to a borrow pit near Bluewater Village, the stream loses water. As Bluewater Creek exits Bluewater Canyon, the streambed consists of boulders and cobbles. The alluvium downstream from the mouth of the canyon probably also consists of coarse material, but finer material probably is brought in by Mitchell Draw, about 2 miles downstream from the mouth of the canyon. The stream flows near the alluvium-San Andres contact. The thickness of the streambed and alluvium, although unknown, varies from zero to possibly as much as 100 feet, and the water table may be in the San Andres-Glorieta aquifer. However, if the water table is below the

bottom of the valley fill in the cavernous San Andres Limestone, the unsaturated limestone may not give much resistance to vertical flow. On April 4, 1986, a streamflow of 4 cubic feet per second measured near the diversion, located in T. 12 N., R. 11 W., sec. 8 about 0.5 mile from the mouth of Bluewater Canyon, disappeared into the ground between the diversion and the borrow pit about 6 miles downstream. The width of the wetted streambed in this reach varied from 40 feet near the diversion to near zero where the flow entered the borrow pit. If there had been more inflow, the wetted streambed would have been wider and streamflow losses could have been greater. The stream flows into the borrow pit, which forms a small lake and probably allows infiltration.

Between the the borrow pit and Milan, the stream probably continues to lose water to the valley fill when there is streamflow, and the water table in the valley fill becomes shallower because the water-table gradient is not as steep as the stream gradient. The stream is normally dry and bottom material is finer than it is upstream. The thickness of the streambed may be the depth from the stream bottom to the water table, which varies from nearly 100 feet between Bluewater and Toltec to 20 feet at Milan. The width of the stream may be about the same as it is upstream. The name of the stream changes from Bluewater Creek to Rio San Jose before it reaches Milan.

Between Milan and Grants the Rio San Jose changes from a losing stream to a gaining stream. However, through Grants to the confluence of Gallo Creek the stream gains very little, if any, flow from ground water. In the vicinity of Grants, the water table in the valley fill is near land surface as indicated by a spring (11.10.26.43) that was observed in 1987. Although this spring had not flowed for decades, it was reported to have been formerly used to irrigate an orchard. The remnants of the orchard still could be seen in 1987. The spring pool was observed at the edge of the basalt above the level of the riverbed in May 1987. Although it is difficult to identify other springs for several miles downstream from this spring, pools of water and white "alkali" in the reach extending downstream from the middle of Grants to the confluence with Gallo Creek probably indicate ground-water discharge from the valley fill. Whereas the basalt is very broken and appears to be very permeable, the alluvium and the streambed consist of fine-grained material such as silt and clay. This may explain the existence of the wet land surface adjacent to the stream that appears to be gaining little, if any, flow. As upstream, the stream width depends on the flow in the stream, but was assumed to be 20 feet.

Ojo del Gallo heads Gallo Creek, about 2 miles south of Grants along the San Rafael fault. Because Ojo del Gallo is a significant feature of the stream-aquifer relation, the geometry and water-yielding characteristics of the aquifer in the immediate vicinity are discussed here.

Ojo del Gallo occurs where the cavernous San Andres Limestone is faulted against the Chinle confining bed and alluvium. Ojo del Gallo emerges from the limestone on the west side of a pool that is dug into the alluvium.

Discharge fluctuates greatly with stage in the pool. On October 8, 1985, when the pool altitude was 6,456 feet, the discharge was approximately 0.8 cubic foot per second, measured with a current meter in a rectangular wooden flume. The accuracy of this measurement is poor because of small streamflow velocity and the unknown effects of the flume. On February 2, 1985, when the pool altitude was 6,455 feet, the flow leaving the pool through steel pipes was estimated, using a pipe-flow equation, to have been almost 2 cubic feet per second. The accuracy of the pipe-flow estimate also is probably poor because the hydraulic characteristics of the pipes are not known. Similar estimates had been made during the previous year. During the time these two estimates were made, the water-level altitude in well 11.10.34.433, approximately 0.8 mile north (upstream) of the spring, was approximately 6,458.5 feet, measured with a float-driven recorder. (The datums at the well and spring were surveyed with an engineering level.) The sensitivity of springflow to pool stage and the small, 3- to 4-foot-per-mile gradient between the well and the spring indicate a very good hydraulic connection between the spring and the upstream aquifer.

Discharge from Ojo del Gallo widens into a swampy, flat area in the northern part of La Vega, and the wet area in 1986 was estimated to be about 100-300 feet wide on the basis of aerial photos taken with a hand-held camera. Although the soil in the swampy area may be fine grained, the area of the streambed probably ensures a very close hydraulic connection between the stream and the valley fill. Gallo Creek narrows as it enters a swale. In 1986, the channel was not well defined probably because it had been dry for decades and apparently had been largely closed by windblown soil. When water flowed in this channel, it probably was narrow and well defined. The effective thickness of the streambed is unknown, but is probably the depth to the water table, which comes to the land surface at springs (10.9.6.442) along Gallo Creek near where the creek enters the Rio San Jose.

The Rio San Jose may gain or lose flow in the reach downstream from Gallo Creek; it is definitely gaining flow near Horace Springs. At Horace Springs, the stream channel is cut into a basalt flow that is very broken and cavernous. The streambed probably offers very little resistance to the upwelling water. The springs emerge along the bottom of the stream channel, flowing about 5 cubic feet per second (Risser, 1982, p. 31). The cavernous basalt flow extends several miles downstream from Horace Springs.

Ground-Water Inflow and Outflow

The rates of ground-water flow into and out of the San Andres-Glorieta aquifer and valley-fill aquifer in the study area are unknown. Although it might be theoretically possible to estimate the net ground-water flow as the residual in a water budget, the errors in the other items of the budget--recharge, streamflows, and evapotranspiration--are potentially much larger than the residual. However, the locations and directions of some flows can be interpreted from hydrologic data. Ground-water flow can be divided into three general categories: underflow in alluvial channels, leakage through the Chinle, and flow through bedrock units. Flows in each of these categories will be represented in the digital model presented later.

Ground water may flow into the simulated part of the valley-fill aquifer as underflow in valley-fill channels of ephemeral streams. Although Mitchell Draw, Grants Canyon, and San Mateo Creek seldom carry surface water to the Rio San Jose, there may be underflow into the valley-fill aquifer at each of these points.

The upstream reaches of San Mateo Creek received an unknown quantity of uranium-mine discharge between the mid-1950's and the 1980's. The mines discharged from rocks of Jurassic and Cretaceous age overlying the Chinle confining unit Ambrosia Lake. Even with the mine discharge, San Mateo Creek remained intermittent and did not flow to the Rio San Jose. The mine discharge probably temporarily increased underflow in the alluvium along San Mateo Creek.

Ground water discharges as underflow in the channel of the Rio San Jose at Horace Springs. As previously mentioned, within 5 miles downstream from Horace Springs, the Rio San Jose gains about 2.5 to 3 cubic feet per second (D.W. Risser and F.P. Lyford, U.S. Geological Survey, written commun., 1984, p. 26). Although some of this flow is discharge from rocks of Jurassic and Cretaceous age, much of it may be underflow from the same source as Horace Springs.

Ground water also leaks through the Chinle Formation. The total area over which leakage might occur is about 5,000 square miles, of which possibly about 3,000 square miles might be a discharge boundary on the San Andres-Glorieta aquifer and 2,000 square miles might be a recharge boundary. Very little water appears to leak through the Chinle where the potential is largest and the Chinle is thinnest. Northwest of Sierra Lucero, the Chinle is less than full thickness underlying a broad valley of about 300 square miles. The potentiometric surface of the San Andres-Glorieta aquifer is about 400 feet above land surface (fig. 6B) over an area that may be half the area of this valley (150 square miles). The small quantity of water that leaks upward to seeps in the Chinle Formation evaporates near the seeps, and the Arroyo Colorado, which drains most of this valley, is normally dry.

Interpretation of ground-water flow implies that discharge of the San Andres-Glorieta aquifer is generally to the east. Although the mechanism and quantity of discharge to the east are unknown, flow may transgress several geologic units. To the east, transmissivity in some of the underlying Pennsylvanian and Permian rocks may be as large or larger than that in the San Andres-Glorieta aquifer. In the Rio Puerco fault zone, north of the Lucero uplift, flow to the east may discharge from the full section of Permian and Pennsylvanian rocks to successively younger rocks, and eventually to the Santa Fe Group in the Rio Grande rift. Near Sierra Lucero, water from the San Andres-Glorieta aquifer may flow through Pennsylvanian rocks and surface in seeps and springs on the east side of Sierra Lucero. Because most of these springs are very small and most of the water may be lost to evaporation in the immediate vicinity, flow from these springs has not been measured (Baldwin and Anderholm, in press). The Rio Salado tributary of the Rio Grande in the southern part of the study area receives about 1 cubic foot per second of water from saline springs (not shown) that discharge from Pennsylvanian rocks (Spiegel, 1955, p. 67).

Ground water may flow into or out of the study area on the southern boundary through more permeable areas of the San Andres-Glorieta aquifer. The area of large transmissivity and cavernous limestone may extend beyond the southern boundary of the study area, but measured water-level altitudes are not precise enough to determine flow direction in this area where the potentiometric surface is flat. However, the most likely destination for this ground water would be the Rio Grande to the east or southeast, and ground-water flow in that area is probably subparallel to the study-area boundary.

On the northwest side of the study area along the Continental Divide, ground-water flow is toward the northeast, assumed to be perpendicular to potentiometric contours (fig. 9) and subparallel to the study-area boundary. As the northeastward flow turns eastward, it approaches the northeast side of the study area obliquely.

This arcuate flow pattern is consistent with the flow pattern found in younger rocks in that area, which is the southeastern part of the San Juan structural basin (Lyford, 1979, figs. 4, 6, and 7), and was considered by Frenzel and Lyford (1982, p. 4) to be controlled by the basinal structure and topography of the San Juan Basin. The same structural/topographic constraint--that is, highland outcrops on the flanks of the Zuni uplift and lowlands to the east (southeast corner of the San Juan structural basin)--probably controls the direction of flow in the San Andres-Glorieta aquifer in this area. The discharge from the San Andres-Glorieta, however, would be laterally across the Puerco fault zone to younger rocks in the Rio Grande rift rather than directly to the land surface. In addition to the structural/topographic constraint, flow in the San Andres-Glorieta aquifer is restricted from proceeding north of the northern corner of the study area by the pinch-out of the aquifer (Baars, 1962, figs. 17 and 18). As the aquifer pinches out, ground water may discharge by way of leakage to other stratigraphic units, but the eventual eastward discharge probably results from structure and topography.

Ground water may flow into the area across the unnamed fault inferred by Thaden and Zech (1984). Although the potentiometric surface (fig. 9) indicates a restriction of flow, some water may cross this boundary especially near the northern end of the fault where offsets may not be the full thickness of the aquifer.

Summary of Predevelopment Ground-Water Flow

On the basis of the simplified interpretation of ground-water flow presented in the preceding section, recharge of the San Andres-Glorieta aquifer occurs mainly around the Zuni uplift on the west side of the study area, and discharge is mainly toward the Rio Grande rift (fig. 2) on the east side. Recharge and discharge result from five main phenomena: (1) recharge of precipitation on outcrop and subcrop areas, (2) discharge of shallow ground water to evapotranspiration, (3) recharge to and discharge from surface water, (4) flow of ground water into and out of the aquifer in the study area, and (5) recharge and discharge associated with water development. Although reliable estimates of these flow rates are not available, approximate estimates of the first three are offered here. Estimates of recharge and discharge associated with water development are discussed in the following History of Water Development section.

Recharge of the valley fill in the Grant-Bluewater and Malpais areas results from precipitation on the surface, infiltration of excess irrigation water, and surface-water outflow from Bluewater Creek and other canyons along the mountain front (Baldwin and Anderholm, in press). Discharge from the valley fill occurs as evapotranspiration from the water table in La Vega and along Gallo Creek downstream from La Vega, and along the Rio San Jose between Grants and Horace Springs (fig. 5).

The main discharge point of the valley fill is at Horace Springs, which emerges along a gaining reach of the Rio San Jose. Discharge at Horace Springs is measured as gain in the Rio San Jose and is about 5 cubic feet per second. Discharge at Horace Springs has not changed much over the years because water-level declines upstream have not greatly changed the slope of the water table, which is largely controlled by topography.

As water flows through the system, the exchanges between surface and ground water are complex and influenced by geology and topography. However, the net exchange between the points where Bluewater and Cottonwood Creeks cross the outcrop of the San Andres-Glorieta and downstream from Horace Springs (gaging station 08343500) is a discharge of 5 cubic feet per second from ground water, resulting from the difference between surface inflow (13 cubic feet per second) and surface outflow (18 cubic feet per second).

The predevelopment water budget is tabulated below. Because the residual is small relative to probable errors in the other estimates, it is not a reliable estimate of net ground-water flow. Flow rates at the individual ground-water flow boundaries will be estimated from simulated results with the digital model described below.

Estimated recharge and discharge prior to development

Description of flow	Estimated rate of flow, in cubic feet per second
Recharge from precipitation	
Zuni uplift	5
Barren basalt	4 to 40
Evapotranspiration from shallow ground water	5 to 15
Net discharge to surface water	5
Residual	Unknown

History of Water Development

The study area has been inhabited by ancestors of the Pueblo Indians since before the arrival of Europeans. The Indians used both dry-land and irrigated agriculture, and diverted water from the Rio San Jose.

Non-Indian settlement of the Grants-Bluewater area began in the late 1800's. Old Fort Wingate was established in 1862 southeast of Ojo del Gallo, and in 1869 when the fort was abandoned in favor of the new location, the community of San Rafael was established (Barela, 1975, p. 9). The community of San Rafael engaged in ranching and irrigated agriculture ("Ojo del Gallo irrigated area" in fig. 2) using the water of Ojo del Gallo until the flow from the spring ceased in 1952 or 1953 after 10 years of decreasing flow (C.V. Theis, Hydrologist, U.S. Geological Survey, written commun., 1949; Gordon, 1961, p. 47 and 51). When the water was available 1,000 to 2,500 acres were irrigated.

The Bluewater area was settled in the 1880's (Gordon, 1961, p. 13) and irrigation water was diverted from the unregulated flow of Bluewater Creek. Grants and Thoreau (Mitchell) were established by the railroad between 1879 and 1883 (Reeve, 1961, v. II, p. 231). Water needed for rail operations generally was supplied by wells, and ground-water withdrawals along the railroad route were consolidated at Grants, reaching a maximum in the 1940's, probably just before steam locomotives were replaced by diesel-electrics. Milan was established in 1957 (Gordon, 1961, p. 15).

At the site of the present (1986) concrete arch dam on Bluewater Creek (fig. 2) was an earthen dam from 1894 to 1905, which was replaced by a rock dam that was washed away in 1909 (Hodges, 1938, p. 360). From 1909 until 1927, irrigation water was diverted from natural streamflow as had been done before the dams. The concrete arch dam was built in 1927 (L.W. Hitchcock, Professional Engineer consultant for Bluewater-Toltec Irrigation District, written commun., 1948). Runoff from upstream of the reservoir was less than expected and the water supply for the planned 10,627 irrigated acres never became available. In 1948 the irrigable area was reduced to 5,488 acres (Bluewater-Toltec Irrigation District in fig. 2) and the difference was permanently excluded from irrigation (Gordon, 1961, p. 14). In 1951 the bottom 20 feet of the reservoir pool (3,500 acre-feet) was reserved for use by the New Mexico Department of Game and Fish (J.H. Bliss, New Mexico State Engineer Office, written commun., 1951).

Water for the Bluewater-Toltec Irrigation District is released from Bluewater Dam and carried in the natural channel through Bluewater Canyon. The point of diversion from the natural channel is about one-half mile southeast of the mouth of Bluewater Canyon.

Major development of water from the San Andres-Glorieta aquifer started in the mid-1940's when the first irrigation wells were drilled in the Grants-Bluewater area. By the end of 1954, 28 irrigation wells, 3 industrial wells, and 4 municipal wells had been drilled (Gordon, 1961, p. 51). The 1950's may have been the time of the greatest ground-water development because only 22 wells were reported in 1977 (Travis Stevenson, U.S. Soil Conservation Service, written commun., 1977). In 1984, the Acoma Tribe drilled a well near the western boundary of the pueblo that produced a good supply of freshwater (Baldwin and Anderholm, in press). The known limit of the freshwater resource in the San Andres-Glorieta aquifer was thereby extended about 4 miles eastward to State Highway 117.

The way in which water has been used in the Grants-Bluewater area has followed economic changes. Before the 1930's, agriculture probably was diversified. In about 1939, agriculture changed to commercial cultivation of vegetables (L.W. Hitchcock, written commun., 1948). In the mid-1950's potato production was attempted, but vegetable production was limited by nearly 10 years of drought. Since the mid-1960's, alfalfa, pasture, and small grains have been the main crops (Joseph Nielson, oral commun., 1986). Industrial and municipal development resulted mainly from the mining and processing of uranium, which started in the early 1950's. Some water withdrawals formerly used for agriculture were transferred to uranium processing. (Uranium-mine dewatering probably had little direct effect on the San Andres-Glorieta aquifer because the mines are in Jurassic rocks that are separated from the San Andres Limestone by about 1,500 feet of siltstone and mudstone of the Triassic Chinle Formation.) Uranium production began to decrease in 1979 due to market conditions. Since 1984, some water withdrawals previously used for uranium processing have been used for electric-power production.

Ground-water withdrawals include water pumped for irrigation, municipal, and industrial uses. Water pumped for stock and individual domestic uses was assumed to be insignificant. Artificial recharge occurs as a result of irrigation, domestic discharges where no municipal sewage system is used, and uranium processing. The following sections estimate the withdrawals and recharge associated with these activities.

These withdrawals and recharges were superimposed on the natural flow system, resulting in changes in the volume of water in storage and in the flow rates for some of the natural recharges and discharges. No attempt was made to estimate these changes here; this is one purpose of the digital model presented later in this report.

Irrigation Ground-Water Withdrawals and Recharge

Irrigation withdrawals from ground water, total ground and surface water applied to fields, and recharge from irrigation were estimated for two irrigation areas (fig. 2): Bluewater-Toltec and south San Raphael. Recharge from irrigation was assumed to be about one-third of the total applied irrigation water at Bluewater-Toltec and south San Rafael. A net withdrawal from the valley-fill aquifer of about one-half of the springflow was assumed for Ojo del Gallo.

The accuracy of estimates of irrigation ground-water withdrawals for the Bluewater-Toltec Irrigation District and south San Rafael area varies greatly. The best estimates are probably those for 1945-57, which are based on electric-power consumption (U.S. Geological Survey, 1949-57) and are tabulated in Gordon (1961, table 7). Estimates for each year were necessary to simulate the system and, therefore, were based on whatever information was available, some of which was conflicting.

Estimation of ground-water withdrawals and recharge in the Bluewater-Toltec Irrigation District (table 1, and fig. 16A) depends primarily on: (1) streamflow, which determines the availability of surface water; (2) reported, estimated, or assumed values for irrigated area, from which is determined the demand for irrigation water; and (3) reported quantities of ground water and surface water applied to irrigated fields during 1932-60 (Gordon, 1961, tables 2 and 7). From reported values for 7 years between 1932 and 1960, a ratio was calculated as the quantity of surface water applied divided by the quantity passing the gage on Bluewater Creek at Bluewater (gaging station 08342000) during the growing season (April to September). This ratio (0.6) and the April-September flow past the gage were used to estimate the quantity of surface water that was applied to irrigated land during years for which no irrigation applications were reported (table 1). The remaining 40 percent of April-September streamflow was assumed to flow downstream, independent of irrigation practices. From reported irrigation applications and acreages for 1932-60, it was estimated that an average of 2.1 acre-feet of water (surface and ground water combined) was applied per irrigated acre. (Approximately the same value, 2.12 acre-feet per acre, apparently was used by Ballance and others, 1962, p. 179.) Thus, the total quantity of water needed for irrigation generally was estimated from reported or assumed values for irrigated acreage, and the quantity of water available from the stream was estimated from measured values of streamflow. After the 1940's when wells were drilled, the remainder of the irrigation water was assumed to have been withdrawn from the San Andres-Glorieta aquifer (table 1). Estimated ground-water withdrawals from the San Andres-Glorieta aquifer for irrigation in the Bluewater-Toltec area occurred mainly during 1945-72 (table 1). During 1973-85, enough surface water was available to satisfy the irrigation demand except for 1977 and 1978, when the lake was drawn down to the conservation pool (U.S. Geological Survey annual data reports) and water was assumed to be supplied from ground water. Because the estimates of water applied to fields during 1973-85 were based on irrigated acreage and the assumption of the adequacy of surface water was based on records of pool elevation, the estimate of surface water applied was independent of the excess-precipitation-based streamflow.

In the Bluewater-Toltec irrigation area, some of the applied irrigation water percolates to the water table and recharges the ground-water reservoir. Where the San Andres-Glorieta aquifer is hydraulically connected to the alluvium, alluvial recharge flows into the San Andres-Glorieta aquifer. In some places where the alluvium is thin, the water table may be in the San Andres-Glorieta aquifer and recharge would be directly to the aquifer. Recharge to the alluvium from applied irrigation water (not shown) was assumed to be one-third of the total applied water (fig. 16A) including surface water and ground water.

Table 1.--Estimated amount of water applied to irrigated fields and recharge from irrigation in the Bluewater-Toltec Irrigation District

[Dashes (--) indicate data not available and no value assumed or estimated]

Year	Irrigated area (acres)	April to September flow past gage[1] (acre-feet)	Water applied to irrigated land: Surface water (acre-feet)	Water applied to irrigated land: Ground water[2] (acre-feet)	Recharge to alluvium from applied irrigation water[3] (acre-feet)
1900-27	[4]2,250	--	[5]4,700	0	1,600
1928	--	2,422	[6]1,500	0	500
1929	--	3,534	[6]2,100	0	700
2930	--	7,026	[6]4,200	0	1,400
1931	--	3,564	[6]2,100	0	700
1932	[7]3,720	10,233	[7]6,000	0	2,000
1933	[7]3,440	9,999	[7]5,300	0	1,800
1934	[7]2,490	3,888	[7]2,100	0	700
1935	--	9,117	[6]5,500	0	1,800
1936	[7]2,740	10,375	[6]6,200	0	2,100
1937	[8]3,100	11,703	[6]7,000	0	2,300
1938	[7]3,080	11,022	[6]6,600	0	2,200
1939	--	8,341	[6]5,000	0	1,700
1940	--	4,200	[6]2,500	0	800
1941	[7]3,770	26,260	[6]7,900	0	2,600
1942	[7]3,920	16,720	[6]10,000	0	3,300
1943	[7]4,300	16,880	[6]10,100	0	3,400
1944	[7]2,100	7,380	[6]4,400	0	1,500
1945	[9]2,700	4,001	[9]2,400	[9]3,500	2,000
1946	[9]4,500	181	[9]0	[9]9,000	3,000
1947	[9]4,500	309	[9]0	[9]10,300	3,400
1948	[9]5,500	7,992	[9]4,600	[9]9,300	4,600
1949	[9]5,700	8,172	[9]4,600	[9]6,900	3,800
1950	[9]6,000	417	[9]0	[9]11,800	3,900
1951	[9]6,000	272	[9]0	[9]12,300	4,000
1952	[9]7,000	6,869	[9]4,500	[9]10,400	5,000
1953	[9]6,000	358	[9]0	[9]12,000	4,000
1954	[9]5,000	410	[9]0	[9]12,600	4,200
1955	[9]4,500	223	[9]0	[9]11,500	3,800

Table 1.--Estimated amount of water applied to irrigated fields and recharge from irrigation in the Bluewater-Toltec Irrigation District--Concluded

Year	Irrigated area (acres)	April to September flow past gage[1] (acre-feet)	Water applied to irrigated land: Surface water (acre-feet)	Water applied to irrigated land: Ground water[2] (acre-feet)	Recharge to alluvium from applied irrigation water[3] (acre-feet)
1956	[9]3,600	104	[9]0	[9]9,200	3,000
1957	[9]3,300	261	[9]0	[9]6,700	2,200
1958	[10]3,300	1,397	[10]300	[5]6,900	2,300
1959	[11]3,300	557	[11]0	[11]7,000	2,300
1960	[11]3,300	1,225	[11]0	[11]7,000	2,300
1961	[12]3,400	922	[6]600	[12]1,900	800
1962	[12]3,400	6,911	[6]4,100	[12]1,900	2,000
1963	[12]3,400	4,115	[6]2,500	[12]1,900	1,500
1964	[12]3,400	5,780	[6]3,500	[12]1,900	1,800
1965	[12]3,400	5,605	[6]3,500	[12]1,900	1,800
1966	--	5,947	[6]3,600	[13]1,900	1,800
1967	[14]2,000	2,058	[6]1,200	[15]3,000	1,400
1968	[14]2,000	457	[16]0	[15]4,200	1,400
1969	[14]2,000	3,989	[6]2,400	[15]1,800	1,400
1970	[14]2,000	545	[16]0	[15]4,200	1,400
1971	[14]2,000	357	[16]0	[15]4,200	1,400
1972	--	243	[16]0	[15]4,200	1,400
1973	[17]2,250	--	[18]5,000	[18]0	1,700
1974	[17]2,250	--	[18]5,000	[18]0	1,700
1975	[17]2,250	--	[18]5,000	[18]0	1,700
1976	[17]2,250	--	[18]5,000	[18]0	1,700
1977	[17]2,250	--	[18]0	[18]5,000	1,700
1978	[17]2,250	--	[16]3,000	[18]2,000	1,700
1979-85	[17]2,250	--	[18]5,000	[18]0	1,700

[1]U.S. Geological Survey station 08342000, Bluewater Creek near Bluewater, discontinued in 1972.

[2]First successful irrigation well drilled in August 1944.

[3]Estimated as one-third of the total amount of irrigation water applied including surface and ground water.

[4]Gordon (1961, p. 13).

[5]Estimated as 2.1 acre-feet per acre times the irrigated acreage, rounded to the nearest 100 acre-feet. The 2.1 value was estimated as the average application rate for 1932-34, 1945-57, and 1959-60.

[6]Sixty percent of summer (April-September) flow past the gage. This was the approximate percentage of summer flow past the gage that was applied to irrigated lands during 1932-35, 1945, 1948-49, and 1952.

[7]Gordon (1961, table 2).

[8]Assumed value based on 1938 value.

[9]Gordon (1961, table 7).

[10]Reeder and others (1962, p. 225). Surface water was used for gardens in the Bluewater area.

[11]Ballance and others (1962, p. 179).

[12]Busch and others (1967, p. 94). The 1,900-acre-foot value may be underestimated if some stream and canal seepage losses are assumed.

[13]Cooper and West (1967, p. 149). They noted "Since 1954 the use of ground water for irrigation use has steadily declined."

[14]Value of 2,000 acres assumed for estimating total amount of water applied to irrigated land. Lansford and others (1973, p. 17) reported 1970 acreage for all of Cibola County to be 2,407 acres, most of which was in the Bluewater-Toltec Irrigation District.

[15]Estimated as 2.1 acre-feet per acre times an assumed acreage of 2,000 acres, minus the reported or estimated surface water applied.

[16]Leo Wolfe, consultant for U.S. Bureau of Indian Affairs, written commun., 1979.

[17]Estimated as the 1986 acreage (2,650 acres) minus 400 acres that were returned to agriculture by Anaconda in 1986 after being idle for many years (Morris Wengert, ditch rider, Bluewater-Toltec Irrigation District, oral commun., Jan. 26, 1987).

[18]Estimated as 2.1 acre-feet per acre times the irrigated acreage, rounded to the nearest 1,000 acre-feet. Precipitation and lake storage were assumed to have been large enough to meet irrigation demands for all of 1973-85 except 1977 and 1978 when the lake was drawn down to the conservation pool (U.S. Geological Survey, annual data reports) and irrigation water was assumed to have been partly supplied by ground water.

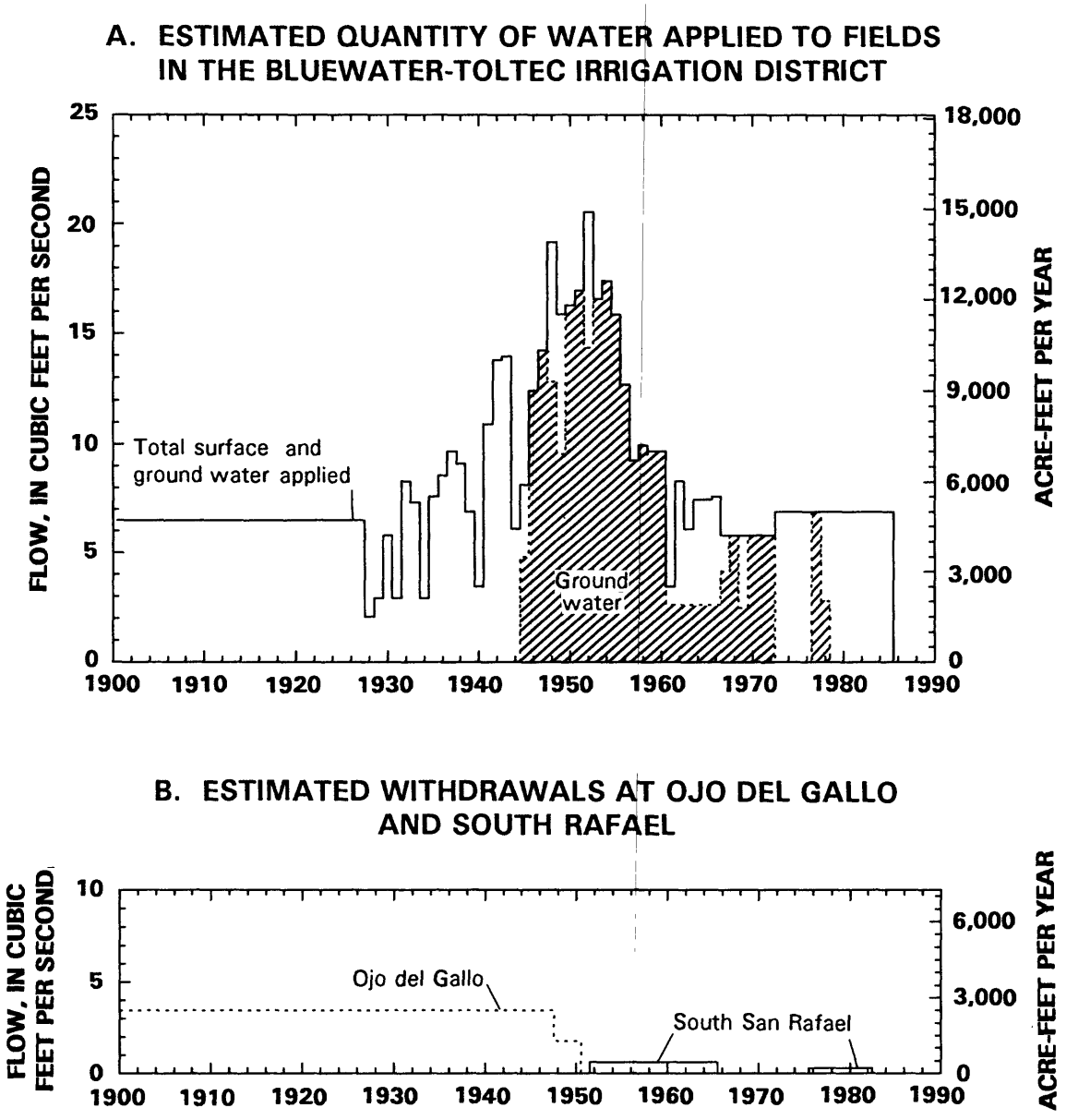

Figure 16.--Estimated quantity of water applied to irrigated fields in the Bluewater-Toltec Irrigation District and withdrawals of water at Ojo Del Gallo and south San Rafael.

The estimated rate of ground-water withdrawal in the south San Rafael area is shown in figure 16B and in the following table:

Years	Estimated withdrawal (acre-feet per year)	Recharge (acre-feet per year)
1952-65	450	150
1966-75	0	0
1976-82	220	75
1983-85	0	0

The value of 450 acre-feet (rounded) was estimated on the basis of 2.1 acre-feet per acre for two fields of 110 and 102 acres (New Mexico State Engineer Office, written commun., 1979). The longest period during which irrigation could have taken place was approximately 1952-82, based on well drilling dates and New Mexico State Engineer Office records. The value of 220 acre-feet (rounded) assumed an acreage reduction of 50 percent. The changes in assumed irrigated acreage were based on semiannual drawdowns at well 10.10.26.331. A hydrograph for well 10.10.26.331 is shown in the Model Adjustments section for convenience of comparison with model-derived hydraulic heads. The summer-drawdown winter-recovery cycle was much more pronounced during 1952-65 than it was later. It was assumed that one-third of the irrigation water percolated to the water table, recharging the valley-fill aquifer.

Using the springflow of Ojo del Gallo, the community of San Rafael irrigated 1,000 to 2,000 acres until the flow from the spring diminished. Ojo del Gallo stopped flowing in 1953. Aerial photographs taken in 1935 show about 1,000 acres of rectangular fields and a large area of meadow and wet land on the north and east sides of these rectangular fields. The meadow and wet land apparently were watered by runoff from the rectangular fields and by winter flow from Ojo del Gallo. Hodges (1938, p. 339) reported that 750 acres were irrigated during the summer using the entire springflow, and that during the winter water was wasted to a meadow and swampy area of about 1,600 acres. Morgan (1938, p. 12) reported 1,200 acres of irrigated land and 1,000 to 1,200 acres of swampy area. Reported springflow in August and November of 1937 was 7 cubic feet per second, and outflow from the meadow-swamp area depended on the season; in June and November of 1937 no flow was leaving the meadow-swamp area, and in January of 1938, the outflow was 3.5 to 4.0 cubic feet per second, which was spread over a second meadow area some distance to the southeast (Hodges, 1938, p. 339). Because of the complexities of year-round irrigation, the information about the Ojo del Gallo irrigated area is not complete enough to estimate how much water was used by evapotranspiration and how much percolated to the water table.

Evapotranspiration from the Ojo del Gallo irrigated area was estimated on the basis of available information and simplifying assumptions. It was assumed that the entire flow of Ojo del Gallo was used for irrigation during the entire year. However, because irrigation occurred outside the growing season and water was transported in earthen channels, much of the irrigation water probably percolated to the water table. It was assumed that 50 percent of the water used in irrigation went to evapotranspiration and the remainder percolated to the water table. Furthermore, it was assumed that the flow of Ojo del Gallo was 7 cubic feet per second (5,000 acre-feet per year, rounded) during 1900-47, 3.5 cubic feet per second during 1948-50, and zero since that time. On the basis of these assumptions, the rate of evapotranspiration from fields and irrigated meadows in the Ojo del Gallo irrigation area was estimated to be:

Years	Evapotranspiration (acre-feet per year)
1900-47	2,500
1948-50	1,300
1951-85	0

In the swampy area downstream from Ojo del Gallo the surface stream and ground water have a close hydraulic connection. Therefore, surface-water diversions were assumed to be hydrologically very similar to ground-water withdrawals. The only distinction is in the point of diversion: surface water is diverted before the water infiltrates into the valley-fill material, whereas ground water is withdrawn further down the flow path. Because the flow from Ojo del Gallo is approximately the same as a ground-water diversion from the valley fill and irrigation would recharge the valley fill, evapotranspiration (fig. 16B) is the net withdrawal from the valley fill.

Municipal and Industrial Ground-Water Withdrawals

Records of municipal and industrial ground-water withdrawals generally are available from the New Mexico State Engineer Office except for some withdrawals that started before 1956. Other withdrawals have been reported or estimated. Locations of municipal and industrial withdrawals are shown in figure 17.

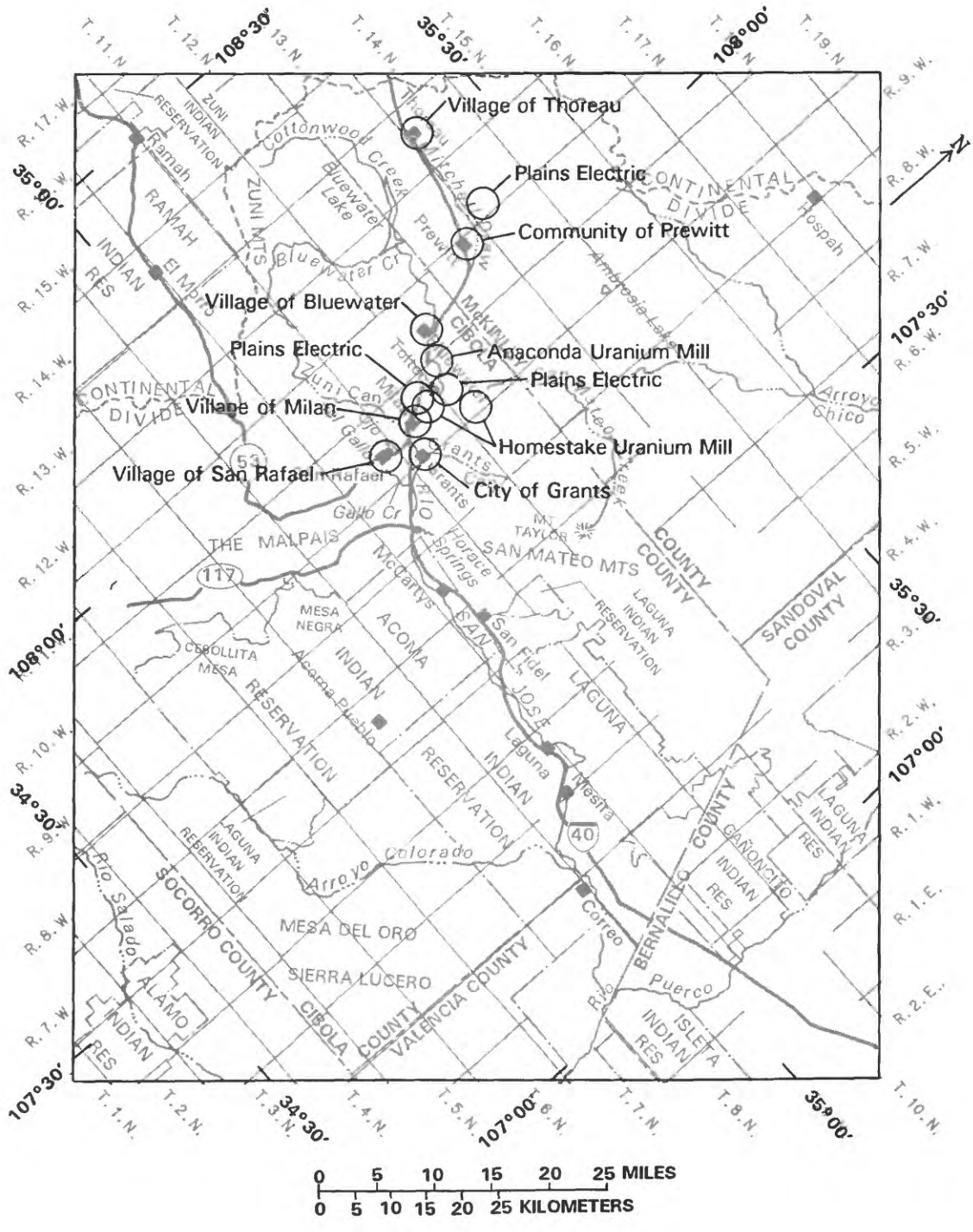

Figure 17.--Locations of municipal and industrial ground-water withdrawals.

Ground-water withdrawals for railroad use date from the late 1800's at various places. Rates of withdrawal from the valley fill at Grants were obtained from a chart in court records that originated in railroad records (deposition by William Turner in Pueblo of Acoma and Pueblo of Laguna, v. City of Grants et al., case CIV-82-1540M, U.S. District Court of New Mexico). Large withdrawals by the railroad ended with installation of diesel-electric locomotives in about 1948-50 (Vernon Glover, oral commun., April 20, 1987). Withdrawals were assumed to have ended in September 1948 and to have remained at a constant 700 acre-feet per year between 1945 and 1948. Although some of the railroad wells drilled at Grants in the 1940's were completed in the San Andres-Glorieta aquifer, railroad withdrawals were assumed for simplicity to be entirely from the valley-fill aquifer. Withdrawals by the railroad constituted most of the municipal and industrial withdrawals (fig. 18) prior to 1950. Approximate railroad ground-water withdrawal rates at Grants were as follows:

Period	Ground-water withdrawal rates (acre-feet per year, rounded)
October 1899 - September 1927	90
October 1927 - September 1931	240
October 1931 - September 1939	200
October 1939 - September 1943	310
October 1943 - March 1944	500
April 1944 - September 1944	570
October 1944 - March 1945	640
April 1945 - September 1948	710

Additional withdrawals by the railroad from the San Andres-Glorieta aquifer at Bluewater and near Thoreau were not considered significant for this study.

Municipal and community ground-water withdrawals are listed in table 2. The values (acre-feet) in table 2 are given for half-water-year periods to correspond with surface-water records and the irrigation season. Total estimated withdrawals for municipal and industrial use, including those for uranium milling and the railroad, are shown in figure 18.

Major industrial ground-water withdrawals and injections are shown in table 3. Ground-water-withdrawal and injection wells are used at the Homestake uranium mill and tailings pile (located in T. 12 N., R. 10 W., sec. 26). This withdrawal-injection system is a pollution-control measure to prevent recharge from leaving the site of the tailings pile. In general, water is withdrawn from the San Andres-Glorieta aquifer, injected into certain alluvial wells, and withdrawn from other alluvial wells. Ultimately, the water is discharged by way of evaporation from the mill and tailings pond. At the Anaconda mill (located in T. 12 N., R. 11 W., sec. 24) the source of supply is the San Andres-Glorieta aquifer and discharge is by way of evaporation from the mill and tailings ponds. At the Plains Electric generating station (located in T. 14 N., R. 12 W., sec. 26), water is used for steam generation and cooling. Some of the supply wells are near the generating station north of Prewitt and some are in the Grants-Bluewater area where the transmissivity of the San Andres-Glorieta aquifer is larger than it is near the generating station.

Table 2.--Reported and estimated municipal and community ground-water withdrawals, in acre-feet

[Dashes (--) indicate no data and an assumed zero value. Section is approximate where several wells are represented by one location. Many data derived from other sources are in calendar-year form, in which case the half-water-year values in this table were calculated from average monthly values]

	City or community					
	Grants	San Rafael	Blue-water	Milan	Thoreau	Prewitt
Township (north)	11	10	12	11	14	13
Range (west)	10	10	11	10	13	11
Section	26	3	23	21	33	18
April 1945-Sept. 1945	[1]100	--	--	--	--	--
Oct. 1945-March 1946	[1]100	--	--	--	--	--
April 1946-Sept. 1946	[1]100	--	--	--	--	--
Oct. 1946-March 1947	[1]100	--	--	--	--	--
April 1947-Sept. 1947	[1]100	--	--	--	--	--
Oct. 1947-March 1948	[1]100	--	--	--	--	--
April 1948-Sept. 1948	[1]100	--	--	--	--	--
Oct. 1948-March 1949	[1]106	--	--	--	--	--
April 1949-Sept. 1949	[1]112	--	--	--	--	--
Oct. 1949-March 1950	[1]119	--	--	--	--	--
April 1950-Sept. 1950	[1]125	--	--	--	--	--
Oct. 1950-March 1951	[1]125	--	--	--	--	--
April 1951-Sept. 1951	[1]125	--	--	--	--	--
Oct. 1951-March 1952	[1]125	[1]5	--	--	--	--
April 1952-Sept. 1952	[1]125	[1]10	--	--	--	--
Oct. 1952-March 1953	[1]137	[1]10	--	--	--	--
April 1953-Sept. 1953	[1]150	[1]10	--	--	--	--
Oct. 1953-March 1954	[1]160	[1]10	[1]5	--	--	--
April 1954-Sept. 1954	[1]175	[1]10	[1]5	--	--	--
Oct. 1954-March 1955	[1]180	[1]10	[1]5	--	--	--
April 1955-Sept. 1955	[1]185	[1]10	[1]5	--	--	--
Oct. 1955-March 1956	[1]195	[1]10	[1]5	[1]5	--	--
April 1956-Sept. 1956	[1]200	[1]10	[1]5	[1]15	--	--
Oct. 1956-March 1957	[1]212	[1]10	[1]5	[1]25	--	--
April 1957-Sept. 1957	[1]225	[1]10	[1]5	[1]35	--	--
Oct. 1957-March 1958	[2]235	[2]11	[2]7	[2]44	--	--
April 1958-Sept. 1958	[2]245	[2]12	[2]8	[2]54	--	--
Oct. 1958-March 1959	[2]255	[2]13	[2]9	[2]63	--	--
April 1959-Sept. 1959	[2]265	[2]14	[2]10	[2]72	--	--
Oct. 1959-March 1960	[2]275	[2]15	[2]11	[2]81	--	--

Table 2.--Reported and estimated municipal and community ground-water withdrawals, in acre-feet--Continued

	City or community					
	Grants	San Rafael	Blue-water	Milan	Thoreau	Prewitt
Township (north)	11	10	12	11	14	13
Range (west)	10	10	11	10	13	11
Section	26	3	23	21	33	18
April 1960-Sept. 1960	[2]285	[2]16	[2]12	[2]91	--	--
Oct. 1960-March 1961	[2]295	[3]17	[3]13	[2]100	[3]17	[3]13
April 1961-Sept. 1961	[2]305	[3]17	[3]13	[4]109	[3]17	[3]13
Oct. 1961-March 1962	[4]316	[3]17	[3]13	[4]135	[3]17	[3]13
April 1962-Sept. 1962	[4]789	[3]17	[3]13	[4]305	[3]17	[3]13
Oct. 1962-March 1963	[4]446	[3]17	[3]13	[4]168	[3]17	[3]13
April 1963-Sept. 1963	[4]707	[3]17	[3]13	[4]260	[3]17	[3]13
Oct. 1963-March 1964	[4]368	[3]17	[3]13	[4]123	[3]17	[3]13
April 1964-Sept. 1964	[4]618	[3]17	[3]13	[4]257	[3]17	[3]13
Oct. 1964-March 1965	[4]372	[3]17	[3]13	[4]137	[3]17	[3]13
April 1965-Sept. 1965	[4]610	[3]17	[3]13	[4]197	[3]17	[3]13
Oct. 1965-March 1966	[4]372	[3]17	[3]13	[4]118	[3]17	[3]13
April 1966-Sept. 1966	[4]693	[3]17	[3]13	[4]192	[3]17	[3]13
Oct. 1966-March 1967	[4]443	[3]17	[3]13	[4]130	[3]17	[3]13
April 1967-Sept. 1967	[4]642	[3]17	[3]13	[4]263	[3]17	[3]13
Oct. 1967-March 1968	[4]410	[3]17	[3]13	[4]117	[3]17	[3]13
April 1968-Sept. 1968	[4]752	[3]17	[3]13	[4]183	[3]17	[3]13
Oct. 1968-March 1969	[4]475	[3]18	[3]13	[4]107	[3]17	[3]13
April 1969-Sept. 1969	[4]803	[3]20	[3]13	[4]100	[3]17	[3]13
Oct. 1969-March 1970	[4]450	[3]18	[3]13	[4]150	[3]17	[3]13
April 1970-Sept. 1970	[4]796	[3]17	[3]13	[4]312	[3]17	[3]13
Oct. 1970-March 1971	[4]565	[3]20	[3]13	[4]223	[3]17	[3]13
April 1971-Sept. 1971	[4]958	[3]24	[3]13	[4]245	[3]17	[3]13
Oct. 1971-March 1972	[4]598	[3]24	[3]13	[4]169	[3]17	[3]13
April 1972-Sept. 1972	[4]887	[3]23	[3]13	[4]78	[3]17	[3]13
Oct. 1972-March 1973	[4]484	[3]23	[3]13	[4]84	[3]19	[3]13
April 1973-Sept. 1973	[4]979	[3]23	[3]13	[4]151	[3]21	[3]13
Oct. 1973-March 1974	[4]694	[3]24	[3]13	[4]96	[3]23	[3]13
April 1974-Sept. 1974	[4]1,032	[3]25	[3]13	[4]143	[3]24	[3]13
Oct. 1974-March 1975	[4]567	[3]24	[3]13	[4]92	[3]27	[3]13
April 1975-Sept. 1975	[4]930	[3]23	[3]13	[4]189	[3]31	[3]13
Oct. 1975-March 1976	[4]733	[3]23	[3]13	[4]142	[3]31	[3]13
April 1976-Sept. 1976	[4]870	[3]23	[3]13	[4]178	[3]31	[3]13
Oct. 1976-March 1977	[4]790	[3]28	[3]13	[4]118	[3]34	[3]13
April 1977-Sept. 1977	[4]1,115	[3]32	[3]13	[4]340	[3]38	[3]13

Table 2.--Reported and estimated municipal and community ground-water withdrawals, in acre-feet--Concluded

	City or community					
	Grants	San Rafael	Blue-water	Milan	Thoreau	Prewitt
Township (north)	11	10	12	11	14	13
Range (west)	10	10	11	10	13	11
Section	26	3	23	21	33	18
Oct. 1977-March 1978	[4]769	[3]36	[3]13	[4]316	[3]38	[3]13
April 1978-Sept. 1978	[4]1,121	[5]40	[3]13	[4]399	[3]39	[3]13
Oct. 1978-March 1979	[4]758	[5]43	[3]13	[4]237	[3]29	[3]13
April 1979-Sept. 1979	[4]1,001	[5]47	[3]13	[4]436	[3]18	[3]13
Oct. 1979-March 1980	[4]2,721	[5]43	[3]13	[4]260	[3]37	[3]13
April 1980-Sept. 1980	[4]1,285	[5]40	[3]13	[4]432	[3]56	[3]13
Oct. 1980-March 1981	[4]882	[5]39	[6]13	[4]311	[2]63	[6]13
April 1981-Sept. 1981	[4]1,246	[5]38	[6]13	[4]423	[2]70	[6]13
Oct. 1981-March 1982	[4]714	[5]38	[6]13	[4]187	[2]77	[6]13
April 1982-Sept. 1982	[4]1,129	[6]40	[6]13	[4]339	[2]84	[6]13
Oct. 1982-March 1983	[4]652	[6]40	[6]13	[4]187	[2]91	[6]13
April 1983-Sept. 1983	[4]1,034	[6]40	[6]13	[4]367	[2]98	[6]13
Oct. 1983-March 1984	[4]607	[6]40	[6]13	[4]181	[2]105	[6]13
April 1984-Sept. 1984	[4]1,114	[6]40	[6]13	[4]385	[2]112	[6]13
Oct. 1984-March 1985	[4]573	[6]40	[6]13	[4]225	[2]119	[6]13
April 1985-Sept. 1985	[4]984	[6]40	[6]13	[4]336	[7]127	[6]13
Oct. 1985-March 1986	[4]651	[6]40	[6]13	[4]162	[6]127	[6]13
Model layer:	2	2	2	2	2	2
Row:	40	43	27	36	3	15
Column:	16	11	17	16	16	22

[1]The total estimated municipal withdrawal reported in Gordon (1961, p. 103) was divided between Grants, Bluewater, and San Rafael on the basis of population. The first San Andres well at San Rafael was assumed to be the one drilled in 1952 (Gordon, 1961, p. 89), and the effects of municipal withdrawals at San Rafael were assumed to be negligible before that time. Withdrawals at Bluewater were assumed to be negligible before 1954.

[2]Interpolated.

[3]Aqua Science, Inc. (1982, table 4.2).

[4]New Mexico State Engineer Office records.

[5]New Mexico State Engineer Office records; research done by Greta Dickerson of U.S. Bureau of Indian Affairs.

[6]Extrapolated.

[7]Estimated as 100 gallons per day per person (based on data in Aqua Science, Inc., 1982, tables 2-1 and 4-2).

Table 3.--Reported and estimated industrial ground-water withdrawals and pumped recharge in the Grants-Bluewater area, in acre-feet

[Negative values indicate pumped recharge. Dashes (--) indicate no data and an assumed zero value. The section is approximate where several wells are represented by one location. In the sources shown, many of these data are in the form of annual (calender-year) values, in which case the half-water-year values given in this table were derived from calculated average monthly values]

	Nuclear firm								
	Ana-conda	Homestake				Plains			Western Nuclear Mine
Township (north)	12	11	12	12	12	14	12	11	15
Range (west)	11	10	10	10	10	12	10	10	13
Section	24	4	26	26	35	23	29	8	25
April 1945-Sept. 1945	--	--	--	--	--	--	--	--	--
Oct. 1945-March 1946	--	--	--	--	--	--	--	--	--
April 1946-Sept. 1946	--	--	--	--	--	--	--	--	--
Oct. 1946-March 1947	--	--	--	--	--	--	--	--	--
April 1947-Sept. 1947	--	--	--	--	--	--	--	--	--
Oct. 1947-March 1948	--	--	--	--	--	--	--	--	--
April 1948-Sept. 1948	--	--	--	--	--	--	--	--	--
Oct. 1948-March 1949	--	--	--	--	--	--	--	--	--
April 1949-Sept. 1949	--	--	--	--	--	--	--	--	--
Oct. 1949-March 1950	--	--	--	--	--	--	--	--	--
April 1950-Sept. 1950	--	--	--	--	--	--	--	--	--
Oct. 1950-March 1951	--	--	--	--	--	--	--	--	--
April 1951-Sept. 1951	--	--	--	--	--	--	--	--	--
Oct. 1951-March 1952	[1]175	--	--	--	--	--	--	--	--
April 1952-Sept. 1952	[1]150	--	--	--	--	--	--	--	--
Oct. 1952-March 1953	[1]325	--	--	--	--	--	--	--	--
April 1953-Sept. 1953	[1]500	--	--	--	--	--	--	--	--
Oct. 1953-March 1954	[1]525	--	--	--	--	--	--	--	--
April 1954-Sept. 1954	[1]550	--	--	--	--	--	--	--	--
Oct. 1954-March 1955	[1]700	--	--	--	--	--	--	--	--
April 1955-Sept. 1955	[1]850	--	--	--	--	--	--	--	--
Oct. 1955-March 1956	[1]1,550	--	--	--	--	--	--	--	--
April 1956-Sept. 1956	[1]2,250	--	--	--	--	--	--	--	--
Oct. 1956-March 1957	[1]2,500	--	--	--	--	--	--	--	--
April 1957-Sept. 1957	[2]2,116	--	--	--	--	--	--	--	--
Oct. 1957-March 1958	[2]1,914	--	--	--	--	--	--	--	--
April 1958-Sept. 1958	[2]1,961	--	--	--	--	--	--	--	--
Oct. 1958-March 1959	[2]1,726	--	[3]300	--	--	--	--	--	--
April 1959-Sept. 1959	[2]1,270	--	[3]300	--	--	--	--	--	--
Oct. 1959-March 1960	[2]1,082	--	[3]300	--	--	--	--	--	--

Table 3.--Reported and estimated industrial ground-water withdrawals and pumped recharge in the Grants-Bluewater area, in acre-feet--Continued

	Nuclear firm								
	Anaconda	Homestake				Plains			Western Nuclear Mine
Township (north)	12	11	12	12	12	14	12	11	15
Range (west)	11	10	10	10	10	12	10	10	13
Section	24	4	26	26	35	23	29	8	25
April 1960-Sept. 1960	[2]1,183	--	[3]300	--	--	--	--	--	--
Oct. 1960-March 1961	[4]1,171	--	[3]300	--	--	--	--	--	--
April 1961-Sept. 1961	[4]1,159	--	[3]300	--	--	--	--	--	--
Oct. 1961-March 1962	[4]1,147	--	[5]372	--	--	--	--	--	--
April 1962-Sept. 1962	[4]1,135	--	[5]409	--	--	--	--	--	--
Oct. 1962-March 1963	[4]1,123	--	[5]338	--	--	--	--	--	--
April 1963-Sept. 1963	[4]1,111	--	[5]618	--	--	--	--	--	--
Oct. 1963-March 1964	[4]1,099	--	[5]397	--	--	--	--	--	--
April 1964-Sept. 1964	[4]1,087	--	[5]508	--	--	--	--	--	--
Oct. 1964-March 1965	[4]1,075	--	[5]347	--	--	--	--	--	--
April 1965-Sept. 1965	[4]1,063	--	[5]418	--	--	--	--	--	--
Oct. 1965-March 1966	[4]1,051	--	[5]346	--	--	--	--	--	--
April 1966-Sept. 1966	[4]1,039	--	[5]359	--	--	--	--	--	--
Oct. 1966-March 1967	[4]1,028	--	[5]493	--	--	--	--	--	--
April 1967-Sept. 1967	[4]1,016	--	[5]479	--	--	--	--	--	--
Oct. 1967-March 1968	[4]1,004	--	[5]454	--	--	--	--	--	--
April 1968-Sept. 1968	[4]992	--	[5]391	--	--	--	--	--	--
Oct. 1968-March 1969	[4]980	--	[5]456	--	--	--	--	--	--
April 1969-Sept. 1969	[4]968	--	[5]435	--	--	--	--	--	--
Oct. 1969-March 1970	[4]956	--	[5]432	--	--	--	--	--	--
April 1970-Sept. 1970	[5]944	--	[5]313	--	--	--	--	--	--
Oct. 1970-March 1971	[5]960	--	[5]408	--	--	--	--	--	--
April 1971-Sept. 1971	[5]975	--	[5]304	--	--	--	--	--	--
Oct. 1971-March 1972	[5]1,012	--	[5]324	--	--	--	--	--	--
April 1972-Sept. 1972	[5]1,049	--	[5]293	--	--	--	--	--	--
Oct. 1972-March 1973	[5]1,112	--	[5]190	--	--	--	--	--	--
April 1973-Sept. 1973	[5]1,174	--	[5]263	--	--	--	--	--	--
Oct. 1973-March 1974	[5]1,132	--	[5]295	--	--	--	--	--	--
April 1974-Sept. 1974	[5]1,089	--	[5]440	--	--	--	--	--	--
Oct. 1974-March 1975	[5]1,091	--	[5]365	--	--	--	--	--	--
April 1975-Sept. 1975	[5]1,094	--	[5]186	--	--	--	--	--	--
Oct. 1975-March 1976	[5]1,086	[5]3	[5]233	--	--	--	--	--	--
April 1976-Sept. 1976	[5]1,078	[5]2	[5]281	--	--	--	--	--	--
Oct. 1976-March 1977	[5]1,129	[5]3	[5]287	--	--	--	--	--	--
April 1977-Sept. 1977	[5]1,181	[5]2	[5]279	--	[5]-19	--	--	--	--

Table 3.--Reported and estimated industrial ground-water withdrawals and pumped recharge in the Grants-Bluewater area, in acre-feet--Concluded

	Nuclear firm								
	Ana-conda	Homestake				Plains			Western Nuclear Mine
Township (north)	12	11	12	12	12	14	12	11	15
Range (west)	11	10	10	10	10	12	10	10	13
Section	24	4	26	26	35	23	29	8	25
Oct. 1977-March 1978	[5]1,390	[5]3	[5]298	--	[5]-28	--	--	--	--
April 1978-Sept. 1978	[5]1,519	[5]3	[5]359	[5]45	[5]-34	--	--	--	--
Oct. 1978-March 1979	[5]1,413	[5]7	[5]348	[5]76	[5]-43	--	--	--	--
April 1979-Sept. 1979	[5]1,558	[5]7	[5]316	[5]68	[5]-38	--	--	--	--
Oct. 1979-March 1980	[5]1,605	[5]7	[5]362	[5]58	[5]-35	--	--	--	0.31
April 1980-Sept. 1980	[5]1,521	[5]8	[5]432	[5]57	[5]-24	[5]48	--	--	0.55
Oct. 1980-March 1981	[5]1,483	[5]6	[5]263	[5]77	[5]-38	[5]52	--	--	1.24
April 1981-Sept. 1981	[5]1,353	[4]5	[5]188	[5]85	[5]-64	[5]56	--	--	1.67
Oct. 1981-March 1982	[5]1,117	[4]4	[5]213	[5]221	[5]-98	[5]49	--	--	1.56
April 1982-Sept. 1982	[5]214	[4]3	[5]352	[5]245	[5]-248	[5]176	--	--	0.65
Oct. 1982-March 1983	[5]322	[5]2	[5]248	[5]211	[5]-162	[5]270	--	--	0.21
April 1983-Sept. 1983	[5]331	[5]1	[5]352	[5]286	[5]-258	[5]275	--	--	0.21
Oct. 1983-March 1984	[5]256	[5]2	[5]577	[5]322	[5]-469	[5]234	--	--	0.34
April 1984-Sept. 1984	[5]181	[5]1	[5]602	[5]314	[5]-485	[5]231	[5]273	--	1.05
Oct. 1984-March 1985	[4]213	[5]0	[5]475	[5]273	[5]-434	[5]159	[5]501	--	0.99
April 1985-Sept. 1985	[4]244	[5]0	[5]490	[5]313	[5]-444	[5]158	[5]616	--	0.13
Oct. 1985-March 1986	[5]276	[5]0	[5]484	[5]297	[5]-454	[5]143	[5]130	[5]951	--
Model layer:	2	2	2	1	1	2	2	2	2
Row:	29	33	34	34	34	8	32	33	2
Column:	19	18	23	23	23	24	20	17	25

[1]Total estimated industrial withdrawal (Gordon, 1961, p. 103), most of which was assumed to be by Anaconda.

[2]New Mexico State Engineer Office records; research done by Greta Dickerson of U.S. Bureau of Indian Affairs.

[3]An extrapolated value based on the assumption that milling operations started within a year after the wells were completed. One well was drilled and another was converted from irrigation to industrial service in 1958 (Gordon, 1961, p. 53).

[4]Interpolated.

[5]New Mexico State Engineer Office records.

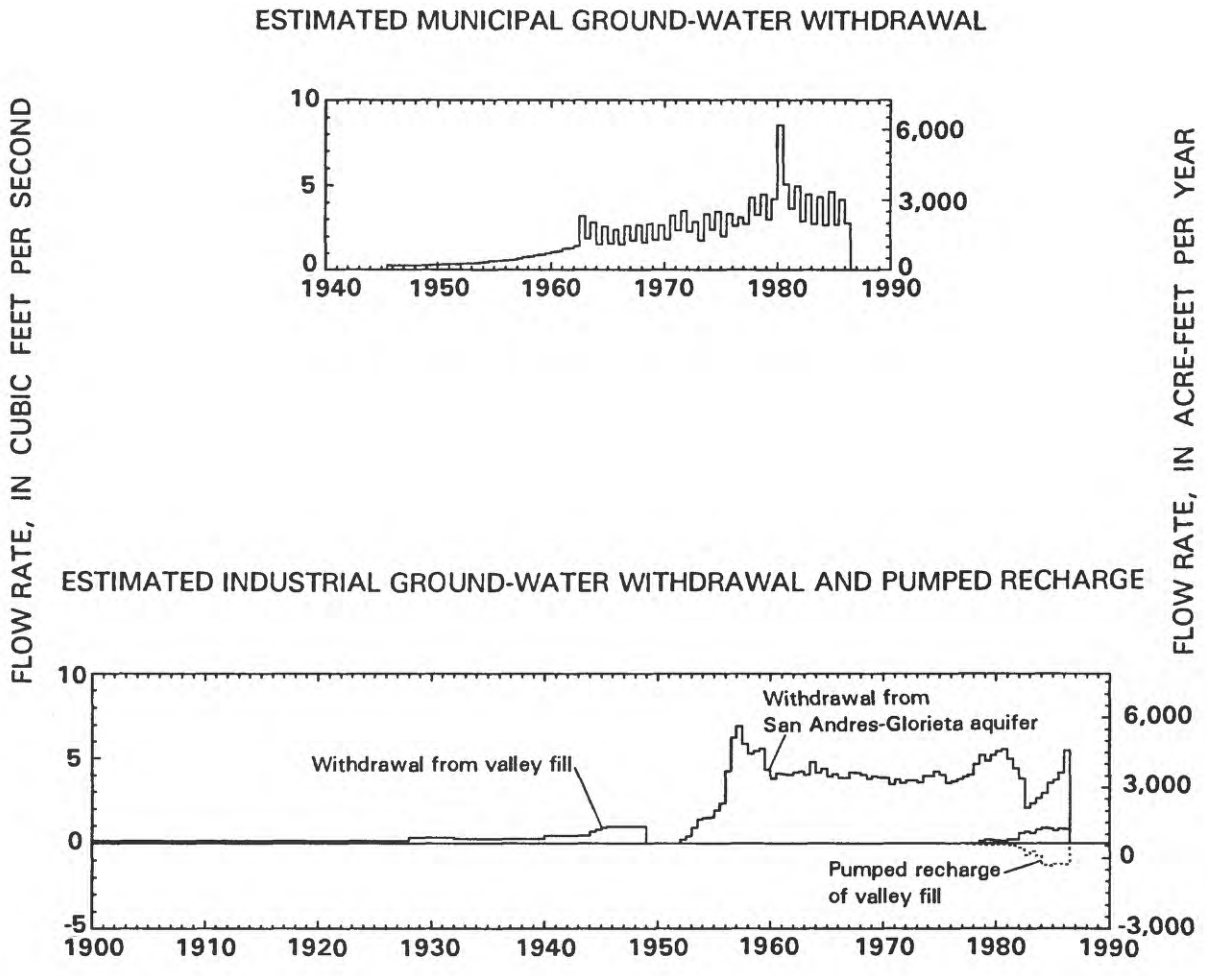

Figure 18.--Estimated municipal and industrial ground-water withdrawals and pumped recharge.

Municipal and Industrial Recharge

Total estimated ground-water recharge of municipal and industrial water from septic drain fields and uranium mill-tailings piles is shown in figure 18. Fifty percent of the water withdrawn by small towns and villages was assumed to recharge the valley fill except at Prewitt and Thoreau. There, discharges were assumed to be evaporation ponds or near-surface septic systems. In either case, return ground-water recharge would be isolated from the San Andres-Glorieta aquifer by the Chinle confining bed. Municipal and industrial effluents at Prewitt and Thoreau were assumed to have been removed from the system completely. At Grants, recharge of the valley fill by septic drain fields was assumed to have occurred between 1946 and 1948. Before 1946, discharge and recharge were assumed to be insignificant by comparison to withdrawals by the railroad. After 1948 a sewage-treatment plant was in use, and 50 percent of city withdrawals were assumed to be discharged to the Rio San Jose. Recharge or effluent of water withdrawn by the railroad was assumed to have been insignificant with respect to the quantity withdrawn because most of the withdrawal probably was used for steam generation.

Recharge beneath the Anaconda tailings pond was assumed to be 66 percent of Anaconda's ground-water withdrawals (table 3) until March 1960. From then until March 1982, recharge was assumed to be 15 percent of ground-water withdrawals and after that 10 percent. These percentages were used because they result in recharge values approximately equal to values used by Dames and Moore (1986, pl. B-13).

Recharge beneath the Homestake tailings pond was assumed to be 20 percent of net ground-water withdrawal. Net withdrawal was the sum of Homestake withdrawals from wells in the San Andres Limestone and alluvial valley fill, and recharge in injection wells in the alluvial valley fill (table 3). The recharge thus derived averaged 140 acre-feet per year, a value between those estimated by Bostick and others (1985) of about 120 acre-feet per year using a two-dimensional model and about 250 acre-feet per year using a water-balance method (Cindy Ardito, New Mexico Environmental Improvement Division, oral commun., April 16, 1987).

The reported ground-water withdrawal at the Western Nuclear supply well is listed in table 3 not because it is large or significant but rather to help explain the large drawdown that was measured in that well. The simulation of this relatively small withdrawal was necessary for completeness.

DIGITAL MODEL OF THE GEOHYDROLOGIC SYSTEM

A two-layer, digital, finite-difference model was constructed to represent the geohydrologic system described in the conceptual model. This section of the report discusses the approach to modeling and describes the model in detail. After the approach to modeling, the characteristics of the aquifers and confining bed are described. The initial conditions and time intervals used for the transient simulation provide a necessary framework for discussing the boundary conditions; some boundaries are time variant. Ground-water withdrawals and artificial recharge imposed as a stress on the system are described after the description of boundaries. Only after this detailed description are the comparisons between simulated and measured hydraulic heads and flows described and the adjustments to represented characteristics discussed. Only the final, adjusted version of the model is presented here.

The purpose of the digital model was to test the internal consistency of the conceptual model and provide a mechanism for estimating the effect of previous and new development on water levels, springflow, and streamflow. The model presented here is consistent with this purpose, with data available to estimate the value of hydrogeologic characteristics, and with data available to compare measured hydraulic heads and flows with those simulated by the model. The model simulates flow in the San Andres-Glorieta aquifer and in the valley fill, with leakage through the intervening Chinle Formation where the Chinle is less than full thickness. Boundary conditions represent interactions between ground water and surface water, evapotranspiration, and ground-water underflow into and out of the modeled area. Although simulation of the valley fill was not the objective of this study, the valley fill lies between the San Andres-Glorieta aquifer and the location of several important boundary conditions such as the surface-water boundary (Horace Springs and parts of Bluewater Creek and the Rio San Jose), and natural evapotranspiration from the water table. A representation of the relation between these boundaries and the San Andres-Glorieta aquifer was needed to meet the objectives for the model.

Approach to Modeling

The general approach was to construct a model that would simulate certain measured characteristics of the hydrologic system while incorporating the other major characteristics of the system in plausible ways. The measured characteristics were springflow at Ojo del Gallo, streamflow downstream from Horace Springs, and hydraulic head measured at selected wells. The other major characteristics of the combined ground-water/surface-water system include aquifer properties such as transmissivity, storage, and leakage; boundary conditions such as Bluewater Creek, Bluewater Lake, and the Rio San Jose; recharge on The Malpais and near the Zuni uplift; and discharge along the Rio Grande rift. Representation of some of these characteristics is, at best, plausible because of the lack of measurements or reliable independent estimates.

Aquifer characteristics and boundary specifications were given values consistent with available data and concepts of the flow system and were then adjusted by trial and error to improve the comparison between model-derived and measured hydraulic heads and flow rates. The plausibility of these characteristics is based on the plausibility of geologic, hydrologic, and water-quality information given in the previous sections and in Baldwin and Anderholm (in press). The details of these comparisons and the adjustments are discussed in following sections of this report.

No claim is made that the resulting model provides a unique solution or an optimal solution; however, the solution provides a reasonable comparison between model-derived and measured hydraulic heads and flows while simulating the geohydrology in a manner that, although simplified, is consistent with available information.

Purpose of Steady-State Simulation

Simulated steady-state conditions provided initial hydraulic heads for transient simulations and an estimate of average pristine flow rates. Because steady-state conditions simulated "average" natural conditions of recharge and streamflow, the model-derived flow from springs and streamflow gains and losses provide estimates for average natural conditions. Also, model-derived evapotranspiration from the water table under steady-state conditions provides an estimate of the average natural rate. Although it might have been theoretically possible to simulate transient conditions as the change from an arbitrary initial condition, steady-state initial conditions facilitated the simulation of stream and evapotranspiration boundaries and allowed the direct comparison of model-derived values of hydraulic head and streamflow with measured values.

Because true steady-state conditions for the study area generally are not known, model adjustments were based on transient simulations. Steady-state and transient simulations were kept consistent; that is, a given transient simulation and the steady-state simulation that provided its initial conditions were identical except for the temporal characteristics, such as storage and stresses. The steady-state simulation was initially adjusted to approximate measured characteristics such as hydraulic heads and springflows, but because almost all of the measured characteristics are time-dependent, these initial adjustments were considered obsolete as soon as adjustment of the transient-state simulation began. Subsequent model adjustments were based only on the transient simulation, and the steady-state simulation was updated simultaneously to provide initial conditions for the transient simulation. Time-dependent boundaries such as recharge and stream inflows were assigned average values for the steady-state simulation.

Transient-State Scenarios

Four transient-state "scenarios" of development were simulated. The following paragraphs give a brief overview of each scenario. Details of the scenarios are given elsewhere in this report.

The "historical" scenario simulated time-varying recharge and modern surface- and ground-water development from 1900 through 1985. All water developments before 1900 were assumed not to have affected the ground-water system, which was assumed to have been under steady-state conditions until 1900. All model adjustments were based on the historical scenario.

The main feature of the "Acoma" scenario was a projected withdrawal of 10,000 acre-feet per year from the San Andres-Glorieta aquifer in the vicinity of T. 9 N., R. 9 W. for irrigation, and a related recharge simulating irrigation-return flow of 3,333 acre-feet to the valley-fill aquifer in the same area. The Acoma scenario simulated 1986 through 2020 and the historical scenario provided the initial conditions for the Acoma scenario. In addition to the 10,000-acre-foot-per-year withdrawal and related irrigation-return flow, the Acoma scenario included a continuation of other water developments at mainly 1986 levels. Irrigation withdrawals and return flows in the Bluewater-Toltec irrigation area were continued at average levels in the Acoma scenario. Together, the historical and Acoma scenarios simulated transient conditions from 1900 through 2020 and are referred to as the "standard scenario."

The "no-Acoma" scenario was the same as the Acoma scenario except that the 10,000-acre-foot-per-year withdrawal and related 3,333-acre-foot-per-year irrigation-return flow were not included. The purpose of the no-Acoma scenario was to provide a basis upon which to assess the effects of the 10,000-acre-foot-per-year withdrawal and related irrigation-return flow. The no-Acoma scenario is a null scenario with respect to the Acoma scenario. However, the name "null" is reserved for another scenario.

The "null" scenario simulated no water development at all during 1900 through 2020. Diversions at Ojo del Gallo, surface-water diversions in the Bluewater-Toltec Irrigation District, ground-water withdrawals, artificial recharge, Bluewater Lake, and regulated streamflows were not simulated in the null scenario. The only time-dependent features simulated in this scenario were precipitation-based recharge and streamflow. The null scenario was used as a basis for estimating the effects of historical and projected development on hydraulic heads, springflows, and streamflows. Because measured hydraulic heads, springflows, and streamflows probably were affected by weather changes as well as development (Baldwin and Anderholm, in press, fig. 2), steady-state simulations were not a suitable basis for estimating the effects of development, making the null scenario necessary.

All simulations of time after September 30, 1985, are projections. Some graphs show measured or estimated model input or output beyond that date. In the case of model input, the value graphed was usually a constant. Some graphs show the comparison of measured values (such as hydraulic head) with model-derived values; where these measured values are more recent than September 30, 1985, the more recent measured values were included to help define a trend. This trend should be compared with the model-derived trend for the time prior to September 30, 1985, because the projections include hypothetical conditions that have not occurred.

Model Program

The model program selected was that of McDonald and Harbaugh (1988) with modifications. The computer program uses an iterative method to solve a finite-difference approximation of the three-dimensional flow equation (McDonald and Harbaugh, 1988, chap. 5, p. 1). The river package (McDonald and Harbaugh, 1988, chap. 6, p. 1) was modified by Miller (1988) to allow a surface-water budget and more control of river leakage than the original code allowed. Also, the block-centered flow package (McDonald and Harbaugh, 1988, chap. 5, p. 1) was modified to avoid model blocks being excluded after the model-derived hydraulic head became lower than the specified altitude of the bottom of the valley fill. (Line 40 of subroutine SBCF1H was changed from "IF(THCK.LE.0.) GO TO 100" to "IF(THCK.LE.4.) THCK=4."; McDonald and Harbaugh, 1988, chap. 5, p. 75.) The McDonald-Harbaugh program as modified was selected because of its ability to simulate a three-dimensional ground-water system with stream and spring boundaries.

Model Grid

The model grid (fig. 19, and table 12) was aligned with the major geohydrologic features of the area. The model was approximately aligned with the mountain front (outcrop of the San Andres-Glorieta aquifer on the northeast side of the Zuni uplift) and the San Rafael fault. The origin of the model grid was at 35°07'30"N. and 108°37'30"W., and the bearing of the first row was N.40°29'24"E. The smallest block size was in the area from Bluewater Lake to Horace Springs where curvilinear flow paths were anticipated. From that area, the block size increased in all directions. The smallest block represented an area 0.5 by 0.5 mile and the largest block an area 7.7 by 6 miles. This grid was adequate for a regional model but may be too coarse to represent local hydrologic features well such as in the immediate vicinity of Bluewater Dam and in the vicinity of closely spaced faults near Bluewater.

The model had two layers. Layer 1 represented the alluvium and basalt valley fill in the area between Prewitt and Horace Springs, and in The Malpais valley. Layer 2 represented the San Andres-Glorieta aquifer. The addition of layers to represent rocks immediately overlying and underlying the San Andres-Glorieta aquifer would give the appearance of greater accuracy without improving the understanding of the primary flow system as described in the conceptual model. Where the Chinle Formation lies between the San Andres and the valley fill, the Chinle was represented by vertical conductance and no storage.

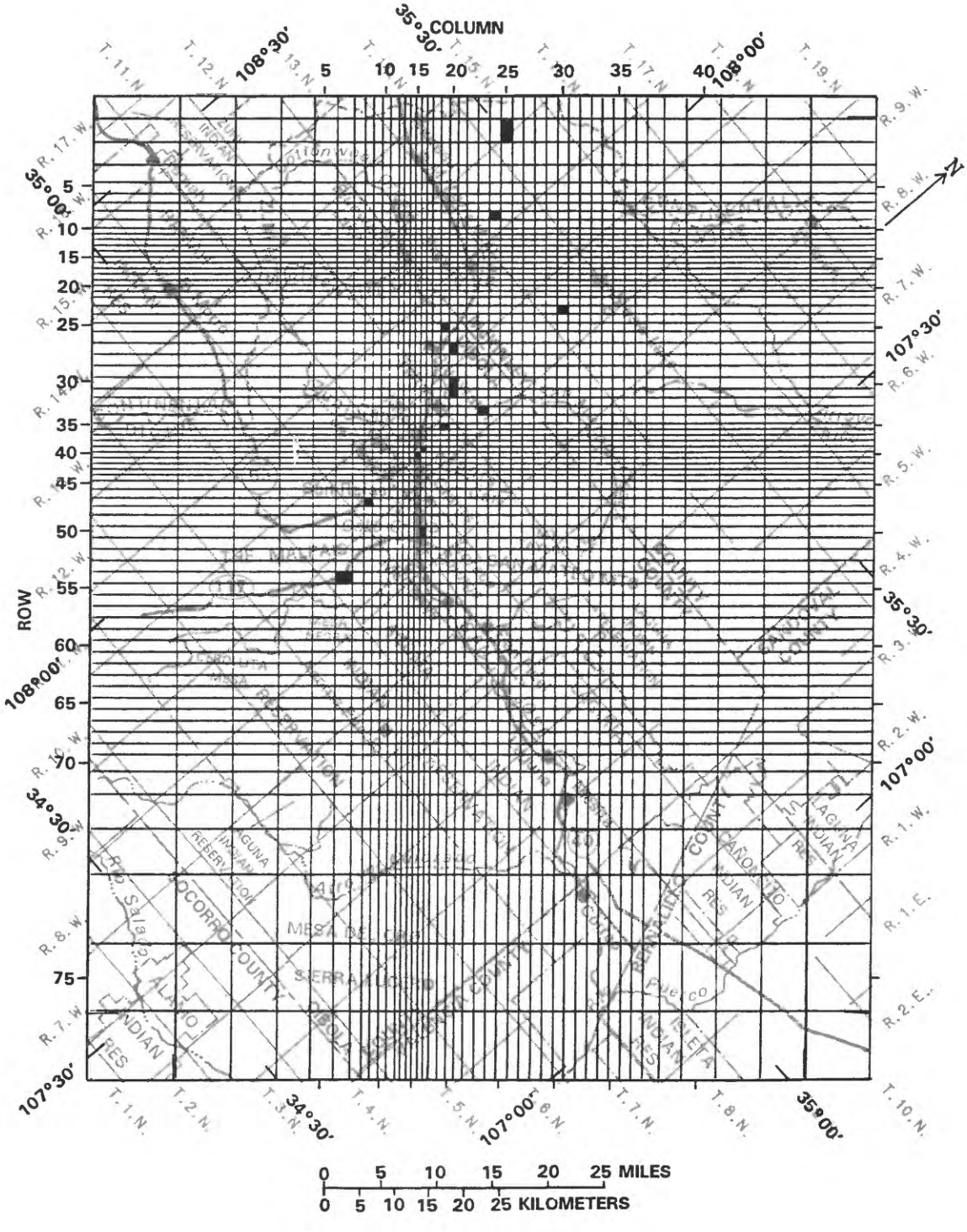

Figure 19.--Model grid and locations of hydraulic-head hydrographs.

Initial Hydraulic Heads and Time Periods

The simulated period of the historical scenario was 1900-85 inclusive. To be consistent with the reporting of water data, water years were used instead of calendar years. The first day of the water year is October 1 (an offset of +0.25 year from the calendar year). The use of water years is advantageous because most ground-water recharge ordinarily occurs during the first half of the water year (October-March), and discharge (irrigation and other evapotranspiration-related withdrawals) ordinarily occurs during the latter half (April-September). To make time calculations simple, decimal years were used. For example, the beginning of water year 1901 (October 1, 1900) is 1901.0, the midpoint of the year (April 1, 1901) is 1901.5, and the end of the water year is September 30, 1901. Water year 1902 begins October 1, 1901. This transition point is referred to as 1902.0. Therefore, the 86-year period of the historical scenario started October 1, 1899 (1900.0), and ended September 30, 1985 (1986.0).

The simulation period of the historical scenario was divided into 70 stress periods of varying lengths depending on the availability of hydrologic information with which to compare the simulation. Stress periods (McDonald and Harbaugh, 1988, chap. 4, p. 5) allow for changes in model input, such as specified fluxes, and in model output, such as hydraulic-head values. Each stress period was divided into five time steps.

The 70 stress periods can be grouped into five time intervals. The first time interval of 28 years, from 1900.0 to 1928.0 (October 1, 1899, through September 30, 1927), was represented by one stress period, approximately simulating the time before the concrete-arch dam was constructed on Bluewater Creek. During this first time interval, detailed information was sparse. The second time interval of 16 years (October 1, 1927, through September 30, 1943) was represented by four stress periods of 4 years each. During the second time interval, recharge rates increased gradually. The third time interval of 20.5 years (October 1, 1943, through March 31, 1964) was represented by 41 stress periods of one-half year each. During the third time interval, semiannual water-level measurements were available, streamflow measurements were made, and for some years, accurate irrigation-withdrawal estimates also were available. The fourth time interval of 19 years (April 1, 1964, through March 31, 1983) was represented by 19 stress periods of 1 year each. During the fourth time interval, annual water-level measurements generally were made during the winter months, and streamflow measurements were made on Bluewater Creek near Bluewater until 1973. The fifth time interval of 2.5 years (April 1, 1983, through September 30, 1985) was represented by five stress periods of one-half year each. During the fifth time interval, semiannual water-level measurements were resumed. Table 4 shows the decimal-water-year end date of each stress period.

Table 4.--End dates of stress periods used to represent 1900.0 (October 1, 1899) through 1986.0 (September 30, 1985), and durations of stress periods used for projections

Stress period	End date	Stress period	End date	Stress period	End date	Stress period	End date
1	1928.0	19	1951.0	37	1960.0	55	1973.5
2	1932.0	20	1951.5	38	1960.5	56	1974.5
3	1936.0	21	1952.0	39	1961.0	57	1975.5
4	1940.0	22	1952.5	40	1961.5	58	1976.5
5	1944.0	23	1953.0	41	1962.0	59	1977.5
6	1944.5	24	1953.5	42	1962.5	60	1978.5
7	1945.0	25	1954.0	43	1963.0	61	1979.5
8	1945.5	26	1954.5	44	1963.5	62	1980.5
9	1946.0	27	1955.0	45	1964.0	63	1981.5
10	1946.5	28	1955.5	46	1964.5	64	1982.5
11	1947.0	29	1956.0	47	1965.5	65	1983.5
12	1947.5	30	1956.5	48	1966.5	66	1984.0
13	1948.0	31	1957.0	49	1967.5	67	1984.5
14	1948.5	32	1957.5	50	1968.5	68	1985.0
15	1949.0	33	1958.0	51	1969.5	69	1985.5
16	1949.5	34	1958.5	52	1970.5	70	1986.0
17	1950.0	35	1959.0	53	1971.5		
18	1950.5	36	1959.5	54	1972.5		

All simulations beyond 1986.0 (September 30, 1985) were projections. All projections simulated 35 years in six stress periods ending in 2021.0 (September 30, 2020). The following table shows the length of each stress period for the projections:

Duration of stress periods used to represent projections

Stress period	Stress period duration (years)	Cumulative duration (years)
71	1	1
72	3	4
73	5	9
74	5	14
75	10	24
76	11	35

Graphical representations of model-derived values start with 1928.0, which is the end of the first stress period. However, it generally would be as correct to interpolate between the steady-state value for 1900.0 and the first transient value for 1928.0 as to interpolate between the ends of the transient stress periods.

Aquifer and Confining-Bed Characteristics

The capacity of the aquifer to transmit water in the horizontal direction was simulated by specifying hydraulic conductivity and bottom altitude for the valley fill (layer 1) and transmissivity for the San Andres-Glorieta (layer 2). The capacity of the aquifer to store water was simulated by specifying specific-yield values for the valley fill (layer 1) and storage coefficient for the San Andres-Glorieta (layer 2). The storage of water under unconfined conditions in the San Andres-Glorieta was simulated by specifying a storage coefficient with a numeric value approximately equal to the specific yield. The capacity to transmit water vertically between the San Andres-Glorieta and the valley fill was simulated by specifying a leakance, which was estimated as a function of the thickness of the intervening confining bed.

All specified values of aquifer and confining-bed characteristics were subject to adjustment to improve the comparison between model-derived and measured hydraulic heads and flow rates. A description of specific comparisons is given in a following section concerning model adjustments. The characteristics described here are those that resulted from the final adjustments.

Hydraulic Conductivity and Transmissivity

Hydraulic-conductivity and transmissivity values assigned to the model are consistent with values presented in the conceptual-model section of this report and resulted in model-derived hydraulic heads that are compared with measured heads in the model-adjustment section. Hydraulic conductivity of alluvium (fig. 20, zone B) was assumed to be generally 40 feet per day on the basis of measurements near the Anaconda and Homestake uranium mills. The hydraulic conductivity of basalt was assumed generally to be greater than that of alluvium because basalt is broken and may have lava tubes. With some exceptions, the hydraulic conductivity of basalt generally was assumed to be 50-60 feet per day (fig. 20, zones C and D). Hydraulic conductivity of 10 feet per day (fig. 20, zone A) was assigned for an area near where San Mateo Creek joins the Rio San Jose. This may be reasonable because fine-grained alluvium may have plugged the fractures in the basalt at the interface between basalt and alluvium (Hydro-Search, Inc., 1981, p. 47). A similar condition may exist in Mitchell Draw. Near Horace Springs and in the northern part of The Malpais, values of hydraulic conductivity for basalt as great as 300 feet per day were based on assumed cavernous basalt.

Horizontal flow from the San Andres-Glorieta aquifer into the alluvium near Ojo del Gallo (fig. 10) was simulated by specifying an arbitrarily large value of hydraulic conductivity in layer 1 on the upstream side of the fault (fig. 20, zone F). This is an area where the San Rafael fault causes the San Andres Limestone to be horizontally adjacent to the alluvium and water flows horizontally from the San Andres-Glorieta aquifer into the alluvium. Zone F extends the active part of layer 1 to the upstream side of the simulated fault, allowing the simulation of flow vertically from layer 2 to layer 1 and then horizontally in layer 1 across the fault, which is simulated as an inactive zone in layer 2.

The transmissivity values specified for layer 2 (fig. 21) generally are similar to values shown in figure 7 for the San Andres-Glorieta aquifer except for transition zones that were specified between areas of very large and very small values of transmissivity to avoid mathematical truncation errors. (Block-by-block transmissivity values are given in table 13 in Supplemental Information.) A transmissivity of 50,000 feet squared per day was assigned to represent cavernous limestone southeast of the San Rafael fault, and 60,000 feet squared per day was assigned to represent cavernous limestone west of San Rafael fault. These areas correspond to zones III and V in figure 7. The transmissivity 10,000 feet squared per day was specified for the area west of the swarm of faults near Bluewater, corresponding to zone II in figure 7. The transmissivity of sandstone was simulated for areas where the San Andres Limestone is not cavernous or is not present; specified values of transmissivity ranged from 100 to 500 feet squared per day for areas corresponding to zones I, VI, VII, and the northern part of zone IV in figure 7. An assumed transmissivity value of 40 feet squared per day represented partly saturated Glorieta Sandstone on the mountain side.

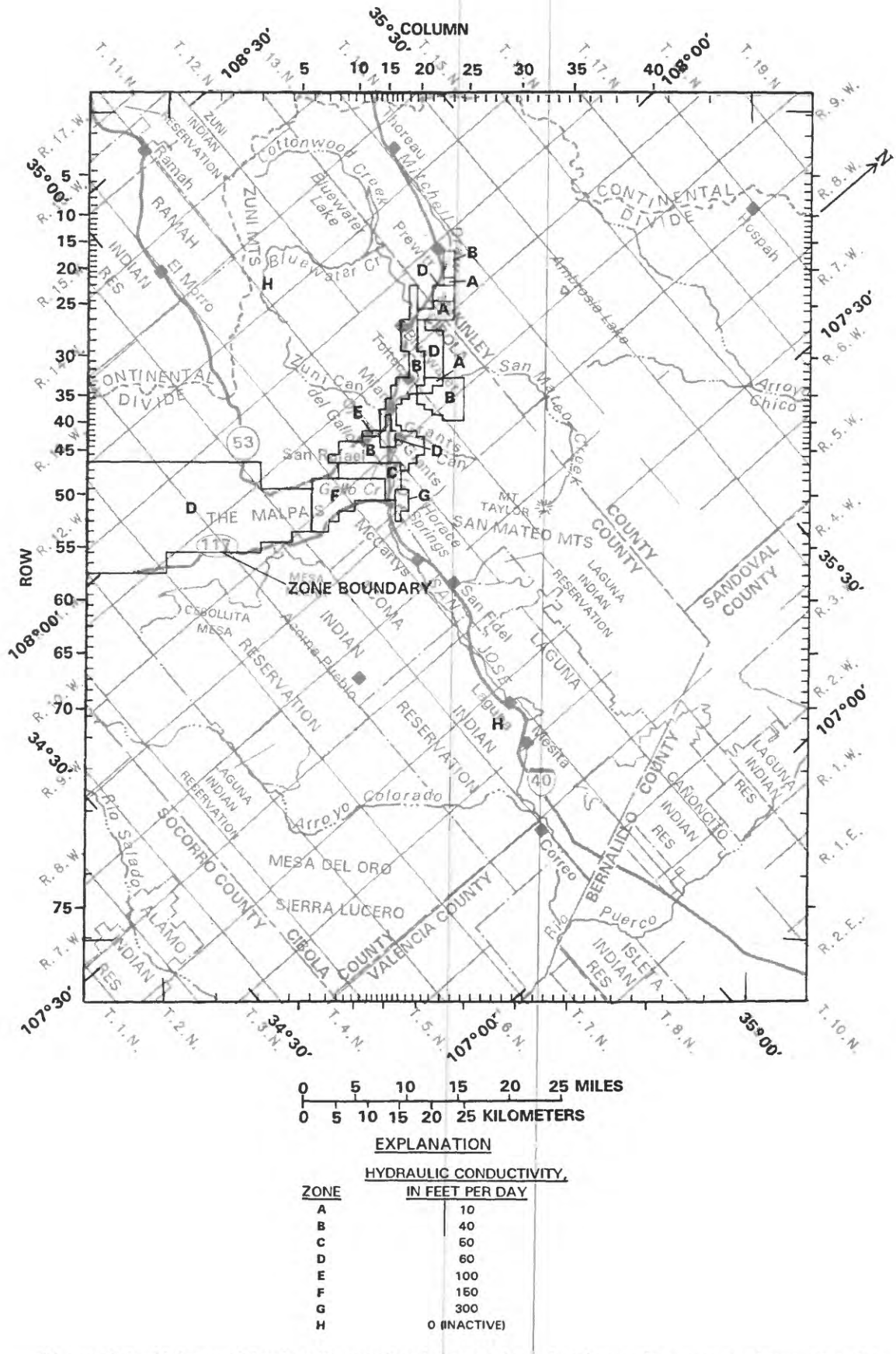

Figure 20.--Values of hydraulic conductivity assigned to layer 1, representing valley fill.

Transmissivity values in transitional zones between the other zones ranged from 100 to 12,500 feet squared per day. This area included the remainder of zone IV of figure 7. The assumed transmissivity of 100 feet squared per day for the northern corner of the model, north of zones I, II, and IV, represented the thinning of the aquifer in that area where no aquifer tests have been made. Where the model was inactive, transmissivity was assigned a value of zero. Large inactive areas include the Zuni uplift where the San Andres-Glorieta aquifer is not present and the eastern corner of the area where ground water flows out of the aquifer to the Rio Grande rift (fig. 2). Smaller inactive areas simulated faults. Simulation of ground-water outflow and faults is described in the Boundary Conditions section.

Two special transmissivity zones were used to simulated specific features. The special transmissivity zone in row 27, columns 18-25 represented a reduced transmissivity (2,000 feet squared per day) northeast of Bluewater where a swarm of faults (fig. 2) are assumed to reduce the horizontal transmissivity of the San Andres-Glorieta aquifer. This assumption is consistent with the hydraulic-head difference (fig. 11) across the faults near Bluewater. The special transmissivity zone near row 16, column 13 was assigned a higher value (coincidentally also 2,000 feet squared per day) than other transmissivity values in the area. This zone was used to simulate the flow of water through the wall of San Andres Limestone between Bluewater Lake and Bluewater Canyon, which runs subparallel to the lake shore as previously described.

Specific Yield and Storage Coefficients

Specific yield for layer 1 (fig. 22) representing the valley fill generally was 0.12. This value, intermediate between the specific yield of unconsolidated sediments and that of dense, fractured rock, may represent interbedded alluvium and basalt. An exception was the area near Bluewater where a value of 0.012 was assigned. In this area, the water table may be in dense, fractured rock. That is, on the northeast side of this area, the water table may have been in basalt, and on the southwest side, the water table may drop temporarily below the bottom of the alluvium into the San Andres Limestone.

Storage coefficients for layer 2 (fig. 23) represent confined and unconfined conditions in the San Andres-Glorieta aquifer. In the area along the mountain front, where the water table probably is in the San Andres-Glorieta aquifer, the storage coefficient represents unconfined conditions. Where the water table was assumed to be in the San Andres Limestone, the storage coefficient was set at 0.015 and where the water table was assumed to be in the Glorieta Sandstone it was set at 0.15. These values are reasonable for the rock types represented. The storage coefficient for the remainder of the active part of layer 2 representing confined conditions in the San Andres-Glorieta aquifer was 4×10^{-4}, a reasonable value for a confined aquifer. Where layer 2 was inactive, the storage coefficient was set to zero.

EXPLANATION

ZONE REPRESENTING CAVERNOUS LIMESTONE--Transmissivity ranges from 50,000 to 60,000 feet squared per day

ZONE REPRESENTING CAVERNOUS LIMESTONE--Transmissivity is equal to 10,000 feet squared per day

ZONE REPRESENTING SANDSTONE--Transmissivity ranges from 100 to 500 feet squared per day

ZONE REPRESENTING PARTLY SATURATED SANDSTONE--Transmissivity is equal to 40 feet squared per day

TRANSITIONAL ZONE--Transmissivity ranges from 100 to 10,000 feet squared per day

ZONES REPRESENTING SPECIFIC FEATURES--Swarm of faults near Bluewater, and San Andres Limestone between Bluewater Lake and Bluewater Canyon. Transmissivity is equal to 2,000 feet squared per day in both zones

INACTIVE ZONES--Transmissivity not used in flow calculations. Zone includes areas where San Andres-Glorieta aquifer not simulated and locations where faults are assumed to restrict flow in the aquifer

BOUNDARY BETWEEN AREAS OF SAME TRANSMISSIVITY

80 VALUE OF TRANSMISSIVITY IN DESIGNATED AREA

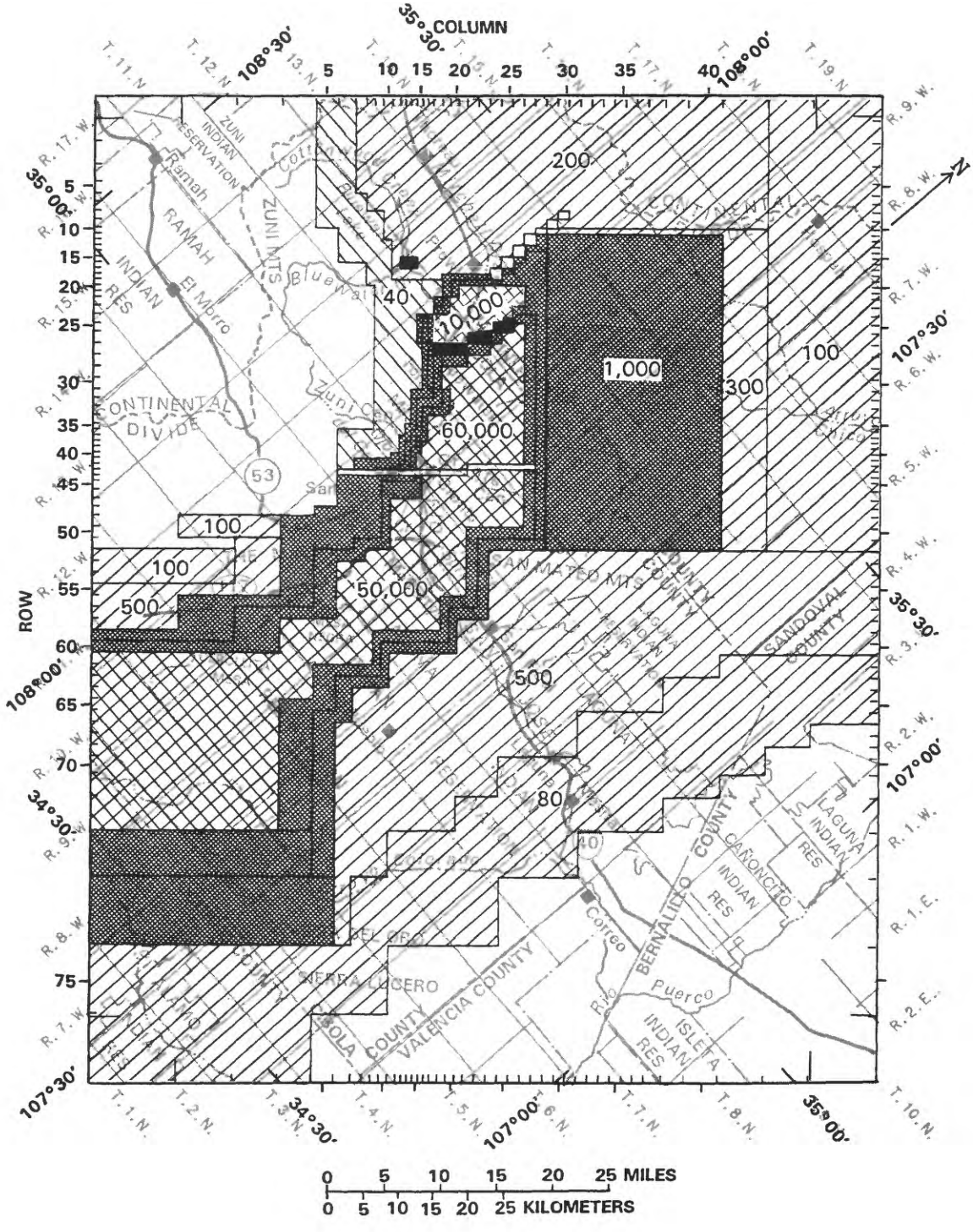

Figure 21.--Values of transmissivity assigned to layer 2, representing the San Andres-Glorieta aquifer.

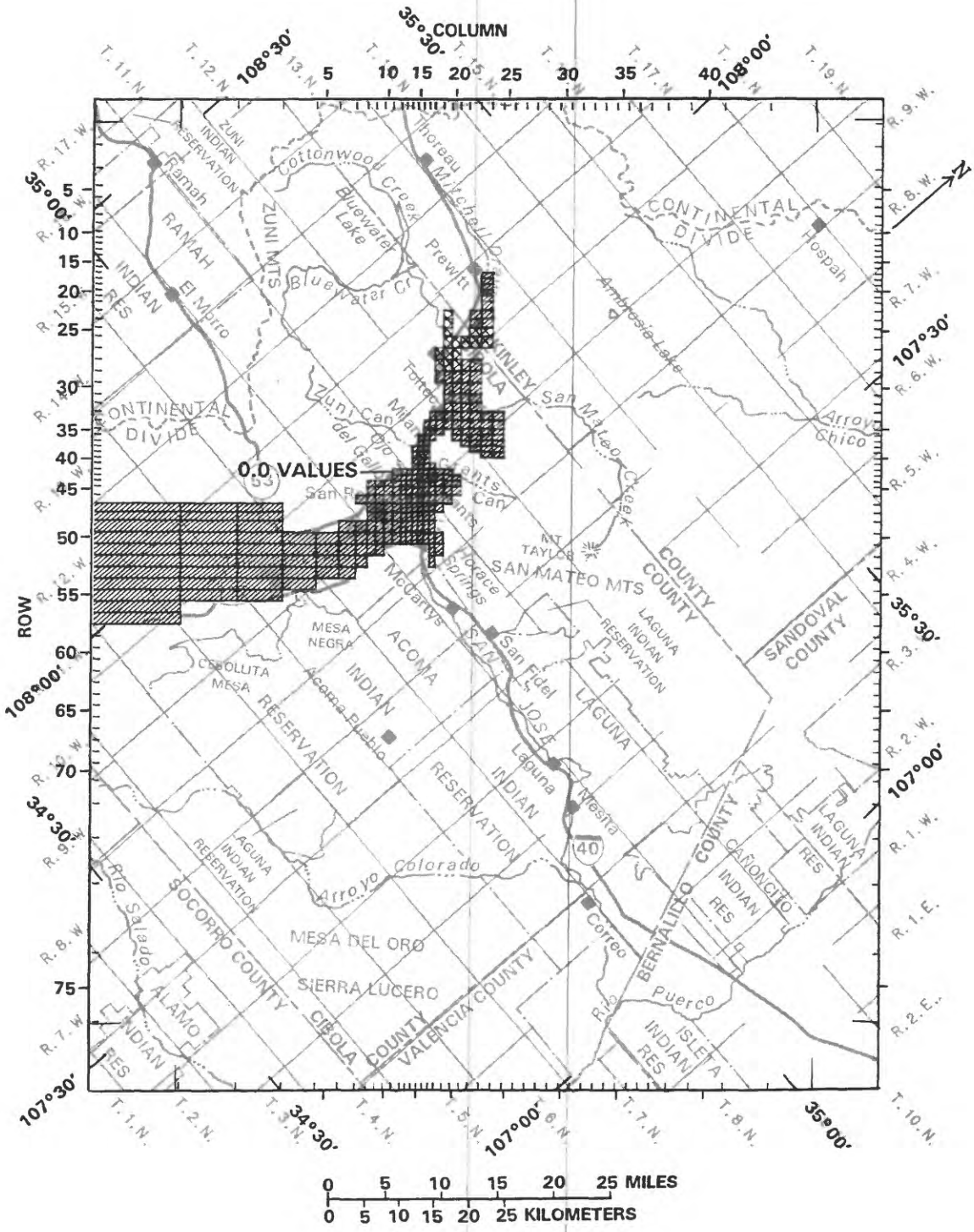

Figure 22.--Specific yields assigned to layer 1, representing valley fill.

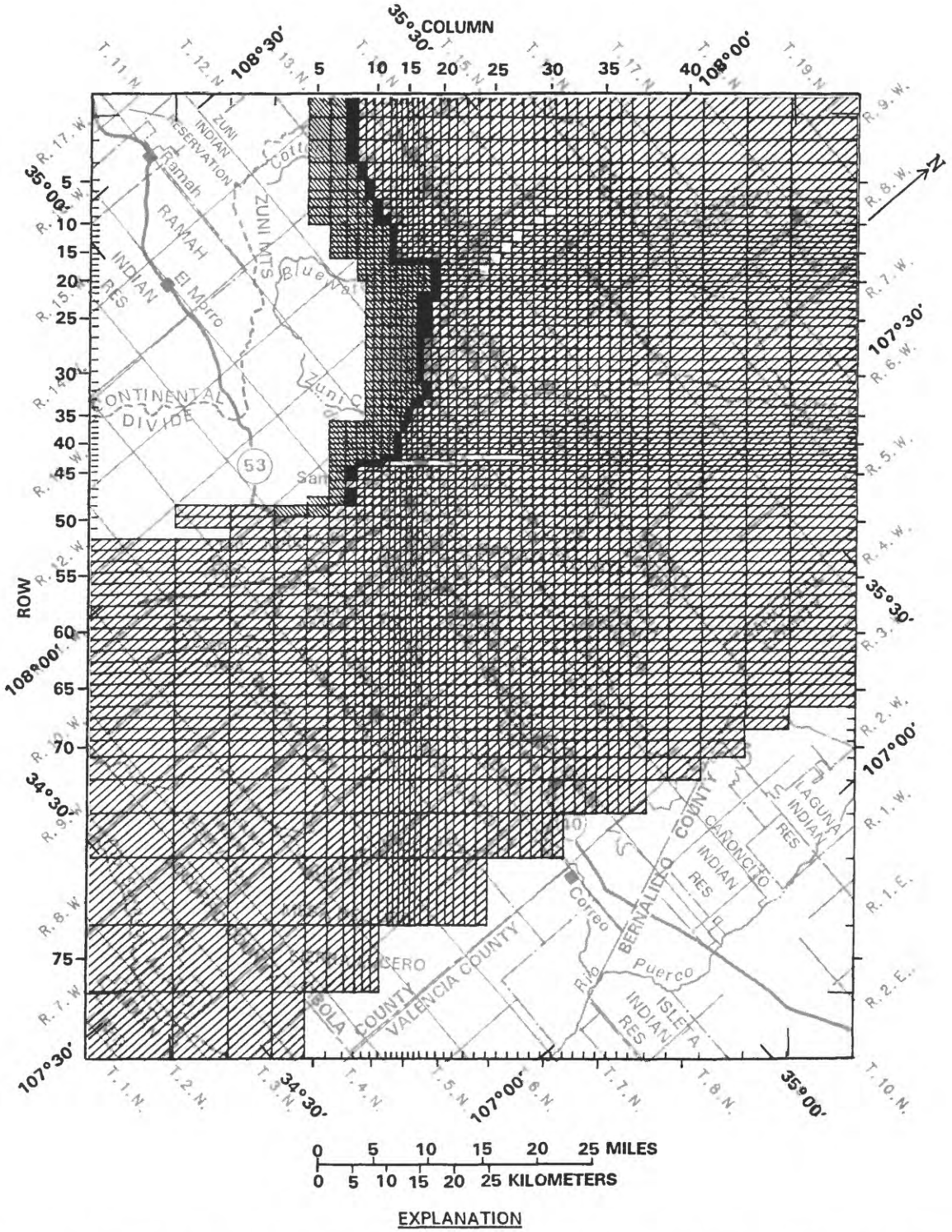

Figure 23.--Storage coefficients assigned to layer 2, representing the San Andres-Glorieta aquifer.

Leakances

Vertical flow of ground water between the valley fill (layer 1) and the San Andres-Glorieta aquifer (layer 2) was simulated by assigning leakance values to layer 1. Leakance through a given confining bed is the vertical hydraulic conductivity of the bed divided by the thickness of the bed. When more than one bed is involved, an "average" leakance may be calculated with a formula having the form of equation 49 of McDonald and Harbaugh (1988). Leakance values were estimated by the equation below, which accounts for variable thickness of the valley fill and Chinle Formation. (Leakance values are given in table 14 of Supplemental Information.) The location of simulated vertical flow is shown in figure 24. Vertical conductance at a given model block is calculated by the model program (McDonald and Harbaugh, 1988, chap. 5, p. 12) as the specified leakance times the horizontal area of the model block.

$$L = \frac{1}{(B1/K1)+(B2/K2)} \qquad (5)$$

where L = leakance (per second) set to zero where both thicknesses are zero;
B1 = saturated thickness of the valley fill, in feet;
K1 = vertical hydraulic conductivity of the valley fill, in feet per second;
B2 = thickness of the Chinle Formation, in feet; and
K2 = vertical hydraulic conductivity of the Chinle Formation, in feet per second.

The small value of vertical hydraulic conductivity of the Chinle Formation tends to determine the leakance value calculated with the above formula. However, where the thickness of the Chinle is zero, the vertical hydraulic conductivity of the valley fill is a significant factor. The thickness and vertical hydraulic conductivity of the San Andres-Glorieta aquifer were not included in the above formula because the resistance to vertical flow in the San Andres-Glorieta aquifer was assumed to be negligible. The vertical hydraulic conductivity of the Chinle Formation was represented as 10^{-11} foot per second (approximately 9×10^{-7} foot per day), and that of the valley fill was represented as 5×10^{-7} foot per second (approximately 0.004 foot per day). Because of the contrast between these values of vertical hydraulic conductivity, most vertical flow was simulated where the leakance was determined by the hydraulic conductivity assigned to the valley fill.

The saturated thickness of the valley fill (Supplemental Information, table 10) was estimated as the water-table altitude (Baldwin and Anderholm, in press, fig. 17) minus the estimated altitude of the bottom of valley fill (fig. 8). Chinle thickness (Supplemental Information, table 15) was estimated from figure 4.

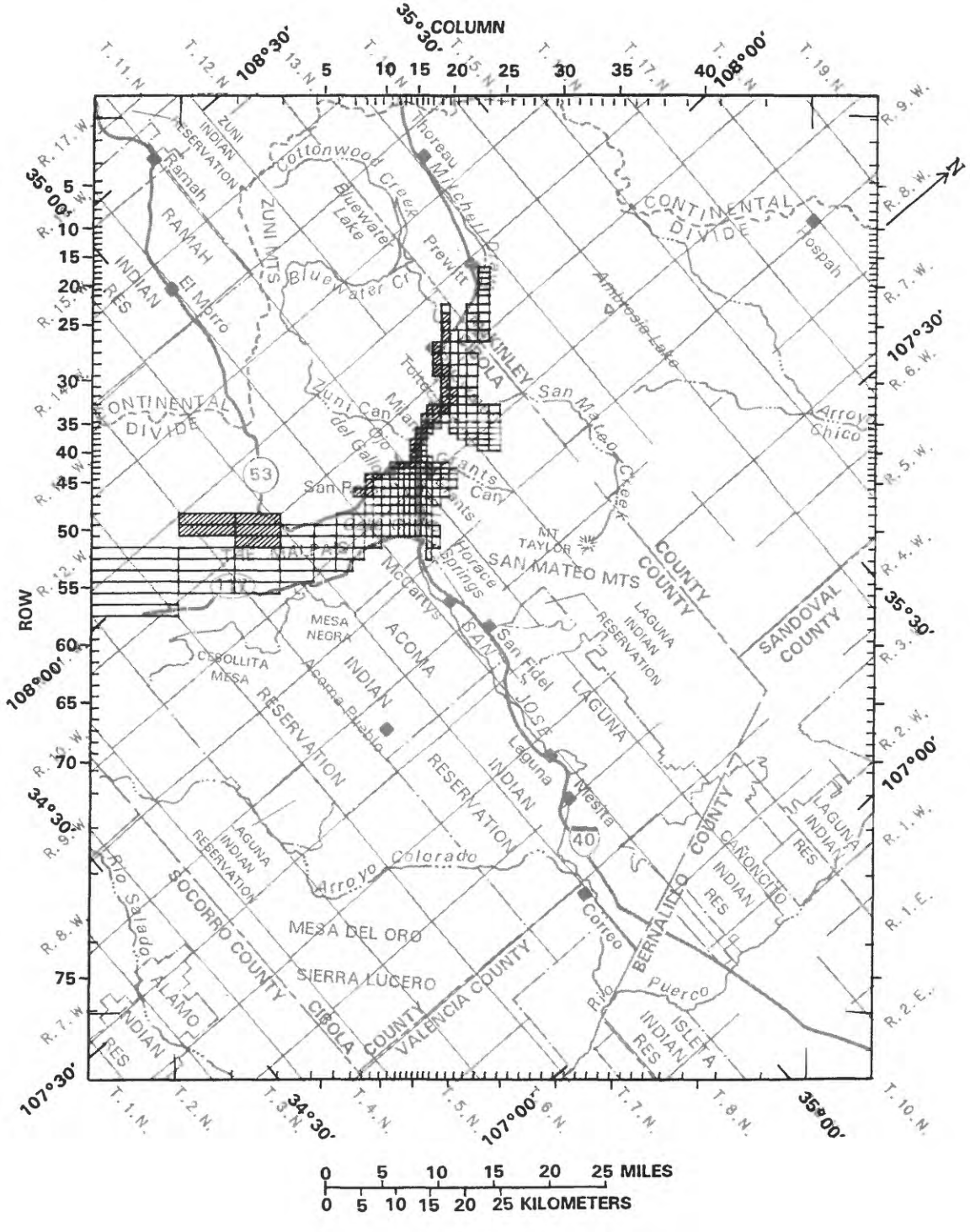

Figure 24.--Location of simulated vertical flow between the San Andres-Glorieta aquifer and the valley fill.

Boundary Conditions

Natural boundary conditions of recharge, discharge, and underflow were simulated by a combination of no-flow, specified-flow, specified-head, general-head, and head-dependent boundaries representing streams and evapotranspiration. The mathematical representation of these boundaries is discussed in detail by McDonald and Harbaugh (1988), except for the stream boundaries, which are described by Miller (1988).

A description of recharge, discharge, and underflow follows a discussion of each type of boundary and appropriate precautions. Ground-water withdrawal and artificial recharge, specified-flow type boundaries, are described under a separate heading.

A no-flow condition is implicitly assumed around the exterior of the grid. Within the model grid, a no-flow boundary consists of inactive cells for which no flow into or out of the cell is permitted. Large drawdowns may be simulated at no-flow boundaries and care is needed in the use of arbitrary no-flow boundaries. If drawdowns are simulated at arbitrary no-flow boundaries, then the effect on the simulation needs to be evaluated and another type of boundary may be considered. Because no vertical flow was simulated where either layer 1 or layer 2 was inactive, a horizontal no-flow boundary on the upper side of layer 2 was simulated in the northern and eastern parts of the model where layer 1 was inactive. No-flow boundaries are essentially specified-flow boundaries where the flow is zero. Within the exterior no-flow boundaries, specified-flow, specified-head, general-head, and head-dependent boundaries simulating streams, and evapotranspiration were defined.

A specified-flow boundary simulates features such as wells that withdraw or inject water at a specified rate during a given stress period. The rate of withdrawal or injection is independent of both the area of the block and the hydraulic head in the block. For convenience in varying the rate with time, recharge was represented as a specified-flow boundary (specified using the "well package," rather than the "recharge package" of McDonald and Harbaugh, 1988). Unreasonably high or low hydraulic heads may develop at specified-flow boundaries. If that occurs and flow is known or estimated with confidence, simulated aquifer characteristics may be changed; if the flow is estimated with less confidence than the aquifer characteristics, the flow may be respecified.

A specified-head boundary includes blocks for which the head is specified in advance and is held at this specified value throughout the simulation; simulated flow to or from a specified-head boundary is not restricted. Because unreasonably large flows may be generated at specified-head boundaries if drawdowns are simulated nearby, care is needed to assure that simulated flows are plausible. If not, the effect on the simulation needs to be evaluated and another type of boundary may be considered.

A general-head boundary is a model block for which flow from or to a source or sink outside the model is calculated in proportion to the difference between the simulated hydraulic head in the block and specified head for the outside source/sink. A general-head boundary is very much like a specified-head boundary except that the exterior source/sink is at some distance. The precautions for using a general-head boundary are the same as those for using a specified-head boundary; simulated flows need to be monitored lest they become unreasonable.

A head-dependent flux boundary was used to simulate the physical stream boundary. This boundary is designated as a "stream boundary" to distinguish it from other head-dependent flux boundaries in this report. A stream boundary is like a general-head boundary except that restrictions are placed on the inflow and outflow and a budget of streamflow is kept (Miller, 1988). Inflow from the stream may be simulated if the model-derived hydraulic head in the block is less than or equal to the specified hydraulic head in the stream. However, inflow from a stream boundary at a given model block is limited to the lesser of (A) the streamflow at that block, or (B) a specified value that is deemed to be a maximum. Outflow to a stream boundary at a given model block is simulated when the model-derived hydraulic head in the aquifer at the block is greater than the specified stream altitude at the block, and is proportional to the difference between the hydraulic head and the stream altitude. Because outflow is not limited it could become unreasonably large and needs to be monitored. The restrictions that are imposed on inflow and outflow at a stream boundary are similar to the restrictions that would be necessary to simulate a spring or lake.

A head-dependent flux boundary was used to simulate the process of evapotranspiration from the water table. This boundary is designated as an "evapotranspiration boundary" to distinguish it from other head-dependent flux boundaries in this report. An evapotranspiration boundary has restrictions on the outflow. (Inflow is not simulated.) An evapotranspiration boundary represents the removal of water from the water table on the basis of the following conventions: when the model-derived water table is at or above a specified altitude (evapotranspiration surface) that might represent the land surface, evapotranspiration loss is at a specified maximum flux (rate per unit area, such as cubic feet per second per foot squared); when the model-derived water table is at a specified depth below the evapotranspiration surface (extinction depth), no ground water is lost to evapotranspiration; and when the water level is between these limits, evapotranspiration from the water table is a linear function of depth to water (McDonald and Harbaugh, 1988, fig. 42).

Unreasonable discharges can be simulated using an evapotranspiration boundary. For example, if the water-table altitude were 6,490 feet and the land-surface altitude were 6,500 feet as determined from measured depth to water and a topographic map with a possible 20-foot error in the datum, a model-derived water-table altitude of 6,499 feet could appear to be close to correct (within one-half the error in the datum) considering only the comparison between the measured and model-derived values of water-table altitude. However, if the depth of zero evapotranspiration were 10 feet, the true discharge to evapotranspiration might be near zero and the model-derived

discharge to evapotranspiration would be near the maximum. The problem is compounded because, although in this example the true depth to water is known, the depth to the water table generally is not known to within a few feet throughout most of the area where it is suspected to be shallow. The problem is further compounded when drawdowns are simulated that cause model-derived evapotranspiration rates to diminish, giving rise to a model-based estimate of salvaged evapotranspiration that, in this example, would be entirely erroneous. Model-derived evapotranspiration rates need to be monitored in view of observed land-surface conditions such as evaporite buildup ("alkali") and vegetation.

Recharge from Precipitation

Recharge from precipitation was simulated as specified-flow boundaries. The locations of simulated recharge are shown in figures 25 and 26. The quantity of simulated recharge at each location is listed in tables 16 and 17 (Supplemental Information) by location and stress period.

In the mountains of the Zuni uplift, recharge was estimated as a function of estimated excess precipitation. The average rate of recharge simulated for the mountains of the Zuni uplift was 4.22 cubic feet per second, about 25 percent of the excess precipitation estimated by the San Juan method and slightly less than the 30 percent estimated in the conceptual-model section of this report. The time variation of simulated recharge on the mountains of the Zuni uplift is shown in figure 27A. The rates shown are proportional to those shown in figure 13F. Most of the mountain recharge was assigned to layer 2 (fig. 26) because the San Andres-Glorieta aquifer crops out over most of the mountain slope where recharge was simulated. Some of the normally dry canyons near Bluewater have been blocked by flood-control structures, and recharge on these watersheds was assigned to layer 2. Near the eastern end of the Zuni uplift (zones 4 and 5 in fig. 12; model rows 32-50, columns 3-8, in tables 16 and 17 in Supplemental Information) where some of the recharge may be by way of surface flows in canyons that debouch onto the valley fill, the mountain recharge was arbitrarily divided with one-half assigned to layer 1 (fig. 25) and one-half assigned to layer 2 (fig. 26). The time variation of recharge near the eastern end of the Zuni uplift is shown in figure 27B.

EXPLANATION

SPECIFIED-HEAD BOUNDARY

SPECIFIED-FLOW BOUNDARY--Represents barren-basalt recharge

SPECIFIED-FLOW BOUNDARY--Represents mountain-front recharge

SPECIFIED-FLOW BOUNDARY--Represents underflow of Mitchell Draw, San Mateo Creek, Grants Canyon, and the Rio San Jose near Horace Springs

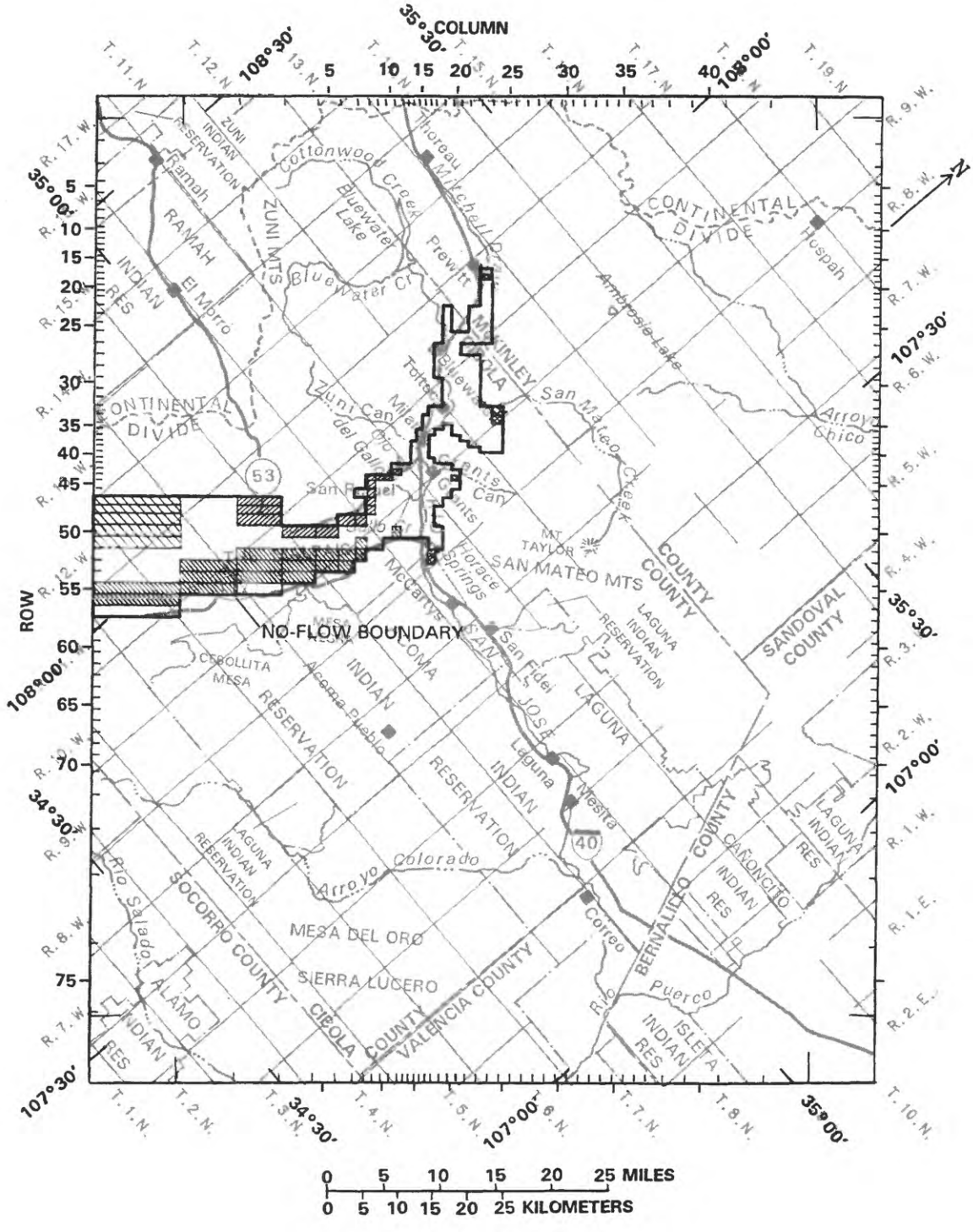

Figure 25.--Specified-flow, no-flow, and specified-head boundaries in layer 1.

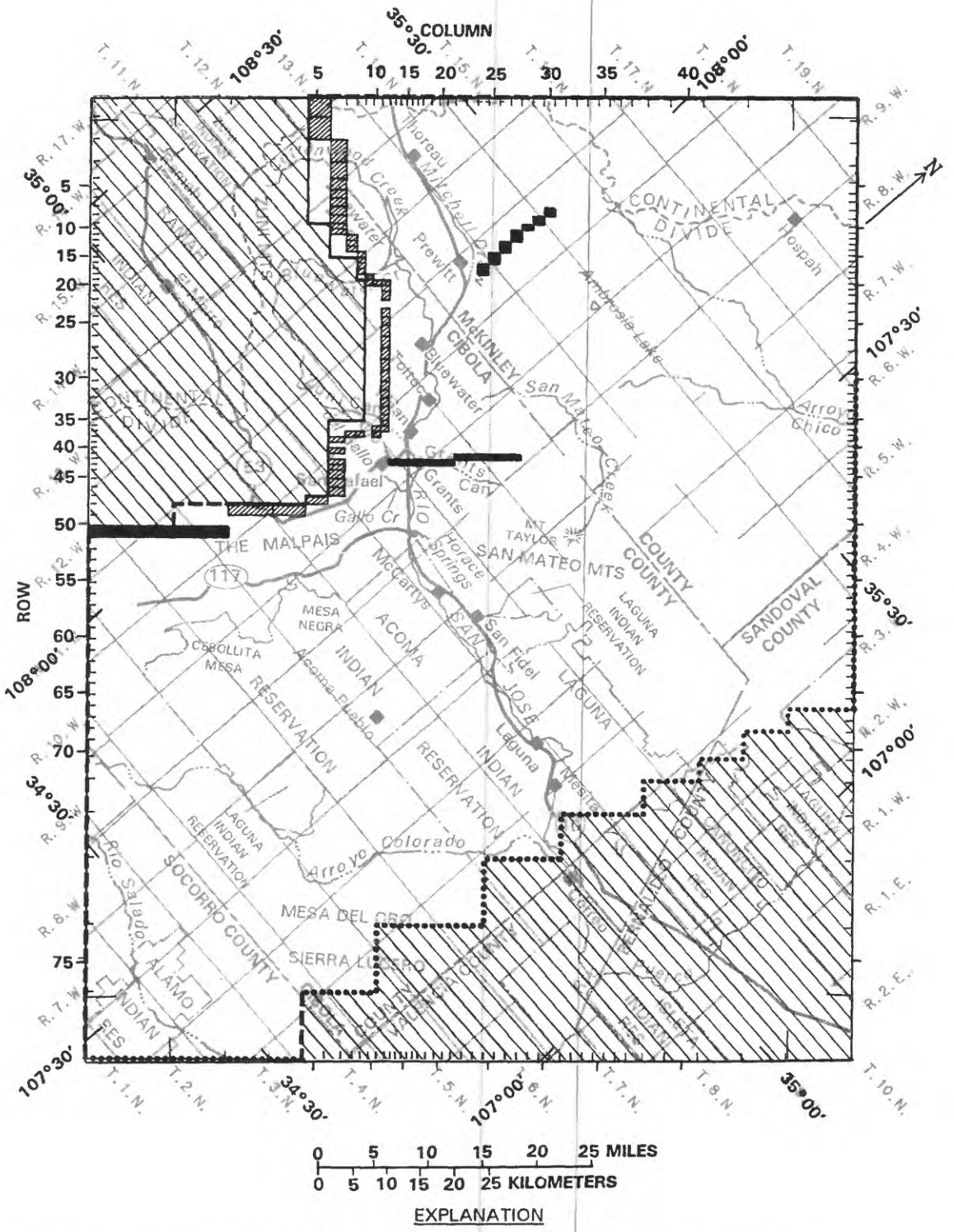

Figure 26.--Specified-flow, no-flow, and general-head boundaries in layer 2.

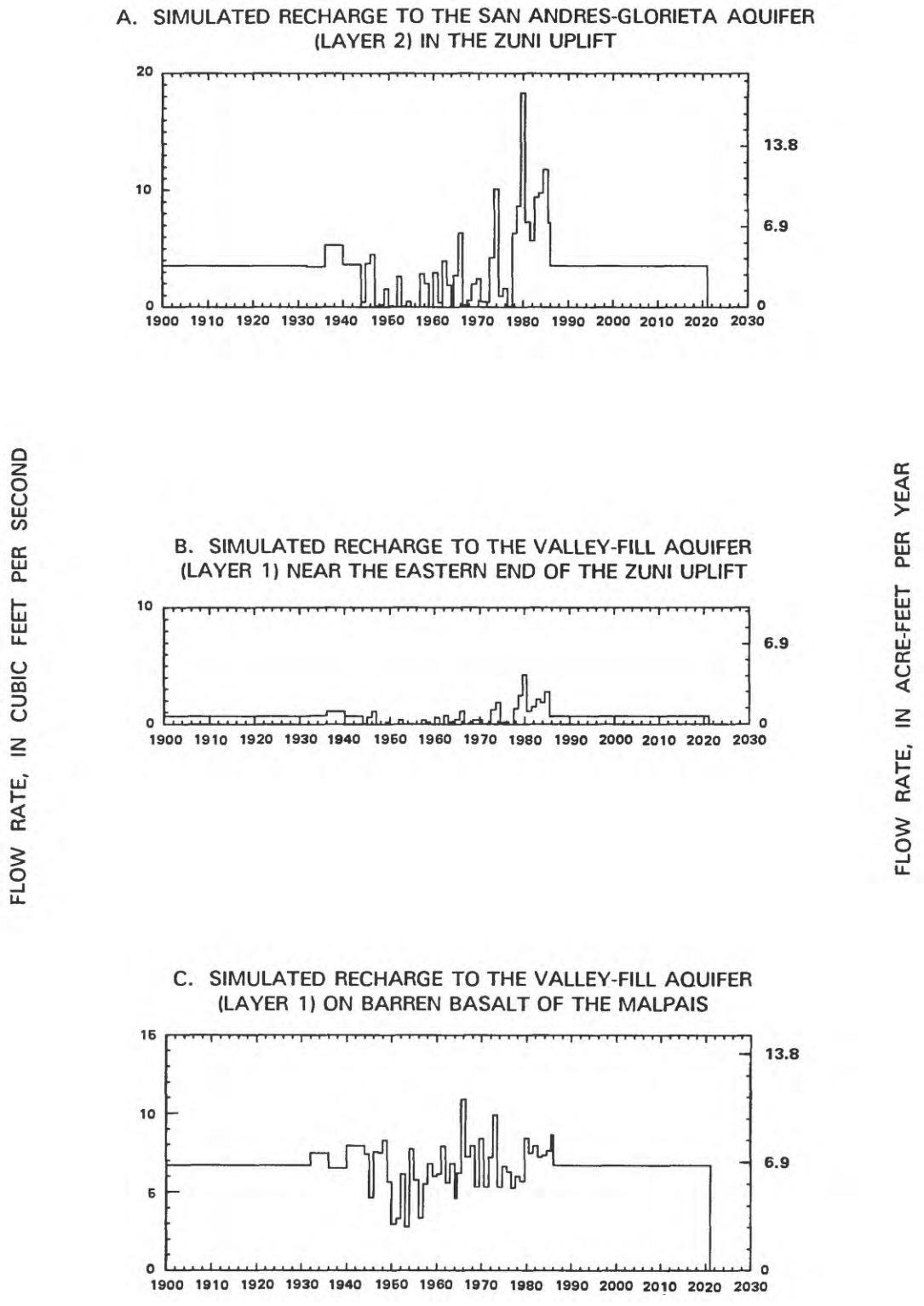

Figure 27.--Specified-flow rates used to represent recharge on the Zuni uplift and The Malpais.

In part of The Malpais where the land surface is barren basalt (fig. 2), recharge was specified as 15 percent of precipitation at Grants. The steady-state flux was 1.5 inches (a flow rate of 6.75 cubic feet per second at 4.5 cubic feet per second per inch of flux). For the transient simulation, the flux was 15 percent of the precipitation at Grants. The flux was multiplied by the area of barren basalt represented in each of the model blocks shown in figure 25, and specified as a flow rate at each block. All of the recharge on barren basalt of The Malpais was assigned to layer 1. The flow specified at each model block is listed in table 16. The time variation of recharge on barren basalt is shown in figure 27C.

A specified-head boundary (fig. 25) was included in The Malpais area as an artifice to make the model calculations more stable, speeding convergence and preventing mathematical oscillations on long time steps. The hydraulic heads specified were selected to represent a water table that may exist near the bottom of the valley fill. This boundary added 0.3 (rounded) cubic foot per second under both steady-state and transient conditions, which is equivalent to 4 percent of the average specified recharge on barren basalt. If flow at this boundary were to become large, the designation as a specified-head boundary may need to be reevaluated. This condition did not develop for simulations described in this report.

Evapotranspiration

Evapotranspiration was simulated where the water table was near land surface in La Vega, along Gallo Creek, and along the Rio San Jose downstream from Grants (figs. 6 and 28). No data are available for evapotranspiration from ground water in the study area. However, to represent this boundary in the model it was necessary to specify an extinction depth, an evapotranspiration surface, and a maximum rate of evapotranspiration. The extinction depth was assumed to be 10 feet, consistent with the discussion in the conceptual model section. The evapotranspiration surface was assumed to be the land surface. Land-surface altitude was taken from U.S. Geological Survey 7.5-minute topographic maps. For each model block, a land-surface altitude was selected to represent the average altitude of the area where evapotranspiration was likely to occur due to a shallow water table. In some model blocks, evapotranspiration from the water table is not likely to occur over the entire area of the block because of an abrupt rise in the topography. For example, for blocks along streams such as Gallo Creek and parts of the Rio San Jose, the land-surface altitude was selected to represent the altitude of the land near the creek, disregarding the higher land in the block. Where the land was more level or gently sloping, it was assumed that evapotranspiration would occur over the entire area of the block, and the altitude selected was the approximate average for the entire block. The maximum evapotranspiration flux (rate per unit area) was assumed generally to equal average annual lake evaporation of 45 inches per year (1.188×10^{-7} feet per second per square foot of area). To avoid the simulation of too much evapotranspiration at blocks where evapotranspiration is not likely to occur over their entire area, the maximum evapotranspiration rate was reduced proportionate to the area. For example, where evapotranspiration is likely to occur over only one-tenth of the area represented by a given model block, the maximum evapotranspiration was set to 4.5 inches per year. The locations of blocks where simulated evapotranspiration was non-zero under steady-state conditions (fig. 28) approximate the area (fig. 5) where evapotranspiration was expected to occur. Model-derived evapotranspiration rates for steady-state and selected transient stress periods are given in a following section on results of simulations.

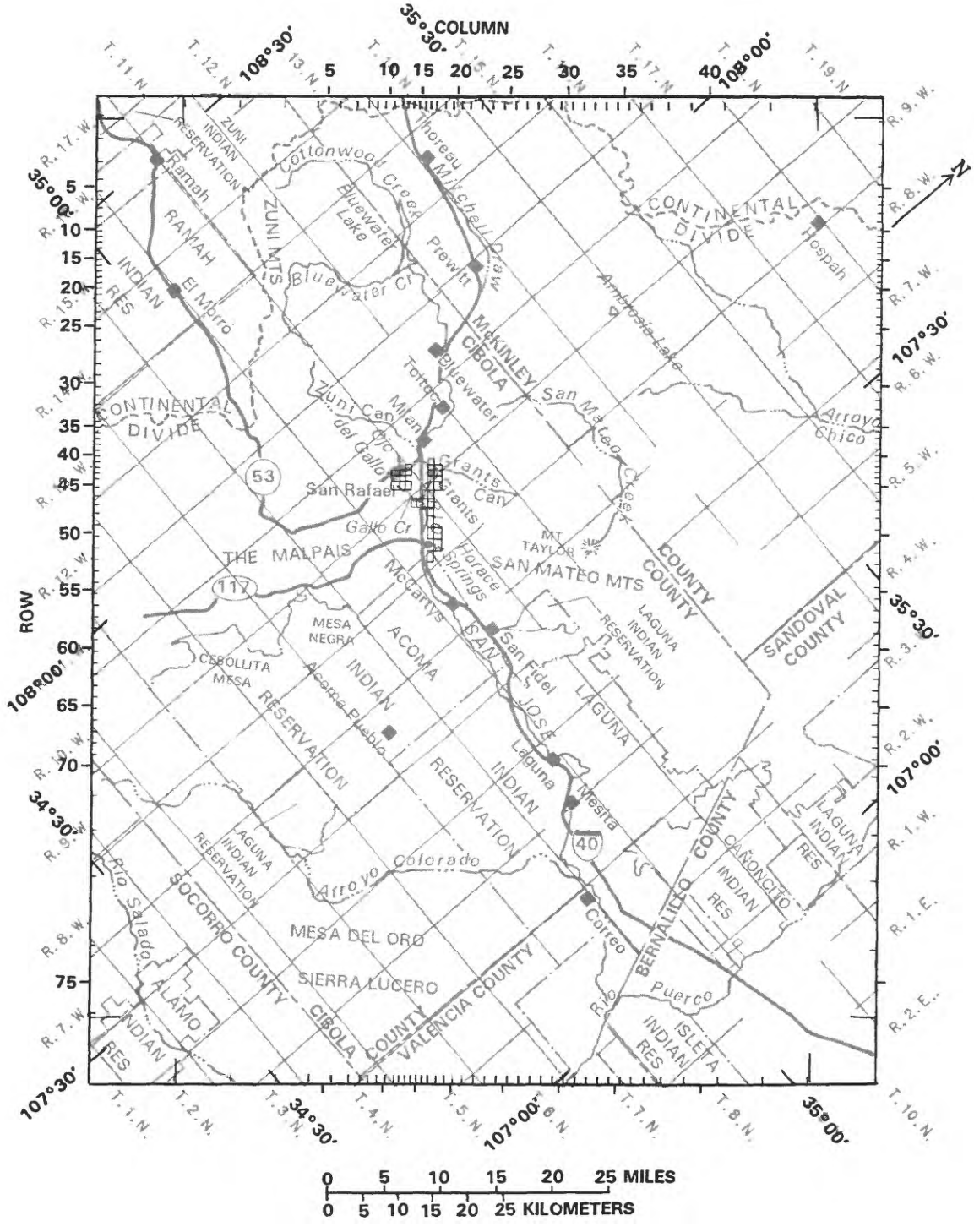

Figure 28.--Location of evapotranspiration represented in layer 1 under steady-state conditions.

The evapotranspiration boundary was used to check for an excessively high model-derived water-table altitude. That is, an evapotranspiration boundary was specified for an area more extensive than the area where evapotranspiration was considered likely to occur. Then the location of model-derived evapotranspiration was monitored to ensure that the area did not become excessive.

Streams

Stream-type boundaries simulated streams and similar natural boundaries. Bluewater Creek, Cottonwood Creek, Gallo Creek, and the Rio San Jose were represented as stream boundaries (fig. 29). Horace Springs was simulated as part of the Rio San Jose. Bluewater Lake was simulated as part of Cottonwood Creek, and Ojo del Gallo and the swampy part of La Vega (the meadow) were simulated as part of Gallo Creek.

The river package as modified by Miller (1988) provides an accounting of streamflow and routing that divides the stream into reaches. (A "reach" in Miller's (1988) usage may include several model blocks.) Miller's (1988) modification allows the simulation of intermittent streams and reporting of the remaining flow in a stream block after the simulated interaction with ground water. Required specifications are: (1) the routing destination of discharge from the reaches; (2) a specified inflow to the upstream end of each reach (which may be zero); (3) the altitude of the stream at each stream block; (4) the conductance of the streambed at each stream block; and (5) the maximum rate of ground-water recharge at each stream block. Conductance was approximated as the hydraulic conductivity divided by the saturated thickness times the area of the stream bottom in each stream block. Simulated stream characteristics are listed in tables 18 and 19 of Supplemental Information. Characteristics that were held constant are shown in table 18 and those that were changed with time are shown in table 19. Many of the values in tables 18 and 19 are estimates and values assigned during model adjustment. The estimates were made not because data are available to verify them, but because they are required input for the stream boundary of the model. The following discussion explains what was done; these methods however, are not a real substitute for data. The reader is advised not to use these estimates for any other purpose.

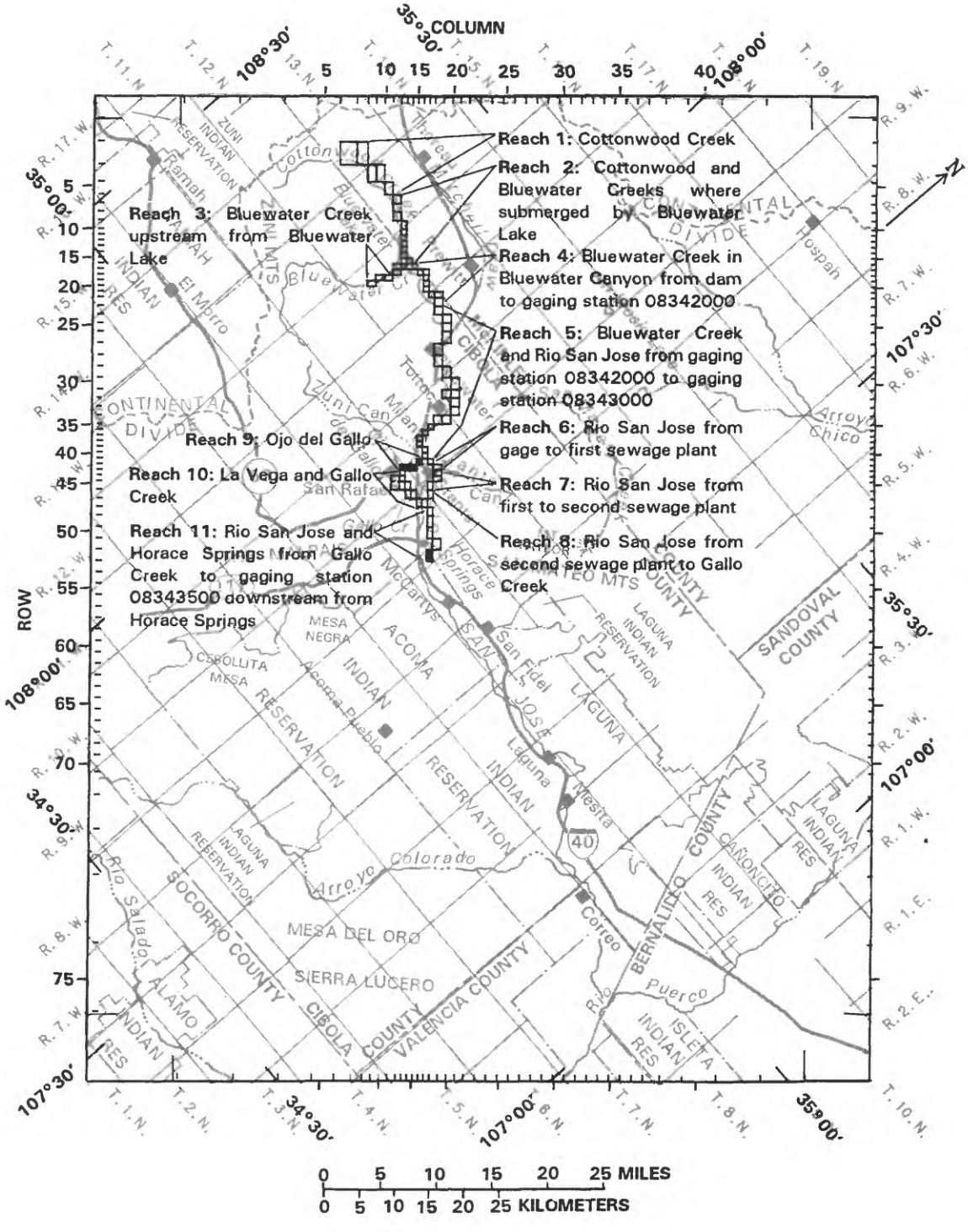

Figure 29.--Location of simulated streams and springs.

Definition of reaches and routing

Reaches (fig. 29) are numbered in downstream order starting with Cottonwood Creek and ending with the part of the Rio San Jose downstream from Gallo Creek that includes Horace Springs. Table 5 gives a brief description of each reach.

Table 5.--Description of simulated stream reaches

Reach	Description
1	Cottonwood Creek from where it crosses the outcrop of the San Andres-Glorieta aquifer to the west end of Bluewater Lake.
2	Cottonwood Creek and Bluewater Creek where submerged by Bluewater Lake.
3	Bluewater Creek from where it crosses the outcrop of the San Andres-Glorieta aquifer to the south end of Bluewater Lake.
4	Bluewater Creek through Bluewater Canyon from Bluewater Dam to gaging station 08342000 at the mouth of Bluewater Canyon.
5	Bluewater Creek and Rio San Jose from gaging station 08342000 to gaging station 08343000 at Grants.
6	Rio San Jose from gaging 08343000 to the first Grants sewage-plant site.
7	Rio San Jose from the first Grants sewage-plant site to the second Grants sewage-plant site.
8	Rio San Jose from the second Grants sewage-plant site to the confluence of Gallo Creek.
9	Ojo del Gallo.
10	The swampy part of La Vega from Ojo del Gallo to Gallo Creek and Gallo Creek to the Rio San Jose.
11	Rio San Jose from Gallo Creek to gaging station 08343500 downstream from Horace Springs.

Outflows from the upstream reaches (reaches 1-4) of the stream system were not routed downstream in transient scenarios. Under steady-state conditions (pre-1900.0), a normal downstream routing order was used. For the historical scenario (1900.0-1986.0), streamflow was interrupted by Bluewater Dam for all but the first stress period (1900.0-1928.0). Also for the first stress period, normal downstream routing order was not used because the inflow to reach 5 was specified directly as the estimated streamflow minus irrigation diversions. During the null scenario, normal downstream routing order was not used because the estimated natural streamflow at the mouth of Bluewater Canyon was considered to be more reliable than the estimated inflows to reaches 1 and 3, which were entirely based on nonstandard methods such as estimated excess precipitation. Normal downstream routing order was used for outflows from reaches 5 through 10 under all conditions. Table 6 lists the routing for the steady-state, historical, and null scenarios.

Table 6.--Streamflow routing

[--, flow not routed downstream]

Streamflow reach	Streamflow reach to which streamflow was routed		
	Steady-state condition	Historical transient condition	Null transient condition
1	2	--	2
2	4	4	4
3	4	--	4
4	5	--	--
5	6	6	6
6	7	7	7
7	8	8	8
8	11	11	11
9	10	10	10
10	11	11	11
11	--	--	--

Inflows

Under steady-state conditions, inflows were specified for reaches 1 and 3 and routed downstream. Inflow to reach 1 was 3.9 cubic feet per second and inflow to reach 3 was 9.1 cubic feet per second (estimated average values).

For the historical scenario, inflows (table 19, in Supplemental Information) were specified for the upstream ends of reaches 1, 2, 3, 5, 7, and 8. Inflows to reaches 1 and 3 were estimated on the basis of excess precipitation as previously explained in the conceptual-model section. The inflow to reach 2 was specified as a round number (20 cubic feet per second) to simulate continuously wet streambed conditions and to make calculation of ground-water recharge and stream capture convenient.

Inflow to reach 5 (table 19) was estimated as the flow passing the mouth of Bluewater Canyon (gaging station 08342000) minus surface water applied to irrigated fields in the Bluewater-Toltec Irrigation District. For stress period 1 (October 1, 1899, through September 30, 1927), the specified inflow was 4.5 cubic feet per second (the estimated average of 11 cubic feet per second minus an estimated 6.49 cubic feet per second applied to irrigated fields). For stress periods 2-53 (through March 1972) inflow to reach 5 was the measured flow (U.S. Geological Survey annual data reports) minus the reported and estimated irrigation application (table 1). For stress periods 54-70 (through October 1985) inflow to reach 5 was estimated streamflow (Supplemental Information, table 11) minus estimated irrigation application.

Inflow to reach 7 included estimated effluent from the first Grants sewage-treatment plant (table 19) in addition to outflow from reach 6. The plant was in operation for about 10 years (1948-58) and the effluent was estimated as one-half of the ground-water withdrawals at Grants and Milan (table 2). The sewage plant was relocated in about 1958 to the second location downstream.

Inflow to reach 8 included estimated sewage-treatment-plant effluent from the second location since about 1958 (table 19) in addition to outflow from reach 7. Again the effluent was estimated as one-half of the ground-water withdrawals at Grants and Milan.

Stream altitudes

The stream altitude (table 18 in Supplemental Information) generally was assumed to be the streambed altitude estimated from topographic maps (U.S. Geological Survey, scale 1:24,000). The accuracy of the assigned altitude may be about plus or minus 10 feet. The altitude assigned to stream blocks in reach 2 was the higher of the streambed altitude or the surface altitude of Bluewater Lake. Streambed altitudes through the lake were estimated by linear interpolation. The lake-surface altitude for a given stress period (table 19, Supplemental Information) was an average of monthly values (U.S. Geological Survey annual data reports) for the stress period. Prior to 1928 and in the null scenario, the lake-surface altitude was set to the streambed altitude of the lowest block in reach 2, thus forcing the assigned altitude to be the streambed altitude. The altitude for blocks in reach 9, representing Ojo del Gallo, was set to 6,453 and 6,452 feet, approximately the water-table altitude in the San Andres-Glorieta aquifer near Ojo del Gallo.

Streambed conductances

Streambed conductances were estimated for each stream block as the area of streambed in the block times the vertical hydraulic conductivity of the streambed divided by the thickness of the streambed. As discussed in the conceptual-model section, measurements of these characteristics generally were not made. The purpose of estimating conductances from approximate streambed characteristics is to show that the conductances are plausible in view of the discussion of streambed conditions in the conceptual-model section. Streambed characteristics listed in tables 18 and 19 should not be used for any other purpose.

The streambed length in each stream block (table 18) was approximately estimated to the nearest 0.25 mile and was often equal to the length of the block. The assigned lengths varied from 0.25 to 1.5 miles (1,320 to 7,920 feet).

The streambed width generally was assumed to be 20 feet (reaches 1, 3, 6, 7, 8, and 11; and parts of reaches 5 and 10) or 40 feet (parts of reaches 4, 5, and 10). Although streambed widths may vary from zero under no-flow conditions to possibly several hundred feet under flood conditions, 20 to 40 feet might be a reasonable approximation for low-flow conditions on the basis of casual observations. The 40-foot streambed width of reach 4 and the upper part of reach 5 was based on measurements when the discharge was about 4 cubic feet per second.

The streambed width of reach 2, representing parts of Cottonwood and Bluewater Creeks flooded by Bluewater Lake, was estimated on the basis of stream or lake altitude. The minimum width (20 feet) for a given stream block was assigned when the stream altitude was the same as the streambed altitude, and the maximum width (table 18) was assigned when the stream altitude was the maximum lake-surface altitude of 7,407 feet (U.S. Geological Survey topographic maps for Prewitt and Pine Canyon, N. Mex.). The widths were interpolated linearly between the minimum and maximum when the lake-surface altitude was between the streambed altitude and 7,407 feet.

The streambed width of the upper part of reach 4, where seepage from Bluewater Lake occurs, was estimated on the basis of lake altitude. The minimum width (40 feet) was assigned when the lake altitude was the streambed altitude, and the maximum width (200 feet) was assigned when the lake altitude was 7,407 feet. The widths were interpolated linearly between the minimum and maximum when the lake-surface altitude was between the streambed altitude and 7,407 feet.

The streambed width of reach 9, representing Ojo del Gallo, was arbitrarily assigned a value of 1 foot. The conductance for reach 9 was set to 1.5 cubic feet per second per foot of difference between the model-derived water-table altitude and the assigned "stream" altitude assigned to reach 9. The streambed width of 1 foot was a convenient value assigned so that the combination of assigned values for length, width, thickness, and hydraulic conductivity would yield a conductance of 1.5 feet squared per second.

The upper part of reach 10 represented the swampy part of La Vega. The streambed width was assumed to be 200 feet, narrowing to 20 feet on the downstream end.

Streambed thicknesses were assumed on the basis of water-table altitudes and streambed conditions. Thicknesses generally were assumed to be the difference between the streambed altitude and the approximate water-table altitude or 5 feet where the water-table altitude is near or above the streambed altitude. Thicknesses of as much as 200 feet assigned to the lower part of reach 1 and as much as 150 feet assigned to the upper part of reach 2 were based on the estimated thickness of Chinle Formation confining bed between the streambed and the San Andres-Glorieta aquifer. Thicknesses as little as 1 foot were assigned to the lower end of reach 2 representing places where Bluewater Lake is directly over San Andres Limestone. Thicknesses of as much as 48 feet were assigned to reach 5 representing places between the mouth of Bluewater Canyon and Toltec where the water table is deep in the valley fill or below the valley fill in the San Andres-Glorieta aquifer. The thickness of 1 foot assigned to reach 9, representing Ojo del Gallo, was an arbitrary value, as was the streambed width, used to derive the previously determined conductance value of 1.5 feet squared per second. An accurate thickness is not critical because other factors of streambed conductance, streambed hydraulic conductivity, and width are not precisely known.

Streambed hydraulic conductivity generally was assigned a value of 8×10^{-7} feet per second. This value and two other values, 8×10^{-6} feet per second assigned to the upper part of reach 4 and 1.2×10^{-6} feet per second assigned to the upper part of reach 5, were derived during model adjustment. A conductivity of 1×10^{-11} was assigned to the lower part of reach 1 and the upper part of reach 2 to represent the Chinle Formation confining bed that intervenes between the streambed and the San Andres-Glorieta aquifer. Conductivities assigned to reach 9, representing Ojo del Gallo, and the lower part of reach 11, representing Horace Springs, were arbitrarily assigned to derive previously determined conductances. As already discussed, the conductance determined for reach 9 was 1.5 feet squared per second (cubic-foot discharge per foot of difference between the model-derived aquifer head and the specified streambed altitude). The conductance for Horace Springs was assumed to be about 2 feet squared per second.

Maximum rate of ground-water recharge

The maximum rate of ground-water recharge from each stream block was assigned a value of 0, 2, or 4 cubic feet per second. The limits of 2 and 4 cubic feet per second generally were large enough to not restrict the flow rate from the stream to ground water. The maximum rate of 0 cubic feet per second was assigned to selected blocks of reach 4 to prevent simulated flow from the stream to the aquifer in places where the streambed is on rocks underlying and less permeable than the San Andres-Glorieta aquifer.

Ground-Water Inflow and Outflow

Ground-water inflow was simulated as underflow in the valley fill of Mitchell Draw, San Mateo Creek, and Grants Canyon (fig. 30). Outflow was simulated as underflow from the valley-fill aquifer at Horace Springs, and as outflow to the Rio Grande rift along the eastern boundary of the study area. Specified-flow and general-head boundaries were used.

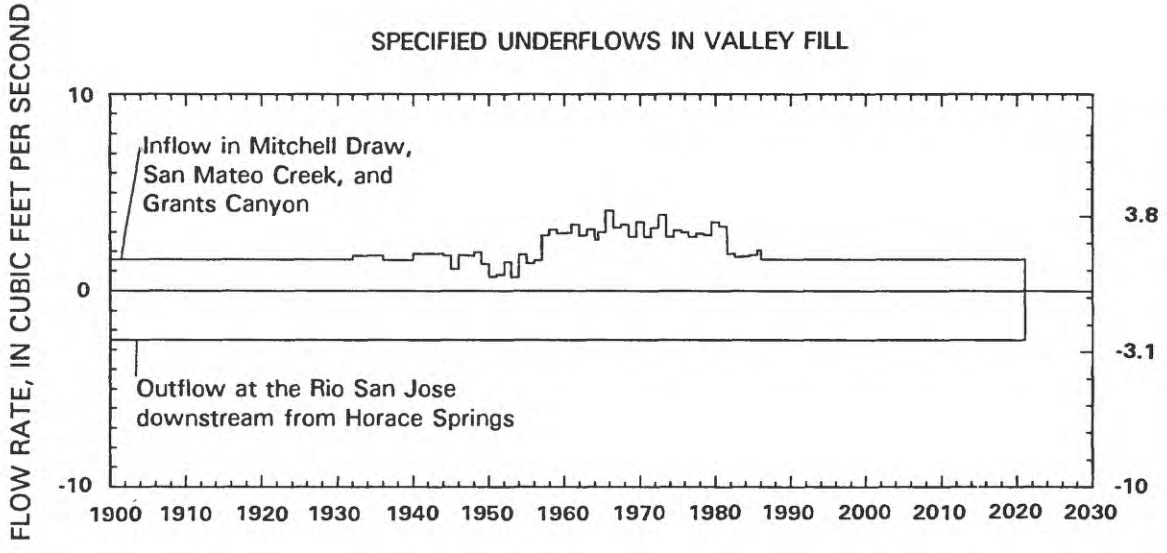

Figure 30.--Specified underflows in valley fill of Mitchell Draw, San Mateo Creek, Grants Canyon, and the Rio San Jose at Horace Springs.

Inflow at Mitchell Draw, San Mateo Creek, and Grants Canyon

Ground-water underflow into the modeled area in Mitchell Draw, San Mateo Creek, and Grants Canyon (locations shown in fig. 25) were simulated with specified-head boundaries in early steady-state simulations; in later steady-state simulations underflows were simulated with specified-flow boundaries. The flows were the same as those derived by the earlier simulations using specified heads. In Mitchell Draw, hydraulic heads specified in earlier simulations were based on measured heads in wells completed in the Chinle Formation because no head data are available for alluvial wells. In San Mateo Creek and Grants Canyon, hydraulic heads specified in the earlier simulations were based on measured heads in the alluvium.

In transient simulations, specified flows simulating natural underflows varied on the basis of rainfall at Grants. That is, specified flows for each stress period were equal to the steady-state flow multiplied by the precipitation at Grants during that period and divided by the average precipitation at Grants.

Additional underflow in San Mateo Creek probably resulted from uranium-mine discharges between the mid-1950's and the early 1980's. An additional flow of 1.5 cubic feet per second during stress periods 31-63 was specified to simulate the effects of uranium-mine discharges. This additional underflow was determined by trial and error, keeping hydraulic heads from becoming unreasonably high or low, as explained under Model Adjustments. The 1.5-cubic-foot-per-second value is not to be interpreted as a reliable estimate of uranium-mine discharges.

If hydraulic heads at these boundaries were to become unreasonably high or low, the designation as specified-flow boundaries would need to be reevaluated. This condition did not develop for simulations described in this report.

Outflow at Horace Springs and the eastern boundary

Ground-water underflow out of the model in the valley-fill aquifer at Horace Springs was simulated as a specified flow of 2.5 cubic feet per second (table 20, Supplemental Information; and fig. 30). This value compares with that reported in the conceptual-model section. Because underflow depends on hydraulic heads and valley-fill aquifer characteristics, neither of which was expected to change much with time, this underflow was assumed to be constant for the entire period of simulation.

A general-head boundary (fig. 26) was used to represent a hydraulic connection between the San Andres-Glorieta aquifer and the basin-fill aquifer in the Rio Grande rift and springs that issue from Pennsylvanian rocks. Although the mechanism by which discharge to the east occurs is unknown, the potentiometric surface (fig. 9) seems to indicate a generally discharging boundary to the east. Because there is no limiting value to bound the flow calculated by the general-head boundary, care needs to be exercised to ensure that unrealistic flows into or out of the system are not simulated. Flow at this boundary, almost a constant 4 cubic feet per second, was monitored during simulations discussed in this report.

The following discussion attempts to relate the boundary to possible values of hydraulic head, hydraulic conductivity, distances, and thicknesses; but does not describe a known flow system. Because of the speculative nature of this mechanism, the discussion is not included in the conceptual-model section. The block faces through which the flux to the general-head boundary was simulated are shown in figure 26. A general-head boundary (McDonald and Harbaugh, 1988, chap. 11, p. 1) requires specified hydraulic heads for the sink area and hydraulic conductance for the material separating the model block from the sink area. The flow is calculated as the hydraulic conductance multiplied by the difference of specified head of the sink minus model-derived head in the aquifer. For model columns 25-43, the specified-head part of the general-head boundary (table 21 in Supplemental Information) was approximated from hydraulic heads measured in wells drilled in the Rio Grande rift area (heads 5,100 to 5,900 feet above sea level). For model columns 1-24, specified head was approximated from altitudes of springs discharging from Pennsylvanian rocks (heads 5,400 and 5,950 feet above sea level).

The hydraulic conductance for each general-head-boundary model block (table 21, Supplemental Information) was estimated as an area approximately perpendicular to the flow field multiplied by hydraulic conductivity divided by distance. (The adjustment for angle of incidence was not significant in view of the speculated values of hydraulic conductivity; however, accounting for angle of incidence provided a convenient way to allow for treating blocks with two sides facing the general-head boundary along with other blocks with one side facing the boundary.) For blocks in columns 25-43, the area was estimated as the block width times the sine of the angle (either approximately 41 degrees for block faces parallel to columns or 49 degrees for block faces parallel to rows) between the face of the block and the easterly direction of flow, times the thickness of the geologic units through which the flow was assumed to occur. For most of the boundary, the effective thickness was assumed to be approximately 2,500 feet representing rocks that might range from Pennsylvanian to Cretaceous age in the Rio Puerco fault belt. The hydraulic conductivity was assumed to be 6×10^{-7} feet per second (about 0.05 foot per day), and the distance was assumed to be 20 miles, approximately the distance across the Rio Puerco fault zone. For the part of the boundary in model columns 11-24, the thickness was assumed to be 500 feet, which corresponds to the thickness of the Pennsylvanian Madera Limestone, although flow may occur in other Permian and Pennsylvanian units; the hydraulic conductivity was assumed to be 4×10^{-6} feet per second (about 0.35 foot per day); and the distance was assumed to be 10 miles, approximately the distance to springs east of Sierra Lucero. The hydraulic conductance for blocks in columns 5-10 was estimated in the same way as for those in columns 11-24 except that the distance was assumed to be 5 miles, approximately the distance to other springs east of Sierra Lucero that are closer along this part of the model boundary. Hydraulic conductance for blocks in columns 1-4 was estimated the same way except that the distance was assumed to be 20 miles, which is approximately the distance to a big spring in the Rio Salado. No angle correction was made for blocks 1-4 because flow to the big spring would be subparallel to the model column, and no flow was assumed for the northeast side of the model block at row 76, column 4.

No-Flow Boundaries

External no-flow boundaries were simulated wherever other boundaries were not specified around the perimeter of the model and where model blocks were inactive. Horizontal no-flow boundaries were simulated below the San Andres-Glorieta aquifer (layer 2) everywhere and above the San Andres-Glorieta aquifer where the aquifer is separated from valley-fill or other aquifers by the full thickness of the Chinle confining bed in the northern and eastern parts of the model where layer 1 is inactive.

No-flow boundaries on layer 1 generally define the extent of the valley-fill aquifer (figs. 5 and 25). The no-flow boundaries do not define the full extent of valley fill in Mitchell Draw, San Mateo Creek, Grants Canyon, and the Rio San Jose at Horace Springs where underflow is simulated by specified-flow boundaries; nor in the southwestern part of The Malpais where the no-flow boundary is arbitrary. Along column 1, rows 46-52, the arbitrary no-flow boundary is defined by the extent of the model grid. In that vicinity, the saturated thickness of the valley fill probably is very small because stock wells produce from bedrock. Similarly, along row 46, columns 1-3, the arbitrary no-flow boundary is in an area where the saturated thickness is very small. Also, the San Andres-Glorieta aquifer was not simulated in much of this area west of the inferred fault of Thaden and Zech (1984). Because the main purpose of simulating the valley fill was to simulate a boundary on the San Andres-Glorieta aquifer, there was little reason to simulate valley fill where the San Andres-Glorieta aquifer was not simulated. These arbitrary boundaries in layer 1 are distant from any pumping centers.

In layer 2, the no-flow condition simulated along row 1, columns 40-43, and along column 43, rows 1-29 (fig. 26) approximates the pinch-out of the San Andres-Glorieta aquifer that crosses the northern corner of the modeled area. In that corner of the model, the direction of flow (assumed perpendicular to potentiometric-surface contours shown in fig. 9) turns from northeastward to eastward.

The no-flow boundaries in layer 2 along row 1, columns 5-39, on the northwest side of the model, and along column 1, rows 52-76, on the southwest side of the model, are arbitrary. The arbitrary boundary along row 1 was distant from the main historical pumping centers and subparallel to flow lines on the basis of potentiometric-surface contours (fig. 9). At the arbitrary no-flow boundary along column 1, where the zone of large transmissivity values (50,000 feet squared per day) abutted the boundary, it was anticipated that drawdowns would be projected at the boundary. Normally in this case, the model would be extended; however, the characteristics of the San Andres-Glorieta aquifer are unknown to the south, and the nature of any boundary in that direction is speculative. Extending the zone of large transmissivity to a more distant arbitrary boundary would result in nearly the same drawdown at the more distant boundary. Extending the model with a small-transmissivity (200-400 feet squared per day) zone would be as arbitrary as not extending the model. Therefore, the model boundary in the vicinity of row 1, columns 52-76 was arbitrarily placed and this problem was addressed in the sensitivity tests.

Three faults, where the offset is greater than the thickness of the San Andres-Glorieta aquifer, were simulated as no-flow boundaries (inactive zones, fig. 26). These faults are marked in figure 2 as Big Draw fault, San Rafael fault, and inferred fault of Thaden and Zech (1984). Flow around the ends of these no-flow boundaries generally was simulated and is discussed in a following section, Model Adjustments. The inferred fault constitutes part of the exterior boundary of the simulated system except near the northern end of the fault. Between the northern end of the fault and the southeastern end of the Zuni uplift (simulated as a recharge boundary) is an arbitrary no-flow boundary. This no-flow boundary excludes most of the flow system west of the inferred fault (fig. 9). However, the no-flow boundary was positioned to include part of the area west of the inferred fault where the valley fill directly overlies the San Andres-Glorieta aquifer (fig. 6), and a direct hydraulic connection was simulated.

Ground-Water Withdrawals and Artificial Recharge

Simulated ground-water withdrawals represent water pumped for irrigation, industrial, and municipal uses. Water pumped for stock and individual domestic uses was assumed to be insignificant. Artificial recharge results from irrigation, uranium processing, and domestic discharges where no municipal sewage system is used.

Irrigation Ground-Water Withdrawals and Recharge

Irrigation was simulated for the Bluewater-Toltec, south San Rafael, and Ojo del Gallo irrigated areas. Ground-water withdrawals were simulated uniformly over the Bluewater-Toltec irrigated area (figs. 2 and 31). In that area, discharge from the San Andres-Glorieta and recharge to the valley fill were simulated. The withdrawals shown in figure 32 are stress-period averages of the values shown in figure 17, and recharge is one-third the total quantity of water applied to fields, including surface water. Block-by-block locations and rates of withdrawal and recharge are shown in table 22 of Supplemental Information. In figure 32 and table 22, discharges are shown as negative values and recharges are shown as positive values. South San Rafael withdrawals from the San Andres-Glorieta aquifer and recharge to the valley fill were simulated, and these values are shown in figure 33 and table 22. In table 22, when half-water-year stress periods were used, the summer rates are double the annual rates and the winter rates are zero.

Ground-water withdrawal was specified for layer 1 in the Ojo del Gallo irrigated area to simulate the diversion of surface water because the model program (Miller, 1988) does not provide for the direct specification of surface-water diversions. As previously discussed, the only difference between surface- and ground-water withdrawals in the Ojo del Gallo area is the point of diversion. Because both withdrawal and recharge would affect the valley-fill aquifer (layer 1), the net withdrawal was simulated, which is the estimated evapotranspiration from irrigated acreage. Accordingly, the simulated ground-water withdrawal was 2,500 acre-feet per year for 1900-47 (3.45 cubic feet per second for stress periods 1-5, and 6.9 cubic feet per second for half-water-year stress periods 7, 9, 11, and 13), 1,300 acre-feet per year for 1948-50 (3.49 cubic feet per second for stress periods 15, 17, and 19), and zero thereafter.

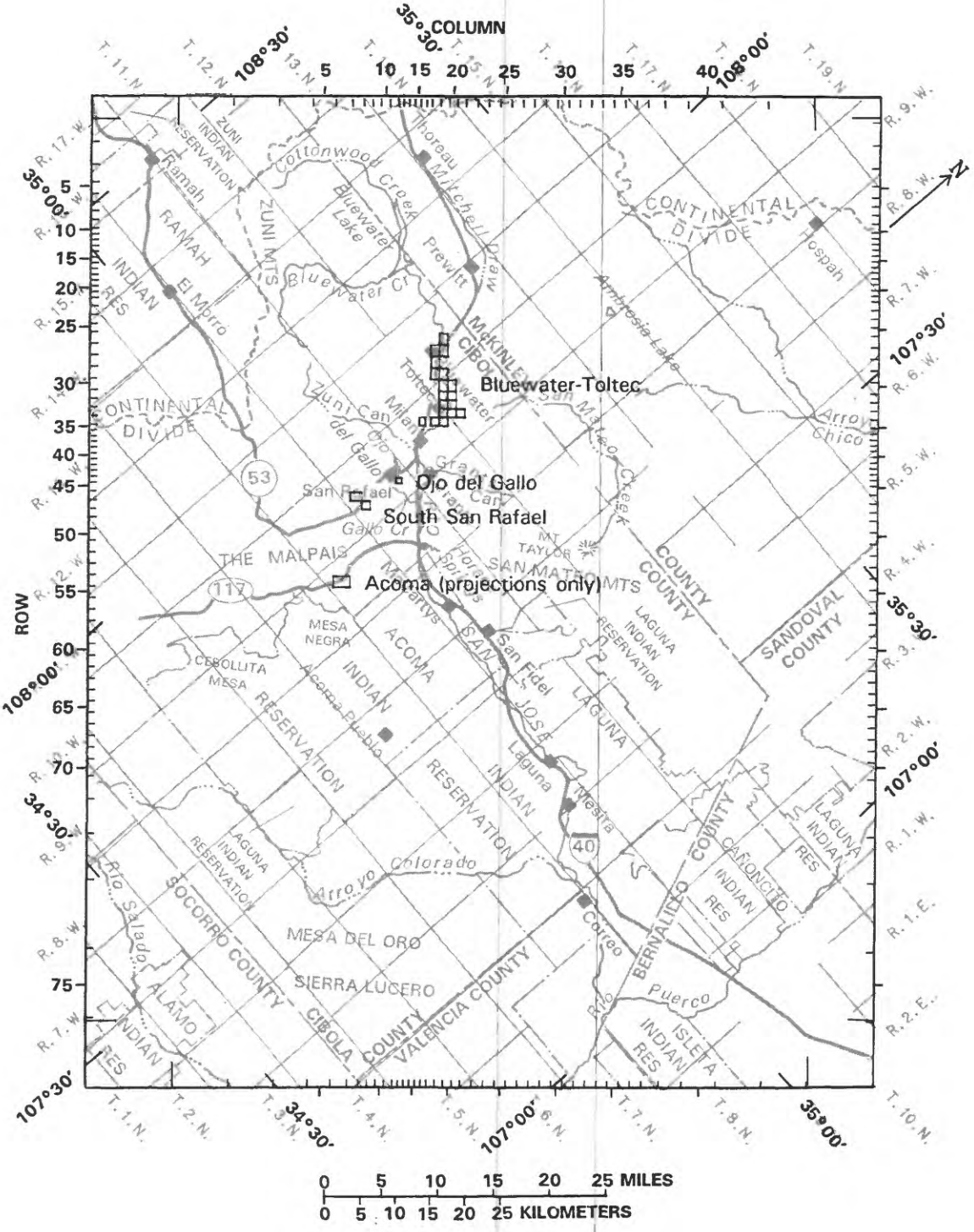

Figure 31.--Locations of simulated irrigation.

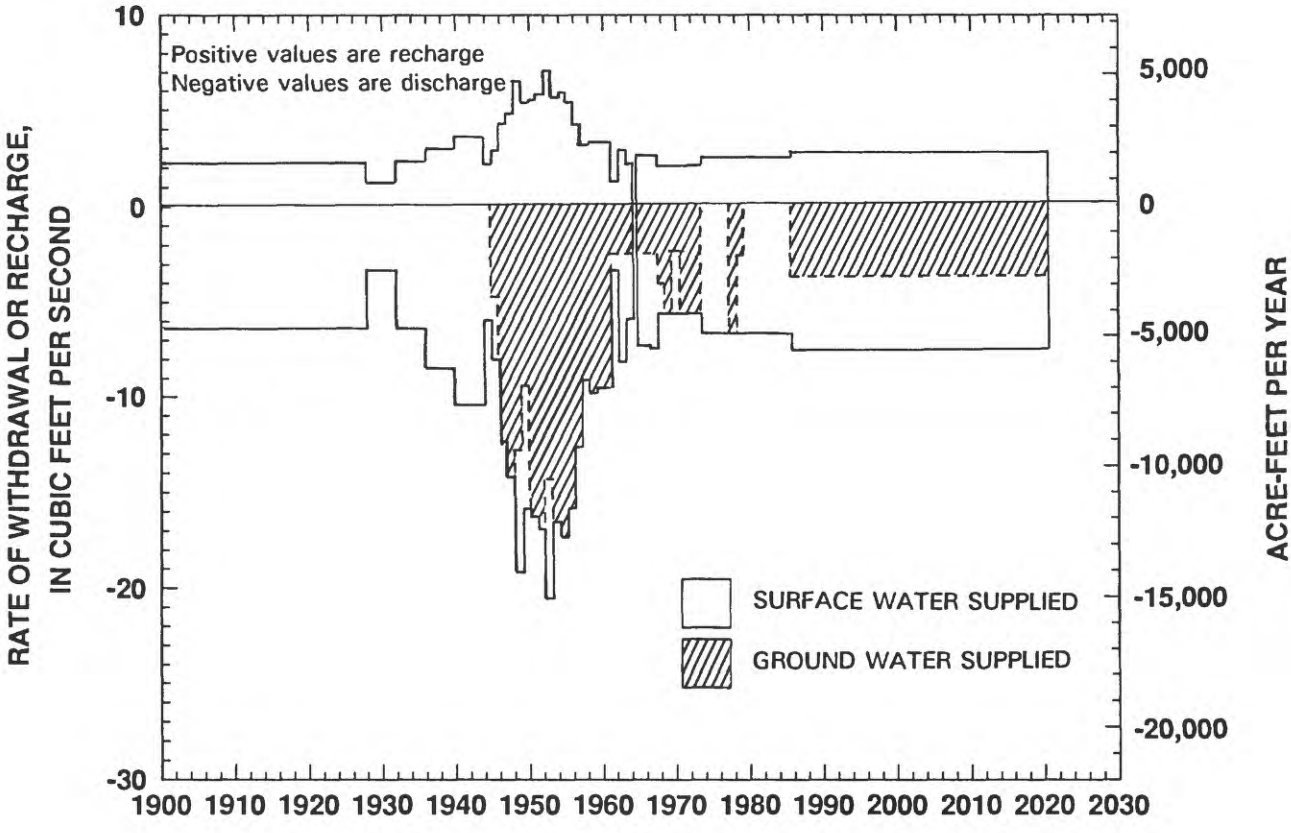

Figure 32.--Specified withdrawal and recharge in the Bluewater-Toltec Irrigation District.

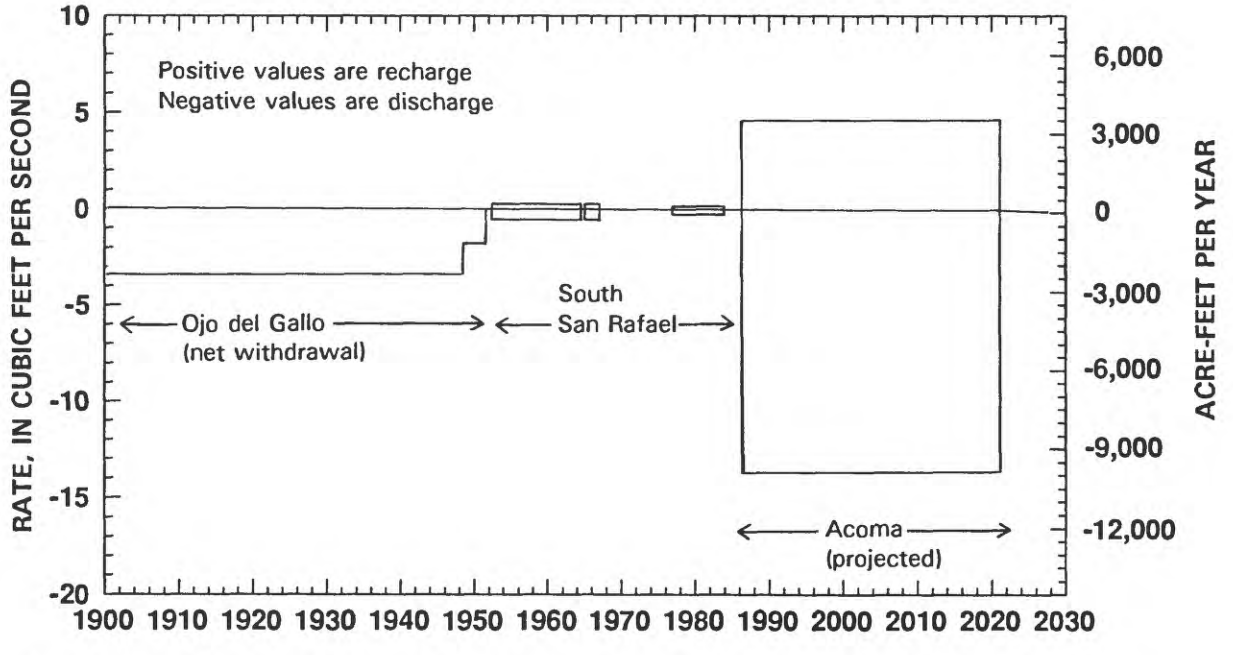

Figure 33.--Specified net withdrawal in the Ojo del Gallo irrigated area and ground-water withdrawal and recharge in the south San Rafael and Acoma irrigated areas.

Municipal and Industrial Ground-Water Withdrawals and Recharge

Previously estimated and reported municipal and industrial ground-water withdrawals (conceptual-model section) were simulated. Locations are shown in figure 17. Total simulated withdrawals for municipal and industrial use are shown in figure 34. Most simulated withdrawals were from the San Andres-Glorieta aquifer. Block-by-block values are listed in table 23 in Supplemental Information.

Previously estimated and reported ground-water recharge (conceptual-model section) was simulated in the same location as the withdrawal except that recharge was always applied to the valley-fill aquifer. Total simulated ground-water recharge of municipal and industrial water from septic drain fields and uranium mill-tailings piles is shown in figure 34.

Model Adjustments

Simulated aquifer characteristics and boundaries were adjusted to make the model-derived hydraulic heads and flows match measured values reasonably well while keeping the simulated values of aquifer characteristics and boundary conditions plausible. The plausibility of these features is based on geologic, hydrologic, and water-quality information given in the conceptual-model section and in Baldwin and Anderholm (in press). The model characteristics described in the previous sections are those of the adjusted model. Because municipal and industrial ground-water withdrawals are mainly reported values, simulated withdrawals were assumed to be correct and were not subject to change during model adjustment.

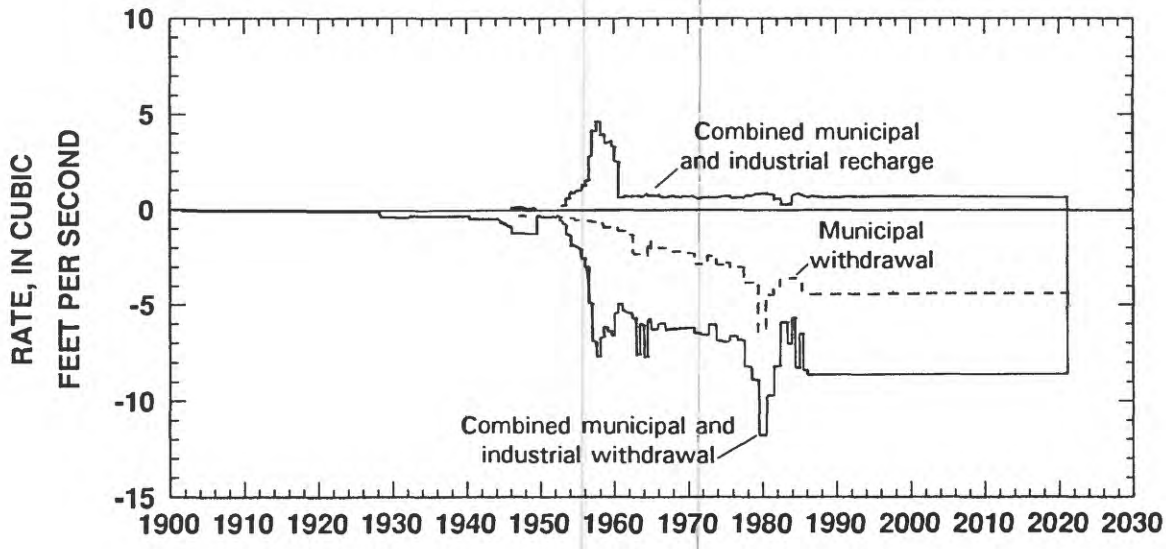

Figure 34.--Specified municipal and industrial ground-water withdrawal and recharge.

Comparison of Model-Derived Values with Measured or Reported Values

Model-derived values were compared with measured hydraulic heads, springflows at Ojo del Gallo, and streamflow downstream from Horace Springs. Streamflows in Bluewater Creek at the mouth of Bluewater Canyon (gaging station 08342000) were not used for comparison because measured values were used to calculate and specify inflow to river reach 5 (fig. 29). Streamflows in the Rio San Jose at Grants (gaging station 08343000) were not used for comparison because they mainly reflect local storms, which were not accounted for in this model.

Hydraulic heads

Measured hydraulic heads for selected wells at selected times were compared with model-derived hydraulic heads. The selection of times (mostly half-year periods) during which a large number of water levels had been measured yielded a wide spatial distribution of measurements. A nearly continuous time distribution of measurements was achieved by selection of a few wells where a long record of annual or semiannual measurements exists. Wells in the Bluewater, Toltec, Milan, and San Rafael areas were selected on the basis of their representation of the area around them and on a relatively long history of water-level measurements. Wells in other parts of the study area (north of Prewitt or east of The Malpais) were selected if the water level had been measured during one of the selected times.

To limit the amount of model output and still include a large percentage of existing hydraulic-head measurements, a limited number of half-year periods were selected. Those selected were the winters of water years 1946, 1956, and 1979, and the summer of 1985. To include more hydraulic-head measurements for the San Andres-Glorieta aquifer in the northern area (northwest of Prewitt), hydraulic heads measured during summer 1984 were compared with model-derived hydraulic heads for September 30, 1984 (1985.0).

To include more hydraulic-head measurements for areas where not many measurements had been made, the duration of time periods of measurement was lengthened from a half-year to several years. For the valley fill, hydraulic heads measured from winter 1956 to winter 1960 were compared with model-derived heads for winter 1958 (1958.5). Hydraulic heads for the valley fill measured during the 1980's were compared with model-derived hydraulic heads for March 31, 1985 (water year 1985.5).

Comparisons with individual measurements and a statistical summary are shown in table 24. The comparison between individual measured and model-derived hydraulic heads was considered good if, due to errors in the datum at each well, minor local conditions, and possible measurement errors, the difference was less than 20 feet. Errors in the datum (land-surface altitude) at each well, as determined from topographic maps, may be as great as 10 feet. Differences of more than 20 feet probably are due to a lack of correspondence between the model and the hydrologic system. Differences northwest of Prewitt (all columns in rows 1-20, table 24) generally are greater than 20 feet. The steepness of the potentiometric surface may have made the 20-foot criterion

unrealistically small. Model node points generally do not fall on the locations of wells, and a slight shift in the location in an area of steep gradients can cause an apparently poor comparison; in addition, steep gradients usually occur in mountainous areas where geologic structure is often much more complex than would be practical to simulate. However, the preponderance of positive differences of model-derived minus measured values could indicate that specified values of recharge were too large, ground-water withdrawals were not large enough, transmissivity was not large enough, or that storage was too large. There may have been some uncontrolled flowing wells in the area that affected the measured heads.

Four statistics were calculated from the differences given in table 24. The mean and median differences indicate the overall comparison, but they tend to mask the largest differences. The root-mean-square difference tends to emphasize the largest differences. The mean absolute difference (mean of the absolute values of the differences) has neither drawback and was considered the primary statistic for judging the degree of adjustment of the model. Because the mean absolute difference cannot be expected to reach zero, model adjustment continued until further adjustments appeared not to yield substantial reduction.

A "scatter diagram" (fig. 35) of the heads in table 24 gives a visual representation of the differences and puts them in the perspective of the overall relief of the potentiometric surface; that is, even the largest differences are small by comparison to the range of measured hydraulic heads. Although the differences between measured and model-derived heads exceed the 20-foot criterion in 21 percent of the comparisons, the differences do not appear excessive in view of the overall scale.

An areawide view of model-derived and measured hydraulic heads for the 1980's is shown in figure 36 in which the model-derived heads are shown as a contoured potentiometric surface. Most measured heads in figure 36 are from the mid-1980's, but three are from previous years as shown. Measured hydraulic heads above 6,600 feet generally are not well matched by model-derived values, as can be seen in figure 35.

Hydrographs of measured hydraulic heads for certain wells were compared with hydrographs of model-derived heads as shown in the following six figures. The locations of hydrographs are shown in figure 19. The hydrographs allow a comparison of heads at selected sites over time. In the following figures, measured hydraulic heads are shown as points and model-derived heads are shown as solid lines. The lines representing the model-derived hydraulic heads are truly representative of only the values at the ends of stress periods. If the values at the ends of each time step had been plotted, the line would have been curved between the beginning and the end of each stress period. Although the only accurate representation would be points for both measured and model-derived hydrographs, the selection of lines for model-derived and symbols for measured heads presents a reasonably clear graph. Graphs start in 1920 because the end of the first transient stress period is 1928.0.

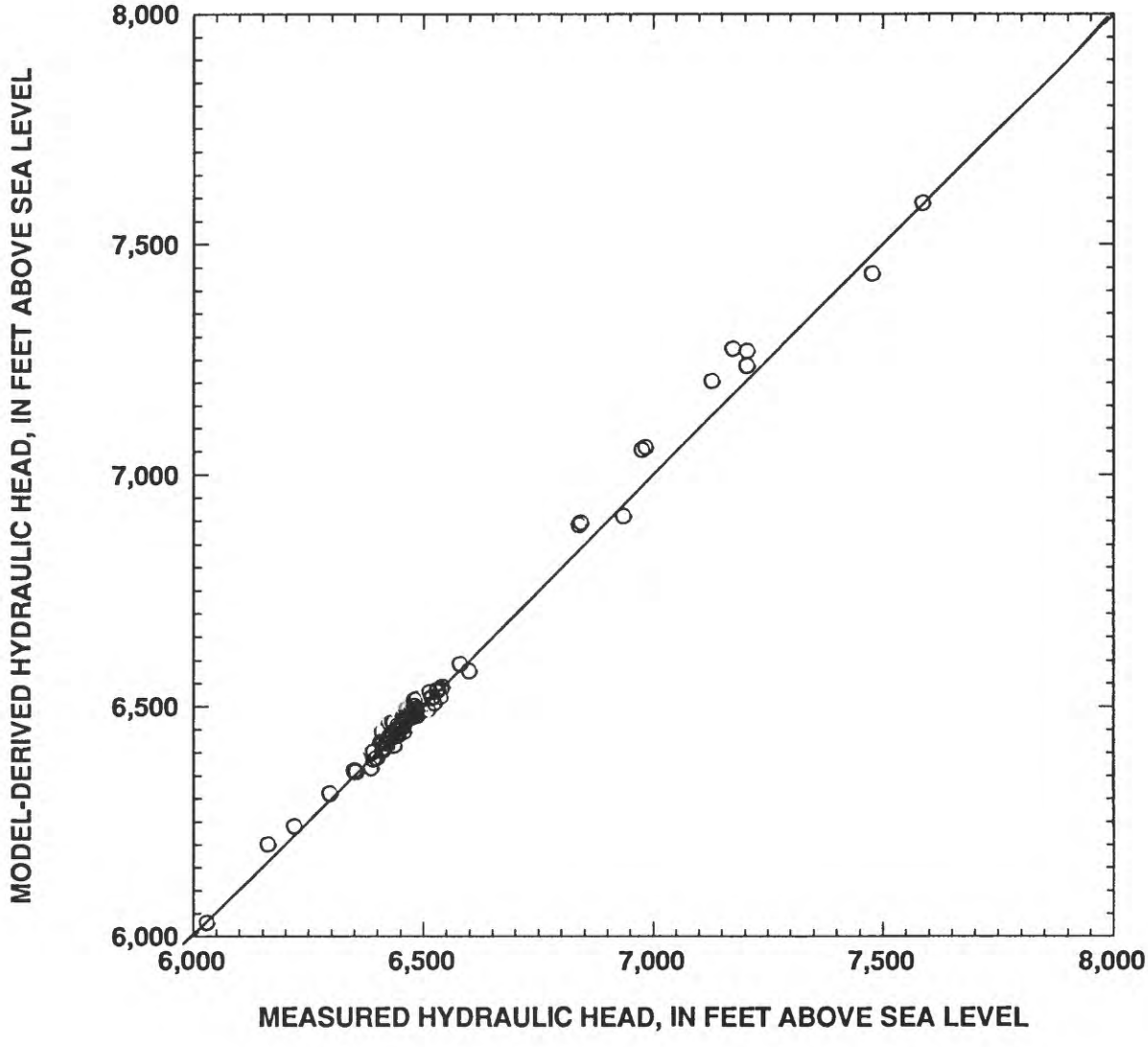

Figure 35.--Relation of model-derived and selected measured hydraulic heads.

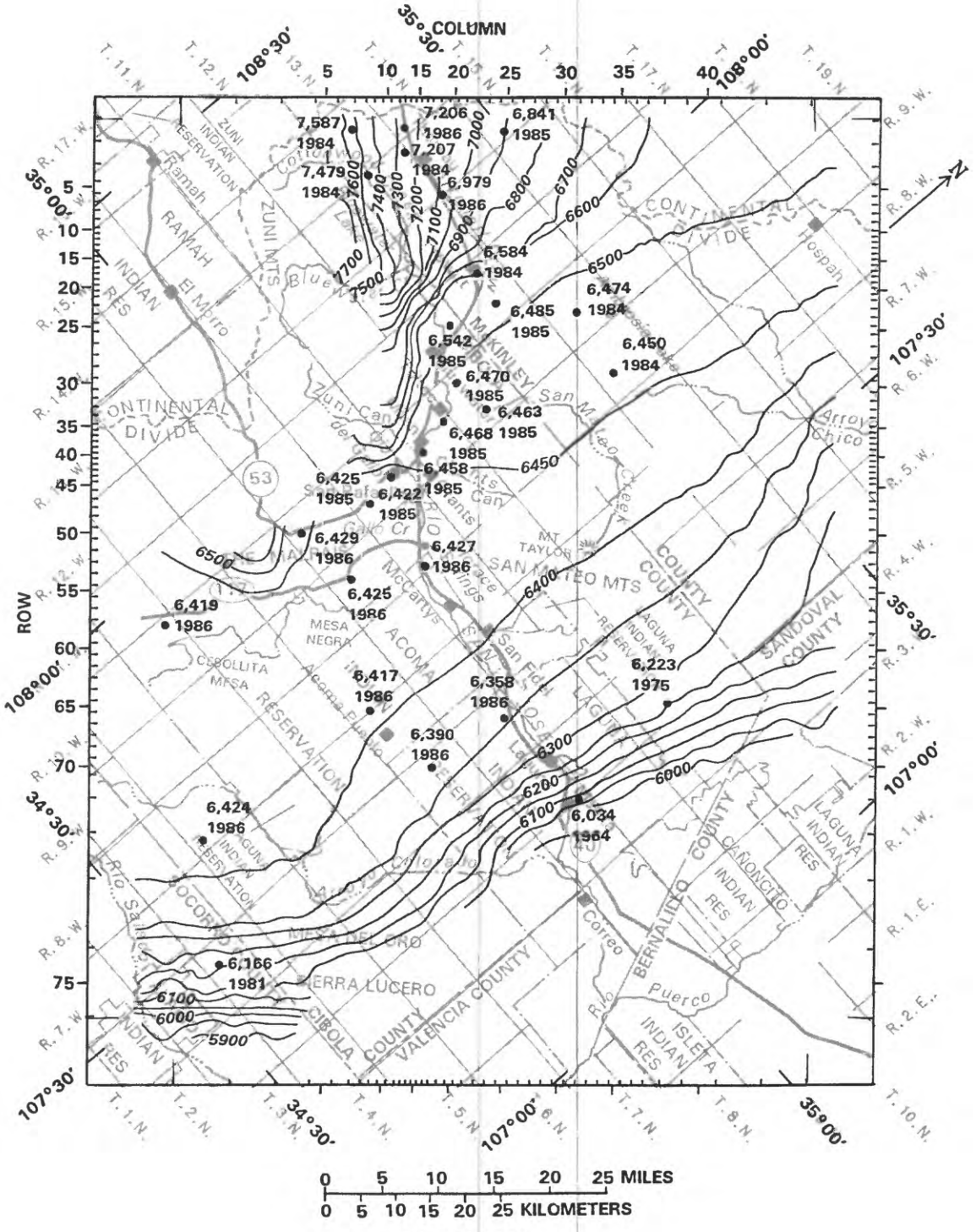

EXPLANATION

5900 — MODEL-DERIVED POTENTIOMETRIC CONTOUR--Shows model-derived altitude of potentiometric surface. Contour interval, in feet, is variable. Datum is sea level

6,166 / 1981 — WELL--Upper number is measured hydraulic head, in feet above sea level. Lower number is calendar year of measurement

Figure 36.--Model-derived 1986 potentiometric surface for layer 2 and selected measured hydraulic heads for the San Andres-Glorieta aquifer.

The comparison of measured and model-derived hydrographs was considered to be good if the shapes of the two hydrographs were similar. Model-derived seasonal fluctuations tend to be more uniform from one area to another than measured fluctuations. The reason for this may be that irrigation withdrawals in the Bluewater-Toltec Irrigation District were simulated as occurring evenly over the irrigated area. Because irrigation wells are in actuality not evenly distributed, it is very likely that more water was withdrawn from one than from another. Another reason for uneven seasonal fluctuations in the measured heads is that the amount of recovery after pumping was probably different for each measurement. However, model-derived seasonal fluctuations shown in the following six figures match measured fluctuations reasonably well overall.

As simulated transmissivity and storage values were adjusted, model-derived seasonal fluctuations depended primarily on simulated transmissivity in the vicinity of the hydrograph whereas long-term (1950's through 1980's) fluctuations depended more on simulated storage. For most hydrographs, the simulated specific yield had a greater effect on long-term fluctuations than did the artesian storage coefficient because most sites are located near the outcrop. The effect of the simulated artesian storage coefficient was relatively greater at distance from the outcrop.

Although long-term measured and model-derived fluctuations generally are similar in these figures, the most dissimilar fluctuations are those for layer 1, row 27, column 20 (fig. 37A). At this location, either the estimated seepage from the Anaconda tailings pile was not correct or local hydrologic characteristics were not well represented. Local hydrologic characteristics, such as the many faults and the extreme heterogeneity of the basaltic valley fill, were not the focus of this regional model. Measured and model-derived long-term fluctuations are more similar in other hydrographs. However, model-derived hydraulic heads for layer 2, row 25, column 19 near Bluewater (fig. 37B) were not as great as the measured heads after 1984. The relatively large fluctuations in figure 37B probably are caused by the close hydraulic connection to Bluewater Creek as well as a locally small storage coefficient.

Model-derived hydraulic heads near Toltec (fig. 38) tended to be greater than measured heads. Figure 38A shows measured and model-derived heads for the valley fill (layer 1). Model-derived heads compare well with measured values except for the late 1950's, early 1960's, and late 1970's when the measured values were approximately 6,453 feet (fig. 38A). This measured head (6,453 feet) may be in error because it results in a departure from the pattern of fluctuations in other hydrographs in this figure and in figure 37B. No attempt was made to simulate the flat parts of the hydrograph in figure 38A. The overall model-derived long-term (1950's through 1980's) drawdown and recovery are approximately the same as measured values indicating that simulated specific yield is approximately correct.

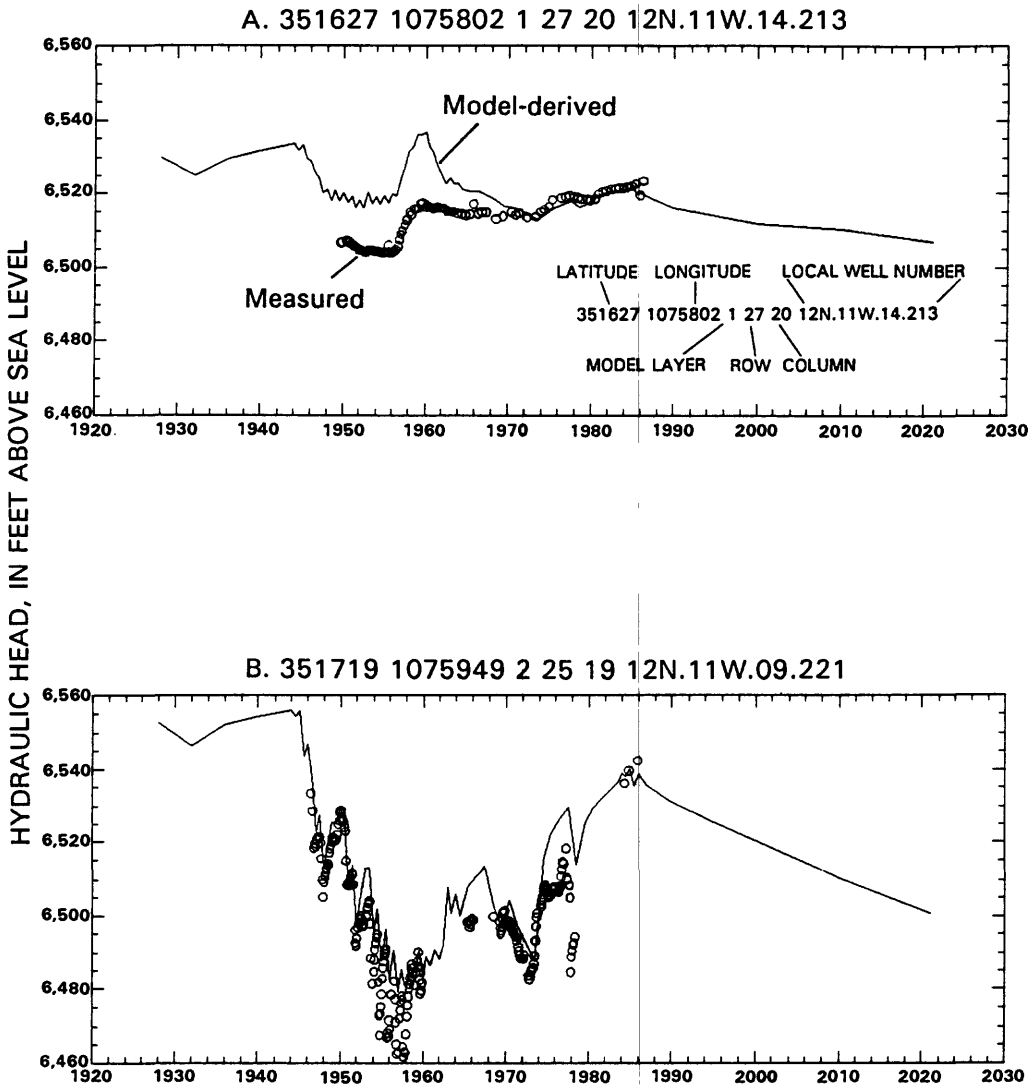

Figure 37.--Measured and model-derived hydraulic heads near Bluewater (locations shown in fig. 19).

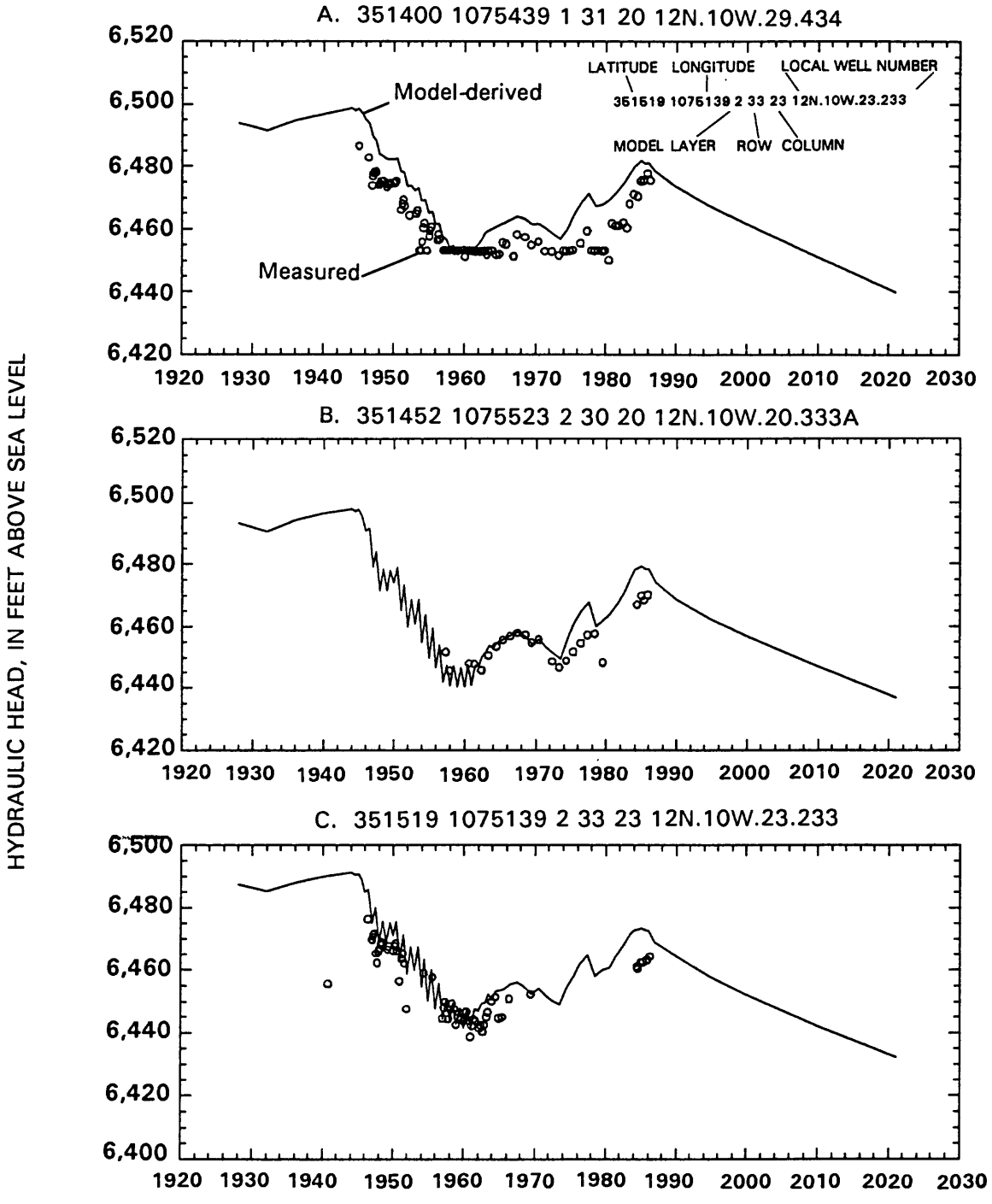

Figure 38.--Measured and model-derived hydraulic heads near Toltec (locations shown in fig. 19).

Measured hydraulic heads in graphs in figure 38B and C were used together to complete the drawdown limb (fig. 38B) and the recovery limb (fig. 38C) of the long-term drawdown-recovery cycle near Toltec. Both the drawdown and recovery limbs of the model-derived curve are a little steeper than the drawdown and recovery limbs of the measured heads. This condition could indicate that storage is not large enough or that the simulated hydraulic connection to Ojo del Gallo is not close enough. Springflow at Ojo del Gallo, which is very sensitive to water-table altitude, tends to limit hydraulic heads in its vicinity. The match between measured and model-derived heads near Toltec shown in figure 38 was deemed acceptable.

Hydrographs for near Milan (not shown) were very similar to those shown in figure 38 except that the fluctuations were not as large as those shown in figure 38. The dampening of fluctuations probably was due to the leveling effect of Ojo del Gallo, which is closer to Milan than to Toltec.

Three hydrographs (figs. 39 and 40) represent the area east of San Rafael fault, although no wells are directly east of the large fault offset. The hydrograph for the south San Rafael irrigation area (fig. 39) has a long-term drawdown that is much less than those in wells west of the fault. A long-term recovery at this site is hardly perceptible in the measured hydraulic heads although a slight recovery was simulated. This near-total lack of recovery could indicate that the hydraulic barrier at San Rafael fault is more complete than was simulated. The seasonal fluctuations are greater than those in most wells west of the fault. The model-derived seasonal fluctuations were increased by a reduction of simulated transmissivity for that locality.

Hydrographs in figure 40 are east of San Rafael fault and relatively distant from the outcrop of the San Andres-Glorieta aquifer. At sites represented in figure 40, the valley-fill aquifer is separated from the San Andres-Glorieta aquifer by the full thickness of the Chinle confining bed and the hydraulic heads are almost totally unrelated.

The hydrograph in figure 40A is for the eastern side of the valley fill. Measured hydraulic heads shown in figure 40A probably are largely controlled by the altitude of Horace Springs. In figure 40A, there is a slight downward trend in the measured heads during the 1950's and 1960's, which is paralleled by the model-derived hydrograph. After that, however, the measured heads are approximately 6,351 feet, a value that also occurs before 1962. The flat trend after the 1960's is not matched by the model-derived heads. Although measured heads that do not change with time may be suspected of not representing a real, dynamic potentiometric surface (as in fig. 38A), the potentiometric surface in this location may not be very dynamic.

The measured hydraulic heads shown in figure 40B have a slight upward trend that is approximately simulated by the model-derived heads. Because the model projection, including the ground-water withdrawals of the Acoma scenario, starts in 1986.0, the model-derived hydrograph does not simulate the trend in heads measured after that time.

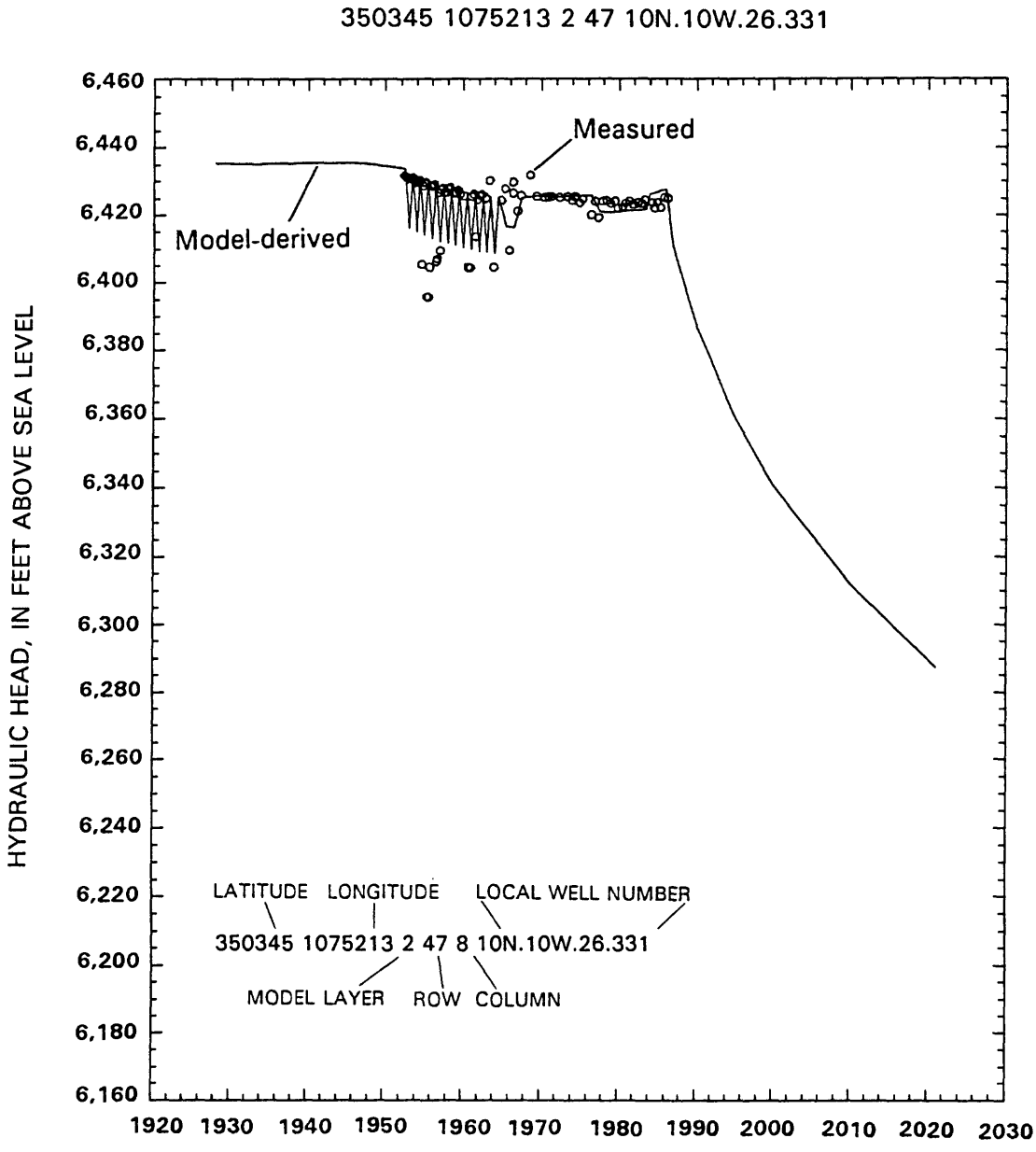

Figure 39.--Measured and model-derived hydraulic heads east of San Rafael fault and near the outcrop of the San Andres-Glorieta aquifer (location shown in fig. 19).

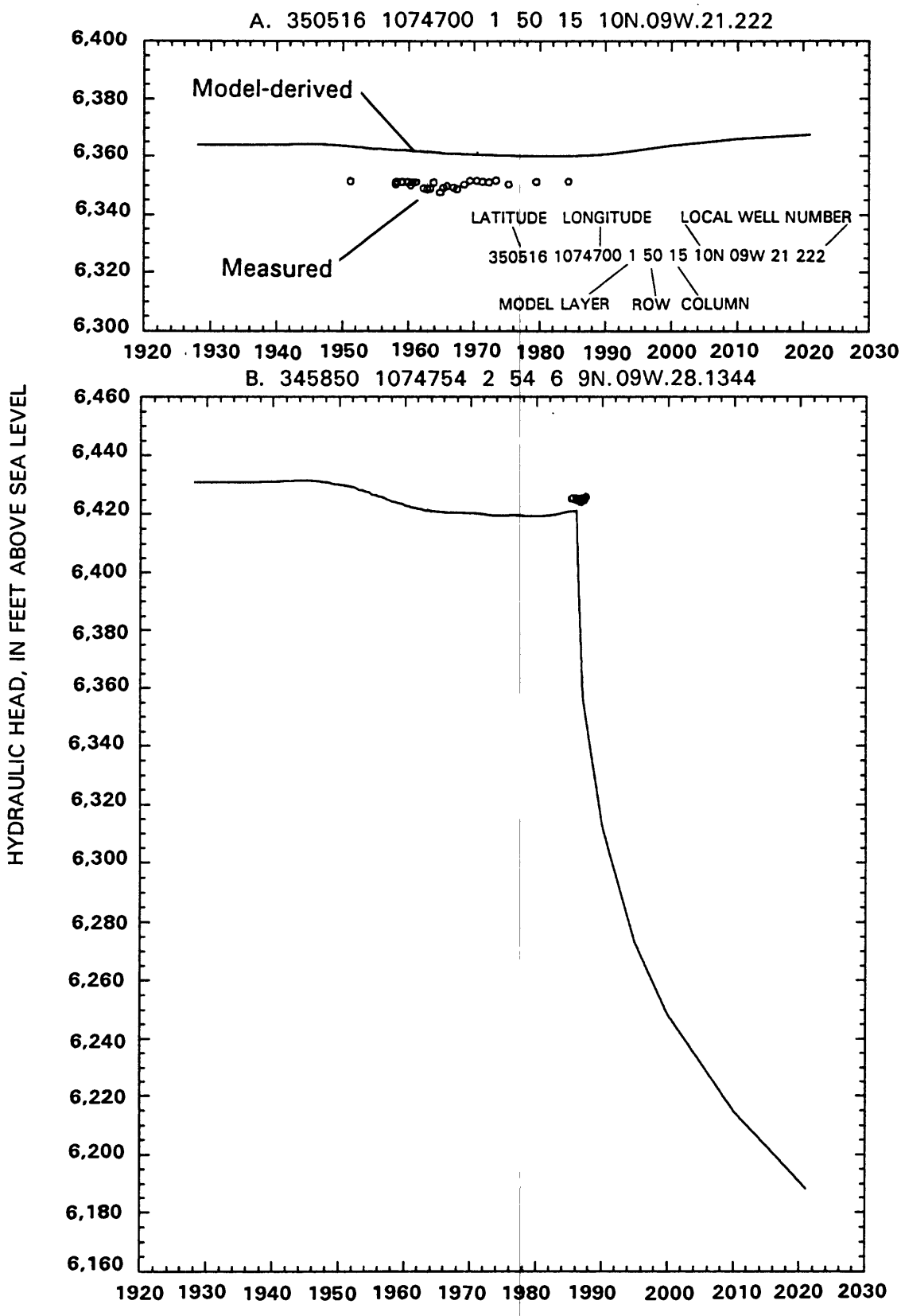

Figure 40.--Measured and model-derived hydraulic heads of San Rafael fault and about 6 to 9 miles from the outcrop of the San Andres-Glorieta aquifer (locations shown in fig.19).

Few hydrographs represent the parts of the study area where the San Andres-Glorieta aquifer is under artesian conditions. Although many of the wells represent the aquifer where it is locally artesian, the hydrographs for the general area of Bluewater, Grants, and San Rafael represent conditions close to the outcrop where the aquifer is unconfined and specific yield dominates the aquifer storage properties. The hydrograph shown in figure 40B, though distant from any water table, has a duration that is too short to be a good indicator of long-term trends and does not have much fluctuation.

Three hydrographs represent the artesian area northeast (downdip) of Thoreau (fig. 41A), northeast (downdip) of Prewitt (fig. 41B), and north of Prewitt (fig. 42). At first, the measured hydraulic heads in figure 41A, showing a very steep decline, were thought to be erroneous because ground-water withdrawals reported for this well were very small (a maximum of about 3 acre-feet for water year 1981, and an average of 1.5 acre-feet per year for the duration of withdrawal shown in table 3) and the closest neighboring ground-water withdrawals were more than 4 miles away. Additionally, because the transmissivity of the San Andres-Glorieta aquifer (fig. 7) is approximately 100 feet squared per day, drawdowns were not expected to spread as rapidly as they would where the aquifer is more transmissive. However, as the measured hydrograph was extended through the 1980's, it developed into a believably consistent drawdown and recovery curve. The nearest simulated ground-water withdrawals were at one of the Plains Electric well fields, about 4.5 miles away, and at Thoreau, about 7 miles away. A very short duration composite hydrograph (fig. 42) at Plains Electric was made up of reported initial measurements at four wells. The difference between the highest and lowest hydraulic heads in figure 42 is about 70 feet, probably indicating a minimum drawdown of about 50 feet considering the possible error of $\pm$ 10 feet in the land-surface datum. No maximum drawdown was estimated. Because true drawdown in the Plains Electric well field is unknown, the model-derived heads in figure 42 were deemed to match measured heads reasonably well.

The hydrographs in figure 41 are more sensitive to artesian storage than the other hydrographs. The drawdown of measured hydraulic heads shown in figure 41A between 1980 and 1986 was not well matched by drawdown of model-derived hydraulic heads. A smaller artesian storage coefficient improved the match from that shown in figure 41A. However, a smaller storage coefficient makes the recovery limb of the model-derived hydrograph in figure 41B steeper than that shown, yielding a poorer match with the measured values. The long-term recovery shown in figure 41B was deemed to be more reliable than the short-term hydrograph shown in figure 41A.

At least two possible explanations of the differences between model-derived and measured hydraulic heads shown in figure 41 might be hypothesized. Horizontal anisotropy could cause an elliptical drawdown cone around a well field oriented so that the major axis is aligned with well 15N.13W.25.1423 (fig. 41A). Another possibility is that the aquifer is highly indurated with fracture permeability, and a small artesian storage coefficient. This could result in a rapid initial spreading of a cone of depression. Possibly most of the transmissivity of the aquifer is derived from fracture permeability and most of the storage capacity is derived from the rocks between the fractures. This could result in an apparently small artesian storage coefficient in the short term and a more normal storage coefficient in the long term. In either case, it was judged that the more long-term effects should be simulated, possibly at the cost of a poor short-term match of measured and model-derived values.

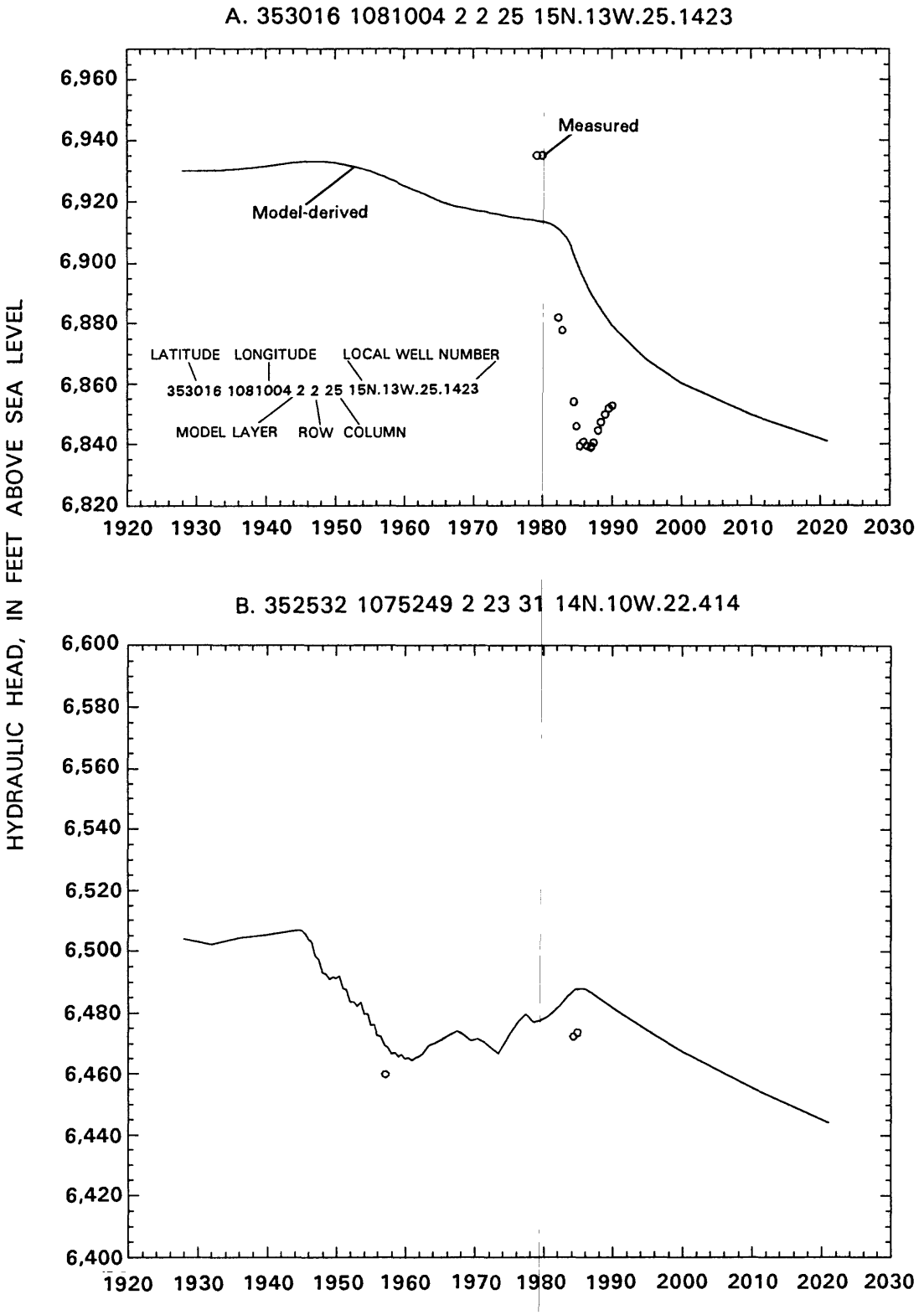

Figure 41.--Measured and model-derived hydraulic heads northeast of Thoreau and Prewitt (locations shown in fig. 19).

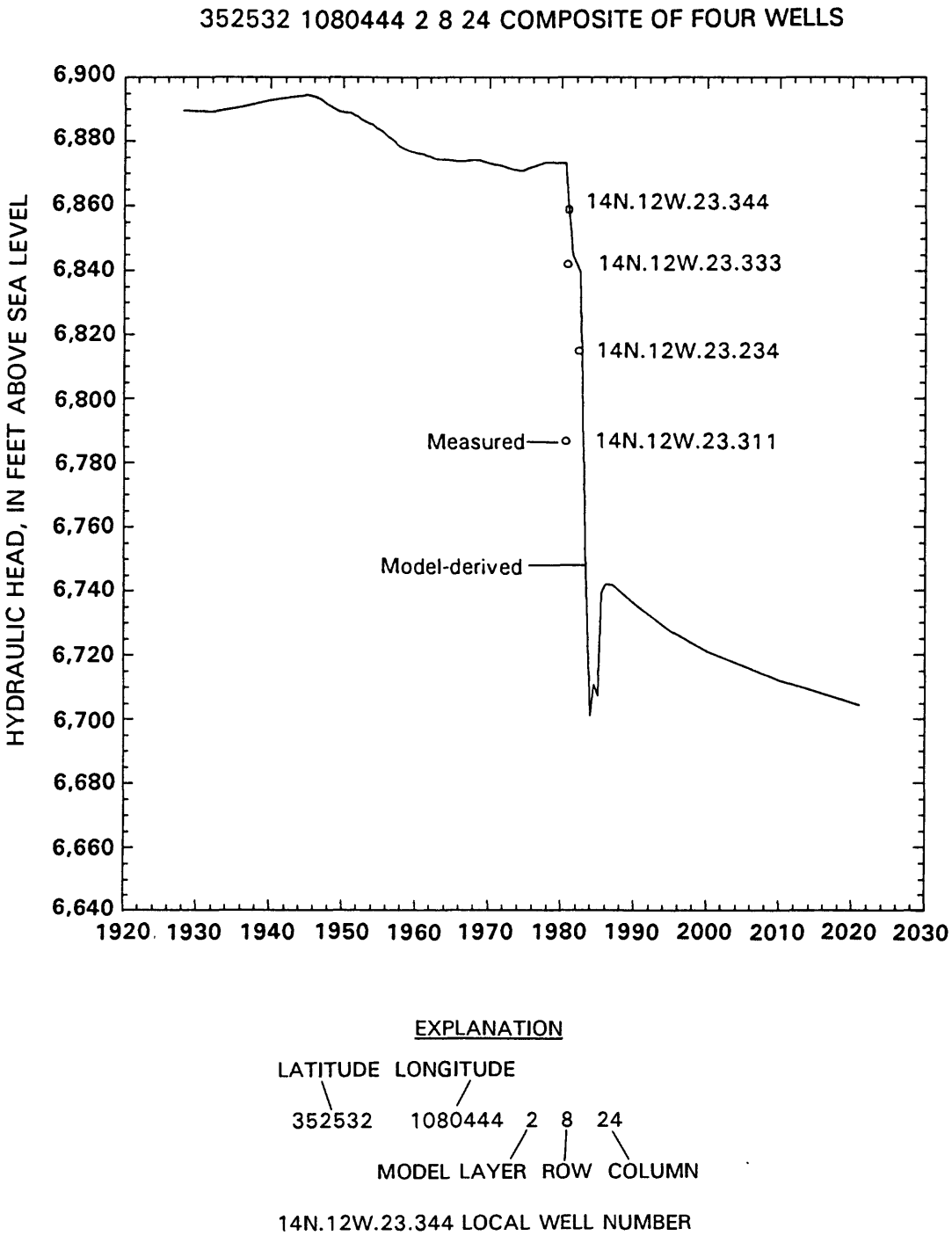

Figure 42.--Measured and model-derived hydraulic heads in the Plains Electric well field north of Prewitt (locations shown in fig. 19).

It may be concluded from these discrepancies that the model is oversimplified. However, added model complexity may not yield a more accurate solution unless it is based on additional knowledge of the physical system. The discrepancies were considered to be acceptable because the shapes of the model-derived hydrographs and measured hydrographs generally are similar.

Springflow and streamflow

Measured and reported springflow at Ojo del Gallo was compared with model-derived flow as shown in figure 43A. Due to the great difficulty of measuring springflow accurately and consistently, the model-derived flow was considered to match measured flow because the discrepancy was 30 percent or less and the date of model-derived flow was within 2 years of the measured flow. Model-derived springflow was substantially greater than one of the values measured during the 1930's. However, the model-derived flows compare well with the maximum measured flows during that time and compare very well with the measured flows after the late 1940's.

Measured streamflow downstream from Horace Springs (U.S. Geological Survey gaging station 08343500 "Rio San Jose near Grants") was compared with model-derived streamflow as shown in figure 43B. At that location, the base flow is made up of springflow and sewage-treatment-plant effluent from the city of Grants. Flow that exceeds the base flow usually is a fast-moving event that cannot be simulated with this ground-water flow model. The comparison was considered to be good when model-derived flows were within about 10 percent of measured flows during base-flow conditions, which occurred during most of the period shown in figure 43B.

Characteristics that were Adjusted

Characteristics that were adjusted were specified recharge, hydraulic conductivity, transmissivity, leakage, streambed hydraulic conductivity, specific yield, storage coefficient, and the extent of the no-flow boundary simulating the blockage of ground-water flow at the San Rafael fault and at the faults near Bluewater. Values for these characteristics were adjusted in a trial-and-error fashion. Often a single objective, such as the simulation of the hydraulic head in a particular place, was approached by the adjustment of several characteristics. This demonstrates not only the complexity of the system but the non-uniqueness of the model.

Characteristics that were not adjusted were municipal and industrial ground-water withdrawal, and most irrigation withdrawals. The exterior boundary of the model was not moved.

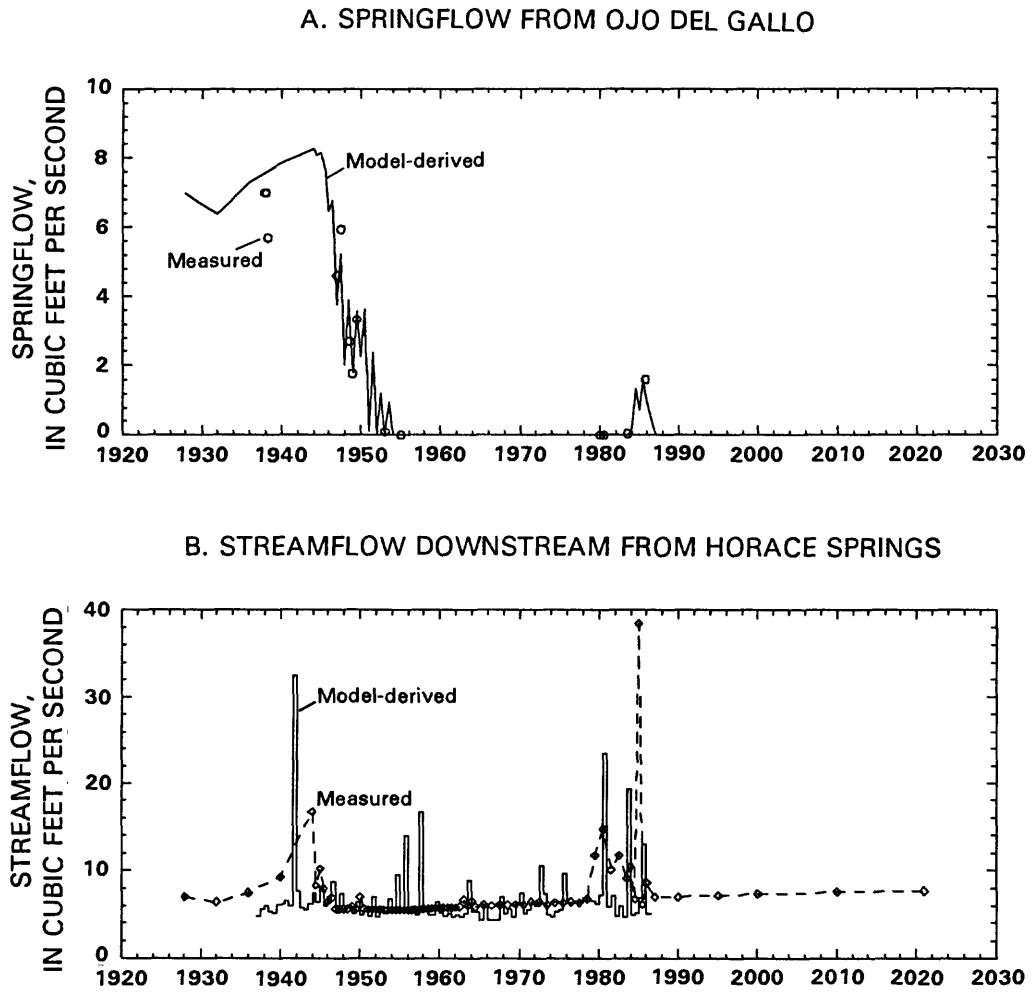

Figure 43.--Measured and model-derived springflow at Ojo del Gallo and measured and model-derived streamflow downstream from Horace Springs.

Recharge

Recharge on the mountains of the Zuni uplift (fig. 27A and B; tables 16 and 17) was reduced to one-fourth of excess precipitation estimated by the San Juan method to reduce model-derived hydraulic heads north and west of Prewitt (figs. 36 and 41; and "north" sites in table 24, Supplemental Information). Adjustments to mountain recharge were made proportionately over the entire mountain-recharge area, thus keeping the patterns shown in figure 13, which were assumed to have been dictated by weather.

Recharge on the barren basalt of The Malpais (fig. 27C) was increased from 0.1 to 0.15 of precipitation at Grants to simulate springflow downstream from Horace Springs (fig. 43B) and to simulate valley-fill hydraulic heads in the north end of The Malpais (fig. 40A and "Malpais" sites in table 24). Because the possible recharge rate could range from near zero to near 100 percent of precipitation, the ratio used (0.15 times precipitation) depended on the simulated transmission rate of water from that area to Horace Springs and, by way of leakage to the San Andres-Glorieta aquifer, to the discharge area along the Rio Grande rift. The discharge at Horace Springs is known, and the underflow at Horace Springs is probably approximately equal to the gain in the Rio San Jose between Horace Springs and McCartys. However, neither the discharge along the Rio Grande rift nor the hydraulic characteristics of the intervening rock formations are known. Therefore, the simulated recharge rate in The Malpais is speculative.

Hydraulic conductivity and transmissivity

Hydraulic conductivity of valley fill (fig. 20) in The Malpais and in the Rio San Jose valley near Grants was adjusted to simulate hydraulic heads in the northern end of The Malpais ("Malpais" sites in table 24), and to simulate springflow and underflow at Horace Springs. A smaller hydraulic conductivity (10 feet per day) than that of the surrounding valley fill represented the interface between the granular permeability of the alluvium and the fracture permeability of the basalt near the Homestake mill. This conductivity was adjusted in order to simulate hydraulic heads in the alluvium north of the interface ("San Mateo" sites in table 24). A similar situation may exist in Mitchell Draw northeast of Prewitt although no measured hydraulic heads have been reported and the existence of a water table in the valley fill is only assumed.

Transmissivity simulated in layer 2 (fig. 21; and table 13 in Supplemental Information) was adjusted from that shown in figure 7. Transmissivity simulated in the Milan-Toltec area was increased from 50,000 to 60,000 feet squared per day to simulate springflow at Ojo del Gallo (fig. 43) and to flatten the model-derived potentiometric surface between Toltec and Milan--that is, to lower the surface near Toltec and raise the surface near Milan (figs. 11, 36, 38; and "Toltec-Milan" sites in table 24). Transmissivity northeast of there was increased from 800 to 1,000 feet squared per day to lower the simulated hydraulic head at row 23, column 31 (fig. 41B), and to reduce the model-derived hydraulic heads in the northwest while increasing the model-derived hydraulic heads on the east end of the modeled

area (fig. 36; and "North" and "East" sites in table 24). Transmissivity along the northwestern side of the modeled area near Thoreau was increased from 140 to 200 feet squared per day to decrease the gradient from column 15 northeastward to column 25 (figs. 36 and 41A; and table 24) and to increase the simulated flow through the modeled area, avoiding a greater reduction in mountain recharge. Transmissivity in the Acoma embayment was increased from 150 to 400 and from 10 to 100 feet squared per day to increase the hydraulic head at row 72, column 31 (fig. 36; and "Mesita" sites in table 24). Values of transmissivity generally were increased from those shown in figure 7, and the overall effect was to flatten the gradient from the Zuni uplift to the Rio Grande rift. An alternative might have been a further reduction of the specified recharge.

The assumed hydraulic conductivity that was used to calculate the conductances of general-head-boundary blocks was adjusted very early in the adjustment procedure. When the conductivity values were all increased by the same multiplier, the change tended to lower model-derived hydraulic heads throughout the model and vice versa. (The specified heads of the general-head boundary were not changed.) The total conductance of the general-head boundary is probably approximately proportional to an "average" transmissivity east of San Rafael fault, which in turn is proportional to the flow through that part of the aquifer, an unknown quantity.

Leakage

Simulated leakage between the valley fill and the San Andres Limestone was adjusted by changing the simulated location of the edge of the Chinle Formation subcrop, which is imprecisely known, and by changing the simulated vertical hydraulic conductivity of the valley fill. These changes were made along the Chinle subcrop between Bluewater and Milan, and south of San Rafael. Generally, the extent of the Chinle was reduced, increasing the leakage between layers, and the vertical hydraulic conductivity representing the valley fill was reduced, having the opposite effect. These adjustments were made to improve the simulation of hydrographs in figures 37-39 by changing the gradient between hydrographs for layer 1 and layer 2, and to improve the overall statistical fit in table 24.

Streambed hydraulic conductivity

The hydraulic conductivity of streambeds was adjusted to simulate hydraulic heads in the valley fill and San Andres-Glorieta aquifer in the Bluewater-Toltec area (figs. 36-38) and to simulate springflow at Ojo del Gallo. Because most of the inflow specified for reach 5 (fig. 29) was simulated as ground-water recharge, the extent of recharge along reach 5 could be shortened by increasing streambed hydraulic conductivity or lengthened by reducing streambed hydraulic conductivity. Occasionally, when a large inflow to reach 5 was specified, simulated surface flow extended the full length of reach 5, and adjustment of streambed hydraulic conductivity had an effect on the total quantity of recharge, which in turn had an effect on springflow at Ojo del Gallo. For consistency, the same value of hydraulic conductivity (8×10^{-7} foot per second) was used except when there was a physical condition to justify a different value. Two other values were introduced during model

adjustment because of physical conditions. (1) At the upper end of reach 5, the first two stream blocks downstream from the mouth of Bluewater Canyon and upstream from the confluence of Mitchell Draw were given a 50 percent larger value (1.2×10^{-6} foot per second) to simulate more leakage from the stream. Bed material may be coarser in this part of reach 5 than in other parts. (2) In the upstream end of reach 4 just downstream from Bluewater Dam, the hydraulic conductivity was set to 8×10^{-6} to increase the simulated flow from the lake to the upstream end of Bluewater Canyon. As previously explained, the seepage face at this location is on the limestone canyon wall, a much different physical condition than those along the rest of the stream system.

Specific yield and storage coefficient

Specific yield for the valley fill and storage coefficient for the San Andres-Glorieta aquifer where it is unconfined were adjusted to simulate the long-term (1940's through 1980's) drawdown and recovery limbs of the hydrographs (figs. 37-39). Larger values for unconfined storage cause the model-derived hydrographs to have smaller long-term drawdown and recovery. Smaller values cause these hydrographs to have larger long-term drawdown and recovery.

To increase the model-derived fluctuation of hydraulic head in the San Andres-Glorieta aquifer near Bluewater (fig. 37), relatively small values of specific yield for the valley fill (0.012 in fig. 22) and of storage coefficient (0.015 in fig. 23) were specified. In this area, the water table may be in basaltic valley fill or in the San Andres Limestone. The porosity of the San Andres Limestone and basalt was assumed to be due to widely spaced fractures. Although the value for the San Andres is small, it is consistent with the discussion in Gordon (1961, p. 56).

Confined storage (artesian storage coefficient for the San Andres-Glorieta aquifer) was adjusted after the unconfined storage values. This sequence is reasonable because most of the hydrographs (figs. 37-39), representing wells in or near a water-table area, are more sensitive to unconfined storage than to confined storage. Also, because unconfined storage constitutes about 95 percent of the total storage in the aquifer system, a small percentage of error in unconfined storage would be larger than a large percentage of error in confined storage.

Confined storage was adjusted (1) on the basis of reducing the overall mean-absolute difference between model-derived and measured hydraulic heads, and (2) on the basis of simulating the slope of the recovery limb of the hydrograph at layer 2, row 23, column 31 (fig. 41B). As previously discussed, the long-term recovery of the hydrograph in figure 41B is a measure of the long-term artesian storage coefficient. The hydrograph in figure 41A may be a measure of a short-term storage coefficient. The overall mean-absolute difference includes a group of measured heads in the northwestern part of the modeled area that tend to be more recent than measured hydraulic heads in the Grants-Bluewater area. Therefore, the mean-absolute difference may be a mixed measure that includes long- and short-term effects of ground-water withdrawals. The mean-absolute difference also includes sites that are mainly influenced by unconfined storage as well as sites that are mainly influenced by confined storage in the aquifer system.

Blockage of ground-water flow

The extent of the blockage of ground-water flow due to the offset of San Rafael fault is not known. The southern end of the blockage probably is somewhere between Grants, where the offset of about 1,000 feet is about three times the aquifer thickness, and Ojo del Gallo, where the offset of about 200 feet is probably less than full aquifer thickness. The northern end of the blockage may be somewhere near the Cibola-McKinley County line. The extent of the no-flow boundary was adjusted to simulate the hydraulic-head difference of about 20 to 30 feet across San Rafael fault near Ojo del Gallo (fig. 11), to simulate flow lines (fig. 44) that might offer an explanation for water-quality differences (reported in Baldwin and Anderholm, in press), and to simulate the shapes of the hydrographs at row 47, column 8 and at row 54, column 6 (figs. 39 and 40B). The response of these hydrographs to ground-water withdrawals in the Grants-Bluewater area appears to be dampened, and the extent of the blockage at San Rafael fault was used to simulate this dampening. The dampening is apparent from a comparison of the hydrograph east of San Rafael fault (fig. 39) with hydrographs near Toltec, which is west of San Rafael fault (fig. 38). The hydrograph in figure 39 has a downward and flattening trend that may indicate a dampened and delayed response to the drawdown that has taken place in the Grants-Bluewater area. The hydrograph shown in figure 40B, although very short, appears to show a slight recovery. The hydrograph for the shorter period probably is more representative of the artesian system than the hydrograph in fig. 39 but may be too short to indicate a trend. The degree of dampening and delaying of the drawdown-recovery cycle may depend on the location of the hydraulic connection between this area and the more developed area west of San Rafael fault.

The simulated location of a stagnation zone (a "stagnation zone" occurs where flow lines converge or diverge abruptly) on the southeast side of San Rafael fault was shifted so that the flow line leading from the stagnation zone would go between model blocks at row 54, column 6 and row 53, column 16, which represent locations of the Acoma-1 and Anzac test wells, respectively (fig. 44), where distinctly different water chemistries were found. The water at Acoma-1 is fresh and the temperature is normal for the aquifer depth, whereas the water at Anzac is brackish and abnormally warm. Simulated flow lines north of the flow line leading from the stagnation zone take a long, basinward route around the northeast end of San Rafael fault where water might be expected to be more mineralized than water near the recharge area. The flow lines southwest of the stagnation zone lead directly from the recharge area. To accomplish the desired change in simulated flow lines, the inactive zone (figs. 23 and 26) that represented the fault was shifted one block to the southwest on both ends--that is, row 42, column 28 was made active, and row 43, column 12 was made inactive. The result was the simulation of more flow passing the northeast end of the fault and less flow passing the southwest end. Although the simulated flow lines may explain the large dissolved-solids concentration at the Anzac well, they may not fully explain the heat content because heat flow lines do not necessarily parallel hydraulic flow lines. Also, the dynamic effects of variable water density in a dipping aquifer (Davies, 1986) are not simulated.

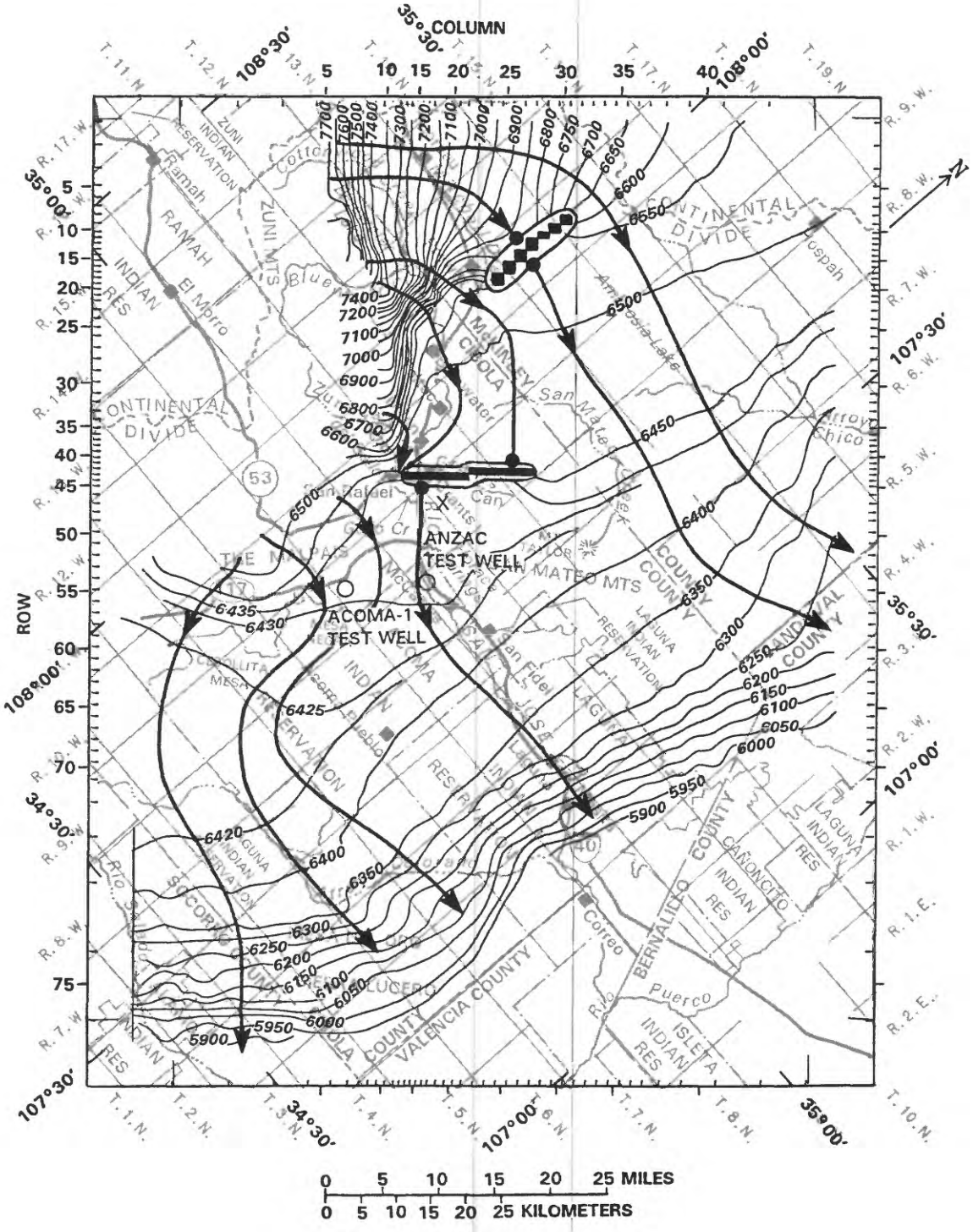

EXPLANATION

5950 — MODEL-DERIVED POTENTIOMETRIC CONTOUR--Shows model-derived altitude of potentiometric surface. Contour interval, in feet, is variable. Datum is sea level

GROUND-WATER FLOW LINE--Drawn from a plot of velocity vectors from each model block

SIMULATED FAULT--Location of blockage of ground-water flow. Solid circles (●) indicate zones of stagnation. X indicates the stagnation zone on the southeast side of San Rafael fault

Figure 44.--Model-derived steady-state potentiometric surface and selected flow lines for layer 2.

Results of Steady-State and Transient Simulations through 1985

The values of some hydrologic characteristics were not estimated independently of the model. To the extent that the model may be judged plausible, the model-derived values fulfill the purpose of this report to estimate the effect of previous (pre-1986) development on water levels, springflow, and streamflow. In addition, the model provides a ground-water budget that was not previously available. Although the accuracy of the model-derived budget is not known, the budget balances and is reasonably consistent with the conceptual model.

A model budget summarizes the sources and destinations of simulated flows. For each stress period, simulated inflows to ground water are divided into six categories: (1) specified fluxes, including wells and recharge; (2) evapotranspiration; (3) river leakage; (4) flow from general-head boundaries; (5) water taken from storage; and (6) flow from specified-head boundaries. For brevity, table 7 shows the budget for only three transient stress periods in addition to the steady-state budget. The model budgets for other transient stress periods are given in table 25 in Supplemental Information. In table 7, specified flows are divided into 11 categories by hydrologic boundary, and river boundary is divided into 11 categories by reach. Although budgets given in table 25 do not have specified flows divided into categories, specified flows are categorized in tables 16, 17, 20, 22, and 23.

In the budget shown in table 7, inflows to the ground-water system are positive values and outflows are negative values. Although this sign convention may seem backwards from the point of view of streamflow, it is consistent throughout the budget. For the purpose of the model budget, the algebraic sign of storage is treated as if storage were another boundary--that is, when flow comes out of storage, the flow rate is a positive value and the quantity of water in storage is reduced. Conversely, flow going into storage is a negative value and the quantity of water in storage is increased.

Simulated Predevelopment Conditions

Because steady-state conditions simulated average natural conditions of recharge and streamflows, the model-derived values in the first column of table 7 constitute estimates of average natural flows to boundaries. All the values in table 7 are model-derived except specified flows.

Ground-water recharge (+) and discharge (-) from or to the stream boundary were model derived, although the simulations of streamflows at Ojo del Gallo and Horace Springs were criteria for model adjustment as previously explained. Ground-water recharge along Cottonwood Creek (reach 1) on the outcrop of the San Andres-Glorieta aquifer and upstream from the reach now occupied by Bluewater Lake was simulated to be 0.17 cubic foot per second. Under steady-state conditions no lake was simulated. Ground-water recharge from those parts of the streams now occupied by Bluewater Lake (reach 2) was 1.42 cubic feet per second. Along Bluewater Creek (reach 3), on the outcrop of the San Andres-Glorieta aquifer upstream from Bluewater Lake, a small quantity (0.07 cubic foot per second) of ground-water discharge to the creek was simulated. Steady-state ground-water recharge from the stream in

Bluewater Canyon (reach 4) was 0.59 cubic foot per second, and ground-water recharge from Bluewater Creek and the Rio San Jose between gaging station 08342000, near the mouth of Bluewater Canyon, and gaging station 08343000, at Grants (reach 5), was 6.37 cubic feet per second. The Rio San Jose was simulated to have gained and lost very small quantities in the three reaches between gaging station 08343000 and Gallo Creek; along reach 6, 0.01 cubic foot per second of ground-water discharge was simulated, and along reaches 7 and 8, 0.09 cubic foot of ground-water recharge was simulated. The simulation of a small quantity of ground-water recharge along the stream (reaches 7 and 8) and ground-water discharge to evapotranspiration from the water table nearby is plausible given the lack of observed streamflow gain along the stream. The simulated 7.17 cubic feet per second of ground-water discharge at Ojo del Gallo (reach 9) under steady-state conditions is an estimate of the average natural springflow. More than half (3.78 cubic feet per second) of the springflow at Ojo del Gallo was simulated as ground-water recharge in La Vega and Gallo Creek (reach 10), leaving a simulated stream discharge of 3.39 cubic feet per second (7.17 minus 3.78) from Gallo Creek to the Rio San Jose. Between Gallo Creek and gaging station 08343500 downstream from Horace Springs (reach 11), simulated ground-water discharge to the Rio San Jose was 5.61 cubic feet per second, mostly at Horace Springs.

Steady-state inflow and outflow for each reach are summarized in the following table, which contains information derived from various places in this report. Inflow routed from upstream reaches and outflow are model-derived quantities. Unlike the sign convention used in the budget table, stream gains are positive and stream losses are negative in this table:

[measurements are in cubic feet per second]

Reach	Specified inflow	Inflow routed from upstream reaches	Stream gain or loss	Outflow
1	3.9	0	-0.2	3.7
2	0	3.7	-1.4	2.3
3	9.1	0	0.1	9.2
4	0	11.5	-0.6	10.9
5	0	10.9	-6.4	4.5
6	0	4.5	0	4.5
7	0	4.5	0	4.5
8	0	4.5	0	4.5
9	0	0	7.2	7.2
10	0	7.2	-3.8	3.4
11	0	[1]7.8	5.6	13.5

[1]The simulated steady-state surface-water inflow to reach 11, the Rio San Jose downstream from Gallo Creek, of 7.8 cubic feet per second was comprised of 4.46 cubic feet per second from reach 8 and 3.39 cubic feet per second from reach 10.

Just as the steady-state simulation provides model-derived values of stream gains and losses, it also provides model-derived flow rates to other simulated geohydrologic boundaries. Average natural evapotranspiration from the water table was simulated to be 5.77 cubic feet per second in La Vega, along Gallo Creek downstream from Ojo del Gallo, and along the Rio San Jose from Grants to Horace Springs. The simulated sources of water discharged as evapotranspiration were underflow in the valley fill and stream losses, especially in La Vega. Discharge of the San Andres-Glorieta aquifer to the Rio Grande rift to the east was simulated by the general-head boundary as 4.08 cubic feet per second. Net ground-water recharge at the specified-head boundary (layer 1, rows 47-51, column 1) was 0.30 cubic foot per second. Although this boundary was used primarily to provide mathematical stability for the model, the recharge or discharge can be regarded as being additional to the specified recharge for the valley fill (fig. 25). This is true as long as transient stresses do not substantially affect flow from the specified-head boundary, a condition that did not occur in this model.

The precision reported here only demonstrates that the model budget balances to within acceptable discrepancies. These model-derived values of streamflows, stream gains and losses, evapotranspiration, and ground-water outflow have an unknown accuracy. Accuracy is further addressed in the Model Evaluation section.

Simulated Effects of Development

A comparison of the historical simulation with the steady-state simulation does not yield the effects of development. Whereas the steady-state simulation included average values for recharge and discharge, natural conditions of recharge and streamflow probably varied during the historical period (1900-85) with changes in precipitation. Precipitation varied (Baldwin and Anderholm, in press, fig. 2) with several years of drought separated by several years of relatively plentiful precipitation. Because measured hydrologic characteristics include the effects of time variation of precipitation in addition to the effects of water development, the historical scenario included variable recharge and streamflows that were estimated on the basis of precipitation in addition to streamflows that were measured.

A "null scenario" included the same recharge on the mountains of the Zuni uplift and barren basalt of The Malpais as that of the historical scenario (table 7). The null scenario differed from the historical scenario in that no surface- or ground-water withdrawals or artificial recharge, including municipal withdrawals, industrial withdrawals, irrigation withdrawals, diversion of springflow, or recharge from irrigation, was simulated, nor was Bluewater Lake simulated. River reach 2 was given stream altitudes that approximated the streambed altitude and a width of 20 feet, and model-derived flows from Bluewater and Cottonwood Creeks were routed to reach 4 (table 6).

Table 7.--Water budget for the steady-state and selected stress periods of the historical and null scenarios

[All items in this budget are in cubic feet per second and are model-derived except for specified flow. Inflows are positive and outflows are negative. Specified flow is divided into 11 hydrologic boundaries. Model-derived flows to and from the river boundary are listed by reach. Reaches are shown in figure 29. Apparent discrepancies in the hundreth's place are rounding errors]

EXPLANATION OF BOUNDARIES SIMULATED BY SPECIFIED FLOWS

(A) Recharge to the valley fill in the barren basalt area of The Malpais;

(B) recharge to the valley fill from flow in canyons that empty onto the valley fill from the eastern end of the mountains of the Zuni uplift;

(C) recharge to the San Andres-Glorieta aquifer in the mountains of the Zuni uplift;

(D) underflow in the valley fill at Mitchell Draw, San Mateo Creek, and Grants Canyon;

(E) underflow in the valley fill downstream from Horace Springs;

(F) ground-water withdrawals in the Bluewater-Toltec Irrigation District;

(G) ground-water recharge in the Bluewater-Toltec Irrigation District;

(H) ground-water withdrawals in the south San Rafael irrigated area and ground-water withdrawals that simulate the net irrigation withdrawal in the Ojo del Gallo irrigated area;

(I) ground-water recharge in the south San Rafael irrigation area;

(J) ground-water withdrawals for municipal and industrial use; and

(K) ground-water recharge by municipal and industrial uses.

Table 7.--Water budget for the steady-state and selected stress periods of the historical and null scenarios--Continued

	Steady state	Stress period 7 (September 30, 1945) Historical	Null	Historical minus null	Stress period 27 (September 30, 1955) Historical	Null	Historical minus null	Stress period 70 (September 30, 1985) Historical	Null	Historical minus null
Storage										
Inflow	0.00	7.68	7.10	0.58	28.39	7.80	20.59	2.45	1.21	1.24
Outflow	0.00	-12.34	-10.01	-2.33	-8.73	-7.80	-0.93	-12.13	-7.35	-4.78
Net	0.00	-4.66	-2.91	-1.75	19.66	0.00	19.66	-9.68	-6.14	-3.54
Specified flow										
Inflow	12.52	23.17	19.03	4.14	28.63	15.60	13.03	21.62	18.57	3.05
Outflow	-2.50	-10.18	-2.50	-7.68	-40.56	-2.50	-38.06	-10.84	-2.50	-8.34
Net	10.02	12.98	16.53	-3.55	-11.93	13.10	-25.03	10.78	16.07	-5.29
	---------- Specified flow subdivided by boundary ----------									
Boundary										
(A)	6.70	14.85	14.85	0.00	12.49	12.49	0.00	8.64	8.64	0.00
(B)	0.70	0.02	0.02	0.00	0.00	0.00	0.00	0.63	0.63	0.00
(C)	3.52	0.62	0.62	0.00	0.14	0.14	0.00	7.24	7.24	0.00
(D)	1.60	3.54	3.54	0.00	2.98	2.98	0.00	2.06	2.06	0.00
(E)	-2.50	-2.50	-2.50	0.00	-2.50	-2.50	0.00	-2.50	-2.50	0.00
(F)	0	0.00	0.00	0.00	-34.78	0.00	-34.78	0.00	0.00	0.00
(G)	0.0	4.14	0.00	4.14	11.59	0.00	11.59	2.35	0.00	2.35
(H)	0.0	-6.90	0.00	-6.90	-1.23	0.00	-1.23	0.00	0.00	0.00
(I)	0.0	0.00	0.00	0.00	0.41	0.00	0.41	0.00	0.00	0.00
(J)	0.0	-0.78	0.00	-0.78	-2.04	0.00	-2.04	-8.34	0.00	-8.34
(K)	0.0	0.00	0.00	0.00	1.02	0.00	1.02	0.70	0.00	0.70

Table 7.--Water budget for the steady-state and selected stress periods of the historical and null scenarios--Continued

	Steady state	Stress period 7 (September 30, 1945) Historical	Null	Historical minus null	Stress period 27 (September 30, 1955) Historical	Null	Historical minus null	Stress period 70 (September 30, 1985) Historical	Null	Historical minus null
River boundary										
Inflow	14.57	17.16	10.38	6.78	5.17	9.44	-4.27	18.23	15.00	3.23
Outflow	-15.03	-17.23	-14.58	-2.65	-7.06	-13.24	6.18	-12.75	-14.43	1.68
Net	-0.46	-0.07	-4.20	4.13	-1.89	-3.80	1.91	5.48	0.57	4.91
	---------- River boundary by reach ----------									
Reach										
1	0.17	0.17	0.17	0.00	0.29	0.30	-0.01	0.13	0.11	0.02
2	1.42	2.24	1.23	1.01	2.30	0.23	2.07	6.28	1.52	4.76
3	-0.07	-0.08	-0.07	-0.01	-0.07	-0.07	0.00	-0.08	-0.07	-0.01
4	0.59	-0.44	0.76	-1.20	-0.26	1.24	-1.50	-3.29	0.68	-3.97
5	6.37	5.92	2.31	3.61	1.13	2.07	-0.94	7.38	6.57	0.81
6	-0.01	0.27	-0.01	0.28	0.00	-0.01	0.01	0.04	-0.01	0.05
7	0.06	0.06	0.01	0.05	0.08	0.01	0.07	0.08	0.06	0.02
8	0.03	0.03	0.00	0.03	0.05	0.00	0.05	0.05	0.03	0.02
9	-7.17	-8.15	-6.77	-1.38	0.00	-5.78	5.78	-0.97	-6.56	5.59
10	3.78	5.51	3.78	1.73	0.00	3.80	-3.80	0.97	3.80	-2.83
11	-5.61	-5.60	-5.62	0.02	-5.42	-5.60	0.18	-5.11	-5.57	0.46
Evapotranspiration from water table										
Inflow	0.00	0.00	0.00	0.00	0.00	0.00	0.00	0.00	0.00	0.00
Outflow	-5.77	-4.30	-5.71	1.41	-2.17	-5.54	3.37	-2.52	-5.80	3.28
Net	-5.77	-4.30	-5.71	1.41	-2.17	-5.54	3.37	-2.52	-5.80	3.28

Table 7.--Water budget for the steady-state and selected stress periods of the historical and null scenarios--Concluded

	Steady state	Stress period 7 (September 30, 1945) Historical	Null	Historical minus null	Stress period 27 (September 30, 1955) Historical	Null	Historical minus null	Stress period 70 (September 30, 1985) Historical	Null	Historical minus null
General-head boundary										
Inflow	0.00	0.00	0.00	0.00	0.00	0.00	0.00	0.00	0.00	0.00
Outflow	-4.08	-4.08	-4.08	0.00	-4.08	-4.08	0.00	-4.02	-4.07	0.05
Net	-4.08	-4.08	-4.08	0.00	-4.08	-4.08	0.00	-4.02	-4.07	0.05
Constant-head boundary										
Inflow	0.44	0.44	0.44	0.00	0.44	0.44	0.00	0.44	0.44	0.00
Outflow	-0.14	-0.14	-0.14	0.00	-0.14	-0.14	0.00	-0.13	-0.13	0.00
Net	0.30	0.30	0.30	0.00	0.30	0.30	0.00	0.31	0.31	0.00
Sum of inflow	27.53	48.45	36.95	11.50	62.63	33.28	29.35	42.74	35.22	7.52
Sum of outflow	-27.52	-48.27	-37.02	-11.25	-62.74	-33.30	-29.44	-42.39	-34.38	-8.01
Discrepancy	0.01	0.18	-0.07	0.25	-0.11	-0.02	-0.09	0.35	0.84	-0.49
Percent discrepancy	0.04	0.37	-0.19	2.20	-0.18	-0.06	-0.31	0.82	2.39	-6.52

Inflow to reach 5 was specified as the estimated natural streamflow at that point (tables 11 and 26, Supplemental Information; and Risser, 1982, table 4) through 1972. Between 1972 and 1986, the specified flow into reach 5 was the estimated basin yield (table 11 of this report); after 1986, the specified flow was the average of Risser's (1982) values. In short, the only transients specified in the null scenario were estimated natural recharge and estimated natural streamflows. The null scenario used steady-state initial conditions and the same time periods as those of the historical scenario.

In the following sections, the comparison of the ground-water budget of the historical scenario with that of the null scenario is used to describe the effects of development. However, because the ground-water budget effectively includes parts of the surface-water budget, its use may be confusing. For example, it was convenient to simulate the withdrawal of water at the Ojo del Gallo irrigated area as a specified flow from ground water. The budget includes a discharge of ground water to Ojo del Gallo, then a recharge from the river boundary in La Vega, and finally a specified discharge to account for the withdrawal of water from the system. In this case, the net discharge to the river boundary is understated in the budget and the net specified ground-water withdrawal is overstated. For the Bluewater-Toltec irrigated area, it was convenient to simulate recharge from partly surface-water-supplied irrigation as a specified flux (specified flow at a given model block calculated on the basis of block area). In this case the net ground-water withdrawal in the model budget may be understated if the effects of ground-water development were to be separated from the effects of surface-water development. However, the biggest effect of surface-water development, the diversion of surface water, is not an item of the model budget.

Had surface-water development been different, the simulated sources of water withdrawn from wells would have been in the same three categories of evapotranspiration, storage, and the river because the constant-head and general-head boundaries are distant from the withdrawals and would be the last of the boundaries affected in any case. However, the proportions of withdrawals derived from each of the three sources would have been different given different surface-water development. No attempt is made to separate historical (pre-1986.0) surface-water development from ground-water development.

Tables 7, 25, and 27 indicate little difference between the historical- and null-scenario flows at the constant-head boundary or at the general-head boundary. It was concluded that almost all simulated effects of development on items of the budget are restricted to changes in ground-water evapotranspiration, ground-water storage, and flow from or to the river boundary. In the following sections, simulated effects on hydraulic heads are determined directly from model output; changes in ground-water evapotranspiration and ground-water storage are determined from the budget; and simulated effects on the river boundary primarily are determined as the difference between historical-scenario and null-scenario streamflows.

Simulated effects on hydraulic heads

Simulated hydraulic heads north of Bluewater (fig. 45A, the same site shown in fig. 37B) generally were greater in the null scenario than in the historical scenario except for a brief period. (In fig. 45 and similar figures, the curve representing the historical scenario is marked "standard" because the curve extends beyond the 1986 endpoint of the historical scenario.) The standard scenario is defined as the historical scenario from 1900.0 through 1985.0 combined with the Acoma scenario from 1986.0 through 2021.0. During the late 1930's and early 1940's, elevated hydraulic heads in the historical scenario were caused by the simulation of recharge from irrigation that predated ground-water withdrawals for irrigation in the Bluewater-Toltec Irrigation District. (The irrigation supply was surface water; table 1.) This effect of irrigation is reasonable because Morgan (1938, p. 12) noted a rise in the water table that he surmised was caused by irrigation. In both the null and historical scenarios, hydraulic heads (fig. 45) during the late 1940's through the 1970's were lower than those before and after that time. This simulation of lowered hydraulic heads was caused by the specification of less-than-normal inflow to reach 5 for many of those years and specification of less-than-normal recharge, both of which were partially based on precipitation. During the late 1970's and early 1980's, specified recharge and stream inflows generally were larger than normal, resulting in the simulated recovery of hydraulic heads. Although the drop in simulated hydraulic heads is present in both the historical and null scenarios, the drop is much less in the null than in the historical scenario. This difference is caused by a combination of simulated ground-water withdrawals in the historical scenario and less specified inflow to reach 5 in the historical scenario than that in the null. The simulated effect of development on hydraulic head near Bluewater was about 50 feet in the late 1950's and about 8 feet in the mid-1980's.

The magnitude of the effect of development near Bluewater is not typical of the entire area west of San Rafael fault. The pattern of fluctuations (fig. 45B) is similar to that near Bluewater but the differences between the historical and null simulations are less for the period of the 1950's and 1960's. The difference was nearly 30 feet in 1960. However, for the mid-1980's, the difference between the standard and the null of about 10 feet is larger than that near Bluewater. Perhaps simulated springflow at Ojo del Gallo tends to reduce the rate of recovery, or perhaps simulated ground-water withdrawals produce the same effect.

East of San Rafael fault, the drawdown and recovery seen west of San Rafael fault before 1986 are dampened and delayed, and the model-derived difference between the historical and null scenarios was a maximum of about 8 feet for 1978 and only slightly less for 1986. This is reasonable because most of the ground-water development was west of San Rafael fault.

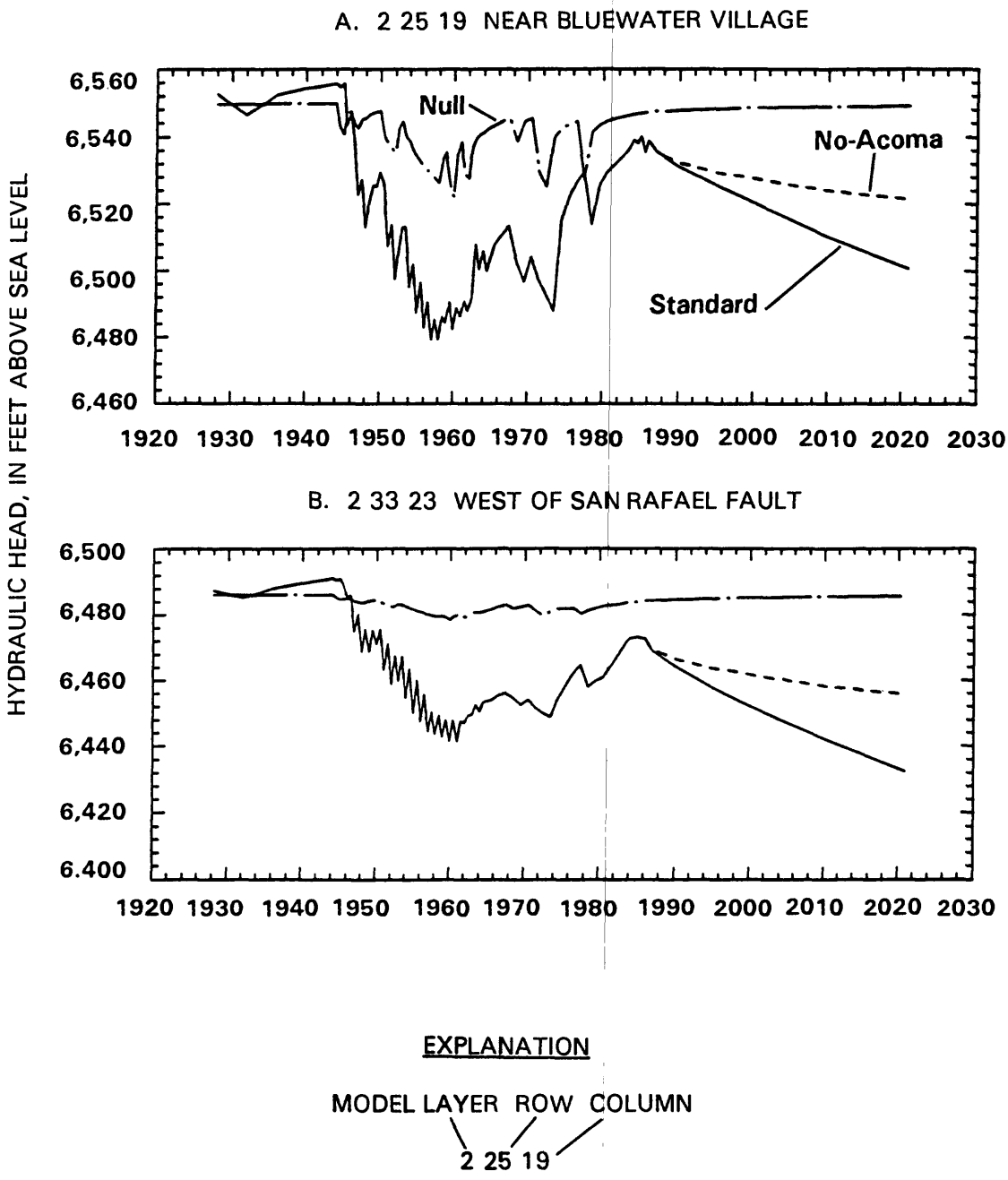

Figure 45.--Model-derived hydraulic heads from the null, standard, and no-Acoma simulations.

C. 2 54 6 EAST OF SAN RAFAEL FAULT

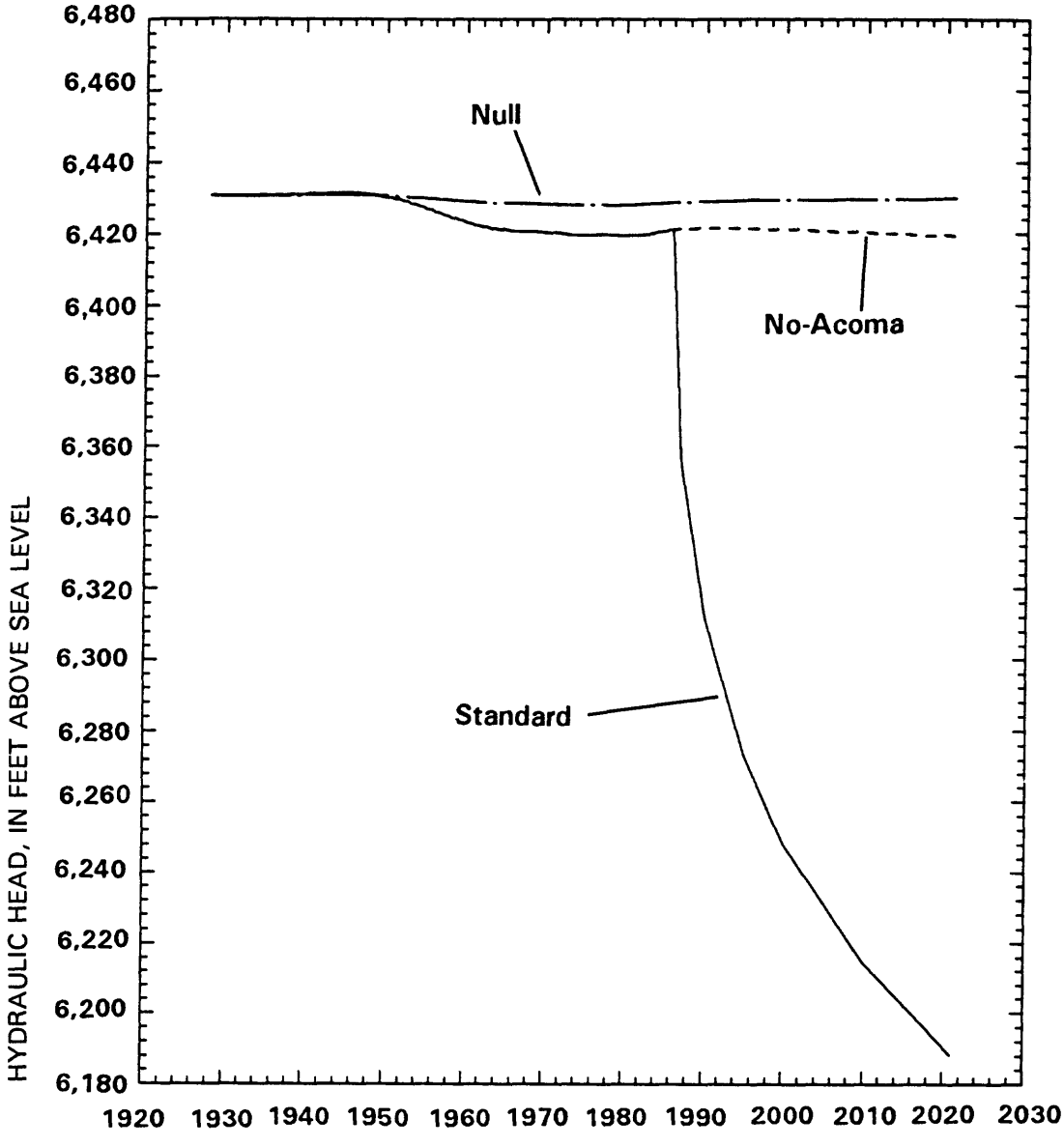

D. 1 44 11 LA VEGA (EAST OF SAN RAFAEL FAULT)

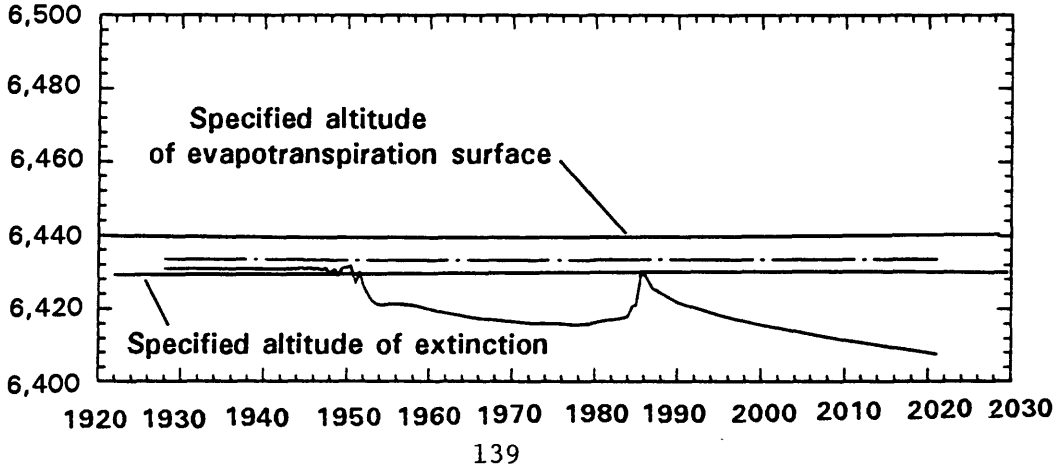

Model-derived hydraulic heads shown in figure 45D are for a location in layer 1, row 44, column 11, where ground-water evapotranspiration is simulated. At this site, the specified altitude of the evapotranspiration surface (representing land surface) is 6,440 feet above sea level and the specified extinction depth is 10 feet, or 6,430 feet above sea level. When the model-derived hydraulic head is below 6,430 feet, no evapotranspiration is simulated. If the model-derived hydraulic head had been equal to or greater than the evapotranspiration surface, the maximum specified flux of evapotranspiration (45 inches per year) would have been simulated. Because the simulated hydraulic head under the conditions of the null scenario was about 6 feet below the specified land surface, the flux was about one-third of the maximum, or about 15 inches per year. This can be verified by dividing the model-derived annual discharge (table 28, Supplemental Information) by the area of the model block (table 12).

Simulated effects on ground-water evapotranspiration

The reduction of ground-water evapotranspiration is the difference between that of the historical scenario and that of the null scenario. The difference is shown for three stress periods in table 7. The rate of discharge to ground-water evapotranspiration for all stress periods is shown in table 28 (Supplemental Information) and in figure 46. During the historical scenario (pre-1986 part of the standard scenario in fig. 46), the ground-water evapotranspiration rate (fig. 46A) changed from that of the steady-state simulation of -5.8 cubic feet per second in 1900.0 (not shown) to -4.5 cubic feet per second for the mid-1940's, subsequently changing steadily to -1.2 for the late 1970's and then to -2.5 for the mid-1980's. During the null scenario (fig. 46B), the rate of ground-water evapotranspiration was near the steady-state value of -5.8, and ranged from -5.8 to -5.5 cubic feet per second. Subtracting the null-scenario rate from the historical-scenario rate (fig. 46C) gives the model-derived effect of development, which is a positive value, indicating a reduced discharge by evapotranspiration in the historical scenario. This simulated reduction in discharge by evapotranspiration is termed "salvaged evapotranspiration" because it results from simulated-development-caused water-table drawdown, and in the budget, it offsets the net specified ground-water withdrawal. Simulated salvaged evapotranspiration increased from zero in 1900.0 to 1.5 cubic feet per second by the end of the first stress period in 1928.0 (fig. 46C), then held steady until about 1945 when ground-water withdrawals began. Simulated salvaged evapotranspiration was as much as 4.5 cubic feet per second by 1980.0 and then decreased to 3.3 cubic feet per second by 1986.0. The increased discharge by evapotranspiration in the 1980's reflects the simulated resaturation of near-surface valley fill, which resulted in turn from the simulated increase of ground-water flow across San Rafael fault from the San Andres-Glorieta aquifer into the valley fill and the simulated resurgence of Ojo del Gallo.

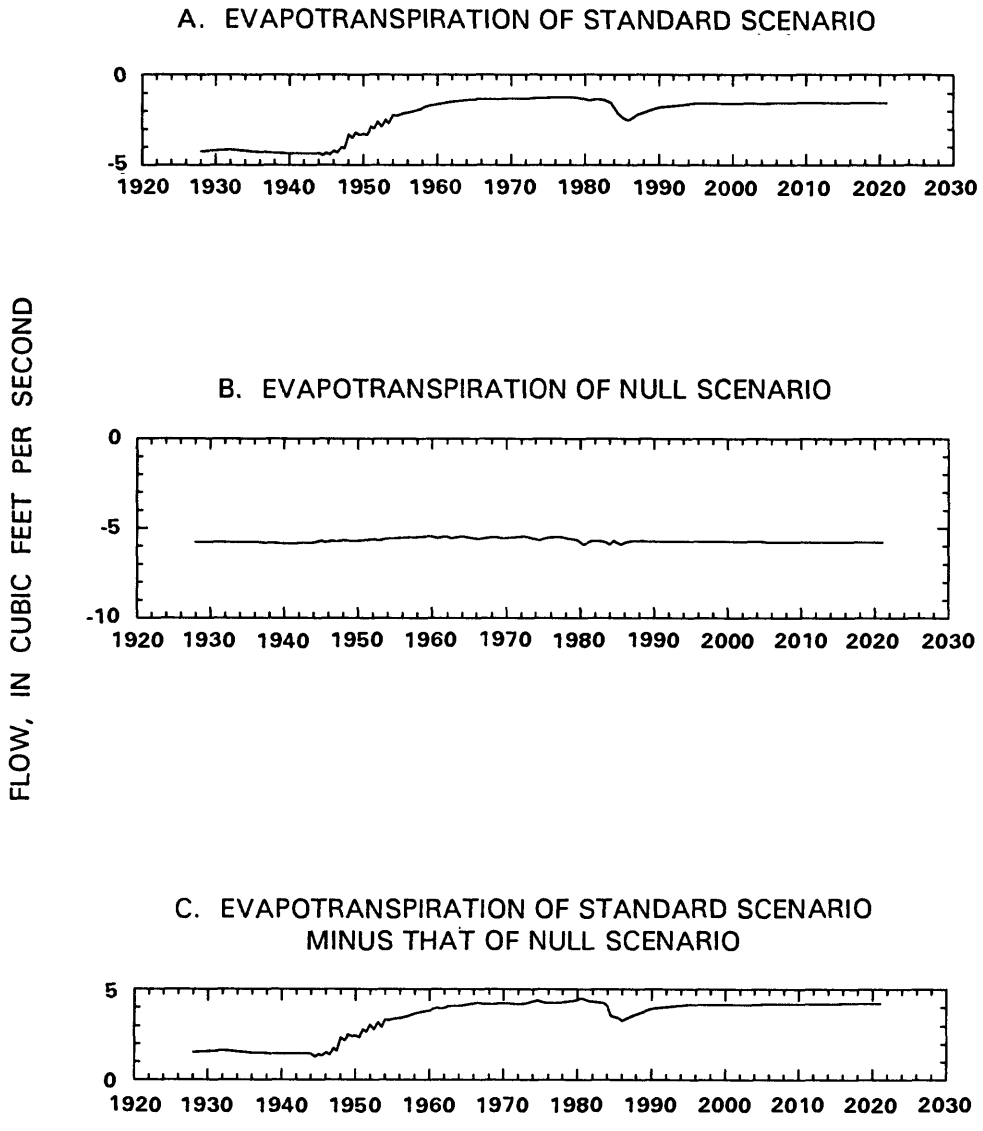

Figure 46.--Model-derived ground-water flow rates to the evapotranspiration boundary, and evapotranspiration of the standard scenario minus that of the null scenario.

As the salvaged evapotranspiration approaches the quantity of null-scenario evapotranspiration, less evapotranspiration remains that may be salvaged by additional drawdown of the water table. However, as previously explained, the model-derived rate of evapotranspiration could be greatly in error by an unknown quantity in all scenarios.

Simulated effect on ground-water storage

The simulated flow rate from ground-water storage attributed to development is shown in figure 47A as the difference between the net flow from ground-water storage in the standard scenario and the net flow from storage in the null scenario. Negative values in figure 47A for the late 1930's show water going into ground-water storage. This is caused by the simulation of surface-water-supplied irrigation during that time. Abruptly in 1946, there is a simulated net withdrawal from ground-water storage that continues through the 1950's, a time when a large part of irrigation water was supplied by ground-water withdrawals. Part of the fluctuations in ground-water storage are the result of seasonal changes in irrigation ground-water withdrawal and recharge. The magnitude and duration of fluctuations are less during the mid-1960's through the early 1980's when seasonal fluctuations were not simulated.

The cumulative change in simulated ground-water storage (fig. 47B) does not have the extreme fluctuations of the flow rate. In figure 47B, the slopes of short (half-year or year) segments of the curve represent the flow rates shown in figure 47A, and the slope of the entire curve represents an average flow rate. Because the historical and null scenarios both started from steady state in 1900.0, the difference in flow rate (fig. 47A) and volume (fig. 47B) would be zero at that time (not shown) and the average flow rate from 1900.0 to 1986.0 would be the 1986.0 volume divided by 86 years (0.24 hundred-thousand acre-feet in 86 years, or 0.4 cubic foot per second). However, the curve in figure 47B is not straight, and the generally negative slope before 1945.0 indicates that the simulated effect of development before 1945 was to increase the quantity of water in ground-water storage. This is consistent with the increase in model-derived hydraulic heads (figs. 37-40) and springflow at Ojo del Gallo (fig. 43) before 1945. The positive slope of the curve in figure 47B from 1945.0 until about 1960.0 indicates that the simulated effect of development in that period was to remove water from ground-water storage. After that, the simulated amount of water in ground-water storage does not change greatly until about 1974.0 when the simulated effect of development is to increase the quantity of water in ground-water storage until the end of the historical scenario. Because the quantity of water in ground-water storage is simulated as being proportional to hydraulic head, the cumulative flow from storage (fig. 47B) is approximately inversely proportional to the hydraulic-head hydrographs (figs. 37-42).

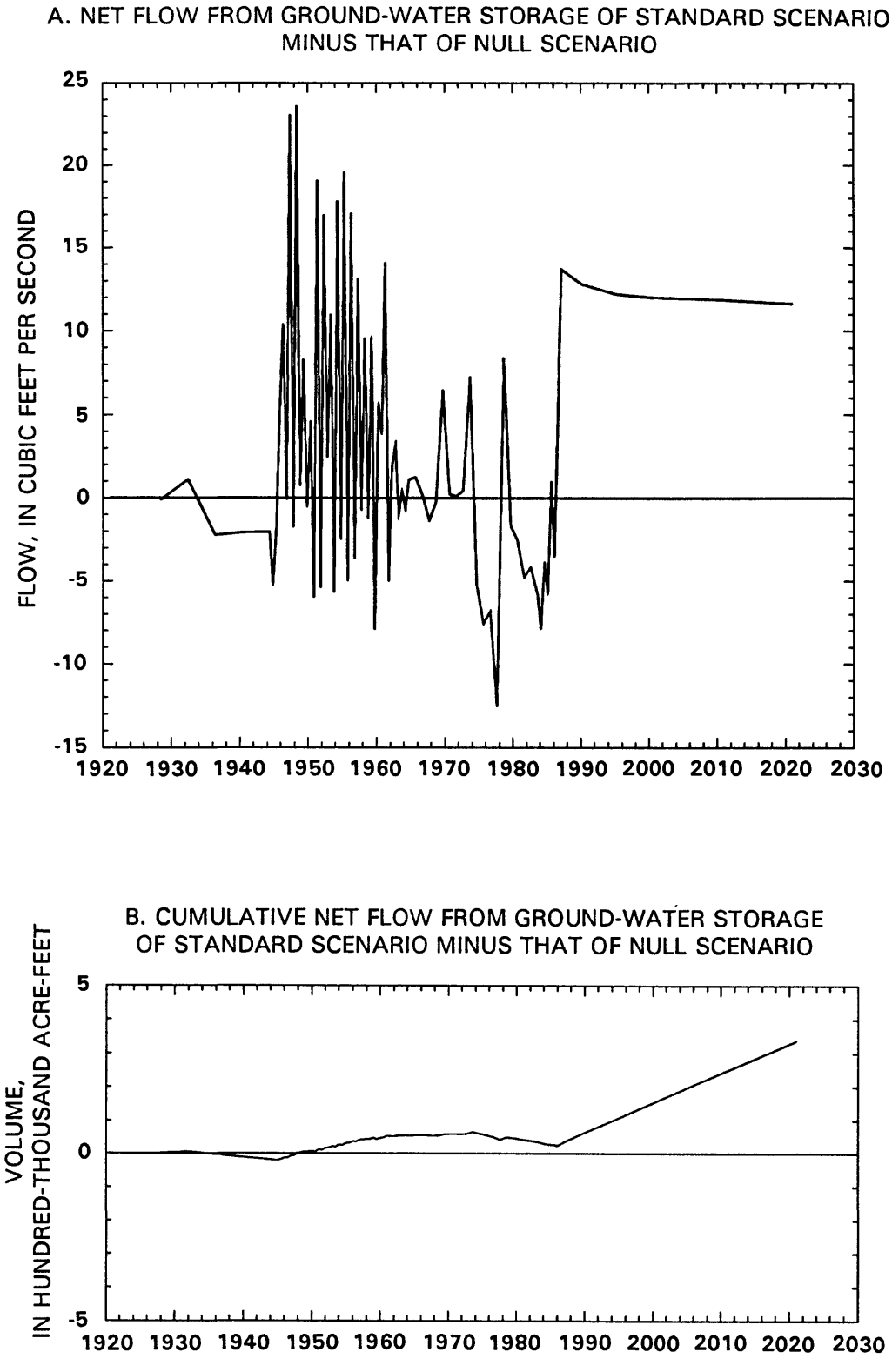

Figure 47.--Net flow from ground-water storage of the standard scenario minus that of the null scenario.

Simulated effects on springflow and streamflow

Estimation of the effects of past water developments was part of the purpose of this project. Past water developments include surface-water developments to the extent that they were accounted for in the river boundary of this model. Because some aspects of surface-water development are simulated by specified flows, separating surface-water development from ground-water development in the model budget was not attempted. The simulated effects of development are shown by the difference between springflows and streamflows of the historical scenario and those of the null.

The effects of development on springflow at Ojo del Gallo and on stream discharge from Gallo Creek and the Rio San Jose downstream from Horace Springs are shown in figure 48. The curve representing the historical scenario is marked "standard" because the curve extends beyond the 1986 endpoint of the historical scenario. The effect of development is the difference between the curve representing the null scenario and the curve representing the historical scenario. For a brief period during the late 1930's and early 1940's, discharge from Ojo del Gallo is greater for the historical scenario than for the null. This is caused by elevated hydraulic heads in the historical scenario that result from simulated irrigation in the Bluewater Toltec Irrigation District, which used only surface water. After the mid-1950's, the simulated effect of development on discharge is the full quantity of springflow simulated in the null scenario, except for a brief period in the mid-1980's.

The simulated effect of development on the discharge of Gallo Creek is the difference between curves representing the null and the historical scenarios in figure 48B. After the late 1940's, when the flow in the historical scenario is zero, the effect is the full quantity simulated in the null scenario, which ranges from as little as 1 cubic foot per second in about 1960 to as much as 2.5 cubic feet per second at the end of the historical scenario in 1986.0.

The simulated effect of development on the discharge of the Rio San Jose downstream from Horace Springs is the difference between curves representing the null and the historical scenarios shown in figure 48C. The difference is much greater and much more variable than the effect on ground-water discharge, which increased gradually to almost 0.5 cubic foot per second by the end of the historical scenario. Streamflow downstream from Horace Springs was about the same in both the historical and the null simulations for the late 1940's through the late 1970's because there was little surface flow into that reach (reach 11) in either simulation. Differences before and after that period were substantial because of surface flow into reach 11 in the null simulation. The effect of development shown in figure 48C averaged about 6 cubic feet per second between 1900.0 and 1986.0.

Simulated surface- and ground-water development affected simulated streamflows in other reaches of the river boundary. However, the effects of development fluctuated greatly, making graphs similar to those shown in figure 48 unintelligible. Therefore, the effects of development are discussed in terms of ground-water recharge and discharge at the stream boundary.

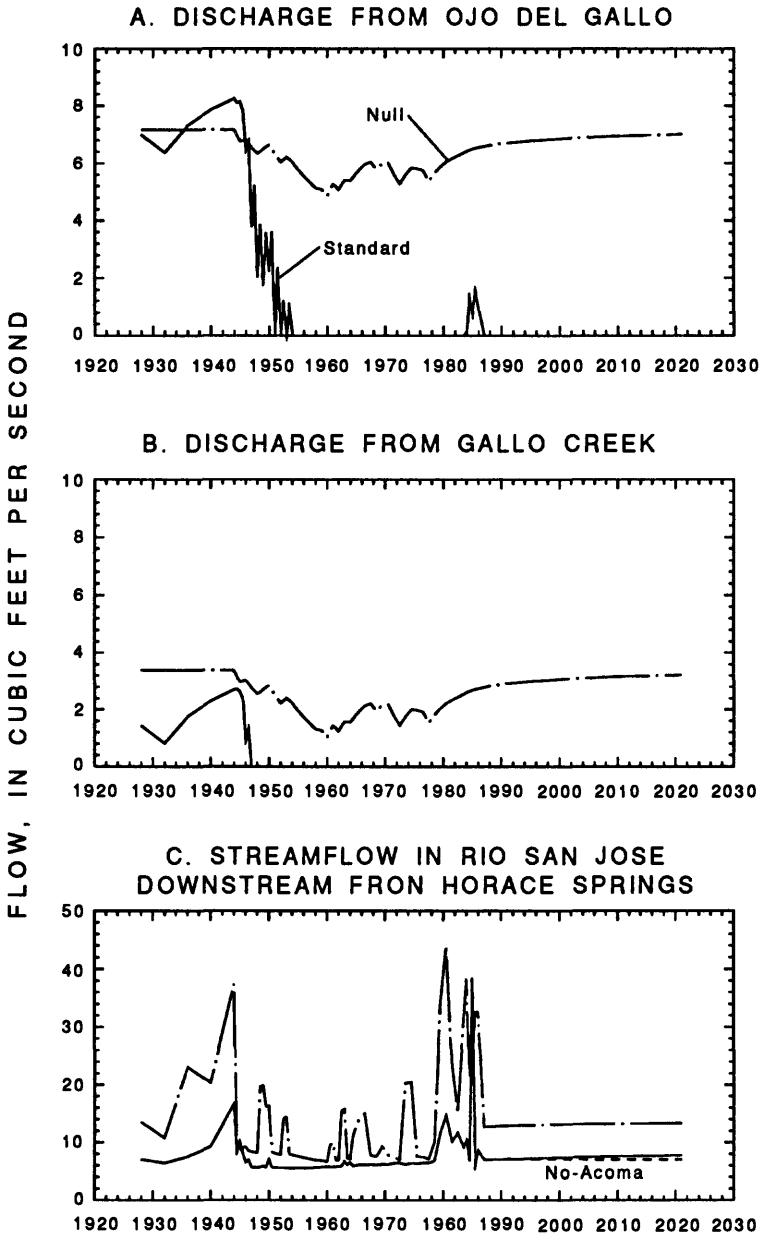

Figure 48.--Model-derived springflow and streamflow from the null, standard, and no-Acoma simulations.

Ground-water recharge (positive values) and discharge (negative values) are shown for the historical scenario in figure 49. For the purpose of comparison, similar recharge-discharge curves are shown for the null scenario in figure 50, and the differences (recharge derived in the historical scenario minus recharge in the null scenario) are shown in figure 51. The effects of development are most clearly shown by the differences in figure 51. Figure 49 shows selected individual reaches and combinations. In some cases, such as where the effects at two reaches are closely related, the combination is possibly more informative than the individual reaches. In these cases, figures 50 and 51 include only the combined reaches. Reaches 9 and 10, representing Ojo del Gallo, and La Vega and Gallo Creek are not included in figures 49-51 because, as previously discussed, simulated ground-water recharge in reach 10 is increased by the rate of simulated diversion for the Ojo del Gallo irrigated area. These reaches are included in figure 48. As in previous figures, the curves representing the historical scenario are marked "standard" because the curves extend beyond the 1986 endpoint of the historical scenario.

The following discussion follows the river boundary generally in downstream order. However, the differences between ground-water recharge derived in the historical scenario minus that in the null scenario are very small for the reaches of Cottonwood and Bluewater Creeks upstream from Bluewater Lake. In both creeks, the differences increased very gradually to 0.01 cubic foot per second by the end of the historical scenario in 1986.0.

Simulated recharge of the San Andres-Glorieta aquifer from Bluewater Lake (reach 2) generally was about 4 cubic feet per second in the historical scenario, ranging from 1 to 7 cubic feet per second (fig. 49A) depending on lake stage. Ground-water discharge to the stream in Bluewater Canyon (negative recharge in fig. 49B) generally was about half of ground-water recharge from Bluewater Lake. Because of the generally opposite sign of the curves in figure 49A and B, and the common dependence of these curves on lake stage, a summation (fig. 49C) was constructed to show a combined net ground-water recharge of about 2.5 cubic feet per second in the lake and canyon reaches in the historical scenario.

During the historical simulation, recharge to ground water (fig. 49D) along Bluewater Creek and the Rio San Jose from gaging station 08342000 near the mouth of Bluewater Canyon to gaging station 08343000 at Grants (reach 5) usually included the entire inflow specified for reach 5 to a maximum of about 6 to 8 cubic feet per second depending on hydraulic head in the underlying aquifer. Only the relatively large inflows of the late 1930's, 1940's, late 1970's, and early 1980's produced simulated outflows from this reach. This is consistent with measurements at these stations, which show almost no correlation between inflow and outflow for this part of the stream.

Very little ground-water interaction (fig. 49E) was simulated along reaches 6, 7, and 8 (from gaging station 08343000 to Gallo Creek). Although a short distance from the stream the water table is generally near or above the level of the streambed, simulated evapotranspiration caused the simulation of very small rates of ground-water recharge at times and the simulation of no flow at other times.

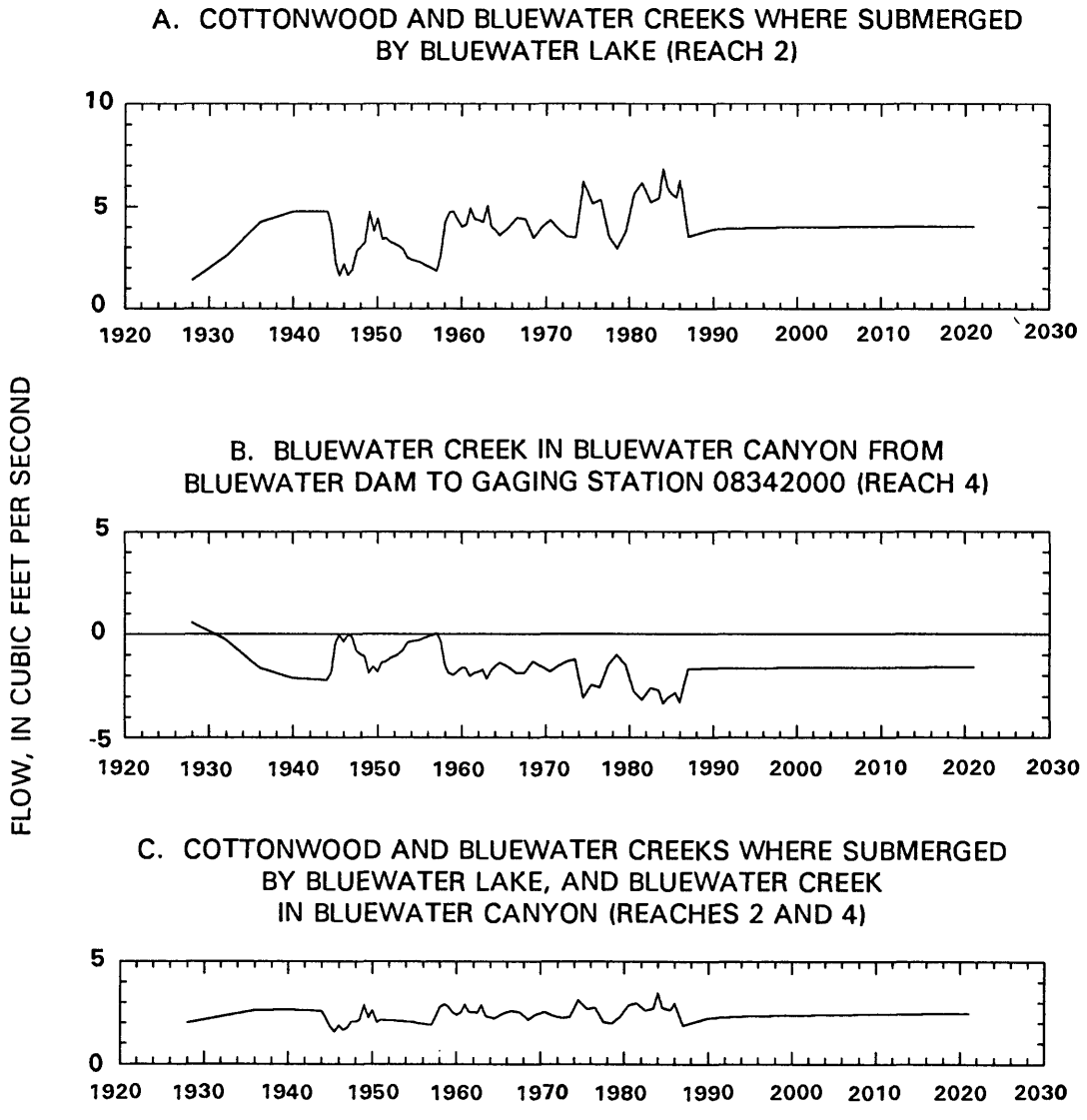

Figure 49.--Model-derived rates of ground-water recharge (positive) and discharge (negative) for selected river reaches and combinations of reaches for the standard model (historical and Acoma scenarios).

D. BLUEWATER CREEK AND RIO SAN JOSE FROM GAGING STATION 08342000 TO GAGING STATION 08343000 (REACH 5)

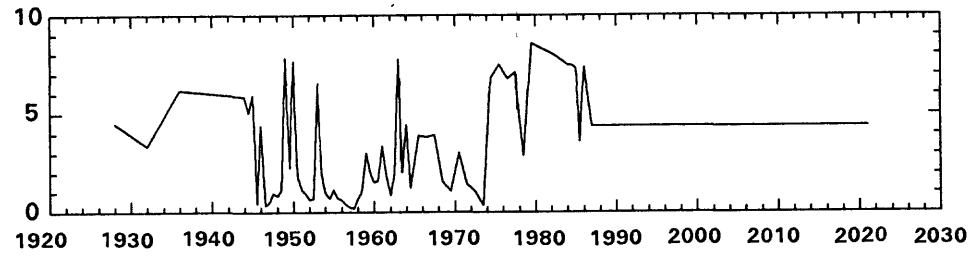

E. RIO SAN JOSE FROM GAGING STATION 08343000 TO GALLO CREEK (REACHES 6, 7, AND 8)

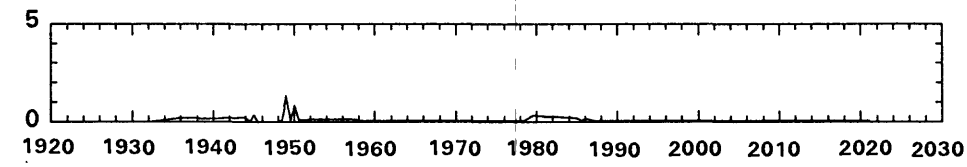

FLOW, IN CUBIC FEET PER SECOND

F. RIO SAN JOSE FROM GALLO CREEK TO GAGING STATION 08343500 DOWNSTREAM FROM HORACE SPRINGS (REACH 11)

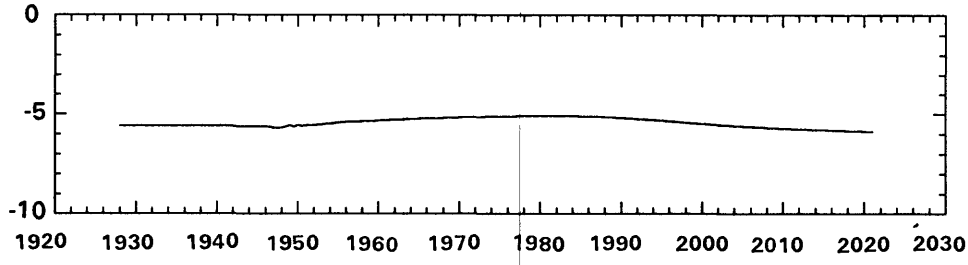

G. RIO SAN JOSE FROM GAGING STATION 08343000 TO GAGING STATION 08343500 DOWNSTREAM FROM HORACE SPRINGS (REACHES 6, 7, 8, AND 11)

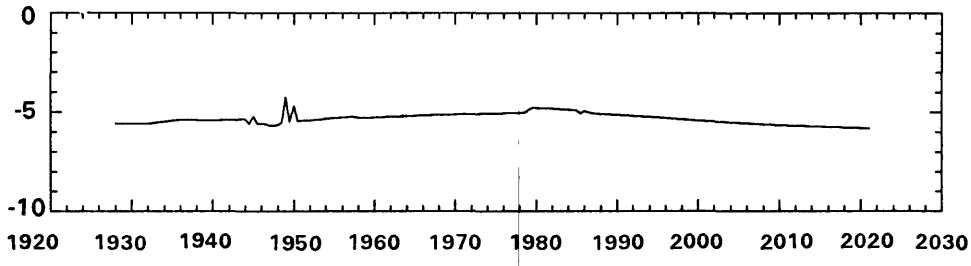

Figure 49.--Concluded.

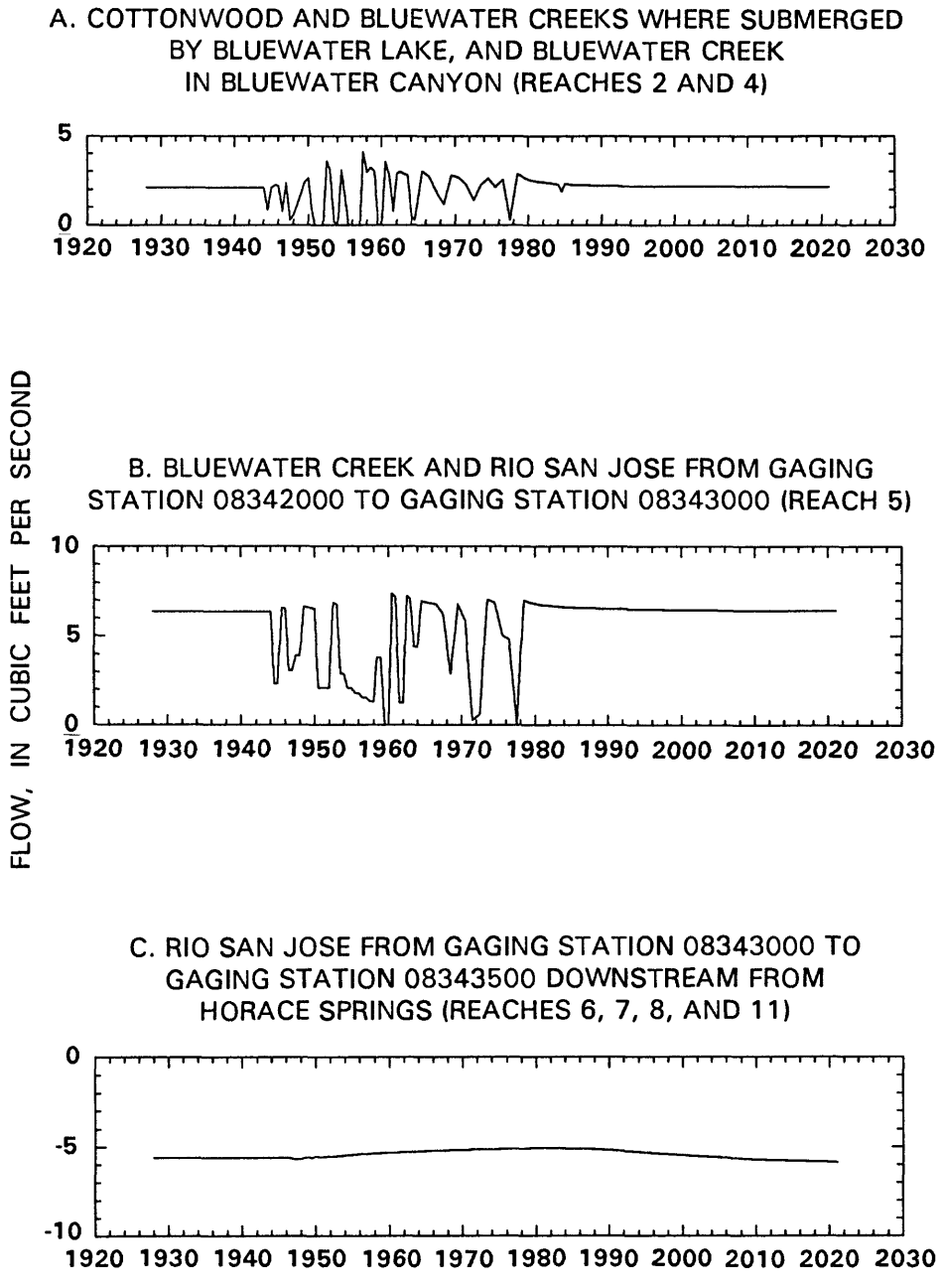

Figure 50.--Model-derived flow rates of ground-water recharge (positive) and discharge (negative) for selected river reaches and combinations of reaches for the null scenario.

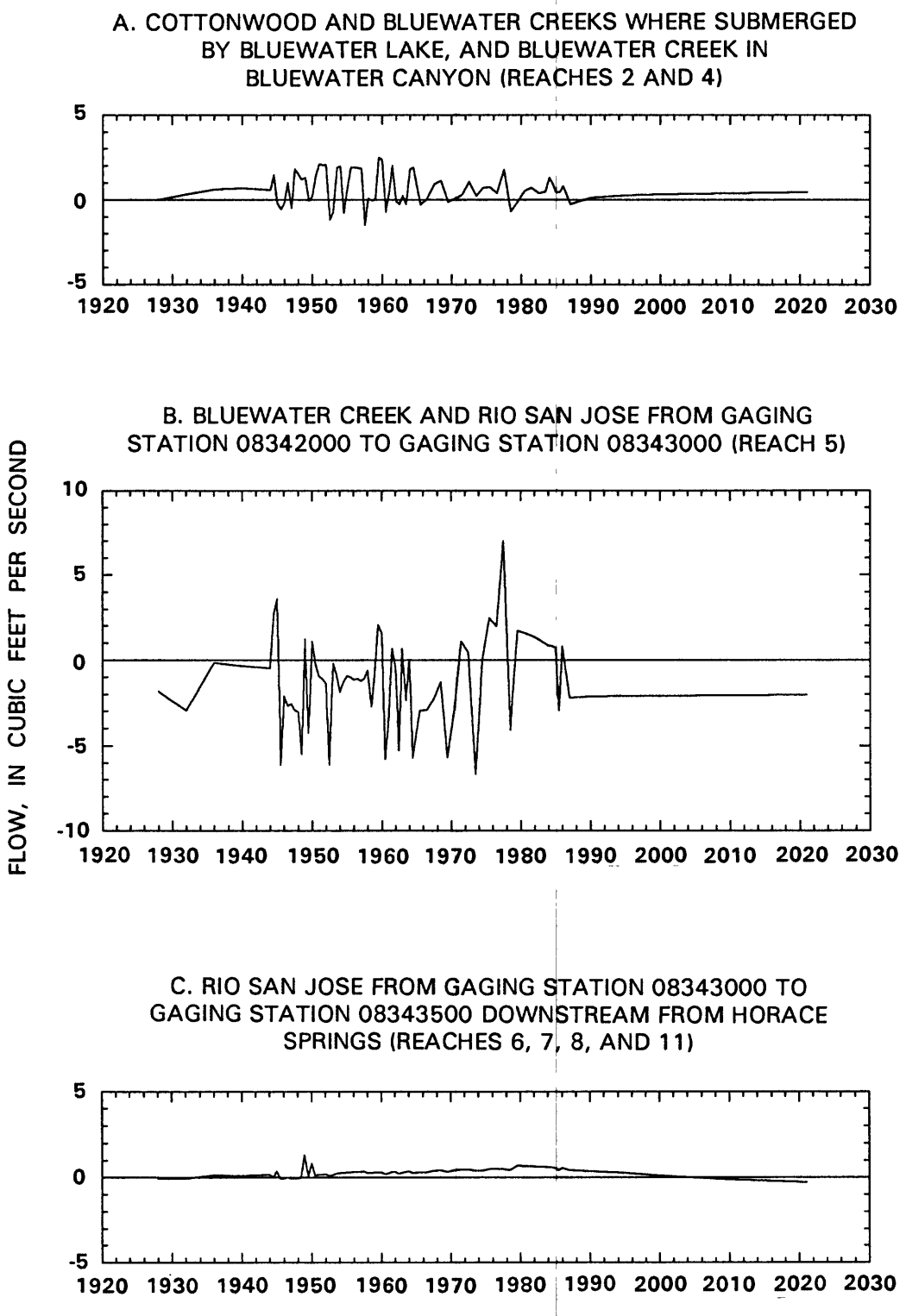

Figure 51.--Model-derived flow rates of ground-water recharge (positive) and discharge (negative) for selected river reaches and combinations of reaches for the standard scenario minus those for the null scenario.

Model-derived values of ground-water discharge (fig. 49F) along the Rio San Jose from Gallo Creek to gaging station 08343500 downstream from Horace Springs generally was about 5.5 cubic feet per second, decreasing gradually to about 5 cubic feet per second (rounded) by 1986.0. Most of the discharge was simulated for the Horace Springs part of the reach. Model-derived values of ground-water recharge and discharge shown in figure 49E and 49F are combined in figures 49G, 50, and 51 for brevity.

For the null scenario, model-derived values of ground-water recharge and discharge along selected reaches and combinations of reaches of the river boundary are shown in figure 50. Ground-water recharge for reaches 2 and 4, representing parts of Cottonwood and Bluewater Creeks submerged by Bluewater Lake, and Bluewater Creek in Bluewater Canyon (fig. 50A) generally was about 2 cubic feet per second, varying from zero to nearly 4 cubic feet per second, depending on streamflow and hydraulic head in the aquifer. Similarly, ground-water recharge (fig. 50B) in Bluewater Creek and the Rio San Jose from gaging station 08342000 to gaging station 08343000 generally was about 6 cubic feet per second except as limited by specified inflow to this reach. Recharge of as much as 7.5 cubic feet per second was simulated for the early 1960's when simulated hydraulic heads in the aquifers were low. The model-derived rate of ground-water discharge along the Rio San Jose from gaging station 08343000 to gaging station 08343500 downstream from Horace Springs (reaches 6, 7, 8, and 11) was generally about 5.5 cubic feet per second (fig. 50C) regardless of model-derived hydraulic heads in the San Andres-Glorieta aquifer. This is because variations in hydraulic head in the San Andres-Glorieta aquifer cause very slight changes in the gradient in the valley-fill aquifer upstream from Horace Springs.

Ground-water recharge in the historical scenario minus that in the null scenario (fig. 51) indicates the effect of water development. The effects of Bluewater Dam and the capture of streamflow along reaches 2 and 4 due to drawdown in the San Andres-Glorieta aquifer are not distinguishable in figure 51. The combined effect simulated was an increase of ground-water recharge of about 1 cubic foot per second (fig. 51A) along the parts of Cottonwood and Bluewater Creeks submerged by Bluewater Lake and Bluewater Creek in Bluewater Canyon (reaches 2 and 4). The simulated effect of development in these reaches varied from as much as 2.5 cubic feet per second of recharge to as much as nearly 2 cubic feet per second of apparent discharge. The apparent discharge is better described as a reduced-recharge effect of development. This is shown when the recharge simulated under the historical scenario is less than that simulated under the null scenario.

The reduced-recharge effect of development is also seen (fig. 51B) for the part of Bluewater Creek and the Rio San Jose from gaging station 08342000 to gaging station 08343000 (reach 5). Ground-water discharge along that reach was never simulated (figs. 49D and 50B). The reduced recharge results from a specified inflow to that reach that is generally less in the historical scenario than in the null. The reduced recharge shown in figure 51B averages 1 cubic foot per second over the 86-year period of the historical scenario.

Very little effect of development is shown (fig. 51C) on ground-water discharge to the Rio San Jose from gaging station 08343000 to gaging station 08343500 downstream from Horace Springs (reaches 6, 7, 8, and 11). The trend in figure 51C is representative of the effect on reach 11, which includes Horace Springs, and the short-term fluctuations are representative of the upstream reaches 6, 7, and 8 through the city of Grants. The reduced-discharge effect on reach 11 increases gradually to almost 0.5 cubic foot per second by the end of the historical scenario (in 1986.0). The minor effects of development depicted in figure 51C do not include the development effect of reduced surface flow into that reach. Because it is often difficult to isolate ground-water discharge from surface flow and because 0.5 cubic foot per second is within the margin of measurement error of the gage, it would be difficult to compare the simulated reduction of ground-water discharge to the stream with similar values estimated from changes in measured streamflow. Therefore, the accuracy of this model-derived quantity is unknown.

Description and Results of Projections

Projections were done to estimate the effects of a hypothetical discharge of 10,000 acre-feet per year from the San Andres-Glorieta aquifer in the vicinity of T. 9 N., R. 9 W. (near Acoma-1 test well 9.9.28.1344, model row 54, column 6). The discharge would be for the purpose of irrigation. Because in this location as much as 1,700 feet of Chinle Formation confines the San Andres-Glorieta aquifer and separates it from the valley fill, deep percolation of irrigation water would recharge the valley fill rather than the San Andres-Glorieta aquifer. Therefore, recharge of the valley fill of 3,300 acre-feet per year was simulated in layer 1, row 53, column 6, assuming one-third of irrigation water would percolate to a depth below the crop root zone. Together, the projected withdrawal of 10,000 acre-feet per year and the associated recharge of 3,300 acre-feet per year (a net withdrawal of 6,700 acre-feet per year) distinguish the "Acoma" scenario from the "no-Acoma" scenario. The no-Acoma scenario was prepared for the purpose of comparison with the Acoma scenario and included all the stresses of the Acoma scenario except for the 10,000-acre-foot withdrawal and the 3,300-acre-foot recharge. The following description of the no-Acoma scenario also applies to the Acoma scenario.

The no-Acoma scenario used the end of the historical scenario as an initial condition. Six stress periods as previously defined (table 4, in text) were appended to those of the historical scenario. The Acoma scenario used the same initial conditions and time descretization as the no-Acoma scenario.

Specified fluxes and streamflows simulating developed conditions were estimated on the basis of the pre-1986 level of water development. A specified altitude of 7,372 feet represented the average altitude for Bluewater Lake, and values of hydraulic conductance along that reach were set corresponding to the width of the lake at that altitude (table 19, Supplemental Information). The specified surface-water inflow for reach 5 representing Bluewater Creek downstream from Bluewater Canyon (4.37 cubic feet per second, table 19; or approximately 3,170 acre-feet per year) was the

average measured streamflow for 1927-72 (5,970 acre-feet per year; Risser, 1982, table 4) minus the average surface water applied to irrigated land in the Bluewater-Toltec Irrigation District for 1927-72 (approximately 2,800 acre-feet per year; table 1). Specified ground-water withdrawal for the Bluewater-Toltec Irrigation District (3.86 cubic feet per second, table 22; or approximately 2,800 acre-feet per year) was estimated as the 1986 irrigated acreage (2,650 acres, table 1, note 17) times the assumed total application rate (2.1 acre-feet per acre per year), minus the surface-water application (2,800 acre-feet per year). Specified recharge for the Bluewater-Toltec Irrigation District (2.58 cubic feet per second, table 22; or 1,869 acre-feet per year) was estimated as approximately one-third of the 1986 acreage times the assumed total application rate. No irrigation was projected for the Ojo del Gallo or south San Rafael areas. Municipal withdrawals (table 23) at Grants and Milan were assigned values equal to the averages for the 1980's, and other municipal and industrial withdrawals were continued without change from the values simulated during the last historical stress period (1985.5-1986.0).

Specified fluxes and streamflows simulating natural features of the geohydrologic system were set to average (steady-state) values. These include mountain and malpais recharge, flows into the upper reaches of Bluewater and Cottonwood Creeks, and underflows.

In short, the no-Acoma scenario projected no changes from the pre-1986 degree of water development and natural recharge and streamflows were specified as average. The only difference between the no-Acoma scenario and the Acoma scenario was the withdrawal of 10,000 acre-feet per year and the recharge of 3,300 acre-feet per year.

Drawdowns from the hydraulic heads of the 1980's were projected by the no-Acoma simulation. Heads simulated by the no-Acoma simulation are shown in figure 45 as dashed lines. Drawdowns of as much as about 17 feet below the 1986.0 hydraulic head were simulated for the area near Bluewater Village (fig. 45A) and generally for the area west of San Rafael fault (fig. 45B). East of San Rafael fault (fig. 45C), drawdowns from the heads of the 1980's were as much as about 3 feet.

The no-Acoma simulation resulted in drawdowns from simulated hydraulic heads for the 1980's because an unusually plentiful water supply was simulated for the late 1970's and early 1980's. The precipitation-based estimate of inflow to reach 5 during the late 1970's and early 1980's was greater than the average inflow, which was based on 1927-72 streamflow measurements. Also, estimated ground-water withdrawals for irrigation during the late 1970's and early 1980's were less than average because surface water was available.

Hydraulic heads simulated by the Acoma scenario are shown in figure 45 as solid lines designated as "standard." The difference between the solid and dashed (no-Acoma) lines in figure 45 is the model-derived drawdown caused by the 10,000-acre-foot withdrawal simulated in the Acoma scenario. This drawdown was projected to be as much as about 20-25 feet by 2020 in the area west of San Rafael fault (fig. 45A and B), and 10 times that east of San Rafael fault (fig. 45C).

The hydraulic heads simulated under the Acoma scenario were subtracted from the heads simulated under the no-Acoma scenario to construct maps of projected drawdown that might result from the 10,000-acre-foot-per-year withdrawal. After 1 year (fig. 52), the drawdown was more than 50 feet in the vicinity of this withdrawal. After 9 years (fig. 53), drawdown exceeded 140 feet in the same location, but was less than 10 feet in the Grants-Bluewater area. After 35 years (fig. 54), the model-derived drawdown was more than 220 feet in the vicinity of the 10,000-acre-foot withdrawal and was as much as 25 feet in the Grants-Bluewater area. In general, the drawdown was much greater east of San Rafael fault than it was west of the fault and drawdown was simulated at the arbitrary no-flow boundaries. The effect of the arbitrary boundaries was investigated by making the projection using other types of boundaries in a series of sensitivity tests.

The items in the model budget of the no-Acoma scenario were subtracted from the items in the model budget of the Acoma scenario to indicate the simulated source of the 10,000-acre-foot withdrawal (table 8). Because recharge was specified to account for irrigation-return flow, however, the 10,000-acre-foot withdrawal (13.8 cubic feet per second) resulted in a recharge of 4.6 cubic feet per second to the valley-fill aquifer and a net withdrawal of 9.2 cubic feet per second (table 8, Acoma minus no-Acoma). Because recharge affects the river and evapotranspiration boundaries, the exact simulated source or destination of the entire withdrawal and the entire recharge cannot be determined from the model budgets. After 1 year, the simulated source of most (13.1 cubic feet per second) of the withdrawal appears to have been storage in the San Andres-Glorieta aquifer and the destination of most (4.0 cubic feet per second) of the recharge appears also to have been storage in the valley-fill aquifer. Ground-water storage was the simulated source of 9.11 cubic feet per second (99 percent) of the net withdrawal. The simulated source of the remainder of the net withdrawal was a reduction of ground-water evapotranspiration. The net values of the other items of the budget, the river, and the general-head and constant-head boundaries were zero. After 9 years, ground-water storage was the simulated source of 9.18 cubic feet per second (99.7 percent of the net withdrawal). However, the simulated destination of some (0.13 cubic foot per second) of the recharge is the river boundary. The simulated source of the remainder was a reduction of ground-water evapotranspiration. After 35 years, the net contribution of ground-water storage (9.6 cubic feet per second) is more than the net withdrawal, whereas both ground-water evapotranspiration and discharge to the river boundary increase due to increasing hydraulic heads (not shown) in part of the valley-fill aquifer near the location of the Acoma irrigation-return flow. The simulated source of most of the 10,000-acre-foot withdrawal is concluded to be aquifer storage. The precision reported here and in table 8 only shows that the budget balances and does not reflect the accuracy of the model-derived values.

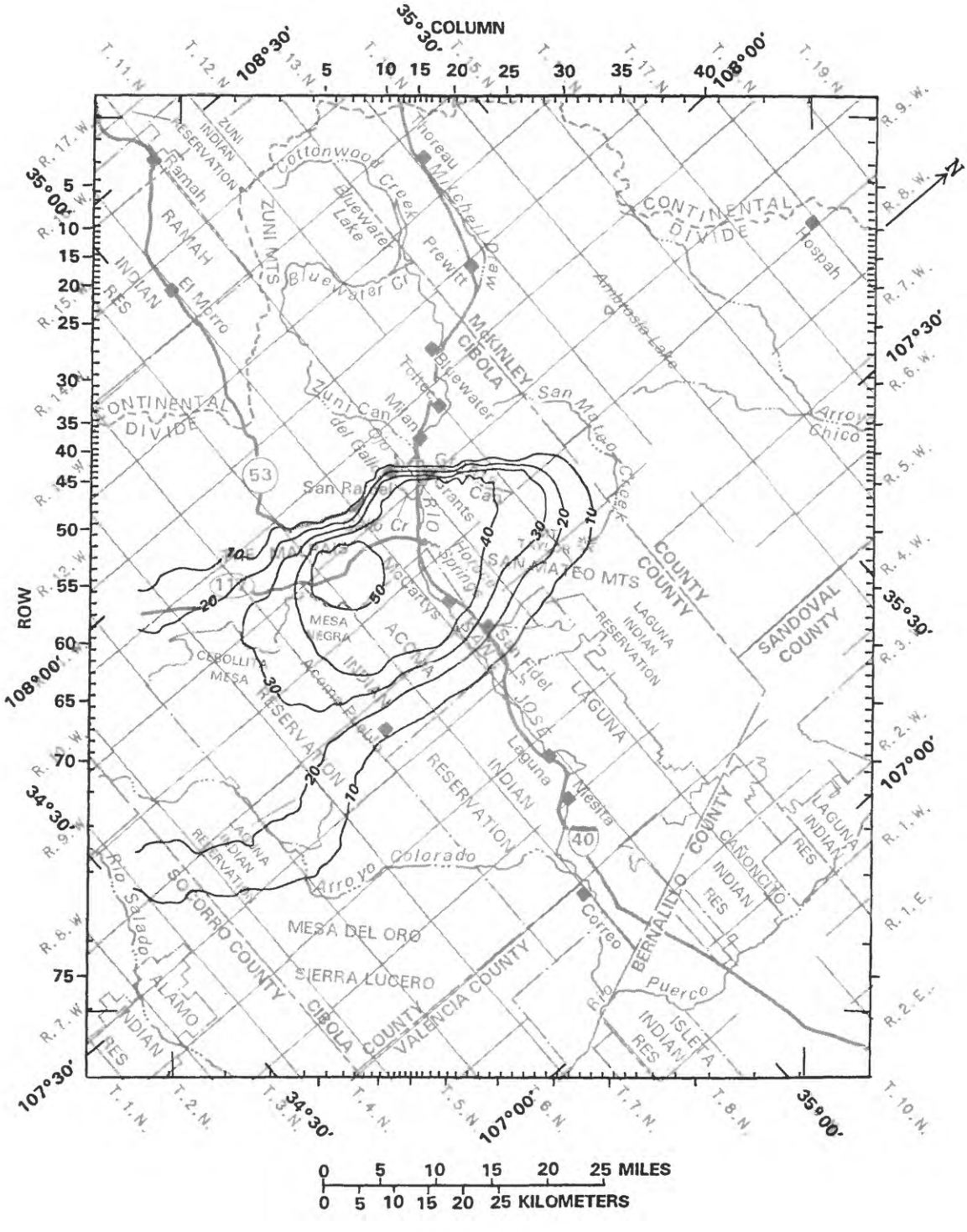

Figure 52.--Projected drawdown after 1 year under the Acoma scenario.

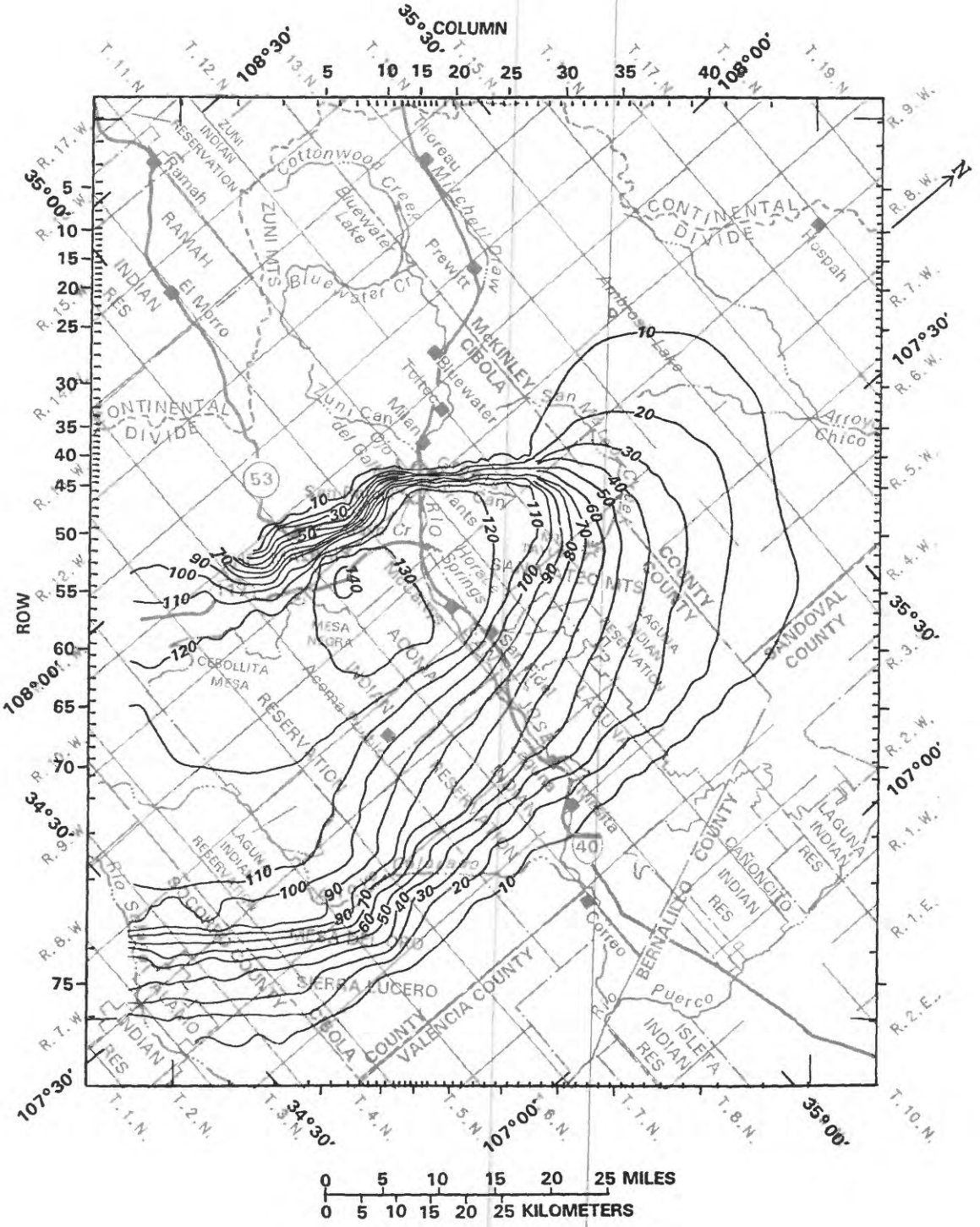

Figure 53.--Projected drawdown after 9 years under the Acoma scenario.

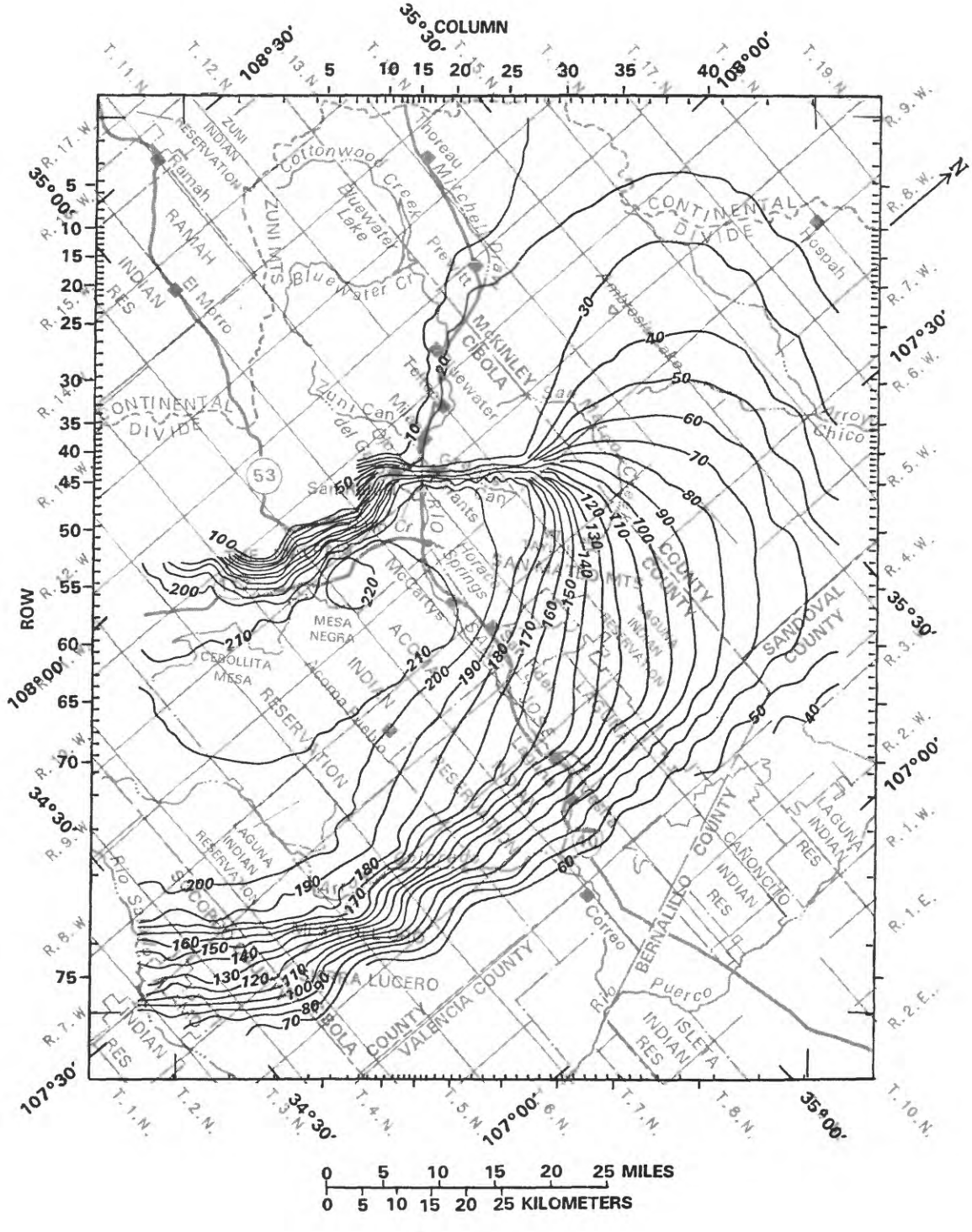

Figure 54.--Projected drawdown after 35 years under the Acoma scenario.

Table 8.--Water budget for selected stress periods of the Acoma and no-Acoma scenarios

[The sum of recharge and discharge by river reach equals the net, allowing for rounding error. Inflows are positive and outflows are negative. Specified flow is divided into 11 hydrologic boundaries. Model-derived flows to and from the river boundary are listed by reach. Reaches are shown in figure 29. Apparent discrepancies in the hundredths place are rounding errors]

EXPLANATION OF BOUNDARIES SIMULATED BY SPECIFIED FLOW

(A) Recharge to the valley fill in the barren basalt area of The Malpais;

(B) recharge to the valley fill from flow in canyons that empty onto the valley fill from the eastern end of the mountains of the Zuni uplift;

(C) recharge to the San Andres-Glorieta aquifer in the mountains of the Zuni uplift;

(D) underflow in the valley fill at Mitchell Draw, San Mateo Creek, and Grants Canyon;

(E) underflow in the valley fill downstream from Horace Springs;

(F) ground-water withdrawals in the Bluewater-Toltec Irrigation District;

(G) ground-water recharge in the Bluewater-Toltec Irrigation District;

(H) ground-water withdrawals in the south San Rafael and Acoma (hypothetical) irrigated area and ground-water withdrawals that simulate the net irrigation withdrawal in the Ojo del Gallo irrigated area;

(I) ground-water recharge in the south San Rafael and Acoma (hypothetical) irrigation area;

(J) ground-water withdrawals for municipal and industrial use; and

(K) ground-water recharge by municipal and industrial uses.

Table 8.--Water budget for selected stress periods of the Acoma and no-Acoma scenarios--Continued

	Stress period 71 after 1 year of projection			Stress period 73 after 9 years of projection			Stress period 76 after 35 years of projection		
	Acoma	No-Acoma	Acoma minus no-Acoma	Acoma	No-Acoma	Acoma minus no-Acoma	Acoma	No-Acoma	Acoma minus no-Acoma
Ground-water storage									
Inflow	19.78	6.67	13.11	16.25	3.23	13.02	12.67	2.14	10.53
Outflow	-6.69	-2.69	-4.00	-4.34	-0.50	-3.84	-1.07	-0.14	-0.93
Net	13.09	3.98	9.11	11.91	2.73	9.18	11.60	2.00	9.60
Specified flow									
Inflow	20.40	15.80	4.60	20.40	15.80	4.60	20.40	15.80	4.60
Outflow	-28.73	-14.92	-13.81	-28.73	-14.92	-13.81	-28.73	-14.92	-13.81
Net	-8.33	0.88	-9.21	-8.33	0.88	-9.21	-8.33	0.88	-9.21
	Specified flow subdivided by boundary								
Boundary									
(A)	6.70	6.70	0.0	6.70	6.70	0.0	6.70	6.70	0.0
(B)	0.70	0.70	0.0	0.70	0.70	0.0	0.70	0.70	0.0
(C)	3.52	3.52	0.0	3.52	3.52	0.0	3.52	3.52	0.0
(D)	1.60	1.60	0.0	1.60	1.60	0.0	1.60	1.60	0.0
(E)	-2.50	-2.50	0.0	-2.50	-2.50	0.0	-2.50	-2.50	0.0
(F)	-3.86	-3.86	0.0	-3.86	-3.86	0.0	-3.86	-3.86	0.0
(G)	2.58	2.58	0.0	2.58	2.58	0.0	2.58	2.58	0.0
(H)	-13.81	0.0	-13.81	-13.80	0.0	-13.81	-13.80	0.0	-13.81
(I)	4.60	0.0	4.60	4.60	0.0	4.60	4.60	0.0	4.60
(J)	-8.20	-8.20	0.0	-8.20	-8.20	0.0	-8.20	-8.20	0.0
(K)	0.34	0.34	0.0	0.34	0.34	0.0	0.34	0.34	0.0

Table 8.--Water budget for selected stress periods of the Acoma and no-Acoma scenarios--Continued

	Stress period 71 after 1 year of projection			Stress period 73 after 9 years of projection			Stress period 76 after 35 years of projection		
	Acoma	No-Acoma	Acoma minus no-Acoma	Acoma	No-Acoma	Acoma minus no-Acoma	Acoma	No-Acoma	Acoma minus no-Acoma
River boundary									
Hydrologic boundary inflow	11.64	11.79	-0.15	10.08	10.10	-0.02	10.13	10.22	-0.09
Hydrologic boundary outflow	-10.38	-10.54	0.16	-8.51	-8.40	-0.11	-8.91	-8.27	-0.64
Net	1.26	1.26	0.00	1.57	1.70	-0.13	1.22	1.95	-0.73
	River boundary by reach								
Reach									
1	0.14	0.14	0.00	0.19	0.19	0.00	0.25	0.25	0.00
2	3.56	3.56	0.00	3.99	3.98	0.01	4.05	4.04	0.01
3	-0.07	-0.07	0.00	-0.08	-0.08	0.00	-0.08	-0.08	0.00
4	-1.66	-1.66	0.00	-1.63	-1.64	0.01	-1.57	-1.60	0.03
5	4.37	4.37	0.00	4.37	4.37	0.00	4.37	4.37	0.00
6	0.00	0.00	0.00	0.00	0.00	0.00	0.00	0.00	0.00
7	0.00	0.00	0.00	0.00	0.00	0.00	0.00	0.00	0.00
8	0.05	0.05	0.00	0.06	0.05	0.01	0.07	0.07	0.00
9	0.00	0.00	0.00	0.00	0.00	0.00	0.00	0.00	0.00
10	0.00	0.00	0.00	0.00	0.00	0.00	0.00	0.00	0.00
11	-5.13	-5.13	0.00	-5.31	-5.18	-0.13	-5.87	-5.09	-0.78

Table 8.--Water budget for selected stress periods of the Acoma and no-Acoma scenarios--Concluded

	Stress period 71 after 1 year of projection			Stress period 73 after 9 years of projection			Stress period 76 after 35 years of projection		
	Acoma	No-Acoma	Acoma minus no-Acoma	Acoma	No-Acoma	Acoma minus no-Acoma	Acoma	No-Acoma	Acoma minus no-Acoma
Evapotranspiration from water table									
Inflow	0.00	0.00	0.00	0.00	0.00	0.00	0.00	0.00	0.00
Outflow	-2.24	-2.34	0.10	-1.60	-1.64	0.04	-1.54	-1.22	-0.32
Net	-2.24	-2.34	0.10	-1.60	-1.64	0.04	-1.54	-1.22	-0.32
General-head boundary									
Inflow	0.00	0.00	0.00	0.00	0.00	0.00	0.00	0.00	0.00
Outflow	-4.02	-4.02	0.00	-3.90	-4.02	0.12	-3.35	-4.01	0.66
Net	-4.02	-4.02	0.00	-3.90	-4.02	0.12	-3.35	-4.01	0.66
Constant-head boundary									
Inflow	0.44	0.44	0.00	0.44	0.44	0.00	0.44	0.44	0.00
Outflow	-0.13	-0.13	0.00	-0.14	-0.14	0.00	-0.14	-0.14	0.00
Net	0.31	0.31	0.00	0.31	0.31	0.00	0.30	0.30	0.00
Sum of inflow	52.26	34.70	17.56	47.17	29.57	17.60	43.64	28.60	15.04
Sum of outflow	-52.19	-34.64	-17.55	-47.22	-29.62	-17.60	-43.74	-28.70	-15.04
Discrepancy	0.07	0.07	0.00	-0.04	-0.04	0.00	-0.10	-0.10	0.00
Percent discrepancy	0.13	0.20	0.00	-0.08	-0.14	0.00	-0.23	-0.35	0.00

The simulated reduction of evapotranspiration in La Vega can be attributed mainly to the level of development simulated in the no-Acoma scenario. In the simulation, the water that is evapotranspired is largely supplied by springflow from Ojo del Gallo. As under the Acoma scenario, simulated flow from Ojo del Gallo under the no-Acoma scenario ceased early in the projection (fig. 43A). That is, projected cessation of discharge from Ojo del Gallo is caused by the no-Acoma level of ground- and surface-water withdrawals, not by the additional 10,000-acre-foot withdrawal of the Acoma scenario. As the simulated discharge from Ojo del Gallo diminishes, simulated water levels decrease in the valley fill downstream from the spring and, as a result, simulated evapotranspiration is also reduced. Because the cessation of discharge from Ojo del Gallo and the accompanying drawdown of the valley-fill aquifer are caused by the no-Acoma withdrawals, the resulting salvage of evapotranspiration also is a result of the no-Acoma withdrawals. It is possible to reduce only the remaining evapotranspiration by additional drawdowns. The model-derived value of evapotranspiration that continues under conditions of the no-Acoma scenario is 2.34 cubic feet per second after 1 year of projection and 1.22 cubic feet per second after 35 years (table 8).

The simulated effect on Horace Springs was very small in both simulations. Simulated ground-water discharge to the part of the stream that includes Horace Springs (reach 11) was reduced by 0.04 cubic foot per second by the end of the 35-year projection under the no-Acoma scenario. Ground-water discharge to the same reach increased by 0.74 cubic foot per second under the Acoma scenario because of the simulation of additional recharge from irrigation.

The simulated resurgence of springflow at Ojo del Gallo during the late 1970's and 1980's is mainly the result of the specification of greater-than-average mountain recharge, greater-than-average streamflow in Bluewater Creek, and less-than-average ground-water withdrawals for irrigation during that time (figs. 27 and 32; and table 19). These factors resulted in model-derived hydraulic heads rising to a temporary high during the late 1970's and early 1980's even though municipal and industrial ground-water withdrawals generally were trending upward (fig. 34). The simulated abrupt reduction of municipal and industrial ground-water withdrawals in the early 1980's allowed simulated flow temporarily at Ojo del Gallo after simulated hydraulic heads already had increased. However, because projected discharge from Ojo del Gallo ceases under the conditions of the no-Acoma scenario, which includes average natural recharge and streamflow and no additional water development, a larger reduction of specified withdrawals would be needed to assure simulated springflow under normal conditions of recharge and streamflow. To the extent that the simulation might accurately represent the natural flow system, these conclusions would apply to the question of continued springflow at Ojo del Gallo.

MODEL EVALUATION

Model evaluation consists of sensitivity tests and a qualitative description of some of the weaknesses and strengths of the model. Sensitivity testing consisted of changing individual model characteristics by a small amount to indicate the effect of these characteristics on model results, such as projected drawdown. Large changes so distort the model that conclusions made from them are illusory.

Sensitivity Tests

After the model had been adjusted to a point where more adjustment did not substantially improve the comparison between measured and model-derived values, sensitivity tests were made. A near-infinite number of tests could be devised, but the limited number of tests described in the following pages seemed to be appropriate on the basis of experience gained while doing model adjustment.

For the historical part of the simulation (before 1986.0), tests were evaluated by comparing the results of the changed model in each test with the unchanged ("standard") model and with measured values. The results compared were the hydrographs of model-derived streamflows and hydraulic heads, and the statistical differences between measured and model-derived hydraulic heads (table 29). The mean absolute difference was given priority over the other statistics as an indicator of sensitivity. Entries in table 29 are in order of increasing mean absolute difference. For the projections, tests were evaluated only by comparison with the standard.

Sensitivity to Specified Values of Recharge and Streamflow

Two tests were conducted to determine the cause of the fluctuations in the model-derived water-level hydrographs for the Grants-Bluewater area. The simulation of these fluctuations was critical in the model-adjustment phase.

In the first test, recharge rates for the Zuni uplift and The Malpais areas were changed from variable, weather-related values to constant, average values. Steady recharge resulted in a slight increase in model-derived streamflow downstream from Horace Springs of 0.1 cubic foot per second between 1966 and 1986. Steady recharge had almost no effect on hydraulic heads with the exception shown in figure 55A. In figure 55B, the curve representing constant recharge is indistinguishable from that of the standard. The mean absolute difference (table 29) was 0.02 foot larger than that of the standard.

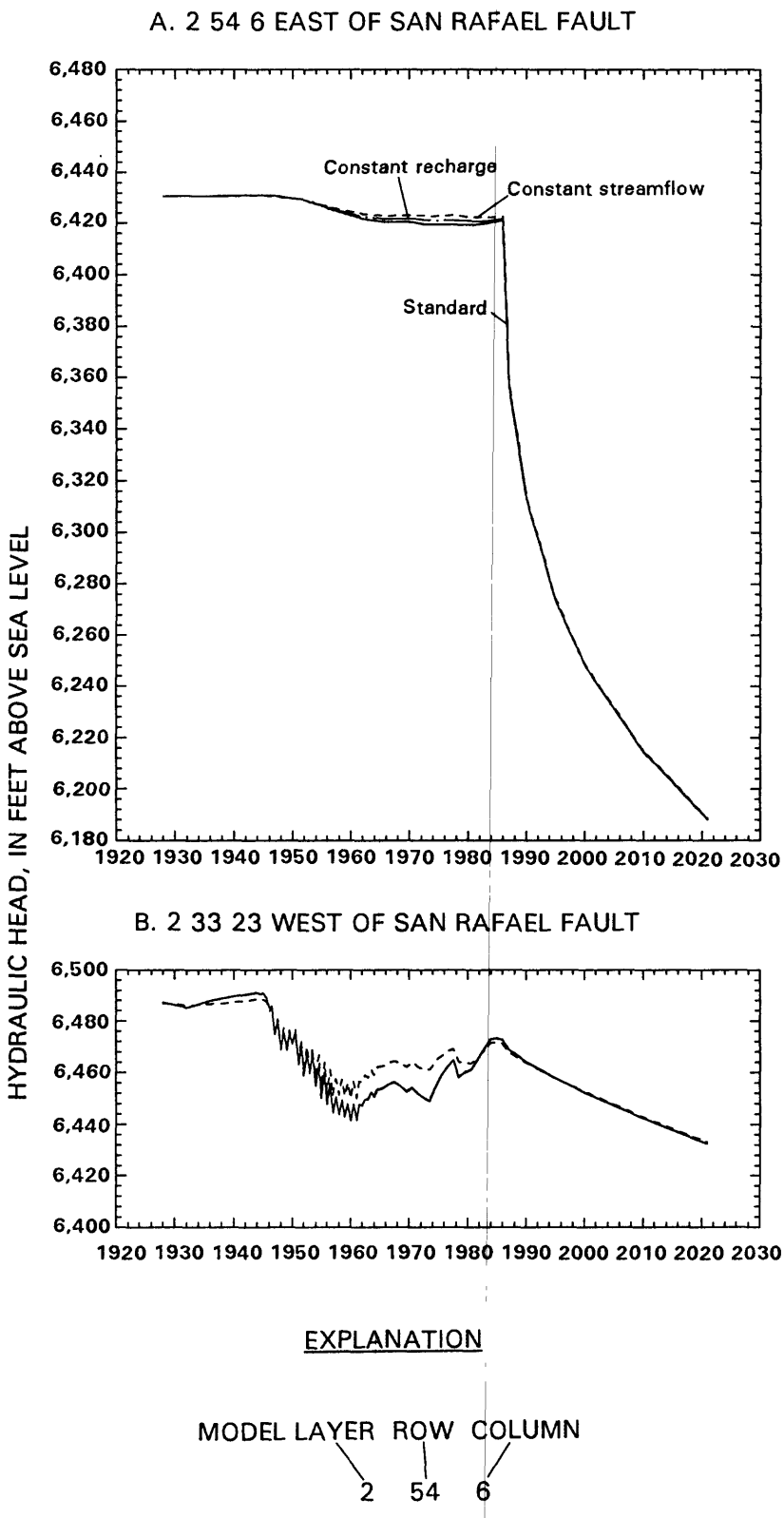

Figure 55.--Hydraulic heads from the standard simulation model and from tests of constant values of specified recharge and streamflow.

In the second test, in addition to the constant recharge, the specified inflow to model reach 5 was changed from variable to a constant, average value of 4.365 cubic feet per second (four-digit precision is not intended to signify accuracy). Model-derived values of streamflow from reach 4 representing Bluewater Canyon (table 30) were increased by 0.1 cubic foot per second for 1958-60. Intermittent flows were simulated for Ojo del Gallo during the 1950's and 1960's (not shown). Flow simulated downstream from Horace Springs was almost unchanged except for large flows, shown as negative values of as much as -31.2 cubic feet per second (table 30). The mean absolute difference between measured and model-derived hydraulic heads (table 29) was 0.24 foot, a value larger than that of the standard.

Model-derived hydraulic-head hydrographs (fig. 55B) were about one-half the variability of those of the standard. This was generally the case for all sites west of San Rafael fault such as in figures 37B, 38, and 41B. Because the slope of the recovery limb of the hydrograph in figure 41B was used to adjust the artesian storage, the variability in specified inflow to reach 5 was critical to adjustment of artesian storage coefficient.

Projections were not directly affected by these tests because average values of recharge and streamflow were specified in the standard. However, projections are indirectly affected to the extent that model adjustment of characteristics, such as artesian storage coefficient, was affected by specified recharge and streamflow.

One conclusion drawn from these tests is that specified changes in discharge from Bluewater Canyon greatly affect simulated hydraulic-head and flow hydrographs; however, specified variations in recharge do not directly affect the hydrographs. The lack of change caused by varying recharge is due to the large amount of aquifer storage simulated for the Zuni uplift area. The remainder of the variability in the hydrographs probably (by elimination) is caused by variations in ground-water withdrawals. Variations in ground-water withdrawals for irrigation (fig. 32 and tables 19 and 22) tend to increase the effect of variations in discharge from Bluewater Canyon. A second conclusion is that measured values of stream discharge and irrigation withdrawals, in addition to measured hydraulic heads, are critical to adjustment of the model.

Sensitivity to No-Flow Boundaries

Two tests of the no-flow boundaries were made because simulated 1985 drawdowns at these boundaries were as much as 36 feet in the northwest (row 1, columns 16-19) and because, as was foreseen, projected drawdowns were very large (as much as 221 feet) where the simulated transmissivity was large in the south (rows 52-76, column 1). The drawdowns projected under the no-flow boundary condition (the standard) probably are the maximum that would be projected under any boundary condition, all other things being equal. A constant-head boundary was tested to estimate minimum drawdown values, and a large-storage boundary (explanation follows) was tested to estimate intermediate drawdown.

The first test consisted of changing the no-flow boundaries to constant-head boundaries. The no-flow boundaries shown in figure 26 (row 1, columns 5-40; rows 49 and 50, column 2; and rows 52-76, column 1; all in layer 2) were changed to constant-head boundaries in the transient simulation and were assigned the hydraulic-head values from the steady-state simulation.

For 1986, flows simulated at these constant-head boundaries were small, both positive and negative, and the net flow from all constant-head boundaries was 0.8 cubic foot per second as compared to the 0.3 cubic foot per second of the standard. The total model inflow for 1986 was increased to 42.8 cubic feet per second, which is 100.07 percent of that of the standard.

After the 35-year projection, however, the net flow from constant-head boundaries was 11.6 cubic feet per second as compared to the 0.3 cubic foot per second of the standard. The total model inflow after the 35-year projection was increased to 45.4 cubic feet per second, 104 percent of that of standard, which was 43.7 cubic feet per second. Most of the additional flow from constant-head boundaries was balanced by less flow from ground-water storage.

This test resulted in slightly larger model-derived values of streamflow downstream from Horace Springs after 1978 (table 30), increasing by 0.2 cubic foot per second by the end of the 35-year projection. The mean absolute difference (table 29) was greater for this test than for that of the standard.

The following table shows the differences, in feet, between model-derived hydraulic-head hydrographs of the constant-head-boundary test (not shown) and those of the standard (figs. 37-42). (Dashes (--) mean hydrographs were indistinguishable):

Figure	1986	After 35-year projection
37A	--	2
37B	--	15
38A	--	18
38B	--	18
38C	--	18
39	5	105
40A	--	1
40B	8	165
41A	12	73
41B	2	25
42	5	35

Generally, hydrographs of this test were approximately the same as those of the standard until 1986, especially in an area between Grants and Bluewater. Figure 56A represents the area west of the San Rafael fault between Grants and Bluewater. The curve representing the constant-head boundary condition is indistinguishable from that representing the standard simulation until the beginning of the projection. However, the hydraulic-head change during the projection, about half of that of the standard, was substantial.

The effect of the constant-head boundaries was much greater near the boundaries. Northeast of Thoreau (fig. 56B) the constant-head boundary stabilizes the model-derived hydraulic head within 2 years of the beginning of the projection. There, the head change during the projection is about one-fifth of that of the standard. The effect of the constant-head boundary in column 1 extends to the site of the 10,000-acre-foot-per-year withdrawal (fig. 56C), where the head change during the projection is about one-third of that of the standard.

The hydraulic heads projected under the constant-head-boundary condition are the minimum that would be projected under any boundary condition, all other things being equal. However, a constant-head boundary is not reasonable in the context of this hydrologic setting. A constant-head boundary effectively simulates a near-infinite storage coefficient and is most appropriate for a perennial river or lake, neither of which exists.

A boundary condition intermediate between the constant-head and no-flow conditions was simulated. It consisted of a large but finite storage coefficient that would account for the storage in a zone of the aquifer from the model boundary to 40 miles beyond the model boundary. To the southwest, the 40-mile extension reaches into the volcanic terrain almost to the Mangas Mountains (not shown). In the volcanic terrain, which includes most of the terrain to the southwest, the existence or nonexistence of structural features that might block ground-water flow is not well known. The caverns in the San Andres Limestone may or may not extend uninterrupted 40 miles to the southwest. To the northwest, the 40-mile extension reaches almost to the Arizona State line through an interval where the existence of hydrologic boundaries is generally unknown. The extensions approximately double the simulated area of the aquifer and include most of the west-central part of the State.

To simulate the storage in an area extended to 40 miles beyond the arbitrary no-flow boundaries, the simulated storage coefficient in blocks along the northwest and southwest sides of the model was increased by factors proportionate to the block size in the direction perpendicular to the boundary. In each case, the factor was $(40 + w)/w$, where w is the width of the block (in miles) in the direction of the extension. The blocks changed were: (1) row 1, columns 5-40, where storage coefficient (4×10^{-4}) was multiplied by a factor of 22; and (2) rows 53-76, column 1, where the factor was 6.2. The factors were compounded in the corner block at row 52, column 1, where the compounded factor was 254. At row 49, column 2, a factor of 82 was used. This change produced less drawdown than a model extended by 40 miles because there is no simulation of the friction loss that would occur in the part of the aquifer simulated by the extension.

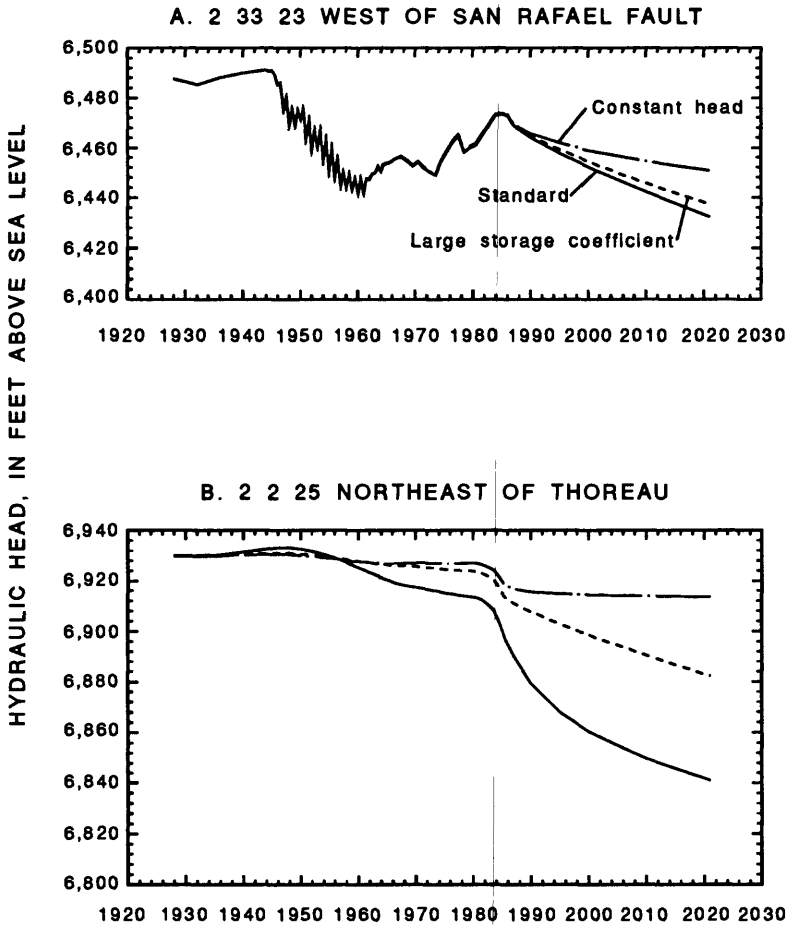

Figure 56.--Hydraulic heads from the standard simulation model and from arbitrary-boundary tests.

C. 2 54 6 EAST OF SAN RAFAEL FAULT

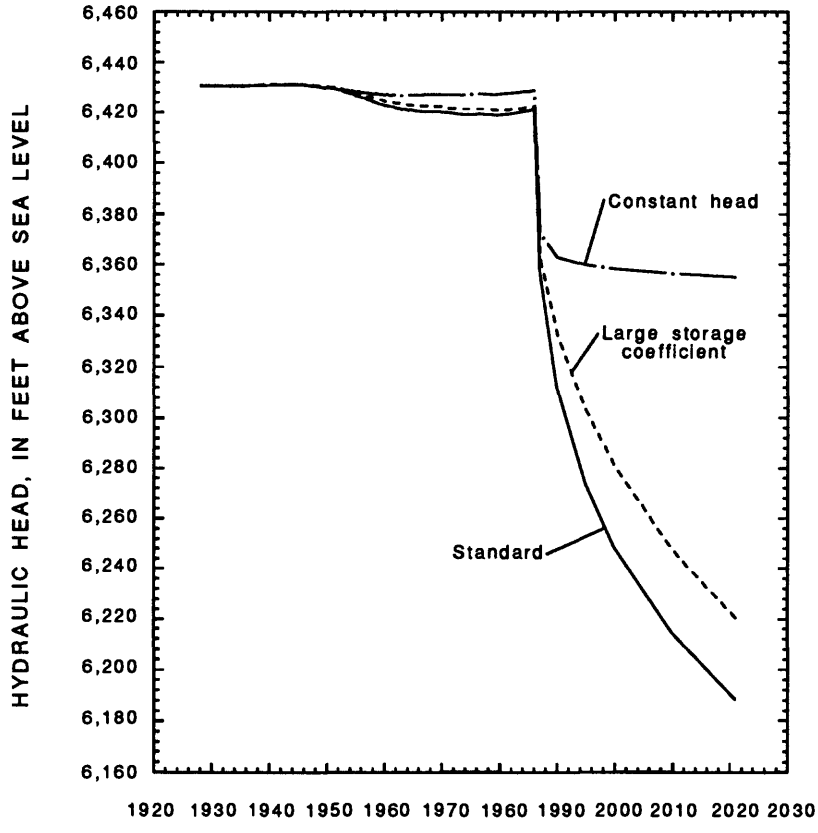

EXPLANATION

MODEL LAYER ROW COLUMN

2 54 6

The historical simulation was slightly affected by this change. Streamflows (table 30) were not affected. The total model inflow was not substantially changed from that of the standard. Although the mean absolute difference (table 29) was greater than that of the standard, the hydrographs for the Grants-Bluewater area such as those in figure 56A were not distinguishable from those of the standard.

The effect of this large-storage-coefficient condition on projected drawdown was substantial near the boundaries. Northeast of Thoreau (fig. 56B) the hydraulic-head change during the projection was about 55 percent of that of the standard. East of the San Rafael fault (fig. 56C), at the site of the 10,000-acre-foot-per-year withdrawal, the head change during the projection was about 85 percent of that of the standard.

The relative appropriateness of any of the three boundary conditions is unknown. For the following reasons, however, the most appropriate boundary may be more like the no-flow boundary than the constant-head boundary. Whereas the constant-head condition does not simulate any known or suspected physical condition in the area, the no-flow boundary condition is possible because an unknown blockage to ground-water flow could exist near the boundary, especially in the southeast (model column 1) where the cavernous character of the San Andres Limestone could end abruptly. In the northwest, ground-water withdrawals beyond the model boundary would tend to draw down hydraulic heads near the boundary. By image-well theory, if the ground-water withdrawals beyond the model boundary constituted an exact mirror image of ground-water withdrawals simulated within the model, a no-flow boundary condition would be exactly correct, assuming that the boundary follows a pristine flow line. Although the location and quantity of ground-water withdrawals beyond the model boundary do not constitute such a mirror image, to some extent they would have a similar effect.

The relative insensitivity of the historical part of the simulation to the arbitrary boundaries does not lend confidence to the projections, which are sensitive to these boundaries. Conditions at the arbitrary boundaries were not accounted for in the adjustment of the model.

Sensitivity to Artesian Storage Coefficient

Two tests of the artesian storage coefficient were conducted. The first test simulated a larger artesian storage coefficient (4×10^{-4} in the standard was increased to 8×10^{-4}) and the second test simulated a smaller coefficient (2×10^{-4}).

Changes in storage coefficient had little effect on streamflow. The larger storage coefficient resulted in an increase in simulated streamflow downstream from Horace Springs of 0.1 cubic foot per second during 1979-82 and at the end of the 35-year projection (table 30). The smaller coefficient resulted in a reduction of streamflow downstream from Horace Springs of 0.1 cubic foot per second during 1979-81.

Neither test resulted in large changes in model-derived hydraulic heads before 1986. The larger artesian storage coefficient resulted in a larger mean absolute difference (table 29) between measured and model-derived hydraulic heads, and the smaller coefficient resulted in a slightly smaller mean absolute difference. Neither change resulted in noticeable changes in the historical parts of most hydrographs (such as hydrographs in figs. 37 and 38) because most of the sites are near the outcrop of the San Andres-Glorieta aquifer where unconfined storage (specific yield) is the dominant storage property of the aquifers. Therefore, adjustment on the basis of hydraulic-head measurements at most sites does not lend confidence to the simulated artesian storage coefficient. However, the simulated artesian storage coefficient has some effect on model-derived hydraulic heads at sites distant from the outcrop. The longest record of measured hydraulic heads distant from the outcrop is northeast of Prewitt (fig. 41B). At this site changes in simulated artesian storage coefficient have a slight effect on model-derived hydraulic heads during the historical scenario (fig. 57A). The smaller artesian storage coefficient was rejected partly on the basis of the comparison between measured and model-derived long-term recovery at this site. At the site northeast of Thoreau (figs. 41A and 57B), although the smaller artesian storage coefficient shows a potentially closer comparison between measured and model-derived hydraulic heads, the smaller coefficient was rejected because the hydrograph of measured values has a relatively short duration and may result from local conditions as previously discussed.

All projected hydraulic heads are sensitive to the specified artesian storage coefficient. With the artesian storage coefficient of 8×10^{-4}, the change in hydraulic head during the projection was about 80 percent of that of the standard. With the artesian storage coefficient of 2×10^{-4}, the change in hydraulic head during the projection ranged from about 110 percent of that of the standard (fig. 57C) to 125 percent (fig. 57A).

It is concluded that the general lack of sensitivity of the comparison of measured and model-derived hydraulic heads, and the sensitivity of projected hydraulic heads to the artesian coefficient does not lead to confidence in the projected heads for sites distant from the outcrop. It could be concluded also that the smaller mean absolute difference that resulted from the smaller artesian storage coefficient signifies that leakage from confining beds is small, assuming that the reaction of the model to leakage would be similar to the reaction to larger storage. However, another specified aquifer characteristic could be in error as previously discussed in the section on model adjustments.

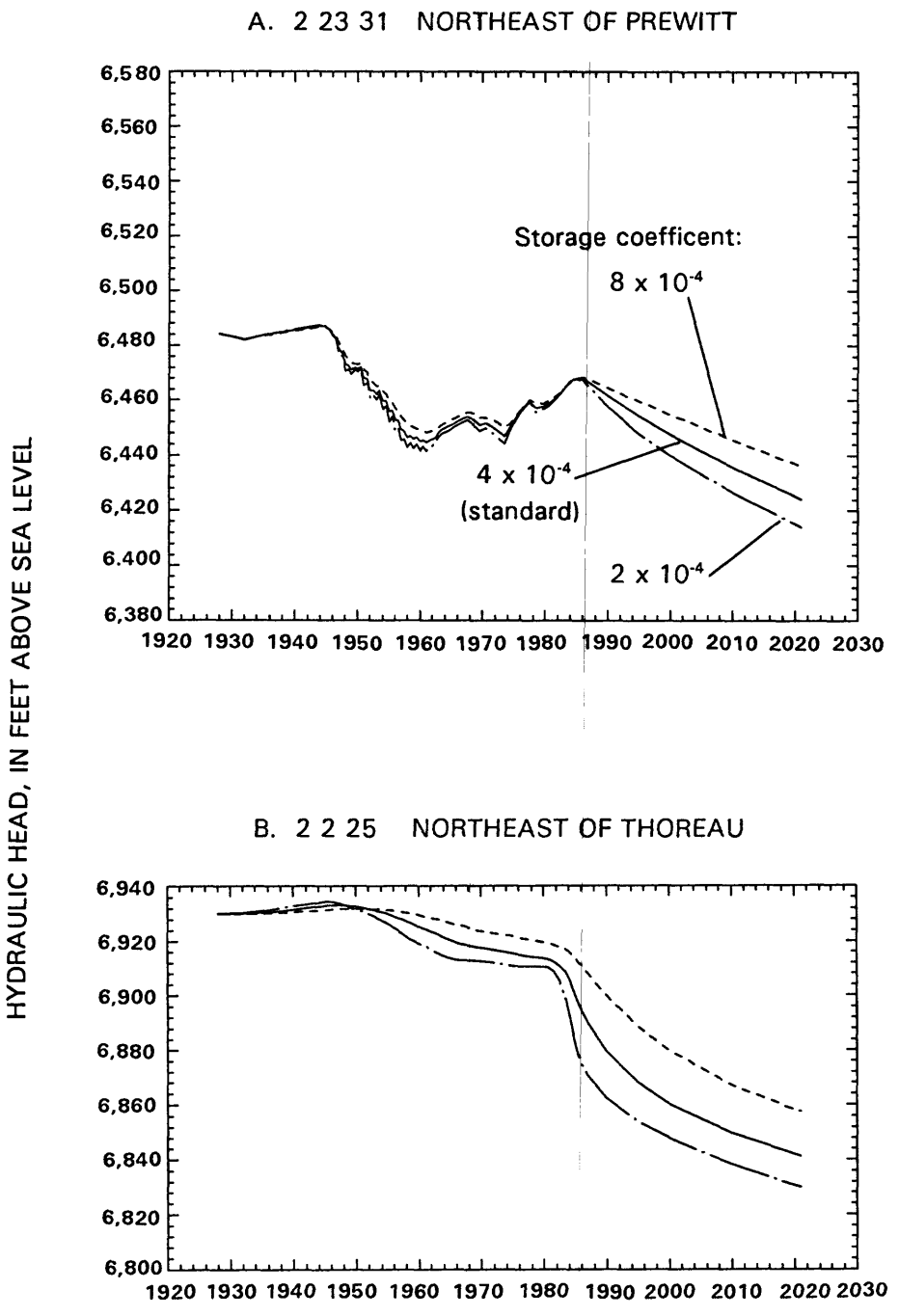

Figure 57.--Hydraulic heads from the standard simulation model and from artesian storage-coefficient tests.

C. 2 54 6 EAST OF SAN RAFAEL FAULT

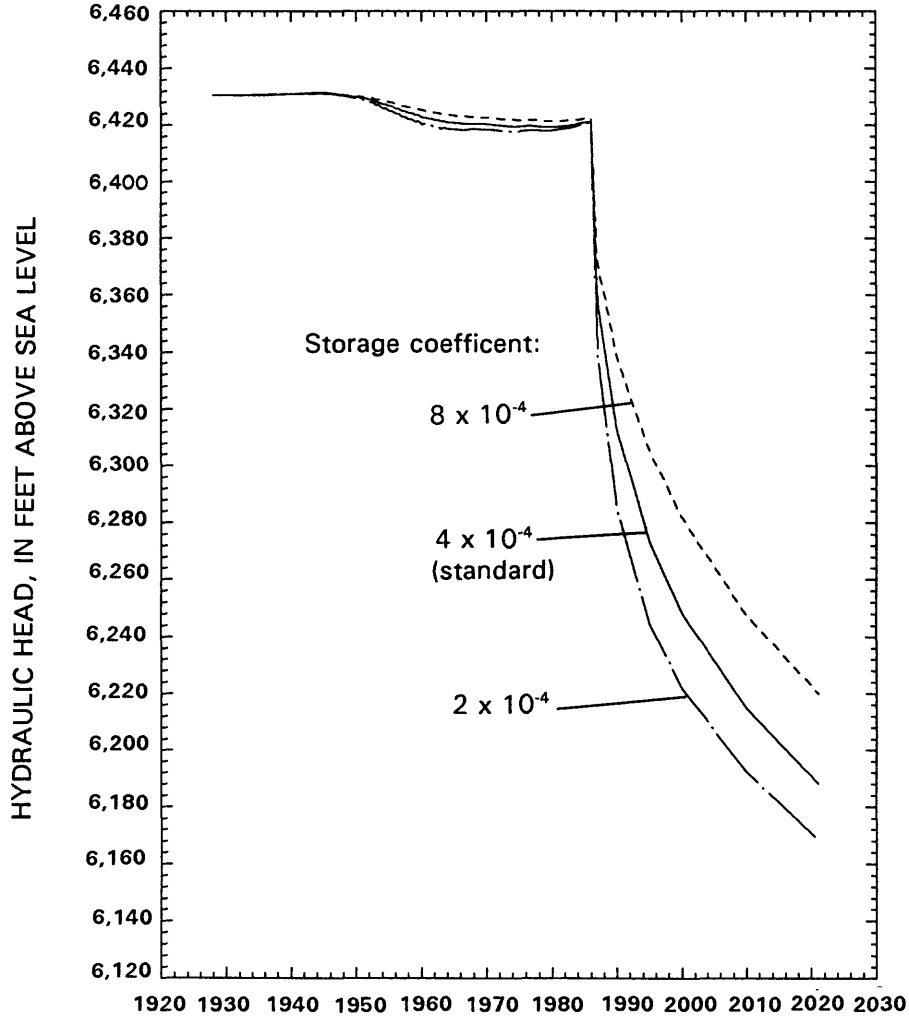

EXPLANATION

MODEL LAYER ROW COLUMN

2 2 25

Sensitivity to Flow from Confining Beds

Three tests of sensitivity to flow from confining beds were conducted. For the purpose of these tests, seven layers ("leakage layers") were added to the model (layers 3-9). Layer 9 was specified entirely as a constant-head boundary to assure mathematical stability of the model and to provide an estimate of leakage from aquifers on the opposite sides of the confining beds. The specified vertical conductances (Vcont) were estimated on the basis of layer thickness, which was increased in the downward direction by a factor of 1.5 as follows:

Layer	Thickness, in feet	Vcont, per second, for test 1
2	0	4.00×10^{-11}
3	50	1.60×10^{-11}
4	75	1.07×10^{-11}
5	112	7.12×10^{-12}
6	169	4.74×10^{-12}
7	253	3.16×10^{-12}
8	380	2.11×10^{-12}
9	570	--

Vcont was calculated by the following formula, which is based on equation 51 of McDonald and Harbaugh (1988):

$$Vcont(k) = \frac{1}{\frac{b(k)/2 + b(k+1)/2}{K}} \qquad (6)$$

where k = the layer number;
b = the layer thickness; and
K = vertical hydraulic conductivity, in feet per second, equal for all layers 3-9.

The thickness of the first leakage layer (layer 3) was arbitrarily selected. However, if errors that might result from layer 3 being too thick are assumed to be proportional to the percentage of confining-bed storage that layer 3 constitutes, the errors should not be great. Given a constant specific storage for all leakage layers, the storage simulated in layer 3 is approximately 5 percent of the storage simulated in layers 3-8.

The transmissivity of all leakage layers was set to zero. The specific storage of all leakage layers was set to 1×10^{-6} per foot. The initial hydraulic head for all leakage layers was set to the steady-state hydraulic head of layer 2 of the standard (two-layer) model. For the first test vertical hydraulic conductivity was set to 1×10^{-9} foot per second, approximately the maximum for shale; for the second test was set to 1×10^{-11} foot per second; and for the third test was set to 1×10^{-13} foot per second, approximately the minimum for shale.

The leakage layers of the model can represent leakage from overlying, underlying, or less permeable beds within the aquifer; or a combination of leakage sources. The model was assumed to respond similarly in any of these cases.

The first test resulted in minor effects on streamflow (table 30). The effect on model-derived discharge from Bluewater Canyon (reach 4) was zero except for the last stress period of the projection when it was 0.1 cubic foot per second. The maximum effect on model-derived discharge of the Rio San Jose downstream from Horace Springs was 0.2 cubic foot per second for 1979-84. The second test resulted in no effect on streamflow except for stress period 47 (1964.5-1965.5) when the streamflow in Bluewater Canyon was 0.4 cubic foot per second less than that of the standard simulation model. The third test had no effect on the model-derived discharge from Bluewater Canyon (reach 4) or on discharge of the Rio San Jose downstream from Horace Springs (reach 11).

The model budget (table 31) indicates that the first test, in which the hydraulic conductivity of confining beds was set to 1×10^{-9}, resulted in a flow from constant-head boundaries of about 1 cubic foot per second by 1986.0, an increase of about 0.6 cubic foot per second over that of the standard (0.44 cubic foot per second from five model blocks in layer 1, column 1; fig. 25). Nine years into the projection, this test resulted in almost 2 cubic feet per second from constant-head boundaries, and at the end of the projection, 5 cubic feet per second. Most of the increase in flow of 5 cubic feet per second from the constant-head boundary was balanced by a decrease of 3 cubic feet per second from storage in the simulated aquifer and confining beds. The second and third tests resulted in no increase in flow from constant-head boundaries over that of the standard.

The cumulative flow from constant-head boundaries of the first test (vertical hydraulic conductivity of 1×10^{-9} foot per second) was 1.1 hundred-thousand acre-feet, 0.8 hundred-thousand acre-feet more that that of the standard by the end of the 35-year projection. This constitutes a model-derived estimate of water taken from aquifers on the opposite sides of the confining beds. If this quantity were all taken from a water-table aquifer having an area of 800 square miles (an area where the largest projected drawdowns occur) and a specific yield of 0.15, it would result in a lowering of the water table by 1 foot. An effect of such small magnitude probably could not be measured because of "noise," fluctuations in water level that result from other human activities and from natural conditions.

The mean absolute difference between measured and model-derived hydraulic heads (table 29) was greater than that of the standard in all three tests. The largest mean absolute difference resulted when vertical hydraulic conductivity of the leakage layers was specified as 1×10^{-9} foot per second.

As with artesian storage, the effects on the historical (pre-1986.0) parts of most hydrographs such as those shown in figures 37 and 38 were so small as to be indistinguishable from the standard. Effects were most noticeable at sites distant from the aquifer outcrop. Increased leakage has an effect on curves in figure 58A that is similar to the effect of increased artesian storage in figure 57A; that is, increased leakage tends to make the recovery curve between the late 1950's and the middle 1980's less steep.

Also, as with artesian storage, the possible effects on projected hydraulic heads could be large if a vertical hydraulic conductivity of 1×10^{-9} foot per second were characteristic of vertical hydraulic conductivity of beds confining the San Andres-Glorieta aquifer. With a confining-bed hydraulic conductivity of 1×10^{-9} the hydraulic-head change during the projection was 60 percent of that of the standard northeast of Prewitt (fig. 58A), 70 percent of that of the standard east of San Rafael fault (fig. 58B), and about 65 percent west of San Rafael fault (not shown).

Tests of vertical hydraulic conductivity of 1×10^{-11} and 1×10^{-13} foot per second resulted in hydraulic heads very similar to those of the standard. The hydraulic-head change during the projection was more than 90 percent of that of the standard with vertical hydraulic conductivity of 1×10^{-11}. Vertical hydraulic conductivity of 1×10^{-13} resulted in curves that are indistinguishable from those shown in figure 58 for the standard model. The general insensitivity to leakage of the comparison of measured and model-derived hydraulic heads, and the sensitivity of projected hydraulic heads to leakage lead to a lack of confidence in the projected heads.

Of practical significance is the 24 hours of central processor time needed to process the nine-layer model. If this size model were required in the future, a faster computer would be desirable especially if the model were to be readjusted.

Sensitivity to the Simulation of San Rafael Fault

Two tests of the simulation of San Rafael fault were conducted to determine the effect of the fault on drawdown. In one test, the inactive zone simulating the fault was extended one model block on both ends to include columns 11-28, and in the other test the inactive zone was shortened to include columns 13-26.

Effects on streamflows with each test tended to be opposite in sign but not equal in magnitude. Model-derived rates of discharge from Ojo del Gallo (not shown) were about 0.2 cubic foot per second more than those of the standard simulation model when the simulated fault was lengthened, and were about 1 cubic foot per second less than those of the standard when the simulated fault was shortened.

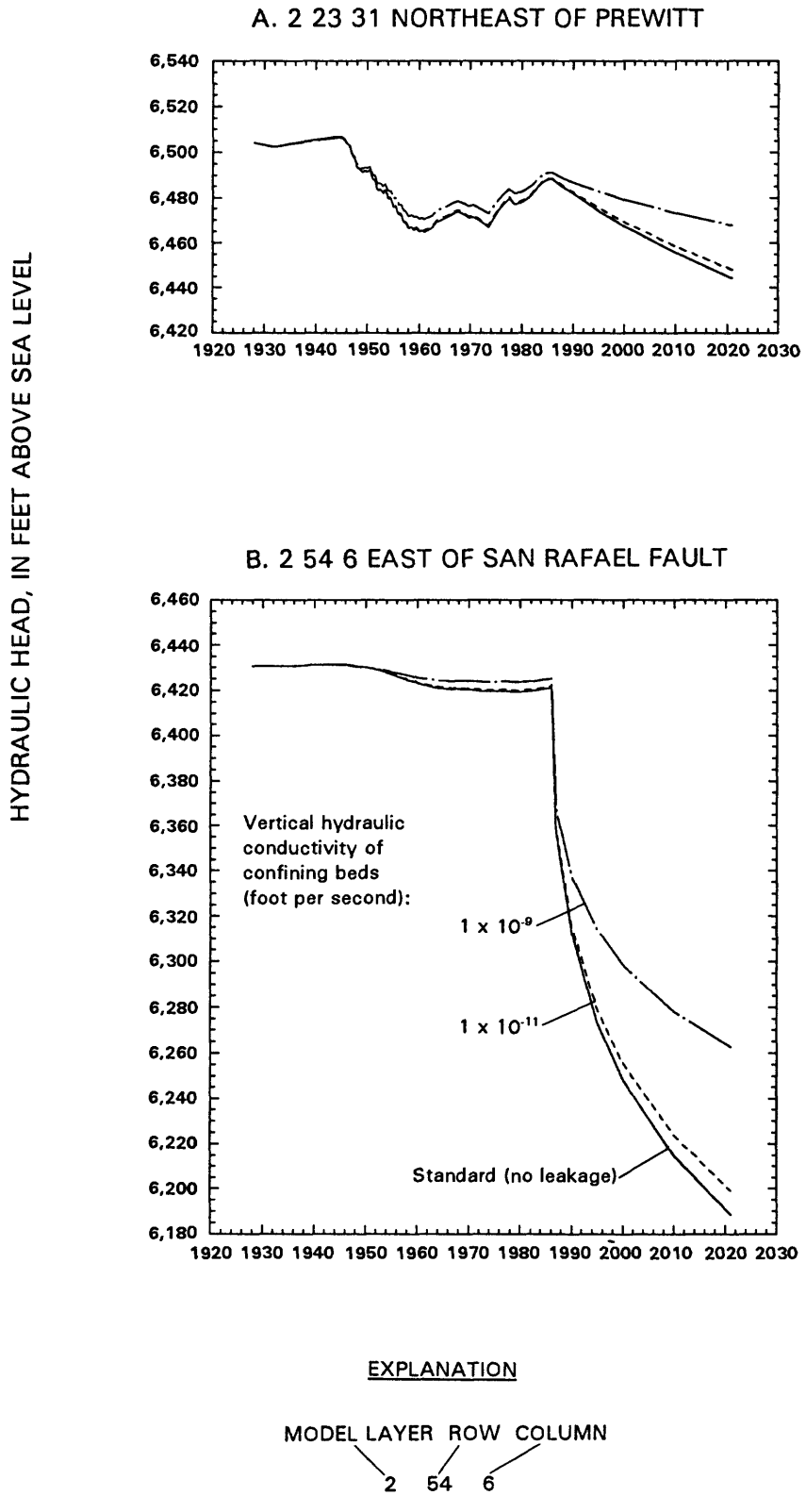

Figure 58.--Hydraulic heads from the standard simulation model and from leakage tests.

With the simulated fault lengthened, model-derived streamflow of the Rio San Jose downstream from Horace Springs (table 30) was 0.2 cubic foot per second more than that of the standard during the first five stress periods. This difference was gradually reduced to -0.1 cubic foot per second by the late 1950's and remained so until the late 1970's. After that, the difference fluctuated between plus and minus 0.1 cubic foot per second.

With the simulated fault shortened, model-derived streamflow of the Rio San Jose downstream from Horace Springs was about 0.5 cubic foot per second less than that of the standard during the first few stress periods. This difference abruptly increased to 0.1 cubic foot per second in the middle 1940's and remained so until the late 1970's. After that, the difference fluctuated between plus and minus 0.1 cubic foot per second.

Neither test affected the model-derived rate of streamflow (table 30) from Bluewater Canyon (reach 4). Both tests resulted in a larger mean absolute difference between measured and model-derived hydraulic heads than that of the standard.

During the historical part of the simulation (pre-1986), the lengthened fault resulted in slightly more dampened and delayed drawdown and recovery east of the fault (fig. 59A and C) during historical time than those of the shortened fault. The adjustment of the simulated length of San Rafael fault was partly based on this tendency and on the measured hydraulic heads shown in figure 39, as previously discussed. The lengthened fault caused lower hydraulic heads east of the fault (fig. 59A and C) and higher heads west of the fault than those of the shortened fault. The hydraulic heads east of the fault depend not only on the fault but also on recharge near the east end of the Zuni uplift, discharge to the Rio Grande rift, and the permeability of rocks along the flow lines between recharge and discharge areas. Therefore, the relatively large vertical offset between curves in figure 59A and C does not determine the length of the fault with certainty. Similarly, the minor differences between the curves representing simulated hydraulic heads west of the fault (fig. 59B) during the historical part of the simulation cannot be used to determine the length of the fault. Although the apparent dampening of the long-term (1950-86) drawdown and recovery cycle is a possible criterion for adjustment of the length of the fault, the measured drawdown and especially the recovery (fig. 39) are very slight, and do not constitute a limiting parameter that can lend great confidence to the model.

Projected hydraulic heads both west and east of San Rafael fault were sensitive to changes in the length of the fault, and the effects were of opposite sign. The changes in model-derived hydraulic heads during the projection were 75-80 percent of those of the standard east of the fault (fig. 59A and C) with the shortened fault and about 110 percent with the lengthened fault. Conversely, west of the fault (fig. 59B), the changes in model-derived hydraulic heads during the projection were 160 percent of those of the standard with the shortened fault and about 75 percent with the lengthened fault.

The fault acted as a partial barrier between two zones of large transmissivity. The exact length of the simulated fault may be no more significant than the simulated aquifer characteristics in the immediate vicinity of the ends of the fault.

Because of the slight sensitivity of the comparison between measured and model-derived hydraulic heads to the length of the fault, the adjustment of the length of the fault is tenuous. However, as the duration of the hydraulic-head record both east and west of the fault increases, the adjustment of the length (or more generally the hydraulic connection) possibly can be made less tenuous. The greater sensitivity of projected hydraulic heads to the length of the fault does not lend confidence to the projected hydraulic heads.

Vertical Hydraulic Conductivity of Stream Bottoms

Two tests of the specified vertical hydraulic conductivity of stream bottoms were made. The vertical hydraulic conductivity was changed from the standard of 8×10^{-7} to 4×10^{-7} foot per second in one test and to 1.6×10^{-6} in the other test. Proportionate changes were made at two blocks (row 23, column 18; and row 24, column 19) where the vertical hydraulic conductivity in the standard was 1.2×10^{-6} foot per second. The specified vertical hydraulic conductivity of the remainder of the simulated stream/spring/lake system was not changed.

Although the mean absolute head difference (table 29) was smaller than that of the standard simulation, when the vertical hydraulic conductivity of the river was decreased, the simulated flow at Ojo del Gallo (fig. 60A) was generally too little, reduced by about 2 cubic feet per second, and no flow was simulated for Ojo del Gallo during the 1980's. When the vertical hydraulic conductivity was increased, the simulated flow at Ojo del Gallo was too large, increased by about 2 cubic feet per second, and the mean absolute head difference was larger than that of the standard simulation.

Model-derived rates of stream discharge from Bluewater Canyon (table 30) generally were within plus or minus 0.1 cubic foot per second of those of the standard simulation model. Discharge was as much as 0.3 cubic foot per second more than that of the standard and as little as 0.2 cubic foot per second less than that of the standard.

Model-derived rates of discharge (fig. 60B) for the Rio San Jose downstream from Horace Springs (reach 11) were the same as those of the standard except for times when surface inflow to reach 11 was simulated. From the mid-1950's to the mid-1970's and during the projection, surface inflow generally was not simulated by the standard or either test. Model-derived discharge ranged from as much as 3.5 cubic feet per second more than that of the standard with the smaller streambed hydraulic conductivity to as little as 5.0 cubic feet per second less than that of the standard with the larger streambed hydraulic conductivity.

Hydraulic heads were quite sensitive to changes in streambed hydraulic conductivity. This was especially true near Bluewater (fig. 60C) where the range was almost 40 feet. Northeast of Prewitt (fig. 60D) the simulated recovery between the mid-1950's and the mid-1980's was steeper when streambed hydraulic conductivity was larger than that of the standard and was less steep when riverbed hydraulic conductivity was smaller than that of the standard.

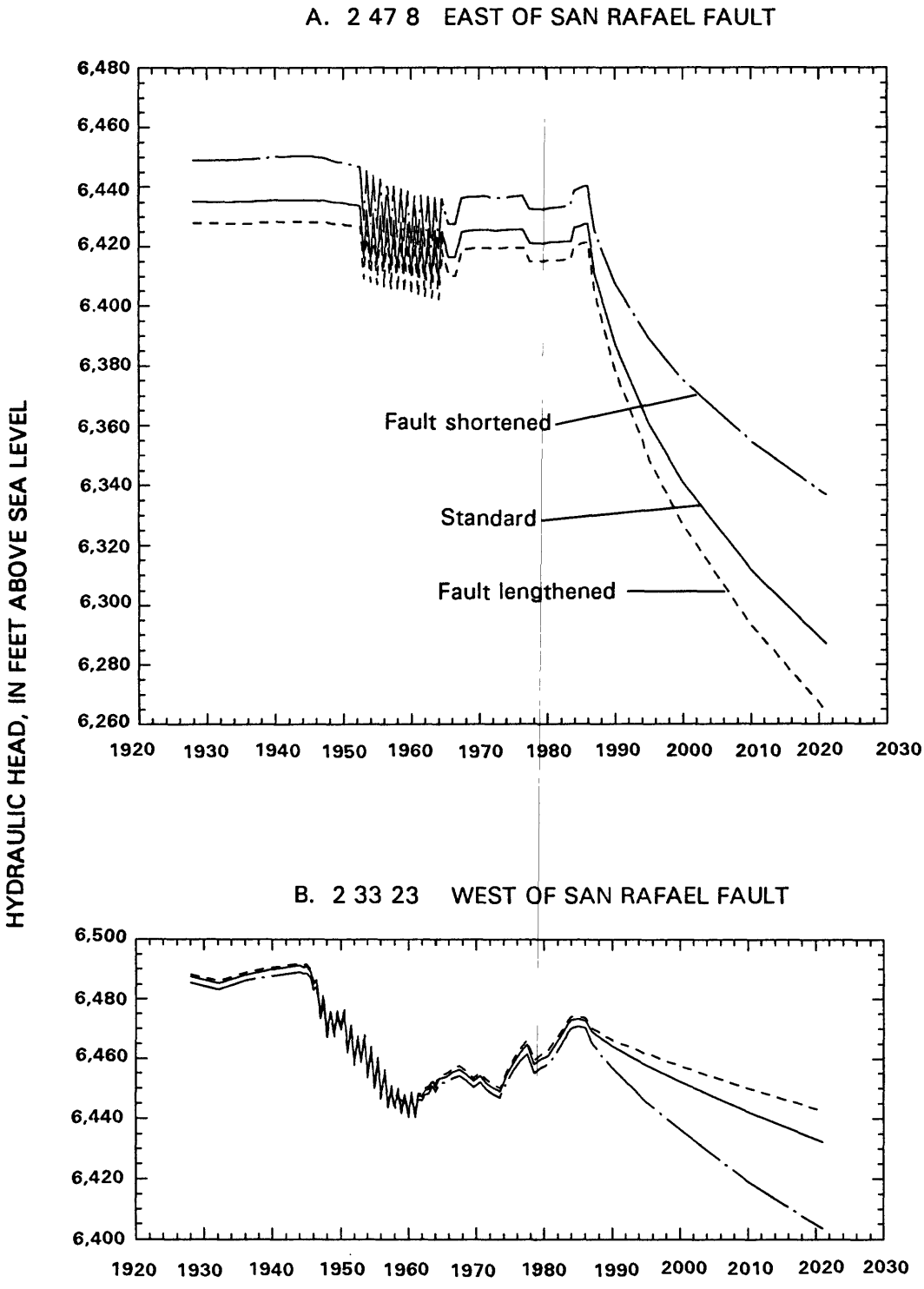

Figure 59.--Hydraulic heads from the standard simulation model and from San Rafael fault tests.

C. 2 54 6 EAST OF SAN RAFAEL FAULT

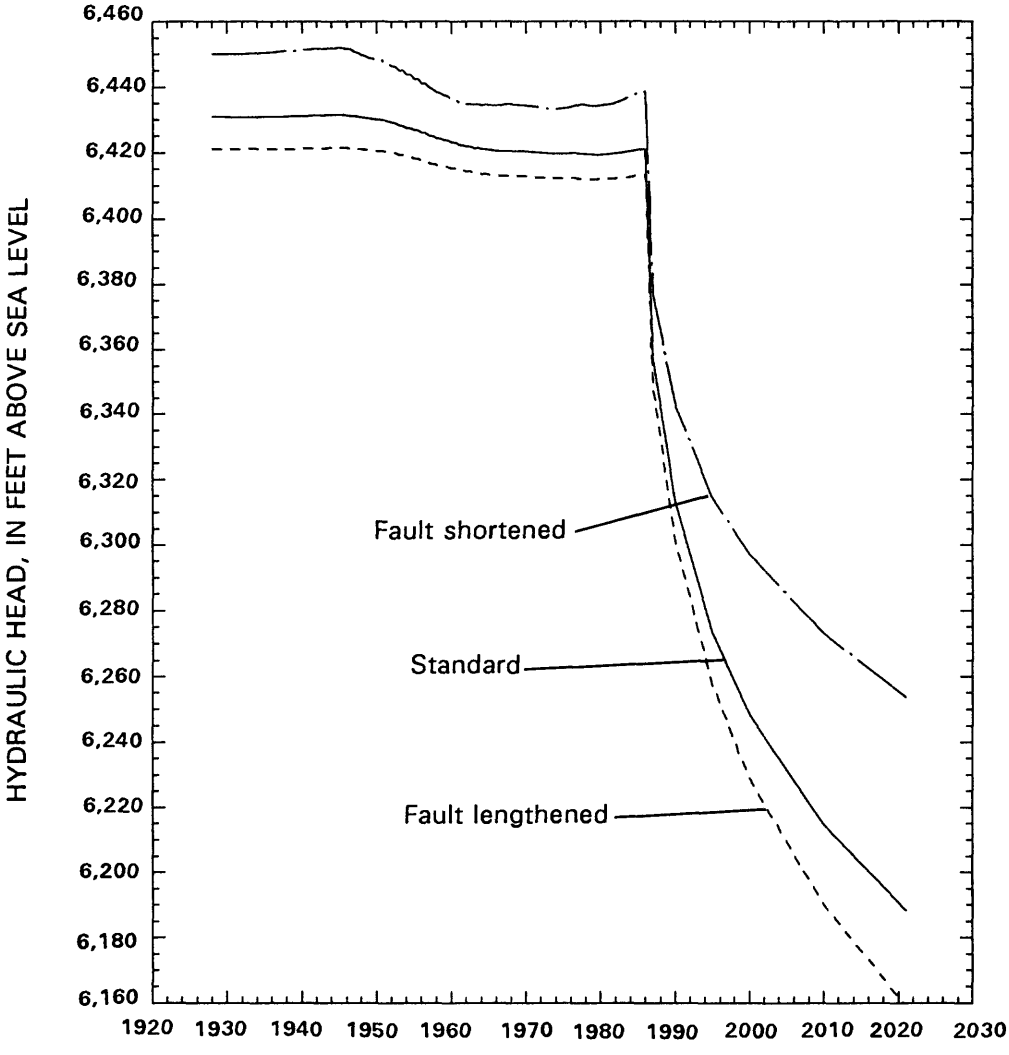

EXPLANATION

MODEL LAYER ROW COLUMN

2 54 6

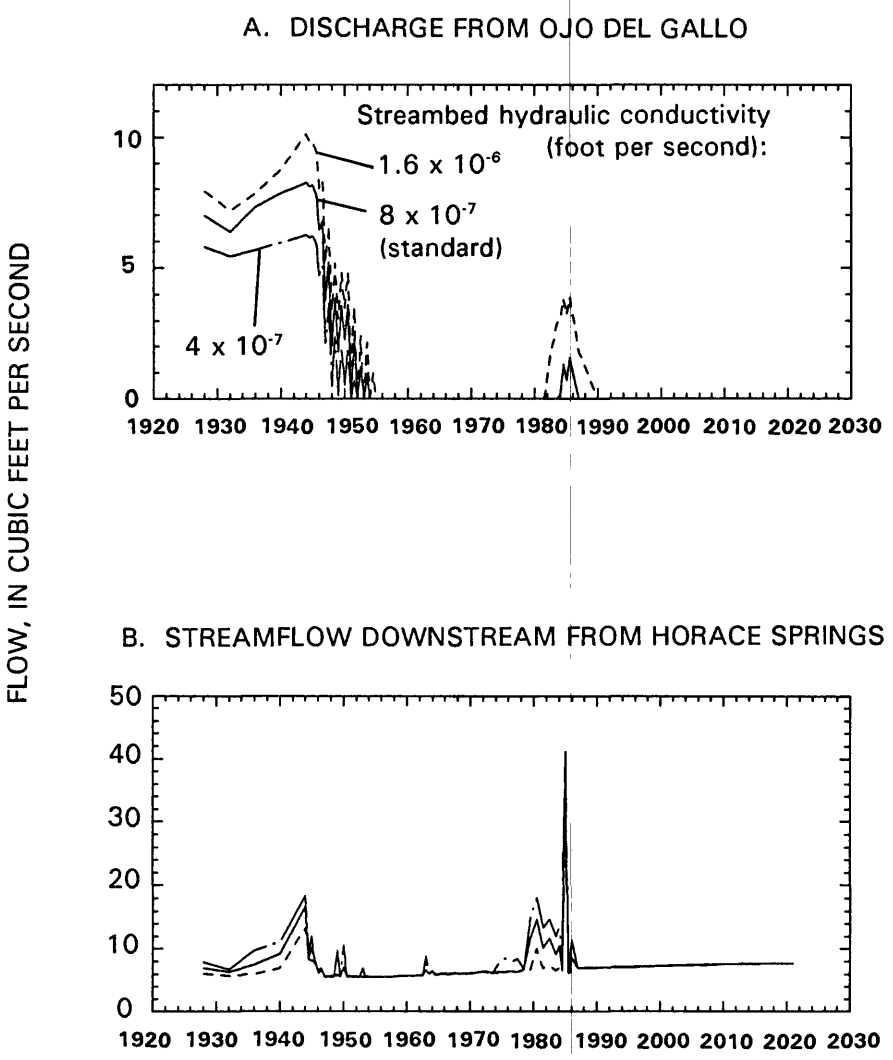

Figure 60.--Flow and hydraulic heads from the standard simulation model and from streambed hydraulic-conductivity tests.

C. 2 25 19 NEAR BLUEWATER

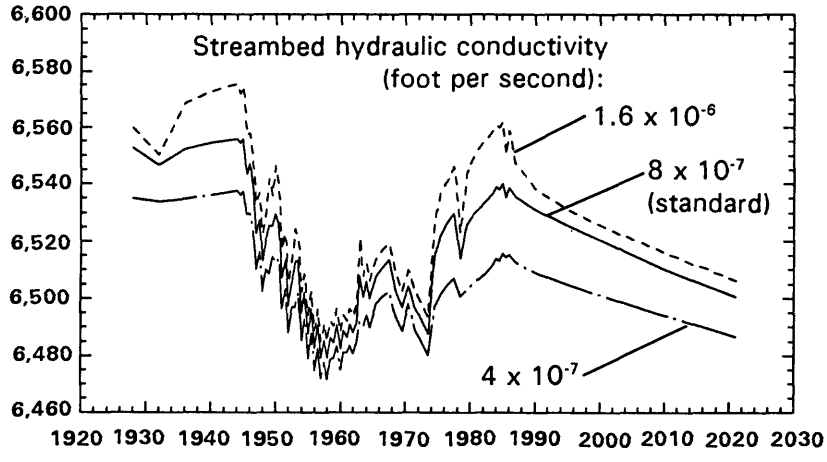

D. 2 23 31 NORTHEAST OF PREWITT

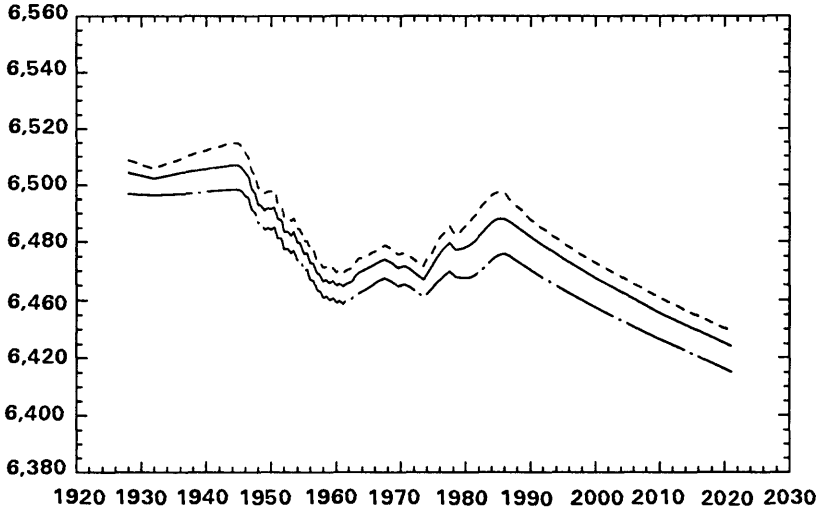

HYDRAULIC HEAD, IN FEET ABOVE SEA LEVEL

EXPLANATION

MODEL LAYER ROW COLUMN

2 23 31

It might be concluded that model adjustment may have yielded an appropriate value of vertical hydraulic conductivity of the streambed because of the great sensitivity of model-derived discharge from Ojo del Gallo and hydraulic heads. However, for consideration of a flow line from the streambed near Bluewater to Ojo del Gallo, there is uncertainty in the specified transmissivity along the flow line as well as in the measured or estimated discharge of Ojo del Gallo. These uncertainties are built into the adjusted value of streambed hydraulic conductivity. Additional uncertainty arises from the fact that probably not all of the stream loss near Bluewater Village resurfaces at Ojo del Gallo. Some is discharged by way of ground-water withdrawals from wells and some probably is discharged to the Rio Grande rift to the east.

Sensitivity to Simulated Flow Through Rocks of the Chinle Formation

Two tests were made to determine sensitivity to flow between the San Andres-Glorieta aquifer and the valley fill through rocks of the Chinle Formation. As previously described, the Chinle Formation confining bed was simulated around the southeastern end of the Zuni uplift where it intervenes between the San Andres-Glorieta aquifer and the valley-fill aquifer; this area constitutes a very small percentage of the area of the Chinle confining bed.

In the first test vertical hydraulic conductivity of the Chinle Formation was set to 0.1 times the value in the standard simulation model. The total flow through the system was 27.52 cubic feet per second, approximately equal to the 27.53 cubic feet per second of the standard. A curve (not shown) representing the site shown in figure 59C was almost indistinguishable from that of the standard.

In the second test vertical hydraulic conductivity was set to 10 times the value in the standard. The total flow through the system was 27.54 cubic feet per second, also approximately equal to that of the standard. A curve (not shown) representing the site shown in figure 59C was indistinguishable from that of the standard.

Summary of Sensitivity Tests

Sensitivity testing is an imprecise way of evaluating the importance of various model features to the adjustment of the model and to projections. Sensitivity tests show the sensitivity of the tested model only. Any change in simulated hydrologic properties tends to make the model maladjusted and alters the sensitivity of the model to other changes. These tests do not show the response of the geohydrologic system. Only by an assumption of the digital model's comparability with the geohydrologic system do these tests provide insight to the behavior of the geohydrologic system.

About half of the variation in hydraulic-head hydrographs was the result of specified inflow to reach 5 (from the mouth of Bluewater Canyon to Grants, which is from gaging station 08342000 to 08343000). The depth of the long-term drawdown (late 1940's to early 1960's) and recovery (mid-1960's to mid-1980's) curves was simulated mainly by the specification of stream-bottom hydraulic-conductivity values and ground-water withdrawal rates, and to a much lesser extent by the specification of storage coefficient and by leakage from confining beds.

Generally the effects on streamflow of the changes made during sensitivity testing were very minor (table 30). One exception was when stream-bottom hydraulic conductivity was tested and model-derived spring discharge at Ojo del Gallo (fig. 60A) was substantially changed.

The changes made in most of the tests did not affect the historical simulation greatly, and with slight additional adjustments in each case, the mean absolute difference probably could have been made as small as that of the standard simulation model. Therefore, the projections made in most of the tests are plausible.

Model Accuracy and Predictive Capability

The model described in this report provides a method for predicting the response to a specified stress. However, the confidence placed in the predicted response results from a subjective judgment of the closeness of the analogy between the San Andres-Glorieta aquifer and the model. Most of the text in this report describes this analogy. The purpose of this section is not to summarize the analogy but to point out some significant parts of the analogy. The analogy rests on three main conditions: the degree of similarity between the geohydrologic system and the conceptual model of the San Andres-Glorieta aquifer described in the first main section of the report, the similarity between the conceptual model and the digital model described in the next main section of the report, and the assumption that the aquifer simulated by the digital model adequately represents the San Andres-Glorieta-aquifer part of the geohydrologic system.

Similarity between the Geohydrologic System and the Conceptual Model

As is generally true of models, the conceptual model is much simpler than the hydrologic system that it attempts to describe. The conceptual model attempts to describe the ground-water system as a subsystem of the hydrologic system using concepts such as aquifers and confining beds that have characteristics such as transmissivity, storage coefficient, and leakage. Each of these concepts leads to additional simplification or distinctions that are somewhat artificial in an attempt to make the conceptual model more comprehensible than the geohydrologic system.

The implied assumption is that the complexities that have not been accounted for are minor or that their effects tend to cancel each other. The complexity caused by variable water density, which was previously noted, is an example. Density variation from place to place in ground water affects the direction of flow in a dipping aquifer. The effect is greater with smaller hydraulic gradient for a given density variation and aquifer dip (Davies, 1986). The gentle slope of the hydraulic gradient on the west and south sides of the Pueblo of Acoma, when combined with the observed density variations and aquifer dips, could cause local flow directions to be much different than those simulated.

Ordinarily in dipping aquifers, more mineralized water is found downdip (figs. 9 and 18 of Baldwin and Anderholm, in press). Greater mineralization contributes to greater density; however, greater temperature with depth decreases the density and tends to cancel the effect of the higher dissolved-mineral concentration. In the case of test wells 10.9.25.324 (Anzac) and 9.9.28.1344 (Acoma-1), in which a discharge test indicates a hydraulic connection between them, the water in the downdip well, although more mineralized, is less dense than water in the updip well because of the temperature effect. These observations seem to indicate a hydrostatically unstable condition, implying that dynamic processes exist that have not been investigated. The overall effects of variations in temperature and dissolved constituents on density are assumed to cancel each other, a convenient assumption because these data are not available for most of the modeled area.

Measured or estimated values presented in the conceptual model may not represent the hydrologic system. This is especially true of the attempted relation of recharge, streamflows, and weather. Other items that are given more credence, such as the hydraulic-head declines and reduced springflows that result from stresses such as reported and estimated ground-water withdrawals, are to some degree inaccurate and are not truly representative of the stress-response relation necessary to project a response to an assumed stress.

Similarity between the Conceptual Model and the Digital Model

The digital model is simpler than the conceptual model. Although some leakage between the San Andres-Glorieta aquifer and other aquifers was considered probable in the conceptual model, the simulation of the intervening confining beds was considered to be impractical. Also, the assumption of no leakage may not be much different than the assumption of leakage if the hydraulic conductivity of confining beds is generally less than 10^{-11} foot per second.

Using stress periods in the digital model of duration that would allow the best simulation of the stream-aquifer boundary was considered to be impractical. Changes in surface-water flow tend to occur over much shorter time periods than do changes in ground-water flow. A result is that simulation of a stream such as the lower reach of Bluewater Creek and the upper reach of the Rio San Jose between Bluewater and Grants (reach 5) tends to require a hydraulic conductance that is dependent on the length of the

stress period. That is, a streambed conductance that works for a long stress period will not work as well for a short stress period. This can best be demonstrated with a hypothetical example. Suppose that a stream reach has an average discharge rate of 10 cubic feet per second for 1 year but that the flow occurs over 1 month during which the average discharge is 120 cubic feet per second. In addition, suppose that the stream loses an average of 1 cubic foot per second over the year or 12 cubic feet per second over the month when the stream actually flowed. The simulated streambed conductance that would work best for a stress period of 1 year would be one-twelfth of the conductance that would work best for a stress period of 1 month, all other things being equal. In this model, which uses variable-length stress periods and a constant conductance, the relation between the conductance used and the physical properties of the streambed is unknown; in addition, the simulated streambed characteristics probably would not be transferable to a similar model with longer or shorter stress periods.

The model is not a unique solution; that is, a different combination of model characteristics could be found that would simulate springflows and hydraulic heads as close to measured values as were simulated. However, an implied assumption is that the model adequately represents the interrelation of major features of this complex system. A simple example might be a system in which flow is proportional to transmissivity and the proportionality is the hydraulic gradient. If the hydraulic gradient were precisely and accurately known throughout the area in terms of hydraulic heads but neither flow nor transmissivity were known, the model could simulate the hydraulic heads with any transmissivity and the corresponding flow. If, in addition to hydraulic heads, transmissivity also were precisely and accurately known throughout the area, the corresponding flow would be accurate; however, neither is true of this hydrologic system. Hydraulic heads are known only in certain places, and values of transmissivity have been estimated only in certain places. Outflows (springflows) have been measured or estimated in some but not all places, and inflows (recharge) have been estimated for the Zuni uplift but not for The Malpais. Other flows through the system, such as underflow, have not been estimated. A large part of the aquifer is unexplored, and where some exploration has taken place, the system is complex.

The sensitivity of the model-derived hydrograph for the site northeast of Prewitt to streambed hydraulic conductivity tends to erode confidence in the artesian storage coefficient, which was adjusted on the basis of the hydrograph northeast of Prewitt. Where a certain measured or estimated value, such as the recovery rate of hydraulic heads, can be matched by a model-derived value by adjusting more than one specified characteristic, the final combination of characteristics depends on the order in which the characteristics are adjusted. In this case, the final specified streambed hydraulic conductivity had been adjusted before the final artesian storage coefficient.

Some information, such as topography and structure, places constraints on the configuration of the flow system, as does geological information. The temporal dimension adds to the complexity of the system. Time is accounted for in terms of time-related values of springflow, hydraulic head, recharge, and ground-water withdrawals, along with what are considered to be reasonable estimates of aquifer storage.

In an attempt to maintain the interrelation of the simulated system, spatial variation of simulated characteristics was minimized. For example, with a few exceptions, the simulated hydraulic conductivity of the stream bottom was 8×10^{-7} foot per second, the hydraulic conductivity of valley fill generally was about 60-70 feet per day for basalt and 40 feet per day for alluvium, and the vertical hydraulic conductivity of the Chinle Formation was 10^{-11} foot per second. Most of the exceptions were individually justified hydrologically, though some justifications are better than others. Probably two examples of the poorest justification are the use of leakances representative of the absence of Chinle Formation in rows 31-32, column 20 and in rows 44-46, column 8. In these two cases, geologic information (fig. 4) seemed to indicate that a significant thickness of Chinle was present, but a thickness of zero was hypothesized to simulate local hydraulic heads. It is possible that undiscovered, buried gullies have breached the Chinle in these places, but the assumption of such local anomalies tends to undermine the uniformity previously assumed.

Assumption that the Aquifer Simulated by the Digital Model Adequately Represents the San Andres-Glorieta-Aquifer Part of the Geohydrologic System

The digital model, which is based on the conceptual model, represents the San Andres-Glorieta-aquifer part of the geohydrologic system. However, that this representation is adequate is an assumption. The adjustment process was an attempt to make the digital model respond like the real system by simulating the measured values of hydraulic head and springflow (responses) while specifying what were thought to be (in the conceptual model) the causes (stresses) of the measured responses--withdrawals of ground and surface water from the system. The likeness of the response is not surprisingly imperfect because of the simplicity of the digital model. In addition, the likeness between the digital model and the geohydrologic system cannot be compared in locations where and times when stresses and responses have not been measured or estimated.

The direct comparison between measured and model-derived hydraulic heads, springflows, and streamflows is an attempt to bridge the gap between the digital model and the geohydrologic system. Model adjustment (sometimes called "calibration") is an attempt to make the digital model behave like the geohydrologic system even though it is structured like the conceptual model. Model adjustment gives the analyst confidence in places and times where measured values exist. Projections are extrapolations in time. The shorter the extrapolation, the more confidence is appropriate. Estimates of aquifer properties in places where measured values do not exist are extrapolations in space. Estimates of responses, such as hydraulic heads in places where aquifer properties are not measured, to measured stresses, such as groundwater withdrawals some distance away or on the opposite side of a major fault, result in the compounding of the uncertainties of extrapolation in space and time. Estimates of responses to hypothetical stresses in places where no stress-response data are available further compound the uncertainties.

Given an accurate scenario of future development, the accuracy of a projection would depend in part on the duration and accuracy of the historical simulation. To the extent that the hydrographs of measured hydraulic heads and hydrographs of measured streamflows for the Grants-Bluewater area have been accurately simulated, the projection for this area would be as accurate as estimates of future stresses. To the extent that the time periods of hydrographs of measured hydraulic heads for the periphery of the modeled area were shorter than those in the Grants-Bluewater area or were nonexistent, the accuracy of projections for those areas is less certain.

The effects of the arbitrary no-flow boundaries near the northern and south-central edges of the modeled area depend on the location, amount, and duration of simulated stresses. Although the historical simulation was shown to not be substantially affected by relocating these boundaries 40 miles farther from simulated pumping centers, projected drawdowns could be significantly magnified by them.

Although the model is not unique and has discrepancies because some features of the hydrologic system could not be measured or estimated, model-derived flows (figs. 43A and B) and hydraulic heads match measured values reasonably well (table 24; and figs. 35-42), and simulated hydraulic characteristics are plausible. Therefore, until more detailed hydrologic information becomes available, the model is plausible and may appropriately be used for estimating the effects of ground-water development on hydraulic heads and streamflows.

CONCLUSIONS

The purpose of the digital model was to test the conceptual model and to provide a mechanism for estimating the effect of previous and new development on water levels, springflow, and streamflow. The following conclusions relate to this purpose.

Internal Consistency of the Conceptual Model

To the extent that the digital model represents the conceptual model, results of the digital model are the logical results of the conceptual model. If these results, as well as the assumptions made at arriving at those results, are found at some future date to have been unreasonable, the internal consistency and assumptions of the conceptual model would need to be reassessed. Where the digital model fails to simulate some measured feature of the geohydrologic system, both the digital model and the conceptual model are subject to question. The following relate to the present assessment of internal consistency.

(1) The estimates of recharge made as part of the conceptual model seemed to indicate that recharge may be three times the quantity simulated by the digital model. However, the hydraulic-head gradient in the aquifer relates the quantity of recharge directly to the transmissivity of the aquifer, so that for a given transmissivity a larger recharge implies a steeper gradient. In the northwestern part of the digital model, the model-derived gradient was generally steeper, the specified transmissivity was larger, and the recharge was less than that of the conceptual model. This implies that the conceptual model may be inconsistent or incomplete. Recharge and transmissivity appear inconsistent with the gradient.

(2) Except for the northwestern part of the modeled area, the model-generated heads generally agree with measured heads.

(3) The postulated existence of blockage of ground-water flow in the San Andres-Glorieta aquifer at the San Rafael fault is supported by successful simulation of hydraulic heads on both sides of the fault. However, the historical simulation was not nearly as sensitive to minor changes in the degree of disconnection as the simulation of projected future withdrawals. This reduces confidence in projected drawdowns as noted below.

(4) Some elements of the water budget not directly derived from the conceptual model are deduced indirectly from the conceptual model on the basis of the digital model simulations and the comparison between the digital and conceptual models. Although the accuracy of these model-derived values is unknown, they are consistent with each other to the extent that the digital model "forces" a balanced water budget. Average natural flows at boundaries derived from the digital model under steady-state conditions are as follows:

(a) Ground-water gains and losses (rounded) at river boundaries:

Reach	Ground-water recharge (+) or discharge (-), in cubic feet per second	Brief description of locale
1	0.2	Cottonwood Creek upstream from Bluewater Lake
2	1	Reaches now occupied by Bluewater Lake
3	-0.1	Bluewater Creek upstream from Bluewater Lake
4	0.6	Bluewater Canyon
5	6	From Bluewater Canyon to Grants
6, 7, 8	0	Rio San Jose, Grants to Gallo Creek
9	-7	Ojo del Gallo
10	4	La Vega and Gallo Creek
11	-6	Rio San Jose including Horace Springs

(b) Ground-water discharge by evapotranspiration was about 7 cubic feet per second.

(c) Discharge to the Rio Grande rift was about 4 cubic feet per second.

Effects of Previous Water Development

The simulated effects of previous water development on hydraulic heads in the San Andres-Glorieta aquifer are most noticeable at a site near Bluewater Village. There, surface-water irrigation led to the simulation of deep percolation of irrigation water, which resulted in an increase in the model-derived hydraulic head calculated under the historical scenario (the historical scenario simulated actual surface- and ground-water development during 1900 through 1985) to a point above that calculated under the null scenario (the null scenario simulated no ground- or surface-water development during 1900 through 2020). However, when the simulation of ground-water withdrawals began, heads calculated under the historical scenario dropped abruptly to levels well below those of the null scenario, but the difference narrowed again to about 10 feet (rounded) by the end of the historical scenario in fall 1985. This pattern of drawdown and recovery generally was simulated for a broad area of development west of San Rafael fault. The difference between heads calculated under the historical scenario and the null scenario for the area east of San Rafael fault gradually increased to about 10 feet by the end of the historical scenario. Hydraulic heads calculated under the historical scenario for the valley-fill aquifer (La Vega) east of Ojo del Gallo dropped abruptly in the mid-1950's and recovered in the early 1980's, resulting in large changes in simulated evapotranspiration.

The simulated effect of previous development on ground-water storage was determined by comparison of water-budget values calculated under the historical and null scenarios. Because the rate of flow to or from ground-water storage varies widely with seasonal changes in hydraulic head, the difference between the flow from storage under the historical scenario and that under the null scenario also varies widely and trends are difficult to determine. However, trends in the cumulative difference are relatively easy to determine. A trend of increased ground-water storage in the early 1940's was reversed in the mid-1940's when large ground-water withdrawals began. Decreases in ground-water storage continued into the 1960's and the trend reversed in the late 1970's. These trends are reasonable because they are inversely proportional to trends in hydraulic heads.

Simulated ground-water evapotranspiration under the historical scenario was generally less than under the null scenario; this difference is termed salvaged evapotranspiration. Salvaged evapotranspiration was about 1.5 cubic feet per second or about 25 percent of the evapotranspiration calculated under the null scenario in the 1930's and early 1940's, then increased as ground-water development began and discharge from Ojo del Gallo decreased. Salvaged evapotranspiration was about 4.5 cubic feet per second during the 1970's or about 80 percent of the evapotranspiration calculated under the null scenario. This would lead to the conclusion that 4 or 5 cubic feet per second of the ground water and surface water withdrawn by development was replaced by salvaged evapotranspiration. A second conclusion would be that additional salvage of evapotranspiration is not likely because most water available for evapotranspiration has been salvaged by previous development. However, because of the large uncertainty of model-derived ground-water evapotranspiration rates, the quantity of salvaged evapotranspiration is likely to be largely in error. The magnitude of this possible error is unknown.

The effect of previous development on springflow at Ojo del Gallo is estimated. Null-scenario springflow was about 7 cubic feet per second through the early 1940's, decreasing to about 5 cubic feet per second by 1960, and increasing after 1960. Historical-scenario springflow increased to as much as about 8 cubic feet per second in the early 1940's, decreasing to zero in the mid-1950's. No springflow was simulated until the mid-1980's. Except for the late 1930's and early 1940's, almost the entire null-scenario flow was extinguished by the development simulated under the historical scenario.

Horace Springs emerges in the lowermost simulated reach of the Rio San Jose (reach 11). The simulated gain in reach 11 was generally about 5.5 cubic feet per second under the null scenario. The simulated stream gain under the historical scenario decreased very gradually to about 90 percent of the null-scenario gain. This small effect is reasonable because simulated development did not change greatly the gradient in the valley-fill aquifer. Simulated water development resulted in drawdowns in the valley-fill aquifer upstream in La Vega where simulated drawdowns of 10-15 feet reduced the average gradient of the water table between there and Horace Springs by about 10 percent.

Although ground-water inflow to reach 11 did not change greatly, changes in streamflow, including the effect of previous development on surface-water inflow to that reach, were substantial. The difference between the discharge from reach 11 simulated under the null scenario and that under the standard scenario averaged about 6 cubic feet per second. The difference in discharge is largely dependent on the difference in specified inflow that was estimated in the conceptual model.

The simulated effect of development on reaches 1 and 3 upstream from Bluewater Lake is very small, about 0.01 cubic foot per second. The combined effect of Bluewater Lake and capture by ground-water withdrawals on reaches 2 and 4 (representing Bluewater Lake and Bluewater Canyon) was about 1 cubic foot per second of increased ground-water recharge. Because specified inflows to reach 5 (representing Bluewater Creek and the Rio San Jose between gaging stations 08342000 and 08343000) were generally less for the historical scenario than for the null scenario, there was a reduction in ground-water recharge along that reach of about 1 cubic foot per second. Ground-water recharge and discharge along reaches 6, 7, and 8 were very small, about 0.2 cubic foot per second. The effect of previous development on reach 10 (La Vega and Gallo Creek) generally was to extinguish the flow as a direct result of the extinguishment of springflow at Ojo del Gallo. Simulated discharge from reach 10 under the historical scenario approached that of the null scenario only in the early 1940's when the effect on Ojo del Gallo was an increase in springflow.

Potential Effects of New Development

A ground-water withdrawal of 10,000 acre-feet per year (13.8 cubic feet per second) was simulated from the San Andres-Glorieta aquifer east of San Rafael fault for 35 years (Acoma scenario). Because this projected withdrawal was for irrigation, 3,333 acre-feet per year (one-third of the withdrawal) was simulated as recharge to the valley-fill aquifer in the same vicinity. The effect of this development was estimated by comparing the heads simulated in the Acoma scenario with the heads simulated without the Acoma scenario. Thus, the simulated heads without the Acoma scenario reverted from a projection of a continuation of the 1980's level of development.

Simulated drawdowns resulted both with and without the Acoma development. The difference between the projected hydraulic heads was attributed to the additional development simulated under the Acoma scenario. The next significant effects of the new development are as follows:

(1) The projected withdrawal of 10,000 acre-feet per year resulted in an estimated 200 feet (rounded) of drawdown at the withdrawal site and about 20 feet (rounded) in the area west of the fault. This distribution of drawdown depends on the degree of hydraulic disconnection at San Rafael fault. These drawdowns may be 20 percent less due to boundary conditions at the lateral extent of the model, especially the unknown boundary to the south of the 10,000-acre-foot withdrawal. These drawdowns may be 30 percent less due to possible leakage from confining beds above and below the San Andres-Glorieta aquifer.

(2) The projected withdrawal of 10,000 acre-feet per year resulted in no significant estimated depletion of streamflow as determined by a comparison of the budget of the Acoma scenarios with that of the simulation without the Acoma development. Almost all of the withdrawal was estimated to have been derived from ground-water storage.

Because the history of springflow and most of the history of hydraulic heads do not include the area of the San Andres-Glorieta aquifer east of San Rafael fault, the close comparison of measured and model-derived hydraulic heads does not lend confidence to the projected drawdowns or the projected source of water for the withdrawal of 10,000 acre-feet per year. Because there is almost no direct comparison between the digital model and the geohydrologic system, any confidence that may exist is based on the comparison between the digital model and the conceptual model, and ultimately on the comparison between the conceptual model and the geohydrologic system.

If large withdrawals from the San Andres-Glorieta aquifer east of San Rafael fault are made, and accurate records kept of the withdrawals (stress) in addition to accurate records of hydraulic heads (response), it would be possible to readjust the digital model to simulate these stress-response relations and increase confidence in projections.

The projection of the 1985 level of development resulted in cessation of springflow at Ojo del Gallo. The simulated resurgence of springflow at Ojo del Gallo during the late 1970's and 1980's is mainly the result of the specification of greater-than-average mountain recharge, greater-than-average streamflow in Bluewater Creek, and less-than-average ground-water withdrawals for irrigation during that time. These factors resulted in model-derived hydraulic heads rising to a temporary high during the late 1970's and early 1980's even though municipal and industrial ground-water withdrawals generally were trending upward. The simulated abrupt reduction of municipal and industrial ground-water withdrawals in the early 1980's allowed simulated flow at Ojo del Gallo temporarily after simulated hydraulic heads already had increased. However, because projected discharge from Ojo del Gallo ceases under the conditions of average natural recharge and streamflow and no additional water development, a larger reduction of specified withdrawals would be needed to assure simulated springflow under normal conditions of recharge and streamflow. To the extent that the simulation might accurately represent the natural flow system, these conclusions would apply to the question of continued springflow at Ojo del Gallo.

Many of the sensitivity tests showed that the projection was much more sensitive to changes in specified aquifer properties (artesian storage coefficient, leakage from confining beds, and hydraulic disconnection at San Rafael fault) than was the historical scenario. This situation does not lend confidence to the projections, and arises because most records of surface- and ground-water withdrawals (stress) and hydraulic heads (response) pertain to a small area (relative to the size of the digital model) west of the San Rafael fault that is relatively close to the outcrop. The main storage property of the aquifer near the outcrop is specific yield, a property that is usually about 1,000 times the artesian storage coefficient. However, the response at a greater distance from the outcrop is relatively more dependent on the artesian storage coefficient. Although records of hydraulic heads for sites east of the San Rafael fault exist, these sites also are near the outcrop and the structurally complex mountainside. The digital model could be more constrained if accurate records of stresses and responses are kept for all areas of interest including areas distant from the outcrop and in the Acoma embayment.

Sensitivity tests showed also that the specified inflow to reach 5 (between the mouth of Bluewater Canyon and Grants) was critical to simulating much of the variability of hydraulic heads in the San Andres-Glorieta aquifer. Accurate records of stream discharge at gaging station 08342000 would be helpful and probably would be less costly than estimates unless records of discharge downstream from Bluewater Dam were kept. Records of streamflow and springflow generally are very useful in constraining the streamflow boundary of the ground-water system, and the cost/effectiveness ratio is probably much less than estimates because the effectiveness of streamflow estimates for constraining the model boundary is near zero. Records of surface-water inflow to Bluewater Lake and of discharge from Ojo del Gallo and the continuing records of streamflow downstream from Horace Springs would be very useful.

REFERENCES

Aqua Science, Inc., 1982, Study of the Rio San Jose basin above the Acoma Indian Reservation: Consultant's report to the Pueblo of Acoma, March 1982, 370 p.

Baars, D.L., 1962, Permian system of Colorado Plateau, in Bulletin of the American Association of Petroleum Geologists, v. 46, no. 2, p. 149-218.

Baldwin, J.A., and Anderholm, S.K., in press, Hydrogeology and ground-water chemistry of the San Andres-Glorieta aquifer in the Acoma embayment and eastern Zuni uplift, west-central New Mexico: U.S. Geological Survey Water-Resources Investigations Report 91-4033.

Ballance, W.C., and others, 1962, Ground-water levels in New Mexico, 1960: New Mexico State Engineer Technical Report 27, 215 p.

Barela, Josephine, 1975, Ojo del Gallo--A nostalgic narrative of historic San Rafael: Grants, New Mexico, Service Printing and Office Supply, 32 p.

Blaney, H.F., and Hanson, E.G., 1965, Consumptive use and water requirements in New Mexico: New Mexico State Engineer Technical Report 32, 85 p.

Bostick, Kent, Hubbel, Joel, and Jercinovic, Devon, 1985, Ground-water discharge plan analysis for Homestake uranium mill near Milan, New Mexico; Homestake Mining Co. Appendix B of Radioactive Materials License Application Analysis: New Mexico Environmental Improvement Division, 83 p.

Busch, F.E., Hudson, J.D., and Sorensen, E.F., 1967, Ground-water levels in New Mexico, 1965, and changes in water levels, 1961-1965: New Mexico State Engineer Technical Report 34, 124 p.

Cooper, J.B., and John, E.C., 1968, Geology and ground-water occurrence in southeastern McKinley County, New Mexico: New Mexico State Engineer Technical Report 35, 108 p.

Cooper, J.B., and West, S.W., 1967, Principal aquifers and uses of water between Laguna Pueblo and Gallup, Valencia and McKinley Counties, New Mexico, in Guidebook of Defiance-Zuni-Mount Taylor region: New Mexico Geological Society, 18th Field Conference, p. 145-149.

Dames and Moore, 1981, Volume XVIII-Pumping test evaluations, Bluewater Uranium Mill vicinity near Grants, New Mexico, for Anaconda Copper Company: October 5, 1981, var. pagination.

_____1986, Ground-water model above-grade tailings impoundment, Bluewater mill and vicinity near Grants, New Mexico for Anaconda Minerals Company: Consultant's report for Anaconda Minerals Company, Grants, New Mexico, March 21, 1986, var. pagination.

Davies, P.B., 1986, Modeling areal, variable-density, ground-water flow using equivalent freshwater head--Analysis of potentially significant errors, in National Water Well Association Conference, Denver, Colorado, February 10-12, 1987: Proceedings, p. 888-903.

Emery, P.A., 1970, Electric analog model evaluation of a water-salvage plan, San Luis Valley, south-central Colorado: Colorado Ground Water Circular 14, 11 p.

Freeze, R.A., and Cherry, J.A., 1979, Groundwater: Englewood Cliffs, N.J., Prentice-Hall, Inc., 604 p.

Frenzel, P.F., 1992, Listings of model input values for the simulation of ground-water flow in the San Andres-Glorieta aquifer in the Acoma embayment and eastern Zuni uplift, west-central New Mexico (Supplement to Water-Resources Investigations Report 91-4099): U.S. Geological Survey Open-File Report 91-236, 4 p., 2 diskettes.

Frenzel, P.F., and Lyford, F.P., 1982, Estimates of vertical hydraulic conductivity and regional ground-water flow rates in rocks of Jurassic and Cretaceous age, San Juan Basin, New Mexico and Colorado: U.S. Geological Survey Water-Resources Investigations Report 82-4015, 59 p.

Geohydrology Associates, Inc., 1981, In the matter of the plan of replacement of Plains Electric Generation and Transmission Cooperative, Inc.: Consultant's report to Plains Electric Generation and Transmission Cooperative, Inc., September 1981, 81 p.

_____1984, Summary of well and aquifer performance test of Plains wells B-18 and B-19, Yager and McBride wells, near Grants, New Mexico: Consultant's report to Plains Electric Generation and Transmission Cooperative, Inc., August 1984, 47 p.

Gordon, E.D., 1961, Geology and ground-water resources of the Grants-Bluewater area, Valencia County, New Mexico, with a section on Aquifer characteristics, by N.L. Reeder, and a section on Chemical quality of the ground water, by J.L. Kunkler: New Mexico State Engineer Technical Report 20, 109 p.

Green, M.W., and Pierson, C.T., 1977, A summary of the stratigraphy and depositional environments of Jurassic and related rocks in the San Juan Basin, Arizona, Colorado, and New Mexico, in Guidebook of the San Juan Basin III: New Mexico Geological Society, 28th Field Conference, p. 147-152.

Hantush, M.S., 1960, Modification of the theory of leaky aquifers: Journal of Geophysical Research, v. 65, no. 11, November 1960, p. 3713-3725.

Hearne, G.A., and Dewey, J.D., 1988, Hydrologic analysis of the Rio Grande basin north of Embudo, New Mexico, Colorado and New Mexico: U.S. Geological Survey Water-Resources Investigations Report 86-4113, 244 p.

Hodges, P.V., 1938, Report on irrigation and water supply of the pueblos of New Mexico in the Rio Grande basin: U.S. Department of the Interior, Indian Irrigation Service, 438 p.

Hydro-Engineering, 1983, Ground-water discharge plan for Homestake's mill near Milan, New Mexico: Consultant's report to Homestake Mining Company, August 31, 1983, var. pagination.

Hydro-Search, Inc., 1977, Hydrogeology of the Bluewater mill tailings pond area, Valencia County, New Mexico: Consultant's report to Anaconda Copper Company, October 17, 1977, 111 p.

_____1978a, Supplement to the hydrogeology report of October 17, 1977, Bluewater mill area, Valencia County, New Mexico: Consultant's report to Anaconda Copper Company, November 15, 1978, 69 p.

_____1978b, Ground-water monitoring program, Bluewater mill area, Valencia County, New Mexico: Consultant's report to Anaconda Copper Company, November 15, 1978, 25 p.

_____1981, Regional ground-water hydrology and water chemistry, Grants-Bluewater area, Valencia County, New Mexico: Consultant's report to Anaconda Copper Company, May 15, 1981, 2 v., 6 appendices, 9 pls., 85 p.

Jobin, D.A., 1962, Relation of the transmissive character of the sedimentary rocks of the Colorado Plateau to the distribution of uranium deposits: U.S. Geological Survey Bulletin 1124, 151 p.

Lansford, R.R., Ben-David, Shaul, Gebhard, T.G., Jr., Brutsaert, W.F., and Creel, B.J., 1973, An analytical interdisciplinary evaluation of the utilization of the water resources of the Rio Grande in New Mexico, middle Rio Grande region: Las Cruces, New Mexico Water Resources Research Institute Report 22, 99 p.

Lohman, S.W., 1972, Ground-water hydraulics: U.S. Geological Survey Professional Paper 708, 70 p.

Lyford, F.P., 1979, Ground water in the San Juan Basin, New Mexico and Colorado: U.S. Geological Survey Water-Resources Investigations 79-73, 22 p.

McDonald, M.G., and Harbaugh, A.W., 1988, A modular three-dimensional finite-difference ground-water flow model: U.S. Geological Survey Techniques of Water-Resources Investigations, book 6, chap. A1, var. pagination.

Miller, R.S., 1988, User's guide for RIV2--A package for routing and accounting of river discharge for a modular, three-dimensional, finite-difference, ground-water flow model: U.S. Geological Survey Open-File Report 88-345, 33 p.

Morgan, A.M., 1938, Ground-water conditions in a portion of the Rio San Jose-Bluewater valley in the vicinity of Grants, New Mexico: U.S. Geological Survey Open-File Report, 16 p.

Pearce, T.M., 1965, New Mexico place names--A geographical dictionary: Albuquerque, University of New Mexico Press, 187 p.

Reeder, H.O., and others, 1962, Ground-water levels in New Mexico, 1958: New Mexico State Engineer Technical Report 23, 288 p.

Reeve, F.D., 1961, History of New Mexico: New York, Lewis Historical Publishing Co., 3 v., 485, 449, and 668 p.

Risser, D.W., 1982, Estimated natural streamflow in the Rio San Jose upstream from the Pueblos of Acoma and Laguna, New Mexico: U.S. Geological Survey Water-Resources Investigations Report 82-4096, 51 p.

Risser, D.W., and Lyford, F.P., 1983, Water resources on the Pueblo of Laguna, west-central New Mexico: U.S. Geological Survey Water-Resources Investigations Report 83-4038, 308 p.

Sorensen, E.F., 1977, Water use by categories in New Mexico, counties and river basins, and irrigated and dry cropland acreage in 1975: New Mexico State Engineer Technical Report 41, 34 p.

_____1982, Water use by categories in New Mexico counties and river basins, and irrigated acreage in 1980: New Mexico State Engineer Technical Report 44, 51 p.

Spiegel, Zane, 1955, Geology and ground-water resources of northeastern Socorro County, New Mexico: Socorro, New Mexico Bureau of Mines and Mineral Resources Ground-Water Report 4, 99 p.

Thaden, R.E., and Zech, R.S., 1984, Preliminary structure-contour map on the base of the Cretaceous Dakota Sandstone in the San Juan Basin and vicinity, New Mexico, Arizona, Colorado, and Utah: U.S. Geological Survey Miscellaneous Field Studies Map MF-1673, scale 1:500,000.

Titus, F.B., Jr., 1963, Geology and ground-water conditions in eastern Valencia County, New Mexico: Socorro, New Mexico Bureau of Mines and Mineral Resources Ground-Water Report 7, 113 p.

U.S. Bureau of Indian Affairs, 1984, Bluewater Basin withdrawals and sources of water: BIA Albuquerque Area Office, Branch of Rights Protection, 36 p.

U.S. Department of Agriculture, 1972, Gross annual lake evaporation, 1 map, in U.S. Bureau of Reclamation, 1973, New Mexico water-resources assessment for planning purposes: v. II, supporting data, 44 p.

_____1985, Cibola National Forest land and resource management plan: U.S. Forest Service, Southwestern Region, 279 p.

U.S. Department of Commerce, no date, Normal October-April precipitation, 1931-1960, state of New Mexico: Environmental Science Services Administration, Weather Bureau, 1 map.

U.S. Geological Survey, 1949-57, Water levels and artesian pressure in observation wells in the United States--Part 6, southwestern States and Territory of Hawaii: Water-Supply Papers 1076, 1101, 1131, 1161, 1170, 1196, 1226, 1270, and 1326, var. pagination.

_____1960, Compilation of records of surface waters of the United States through September 1950--Part 8, Western Gulf of Mexico Basins: U.S. Geological Survey Water-Supply Paper 1312, 633 p.

_____[1952-61], Surface water supply of the United States--Part 8, Western Gulf of Mexico Basins, annual reports as follows: 1951, Water-Supply Paper 1212; 1952, Water-Supply Paper 1242; 1953, Water-Supply Paper 1282; 1954, Water-Supply Paper 1342; 1955, Water-Supply Paper 1392; 1956, Water-Supply Paper 1442; 1957, Water-Supply Paper 1512; 1958, Water-Supply Paper 1562; 1959, Water-Supply Paper 1632; 1960, Water-Supply Paper 1712.

_____1964, Compilation of records of surface waters of the United States, October 1950 to September 1960--Part 8, Western Gulf of Mexico Basins: U.S. Geological Survey Water-Supply Paper 1732, 573 p.

_____[1962-65], Surface-water records of New Mexico, water years 1961-64 (published annually).

_____1966-75, Water-resources data for New Mexico, water years 1965-74--Part 1, surface-water records (published annually).

_____1976-87, Water-resources data for New Mexico, water years 1975-86: U.S. Geological Survey Water-Data Reports NM-75-1 to NM-86-1 (published annually).

West, S.A., 1972, Disposal of uranium-mill effluent by well injection in the Grants area, Valencia County, New Mexico: U.S. Geological Survey Professional Paper 386-D, 28 p.

SUPPLEMENTAL INFORMATION

Excess precipitation, that part of precipitation not used by evapotranspiration, was estimated for part of the Zuni uplift area by a method developed for the San Juan Mountains of Colorado by J.D. Dewey (Hearne and Dewey, 1988, p. 14-29). This method estimates a water balance (figs. 61 and 62) that accounts for precipitation, storage in the snowpack and root zone, sublimation from the snowpack, and evapotranspiration. The remainder is excess precipitation.

The Zuni uplift area was divided into 53 drainage basins (fig. 63). Each drainage basin was divided into subbasins (not shown) on the basis of altitude (U.S. Geological Survey topographic maps, scale 1:24,000) and average annual winter precipitation (U.S. Department of Commerce, no date).

Daily precipitation in a subbasin was estimated as a function of daily precipitation at McGaffey, the average annual winter precipitation in the subbasin (U.S. Department of Commerce, no date), the average annual winter precipitation at McGaffey, and, during May to September, a regression coefficient relating average annual winter precipitation to average monthly precipitation for six nearby stations (table 32). Hearne and Dewey (1988) found that daily precipitation was more closely correlated to average winter precipitation than to average annual or average summer precipitation for the San Juan Mountains. The same was assumed to hold true for the mountains of the Zuni uplift.

Buildup and melting of the snowpack were estimated on the basis of temperature. Temperature was estimated by adjusting the temperature measured at McGaffey on the basis of a regression coefficient relating temperature to altitude at six nearby stations (table 33). (McGaffey, due north of Ramah and due west of Thoreau, is outside of the study area on the northwestern end of the Zuni uplift. Fort Wingate and Gamerco are farther to the northwest.) Gaps in the temperature records at McGaffey were filled by adjusting records for the Fort Wingate and Gamerco stations. McGaffey was considered to be the most representative station for the mountains in the Zuni uplift. Tables 32 and 33 reflect similar tables in Hearne and Dewey (1988).

When a snowpack was not simulated, evapotranspiration was simulated. Sublimation of the snowpack was assumed to be 0.011 inch per day, the same as was simulated for the San Juan Mountains. The rate of evapotranspiration was estimated on the basis of temperature, altitude, solar radiation, vegetation type, and soil moisture.

Storage of the root zone was 0.2 times the depth of the root zone, which was assumed to be dependent on vegetation type. The vegetation types were grass (soil depth 2 feet), piñon-juniper (soil depth 3 feet), and ponderosa (soil depth 3.5 feet). Timber type was determined for each subbasin on the basis of altitudes estimated from unpublished U.S. Forest Service planning maps. Generally, similar timber-type information is on a published map showing the forest plan (U.S. Department of Agriculture, 1985). Grass areas were determined from U.S. Geological Survey 7 1/2-minute topographic maps. During field observation full tree cover was assumed where 20 percent or more timber cover was indicated on the topographic maps.

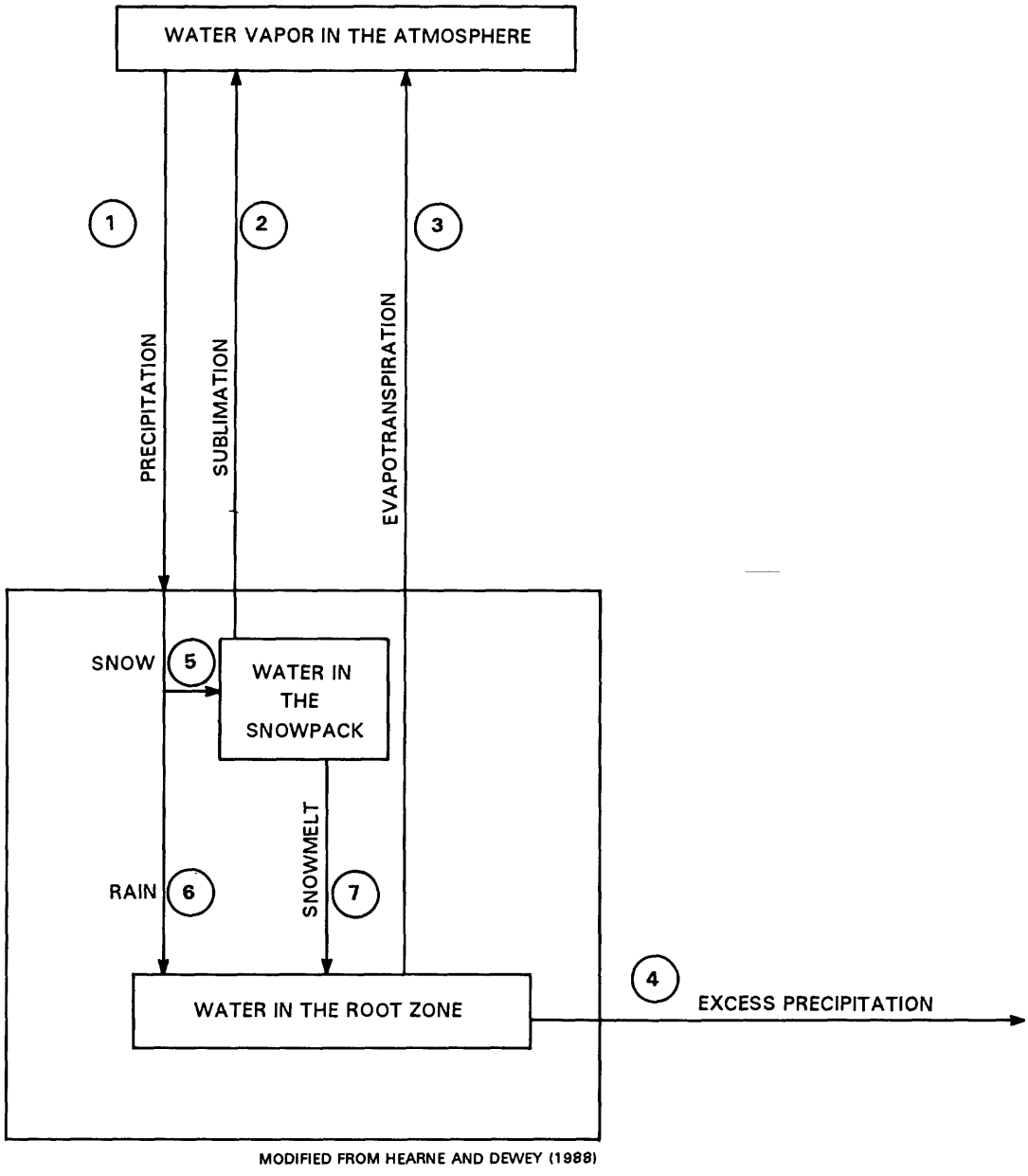

Figure 61.--Movement of water as represented in the water-budget model of the Zuni uplift.

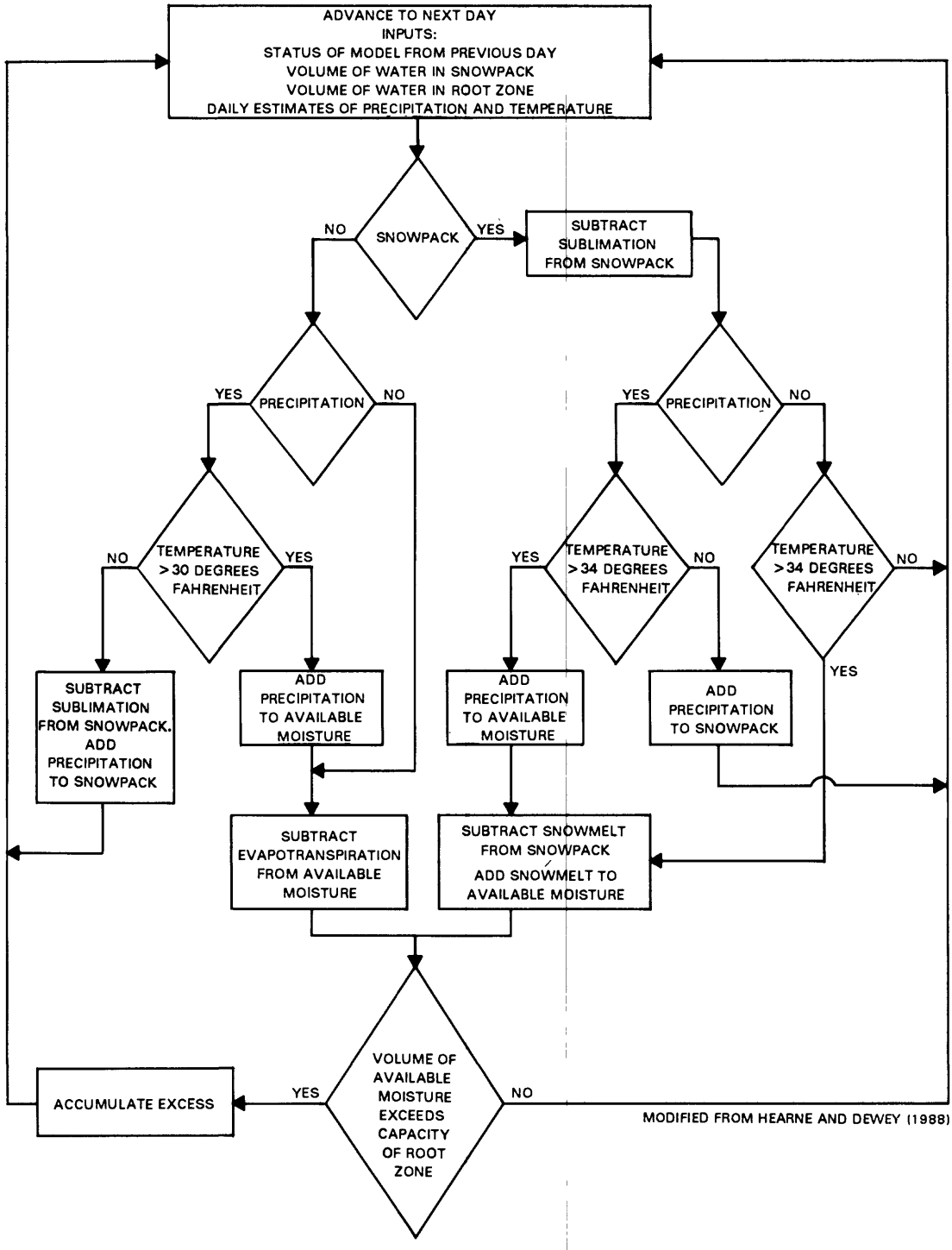

Figure 62.--Flow chart of the water-budget model of the Zuni uplift.

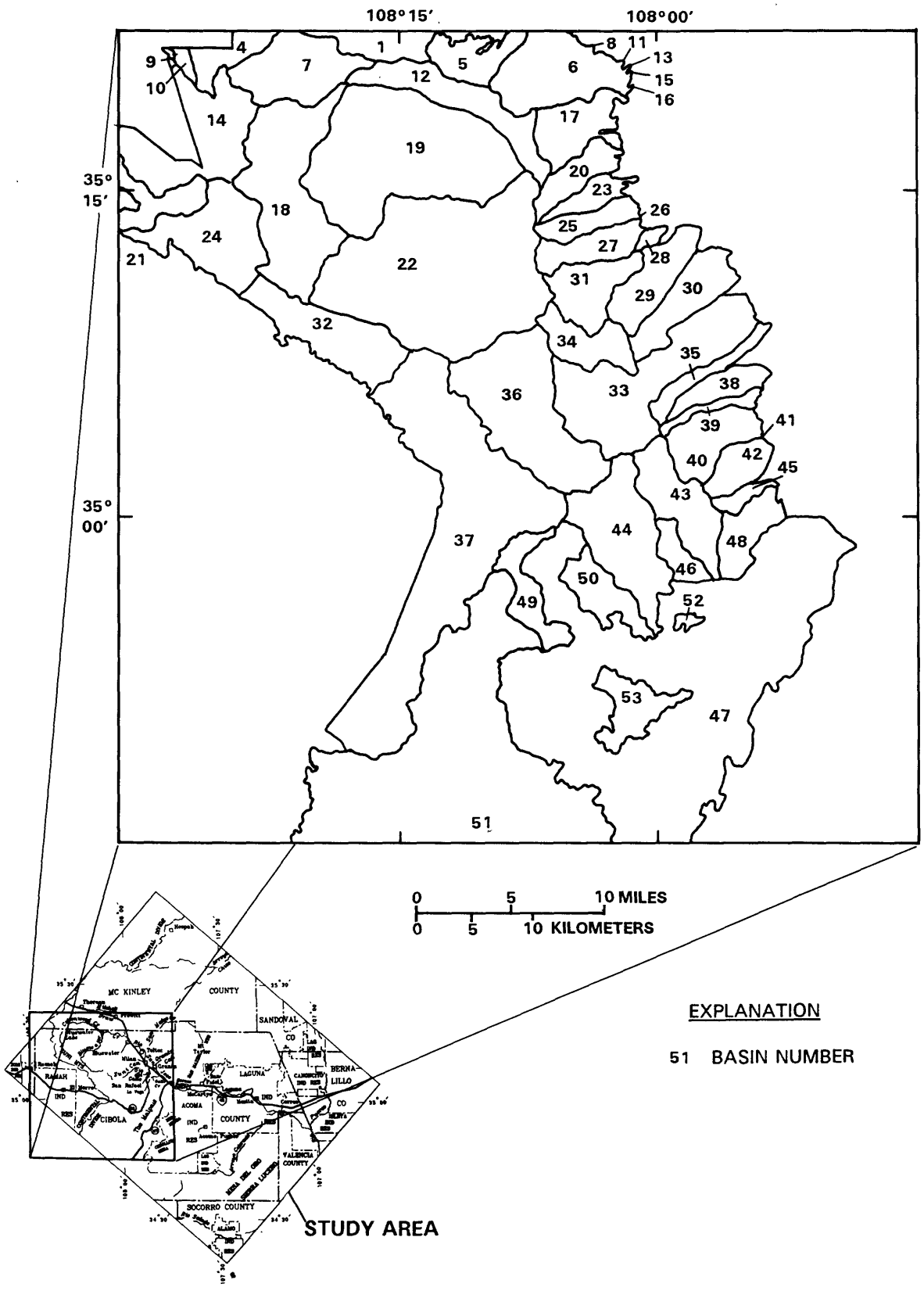

Figure 63.--Drainage basins as defined for the water-budget model of the Zuni uplift.

Table 9.--Specified bottom altitude for layer 1, in feet

[Zero values are shown where layer 1 is inactive. Layer 1 is inactive in rows 1-16 and 58-76 (not shown)]

	Columns									
	1	2	3	4	5	6	7	8	9	10
	11	12	13	14	15	16	17	18	19	20
	21	22	23	24	25	26	27	28	29	30
	31	32	33	34	35	36	37	38	39	40
Rows	41	42	43							
17	0.0000	0.0000	0.0000	0.0000	0.0000	0.0000	0.0000	0.0000	0.0000	0.0000
	0.0000	0.0000	0.0000	0.0000	0.0000	0.0000	0.0000	0.0000	0.0000	0.0000
	0.0000	0.0000	6,640	0.0000	0.0000	0.0000	0.0000	0.0000	0.0000	0.0000
	0.0000	0.0000	0.0000	0.0000	0.0000	0.0000	0.0000	0.0000	0.0000	0.0000
	0.0000	0.0000	0.0000							
18	0.0000	0.0000	0.0000	0.0000	0.0000	0.0000	0.0000	0.0000	0.0000	0.0000
	0.0000	0.0000	0.0000	0.0000	0.0000	0.0000	0.0000	0.0000	0.0000	0.0000
	0.0000	0.0000	6,620	0.0000	0.0000	0.0000	0.0000	0.0000	0.0000	0.0000
	0.0000	0.0000	0.0000	0.0000	0.0000	0.0000	0.0000	0.0000	0.0000	0.0000
	0.0000	0.0000	0.0000							
19	0.0000	0.0000	0.0000	0.0000	0.0000	0.0000	0.0000	0.0000	0.0000	0.0000
	0.0000	0.0000	0.0000	0.0000	0.0000	0.0000	0.0000	0.0000	0.0000	0.0000
	0.0000	0.0000	6,600	0.0000	0.0000	0.0000	0.0000	0.0000	0.0000	0.0000
	0.0000	0.0000	0.0000	0.0000	0.0000	0.0000	0.0000	0.0000	0.0000	0.0000
	0.0000	0.0000	0.0000							
20	0.0000	0.0000	0.0000	0.0000	0.0000	0.0000	0.0000	0.0000	0.0000	0.0000
	0.0000	0.0000	0.0000	0.0000	0.0000	0.0000	0.0000	0.0000	0.0000	0.0000
	0.0000	0.0000	6,580	0.0000	0.0000	0.0000	0.0000	0.0000	0.0000	0.0000
	0.0000	0.0000	0.0000	0.0000	0.0000	0.0000	0.0000	0.0000	0.0000	0.0000
	0.0000	0.0000	0.0000							

Table 9.--Specified bottom altitude for layer 1, in feet--Continued

Rows	Columns 1	2	3	4	5	6	7	8	9	10
	11	12	13	14	15	16	17	18	19	20
	21	22	23	24	25	26	27	28	29	30
	31	32	33	34	35	36	37	38	39	40
	41	42	43							
21	0.0000	0.0000	0.0000	0.0000	0.0000	0.0000	0.0000	0.0000	0.0000	0.0000
	0.0000	0.0000	0.0000	0.0000	0.0000	0.0000	0.0000	0.0000	0.0000	0.0000
	0.0000	6,630	6,560	6,700	0.0000	0.0000	0.0000	0.0000	0.0000	0.0000
	0.0000	0.0000	0.0000	0.0000	0.0000	0.0000	0.0000	0.0000	0.0000	0.0000
	0.0000	0.0000	0.0000							
22	0.0000	0.0000	0.0000	0.0000	0.0000	0.0000	0.0000	0.0000	0.0000	0.0000
	0.0000	0.0000	0.0000	0.0000	0.0000	0.0000	0.0000	0.0000	0.0000	0.0000
	0.0000	6,600	6,550	6,600	0.0000	0.0000	0.0000	0.0000	0.0000	0.0000
	0.0000	0.0000	0.0000	0.0000	0.0000	0.0000	0.0000	0.0000	0.0000	0.0000
	0.0000	0.0000	0.0000							
23	0.0000	0.0000	0.0000	0.0000	0.0000	0.0000	0.0000	0.0000	0.0000	0.0000
	0.0000	0.0000	0.0000	0.0000	0.0000	0.0000	0.0000	0.0000	6,520	0.0000
	0.0000	6,540	6,540	6,600	0.0000	0.0000	0.0000	0.0000	0.0000	0.0000
	0.0000	0.0000	0.0000	0.0000	0.0000	0.0000	0.0000	0.0000	0.0000	0.0000
	0.0000	0.0000	0.0000							
24	0.0000	0.0000	0.0000	0.0000	0.0000	0.0000	0.0000	0.0000	0.0000	0.0000
	0.0000	0.0000	0.0000	0.0000	0.0000	0.0000	0.0000	0.0000	6,519	0.0000
	0.0000	6,520	6,560	6,600	0.0000	0.0000	0.0000	0.0000	0.0000	0.0000
	0.0000	0.0000	0.0000	0.0000	0.0000	0.0000	0.0000	0.0000	0.0000	0.0000
	0.0000	0.0000	0.0000							

Table 9.--Specified bottom altitude for layer 1, in feet--Continued

Rows	Columns 1	2	3	4	5	6	7	8	9	10
	11	12	13	14	15	16	17	18	19	20
	21	22	23	24	25	26	27	28	29	30
	31	32	33	34	35	36	37	38	39	40
	41	42	43							
25	0.0000	0.0000	0.0000	0.0000	0.0000	0.0000	0.0000	0.0000	0.0000	0.0000
	0.0000	0.0000	0.0000	0.0000	0.0000	0.0000	0.0000	0.0000	6,514	6,514
	6,500	6,500	6,560	6,600	0.0000	0.0000	0.0000	0.0000	0.0000	0.0000
	0.0000	0.0000	0.0000	0.0000	0.0000	0.0000	0.0000	0.0000	0.0000	0.0000
	0.0000	0.0000	0.0000							
26	0.0000	0.0000	0.0000	0.0000	0.0000	0.0000	0.0000	0.0000	0.0000	0.0000
	0.0000	0.0000	0.0000	0.0000	0.0000	0.0000	0.0000	0.0000	6,500	6,490
	6,490	6,500	6,600	6,600	0.0000	0.0000	0.0000	0.0000	0.0000	0.0000
	0.0000	0.0000	0.0000	0.0000	0.0000	0.0000	0.0000	0.0000	0.0000	0.0000
	0.0000	0.0000	0.0000							
27	0.0000	0.0000	0.0000	0.0000	0.0000	0.0000	0.0000	0.0000	0.0000	0.0000
	0.0000	0.0000	0.0000	0.0000	0.0000	0.0000	0.0000	6,500	6,480	6,470
	0.0000	0.0000	0.0000	0.0000	0.0000	0.0000	0.0000	0.0000	0.0000	0.0000
	0.0000	0.0000	0.0000	0.0000	0.0000	0.0000	0.0000	0.0000	0.0000	0.0000
	0.0000	0.0000	0.0000							
28	0.0000	0.0000	0.0000	0.0000	0.0000	0.0000	0.0000	0.0000	0.0000	0.0000
	0.0000	0.0000	0.0000	0.0000	0.0000	0.0000	0.0000	6,500	6,470	6,460
	6,500	6,600	0.0000	0.0000	0.0000	0.0000	0.0000	0.0000	0.0000	0.0000
	0.0000	0.0000	0.0000	0.0000	0.0000	0.0000	0.0000	0.0000	0.0000	0.0000
	0.0000	0.0000	0.0000							

Table 9.--Specified bottom altitude for layer 1, in feet--Continued

Rows	Columns 1	2	3	4	5	6	7	8	9	10
	11	12	13	14	15	16	17	18	19	20
	21	22	23	24	25	26	27	28	29	30
	31	32	33	34	35	36	37	38	39	40
	41	42	43							
29	0.0000	0.0000	0.0000	0.0000	0.0000	0.0000	0.0000	0.0000	0.0000	0.0000
	0.0000	0.0000	0.0000	0.0000	0.0000	0.0000	0.0000	6,500	6,460	6,450
	6,450	6,500	0.0000	0.0000	0.0000	0.0000	0.0000	0.0000	0.0000	0.0000
	0.0000	0.0000	0.0000	0.0000	0.0000	0.0000	0.0000	0.0000	0.0000	0.0000
	0.0000	0.0000	0.0000							
30	0.0000	0.0000	0.0000	0.0000	0.0000	0.0000	0.0000	0.0000	0.0000	0.0000
	0.0000	0.0000	0.0000	0.0000	0.0000	0.0000	0.0000	0.0000	6,480	6,440
	6,440	6,500	0.0000	0.0000	0.0000	0.0000	0.0000	0.0000	0.0000	0.0000
	0.0000	0.0000	0.0000	0.0000	0.0000	0.0000	0.0000	0.0000	0.0000	0.0000
	0.0000	0.0000	0.0000							
31	7,000	7,000	0.0000	0.0000	0.0000	0.0000	0.0000	0.0000	0.0000	0.0000
	0.0000	0.0000	0.0000	0.0000	0.0000	0.0000	0.0000	0.0000	6,484	6,430
	6,440	6,490	0.0000	0.0000	0.0000	0.0000	0.0000	0.0000	0.0000	0.0000
	0.0000	0.0000	0.0000	0.0000	0.0000	0.0000	0.0000	0.0000	0.0000	0.0000
	0.0000	0.0000	0.0000							
32	7,000	7,000	0.0000	0.0000	0.0000	0.0000	0.0000	0.0000	0.0000	0.0000
	0.0000	0.0000	0.0000	0.0000	0.0000	0.0000	0.0000	0.0000	6,480	6,420
	6,440	6,470	0.0000	0.0000	0.0000	0.0000	0.0000	0.0000	0.0000	0.0000
	0.0000	0.0000	0.0000	0.0000	0.0000	0.0000	0.0000	0.0000	0.0000	0.0000
	0.0000	0.0000	0.0000							

Table 9.--Specified bottom altitude for layer 1, in feet--Continued

Rows	Columns 1	2	3	4	5	6	7	8	9	10
	11	12	13	14	15	16	17	18	19	20
	21	22	23	24	25	26	27	28	29	30
	31	32	33	34	35	36	37	38	39	40
	41	42	43							
33	7,000	7,000	0.0000	0.0000	0.0000	0.0000	0.0000	0.0000	0.0000	0.0000
	0.0000	0.0000	0.0000	0.0000	0.0000	0.0000	6,380	6,390	6,400	6,420
	6,430	6,440	6,450	6,450	0.0000	0.0000	0.0000	0.0000	0.0000	0.0000
	0.0000	0.0000	0.0000	0.0000	0.0000	0.0000	0.0000	0.0000	0.0000	0.0000
	0.0000	0.0000	0.0000							
34	7,000	7,000	0.0000	0.0000	0.0000	0.0000	0.0000	0.0000	0.0000	0.0000
	0.0000	0.0000	0.0000	0.0000	0.0000	6,370	6,370	6,380	6,390	6,430
	6,430	6,450	6,450	6,540	0.0000	0.0000	0.0000	0.0000	0.0000	0.0000
	0.0000	0.0000	0.0000	0.0000	0.0000	0.0000	0.0000	0.0000	0.0000	0.0000
	0.0000	0.0000	0.0000							
35	7,000	7,000	0.0000	0.0000	0.0000	0.0000	0.0000	0.0000	0.0000	0.0000
	0.0000	0.0000	0.0000	0.0000	0.0000	6,360	6,360	6,360	0.0000	6,499
	6,490	6,470	6,470	6,500	0.0000	0.0000	0.0000	0.0000	0.0000	0.0000
	0.0000	0.0000	0.0000	0.0000	0.0000	0.0000	0.0000	0.0000	0.0000	0.0000
	0.0000	0.0000	0.0000							
36	7,000	7,000	0.0000	0.0000	0.0000	0.0000	0.0000	0.0000	0.0000	0.0000
	0.0000	0.0000	0.0000	0.0000	6,350	6,350	6,350	0.0000	0.0000	6,600
	6,550	6,500	6,500	6,550	0.0000	0.0000	0.0000	0.0000	0.0000	0.0000
	0.0000	0.0000	0.0000	0.0000	0.0000	0.0000	0.0000	0.0000	0.0000	0.0000
	0.0000	0.0000	0.0000							

Table 9.--Specified bottom altitude for layer 1, in feet--Continued

Rows	Columns 1	2	3	4	5	6	7	8	9	10
	11	12	13	14	15	16	17	18	19	20
	21	22	23	24	25	26	27	28	29	30
	31	32	33	34	35	36	37	38	39	40
	41	42	43							
37	7,000	7,000	0.0000	0.0000	0.0000	0.0000	0.0000	0.0000	0.0000	0.0000
	0.0000	0.0000	0.0000	0.0000	6,340	6,340	0.0000	0.0000	0.0000	0.0000
	6,650	6,600	6,600	6,600	0.0000	0.0000	0.0000	0.0000	0.0000	0.0000
	0.0000	0.0000	0.0000	0.0000	0.0000	0.0000	0.0000	0.0000	0.0000	0.0000
	0.0000	0.0000	0.0000							
38	7,000	7,000	0.0000	0.0000	0.0000	0.0000	0.0000	0.0000	0.0000	0.0000
	0.0000	0.0000	0.0000	6,330	6,330	6,380	0.0000	0.0000	0.0000	0.0000
	0.0000	6,650	6,640	6,630	0.0000	0.0000	0.0000	0.0000	0.0000	0.0000
	0.0000	0.0000	0.0000	0.0000	0.0000	0.0000	0.0000	0.0000	0.0000	0.0000
	0.0000	0.0000	0.0000							
39	7,000	7,000	0.0000	0.0000	0.0000	0.0000	0.0000	0.0000	0.0000	0.0000
	0.0000	0.0000	0.0000	6,320	6,320	6,380	0.0000	0.0000	0.0000	0.0000
	0.0000	0.0000	6,680	6,660	0.0000	0.0000	0.0000	0.0000	0.0000	0.0000
	0.0000	0.0000	0.0000	0.0000	0.0000	0.0000	0.0000	0.0000	0.0000	0.0000
	0.0000	0.0000	0.0000							
40	7,000	7,000	0.0000	0.0000	0.0000	0.0000	0.0000	0.0000	0.0000	0.0000
	0.0000	0.0000	0.0000	6,310	6,310	6,390	0.0000	0.0000	0.0000	0.0000
	0.0000	0.0000	0.0000	6,690	0.0000	0.0000	0.0000	0.0000	0.0000	0.0000
	0.0000	0.0000	0.0000	0.0000	0.0000	0.0000	0.0000	0.0000	0.0000	0.0000
	0.0000	0.0000	0.0000							

Table 9.--Specified bottom altitude for layer 1, in feet--Continued

	Columns									
	1	2	3	4	5	6	7	8	9	10
	11	12	13	14	15	16	17	18	19	20
	21	22	23	24	25	26	27	28	29	30
	31	32	33	34	35	36	37	38	39	40
Rows	41	42	43							
41	7,000	7,000	0.0000	0.0000	0.0000	0.0000	0.0000	0.0000	0.0000	0.0000
	0.0000	0.0000	0.0000	6300	6,300	6,330	6,400	0.0000	0.0000	0.0000
	0.0000	0.0000	0.0000	0.0000	0.0000	0.0000	0.0000	0.0000	0.0000	0.0000
	0.0000	0.0000	0.0000	0.0000	0.0000	0.0000	0.0000	0.0000	0.0000	0.0000
	0.0000	0.0000	0.0000							
42	7,000	7,000	0.0000	0.0000	0.0000	0.0000	0.0000	0.0000	0.0000	0.0000
	6,444	6,400	6,350	6,300	6,290	6,350	6,400	6,430	6,450	0.0000
	0.0000	0.0000	0.0000	0.0000	0.0000	0.0000	0.0000	0.0000	0.0000	0.0000
	0.0000	0.0000	0.0000	0.0000	0.0000	0.0000	0.0000	0.0000	0.0000	0.0000
	0.0000	0.0000	0.0000							
43	7,000	7,000	0.0000	0.0000	0.0000	0.0000	0.0000	0.0000	0.0000	0.0000
	6,444	6,400	6,350	6,300	6,280	6,340	6,370	6,400	6,434	6,439
	0.0000	0.0000	0.0000	0.0000	0.0000	0.0000	0.0000	0.0000	0.0000	0.0000
	0.0000	0.0000	0.0000	0.0000	0.0000	0.0000	0.0000	0.0000	0.0000	0.0000
	0.0000	0.0000	0.0000							
44	7,000	7,000	0.0000	0.0000	0.0000	0.0000	0.0000	6,429	6,434	6,439
	6,400	6,390	6,340	6,300	6,270	6,290	6,320	6,350	6,350	6,400
	0.0000	0.0000	0.0000	0.0000	0.0000	0.0000	0.0000	0.0000	0.0000	0.0000
	0.0000	0.0000	0.0000	0.0000	0.0000	0.0000	0.0000	0.0000	0.0000	0.0000
	0.0000	0.0000	0.0000							

Table 9.--Specified bottom altitude for layer 1, in feet--Continued

	Columns									
	1	2	3	4	5	6	7	8	9	10
	11	12	13	14	15	16	17	18	19	20
	21	22	23	24	25	26	27	28	29	30
	31	32	33	34	35	36	37	38	39	40
Rows	41	42	43							
45	7,000	7,000	0.0000	0.0000	0.0000	0.0000	0.0000	6,424	6,400	6,390
	6,370	6,370	6,330	6,300	6,260	6,260	6,280	6,290	6,300	6,400
	0.0000	0.0000	0.0000	0.0000	0.0000	0.0000	0.0000	0.0000	0.0000	0.0000
	0.0000	0.0000	0.0000	0.0000	0.0000	0.0000	0.0000	0.0000	0.0000	0.0000
	0.0000	0.0000	0.0000							
46	7,000	6,800	0.0000	0.0000	0.0000	0.0000	6,419	6,400	6,370	6,370
	6,350	6,330	6,300	6,270	6,240	6,230	6,270	6,300	6,400	0.0000
	0.0000	0.0000	0.0000	0.0000	0.0000	0.0000	0.0000	0.0000	0.0000	0.0000
	0.0000	0.0000	0.0000	0.0000	0.0000	0.0000	0.0000	0.0000	0.0000	0.0000
	0.0000	0.0000	0.0000							
47	7,000	6,800	6,600	0.0000	0.0000	0.0000	0.0000	6,400	6,400	6,350
	6,300	6,300	6,280	6,240	622,0	620,0	630,0	6,400	0.0000	0.0000
	0.0000	0.0000	0.0000	0.0000	0.0000	0.0000	0.0000	0.0000	0.0000	0.0000
	0.0000	0.0000	0.0000	0.0000	0.0000	0.0000	0.0000	0.0000	0.0000	0.0000
	0.0000	0.0000	0.0000							
48	7,000	6,800	6,600	0.0000	0.0000	0.0000	0.0000	6,400	6,350	6,300
	6,280	6,270	6,220	6,230	6,200	6,180	6,300	0.0000	0.0000	0.0000
	0.0000	0.0000	0.0000	0.0000	0.0000	0.0000	0.0000	0.0000	0.0000	0.0000
	0.0000	0.0000	0.0000	0.0000	0.0000	0.0000	0.0000	0.0000	0.0000	0.0000
	0.0000	0.0000	0.0000							

Table 9.--Specified bottom altitude for layer 1, in feet--Continued

Rows	Columns 1	2	3	4	5	6	7	8	9	10
	11	12	13	14	15	16	17	18	19	20
	21	22	23	24	25	26	27	28	29	30
	31	32	33	34	35	36	37	38	39	40
	41	42	43							
49	7,000	6,800	6,600	0.0000	0.0000	6,370	6,350	6,350	6,280	6,270
	6,260	6,250	6,240	6,230	6,220	6,160	6,200	0.0000	0.0000	0.0000
	0.0000	0.0000	0.0000	0.0000	0.0000	0.0000	0.0000	0.0000	0.0000	0.0000
	0.0000	0.0000	0.0000	0.0000	0.0000	0.0000	0.0000	0.0000	0.0000	0.0000
	0.0000	0.0000	0.0000							
50	7,000	6,800	6,600	6,500	6,400	6,370	6,330	6,300	6,290	6,280
	6,290	6,300	6,280	6,250	6,200	6,150	6,130	6,300	0.0000	0.0000
	0.0000	0.0000	0.0000	0.0000	0.0000	0.0000	0.0000	0.0000	0.0000	0.0000
	0.0000	0.0000	0.0000	0.0000	0.0000	0.0000	0.0000	0.0000	0.0000	0.0000
	0.0000	0.0000	0.0000							
51	7,000	6,800	6,600	6,500	6,400	6,370	6,400	6,400	6,400	0.0000
	0.0000	0.0000	0.0000	0.0000	0.0000	0.0000	6,100	6,200	0.0000	0.0000
	0.0000	0.0000	0.0000	0.0000	0.0000	0.0000	0.0000	0.0000	0.0000	0.0000
	0.0000	0.0000	0.0000	0.0000	0.0000	0.0000	0.0000	0.0000	0.0000	0.0000
	0.0000	0.0000	0.0000							
52	7,000	6,800	6,600	6,500	6,400	6,400	6,400	0.0000	0.0000	0.0000
	0.0000	0.0000	0.0000	0.0000	0.0000	0.0000	6,070	0.0000	0.0000	0.0000
	0.0000	0.0000	0.0000	0.0000	0.0000	0.0000	0.0000	0.0000	0.0000	0.0000
	0.0000	0.0000	0.0000	0.0000	0.0000	0.0000	0.0000	0.0000	0.0000	0.0000
	0.0000	0.0000	0.0000							

Table 9.--Specified bottom altitude for layer 1, in feet--Concluded

Rows	Columns 1	2	3	4	5	6	7	8	9	10
	11	12	13	14	15	16	17	18	19	20
	21	22	23	24	25	26	27	28	29	30
	31	32	33	34	35	36	37	38	39	40
	41	42	43							
53	7,000	6,800	6,600	6,500	6,400	6,400	0.0000	0.0000	0.0000	0.0000
	0.0000	0.0000	0.0000	0.0000	0.0000	0.0000	0.0000	0.0000	0.0000	0.0000
	0.0000	0.0000	0.0000	0.0000	0.0000	0.0000	0.0000	0.0000	0.0000	0.0000
	0.0000	0.0000	0.0000	0.0000	0.0000	0.0000	0.0000	0.0000	0.0000	0.0000
	0.0000	0.0000	0.0000							
54	7,000	6,800	6,600	6,500	0.0000	0.0000	0.0000	0.0000	0.0000	0.0000
	0.0000	0.0000	0.0000	0.0000	0.0000	0.0000	0.0000	0.0000	0.0000	0.0000
	0.0000	0.0000	0.0000	0.0000	0.0000	0.0000	0.0000	0.0000	0.0000	0.0000
	0.0000	0.0000	0.0000	0.0000	0.0000	0.0000	0.0000	0.0000	0.0000	0.0000
	0.0000	0.0000	0.0000							
55	7,000	6,800	6,600	0.0000	0.0000	0.0000	0.0000	0.0000	0.0000	0.0000
	0.0000	0.0000	0.0000	0.0000	0.0000	0.0000	0.0000	0.0000	0.0000	0.0000
	0.0000	0.0000	0.0000	0.0000	0.0000	0.0000	0.0000	0.0000	0.0000	0.0000
	0.0000	0.0000	0.0000	0.0000	0.0000	0.0000	0.0000	0.0000	0.0000	0.0000
	0.0000	0.0000	0.0000							
56	7,000	0.0000	0.0000	0.0000	0.0000	0.0000	0.0000	0.0000	0.0000	0.0000
	0.0000	0.0000	0.0000	0.0000	0.0000	0.0000	0.0000	0.0000	0.0000	0.0000
	0.0000	0.0000	0.0000	0.0000	0.0000	0.0000	0.0000	0.0000	0.0000	0.0000
	0.0000	0.0000	0.0000	0.0000	0.0000	0.0000	0.0000	0.0000	0.0000	0.0000
	0.0000	0.0000	0.0000							
57	7,000	0.0000	0.0000	0.0000	0.0000	0.0000	0.0000	0.0000	0.0000	0.0000
	0.0000	0.0000	0.0000	0.0000	0.0000	0.0000	0.0000	0.0000	0.0000	0.0000
	0.0000	0.0000	0.0000	0.0000	0.0000	0.0000	0.0000	0.0000	0.0000	0.0000
	0.0000	0.0000	0.0000	0.0000	0.0000	0.0000	0.0000	0.0000	0.0000	0.0000
	0.0000	0.0000	0.0000							

Table 10.--Estimated thickness of saturated valley fill, in feet

[Zero values are shown where layer 1 is inactive.
Values not shown for rows 1-16 and 58-76 are all zero]

Row	Columns											
	1	2	3	4	5	6	7	8	9	10	11	12
	13	14	15	16	17	18	19	20	21	22	23	24
	25	26	27	28	29	30	31	32	33	34	35	36
	37	38	39	40	41	42	43					
17	0	0	0	0	0	0	0	0	0	0	0	0
	0	0	0	0	0	0	0	0	0	0	10	0
	0	0	0	0	0	0	0	0	0	0	0	0
	0	0	0	0	0	0	0					
18	0	0	0	0	0	0	0	0	0	0	0	0
	0	0	0	0	0	0	0	0	0	0	10	0
	0	0	0	0	0	0	0	0	0	0	0	0
	0	0	0	0	0	0	0					
19	0	0	0	0	0	0	0	0	0	0	0	0
	0	0	0	0	0	0	0	0	0	0	10	0
	0	0	0	0	0	0	0	0	0	0	0	0
	0	0	0	0	0	0	0					
20	0	0	0	0	0	0	0	0	0	0	0	0
	0	0	0	0	0	0	0	0	0	0	10	0
	0	0	0	0	0	0	0	0	0	0	0	0
	0	0	0	0	0	0	0					
21	0	0	0	0	0	0	0	0	0	0	0	0
	0	0	0	0	0	0	0	0	0	0	20	0
	0	0	0	0	0	0	0	0	0	0	0	0
	0	0	0	0	0	0	0					
22	0	0	0	0	0	0	0	0	0	0	0	0
	0	0	0	0	0	0	0	0	0	0	20	0
	0	0	0	0	0	0	0	0	0	0	0	0
	0	0	0	0	0	0	0					
23	0	0	0	0	0	0	0	0	0	0	0	0
	0	0	0	0	0	0	1	0	0	20	20	0
	0	0	0	0	0	0	0	0	0	0	0	0
	0	0	0	0	0	0	0					
24	0	0	0	0	0	0	0	0	0	0	0	0
	0	0	0	0	0	0	1	0	0	40	40	10
	0	0	0	0	0	0	0	0	0	0	0	0
	0	0	0	0	0	0	0					

Table 10.--Estimated thickness of saturated valley fill, in feet--Continued

Row	Columns 1	2	3	4	5	6	7	8	9	10	11	12
	13	14	15	16	17	18	19	20	21	22	23	24
	25	26	27	28	29	30	31	32	33	34	35	36
	37	38	39	40	41	42	43					
25	0	0	0	0	0	0	0	0	0	0	0	0
	0	0	0	0	0	0	1	1	20	40	10	1
	0	0	0	0	0	0	0	0	0	0	0	0
	0	0	0	0	0	0	0					
26	0	0	0	0	0	0	0	0	0	0	0	0
	0	0	0	0	0	0	10	20	20	30	1	1
	0	0	0	0	0	0	0	0	0	0	0	0
	0	0	0	0	0	0	0					
27	0	0	0	0	0	0	0	0	0	0	0	0
	0	0	0	0	0	5	25	35	0	0	0	0
	0	0	0	0	0	0	0	0	0	0	0	0
	0	0	0	0	0	0	0					
28	0	0	0	0	0	0	0	0	0	0	0	0
	0	0	0	0	0	1	30	45	50	1	0	0
	0	0	0	0	0	0	0	0	0	0	0	0
	0	0	0	0	0	0	0					
29	0	0	0	0	0	0	0	0	0	0	0	0
	0	0	0	0	0	1	1	30	60	50	0	0
	0	0	0	0	0	0	0	0	0	0	0	0
	0	0	0	0	0	0	0					
30	0	0	0	0	0	0	0	0	0	0	0	0
	0	0	0	0	0	0	10	50	60	10	0	0
	0	0	0	0	0	0	0	0	0	0	0	0
	0	0	0	0	0	0	0					
31	50	50	0	0	0	0	0	0	0	0	0	0
	0	0	0	0	0	0	1	60	60	20	0	0
	0	0	0	0	0	0	0	0	0	0	0	0
	0	0	0	0	0	0	0					
32	0	0	0	0	0	0	0	0	0	0	0	0
	0	0	0	0	0	0	5	70	60	50	0	0
	0	0	0	0	0	0	0	0	0	0	0	0
	0	0	0	0	0	0	0					
33	0	0	0	0	0	0	0	0	0	0	0	0
	0	0	0	0	95	90	80	65	70	85	90	105
	0	0	0	0	0	0	0	0	0	0	0	0
	0	0	0	0	0	0	0					

Table 10.--Estimated thickness of saturated valley fill, in feet--Continued

Row	Columns 1	2	3	4	5	6	7	8	9	10	11	12
	13	14	15	16	17	18	19	20	21	22	23	24
	25	26	27	28	29	30	31	32	33	34	35	36
	37	38	39	40	41	42	43					
34	0	0	0	0	0	0	0	0	0	0	0	0
	0	0	0	205	105	100	90	60	80	80	90	15
	0	0	0	0	0	0	0	0	0	0	0	0
	0	0	0	0	0	0	0					
35	0	0	0	0	0	0	0	0	0	0	0	0
	0	0	0	110	115	120	0	1	35	60	75	55
	0	0	0	0	0	0	0	0	0	0	0	0
	0	0	0	0	0	0	0					
36	0	0	0	0	0	0	0	0	0	0	0	0
	0	0	132	120	120	0	0	1	1	35	45	5
	0	0	0	0	0	0	0	0	0	0	0	0
	0	0	0	0	0	0	0					
37	0	0	0	0	0	0	0	0	0	0	0	0
	0	0	125	125	0	0	0	0	1	1	1	1
	0	0	0	0	0	0	0	0	0	0	0	0
	0	0	0	0	0	0	0					
38	0	0	0	0	0	0	0	0	0	0	0	0
	0	135	135	85	0	0	0	0	0	1	1	1
	0	0	0	0	0	0	0	0	0	0	0	0
	0	0	0	0	0	0	0					
39	0	0	0	0	0	0	0	0	0	0	0	0
	0	140	140	80	0	0	0	0	0	0	1	1
	0	0	0	0	0	0	0	0	0	0	0	0
	0	0	0	0	0	0	0					
40	0	0	0	0	0	0	0	0	0	0	0	0
	0	150	150	65	0	0	0	0	0	0	0	1
	0	0	0	0	0	0	0	0	0	0	0	0
	0	0	0	0	0	0	0					
41	0	0	0	0	0	0	0	0	0	0	0	0
	0	155	155	120	50	0	0	0	0	0	0	0
	0	0	0	0	0	0	0	0	0	0	0	0
	0	0	0	0	0	0	0					
42	0	0	0	0	0	0	0	0	0	1	1	1
	1	150	160	90	35	5	1	0	0	0	0	0
	0	0	0	0	0	0	0	0	0	0	0	0
	0	0	0	0	0	0	0					

Table 10.--Estimated thickness of saturated valley fill, in feet--Continued

Row	Columns											
	1	2	3	4	5	6	7	8	9	10	11	12
	13	14	15	16	17	18	19	20	21	22	23	24
	25	26	27	28	29	30	31	32	33	34	35	36
	37	38	39	40	41	42	43					
43	0	0	0	0	0	0	0	0	0	0	1	50
	100	145	160	95	60	25	1	1	0	0	0	0
	0	0	0	0	0	0	0	0	0	0	0	0
	0	0	0	0	0	0	0					
44	0	0	0	0	0	0	0	1	1	1	40	50
	100	135	160	145	100	70	80	40	0	0	0	0
	0	0	0	0	0	0	0	0	0	0	0	0
	0	0	0	0	0	0	0					
45	0	0	0	0	0	0	0	1	30	40	60	60
	100	125	160	160	135	125	130	40	0	0	0	0
	0	0	0	0	0	0	0	0	0	0	0	0
	0	0	0	0	0	0	0					
46	0	0	0	0	0	0	1	20	50	50	70	90
	115	145	175	185	145	115	25	0	0	0	0	0
	0	0	0	0	0	0	0	0	0	0	0	0
	0	0	0	0	0	0	0					
47	0	0	0	0	0	0	0	15	15	65	115	115
	130	170	185	205	105	10	0	0	0	0	0	0
	0	0	0	0	0	0	0	0	0	0	0	0
	0	0	0	0	0	0	0					
48	0	0	0	0	0	0	0	15	65	115	130	135
	180	170	195	215	100	0	0	0	0	0	0	0
	0	0	0	0	0	0	0	0	0	0	0	0
	0	0	0	0	0	0	0					
49	0	10	10	0	0	60	70	65	135	140	140	140
	150	150	155	210	170	0	0	0	0	0	0	0
	0	0	0	0	0	0	0	0	0	0	0	0
	0	0	0	0	0	0	0					
50	0	10	10	10	10	60	90	120	125	130	110	85
	100	120	150	180	180	0	0	0	0	0	0	0
	0	0	0	0	0	0	0	0	0	0	0	0
	0	0	0	0	0	0	0					
51	10	10	10	10	10	60	25	20	15	0	0	0
	0	0	0	0	185	85	0	0	0	0	0	0
	0	0	0	0	0	0	0	0	0	0	0	0
	0	0	0	0	0	0	0					

Table 10.--Estimated thickness of saturated valley fill, in feet--Concluded

Row	Columns											
	1	2	3	4	5	6	7	8	9	10	11	12
	13	14	15	16	17	18	19	20	21	22	23	24
	25	26	27	28	29	30	31	32	33	34	35	36
	37	38	39	40	41	42	43					
52	10	10	10	10	10	30	30	0	0	0	0	0
	0	0	0	0	210	0	0	0	0	0	0	0
	0	0	0	0	0	0	0	0	0	0	0	0
	0	0	0	0	0	0	0					
53	10	10	10	10	10	35	0	0	0	0	0	0
	0	0	0	0	0	0	0	0	0	0	0	0
	0	0	0	0	0	0	0	0	0	0	0	0
	0	0	0	0	0	0	0					
54	10	10	10	10	0	0	0	0	0	0	0	0
	0	0	0	0	0	0	0	0	0	0	0	0
	0	0	0	0	0	0	0	0	0	0	0	0
	0	0	0	0	0	0	0					
55	10	10	10	0	0	0	0	0	0	0	0	0
	0	0	0	0	0	0	0	0	0	0	0	0
	0	0	0	0	0	0	0	0	0	0	0	0
	0	0	0	0	0	0	0					
56	10	0	0	0	0	0	0	0	0	0	0	0
	0	0	0	0	0	0	0	0	0	0	0	0
	0	0	0	0	0	0	0	0	0	0	0	0
	0	0	0	0	0	0	0					
57	10	0	0	0	0	0	0	0	0	0	0	0
	0	0	0	0	0	0	0	0	0	0	0	0
	0	0	0	0	0	0	0	0	0	0	0	0
	0	0	0	0	0	0	0					

Table 11.--Estimates of annual flow past the gaging station 08342000, Bluewater Creek near Bluewater, and estimated yield of the watershed upstream from the gage

[This station is in the lower end of Bluewater Canyon and measurements were discontinued in 1973. All values are in acre-feet. Dashes (--) indicate negative value, or in the absence of a number indicate no estimate was made or reported]

Water year	Excess precip-itation[1]	Reported estimate of basin yield[2]	Estimated basin yield[3]	Differ-ence[4]	Estimated net evapo-ration from lake[5]	Estimated change in lake contents[6]	Estimated flow past gage[7]
1959	2,968	0	305	-305	--	--	--
1960	20,542	6,640	6,540	100	--	--	--
1961	5,283	810	1,126	-316	--	--	--
1962	27,309	10,310	8,941	1,369	--	--	--
1963	18,035	2,880	5,651	-2,771	--	--	--
1964	14,293	7,190	4,323	2,867	--	--	--
1965	30,502	10,380	10,074	306	--	--	--
1966	25,785	8,110	8,400	-290	--	--	--
1967	64	0	-726	726	--	--	--
1968	14,848	3,760	4,520	-760	--	--	--
1969	23,761	7,210	7,682	-472	--	--	--
1970	6,845	400	1,680	-1,280	--	--	--
1971	752	14	-482	496	--	--	--
1972	3,373	778	448	330	--	--	--
1973	82,143	--	28,397	--	2,926	25,240	231
1974	3,077	--	343	--	2,967	-14,550	11,926
1975	21,700	--	6,951	--	2,595	3,460	896
1976	10	--	-745	--	1,974	-13,620	11,646
1977	2,496	--	137	--	681	-1,030	486
1978	41,811	--	14,087	--	1,077	610	12,400
1979	97,534	--	33,858	--	2,608	24,790	6,460
1980	82,828	--	28,639	--	3,531	12,030	13,078
1981	12,795	--	3,791	--	2,728	-13,590	14,653
1982	48,396	--	16,422	--	2,508	1,130	12,784
1983	77,195	--	26,641	--	3,328	12,890	10,423
1984	42,200	--	14,224	--	2,735	-10,530	22,019
1985	65,409	--	22,459	--	3,270	9,530	9,659

[1]Excess precipitation estimated by the Hearne and Dewey (1988) method for the watersheds upstream from gaging station "Bluewater Creek near Bluewater."

[2]Reported yield (Risser, 1982, table 4) of the watersheds upstream from the gage estimated as the measured discharge plus the net evaporation from Bluewater Lake plus the change in lake contents. Negative values were changed to zero values.

[3]Yield of the watersheds upstream from gaging station 08342000 estimated from excess precipitation as minus 748.6 acre-feet plus 0.3548 times excess precipitation.

[4]Difference in the two estimates of basin yield. Assuming Risser's (1982, table 4) estimate to be true, the standard error of the estimate derived from excess precipitation is 1,340 acre-feet.

[5]Net evaporation from Bluewater Lake estimated by the method of Risser (1982).

[6]Change in lake contents estimated from published data (U.S. Geological Survey, 1972-86). Positive values indicate a net gain in lake contents.

[7]Flow past gaging station 08342000 estimated as the basin yield minus the net evaporation minus the change in lake contents. Negative value of basin yield for 1976 was changed to zero.

Table 12.--Horizontal grid dimensions, in feet

[DELR (McDonald and Harbaugh, 1988, p. 5-39) is the model block width along rows. DELR is a vector with one value for each model column. DELC is the model block width along columns. DELC has one value for each model row]

DELR

Columns									
1	2	3	4	5	6	7	8	9	10
11	12	13	14	15	16	17	18	19	20
21	22	23	24	25	26	27	28	29	30
31	32	33	34	35	36	37	38	39	40
41	42	43							
40,573	26,400	21,120	15,840	10,560	7,920.0	5,280.0	3,960.0	39,60.0	3,960.0
3,960.0	2,640.0	2,640.0	2,640.0	2,640.0	2,640.0	2,640.0	3,960.0	39,60.0	3,960.0
3,960.0	5,280.0	5,280.0	5,280.0	5,280.0	5,280.0	5,280.0	5,280.0	52,80.0	5,280.0
5,280.0	5,280.0	5,280.0	5,280.0	5,280.0	5,280.0	5,280.0	7,920.0	10,560	15,840
21,120	21,120	31,680							

DELC

Rows									
1	2	3	4	5	6	7	8	9	10
11	12	13	14	15	16	17	18	19	20
21	22	23	24	25	26	27	28	29	30
31	32	33	34	35	36	37	38	39	40
41	42	43	44	45	46	47	48	49	50
51	52	53	54	55	56	57	58	59	60
61	62	63	64	65	66	67	68	69	70
71	72	73	74	75	76				
10,006	10,560	10,560	7,920.0	5,280.0	3,960.0	3,960.0	3,960.0	3,960.0	2,640.0
2,640.0	2,640.0	2,640.0	2,640.0	2,640.0	2,640.0	2,640.0	2,640.0	2,640.0	2,640.0
2,640.0	3,960.0	3,960.0	3,960.0	3,960.0	5,280.0	5,280.0	5,280.0	5,280.0	5,280.0
3,960.0	3,960.0	3,960.0	3,960.0	2,640.0	2,640.0	2,640.0	2,640.0	2,640.0	2,640.0
2.640.0	2,640.0	2,640.0	2,640.0	3,960.0	3,960.0	3,960.0	3,960.0	5,280.0	5,280.0
5.280.0	5,280.0	5,280.0	5,280.0	5,280.0	5,280.0	5,280.0	5,280.0	5,280.0	5,280.0
5.280.0	5,280.0	5,280.0	5,280.0	5,280.0	5,280.0	5,280.0	5,280.0	5,280.0	7,820.0
10.560	15,840	21,120	31,680	31,680	31,680				

Table 13.--Specified transmissivity values for layer 2, representing the San Andres-Glorieta aquifer

[Values are in feet squared per second. Zero values are shown where layer 2 is inactive]

Rows	Columns									
	1	2	3	4	5	6	7	8	9	10
	11	12	13	14	15	16	17	18	19	20
	21	22	23	24	25	26	27	28	29	30
	31	32	33	34	35	36	37	38	39	40
	41	42	43							
1	0.0000	0.0000	0.0000	0.0000	4.6280E-04	4.6280E-04	2.3140E-03	2.3140E-03	2.3140E-03	2.3140E-03
	2.3140E-03	2.3140E-03	2.3140E-03	2.3140E-03	2.3140E-03	2.3140E-03	2.3140E-03	2.3140E-03	2.3140E-03	2.3140E-03
	2.3140E-03	2.3140E-03	2.3140E-03	2.3140E-03	2.3140E-03	2.3140E-03	2.3140E-03	2.3140E-03	2.3140E-03	2.3140E-03
	2.3140E-03	2.3140E-03	2.3140E-03	2.3140E-03	2.3140E-03	2.3140E-03	2.3140E-03	2.3140E-03	2.3140E-03	2.3140E-03
	2.3140E-03	1.1570E-03	1.1570E-03							
2	0.0000	0.0000	0.0000	0.0000	4.6280E-04	4.6280E-04	2.3140E-03	2.3140E-03	2.3140E-03	2.3140E-03
	2.3140E-03	2.3140E-03	2.3140E-03	2.3140E-03	2.3140E-03	2.3140E-03	2.3140E-03	2.3140E-03	2.3140E-03	2.3140E-03
	2.3140E-03	2.3140E-03	2.3140E-03	2.3140E-03	2.3140E-03	2.3140E-03	2.3140E-03	2.3140E-03	2.3140E-03	2.3140E-03
	2.3140E-03	2.3140E-03	2.3140E-03	2.3140E-03	2.3140E-03	2.3140E-03	2.3140E-03	2.3140E-03	2.3140E-03	2.3140E-03
	2.3140E-03	1.1570E-03	1.1570E-03							
3	0.0000	0.0000	0.0000	0.0000	4.6280E-04	4.6280E-04	2.3140E-03	2.3140E-03	2.3140E-03	2.3140E-03
	2.3140E-03	2.3140E-03	2.3140E-03	2.3140E-03	2.3140E-03	2.3140E-03	2.3140E-03	2.3140E-03	2.3140E-03	2.3140E-03
	2.3140E-03	2.3140E-03	2.3140E-03	2.3140E-03	2.3140E-03	2.3140E-03	2.3140E-03	2.3140E-03	2.3140E-03	2.3140E-03
	2.3140E-03	2.3140E-03	2.3140E-03	2.3140E-03	2.3140E-03	2.3140E-03	2.3140E-03	2.3140E-03	2.3140E-03	2.3140E-03
	2.3140E-03	1.1570E-03	1.1570E-03							
4	0.0000	0.0000	0.0000	0.0000	4.6280E-04	4.6280E-04	2.3140E-03	2.3140E-03	2.3140E-03	2.3140E-03
	2.3140E-03	2.3140E-03	2.3140E-03	2.3140E-03	2.3140E-03	2.3140E-03	2.3140E-03	2.3140E-03	2.3140E-03	2.3140E-03
	2.3140E-03	2.3140E-03	2.3140E-03	2.3140E-03	2.3140E-03	2.3140E-03	2.3140E-03	2.3140E-03	2.3140E-03	2.3140E-03
	2.3140E-03	2.3140E-03	2.3140E-03	2.3140E-03	2.3140E-03	2.3140E-03	2.3140E-03	2.3140E-03	2.3140E-03	2.3140E-03
	2.3140E-03	1.1570E-03	1.1570E-03							

Table 13.--Specified transmissivity values for layer 2, representing the San Andres-Glorieta aquifer--Continued

Rows	Columns									
	1 11 21 31 41	2 12 22 32 42	3 13 23 33 43	4 14 24 34	5 15 25 35	6 16 26 36	7 17 27 37	8 18 28 38	9 19 29 39	10 20 30 40
5	0.0000	0.0000	0.0000	0.0000	4.6280E-04	4.6280E-04	2.3140E-03	2.3140E-03	2.3140E-03	2.3140E-03
	2.3140E-03	2.3140E-03	2.3140E-03	2.3140E-03	2.3140E-03	2.3140E-03	2.3140E-03	2.3140E-03	2.3140E-03	2.3140E-03
	2.3140E-03	2.3140E-03	2.3140E-03	2.3140E-03	2.3140E-03	2.3140E-03	2.3140E-03	2.3140E-03	2.3140E-03	2.3140E-03
	2.3140E-03	2.3140E-03	2.3140E-03	2.3140E-03	2.3140E-03	2.3140E-03	2.3140E-03	2.3140E-03	2.3140E-03	2.3140E-03
	2.3140E-03	1.1570E-03	1.1570E-03							
6	0.0000	0.0000	0.0000	0.0000	4.6280E-04	4.6280E-04	4.6280E-04	2.3140E-03	2.3140E-03	2.3140E-03
	2.3140E-03	2.3140E-03	2.3140E-03	2.3140E-03	2.3140E-03	2.3140E-03	2.3140E-03	2.3140E-03	2.3140E-03	2.3140E-03
	2.3140E-03	2.3140E-03	2.3140E-03	2.3140E-03	2.3140E-03	2.3140E-03	2.3140E-03	2.3140E-03	2.3140E-03	2.3140E-03
	2.3140E-03	2.3140E-03	2.3140E-03	2.3140E-03	2.3140E-03	2.3140E-03	2.3140E-03	2.3140E-03	2.3140E-03	2.3140E-03
	2.3140E-03	1.1570E-03	1.1570E-03							
7	0.0000	0.0000	0.0000	0.0000	4.6280E-04	4.6280E-04	4.6280E-04	2.3140E-03	2.3140E-03	2.3140E-03
	2.3140E-03	2.3140E-03	2.3140E-03	2.3140E-03	2.3140E-03	2.3140E-03	2.3140E-03	2.3140E-03	2.3140E-03	2.3140E-03
	2.3140E-03	2.3140E-03	2.3140E-03	2.3140E-03	2.3140E-03	2.3140E-03	2.3140E-03	2.3140E-03	2.3140E-03	2.3140E-03
	2.3140E-03	2.3140E-03	2.3140E-03	2.3140E-03	2.3140E-03	2.3140E-03	2.3140E-03	2.3140E-03	2.3140E-03	2.3140E-03
	2.3140E-03	1.1570E-03	1.1570E-03							
8	0.0000	0.0000	0.0000	0.0000	4.6280E-04	4.6280E-04	4.6280E-04	4.6280E-04	4.6280E-04	2.3140E-03
	2.3140E-03	2.3140E-03	2.3140E-03	2.3140E-03	2.3140E-03	2.3140E-03	2.3140E-03	2.3140E-03	2.3140E-03	2.3140E-03
	2.3140E-03	2.3140E-03	2.3140E-03	2.3140E-03	2.3140E-03	2.3140E-03	2.3140E-03	2.3140E-03	2.3140E-03	0.0000
	2.3140E-03	2.3140E-03	2.3140E-03	2.3140E-03	2.3140E-03	2.3140E-03	2.3140E-03	2.3140E-03	2.3140E-03	2.3140E-03
	2.3140E-03	1.1570E-03	1.1570E-03							

Table 13.--Specified transmissivity values for layer 2, representing the San Andres-Glorieta aquifer--Continued

Rows	Columns 1	2	3	4	5	6	7	8	9	10
	11	12	13	14	15	16	17	18	19	20
	21	22	23	24	25	26	27	28	29	30
	31	32	33	34	35	36	37	38	39	40
	41	42	43							
9	0.0000	0.0000	0.0000	0.0000	4.6280E-04	4.6280E-04	4.6280E-04	4.6280E-04	4.6280E-04	2.3140E-03
	2.3140E-03	2.3140E-03	2.3140E-03	2.3140E-03	2.3140E-03	2.3140E-03	2.3140E-03	2.3140E-03	2.3140E-03	2.3140E-03
	2.3140E-03	2.3140E-03	2.3140E-03	2.3140E-03	2.3140E-03	2.3140E-03	2.3140E-03	2.3140E-03	0.0000	2.3140E-03
	2.3140E-03	2.3140E-03	2.3140E-03	2.3140E-03	2.3140E-03	2.3140E-03	2.3140E-03	2.3140E-03	2.3140E-03	2.3140E-03
	2.3140E-03	1.1570E-03	1.1570E-03							
10	0.0000	0.0000	0.0000	0.0000	0.0000	4.6280E-04	4.6280E-04	4.6280E-04	4.6280E-04	2.3140E-03
	2.3140E-03	2.3140E-03	2.3140E-03	2.3140E-03	2.3140E-03	2.3140E-03	2.3140E-03	2.3140E-03	2.3140E-03	2.3140E-03
	2.3140E-03	2.3140E-03	2.3140E-03	2.3140E-03	2.3140E-03	2.3140E-03	2.3140E-03	3.4710E-03	3.4710E-03	3.4710E-03
	3.4710E-03	3.4710E-03	3.4710E-03	3.4710E-03	3.4710E-03	3.4710E-03	3.4710E-03	3.4710E-03	3.4710E-03	3.4710E-03
	3.4710E-03	1.1570E-03	1.1570E-03							
11	0.0000	0.0000	0.0000	0.0000	0.0000	4.6280E-04	4.6280E-04	4.6280E-04	4.6280E-04	2.3140E-03
	2.3140E-03	2.3140E-03	2.3140E-03	2.3140E-03	2.3140E-03	2.3140E-03	2.3140E-03	2.3140E-03	2.3140E-03	2.3140E-03
	2.3140E-03	2.3140E-03	2.3140E-03	2.3140E-03	2.3140E-03	2.3140E-03	0.0000	5.7850E-03	1.1570E-02	1.1570E-02
	1.1570E-02	1.1570E-02	1.1570E-02	1.1570E-02	1.1570E-02	1.1570E-02	1.1570E-02	1.1570E-02	1.1570E-02	1.1570E-02
	3.4710E-03	1.1570E-03	1.1570E-03							
12	0.0000	0.0000	0.0000	0.0000	0.0000	4.6280E-04	4.6280E-04	4.6280E-04	4.6280E-04	4.6280E-04
	2.3140E-03	2.3140E-03	2.3140E-03	2.3140E-03	2.3140E-03	2.3140E-03	2.3140E-03	2.3140E-03	2.3140E-03	2.3140E-03
	2.3140E-03	2.3140E-03	2.3140E-03	2.3140E-03	2.3140E-03	2.3140E-03	0.0000	5.7850E-03	1.1570E-02	1.1570E-02
	1.1570E-02	1.1570E-02	1.1570E-02	1.1570E-02	1.1570E-02	1.1570E-02	1.1570E-02	1.1570E-02	1.1570E-02	1.1570E-02
	3.4710E-03	1.1570E-03	1.1570E-03							

Table 13.--Specified transmissivity values for layer 2, representing the San Andres-Glorieta aquifer--Continued

Rows	Columns 1	2	3	4	5	6	7	8	9	10
	11	12	13	14	15	16	17	18	19	20
	21	22	23	24	25	26	27	28	29	30
	31	32	33	34	35	36	37	38	39	40
	41	42	43							
13	0.0000	0.0000	0.0000	0.0000	0.0000	4.6280E-04	4.6280E-04	4.6280E-04	4.6280E-04	4.6280E-04
	2.3140E-03	2.3140E-03	2.3140E-03	2.3140E-03	2.3140E-03	2.3140E-03	2.3140E-03	2.3140E-03	2.3140E-03	2.3140E-03
	2.3140E-03	2.3140E-03	2.3140E-03	2.3140E-03	2.3140E-03	0.0000	5.7850E-03	5.7850E-03	1.1570E-02	1.1570E-02
	1.1570E-02	1.1570E-02	1.1570E-02	1.1570E-02	1.1570E-02	1.1570E-02	1.1570E-02	1.1570E-02	1.1570E-02	1.1570E-02
	3.4710E-03	1.1570E-03	1.1570E-03							
14	0.0000	0.0000	0.0000	0.0000	0.0000	4.6280E-04	4.6280E-04	4.6280E-04	4.6280E-04	4.6280E-04
	2.3140E-03	2.3140E-03	2.3140E-03	2.3140E-03	2.3140E-03	2.3140E-03	2.3140E-03	2.3140E-03	2.3140E-03	2.3140E-03
	2.3140E-03	2.3140E-03	2.3140E-03	2.3140E-03	2.3140E-03	0.0000	2.3140E-02	2.3140E-02	1.1570E-02	1.1570E-02
	1.1570E-02	1.1570E-02	1.1570E-02	1.1570E-02	1.1570E-02	1.1570E-02	1.1570E-02	1.1570E-02	1.1570E-02	1.1570E-02
	3.4710E-03	1.1570E-03	1.1570E-03							
15	0.0000	0.0000	0.0000	0.0000	0.0000	4.6280E-04	4.6280E-04	4.6280E-04	4.6280E-04	4.6280E-04
	2.3140E-03	2.3140E-02	2.3140E-02	2.3140E-02	2.3140E-03	2.3140E-03	2.3140E-03	2.3140E-03	2.3140E-03	2.3140E-03
	2.3140E-03	2.3140E-03	2.3140E-03	2.3140E-03	0.0000	5.7850E-03	2.3140E-02	2.3140E-02	1.1570E-02	1.1570E-02
	1.1570E-02	1.1570E-02	1.1570E-02	1.1570E-02	1.1570E-02	1.1570E-02	1.1570E-02	1.1570E-02	1.1570E-02	1.1570E-02
	3.4710E-03	1.1570E-03	1.1570E-03							
16	0.0000	0.0000	0.0000	0.0000	0.0000	0.0000	0.0000	4.6280E-04	4.6280E-04	4.6280E-04
	2.3140E-03	2.3140E-02	2.3140E-02	2.3140E-02	2.3140E-03	2.3140E-03	2.3140E-03	2.3140E-03	2.3140E-03	2.3140E-03
	2.3140E-03	2.3140E-03	2.3140E-03	2.3140E-03	0.0000	2.3140E-02	2.3140E-02	2.3140E-02	1.1570E-02	1.1570E-02
	1.1570E-02	1.1570E-02	1.1570E-02	1.1570E-02	1.1570E-02	1.1570E-02	1.1570E-02	1.1570E-02	1.1570E-02	1.1570E-02
	3.4710E-03	1.1570E-03	1.1570E-03							

Table 13.--Specified transmissivity values for layer 2, representing the San Andres-Glorieta aquifer--Continued

	Columns									
	1	2	3	4	5	6	7	8	9	10
	11	12	13	14	15	16	17	18	19	20
	21	22	23	24	25	26	27	28	29	30
	31	32	33	34	35	36	37	38	39	40
Rows	41	42	43							
17	0.0000	0.0000	0.0000	0.0000	0.0000	0.0000	0.0000	4.6280E-04	4.6280E-04	4.6280E-04
	2.3140E-03	2.3140E-03	2.3140E-03	2.3140E-03	2.3140E-03	2.3140E-03	2.3140E-03	2.3140E-03	2.3140E-03	2.3140E-03
	2.3140E-03	2.3140E-03	2.3140E-03	0.0000	5.7850E-03	2.3140E-02	2.3140E-02	2.3140E-02	1.1570E-02	1.1570E-02
	1.1570E-02	1.1570E-02	1.1570E-02	1.1570E-02	1.1570E-02	1.1570E-02	1.1570E-02	1.1570E-02	1.1570E-02	1.1570E-02
	3.4710E-03	1.1570E-03	1.1570E-03							
18	0.0000	0.0000	0.0000	0.0000	0.0000	0.0000	0.0000	4.6280E-04	4.6280E-04	4.6280E-04
	2.3140E-03	2.3140E-03	2.3140E-03	2.3140E-03	2.3140E-03	2.3140E-03	2.3140E-03	2.3140E-03	5.7850E-03	5.7850E-03
	5.7850E-03	5.7850E-03	5.7850E-03	0.0000	2.3140E-02	2.3140E-02	2.3140E-02	2.3140E-02	1.1570E-02	1.1570E-02
	1.1570E-02	1.1570E-02	1.1570E-02	1.1570E-02	1.1570E-02	1.1570E-02	1.1570E-02	1.1570E-02	1.1570E-02	1.1570E-02
	3.4710E-03	1.1570E-03	1.1570E-03							
19	0.0000	0.0000	0.0000	0.0000	0.0000	0.0000	0.0000	4.6280E-04	4.6280E-04	4.6280E-04
	4.6280E-04	4.6280E-04	4.6280E-04	4.6280E-04	4.6280E-04	4.6280E-04	4.6280E-04	4.6280E-04	5.7850E-03	2.3140E-02
	2.3140E-02	2.3140E-02	2.3140E-02	2.3140E-02	2.3140E-02	2.3140E-02	2.3140E-02	2.3140E-02	1.1570E-02	1.1570E-02
	1.1570E-02	1.1570E-02	1.1570E-02	1.1570E-02	1.1570E-02	1.1570E-02	1.1570E-02	1.1570E-02	1.1570E-02	1.1570E-02
	3.4710E-03	1.1570E-03	1.1570E-03							
20	0.0000	0.0000	0.0000	0.0000	0.0000	0.0000	0.0000	0.0000	4.6280E-04	4.6280E-04
	4.6280E-04	4.6280E-04	4.6280E-04	4.6280E-04	4.6280E-04	4.6280E-04	4.6280E-04	4.6280E-04	5.7850E-03	2.3140E-02
	0.1157	0.1157	0.1157	0.1157	0.1157	0.1157	2.3140E-02	2.3140E-02	1.1570E-02	1.1570E-02
	1.1570E-02	1.1570E-02	1.1570E-02	1.1570E-02	1.1570E-02	1.1570E-02	1.1570E-02	1.1570E-02	1.1570E-02	1.1570E-02
	3.4710E-03	1.1570E-03	1.1570E-03							

Table 13.--Specified transmissivity values for layer 2, representing the San Andres-Glorieta aquifer--Continued

	Columns									
	1	2	3	4	5	6	7	8	9	10
	11	12	13	14	15	16	17	18	19	20
	21	22	23	24	25	26	27	28	29	30
	31	32	33	34	35	36	37	38	39	40
Rows	41	42	43							
21	0.0000	0.0000	0.0000	0.0000	0.0000	0.0000	0.0000	0.0000	4.6280E-04	4.6280E-04
	4.6280E-04	4.6280E-04	4.6280E-04	4.6280E-04	4.6280E-04	4.6280E-04	4.6280E-04	4.6280E-04	5.7850E-03	2.3140E-02
	0.1157	0.1157	0.1157	0.1157	0.1157	0.1157	2.3140E-02	2.3140E-02	1.1570E-02	1.1570E-02
	1.1570E-02	1.1570E-02	1.1570E-02	1.1570E-02	1.1570E-02	1.1570E-02	1.1570E-02	1.1570E-02	1.1570E-02	1.1570E-02
	3.4710E-03	1.1570E-03	1.1570E-03							
22	0.0000	0.0000	0.0000	0.0000	0.0000	0.0000	0.0000	0.0000	4.6280E-04	4.6280E-04
	4.6280E-04	4.6280E-04	4.6280E-04	4.6280E-04	4.6280E-04	4.6280E-04	4.6280E-04	1.3880E-02	8.0990E-02	0.1157
	0.1157	0.1157	0.1157	0.1157	0.1157	0.1157	2.3140E-02	2.3140E-02	1.1570E-02	1.1570E-02
	1.1570E-02	1.1570E-02	1.1570E-02	1.1570E-02	1.1570E-02	1.1570E-02	1.1570E-02	1.1570E-02	1.1570E-02	1.1570E-02
	3.4710E-03	1.1570E-03	1.1570E-03							
23	0.0000	0.0000	0.0000	0.0000	0.0000	0.0000	0.0000	0.0000	4.6280E-04	4.6280E-04
	4.6280E-04	4.6280E-04	4.6280E-04	4.6280E-04	4.6280E-04	4.6280E-04	4.6280E-04	8.0990E-02	8.0990E-02	0.1157
	0.1157	0.1157	0.1157	0.1157	0.1157	2.3140E-02	2.3140E-02	2.3140E-02	1.1570E-02	1.1570E-02
	1.1570E-02	1.1570E-02	1.1570E-02	1.1570E-02	1.1570E-02	1.1570E-02	1.1570E-02	1.1570E-02	1.1570E-02	1.1570E-02
	3.4710E-03	1.1570E-03	1.1570E-03							
24	0.0000	0.0000	0.0000	0.0000	0.0000	0.0000	0.0000	0.0000	4.6280E-04	4.6280E-04
	4.6280E-04	4.6280E-04	4.6280E-04	4.6280E-04	1.1570E-03	1.3880E-02	8.0990E-02	0.1157	0.1157	0.1157
	0.1157	0.1157	0.1157	0.1157	2.3140E-02	0.1157	0.1157	2.3140E-02	1.1570E-02	1.1570E-02
	1.1570E-02	1.1570E-02	1.1570E-02	1.1570E-02	1.1570E-02	1.1570E-02	1.1570E-02	1.1570E-02	1.1570E-02	1.1570E-02
	3.4710E-03	1.1570E-03	1.1570E-03							

Table 13.--Specified transmissivity values for layer 2, representing the San Andres-Glorieta aquifer--Continued

	Columns									
	1	2	3	4	5	6	7	8	9	10
	11	12	13	14	15	16	17	18	19	20
	21	22	23	24	25	26	27	28	29	30
	31	32	33	34	35	36	37	38	39	40
Rows	41	42	43							
25	0.0000	0.0000	0.0000	0.0000	0.0000	0.0000	0.0000	0.0000	4.6280E-04	4.6280E-04
	4.6280E-04	4.6280E-04	4.6280E-04	4.6280E-04	1.1570E-03	1.3880E-02	8.0990E-02	0.1157	0.1157	0.1157
	0.1157	0.1157	0.1157	2.3140E-02	0.1157	0.6942	0.1157	2.3140E-02	1.1570E-02	1.1570E-02
	1.1570E-02	1.1570E-02	1.1570E-02	1.1570E-02	1.1570E-02	1.1570E-02	1.1570E-02	1.1570E-02	1.1570E-02	1.1570E-02
	3.4710E-03	1.1570E-03	1.1570E-03							
26	0.0000	0.0000	0.0000	0.0000	0.0000	0.0000	0.0000	0.0000	4.6280E-04	4.6280E-04
	4.6280E-04	4.6280E-04	4.6280E-04	4.6280E-04	1.1570E-03	1.3880E-02	8.0990E-02	0.1157	0.1157	0.1157
	0.1157	2.3140E-02	2.3140E-02	0.1157	0.6942	0.6942	0.1157	2.3140E-02	1.1570E-02	1.1570E-02
	1.1570E-02	1.1570E-02	1.1570E-02	1.1570E-02	1.1570E-02	1.1570E-02	1.1570E-02	1.1570E-02	1.1570E-02	1.1570E-02
	3.4710E-03	1.1570E-03	1.1570E-03							
27	0.0000	0.0000	0.0000	0.0000	0.0000	0.0000	0.0000	0.0000	4.6280E-04	4.6280E-04
	4.6280E-04	4.6280E-04	4.6280E-04	4.6280E-04	4.6280E-04	1.1570E-03	1.3880E-02	2.3140E-02	2.3140E-02	2.3140E-02
	2.3140E-02	0.1157	0.1157	0.6942	0.6942	0.6942	0.1157	2.3140E-02	1.1570E-02	1.1570E-02
	1.1570E-02	1.1570E-02	1.1570E-02	1.1570E-02	1.1570E-02	1.1570E-02	1.1570E-02	1.1570E-02	1.1570E-02	1.1570E-02
	3.4710E-03	1.1570E-03	1.1570E-03							
28	0.0000	0.0000	0.0000	0.0000	0.0000	0.0000	0.0000	0.0000	4.6280E-04	4.6280E-04
	4.6280E-04	4.6280E-04	4.6280E-04	4.6280E-04	4.6280E-04	1.1570E-03	1.3880E-02	8.0990E-02	0.1157	0.1157
	0.1157	0.6942	0.6942	0.6942	0.6942	0.6942	0.1157	2.3140E-02	1.1570E-02	1.1570E-02
	1.1570E-02	1.1570E-02	1.1570E-02	1.1570E-02	1.1570E-02	1.1570E-02	1.1570E-02	1.1570E-02	1.1570E-02	1.1570E-02
	3.4710E-03	1.1570E-03	1.1570E-03							

Table 13.--Specified transmissivity values for layer 2, representing the San Andres-Glorieta aquifer--Continued

	Columns									
	1	2	3	4	5	6	7	8	9	10
	11	12	13	14	15	16	17	18	19	20
	21	22	23	24	25	26	27	28	29	30
	31	32	33	34	35	36	37	38	39	40
Rows	41	42	43							
29	0.0000	0.0000	0.0000	0.0000	0.0000	0.0000	0.0000	0.0000	4.6280E-04	4.6280E-04
	4.6280E-04	4.6280E-04	4.6280E-04	4.6280E-04	4.6280E-04	1.1570E-03	1.3880E-02	8.0990E-02	0.6942	0.6942
	0.6942	0.6942	0.6942	0.6942	0.6942	0.6942	0.1157	2.3140E-02	1.1570E-02	1.1570E-02
	1.1570E-02	1.1570E-02	1.1570E-02	1.1570E-02	1.1570E-02	1.1570E-02	1.1570E-02	1.1570E-02	1.1570E-02	1.1570E-02
	3.4710E-03	1.1570E-03	1.1570E-03							
30	0.0000	0.0000	0.0000	0.0000	0.0000	0.0000	0.0000	0.0000	4.6280E-04	4.6280E-04
	4.6280E-04	4.6280E-04	4.6280E-04	4.6280E-04	4.6280E-04	1.1570E-03	1.3880E-02	8.0990E-02	0.6942	0.6942
	0.6942	0.6942	0.6942	0.6942	0.6942	0.6942	0.1157	2.3140E-02	1.1570E-02	1.1570E-02
	1.1570E-02	1.1570E-02	1.1570E-02	1.1570E-02	1.1570E-02	1.1570E-02	1.1570E-02	1.1570E-02	1.1570E-02	1.1570E-02
	3.4710E-03	1.1570E-03	1.1570E-03							
31	0.0000	0.0000	0.0000	0.0000	0.0000	0.0000	0.0000	0.0000	4.6280E-04	4.6280E-04
	4.6280E-04	4.6280E-04	4.6280E-04	1.1570E-03	1.1570E-03	1.1570E-03	1.1570E-03	1.3880E-02	8.0990E-02	0.6942
	0.6942	0.6942	0.6942	0.6942	0.6942	0.6942	0.1157	2.3140E-02	1.1570E-02	1.1570E-02
	1.1570E-02	1.1570E-02	1.1570E-02	1.1570E-02	1.1570E-02	1.1570E-02	1.1570E-02	1.1570E-02	1.1570E-02	1.1570E-02
	3.4710E-03	1.1570E-03	1.1570E-03							
32	0.0000	0.0000	0.0000	0.0000	0.0000	0.0000	0.0000	0.0000	4.6280E-04	4.6280E-04
	4.6280E-04	4.6280E-04	4.6280E-04	1.1570E-03	1.3880E-02	1.3880E-02	1.3880E-02	1.3880E-02	8.0990E-02	0.6942
	0.6942	0.6942	0.6942	0.6942	0.6942	0.6942	0.1157	2.3140E-02	1.1570E-02	1.1570E-02
	1.1570E-02	1.1570E-02	1.1570E-02	1.1570E-02	1.1570E-02	1.1570E-02	1.1570E-02	1.1570E-02	1.1570E-02	1.1570E-02
	3.4710E-03	1.1570E-03	1.1570E-03							

Table 13.--Specified transmissivity values for layer 2, representing the San Andres-Glorieta aquifer--Continued

Rows	Columns									
	1	2	3	4	5	6	7	8	9	10
	11	12	13	14	15	16	17	18	19	20
	21	22	23	24	25	26	27	28	29	30
	31	32	33	34	35	36	37	38	39	40
	41	42	43							
33	0.0000	0.0000	0.0000	0.0000	0.0000	0.0000	0.0000	0.0000	4.6280E-04	4.6280E-04
	4.6280E-04	4.6280E-04	4.6280E-04	1.1570E-03	1.3880E-02	8.0990E-02	8.0990E-02	8.0990E-02	8.0990E-02	0.6942
	0.6942	0.6942	0.6942	0.6942	0.6942	0.6942	0.1157	2.3140E-02	1.1570E-02	1.1570E-02
	1.1570E-02	1.1570E-02	1.1570E-02	1.1570E-02	1.1570E-02	1.1570E-02	1.1570E-02	1.1570E-02	1.1570E-02	1.1570E-02
	3.4710E-03	1.1570E-03	1.1570E-03							
34	0.0000	0.0000	0.0000	0.0000	0.0000	0.0000	0.0000	0.0000	4.6280E-04	4.6280E-04
	4.6280E-04	4.6280E-04	4.6280E-04	1.1570E-03	1.3880E-02	8.0990E-02	0.6942	0.6942	0.6942	0.6942
	0.6942	0.6942	0.6942	0.6942	0.6942	0.6942	0.1157	2.3140E-02	1.1570E-02	1.1570E-02
	1.1570E-02	1.1570E-02	1.1570E-02	1.1570E-02	1.1570E-02	1.1570E-02	1.1570E-02	1.1570E-02	1.1570E-02	1.1570E-02
	3.4710E-03	1.1570E-03	1.1570E-03							
35	0.0000	0.0000	0.0000	0.0000	0.0000	0.0000	0.0000	0.0000	4.6280E-04	4.6280E-04
	4.6280E-04	4.6280E-04	1.1570E-03	1.1570E-03	1.3880E-02	8.0990E-02	0.6942	0.6942	0.6942	0.6942
	0.6942	0.6942	0.6942	0.6942	0.6942	0.6942	0.1157	2.3140E-02	1.1570E-02	1.1570E-02
	1.1570E-02	1.1570E-02	1.1570E-02	1.1570E-02	1.1570E-02	1.1570E-02	1.1570E-02	1.1570E-02	1.1570E-02	1.1570E-02
	3.4710E-03	1.1570E-03	1.1570E-03							
36	0.0000	0.0000	0.0000	0.0000	0.0000	4.6280E-04	4.6280E-04	4.6280E-04	4.6280E-04	4.6280E-04
	4.6280E-04	4.6280E-04	1.1570E-03	1.3880E-02	1.3880E-02	8.0990E-02	0.6942	0.6942	0.6942	0.6942
	0.6942	0.6942	0.6942	0.6942	0.6942	0.6942	0.1157	2.3140E-02	1.1570E-02	1.1570E-02
	1.1570E-02	1.1570E-02	1.1570E-02	1.1570E-02	1.1570E-02	1.1570E-02	1.1570E-02	1.1570E-02	1.1570E-02	1.1570E-02
	3.4710E-03	1.1570E-03	1.1570E-03							

Table 13.--Specified transmissivity values for layer 2, representing the San Andres-Glorieta aquifer--Continued

	Columns									
	1	2	3	4	5	6	7	8	9	10
	11	12	13	14	15	16	17	18	19	20
	21	22	23	24	25	26	27	28	29	30
	31	32	33	34	35	36	37	38	39	40
Rows	41	42	43							
37	0.0000	0.0000	0.0000	0.0000	0.0000	4.6280E-04	4.6280E-04	4.6280E-04	4.6280E-04	4.6280E-04
	4.6280E-04	1.1570E-03	1.1570E-03	1.3880E-02	8.0990E-02	8.0990E-02	0.6942	0.6942	0.6942	0.6942
	0.6942	0.6942	0.6942	0.6942	0.6942	0.6942	0.1157	2.3140E-02	1.1570E-02	1.1570E-02
	1.1570E-02	1.1570E-02	1.1570E-02	1.1570E-02	1.1570E-02	1.1570E-02	1.1570E-02	1.1570E-02	1.1570E-02	1.1570E-02
	3.4710E-03	1.1570E-03	1.1570E-03							
38	0.0000	0.0000	0.0000	0.0000	0.0000	4.6280E-04	4.6280E-04	4.6280E-04	4.6280E-04	4.6280E-04
	4.6280E-04	1.1570E-03	1.3880E-02	1.3880E-02	8.0990E-02	0.6942	0.6942	0.6942	0.6942	0.6942
	0.6942	0.6942	0.6942	0.6942	0.6942	0.6942	0.1157	2.3140E-02	1.1570E-02	1.1570E-02
	1.1570E-02	1.1570E-02	1.1570E-02	1.1570E-02	1.1570E-02	1.1570E-02	1.1570E-02	1.1570E-02	1.1570E-02	1.1570E-02
	3.4710E-03	1.1570E-03	1.1570E-03							
39	0.0000	0.0000	0.0000	0.0000	0.0000	4.6280E-04	4.6280E-04	4.6280E-04	4.6280E-04	4.6280E-04
	4.6280E-04	1.1570E-03	1.3880E-02	8.0990E-02	8.0990E-02	0.6942	0.6942	0.6942	0.6942	0.6942
	0.6942	0.6942	0.6942	0.6942	0.6942	0.6942	0.1157	2.3140E-02	1.1570E-02	1.1570E-02
	1.1570E-02	1.1570E-02	1.1570E-02	1.1570E-02	1.1570E-02	1.1570E-02	1.1570E-02	1.1570E-02	1.1570E-02	1.1570E-02
	3.4710E-03	1.1570E-03	1.1570E-03							
40	0.0000	0.0000	0.0000	0.0000	0.0000	4.6280E-04	4.6280E-04	4.6280E-04	4.6280E-04	4.6280E-04
	1.1570E-03	1.1570E-03	1.3880E-02	8.0990E-02	0.6942	0.6942	0.6942	0.6942	0.6942	0.6942
	0.6942	0.6942	0.6942	0.6942	0.6942	0.6942	0.1157	2.3140E-02	1.1570E-02	1.1570E-02
	1.1570E-02	1.1570E-02	1.1570E-02	1.1570E-02	1.1570E-02	1.1570E-02	1.1570E-02	1.1570E-02	1.1570E-02	1.1570E-02
	3.4710E-03	1.1570E-03	1.1570E-03							

Table 13.--Specified transmissivity values for layer 2, representing the San Andres-Glorieta aquifer--Continued

	Columns									
	1	2	3	4	5	6	7	8	9	10
	11	12	13	14	15	16	17	18	19	20
	21	22	23	24	25	26	27	28	29	30
	31	32	33	34	35	36	37	38	39	40
Rows	41	42	43							
41	0.0000	0.0000	0.0000	0.0000	0.0000	4.6280E-04	1.1570E-03	1.1570E-03	1.1570E-03	1.1570E-03
	1.1570E-03	1.1570E-03	1.3880E-02	8.0990E-02	0.6942	0.6942	0.6942	0.6942	0.6942	0.6942
	0.6942	0.6942	0.6942	0.6942	0.6942	0.6942	0.1157	2.3140E-02	1.1570E-02	1.1570E-02
	1.1570E-02	1.1570E-02	1.1570E-02	1.1570E-02	1.1570E-02	1.1570E-02	1.1570E-02	1.1570E-02	1.1570E-02	1.1570E-02
	3.4710E-03	1.1570E-03	1.1570E-03							
42	0.0000	0.0000	0.0000	0.0000	0.0000	4.6280E-04	1.1570E-03	1.1570E-03	1.1570E-03	1.1570E-03
	1.1570E-03	1.3880E-02	1.3880E-02	8.0990E-02	0.6942	0.6942	0.6942	0.6942	0.6942	0.6942
	0.6942	0.0000	0.0000	0.0000	0.0000	0.0000	0.0000	2.3140E-02	1.1570E-02	1.1570E-02
	1.1570E-02	1.1570E-02	1.1570E-02	1.1570E-02	1.1570E-02	1.1570E-02	1.1570E-02	1.1570E-02	1.1570E-02	1.1570E-02
	3.4710E-03	1.1570E-03	1.1570E-03							
43	0.0000	0.0000	0.0000	0.0000	0.0000	5.7850E-03	5.7850E-03	5.7850E-03	5.7850E-03	5.7850E-03
	5.7850E-03	0.0000	0.0000	0.0000	0.0000	0.0000	0.0000	0.0000	0.0000	0.0000
	0.0000	0.5785	0.5785	0.5785	0.5785	0.5785	0.1157	2.3140E-02	1.1570E-02	1.1570E-02
	1.1570E-02	1.1570E-02	1.1570E-02	1.1570E-02	1.1570E-02	1.1570E-02	1.1570E-02	1.1570E-02	1.1570E-02	1.1570E-02
	3.4710E-03	1.1570E-03	1.1570E-03							
44	0.0000	0.0000	0.0000	0.0000	0.0000	1.1570E-02	1.1570E-02	1.1570E-02	1.1570E-02	1.1570E-02
	1.1570E-02	1.1570E-02	1.1570E-02	1.1570E-02	0.1157	0.5785	0.5785	0.5785	0.5785	0.5785
	0.5785	0.5785	0.5785	0.5785	0.5785	0.5785	0.1157	2.3140E-02	1.1570E-02	1.1570E-02
	1.1570E-02	1.1570E-02	1.1570E-02	1.1570E-02	1.1570E-02	1.1570E-02	1.1570E-02	1.1570E-02	1.1570E-02	1.1570E-02
	3.4710E-03	1.1570E-03	1.1570E-03							

Table 13.--Specified transmissivity values for layer 2, representing the San Andres-Glorieta aquifer--Continued

	Columns									
	1	2	3	4	5	6	7	8	9	10
	11	12	13	14	15	16	17	18	19	20
	21	22	23	24	25	26	27	28	29	30
	31	32	33	34	35	36	37	38	39	40
Rows	41	42	43							
45	0.0000	0.0000	0.0000	0.0000	0.0000	1.1570E-02	1.1570E-02	1.1570E-02	1.1570E-02	0.1157
	0.1157	0.1157	0.1157	0.1157	0.1157	0.5785	0.5785	0.5785	0.5785	0.5785
	0.5785	0.5785	0.5785	0.5785	0.5785	0.5785	0.1157	2.3140E-02	1.1570E-02	1.1570E-02
	1.1570E-02	1.1570E-02	1.1570E-02	1.1570E-02	1.1570E-02	1.1570E-02	1.1570E-02	1.1570E-02	1.1570E-02	1.1570E-02
	3.4710E-03	1.1570E-03	1.1570E-03							
46	0.0000	0.0000	0.0000	0.0000	0.0000	1.1570E-02	1.1570E-02	1.1570E-02	1.1570E-02	0.1157
	0.1157	0.1157	0.1157	0.1157	0.1157	0.5785	0.5785	0.5785	0.5785	0.5785
	0.5785	0.5785	0.5785	0.5785	0.5785	0.5785	0.1157	2.3140E-02	1.1570E-02	1.1570E-02
	1.1570E-02	1.1570E-02	1.1570E-02	1.1570E-02	1.1570E-02	1.1570E-02	1.1570E-02	1.1570E-02	1.1570E-02	1.1570E-02
	3.4710E-03	1.1570E-03	1.1570E-03							
47	0.0000	0.0000	0.0000	0.0000	0.0000	1.1570E-02	1.1570E-02	1.1570E-02	1.1570E-02	0.1157
	0.5785	0.5785	0.5785	0.5785	0.5785	0.5785	0.5785	0.5785	0.5785	0.5785
	0.5785	0.5785	0.5785	0.5785	0.5785	0.5785	0.1157	2.3140E-02	1.1570E-02	1.1570E-02
	1.1570E-02	1.1570E-02	1.1570E-02	1.1570E-02	1.1570E-02	1.1570E-02	1.1570E-02	1.1570E-02	1.1570E-02	1.1570E-02
	3.4710E-03	1.1570E-03	1.1570E-03							
48	0.0000	0.0000	0.0000	0.0000	1.1570E-02	1.1570E-02	1.1570E-02	1.1570E-02	1.1570E-02	0.1157
	0.5785	0.5785	0.5785	0.5785	0.5785	0.5785	0.5785	0.5785	0.5785	0.5785
	0.5785	0.5785	0.5785	0.5785	0.5785	0.5785	0.1157	2.3140E-02	1.1570E-02	1.1570E-02
	1.1570E-02	1.1570E-02	1.1570E-02	1.1570E-02	1.1570E-02	1.1570E-02	1.1570E-02	1.1570E-02	1.1570E-02	1.1570E-02
	3.4710E-03	1.1570E-03	1.1570E-03							

Table 13.--Specified transmissivity values for layer 2, representing the San Andres-Glorieta aquifer--Continued

	Columns									
	1	2	3	4	5	6	7	8	9	10
	11	12	13	14	15	16	17	18	19	20
	21	22	23	24	25	26	27	28	29	30
	31	32	33	34	35	36	37	38	39	40
Rows	41	42	43							
49	0.0000	1.1570E-03	1.1570E-03	1.1570E-02	1.1570E-02	1.1570E-02	1.1570E-02	1.1570E-02	1.1570E-02	0.1157
	0.5785	0.5785	0.5785	0.5785	0.5785	0.5785	0.5785	0.5785	0.5785	0.5785
	0.5785	0.5785	0.5785	0.5785	0.5785	0.5785	0.1157	2.3140E-02	1.1570E-02	1.1570E-02
	1.1570E-02	1.1570E-02	1.1570E-02	1.1570E-02	1.1570E-02	1.1570E-02	1.1570E-02	1.1570E-02	1.1570E-02	1.1570E-02
	3.4710E-03	1.1570E-03	1.1570E-03							
50	0.0000	1.1570E-03	1.1570E-03	1.1570E-02	1.1570E-02	1.1570E-02	1.1570E-02	1.1570E-02	1.1570E-02	0.1157
	0.5785	0.5785	0.5785	0.5785	0.5785	0.5785	0.5785	0.5785	0.5785	0.5785
	0.5785	0.1157	0.1157	0.1157	0.1157	0.1157	0.1157	2.3140E-02	1.1570E-02	1.1570E-02
	1.1570E-02	1.1570E-02	1.1570E-02	1.1570E-02	1.1570E-02	1.1570E-02	1.1570E-02	1.1570E-02	1.1570E-02	1.1570E-02
	3.4710E-03	1.1570E-03	1.1570E-03							
51	0.0000	0.0000	5.7850E-03	1.1570E-02	1.1570E-02	1.1570E-02	0.1157	0.1157	0.1157	0.1157
	0.5785	0.5785	0.5785	0.5785	0.5785	0.5785	0.5785	0.5785	0.5785	0.5785
	0.5785	0.1157	1.3880E-02	1.3880E-02	1.3880E-02	1.3880E-02	1.3880E-02	1.3880E-02	1.1570E-02	1.1570E-02
	1.1570E-02	1.1570E-02	1.1570E-02	1.1570E-02	1.1570E-02	1.1570E-02	1.1570E-02	1.1570E-02	1.1570E-02	1.1570E-02
	3.4710E-03	1.1570E-03	1.1570E-03							
52	1.1570E-03	1.1570E-03	5.7850E-03	1.1570E-02	0.1157	0.1157	0.1157	0.5785	0.5785	0.5785
	0.5785	0.5785	0.5785	0.5785	0.5785	0.5785	0.5785	0.5785	0.5785	0.5785
	0.5785	0.1157	1.3880E-02	5.7850E-03	5.7850E-03	5.7850E-03	5.7850E-03	5.7850E-03	5.7850E-03	5.7850E-03
	5.7850E-03	5.7850E-03	5.7850E-03	5.7850E-03	5.7850E-03	5.7850E-03	5.7850E-03	5.7850E-03	5.7850E-03	5.7850E-03
	5.7850E-03	5.7850E-03	5.7850E-03							

Table 13.--Specified transmissivity values for layer 2, representing the San Andres-Glorieta aquifer--Continued

Rows	Columns 1	2	3	4	5	6	7	8	9	10
	11	12	13	14	15	16	17	18	19	20
	21	22	23	24	25	26	27	28	29	30
	31	32	33	34	35	36	37	38	39	40
	41	42	43							
53	1.1570E-03	1.1570E-03	5.7850E-03	1.1570E-02	0.1157	0.5785	0.5785	0.5785	0.5785	0.5785
	0.5785	0.5785	0.5785	0.5785	0.5785	0.5785	0.5785	0.5785	0.5785	0.5785
	0.5785	0.1157	1.3880E-02	5.7850E-03	5.7850E-03	5.7850E-03	5.7850E-03	5.7850E-03	5.7850E-03	5.7850E-03
	5.7850E-03	5.7850E-03	5.7850E-03	5.7850E-03	5.7850E-03	5.7850E-03	5.7850E-03	5.7850E-03	5.7850E-03	5.7850E-03
	5.7850E-03	5.7850E-03	5.7850E-03							
54	1.1570E-03	1.1570E-03	5.7850E-03	1.1570E-02	0.1157	0.5785	0.5785	0.5785	0.5785	0.5785
	0.5785	0.5785	0.5785	0.5785	0.5785	0.5785	0.5785	0.5785	0.5785	0.5785
	0.5785	0.1157	1.3880E-02	5.7850E-03	5.7850E-03	5.7850E-03	5.7850E-03	5.7850E-03	5.7850E-03	5.7850E-03
	5.7850E-03	5.7850E-03	5.7850E-03	5.7850E-03	5.7850E-03	5.7850E-03	5.7850E-03	5.7850E-03	5.7850E-03	5.7850E-03
	5.7850E-03	5.7850E-03	5.7850E-03							
55	5.7850E-03	5.7850E-03	5.7850E-03	1.1570E-02	0.1157	0.5785	0.5785	0.5785	0.5785	0.5785
	0.5785	0.5785	0.5785	0.5785	0.5785	0.5785	0.5785	0.5785	0.5785	0.5785
	0.5785	0.1157	1.3880E-02	5.7850E-03	5.7850E-03	5.7850E-03	5.7850E-03	5.7850E-03	5.7850E-03	5.7850E-03
	5.7850E-03	5.7850E-03	5.7850E-03	5.7850E-03	5.7850E-03	5.7850E-03	5.7850E-03	5.7850E-03	5.7850E-03	5.7850E-03
	5.7850E-03	5.7850E-03	5.7850E-03							
56	5.7850E-03	1.1570E-02	1.1570E-02	1.1570E-02	0.1157	0.5785	0.5785	0.5785	0.5785	0.5785
	0.5785	0.5785	0.5785	0.5785	0.5785	0.5785	0.5785	0.5785	0.1157	0.1157
	0.1157	0.1157	1.3880E-02	5.7850E-03	5.7850E-03	5.7850E-03	5.7850E-03	5.7850E-03	5.7850E-03	5.7850E-03
	5.7850E-03	5.7850E-03	5.7850E-03	5.7850E-03	5.7850E-03	5.7850E-03	5.7850E-03	5.7850E-03	5.7850E-03	5.7850E-03
	5.7850E-03	5.7850E-03	5.7850E-03							

Table 13.--Specified transmissivity values for layer 2, representing the San Andres-Glorieta aquifer--Continued

Rows	Columns 1	2	3	4	5	6	7	8	9	10
	11	12	13	14	15	16	17	18	19	20
	21	22	23	24	25	26	27	28	29	30
	31	32	33	34	35	36	37	38	39	40
	41	42	43							
57	5.7850E-03	1.1570E-02	0.1157	0.1157	0.1157	0.5785	0.5785	0.5785	0.5785	0.5785
	0.5785	0.5785	0.5785	0.5785	0.5785	0.5785	0.5785	0.5785	0.1157	1.3880E-02
	1.3880E-02	1.3880E-02	1.3880E-02	5.7850E-03	5.7850E-03	5.7850E-03	5.7850E-03	5.7850E-03	5.7850E-03	5.7850E-03
	5.7850E-03	5.7850E-03	5.7850E-03	5.7850E-03	5.7850E-03	5.7850E-03	5.7850E-03	5.7850E-03	5.7850E-03	5.7850E-03
	5.7850E-03	5.7850E-03	5.7850E-03							
58	5.7850E-03	1.1570E-02	0.1157	0.5785	0.5785	0.5785	0.5785	0.5785	0.5785	0.5785
	0.5785	0.5785	0.5785	0.5785	0.5785	0.5785	0.5785	0.5785	0.1157	1.3880E-02
	5.7850E-03	5.7850E-03	5.7850E-03	5.7850E-03	5.7850E-03	5.7850E-03	5.7850E-03	5.7850E-03	5.7850E-03	5.7850E-03
	5.7850E-03	5.7850E-03	5.7850E-03	5.7850E-03	5.7850E-03	5.7850E-03	5.7850E-03	5.7850E-03	5.7850E-03	5.7850E-03
	5.7850E-03	5.7850E-03	5.7850E-03							
59	1.1570E-02	1.1570E-02	0.1157	0.5785	0.5785	0.5785	0.5785	0.5785	0.1157	0.1157
	0.1157	0.1157	0.1157	0.1157	0.1157	0.1157	0.1157	0.1157	0.1157	1.3880E-02
	5.7850E-03	5.7850E-03	5.7850E-03	5.7850E-03	5.7850E-03	5.7850E-03	5.7850E-03	5.7850E-03	5.7850E-03	5.7850E-03
	5.7850E-03	5.7850E-03	5.7850E-03	5.7850E-03	5.7850E-03	5.7850E-03	5.7850E-03	5.7850E-03	5.7850E-03	5.7850E-03
	5.7850E-03	5.7850E-03	5.7850E-03							
60	0.1157	0.1157	0.1157	0.5785	0.5785	0.5785	0.5785	0.5785	0.1157	1.3880E-02
	1.3880E-02	1.3880E-02	1.3880E-02	1.3880E-02	1.3880E-02	1.3880E-02	1.3880E-02	1.3880E-02	1.3880E-02	1.3880E-02
	5.7850E-03	5.7850E-03	5.7850E-03	5.7850E-03	5.7850E-03	5.7850E-03	5.7850E-03	5.7850E-03	5.7850E-03	5.7850E-03
	5.7850E-03	5.7850E-03	5.7850E-03	5.7850E-03	5.7850E-03	5.7850E-03	5.7850E-03	5.7850E-03	5.7850E-03	5.7850E-03
	5.7850E-03	5.7850E-03	5.7850E-03							

Table 13.--Specified transmissivity values for layer 2, representing the San Andres-Glorieta aquifer--Continued

	Columns									
	1	2	3	4	5	6	7	8	9	10
	11	12	13	14	15	16	17	18	19	20
	21	22	23	24	25	26	27	28	29	30
	31	32	33	34	35	36	37	38	39	40
Rows	41	42	43							
61	0.5785	0.5785	0.5785	0.5785	0.5785	0.5785	0.5785	0.5785	0.1157	1.3880E-02
	5.7850E-03	5.7850E-03	5.7850E-03	5.7850E-03	5.7850E-03	5.7850E-03	5.7850E-03	5.7850E-03	5.7850E-03	5.7850E-03
	5.7850E-03	5.7850E-03	5.7850E-03	5.7850E-03	5.7850E-03	5.7850E-03	5.7850E-03	5.7850E-03	5.7850E-03	5.7850E-03
	5.7850E-03	5.7850E-03	5.7850E-03	5.7850E-03	5.7850E-03	5.7850E-03	5.7850E-03	5.7850E-03	5.7850E-03	5.7850E-03
	9.2560E-04	9.2560E-04	9.2560E-04							
62	0.5785	0.5785	0.5785	0.5785	0.1157	0.1157	0.1157	0.1157	0.1157	1.3880E-02
	5.7850E-03	5.7850E-03	5.7850E-03	5.7850E-03	5.7850E-03	5.7850E-03	5.7850E-03	5.7850E-03	5.7850E-03	5.7850E-03
	5.7850E-03	5.7850E-03	5.7850E-03	5.7850E-03	5.7850E-03	5.7850E-03	5.7850E-03	5.7850E-03	5.7850E-03	5.7850E-03
	5.7850E-03	5.7850E-03	5.7850E-03	5.7850E-03	5.7850E-03	5.7850E-03	5.7850E-03	5.7850E-03	5.7850E-03	5.7850E-03
	9.2560E-04	9.2560E-04	9.2560E-04							
63	0.5785	0.5785	0.5785	0.5785	0.1157	1.3880E-02	1.3880E-02	1.3880E-02	1.3880E-02	1.3880E-02
	5.7850E-03	5.7850E-03	5.7850E-03	5.7850E-03	5.7850E-03	5.7850E-03	5.7850E-03	5.7850E-03	5.7850E-03	5.7850E-03
	5.7850E-03	5.7850E-03	5.7850E-03	5.7850E-03	5.7850E-03	5.7850E-03	5.7850E-03	5.7850E-03	5.7850E-03	5.7850E-03
	5.7850E-03	5.7850E-03	5.7850E-03	5.7850E-03	5.7850E-03	5.7850E-03	5.7850E-03	5.7850E-03	9.2560E-04	9.2560E-04
	9.2560E-04	9.2560E-04	9.2560E-04							
64	0.5785	0.5785	0.5785	0.5785	0.1157	1.3880E-02	5.7850E-03	5.7850E-03	5.7850E-03	5.7850E-03
	5.7850E-03	5.7850E-03	5.7850E-03	5.7850E-03	5.7850E-03	5.7850E-03	5.7850E-03	5.7850E-03	5.7850E-03	5.7850E-03
	5.7850E-03	5.7850E-03	5.7850E-03	5.7850E-03	5.7850E-03	5.7850E-03	5.7850E-03	5.7850E-03	5.7850E-03	5.7850E-03
	5.7850E-03	5.7850E-03	5.7850E-03	5.7850E-03	5.7850E-03	5.7850E-03	5.7850E-03	5.7850E-03	9.2560E-04	9.2560E-04
	9.2560E-04	9.2560E-04	9.2560E-04							

Table 13.--Specified transmissivity values for layer 2, representing the San Andres-Glorieta aquifer--Continued

	Columns									
	1	2	3	4	5	6	7	8	9	10
	11	12	13	14	15	16	17	18	19	20
	21	22	23	24	25	26	27	28	29	30
	31	32	33	34	35	36	37	38	39	40
Rows	41	42	43							
65	0.5785	0.5785	0.5785	0.1157	0.1157	1.3880E-02	5.7850E-03	5.7850E-03	5.7850E-03	5.7850E-03
	5.7850E-03	5.7850E-03	5.7850E-03	5.7850E-03	5.7850E-03	5.7850E-03	5.7850E-03	5.7850E-03	5.7850E-03	5.7850E-03
	5.7850E-03	5.7850E-03	5.7850E-03	5.7850E-03	5.7850E-03	5.7850E-03	5.7850E-03	5.7850E-03	5.7850E-03	5.7850E-03
	5.7850E-03	5.7850E-03	5.7850E-03	5.7850E-03	5.7850E-03	5.7850E-03	5.7850E-03	5.7850E-03	9.2560E-04	9.2560E-04
	9.2560E-04	9.2560E-04	9.2560E-04							
66	0.5785	0.5785	0.5785	0.1157	1.3880E-02	1.3880E-02	5.7850E-03	5.7850E-03	5.7850E-03	5.7850E-03
	5.7850E-03	5.7850E-03	5.7850E-03	5.7850E-03	5.7850E-03	5.7850E-03	5.7850E-03	5.7850E-03	5.7850E-03	5.7850E-03
	5.7850E-03	5.7850E-03	5.7850E-03	5.7850E-03	5.7850E-03	5.7850E-03	5.7850E-03	5.7850E-03	5.7850E-03	5.7850E-03
	5.7850E-03	9.2560E-04	9.2560E-04	9.2560E-04	9.2560E-04	9.2560E-04	9.2560E-04	9.2560E-04	9.2560E-04	9.2560E-04
	9.2560E-04	9.2560E-04	9.2560E-04							
67	0.5785	0.5785	0.5785	0.1157	1.3880E-02	5.7850E-03	5.7850E-03	5.7850E-03	5.7850E-03	5.7850E-03
	5.7850E-03	5.7850E-03	5.7850E-03	5.7850E-03	5.7850E-03	5.7850E-03	5.7850E-03	5.7850E-03	5.7850E-03	5.7850E-03
	5.7850E-03	5.7850E-03	5.7850E-03	5.7850E-03	5.7850E-03	5.7850E-03	5.7850E-03	5.7850E-03	5.7850E-03	5.7850E-03
	5.7850E-03	9.2560E-04	9.2560E-04	9.2560E-04	9.2560E-04	9.2560E-04	9.2560E-04	9.2560E-04	9.2560E-04	9.2560E-04
	9.2560E-04	9.2560E-04	0.0000							
68	0.5785	0.5785	0.5785	0.1157	1.3880E-02	5.7850E-03	5.7850E-03	5.7850E-03	5.7850E-03	5.7850E-03
	5.7850E-03	5.7850E-03	5.7850E-03	5.7850E-03	5.7850E-03	5.7850E-03	5.7850E-03	5.7850E-03	5.7850E-03	5.7850E-03
	5.7850E-03	5.7850E-03	5.7850E-03	5.7850E-03	5.7850E-03	5.7850E-03	5.7850E-03	5.7850E-03	5.7850E-03	5.7850E-03
	5.7850E-03	9.2560E-04	9.2560E-04	9.2560E-04	9.2560E-04	9.2560E-04	9.2560E-04	9.2560E-04	9.2560E-04	9.2560E-04
	9.2560E-04	9.2560E-04	0.0000							

Table 13.--Specified transmissivity values for layer 2, representing the San Andres-Glorieta aquifer--Continued

	Columns									
	1	2	3	4	5	6	7	8	9	10
	11	12	13	14	15	16	17	18	19	20
	21	22	23	24	25	26	27	28	29	30
	31	32	33	34	35	36	37	38	39	40
Rows	41	42	43							
69	0.5785	0.5785	0.5785	0.1157	1.3880E-02	5.7850E-03	5.7850E-03	5.7850E-03	5.7850E-03	5.7850E-03
	5.7850E-03	5.7850E-03	5.7850E-03	5.7850E-03	5.7850E-03	5.7850E-03	5.7850E-03	5.7850E-03	5.7850E-03	5.7850E-03
	5.7850E-03	5.7850E-03	5.7850E-03	5.7850E-03	5.7850E-03	5.7850E-03	5.7850E-03	5.7850E-03	5.7850E-03	5.7850E-03
	5.7850E-03	9.2560E-04	9.2560E-04	9.2560E-04	9.2560E-04	9.2560E-04	9.2560E-04	9.2560E-04	9.2560E-04	9.2560E-04
	9.2560E-04	0.0000	0.0000							
70	0.5785	0.5785	0.5785	0.1157	1.3880E-02	5.7850E-03	5.7850E-03	5.7850E-03	5.7850E-03	5.7850E-03
	5.7850E-03	5.7850E-03	5.7850E-03	5.7850E-03	5.7850E-03	5.7850E-03	5.7850E-03	5.7850E-03	5.7850E-03	5.7850E-03
	5.7850E-03	5.7850E-03	5.7850E-03	5.7850E-03	9.2560E-04	9.2560E-04	9.2560E-04	9.2560E-04	9.2560E-04	9.2560E-04
	9.2560E-04	9.2560E-04	9.2560E-04	9.2560E-04	9.2560E-04	9.2560E-04	9.2560E-04	9.2560E-04	9.2560E-04	9.2560E-04
	9.2560E-04	0.0000	0.0000							
71	0.5785	0.5785	0.5785	0.1157	1.3880E-02	5.7850E-03	5.7850E-03	5.7850E-03	5.7850E-03	5.7850E-03
	5.7850E-03	5.7850E-03	5.7850E-03	5.7850E-03	5.7850E-03	5.7850E-03	5.7850E-03	5.7850E-03	5.7850E-03	5.7850E-03
	5.7850E-03	5.7850E-03	5.7850E-03	5.7850E-03	9.2560E-04	9.2560E-04	9.2560E-04	9.2560E-04	9.2560E-04	9.2560E-04
	9.2560E-04	9.2560E-04	9.2560E-04	9.2560E-04	9.2560E-04	9.2560E-04	9.2560E-04	9.2560E-04	9.2560E-04	9.2560E-04
	0.0000	0.0000	0.0000							
72	0.5785	0.5785	0.5785	0.1157	1.3880E-02	5.7850E-03	5.7850E-03	5.7850E-03	5.7850E-03	5.7850E-03
	5.7850E-03	5.7850E-03	5.7850E-03	5.7850E-03	5.7850E-03	5.7850E-03	5.7850E-03	5.7850E-03	5.7850E-03	5.7850E-03
	9.2560E-04	9.2560E-04	9.2560E-04	9.2560E-04	9.2560E-04	9.2560E-04	9.2560E-04	9.2560E-04	9.2560E-04	9.2560E-04
	9.2560E-04	9.2560E-04	9.2560E-04	9.2560E-04	9.2560E-04	9.2560E-04	9.2560E-04	9.2560E-04	0.0000	0.0000
	0.0000	0.0000	0.0000							

Table 13.--Specified transmissivity values for layer 2, representing the San Andres-Glorieta aquifer--Concluded

	Columns									
	1	2	3	4	5	6	7	8	9	10
	11	12	13	14	15	16	17	18	19	20
	21	22	23	24	25	26	27	28	29	30
	31	32	33	34	35	36	37	38	39	40
Rows	41	42	43							
73	8.0990E-02	8.0990E-02	8.0990E-02	8.0990E-02	1.3880E-02	5.7850E-03	5.7850E-03	5.7850E-03	5.7850E-03	5.7850E-03
	9.2560E-04	9.2560E-04	9.2560E-04	9.2560E-04	9.2560E-04	9.2560E-04	9.2560E-04	9.2560E-04	9.2560E-04	9.2560E-04
	9.2560E-04	9.2560E-04	9.2560E-04	9.2560E-04	9.2560E-04	9.2560E-04	9.2560E-04	9.2560E-04	9.2560E-04	9.2560E-04
	9.2560E-04	0.0000	0.0000	0.0000	0.0000	0.0000	0.0000	0.0000	0.0000	0.0000
	0.0000	0.0000	0.0000							
74	8.0990E-03	8.0990E-03	8.0990E-03	8.0990E-03	8.0990E-03	5.7850E-03	9.2560E-04	9.2560E-04	9.2560E-04	9.2560E-04
	9.2560E-04	9.2560E-04	9.2560E-04	9.2560E-04	9.2560E-04	9.2560E-04	9.2560E-04	9.2560E-04	9.2560E-04	9.2560E-04
	9.2560E-04	9.2560E-04	9.2560E-04	9.2560E-04	0.0000	0.0000	0.0000	0.0000	0.0000	0.0000
	0.0000	0.0000	0.0000	0.0000	0.0000	0.0000	0.0000	0.0000	0.0000	0.0000
	0.0000	0.0000	0.0000							
75	9.2560E-04	9.2560E-04	9.2560E-04	9.2560E-04	9.2560E-04	9.2560E-04	9.2560E-04	9.2560E-04	9.2560E-04	9.2560E-04
	0.0000	0.0000	0.0000	0.0000	0.0000	0.0000	0.0000	0.0000	0.0000	0.0000
	0.0000	0.0000	0.0000	0.0000	0.0000	0.0000	0.0000	0.0000	0.0000	0.0000
	0.0000	0.0000	0.0000	0.0000	0.0000	0.0000	0.0000	0.0000	0.0000	0.0000
	0.0000	0.0000	0.0000							
76	9.2560E-04	9.2560E-04	9.2560E-04	9.2560E-04	0.0000	0.0000	0.0000	0.0000	0.0000	0.0000
	0.0000	0.0000	0.0000	0.0000	0.0000	0.0000	0.0000	0.0000	0.0000	0.0000
	0.0000	0.0000	0.0000	0.0000	0.0000	0.0000	0.0000	0.0000	0.0000	0.0000
	0.0000	0.0000	0.0000	0.0000	0.0000	0.0000	0.0000	0.0000	0.0000	0.0000
	0.0000	0.0000	0.0000							

Table 14.--Specified leakance values for layer 1, in per second

[Zero values are shown where layer 1 is inactive. Layer 1 is inactive in rows 1-16 and 58-76 (not shown)]

	Columns									
	1	2	3	4	5	6	7	8	9	10
	11	12	13	14	15	16	17	18	19	20
	21	22	23	24	25	26	27	28	29	30
	31	32	33	34	35	36	37	38	39	40
Rows	41	42	43							
17	0.0000	0.0000	0.0000	0.0000	0.0000	0.0000	0.0000	0.0000	0.0000	0.0000
	0.0000	0.0000	0.0000	0.0000	0.0000	0.0000	0.0000	0.0000	0.0000	0.0000
	0.0000	0.0000	0.9091E-14	0.0000	0.0000	0.0000	0.0000	0.0000	0.0000	0.0000
	0.0000	0.0000	0.0000	0.0000	0.0000	0.0000	0.0000	0.0000	0.0000	0.0000
	0.0000	0.0000	0.0000							
18	0.0000	0.0000	0.0000	0.0000	0.0000	0.0000	0.0000	0.0000	0.0000	0.0000
	0.0000	0.0000	0.0000	0.0000	0.0000	0.0000	0.0000	0.0000	0.0000	0.0000
	0.0000	0.0000	0.9091E-14	0.0000	0.0000	0.0000	0.0000	0.0000	0.0000	0.0000
	0.0000	0.0000	0.0000	0.0000	0.0000	0.0000	0.0000	0.0000	0.0000	0.0000
	0.0000	0.0000	0.0000							
19	0.0000	0.0000	0.0000	0.0000	0.0000	0.0000	0.0000	0.0000	0.0000	0.0000
	0.0000	0.0000	0.0000	0.0000	0.0000	0.0000	0.0000	0.0000	0.0000	0.0000
	0.0000	0.0000	0.9091E-14	0.0000	0.0000	0.0000	0.0000	0.0000	0.0000	0.0000
	0.0000	0.0000	0.0000	0.0000	0.0000	0.0000	0.0000	0.0000	0.0000	0.0000
	0.0000	0.0000	0.0000							
20	0.0000	0.0000	0.0000	0.0000	0.0000	0.0000	0.0000	0.0000	0.0000	0.0000
	0.0000	0.0000	0.0000	0.0000	0.0000	0.0000	0.0000	0.0000	0.0000	0.0000
	0.0000	0.0000	0.9091E-14	0.0000	0.0000	0.0000	0.0000	0.0000	0.0000	0.0000
	0.0000	0.0000	0.0000	0.0000	0.0000	0.0000	0.0000	0.0000	0.0000	0.0000
	0.0000	0.0000	0.0000							

Table 14.--Specified leakance values for layer 1, in per second--Continued

	Columns									
	1	2	3	4	5	6	7	8	9	10
	11	12	13	14	15	16	17	18	19	20
	21	22	23	24	25	26	27	28	29	30
	31	32	33	34	35	36	37	38	39	40
Rows	41	42	43							
21	0.0000	0.0000	0.0000	0.0000	0.0000	0.0000	0.0000	0.0000	0.0000	0.0000
	0.0000	0.0000	0.0000	0.0000	0.0000	0.0000	0.0000	0.0000	0.0000	0.0000
	0.0000	0.0000	0.1111E-13	0.0000	0.0000	0.0000	0.0000	0.0000	0.0000	0.0000
	0.0000	0.0000	0.0000	0.0000	0.0000	0.0000	0.0000	0.0000	0.0000	0.0000
	0.0000	0.0000	0.0000							
22	0.0000	0.0000	0.0000	0.0000	0.0000	0.0000	0.0000	0.0000	0.0000	0.0000
	0.0000	0.0000	0.0000	0.0000	0.0000	0.0000	0.0000	0.0000	0.0000	0.0000
	0.0000	0.0000	0.1111E-13	0.0000	0.0000	0.0000	0.0000	0.0000	0.0000	0.0000
	0.0000	0.0000	0.0000	0.0000	0.0000	0.0000	0.0000	0.0000	0.0000	0.0000
	0.0000	0.0000	0.0000							
23	0.0000	0.0000	0.0000	0.0000	0.0000	0.0000	0.0000	0.0000	0.0000	0.0000
	0.0000	0.0000	0.0000	0.0000	0.0000	0.0000	0.0000	0.0000	0.5000E-13	0.0000
	0.0000	0.1429E-13	0.1111E-13	0.0000	0.0000	0.0000	0.0000	0.0000	0.0000	0.0000
	0.0000	0.0000	0.0000	0.0000	0.0000	0.0000	0.0000	0.0000	0.0000	0.0000
	0.0000	0.0000	0.0000							
24	0.0000	0.0000	0.0000	0.0000	0.0000	0.0000	0.0000	0.0000	0.0000	0.0000
	0.0000	0.0000	0.0000	0.0000	0.0000	0.0000	0.0000	0.0000	0.5000E-06	0.0000
	0.0000	0.2000E-13	0.1250E-13	0.0000	0.0000	0.0000	0.0000	0.0000	0.0000	0.0000
	0.0000	0.0000	0.0000	0.0000	0.0000	0.0000	0.0000	0.0000	0.0000	0.0000
	0.0000	0.0000	0.0000							

Table 14.--Specified leakance values for layer 1, in per second--Continued

Rows	Columns 1	2	3	4	5	6	7	8	9	10
	11	12	13	14	15	16	17	18	19	20
	21	22	23	24	25	26	27	28	29	30
	31	32	33	34	35	36	37	38	39	40
	41	42	43							
25	0.0000	0.0000	0.0000	0.0000	0.0000	0.0000	0.0000	0.0000	0.0000	0.0000
	0.0000	0.0000	0.0000	0.0000	0.0000	0.0000	0.0000	0.0000	0.5000E-06	0.0000
	0.0000	0.2000E-13	0.1250E-13	0.0000	0.0000	0.0000	0.0000	0.0000	0.0000	0.0000
	0.0000	0.0000	0.0000	0.0000	0.0000	0.0000	0.0000	0.0000	0.0000	0.0000
	0.0000	0.0000	0.0000							
26	0.0000	0.0000	0.0000	0.0000	0.0000	0.0000	0.0000	0.0000	0.0000	0.0000
	0.0000	0.0000	0.0000	0.0000	0.0000	0.0000	0.0000	0.0000	0.5000E-07	0.5000E-13
	0.2500E-13	0.2000E-13	0.1250E-13	0.0000	0.0000	0.0000	0.0000	0.0000	0.0000	0.0000
	0.0000	0.0000	0.0000	0.0000	0.0000	0.0000	0.0000	0.0000	0.0000	0.0000
	0.0000	0.0000	0.0000							
27	0.0000	0.0000	0.0000	0.0000	0.0000	0.0000	0.0000	0.0000	0.0000	0.0000
	0.0000	0.0000	0.0000	0.0000	0.0000	0.0000	0.0000	0.1000E-06	0.1000E-12	0.3333E-13
	0.0000	0.0000	0.0000	0.0000	0.0000	0.0000	0.0000	0.0000	0.0000	0.0000
	0.0000	0.0000	0.0000	0.0000	0.0000	0.0000	0.0000	0.0000	0.0000	0.0000
	0.0000	0.0000	0.0000							
28	0.0000	0.0000	0.0000	0.0000	0.0000	0.0000	0.0000	0.0000	0.0000	0.0000
	0.0000	0.0000	0.0000	0.0000	0.0000	0.0000	0.0000	0.5000E-06	0.1000E-12	0.5000E-13
	0.3333E-13	0.2500E-13	0.0000	0.0000	0.0000	0.0000	0.0000	0.0000	0.0000	0.0000
	0.0000	0.0000	0.0000	0.0000	0.0000	0.0000	0.0000	0.0000	0.0000	0.0000
	0.0000	0.0000	0.0000							

Table 14.--Specified leakance values for layer 1, in per second--Continued

Rows	Columns 1	2	3	4	5	6	7	8	9	10
	11	12	13	14	15	16	17	18	19	20
	21	22	23	24	25	26	27	28	29	30
	31	32	33	34	35	36	37	38	39	40
	41	42	43							
29	0.0000	0.0000	0.0000	0.0000	0.0000	0.0000	0.0000	0.0000	0.0000	0.0000
	0.0000	0.0000	0.0000	0.0000	0.0000	0.0000	0.0000	0.5000E-06	0.5000E-06	0.1000E-12
	0.7692E-13	0.5000E-13	0.0000	0.0000	0.0000	0.0000	0.0000	0.0000	0.0000	0.0000
	0.0000	0.0000	0.0000	0.0000	0.0000	0.0000	0.0000	0.0000	0.0000	0.0000
	0.0000	0.0000	0.0000							
30	0.0000	0.0000	0.0000	0.0000	0.0000	0.0000	0.0000	0.0000	0.0000	0.0000
	0.0000	0.0000	0.0000	0.0000	0.0000	0.0000	0.0000	0.0000	0.5000E-07	0.5263E-13
	0.3333E-13	0.2500E-13	0.0000	0.0000	0.0000	0.0000	0.0000	0.0000	0.0000	0.0000
	0.0000	0.0000	0.0000	0.0000	0.0000	0.0000	0.0000	0.0000	0.0000	0.0000
	0.0000	0.0000	0.0000							
31	0.0000	0.0000	0.0000	0.0000	0.0000	0.0000	0.0000	0.0000	0.0000	0.0000
	0.0000	0.0000	0.0000	0.0000	0.0000	0.0000	0.0000	0.0000	0.5000E-06	0.8333E-08
	0.5000E-13	0.2500E-13	0.0000	0.0000	0.0000	0.0000	0.0000	0.0000	0.0000	0.0000
	0.0000	0.0000	0.0000	0.0000	0.0000	0.0000	0.0000	0.0000	0.0000	0.0000
	0.0000	0.0000	0.0000							
32	0.0000	0.0000	0.0000	0.0000	0.0000	0.0000	0.0000	0.0000	0.0000	0.0000
	0.0000	0.0000	0.0000	0.0000	0.0000	0.0000	0.0000	0.0000	0.1000E-06	0.7143E-08
	0.4348E-13	0.2500E-13	0.0000	0.0000	0.0000	0.0000	0.0000	0.0000	0.0000	0.0000
	0.0000	0.0000	0.0000	0.0000	0.0000	0.0000	0.0000	0.0000	0.0000	0.0000
	0.0000	0.0000	0.0000							

Table 14.--Specified leakance values for layer 1, in per second--Continued

	Columns									
	1	2	3	4	5	6	7	8	9	10
	11	12	13	14	15	16	17	18	19	20
	21	22	23	24	25	26	27	28	29	30
	31	32	33	34	35	36	37	38	39	40
Rows	41	42	43							
33	0.0000	0.0000	0.0000	0.0000	0.0000	0.0000	0.0000	0.0000	0.0000	0.0000
	0.0000	0.0000	0.0000	0.0000	0.0000	0.0000	0.5263E-08	0.5556E-08	0.6250E-08	0.5000E-13
	0.3333E-13	0.2500E-13	0.1667E-13	0.1250E-13	0.0000	0.0000	0.0000	0.0000	0.0000	0.0000
	0.0000	0.0000	0.0000	0.0000	0.0000	0.0000	0.0000	0.0000	0.0000	0.0000
	0.0000	0.0000	0.0000							
34	0.0000	0.0000	0.0000	0.0000	0.0000	0.0000	0.0000	0.0000	0.0000	0.0000
	0.0000	0.0000	0.0000	0.0000	0.0000	0.2439E-08	0.4762E-08	0.5000E-08	0.3333E-13	0.2000E-13
	0.1429E-13	0.1429E-13	0.1250E-13	0.1176E-13	0.0000	0.0000	0.0000	0.0000	0.0000	0.0000
	0.0000	0.0000	0.0000	0.0000	0.0000	0.0000	0.0000	0.0000	0.0000	0.0000
	0.0000	0.0000	0.0000							
35	0.0000	0.0000	0.0000	0.0000	0.0000	0.0000	0.0000	0.0000	0.0000	0.0000
	0.0000	0.0000	0.0000	0.0000	0.0000	0.4545E-08	0.4348E-08	0.3333E-13	0.0000	0.1250E-13
	0.1205E-13	0.1176E-13	0.1176E-13	0.1111E-13	0.0000	0.0000	0.0000	0.0000	0.0000	0.0000
	0.0000	0.0000	0.0000	0.0000	0.0000	0.0000	0.0000	0.0000	0.0000	0.0000
	0.0000	0.0000	0.0000							
36	0.0000	0.0000	0.0000	0.0000	0.0000	0.0000	0.0000	0.0000	0.0000	0.0000
	0.0000	0.0000	0.0000	0.0000	0.3788E-08	0.4167E-08	0.3333E-13	0.0000	0.0000	0.1053E-13
	0.1111E-13	0.1111E-13	0.1111E-13	0.1053E-13	0.0000	0.0000	0.0000	0.0000	0.0000	0.0000
	0.0000	0.0000	0.0000	0.0000	0.0000	0.0000	0.0000	0.0000	0.0000	0.0000
	0.0000	0.0000	0.0000							

Table 14.--Specified leakance values for layer 1, in per second--Continued

Rows	Columns 1	2	3	4	5	6	7	8	9	10
	11	12	13	14	15	16	17	18	19	20
	21	22	23	24	25	26	27	28	29	30
	31	32	33	34	35	36	37	38	39	40
	41	42	43							
37	0.0000	0.0000	0.0000	0.0000	0.0000	0.0000	0.0000	0.0000	0.0000	0.0000
	0.0000	0.0000	0.0000	0.0000	0.4000E-08	0.4000E-08	0.0000	0.0000	0.0000	0.0000
	0.1000E-13	0.1020E-13	0.1020E-13	0.9804E-14	0.0000	0.0000	0.0000	0.0000	0.0000	0.0000
	0.0000	0.0000	0.0000	0.0000	0.0000	0.0000	0.0000	0.0000	0.0000	0.0000
	0.0000	0.0000	0.0000							
38	0.0000	0.0000	0.0000	0.0000	0.0000	0.0000	0.0000	0.0000	0.0000	0.0000
	0.0000	0.0000	0.0000	0.3704E-08	0.3704E-08	0.3333E-13	0.0000	0.0000	0.0000	0.0000
	0.0000	0.9434E-14	0.9434E-14	0.9091E-14	0.0000	0.0000	0.0000	0.0000	0.0000	0.0000
	0.0000	0.0000	0.0000	0.0000	0.0000	0.0000	0.0000	0.0000	0.0000	0.0000
	0.0000	0.0000	0.0000							
39	0.0000	0.0000	0.0000	0.0000	0.0000	0.0000	0.0000	0.0000	0.0000	0.0000
	0.0000	0.0000	0.0000	0.3571E-08	0.3571E-08	0.3333E-13	0.0000	0.0000	0.0000	0.0000
	0.0000	0.0000	0.8621E-14	0.8547E-14	0.0000	0.0000	0.0000	0.0000	0.0000	0.0000
	0.0000	0.0000	0.0000	0.0000	0.0000	0.0000	0.0000	0.0000	0.0000	0.0000
	0.0000	0.0000	0.0000							
40	0.0000	0.0000	0.0000	0.0000	0.0000	0.0000	0.0000	0.0000	0.0000	0.0000
	0.0000	0.0000	0.0000	0.3333E-08	0.3333E-08	0.1000E-12	0.0000	0.0000	0.0000	0.0000
	0.0000	0.0000	0.0000	0.0000	0.0000	0.0000	0.0000	0.0000	0.0000	0.0000
	0.0000	0.0000	0.0000	0.0000	0.0000	0.0000	0.0000	0.0000	0.0000	0.0000
	0.0000	0.0000	0.0000							

Table 14.--Specified leakance values for layer 1, in per second--Continued

Rows	Columns 1	2	3	4	5	6	7	8	9	10
	11	12	13	14	15	16	17	18	19	20
	21	22	23	24	25	26	27	28	29	30
	31	32	33	34	35	36	37	38	39	40
	41	42	43							
41	0.0000	0.0000	0.0000	0.0000	0.0000	0.0000	0.0000	0.0000	0.0000	0.0000
	0.0000	0.0000	0.0000	0.3226E-08	0.3226E-08	0.6667E-13	0.3333E-13	0.0000	0.0000	0.0000
	0.0000	0.0000	0.0000	0.0000	0.0000	0.0000	0.0000	0.0000	0.0000	0.0000
	0.0000	0.0000	0.0000	0.0000	0.0000	0.0000	0.0000	0.0000	0.0000	0.0000
	0.0000	0.0000	0.0000							
42	0.0000	0.0000	0.0000	0.0000	0.0000	0.0000	0.0000	0.0000	0.0000	0.0000
	0.5000E-06	0.5000E-06	0.5000E-06	0.3333E-08	0.1000E-12	0.4000E-13	0.2857E-13	0.1818E-13	0.1429E-13	0.0000
	0.0000	0.0000	0.0000	0.0000	0.0000	0.0000	0.0000	0.0000	0.0000	0.0000
	0.0000	0.0000	0.0000	0.0000	0.0000	0.0000	0.0000	0.0000	0.0000	0.0000
	0.0000	0.0000	0.0000							
43	0.0000	0.0000	0.0000	0.0000	0.0000	0.0000	0.0000	0.0000	0.0000	0.0000
	0.2857E-13	0.2083E-13	0.1818E-13	0.1429E-13	0.1250E-13	0.1111E-13	0.9524E-14	0.8000E-14	0.6667E-14	0.6250E-14
	0.0000	0.0000	0.0000	0.0000	0.0000	0.0000	0.0000	0.0000	0.0000	0.0000
	0.0000	0.0000	0.0000	0.0000	0.0000	0.0000	0.0000	0.0000	0.0000	0.0000
	0.0000	0.0000	0.0000							
44	0.0000	0.0000	0.0000	0.0000	0.0000	0.0000	0.0000	0.5000E-06	0.5000E-06	0.5000E-13
	0.2857E-13	0.2083E-13	0.1786E-13	0.1429E-13	0.1250E-13	0.1111E-13	0.9091E-14	0.7692E-14	0.6452E-14	0.6250E-14
	0.0000	0.0000	0.0000	0.0000	0.0000	0.0000	0.0000	0.0000	0.0000	0.0000
	0.0000	0.0000	0.0000	0.0000	0.0000	0.0000	0.0000	0.0000	0.0000	0.0000
	0.0000	0.0000	0.0000							

Table 14.--Specified leakance values for layer 1, in per second--Continued

	Columns									
	1	2	3	4	5	6	7	8	9	10
	11	12	13	14	15	16	17	18	19	20
	21	22	23	24	25	26	27	28	29	30
	31	32	33	34	35	36	37	38	39	40
Rows	41	42	43							
45	0.0000	0.0000	0.0000	0.0000	0.0000	0.0000	0.0000	0.5000E-06	0.5000E-13	0.3846E-13
	0.2632E-13	0.2000E-13	0.1667E-13	0.1389E-13	0.1205E-13	0.1053E-13	0.8696E-14	0.7143E-14	0.6250E-14	0.6250E-14
	0.0000	0.0000	0.0000	0.0000	0.0000	0.0000	0.0000	0.0000	0.0000	0.0000
	0.0000	0.0000	0.0000	0.0000	0.0000	0.0000	0.0000	0.0000	0.0000	0.0000
	0.0000	0.0000	0.0000							
46	0.0000	0.0000	0.0000	0.0000	0.0000	0.0000	0.5000E-06	0.2500E-07	0.4545E-13	0.3125E-13
	0.2326E-13	0.1923E-13	0.1538E-13	0.1282E-13	0.1163E-13	0.1000E-13	0.8000E-14	0.6667E-14	0.6250E-14	0.0000
	0.0000	0.0000	0.0000	0.0000	0.0000	0.0000	0.0000	0.0000	0.0000	0.0000
	0.0000	0.0000	0.0000	0.0000	0.0000	0.0000	0.0000	0.0000	0.0000	0.0000
	0.0000	0.0000	0.0000							
47	0.0000	0.0000	0.0000	0.0000	0.0000	0.0000	0.0000	0.5000E-13	0.3571E-13	0.2632E-13
	0.2000E-13	0.1667E-13	0.1429E-13	0.1250E-13	0.1111E-13	0.9091E-14	0.7143E-14	0.6250E-14	0.0000	0.0000
	0.0000	0.0000	0.0000	0.0000	0.0000	0.0000	0.0000	0.0000	0.0000	0.0000
	0.0000	0.0000	0.0000	0.0000	0.0000	0.0000	0.0000	0.0000	0.0000	0.0000
	0.0000	0.0000	0.0000							
48	0.0000	0.0000	0.0000	0.0000	0.0000	0.0000	0.0000	0.5000E-13	0.2857E-13	0.2128E-13
	0.1786E-13	0.1429E-13	0.1250E-13	0.1111E-13	0.1000E-13	0.8333E-14	0.6667E-14	0.0000	0.0000	0.0000
	0.0000	0.0000	0.0000	0.0000	0.0000	0.0000	0.0000	0.0000	0.0000	0.0000
	0.0000	0.0000	0.0000	0.0000	0.0000	0.0000	0.0000	0.0000	0.0000	0.0000
	0.0000	0.0000	0.0000							

Table 14.--Specified leakance values for layer 1, in per second--Continued

	Columns									
	1	2	3	4	5	6	7	8	9	10
	11	12	13	14	15	16	17	18	19	20
	21	22	23	24	25	26	27	28	29	30
	31	32	33	34	35	36	37	38	39	40
Rows	41	42	43							
49	0.0000	0.5000E-07	0.5000E-07	0.0000	0.0000	0.1000E-12	0.3333E-13	0.2500E-13	0.2000E-13	0.1538E-13
	0.1250E-13	0.1176E-13	0.1111E-13	0.1053E-13	0.8333E-14	0.7143E-14	0.6250E-14	0.0000	0.0000	0.0000
	0.0000	0.0000	0.0000	0.0000	0.0000	0.0000	0.0000	0.0000	0.0000	0.0000
	0.0000	0.0000	0.0000	0.0000	0.0000	0.0000	0.0000	0.0000	0.0000	0.0000
	0.0000	0.0000	0.0000							
50	0.0000	0.5000E-07	0.5000E-07	0.5000E-13	0.5000E-13	0.2857E-13	0.2500E-13	0.1538E-13	0.1250E-13	0.1176E-13
	0.1111E-13	0.8333E-14	0.6250E-14	0.6250E-14	0.6250E-14	0.6250E-14	0.6250E-14	0.6250E-14	0.0000	0.0000
	0.0000	0.0000	0.0000	0.0000	0.0000	0.0000	0.0000	0.0000	0.0000	0.0000
	0.0000	0.0000	0.0000	0.0000	0.0000	0.0000	0.0000	0.0000	0.0000	0.0000
	0.0000	0.0000	0.0000							
51	0.5000E-07	0.5000E-07	0.5000E-07	0.1667E-13	0.2000E-13	0.1667E-13	0.1250E-13	0.1111E-13	0.1000E-13	0.0000
	0.0000	0.0000	0.0000	0.0000	0.0000	0.0000	0.6250E-14	0.6250E-14	0.0000	0.0000
	0.0000	0.0000	0.0000	0.0000	0.0000	0.0000	0.0000	0.0000	0.0000	0.0000
	0.0000	0.0000	0.0000	0.0000	0.0000	0.0000	0.0000	0.0000	0.0000	0.0000
	0.0000	0.0000	0.0000							
52	0.7692E-14	0.1111E-13	0.2500E-13	0.1111E-13	0.1250E-13	0.1000E-13	0.6667E-14	0.0000	0.0000	0.0000
	0.0000	0.0000	0.0000	0.0000	0.0000	0.0000	0.6250E-14	0.0000	0.0000	0.0000
	0.0000	0.0000	0.0000	0.0000	0.0000	0.0000	0.0000	0.0000	0.0000	0.0000
	0.0000	0.0000	0.0000	0.0000	0.0000	0.0000	0.0000	0.0000	0.0000	0.0000
	0.0000	0.0000	0.0000							

Table 14.--Specified leakance values for layer 1, in per second--Continued

Rows	Columns 1	2	3	4	5	6	7	8	9	10
	11	12	13	14	15	16	17	18	19	20
	21	22	23	24	25	26	27	28	29	30
	31	32	33	34	35	36	37	38	39	40
	41	42	43							
53	0.7692E-14	0.9091E-14	0.1111E-13	0.7692E-14	0.7143E-14	0.6667E-14	0.0000	0.0000	0.0000	0.0000
	0.0000	0.0000	0.0000	0.0000	0.0000	0.0000	0.0000	0.0000	0.0000	0.0000
	0.0000	0.0000	0.0000	0.0000	0.0000	0.0000	0.0000	0.0000	0.0000	0.0000
	0.0000	0.0000	0.0000	0.0000	0.0000	0.0000	0.0000	0.0000	0.0000	0.0000
	0.0000	0.0000	0.0000							
54	0.6667E-14	0.7143E-14	0.8333E-14	0.6667E-14	0.0000	0.0000	0.0000	0.0000	0.0000	0.0000
	0.0000	0.0000	0.0000	0.0000	0.0000	0.0000	0.0000	0.0000	0.0000	0.0000
	0.0000	0.0000	0.0000	0.0000	0.0000	0.0000	0.0000	0.0000	0.0000	0.0000
	0.0000	0.0000	0.0000	0.0000	0.0000	0.0000	0.0000	0.0000	0.0000	0.0000
	0.0000	0.0000	0.0000							
55	0.6250E-14	0.6250E-14	0.5882E-14	0.0000	0.0000	0.0000	0.0000	0.0000	0.0000	0.0000
	0.0000	0.0000	0.0000	0.0000	0.0000	0.0000	0.0000	0.0000	0.0000	0.0000
	0.0000	0.0000	0.0000	0.0000	0.0000	0.0000	0.0000	0.0000	0.0000	0.0000
	0.0000	0.0000	0.0000	0.0000	0.0000	0.0000	0.0000	0.0000	0.0000	0.0000
	0.0000	0.0000	0.0000							

Table 14.--Specified leakance values for layer 1, in per second--Concluded

	Columns									
	1	2	3	4	5	6	7	8	9	10
	11	12	13	14	15	16	17	18	19	20
	21	22	23	24	25	26	27	28	29	30
	31	32	33	34	35	36	37	38	39	40
Rows	41	42	43							
56	0.6250E-14	0.0000	0.0000	0.0000	0.0000	0.0000	0.0000	0.0000	0.0000	0.0000
	0.0000	0.0000	0.0000	0.0000	0.0000	0.0000	0.0000	0.0000	0.0000	0.0000
	0.0000	0.0000	0.0000	0.0000	0.0000	0.0000	0.0000	0.0000	0.0000	0.0000
	0.0000	0.0000	0.0000	0.0000	0.0000	0.0000	0.0000	0.0000	0.0000	0.0000
	0.0000	0.0000	0.0000							
57	0.6250E-14	0.0000	0.0000	0.0000	0.0000	0.0000	0.0000	0.0000	0.0000	0.0000
	0.0000	0.0000	0.0000	0.0000	0.0000	0.0000	0.0000	0.0000	0.0000	0.0000
	0.0000	0.0000	0.0000	0.0000	0.0000	0.0000	0.0000	0.0000	0.0000	0.0000
	0.0000	0.0000	0.0000	0.0000	0.0000	0.0000	0.0000	0.0000	0.0000	0.0000
	0.0000	0.0000	0.0000							

Table 15.--Estimated thickness of Chinle confining bed between the San Andres-Glorieta aquifer and the valley-fill aquifer, in feet

[Zero values are shown where layer 1 is inactive.
Layer 1 is inactive in rows 1-16 and 58-76 (not shown)]

	Column											
	1	2	3	4	5	6	7	8	9	10	11	12
	13	14	15	16	17	18	19	20	21	22	23	24
	25	26	27	28	29	30	31	32	33	34	35	36
Row	37	38	39	40	41	42	43					
17	0	0	0	0	0	0	0	0	0	0	0	0
	0	0	0	0	0	0	0	0	0	0	1,100	0
	0	0	0	0	0	0	0	0	0	0	0	0
	0	0	0	0	0	0	0					
18	0	0	0	0	0	0	0	0	0	0	0	0
	0	0	0	0	0	0	0	0	0	0	1,100	0
	0	0	0	0	0	0	0	0	0	0	0	0
	0	0	0	0	0	0	0					
19	0	0	0	0	0	0	0	0	0	0	0	0
	0	0	0	0	0	0	0	0	0	0	1,100	0
	0	0	0	0	0	0	0	0	0	0	0	0
	0	0	0	0	0	0	0					
20	0	0	0	0	0	0	0	0	0	0	0	0
	0	0	0	0	0	0	0	0	0	0	1,100	0
	0	0	0	0	0	0	0	0	0	0	0	0
	0	0	0	0	0	0	0					
21	0	0	0	0	0	0	0	0	0	0	0	0
	0	0	0	0	0	0	0	0	0	0	900	0
	0	0	0	0	0	0	0	0	0	0	0	0
	0	0	0	0	0	0	0					
22	0	0	0	0	0	0	0	0	0	0	0	0
	0	0	0	0	0	0	0	0	0	0	900	0
	0	0	0	0	0	0	0	0	0	0	0	0
	0	0	0	0	0	0	0					
23	0	0	0	0	0	0	0	0	0	0	0	0
	0	0	0	0	0	0	200	0	0	700	900	0
	0	0	0	0	0	0	0	0	0	0	0	0
	0	0	0	0	0	0	0					
24	0	0	0	0	0	0	0	0	0	0	0	0
	0	0	0	0	0	0	0	0	0	500	800	0
	0	0	0	0	0	0	0	0	0	0	0	0
	0	0	0	0	0	0	0					

Table 15.--Estimated thickness of Chinle confining bed between the San Andres-Glorieta aquifer and the valley-fill aquifer, in feet--Continued

Row	Column 1	2	3	4	5	6	7	8	9	10	11	12
	13	14	15	16	17	18	19	20	21	22	23	24
	25	26	27	28	29	30	31	32	33	34	35	36
	37	38	39	40	41	42	43					
25	0	0	0	0	0	0	0	0	0	0	0	0
	0	0	0	0	0	0	0	0	0	500	800	0
	0	0	0	0	0	0	0	0	0	0	0	0
	0	0	0	0	0	0	0					
26	0	0	0	0	0	0	0	0	0	0	0	0
	0	0	0	0	0	0	0	200	400	500	800	0
	0	0	0	0	0	0	0	0	0	0	0	0
	0	0	0	0	0	0	0					
27	0	0	0	0	0	0	0	0	0	0	0	0
	0	0	0	0	0	0	100	300	0	0	0	0
	0	0	0	0	0	0	0	0	0	0	0	0
	0	0	0	0	0	0	0					
28	0	0	0	0	0	0	0	0	0	0	0	0
	0	0	0	0	0	0	100	200	300	400	0	0
	0	0	0	0	0	0	0	0	0	0	0	0
	0	0	0	0	0	0	0					
29	0	0	0	0	0	0	0	0	0	0	0	0
	0	0	0	0	0	0	0	100	130	200	0	0
	0	0	0	0	0	0	0	0	0	0	0	0
	0	0	0	0	0	0	0					
30	0	0	0	0	0	0	0	0	0	0	0	0
	0	0	0	0	0	0	0	190	300	400	0	0
	0	0	0	0	0	0	0	0	0	0	0	0
	0	0	0	0	0	0	0					
31	0	0	0	0	0	0	0	0	0	0	0	0
	0	0	0	0	0	0	0	0	200	400	0	0
	0	0	0	0	0	0	0	0	0	0	0	0
	0	0	0	0	0	0	0					
32	0	0	0	0	0	0	0	0	0	0	0	0
	0	0	0	0	0	0	0	0	230	400	0	0
	0	0	0	0	0	0	0	0	0	0	0	0
	0	0	0	0	0	0	0					

Table 15.--Estimated thickness of Chinle confining bed between the San Andres-Glorieta aquifer and the valley-fill aquifer, in feet--Continued

Row	Column 1	2	3	4	5	6	7	8	9	10	11	12
	13	14	15	16	17	18	19	20	21	22	23	24
	25	26	27	28	29	30	31	32	33	34	35	36
	37	38	39	40	41	42	43					
33	0	0	0	0	0	0	0	0	0	0	0	0
	0	0	0	0	0	0	0	200	300	400	600	800
	0	0	0	0	0	0	0	0	0	0	0	0
	0	0	0	0	0	0	0					
34	0	0	0	0	0	0	0	0	0	0	0	0
	0	0	0	0	0	0	300	500	700	700	800	850
	0	0	0	0	0	0	0	0	0	0	0	0
	0	0	0	0	0	0	0					
35	0	0	0	0	0	0	0	0	0	0	0	0
	0	0	0	0	0	300	0	800	830	850	850	900
	0	0	0	0	0	0	0	0	0	0	0	0
	0	0	0	0	0	0	0					
36	0	0	0	0	0	0	0	0	0	0	0	0
	0	0	0	0	300	0	0	950	900	900	900	950
	0	0	0	0	0	0	0	0	0	0	0	0
	0	0	0	0	0	0	0					
37	0	0	0	0	0	0	0	0	0	0	0	0
	0	0	0	0	0	0	0	0	1,000	980	980	1,020
	0	0	0	0	0	0	0	0	0	0	0	0
	0	0	0	0	0	0	0					
38	0	0	0	0	0	0	0	0	0	0	0	0
	0	0	0	300	0	0	0	0	0	1,060	1,060	1,100
	0	0	0	0	0	0	0	0	0	0	0	0
	0	0	0	0	0	0	0					
39	0	0	0	0	0	0	0	0	0	0	0	0
	0	0	0	300	0	0	0	0	0	0	1,160	1,170
	0	0	0	0	0	0	0	0	0	0	0	0
	0	0	0	0	0	0	0					
40	0	0	0	0	0	0	0	0	0	0	0	0
	0	0	0	100	0	0	0	0	0	0	0	0
	0	0	0	0	0	0	0	0	0	0	0	0
	0	0	0	0	0	0	0					

Table 15.--Estimated thickness of Chinle confining bed between the San Andres-Glorieta aquifer and the valley-fill aquifer, in feet--Continued

Row	Column 1	2	3	4	5	6	7	8	9	10	11	12
	13	14	15	16	17	18	19	20	21	22	23	24
	25	26	27	28	29	30	31	32	33	34	35	36
	37	38	39	40	41	42	43					
41	0	0	0	0	0	0	0	0	0	0	0	0
	0	0	0	150	300	0	0	0	0	0	0	0
	0	0	0	0	0	0	0	0	0	0	0	0
	0	0	0	0	0	0	0					
42	0	0	0	0	0	0	0	0	0	0	0	0
	0	0	100	250	350	550	700	0	0	0	0	0
	0	0	0	0	0	0	0	0	0	0	0	0
	0	0	0	0	0	0	0					
43	0	0	0	0	0	0	0	0	0	0	350	480
	550	700	800	900	1,050	1,250	1,500	1,600	0	0	0	0
	0	0	0	0	0	0	0	0	0	0	0	0
	0	0	0	0	0	0	0					
44	0	0	0	0	0	0	0	0	0	200	350	480
	560	700	800	900	1,100	1,300	1,550	1,600	0	0	0	0
	0	0	0	0	0	0	0	0	0	0	0	0
	0	0	0	0	0	0	0					
45	0	0	0	0	0	0	0	0	200	260	380	500
	600	720	830	950	1,150	1,400	1,600	1,600	0	0	0	0
	0	0	0	0	0	0	0	0	0	0	0	0
	0	0	0	0	0	0	0					
46	0	0	0	0	0	0	0	0	220	320	430	520
	650	780	860	1,000	1,250	1,500	1,600	0	0	0	0	0
	0	0	0	0	0	0	0	0	0	0	0	0
	0	0	0	0	0	0	0					
47	0	0	0	0	0	0	0	200	280	380	500	600
	700	800	900	1,100	1,400	1,600	0	0	0	0	0	0
	0	0	0	0	0	0	0	0	0	0	0	0
	0	0	0	0	0	0	0					
48	0	0	0	0	0	0	0	200	350	470	560	700
	800	900	1,000	1,200	1,500	0	0	0	0	0	0	0
	0	0	0	0	0	0	0	0	0	0	0	0
	0	0	0	0	0	0	0					

Table 15.--Estimated thickness of Chinle confining bed between the San Andres-Glorieta aquifer and the valley-fill aquifer, in feet--Concluded

Row	Column 1	2	3	4	5	6	7	8	9	10	11	12
	13	14	15	16	17	18	19	20	21	22	23	24
	25	26	27	28	29	30	31	32	33	34	35	36
	37	38	39	40	41	42	43					
49	0	0	0	0	0	100	300	400	500	650	800	850
	900	950	1,200	1,400	1,600	0	0	0	0	0	0	0
	0	0	0	0	0	0	0	0	0	0	0	0
	0	0	0	0	0	0	0					
50	0	0	0	200	200	350	400	650	800	850	900	1,200
	1,600	1,600	1,600	1,600	1,600	1,600	0	0	0	0	0	0
	0	0	0	0	0	0	0	0	0	0	0	0
	0	0	0	0	0	0	0					
51	0	0	0	600	500	600	800	900	1,000	0	0	0
	0	0	0	0	1,600	1,600	0	0	0	0	0	0
	0	0	0	0	0	0	0	0	0	0	0	0
	0	0	0	0	0	0	0					
52	1,300	900	400	900	800	1,000	1,500	0	0	0	0	0
	0	0	0	0	1,600	0	0	0	0	0	0	0
	0	0	0	0	0	0	0	0	0	0	0	0
	0	0	0	0	0	0	0					
53	1,300	1,100	900	1,300	1,400	1,500	0	0	0	0	0	0
	0	0	0	0	0	0	0	0	0	0	0	0
	0	0	0	0	0	0	0	0	0	0	0	0
	0	0	0	0	0	0	0					
54	1,500	1,400	1,200	1,500	0	0	0	0	0	0	0	0
	0	0	0	0	0	0	0	0	0	0	0	0
	0	0	0	0	0	0	0	0	0	0	0	0
	0	0	0	0	0	0	0					
55	1,600	1,600	1,700	0	0	0	0	0	0	0	0	0
	0	0	0	0	0	0	0	0	0	0	0	0
	0	0	0	0	0	0	0	0	0	0	0	0
	0	0	0	0	0	0	0					
56	1,600	0	0	0	0	0	0	0	0	0	0	0
	0	0	0	0	0	0	0	0	0	0	0	0
	0	0	0	0	0	0	0	0	0	0	0	0
	0	0	0	0	0	0	0					
57	1,600	0	0	0	0	0	0	0	0	0	0	0
	0	0	0	0	0	0	0	0	0	0	0	0
	0	0	0	0	0	0	0	0	0	0	0	0
	0	0	0	0	0	0	0					

Table 16.--Specified recharge for the barren basalt area of the valley-fill aquifer, represented by layer 1, in cubic feet per second

[Locations are shown in figure 25. Recharge is the same for all scenarios]

Stress period															
1	2	3	4	5	6	7	8	9	10	11	12	13	14	15	16
17	18	19	20	21	22	23	24	25	26	27	28	29	30	31	32
33	34	35	36	37	38	39	40	41	42	43	44	45	46	47	48
49	50	51	52	53	54	55	56	57	58	59	60	61	62	63	64
65	66	67	68	69	70	71	72	73	74	75	76				

Row 55, column 1

0.843	0.843	0.940	0.823	0.997	0.000	1.867	0.000	1.171	0.000	1.901	0.000	1.884	0.000	2.088	0.000
1.426	0.000	0.747	0.000	0.832	0.000	1.545	0.000	0.703	0.370	1.570	0.221	1.227	0.373	0.470	0.397
0.990	0.805	0.912	0.433	1.081	0.862	0.686	0.918	1.066	0.592	0.815	0.594	1.119	0.582	0.781	1.372
0.912	0.998	0.668	1.053	0.668	0.904	1.244	0.671	0.833	0.792	0.662	0.757	0.716	1.058	0.939	0.996
0.910	1.142	0.706	1.059	0.857	1.086	0.843	0.843	0.843	0.843	0.843	0.843				

Row 56, column 1

0.843	0.843	0.940	0.823	0.997	0.000	1.867	0.000	1.171	0.000	1.901	0.000	1.884	0.000	2.088	0.000
1.426	0.000	0.747	0.000	0.832	0.000	1.545	0.000	0.703	0.370	1.570	0.221	1.227	0.373	0.470	0.397
0.990	0.805	0.912	0.433	1.081	0.862	0.686	0.918	1.066	0.592	0.815	0.594	1.119	0.582	0.781	1.372
0.912	0.998	0.668	1.053	0.668	0.904	1.244	0.671	0.833	0.792	0.662	0.757	0.716	1.058	0.939	0.996
0.910	1.142	0.706	1.059	0.857	1.086	0.843	0.843	0.843	0.843	0.843	0.843				

Row 53, column 2

0.549	0.549	0.612	0.536	0.649	0.000	1.216	0.000	0.762	0.000	1.238	0.000	1.227	0.000	1.359	0.000
0.928	0.000	0.486	0.000	0.541	0.000	1.006	0.000	0.457	0.241	1.022	0.144	0.799	0.243	0.306	0.259
0.644	0.524	0.593	0.282	0.704	0.561	0.446	0.598	0.694	0.386	0.530	0.387	0.728	0.379	0.508	0.893
0.593	0.650	0.435	0.686	0.435	0.588	0.810	0.436	0.543	0.515	0.431	0.493	0.466	0.688	0.611	0.648
0.592	0.744	0.460	0.690	0.558	0.707	0.549	0.549	0.549	0.549	0.549	0.549				

Table 16.--Specified recharge for the barren basalt area of the valley-fill aquifer, represented by layer 1, in cubic feet per second--Continued

Stress period															
1	2	3	4	5	6	7	8	9	10	11	12	13	14	15	16
17	18	19	20	21	22	23	24	25	26	27	28	29	30	31	32
33	34	35	36	37	38	39	40	41	42	43	44	45	46	47	48
49	50	51	52	53	54	55	56	57	58	59	60	61	62	63	64
65	66	67	68	69	70	71	72	73	74	75	76				
Row 54, column 2															
0.549	0.549	0.612	0.536	0.649	0.000	1.216	0.000	0.762	0.000	1.238	0.000	1.227	0.000	1.359	0.000
0.928	0.000	0.486	0.000	0.541	0.000	1.006	0.000	0.457	0.241	1.022	0.144	0.799	0.243	0.306	0.259
0.644	0.524	0.593	0.282	0.704	0.561	0.446	0.598	0.694	0.386	0.530	0.387	0.728	0.379	0.508	0.893
0.593	0.650	0.435	0.686	0.435	0.588	0.810	0.436	0.543	0.515	0.431	0.493	0.466	0.688	0.611	0.648
0.592	0.744	0.460	0.690	0.558	0.707	0.549	0.549	0.549	0.549	0.549	0.549				
Row 55, column 2															
0.549	0.549	0.612	0.536	0.649	0.000	1.216	0.000	0.762	0.000	1.238	0.000	1.227	0.000	1.359	0.000
0.928	0.000	0.486	0.000	0.541	0.000	1.006	0.000	0.457	0.241	1.022	0.144	0.799	0.243	0.306	0.259
0.644	0.524	0.593	0.282	0.704	0.561	0.446	0.598	0.694	0.386	0.530	0.387	0.728	0.379	0.508	0.893
0.593	0.650	0.435	0.686	0.435	0.588	0.810	0.436	0.543	0.515	0.431	0.493	0.466	0.688	0.611	0.648
0.592	0.744	0.460	0.690	0.558	0.707	0.549	0.549	0.549	0.549	0.549	0.549				
Row 52, column 3															
0.438	0.438	0.489	0.428	0.518	0.000	0.971	0.000	0.609	0.000	0.988	0.000	0.980	0.000	1.085	0.000
0.741	0.000	0.388	0.000	0.432	0.000	0.803	0.000	0.365	0.192	0.816	0.115	0.638	0.194	0.244	0.207
0.514	0.418	0.474	0.225	0.562	0.448	0.357	0.477	0.554	0.308	0.424	0.309	0.582	0.303	0.406	0.714
0.474	0.519	0.347	0.548	0.347	0.470	0.647	0.349	0.433	0.412	0.344	0.394	0.372	0.550	0.488	0.518
0.473	0.594	0.367	0.551	0.446	0.565	0.438	0.438	0.438	0.438	0.438	0.438				

Table 16.--Specified recharge for the barren basalt area of the valley-fill aquifer, represented by layer 1, in cubic feet per second--Continued

Stress period															
1	2	3	4	5	6	7	8	9	10	11	12	13	14	15	16
17	18	19	20	21	22	23	24	25	26	27	28	29	30	31	32
33	34	35	36	37	38	39	40	41	42	43	44	45	46	47	48
49	50	51	52	53	54	55	56	57	58	59	60	61	62	63	64
65	66	67	68	69	70	71	72	73	74	75	76				
Row 53, column 3															
0.438	0.438	0.489	0.428	0.518	0.000	0.971	0.000	0.609	0.000	0.988	0.000	0.980	0.000	1.085	0.000
0.741	0.000	0.388	0.000	0.432	0.000	0.803	0.000	0.365	0.192	0.816	0.115	0.638	0.194	0.244	0.207
0.514	0.418	0.474	0.225	0.562	0.448	0.357	0.477	0.554	0.308	0.424	0.309	0.582	0.303	0.406	0.714
0.474	0.519	0.347	0.548	0.347	0.470	0.647	0.349	0.433	0.412	0.344	0.394	0.372	0.550	0.488	0.518
0.473	0.594	0.367	0.551	0.446	0.565	0.438	0.438	0.438	0.438	0.438	0.438				
Row 54, column 3															
0.438	0.438	0.489	0.428	0.518	0.000	0.971	0.000	0.609	0.000	0.988	0.000	0.980	0.000	1.085	0.000
0.741	0.000	0.388	0.000	0.432	0.000	0.803	0.000	0.365	0.192	0.816	0.115	0.638	0.194	0.244	0.207
0.514	0.418	0.474	0.225	0.562	0.448	0.357	0.477	0.554	0.308	0.424	0.309	0.582	0.303	0.406	0.714
0.474	0.519	0.347	0.548	0.347	0.470	0.647	0.349	0.433	0.412	0.344	0.394	0.372	0.550	0.488	0.518
0.473	0.594	0.367	0.551	0.446	0.565	0.438	0.438	0.438	0.438	0.438	0.438				
Row 52, column 4															
0.329	0.329	0.367	0.321	0.389	0.000	0.729	0.000	0.457	0.000	0.742	0.000	0.735	0.000	0.815	0.000
0.557	0.000	0.292	0.000	0.325	0.000	0.603	0.000	0.274	0.144	0.613	0.086	0.479	0.146	0.184	0.155
0.386	0.314	0.356	0.169	0.422	0.337	0.268	0.358	0.416	0.231	0.318	0.232	0.437	0.227	0.305	0.536
0.356	0.390	0.261	0.411	0.261	0.353	0.486	0.262	0.325	0.309	0.258	0.295	0.279	0.413	0.366	0.389
0.355	0.446	0.276	0.413	0.335	0.424	0.329	0.329	0.329	0.329	0.329	0.329				

Table 16.--Specified recharge for the barren basalt area of the valley-fill aquifer, represented by layer 1, in cubic feet per second--Continued

Stress period															
1	2	3	4	5	6	7	8	9	10	11	12	13	14	15	16
17	18	19	20	21	22	23	24	25	26	27	28	29	30	31	32
33	34	35	36	37	38	39	40	41	42	43	44	45	46	47	48
49	50	51	52	53	54	55	56	57	58	59	60	61	62	63	64
65	66	67	68	69	70	71	72	73	74	75	76				
Row 53, column 4															
0.329	0.329	0.367	0.321	0.389	0.000	0.729	0.000	0.457	0.000	0.742	0.000	0.735	0.000	0.815	0.000
0.557	0.000	0.292	0.000	0.325	0.000	0.603	0.000	0.274	0.144	0.613	0.086	0.479	0.146	0.184	0.155
0.386	0.314	0.356	0.169	0.422	0.337	0.268	0.358	0.416	0.231	0.318	0.232	0.437	0.227	0.305	0.536
0.356	0.390	0.261	0.411	0.261	0.353	0.486	0.262	0.325	0.309	0.258	0.295	0.279	0.413	0.366	0.389
0.355	0.446	0.276	0.413	0.335	0.424	0.329	0.329	0.329	0.329	0.329	0.329				
Row 54, column 4															
0.329	0.329	0.367	0.321	0.389	0.000	0.729	0.000	0.457	0.000	0.742	0.000	0.735	0.000	0.815	0.000
0.557	0.000	0.292	0.000	0.325	0.000	0.603	0.000	0.274	0.144	0.613	0.086	0.479	0.146	0.184	0.155
0.386	0.314	0.356	0.169	0.422	0.337	0.268	0.358	0.416	0.231	0.318	0.232	0.437	0.227	0.305	0.536
0.356	0.390	0.261	0.411	0.261	0.353	0.486	0.262	0.325	0.309	0.258	0.295	0.279	0.413	0.366	0.389
0.355	0.446	0.276	0.413	0.335	0.424	0.329	0.329	0.329	0.329	0.329	0.329				
Row 52, column 5															
0.220	0.220	0.245	0.215	0.260	0.000	0.487	0.000	0.305	0.000	0.496	0.000	0.491	0.000	0.544	0.000
0.372	0.000	0.195	0.000	0.217	0.000	0.403	0.000	0.183	0.096	0.409	0.058	0.320	0.097	0.123	0.104
0.258	0.210	0.238	0.113	0.282	0.225	0.179	0.239	0.278	0.154	0.212	0.155	0.292	0.152	0.204	0.358
0.238	0.260	0.174	0.275	0.174	0.236	0.324	0.175	0.217	0.206	0.173	0.197	0.187	0.276	0.245	0.260
0.237	0.298	0.184	0.276	0.223	0.283	0.220	0.220	0.220	0.220	0.220	0.220				

Table 16.--Specified recharge for the barren basalt area of the valley-fill aquifer, represented by layer 1, in cubic feet per second--Continued

Stress period															
1	2	3	4	5	6	7	8	9	10	11	12	13	14	15	16
17	18	19	20	21	22	23	24	25	26	27	28	29	30	31	32
33	34	35	36	37	38	39	40	41	42	43	44	45	46	47	48
49	50	51	52	53	54	55	56	57	58	59	60	61	62	63	64
65	66	67	68	69	70	71	72	73	74	75	76				
Row 53, column 5															
0.220	0.220	0.245	0.215	0.260	0.000	0.487	0.000	0.305	0.000	0.496	0.000	0.491	0.000	0.544	0.000
0.372	0.000	0.195	0.000	0.217	0.000	0.403	0.000	0.183	0.096	0.409	0.058	0.320	0.097	0.123	0.104
0.258	0.210	0.238	0.113	0.282	0.225	0.179	0.239	0.278	0.154	0.212	0.155	0.292	0.152	0.204	0.358
0.238	0.260	0.174	0.275	0.174	0.236	0.324	0.175	0.217	0.206	0.173	0.197	0.187	0.276	0.245	0.260
0.237	0.298	0.184	0.276	0.223	0.283	0.220	0.220	0.220	0.220	0.220	0.220				
Row 52, column 6															
0.165	0.165	0.184	0.161	0.195	0.000	0.366	0.000	0.229	0.000	0.372	0.000	0.369	0.000	0.409	0.000
0.279	0.000	0.146	0.000	0.163	0.000	0.303	0.000	0.138	0.072	0.308	0.043	0.240	0.073	0.092	0.078
0.194	0.158	0.179	0.085	0.212	0.169	0.134	0.180	0.209	0.116	0.160	0.116	0.219	0.114	0.153	0.269
0.179	0.196	0.131	0.206	0.131	0.177	0.244	0.131	0.163	0.155	0.130	0.148	0.140	0.207	0.184	0.195
0.178	0.224	0.138	0.207	0.168	0.213	0.165	0.165	0.165	0.165	0.165	0.165				
Row 53, column 6															
0.165	0.165	0.184	0.161	0.195	0.000	0.366	0.000	0.229	0.000	0.372	0.000	0.369	0.000	0.409	0.000
0.279	0.000	0.146	0.000	0.163	0.000	0.303	0.000	0.138	0.072	0.308	0.043	0.240	0.073	0.092	0.078
0.194	0.158	0.179	0.085	0.212	0.169	0.134	0.180	0.209	0.116	0.160	0.116	0.219	0.114	0.153	0.269
0.179	0.196	0.131	0.206	0.131	0.177	0.244	0.131	0.163	0.155	0.130	0.148	0.140	0.207	0.184	0.195
0.178	0.224	0.138	0.207	0.168	0.213	0.165	0.165	0.165	0.165	0.165	0.165				

Table 16.--Specified recharge for the barren basalt area of the valley-fill aquifer, represented by layer 1, in cubic feet per second--Continued

Stress period															
1	2	3	4	5	6	7	8	9	10	11	12	13	14	15	16
17	18	19	20	21	22	23	24	25	26	27	28	29	30	31	32
33	34	35	36	37	38	39	40	41	42	43	44	45	46	47	48
49	50	51	52	53	54	55	56	57	58	59	60	61	62	63	64
65	66	67	68	69	70	71	72	73	74	75	76				

Row 51, column 7

0.109	0.109	0.122	0.107	0.129	0.000	0.242	0.000	0.152	0.000	0.246	0.000	0.244	0.000	0.271	0.000
0.185	0.000	0.097	0.000	0.108	0.000	0.200	0.000	0.091	0.048	0.203	0.029	0.159	0.048	0.061	0.051
0.128	0.104	0.118	0.056	0.140	0.112	0.089	0.119	0.138	0.077	0.106	0.077	0.145	0.075	0.101	0.178
0.118	0.129	0.087	0.137	0.087	0.117	0.161	0.087	0.108	0.103	0.086	0.098	0.093	0.137	0.122	0.129
0.118	0.148	0.092	0.137	0.111	0.141	0.109	0.109	0.109	0.109	0.109	0.109				

Row 52, column 7

0.109	0.109	0.122	0.107	0.129	0.000	0.242	0.000	0.152	0.000	0.246	0.000	0.244	0.000	0.271	0.000
0.185	0.000	0.097	0.000	0.108	0.000	0.200	0.000	0.091	0.048	0.203	0.029	0.159	0.048	0.061	0.051
0.128	0.104	0.118	0.056	0.140	0.112	0.089	0.119	0.138	0.077	0.106	0.077	0.145	0.075	0.101	0.178
0.118	0.129	0.087	0.137	0.087	0.117	0.161	0.087	0.108	0.103	0.086	0.098	0.093	0.137	0.122	0.129
0.118	0.148	0.092	0.137	0.111	0.141	0.109	0.109	0.109	0.109	0.109	0.109				

Table 16.--Specified recharge for the barren basalt area of the valley-fill aquifer, represented by layer 1, in cubic feet per second--Concluded

Stress period															
1	2	3	4	5	6	7	8	9	10	11	12	13	14	15	16
17	18	19	20	21	22	23	24	25	26	27	28	29	30	31	32
33	34	35	36	37	38	39	40	41	42	43	44	45	46	47	48
49	50	51	52	53	54	55	56	57	58	59	60	61	62	63	64
65	66	67	68	69	70	71	72	73	74	75	76				
Row 50, column 11															
0.082	0.082	0.091	0.080	0.097	0.000	0.181	0.000	0.114	0.000	0.185	0.000	0.183	0.000	0.203	0.000
0.139	0.000	0.073	0.000	0.081	0.000	0.150	0.000	0.068	0.036	0.153	0.021	0.119	0.036	0.046	0.039
0.096	0.078	0.089	0.042	0.105	0.084	0.067	0.089	0.104	0.058	0.079	0.058	0.109	0.057	0.076	0.133
0.089	0.097	0.065	0.102	0.065	0.088	0.121	0.065	0.081	0.077	0.064	0.074	0.070	0.103	0.091	0.097
0.088	0.111	0.069	0.103	0.083	0.106	0.082	0.082	0.082	0.082	0.082	0.082				
Total specified recharge for the barren basalt area of the valley-fill aquifer, represented by layer 1.															
6.70	6.70	7.48	6.55	7.93	0.00	14.85	0.00	9.32	0.00	15.12	0.00	14.99	0.00	16.61	0.00
11.34	0.00	5.94	0.00	6.62	0.00	12.29	0.00	5.59	2.94	12.49	1.76	9.76	2.97	3.74	3.16
7.87	6.40	7.25	3.44	8.60	6.86	5.45	7.30	8.48	4.71	6.48	4.73	8.90	4.63	6.21	10.92
7.25	7.94	5.31	8.38	5.31	7.19	9.90	5.33	6.63	6.30	5.27	6.02	5.69	8.41	7.47	7.92
7.24	9.09	5.62	8.42	6.82	8.64	6.70	6.70	6.70	6.70	6.70	6.70				

Table 17.--Specified recharge for the mountains of the Zuni uplift, in cubic feet per second

[Locations shown in figures 25 and 26. Zones shown in figure 12. Recharge is the same for all scenarios]

Stress period															
1	2	3	4	5	6	7	8	9	10	11	12	13	14	15	16
17	18	19	20	21	22	23	24	25	26	27	28	29	30	31	32
33	34	35	36	37	38	39	40	41	42	43	44	45	46	47	48
49	50	51	52	53	54	55	56	57	58	59	60	61	62	63	64
65	66	67	68	69	70	71	72	73	74	75	76	77			

Specified recharge for the San Andres-Glorieta aquifer in the mountains of the Zuni uplift, represented by layer 2

Row 1, column 5, zone 1

0.163	0.163	0.151	0.229	0.174	0.030	0.057	0.295	0.132	0.016	0.290	0.007	0.018	0.032	0.006	0.104
0.120	0.019	0.000	0.000	0.000	0.185	0.141	0.005	0.000	0.074	0.011	0.000	0.000	0.000	0.000	0.333
0.027	0.124	0.182	0.000	0.000	0.274	0.028	0.009	0.061	0.263	0.142	0.262	0.001	0.012	0.169	0.330
0.011	0.042	0.104	0.133	0.046	0.037	0.094	0.503	0.065	0.097	0.008	0.287	0.181	0.715	0.408	0.204
0.359	0.831	0.117	0.488	0.434	0.490	0.163	0.163	0.163	0.163	0.163	0.163				

Row 2, column 5, zone 1

0.172	0.172	0.159	0.242	0.184	0.031	0.060	0.311	0.140	0.017	0.307	0.008	0.019	0.034	0.007	0.110
0.126	0.020	0.000	0.000	0.000	0.195	0.149	0.005	0.000	0.078	0.012	0.000	0.000	0.000	0.000	0.351
0.029	0.131	0.192	0.000	0.000	0.289	0.030	0.009	0.064	0.278	0.150	0.277	0.001	0.013	0.179	0.348
0.011	0.045	0.109	0.140	0.048	0.039	0.099	0.531	0.069	0.102	0.009	0.303	0.191	0.755	0.431	0.215
0.379	0.877	0.124	0.515	0.458	0.517	0.172	0.172	0.172	0.172	0.172	0.172				

Row 3, column 6, zone 1

0.172	0.172	0.159	0.242	0.184	0.031	0.060	0.311	0.140	0.017	0.307	0.008	0.019	0.034	0.007	0.110
0.126	0.020	0.000	0.000	0.000	0.195	0.149	0.005	0.000	0.078	0.012	0.000	0.000	0.000	0.000	0.351
0.029	0.131	0.192	0.000	0.000	0.289	0.030	0.009	0.064	0.278	0.150	0.277	0.001	0.013	0.179	0.348
0.011	0.045	0.109	0.140	0.048	0.039	0.099	0.531	0.069	0.102	0.009	0.303	0.191	0.755	0.431	0.215
0.379	0.877	0.124	0.515	0.458	0.517	0.172	0.172	0.172	0.172	0.172	0.172				

Table 17.--Specified recharge for the mountains of the Zuni uplift, in cubic feet per second--Continued

Stress period															
1	2	3	4	5	6	7	8	9	10	11	12	13	14	15	16
17	18	19	20	21	22	23	24	25	26	27	28	29	30	31	32
33	34	35	36	37	38	39	40	41	42	43	44	45	46	47	48
49	50	51	52	53	54	55	56	57	58	59	60	61	62	63	64
65	66	67	68	69	70	71	72	73	74	75	76	77			

Specified recharge for the San Andres-Glorieta aquifer in the mountains of the Zuni uplift, represented by layer 2

Row 4, column 6, zone 1

0.129	0.129	0.119	0.181	0.138	0.023	0.045	0.233	0.105	0.012	0.230	0.006	0.014	0.026	0.005	0.082
0.095	0.015	0.000	0.000	0.000	0.146	0.112	0.004	0.000	0.059	0.009	0.000	0.000	0.000	0.000	0.263
0.022	0.098	0.144	0.000	0.000	0.217	0.022	0.007	0.048	0.208	0.113	0.207	0.001	0.009	0.134	0.261
0.009	0.033	0.082	0.105	0.036	0.029	0.074	0.398	0.052	0.077	0.006	0.228	0.144	0.566	0.323	0.161
0.284	0.658	0.093	0.386	0.344	0.388	0.129	0.129	0.129	0.129	0.129	0.129				

Row 5, column 6, zone 1

0.086	0.086	0.080	0.121	0.092	0.016	0.030	0.156	0.070	0.008	0.153	0.004	0.009	0.017	0.003	0.055
0.063	0.010	0.000	0.000	0.000	0.098	0.074	0.003	0.000	0.039	0.006	0.000	0.000	0.000	0.000	0.175
0.014	0.065	0.096	0.000	0.000	0.144	0.015	0.005	0.032	0.139	0.075	0.138	0.001	0.006	0.089	0.174
0.006	0.022	0.055	0.070	0.024	0.019	0.049	0.266	0.034	0.051	0.004	0.152	0.096	0.378	0.215	0.107
0.189	0.438	0.062	0.258	0.229	0.258	0.086	0.086	0.086	0.086	0.086	0.086				

Row 6, column 6, zone 1

0.065	0.065	0.060	0.091	0.069	0.012	0.022	0.117	0.052	0.006	0.115	0.003	0.007	0.013	0.003	0.041
0.047	0.007	0.000	0.000	0.000	0.073	0.056	0.002	0.000	0.029	0.004	0.000	0.000	0.000	0.000	0.132
0.011	0.049	0.072	0.000	0.000	0.108	0.011	0.003	0.024	0.104	0.056	0.104	0.000	0.005	0.067	0.130
0.004	0.017	0.041	0.053	0.018	0.014	0.037	0.199	0.026	0.038	0.003	0.114	0.072	0.283	0.162	0.081
0.142	0.329	0.046	0.193	0.172	0.194	0.065	0.065	0.065	0.065	0.065	0.065				

Table 17.--Specified recharge for the mountains of the Zuni uplift, in cubic feet per second--Continued

Stress period															
1	2	3	4	5	6	7	8	9	10	11	12	13	14	15	16
17	18	19	20	21	22	23	24	25	26	27	28	29	30	31	32
33	34	35	36	37	38	39	40	41	42	43	44	45	46	47	48
49	50	51	52	53	54	55	56	57	58	59	60	61	62	63	64
65	66	67	68	69	70	71	72	73	74	75	76	77			

Specified recharge for the San Andres-Glorieta aquifer in the mountains of the Zuni uplift, represented by layer 2

Row 7, column 6, zone 1

0.065	0.065	0.060	0.091	0.069	0.012	0.022	0.117	0.052	0.006	0.115	0.003	0.007	0.013	0.003	0.041
0.047	0.007	0.000	0.000	0.000	0.073	0.056	0.002	0.000	0.029	0.004	0.000	0.000	0.000	0.000	0.132
0.011	0.049	0.072	0.000	0.000	0.108	0.011	0.003	0.024	0.104	0.056	0.104	0.000	0.005	0.067	0.130
0.004	0.017	0.041	0.053	0.018	0.014	0.037	0.199	0.026	0.038	0.003	0.114	0.072	0.283	0.162	0.081
0.142	0.329	0.046	0.193	0.172	0.194	0.065	0.065	0.065	0.065	0.065	0.065				

Row 8, column 6, zone 1

0.065	0.065	0.060	0.091	0.069	0.012	0.022	0.117	0.052	0.006	0.115	0.003	0.007	0.013	0.003	0.041
0.047	0.007	0.000	0.000	0.000	0.073	0.056	0.002	0.000	0.029	0.004	0.000	0.000	0.000	0.000	0.132
0.011	0.049	0.072	0.000	0.000	0.108	0.011	0.003	0.024	0.104	0.056	0.104	0.000	0.005	0.067	0.130
0.004	0.017	0.041	0.053	0.018	0.014	0.037	0.199	0.026	0.038	0.003	0.114	0.072	0.283	0.162	0.081
0.142	0.329	0.046	0.193	0.172	0.194	0.065	0.065	0.065	0.065	0.065	0.065				

Row 9, column 6, zone 1

0.065	0.065	0.060	0.091	0.069	0.012	0.022	0.117	0.052	0.006	0.115	0.003	0.007	0.013	0.003	0.041
0.047	0.007	0.000	0.000	0.000	0.073	0.056	0.002	0.000	0.029	0.004	0.000	0.000	0.000	0.000	0.132
0.011	0.049	0.072	0.000	0.000	0.108	0.011	0.003	0.024	0.104	0.056	0.104	0.000	0.005	0.067	0.130
0.004	0.017	0.041	0.053	0.018	0.014	0.037	0.199	0.026	0.038	0.003	0.114	0.072	0.283	0.162	0.081
0.142	0.329	0.046	0.193	0.172	0.194	0.065	0.065	0.065	0.065	0.065	0.065				

Table 17.--Specified recharge for the mountains of the Zuni uplift, in cubic feet per second--Continued

Stress period															
1	2	3	4	5	6	7	8	9	10	11	12	13	14	15	16
17	18	19	20	21	22	23	24	25	26	27	28	29	30	31	32
33	34	35	36	37	38	39	40	41	42	43	44	45	46	47	48
49	50	51	52	53	54	55	56	57	58	59	60	61	62	63	64
65	66	67	68	69	70	71	72	73	74	75	76	77			

Specified recharge for the San Andres-Glorieta aquifer in the mountains of the Zuni uplift, represented by layer 2

Row 10, column 6, zone 1

0.043	0.043	0.040	0.060	0.046	0.008	0.015	0.078	0.035	0.004	0.077	0.002	0.005	0.009	0.002	0.027
0.032	0.005	0.000	0.000	0.000	0.049	0.037	0.001	0.000	0.020	0.003	0.000	0.000	0.000	0.000	0.088
0.007	0.033	0.048	0.000	0.000	0.072	0.007	0.002	0.016	0.069	0.038	0.069	0.000	0.003	0.045	0.087
0.003	0.011	0.027	0.035	0.012	0.010	0.025	0.133	0.017	0.026	0.002	0.076	0.048	0.189	0.108	0.054
0.095	0.219	0.031	0.129	0.115	0.129	0.043	0.043	0.043	0.043	0.043	0.043				

Row 11, column 6, zone 1

0.043	0.043	0.040	0.060	0.046	0.008	0.015	0.078	0.035	0.004	0.077	0.002	0.005	0.009	0.002	0.027
0.032	0.005	0.000	0.000	0.000	0.049	0.037	0.001	0.000	0.020	0.003	0.000	0.000	0.000	0.000	0.088
0.007	0.033	0.048	0.000	0.000	0.072	0.007	0.002	0.016	0.069	0.038	0.069	0.000	0.003	0.045	0.087
0.003	0.011	0.027	0.035	0.012	0.010	0.025	0.133	0.017	0.026	0.002	0.076	0.048	0.189	0.108	0.054
0.095	0.219	0.031	0.129	0.115	0.129	0.043	0.043	0.043	0.043	0.043	0.043				

Row 12, column 7, zone 1

0.043	0.043	0.040	0.060	0.046	0.008	0.015	0.078	0.035	0.004	0.077	0.002	0.005	0.009	0.002	0.027
0.032	0.005	0.000	0.000	0.000	0.049	0.037	0.001	0.000	0.020	0.003	0.000	0.000	0.000	0.000	0.088
0.007	0.033	0.048	0.000	0.000	0.072	0.007	0.002	0.016	0.069	0.038	0.069	0.000	0.003	0.045	0.087
0.003	0.011	0.027	0.035	0.012	0.010	0.025	0.133	0.017	0.026	0.002	0.076	0.048	0.189	0.108	0.054
0.095	0.219	0.031	0.129	0.115	0.129	0.043	0.043	0.043	0.043	0.043	0.043				

Table 17.--Specified recharge for the mountains of the Zuni uplift, in cubic feet per second--Continued

Stress period															
1	2	3	4	5	6	7	8	9	10	11	12	13	14	15	16
17	18	19	20	21	22	23	24	25	26	27	28	29	30	31	32
33	34	35	36	37	38	39	40	41	42	43	44	45	46	47	48
49	50	51	52	53	54	55	56	57	58	59	60	61	62	63	64
65	66	67	68	69	70	71	72	73	74	75	76	77			

Specified recharge for the San Andres-Glorieta aquifer in the mountains of the Zuni uplift, represented by layer 2

Row 13, column 7, zone 1

0.043	0.043	0.040	0.060	0.046	0.008	0.015	0.078	0.035	0.004	0.077	0.002	0.005	0.009	0.002	0.027
0.032	0.005	0.000	0.000	0.000	0.049	0.037	0.001	0.000	0.020	0.003	0.000	0.000	0.000	0.000	0.088
0.007	0.033	0.048	0.000	0.000	0.072	0.007	0.002	0.016	0.069	0.038	0.069	0.000	0.003	0.045	0.087
0.003	0.011	0.027	0.035	0.012	0.010	0.025	0.133	0.017	0.026	0.002	0.076	0.048	0.189	0.108	0.054
0.095	0.219	0.031	0.129	0.115	0.129	0.043	0.043	0.043	0.043	0.043	0.043				

Row 14, column 7, zone 1

0.043	0.043	0.040	0.060	0.046	0.008	0.015	0.078	0.035	0.004	0.077	0.002	0.005	0.009	0.002	0.027
0.032	0.005	0.000	0.000	0.000	0.049	0.037	0.001	0.000	0.020	0.003	0.000	0.000	0.000	0.000	0.088
0.007	0.033	0.048	0.000	0.000	0.072	0.007	0.002	0.016	0.069	0.038	0.069	0.000	0.003	0.045	0.087
0.003	0.011	0.027	0.035	0.012	0.010	0.025	0.133	0.017	0.026	0.002	0.076	0.048	0.189	0.108	0.054
0.095	0.219	0.031	0.129	0.115	0.129	0.043	0.043	0.043	0.043	0.043	0.043				

Row 15, column 8, zone 1

0.043	0.043	0.040	0.060	0.046	0.008	0.015	0.078	0.035	0.004	0.077	0.002	0.005	0.009	0.002	0.027
0.032	0.005	0.000	0.000	0.000	0.049	0.037	0.001	0.000	0.020	0.003	0.000	0.000	0.000	0.000	0.088
0.007	0.033	0.048	0.000	0.000	0.072	0.007	0.002	0.016	0.069	0.038	0.069	0.000	0.003	0.045	0.087
0.003	0.011	0.027	0.035	0.012	0.010	0.025	0.133	0.017	0.026	0.002	0.076	0.048	0.189	0.108	0.054
0.095	0.219	0.031	0.129	0.115	0.129	0.043	0.043	0.043	0.043	0.043	0.043				

Table 17.--Specified recharge for the mountains of the Zuni uplift, in cubic feet per second--Continued

Stress period															
1	2	3	4	5	6	7	8	9	10	11	12	13	14	15	16
17	18	19	20	21	22	23	24	25	26	27	28	29	30	31	32
33	34	35	36	37	38	39	40	41	42	43	44	45	46	47	48
49	50	51	52	53	54	55	56	57	58	59	60	61	62	63	64
65	66	67	68	69	70	71	72	73	74	75	76	77			

Specified recharge for the San Andres-Glorieta aquifer in the mountains of the Zuni uplift, represented by layer 2

Row 16, column 8, zone 1

0.043	0.043	0.040	0.060	0.046	0.008	0.015	0.078	0.035	0.004	0.077	0.002	0.005	0.009	0.002	0.027
0.032	0.005	0.000	0.000	0.000	0.049	0.037	0.001	0.000	0.020	0.003	0.000	0.000	0.000	0.000	0.088
0.007	0.033	0.048	0.000	0.000	0.072	0.007	0.002	0.016	0.069	0.038	0.069	0.000	0.003	0.045	0.087
0.003	0.011	0.027	0.035	0.012	0.010	0.025	0.133	0.017	0.026	0.002	0.076	0.048	0.189	0.108	0.054
0.095	0.219	0.031	0.129	0.115	0.129	0.043	0.043	0.043	0.043	0.043	0.043				

Row 17, column 8, zone 1

0.043	0.043	0.040	0.060	0.046	0.008	0.015	0.078	0.035	0.004	0.077	0.002	0.005	0.009	0.002	0.027
0.032	0.005	0.000	0.000	0.000	0.049	0.037	0.001	0.000	0.020	0.003	0.000	0.000	0.000	0.000	0.088
0.007	0.033	0.048	0.000	0.000	0.072	0.007	0.002	0.016	0.069	0.038	0.069	0.000	0.003	0.045	0.087
0.003	0.011	0.027	0.035	0.012	0.010	0.025	0.133	0.017	0.026	0.002	0.076	0.048	0.189	0.108	0.054
0.095	0.219	0.031	0.129	0.115	0.129	0.043	0.043	0.043	0.043	0.043	0.043				

Row 18, column 8, zone 1

0.043	0.043	0.040	0.060	0.046	0.008	0.015	0.078	0.035	0.004	0.077	0.002	0.005	0.009	0.002	0.027
0.032	0.005	0.000	0.000	0.000	0.049	0.037	0.001	0.000	0.020	0.003	0.000	0.000	0.000	0.000	0.088
0.007	0.033	0.048	0.000	0.000	0.072	0.007	0.002	0.016	0.069	0.038	0.069	0.000	0.003	0.045	0.087
0.003	0.011	0.027	0.035	0.012	0.010	0.025	0.133	0.017	0.026	0.002	0.076	0.048	0.189	0.108	0.054
0.095	0.219	0.031	0.129	0.115	0.129	0.043	0.043	0.043	0.043	0.043	0.043				

Table 17.--Specified recharge for the mountains of the Zuni uplift, in cubic feet per second--Continued

Stress period															
1	2	3	4	5	6	7	8	9	10	11	12	13	14	15	16
17	18	19	20	21	22	23	24	25	26	27	28	29	30	31	32
33	34	35	36	37	38	39	40	41	42	43	44	45	46	47	48
49	50	51	52	53	54	55	56	57	58	59	60	61	62	63	64
65	66	67	68	69	70	71	72	73	74	75	76	77			

Specified recharge for the San Andres-Glorieta aquifer in the mountains of the Zuni uplift, represented by layer 2

Row 19, column 9, zone 2

0.040	0.040	0.041	0.064	0.040	0.001	0.001	0.069	0.005	0.000	0.127	0.000	0.000	0.000	0.000	0.012
0.008	0.000	0.000	0.000	0.000	0.038	0.007	0.000	0.000	0.002	0.000	0.000	0.000	0.000	0.000	0.048
0.000	0.006	0.014	0.000	0.000	0.062	0.000	0.000	0.000	0.081	0.006	0.024	0.000	0.000	0.024	0.066
0.000	0.003	0.020	0.023	0.000	0.001	0.064	0.114	0.007	0.014	0.000	0.074	0.135	0.241	0.068	0.075
0.121	0.195	0.027	0.115	0.192	0.052	0.040	0.040	0.040	0.040	0.040	0.040				

Row 20, column 9, zone 2

0.040	0.040	0.041	0.064	0.040	0.001	0.001	0.069	0.005	0.000	0.127	0.000	0.000	0.000	0.000	0.012
0.008	0.000	0.000	0.000	0.000	0.038	0.007	0.000	0.000	0.002	0.000	0.000	0.000	0.000	0.000	0.048
0.000	0.006	0.014	0.000	0.000	0.062	0.000	0.000	0.000	0.081	0.006	0.024	0.000	0.000	0.024	0.066
0.000	0.003	0.020	0.023	0.000	0.001	0.064	0.114	0.007	0.014	0.000	0.074	0.135	0.241	0.068	0.075
0.121	0.195	0.027	0.115	0.192	0.052	0.040	0.040	0.040	0.040	0.040	0.040				

Row 20, column 10, zone 2

0.061	0.061	0.061	0.096	0.061	0.001	0.001	0.104	0.007	0.000	0.190	0.000	0.000	0.000	0.000	0.018
0.012	0.000	0.000	0.000	0.000	0.057	0.011	0.000	0.000	0.002	0.000	0.000	0.000	0.000	0.000	0.072
0.000	0.009	0.022	0.000	0.000	0.092	0.000	0.000	0.000	0.122	0.009	0.037	0.000	0.000	0.037	0.100
0.000	0.005	0.031	0.034	0.001	0.002	0.097	0.171	0.011	0.020	0.000	0.112	0.203	0.362	0.102	0.113
0.181	0.293	0.041	0.173	0.288	0.078	0.061	0.061	0.061	0.061	0.061	0.061				

Table 17.--Specified recharge for the mountains of the Zuni uplift, in cubic feet per second--Continued

Stress period															
1	2	3	4	5	6	7	8	9	10	11	12	13	14	15	16
17	18	19	20	21	22	23	24	25	26	27	28	29	30	31	32
33	34	35	36	37	38	39	40	41	42	43	44	45	46	47	48
49	50	51	52	53	54	55	56	57	58	59	60	61	62	63	64
65	66	67	68	69	70	71	72	73	74	75	76	77			

Specified recharge for the San Andres-Glorieta aquifer in the mountains of the Zuni uplift, represented by layer 2

Row 20, column 11, zone 2

0.101	0.101	0.102	0.160	0.101	0.001	0.002	0.173	0.011	0.000	0.317	0.000	0.000	0.000	0.000	0.031
0.020	0.000	0.000	0.000	0.000	0.095	0.018	0.000	0.000	0.004	0.000	0.000	0.000	0.000	0.000	0.120
0.000	0.016	0.036	0.000	0.000	0.154	0.000	0.000	0.000	0.203	0.015	0.061	0.000	0.000	0.061	0.166
0.000	0.009	0.051	0.056	0.001	0.003	0.161	0.285	0.018	0.034	0.000	0.186	0.338	0.603	0.170	0.188
0.302	0.488	0.068	0.289	0.479	0.131	0.101	0.101	0.101	0.101	0.101	0.101				

Row 21, column 11, zone 2

0.040	0.040	0.041	0.064	0.040	0.001	0.001	0.069	0.005	0.000	0.127	0.000	0.000	0.000	0.000	0.012
0.008	0.000	0.000	0.000	0.000	0.038	0.007	0.000	0.000	0.002	0.000	0.000	0.000	0.000	0.000	0.048
0.000	0.006	0.014	0.000	0.000	0.062	0.000	0.000	0.000	0.081	0.006	0.024	0.000	0.000	0.024	0.066
0.000	0.003	0.020	0.023	0.000	0.001	0.064	0.114	0.007	0.014	0.000	0.074	0.135	0.241	0.068	0.075
0.121	0.195	0.027	0.115	0.192	0.052	0.040	0.040	0.040	0.040	0.040	0.040				

Row 22, column 11, zone 2

0.061	0.061	0.061	0.096	0.061	0.001	0.001	0.104	0.007	0.000	0.190	0.000	0.000	0.000	0.000	0.018
0.012	0.000	0.000	0.000	0.000	0.057	0.011	0.000	0.000	0.002	0.000	0.000	0.000	0.000	0.000	0.072
0.000	0.009	0.022	0.000	0.000	0.092	0.000	0.000	0.000	0.122	0.009	0.037	0.000	0.000	0.037	0.100
0.000	0.005	0.031	0.034	0.001	0.002	0.097	0.171	0.011	0.020	0.000	0.112	0.203	0.362	0.102	0.113
0.181	0.293	0.041	0.173	0.288	0.078	0.061	0.061	0.061	0.061	0.061	0.061				

Table 17.--Specified recharge for the mountains of the Zuni uplift, in cubic feet per second--Continued

Stress period															
1	2	3	4	5	6	7	8	9	10	11	12	13	14	15	16
17	18	19	20	21	22	23	24	25	26	27	28	29	30	31	32
33	34	35	36	37	38	39	40	41	42	43	44	45	46	47	48
49	50	51	52	53	54	55	56	57	58	59	60	61	62	63	64
65	66	67	68	69	70	71	72	73	74	75	76	77			

Specified recharge for the San Andres-Glorieta aquifer in the mountains of the Zuni uplift, represented by layer 2

Row 24, column 11, zone 2

0.061	0.061	0.061	0.096	0.061	0.001	0.001	0.104	0.007	0.000	0.190	0.000	0.000	0.000	0.000	0.018
0.012	0.000	0.000	0.000	0.000	0.057	0.011	0.000	0.000	0.002	0.000	0.000	0.000	0.000	0.000	0.072
0.000	0.009	0.022	0.000	0.000	0.092	0.000	0.000	0.000	0.122	0.009	0.037	0.000	0.000	0.037	0.100
0.000	0.005	0.031	0.034	0.001	0.002	0.097	0.171	0.011	0.020	0.000	0.112	0.203	0.362	0.102	0.113
0.181	0.293	0.041	0.173	0.288	0.078	0.061	0.061	0.061	0.061	0.061	0.061				

Row 25, column 11, zone 3

0.066	0.066	0.066	0.102	0.067	0.000	0.008	0.097	0.027	0.000	0.191	0.000	0.000	0.000	0.003	0.020
0.025	0.000	0.000	0.000	0.000	0.054	0.032	0.000	0.000	0.010	0.003	0.000	0.000	0.000	0.000	0.085
0.008	0.020	0.036	0.000	0.000	0.097	0.009	0.001	0.008	0.111	0.027	0.055	0.000	0.000	0.039	0.114
0.003	0.006	0.034	0.045	0.006	0.003	0.098	0.181	0.013	0.027	0.000	0.115	0.207	0.355	0.127	0.111
0.190	0.310	0.045	0.179	0.269	0.124	0.066	0.066	0.066	0.066	0.066	0.066				

Row 26, column 11, zone 3

0.087	0.087	0.088	0.136	0.090	0.000	0.010	0.130	0.036	0.000	0.255	0.000	0.000	0.000	0.004	0.027
0.033	0.000	0.000	0.000	0.000	0.072	0.042	0.000	0.000	0.013	0.003	0.000	0.000	0.000	0.000	0.114
0.010	0.027	0.048	0.000	0.000	0.130	0.012	0.001	0.011	0.147	0.036	0.073	0.001	0.000	0.052	0.152
0.004	0.008	0.046	0.060	0.008	0.004	0.130	0.241	0.017	0.037	0.000	0.154	0.276	0.474	0.170	0.148
0.254	0.414	0.061	0.239	0.359	0.165	0.087	0.087	0.087	0.087	0.087	0.087				

Table 17.--Specified recharge for the mountains of the Zuni uplift, in cubic feet per second--Continued

Stress period															
1	2	3	4	5	6	7	8	9	10	11	12	13	14	15	16
17	18	19	20	21	22	23	24	25	26	27	28	29	30	31	32
33	34	35	36	37	38	39	40	41	42	43	44	45	46	47	48
49	50	51	52	53	54	55	56	57	58	59	60	61	62	63	64
65	66	67	68	69	70	71	72	73	74	75	76	77			

Specified recharge for the San Andres-Glorieta aquifer in the mountains of the Zuni uplift, represented by layer 2

Row 27, column 11, zone 3

0.087	0.087	0.088	0.136	0.090	0.000	0.010	0.130	0.036	0.000	0.255	0.000	0.000	0.000	0.004	0.027
0.033	0.000	0.000	0.000	0.000	0.072	0.042	0.000	0.000	0.013	0.003	0.000	0.000	0.000	0.000	0.114
0.010	0.027	0.048	0.000	0.000	0.130	0.012	0.001	0.011	0.147	0.036	0.073	0.001	0.000	0.052	0.152
0.004	0.008	0.046	0.060	0.008	0.004	0.130	0.241	0.017	0.037	0.000	0.154	0.276	0.474	0.170	0.148
0.254	0.414	0.061	0.239	0.359	0.165	0.087	0.087	0.087	0.087	0.087	0.087				

Row 28, column 11, zone 3

0.087	0.087	0.088	0.136	0.090	0.000	0.010	0.130	0.036	0.000	0.255	0.000	0.000	0.000	0.004	0.027
0.033	0.000	0.000	0.000	0.000	0.072	0.042	0.000	0.000	0.013	0.003	0.000	0.000	0.000	0.000	0.114
0.010	0.027	0.048	0.000	0.000	0.130	0.012	0.001	0.011	0.147	0.036	0.073	0.001	0.000	0.052	0.152
0.004	0.008	0.046	0.060	0.008	0.004	0.130	0.241	0.017	0.037	0.000	0.154	0.276	0.474	0.170	0.148
0.254	0.414	0.061	0.239	0.359	0.165	0.087	0.087	0.087	0.087	0.087	0.087				

Row 29, column 11, zone 3

0.087	0.087	0.088	0.136	0.090	0.000	0.010	0.130	0.036	0.000	0.255	0.000	0.000	0.000	0.004	0.027
0.033	0.000	0.000	0.000	0.000	0.072	0.042	0.000	0.000	0.013	0.003	0.000	0.000	0.000	0.000	0.114
0.010	0.027	0.048	0.000	0.000	0.130	0.012	0.001	0.011	0.147	0.036	0.073	0.001	0.000	0.052	0.152
0.004	0.008	0.046	0.060	0.008	0.004	0.130	0.241	0.017	0.037	0.000	0.154	0.276	0.474	0.170	0.148
0.254	0.414	0.061	0.239	0.359	0.165	0.087	0.087	0.087	0.087	0.087	0.087				

Table 17.--Specified recharge for the mountains of the Zuni uplift, in cubic feet per second--Continued

Stress period															
1	2	3	4	5	6	7	8	9	10	11	12	13	14	15	16
17	18	19	20	21	22	23	24	25	26	27	28	29	30	31	32
33	34	35	36	37	38	39	40	41	42	43	44	45	46	47	48
49	50	51	52	53	54	55	56	57	58	59	60	61	62	63	64
65	66	67	68	69	70	71	72	73	74	75	76	77			

Specified recharge for the San Andres-Glorieta aquifer in the mountains of the Zuni uplift, represented by layer 2

Row 30, column 11, zone 3

0.087	0.087	0.088	0.136	0.090	0.000	0.010	0.130	0.036	0.000	0.255	0.000	0.000	0.000	0.004	0.027
0.033	0.000	0.000	0.000	0.000	0.072	0.042	0.000	0.000	0.013	0.003	0.000	0.000	0.000	0.000	0.114
0.010	0.027	0.048	0.000	0.000	0.130	0.012	0.001	0.011	0.147	0.036	0.073	0.001	0.000	0.052	0.152
0.004	0.008	0.046	0.060	0.008	0.004	0.130	0.241	0.017	0.037	0.000	0.154	0.276	0.474	0.170	0.148
0.254	0.414	0.061	0.239	0.359	0.165	0.087	0.087	0.087	0.087	0.087	0.087				

Row 31, column 11, zone 3

0.066	0.066	0.066	0.102	0.067	0.000	0.008	0.097	0.027	0.000	0.191	0.000	0.000	0.000	0.003	0.020
0.025	0.000	0.000	0.000	0.000	0.054	0.032	0.000	0.000	0.010	0.003	0.000	0.000	0.000	0.000	0.085
0.008	0.020	0.036	0.000	0.000	0.097	0.009	0.001	0.008	0.111	0.027	0.055	0.000	0.000	0.039	0.114
0.003	0.006	0.034	0.045	0.006	0.003	0.098	0.181	0.013	0.027	0.000	0.115	0.207	0.355	0.127	0.111
0.190	0.310	0.045	0.179	0.269	0.124	0.066	0.066	0.066	0.066	0.066	0.066				

Row 32, column 11, zone 3

0.066	0.066	0.066	0.102	0.067	0.000	0.008	0.097	0.027	0.000	0.191	0.000	0.000	0.000	0.003	0.020
0.025	0.000	0.000	0.000	0.000	0.054	0.032	0.000	0.000	0.010	0.003	0.000	0.000	0.000	0.000	0.085
0.008	0.020	0.036	0.000	0.000	0.097	0.009	0.001	0.008	0.111	0.027	0.055	0.000	0.000	0.039	0.114
0.003	0.006	0.034	0.045	0.006	0.003	0.098	0.181	0.013	0.027	0.000	0.115	0.207	0.355	0.127	0.111
0.190	0.310	0.045	0.179	0.269	0.124	0.066	0.066	0.066	0.066	0.066	0.066				

Table 17.--Specified recharge for the mountains of the Zuni uplift, in cubic feet per second--Continued

Stress period															
1	2	3	4	5	6	7	8	9	10	11	12	13	14	15	16
17	18	19	20	21	22	23	24	25	26	27	28	29	30	31	32
33	34	35	36	37	38	39	40	41	42	43	44	45	46	47	48
49	50	51	52	53	54	55	56	57	58	59	60	61	62	63	64
65	66	67	68	69	70	71	72	73	74	75	76	77			

Specified recharge for the San Andres-Glorieta aquifer in the mountains of the Zuni uplift, represented by layer 2

Row 33, column 11, zone 3

0.066	0.066	0.066	0.102	0.067	0.000	0.008	0.097	0.027	0.000	0.191	0.000	0.000	0.000	0.003	0.020
0.025	0.000	0.000	0.000	0.000	0.054	0.032	0.000	0.000	0.010	0.003	0.000	0.000	0.000	0.000	0.085
0.008	0.020	0.036	0.000	0.000	0.097	0.009	0.001	0.008	0.111	0.027	0.055	0.000	0.000	0.039	0.114
0.003	0.006	0.034	0.045	0.006	0.003	0.098	0.181	0.013	0.027	0.000	0.115	0.207	0.355	0.127	0.111
0.190	0.310	0.045	0.179	0.269	0.124	0.066	0.066	0.066	0.066	0.066	0.066				

Row 34, column 11, zone 3

0.066	0.066	0.066	0.102	0.067	0.000	0.008	0.097	0.027	0.000	0.191	0.000	0.000	0.000	0.003	0.020
0.025	0.000	0.000	0.000	0.000	0.054	0.032	0.000	0.000	0.010	0.003	0.000	0.000	0.000	0.000	0.085
0.008	0.020	0.036	0.000	0.000	0.097	0.009	0.001	0.008	0.111	0.027	0.055	0.000	0.000	0.039	0.114
0.003	0.006	0.034	0.045	0.006	0.003	0.098	0.181	0.013	0.027	0.000	0.115	0.207	0.355	0.127	0.111
0.190	0.310	0.045	0.179	0.269	0.124	0.066	0.066	0.066	0.066	0.066	0.066				

Row 35, column 11, zone 3

0.044	0.044	0.044	0.068	0.045	0.000	0.005	0.065	0.018	0.000	0.128	0.000	0.000	0.000	0.002	0.014
0.016	0.000	0.000	0.000	0.000	0.036	0.021	0.000	0.000	0.006	0.002	0.000	0.000	0.000	0.000	0.057
0.005	0.013	0.024	0.000	0.000	0.065	0.006	0.000	0.005	0.074	0.018	0.036	0.000	0.000	0.026	0.076
0.002	0.004	0.023	0.030	0.004	0.002	0.065	0.121	0.008	0.018	0.000	0.077	0.138	0.237	0.085	0.074
0.127	0.207	0.030	0.119	0.180	0.082	0.044	0.044	0.044	0.044	0.044	0.044				

Table 17.--Specified recharge for the mountains of the Zuni uplift, in cubic feet per second--Continued

Stress period															
1	2	3	4	5	6	7	8	9	10	11	12	13	14	15	16
17	18	19	20	21	22	23	24	25	26	27	28	29	30	31	32
33	34	35	36	37	38	39	40	41	42	43	44	45	46	47	48
49	50	51	52	53	54	55	56	57	58	59	60	61	62	63	64
65	66	67	68	69	70	71	72	73	74	75	76	77			

Specified recharge for the San Andres-Glorieta aquifer in the mountains of the Zuni uplift, represented by layer 2

Row 36, column 11, zone 3

0.044	0.044	0.044	0.068	0.045	0.000	0.005	0.065	0.018	0.000	0.128	0.000	0.000	0.000	0.002	0.014
0.016	0.000	0.000	0.000	0.000	0.036	0.021	0.000	0.000	0.006	0.002	0.000	0.000	0.000	0.000	0.057
0.005	0.013	0.024	0.000	0.000	0.065	0.006	0.000	0.005	0.074	0.018	0.036	0.000	0.000	0.026	0.076
0.002	0.004	0.023	0.030	0.004	0.002	0.065	0.121	0.008	0.018	0.000	0.077	0.138	0.237	0.085	0.074
0.127	0.207	0.030	0.119	0.180	0.082	0.044	0.044	0.044	0.044	0.044	0.044				

Row 37, column 11, zone 3

0.044	0.044	0.044	0.068	0.045	0.000	0.005	0.065	0.018	0.000	0.128	0.000	0.000	0.000	0.002	0.014
0.016	0.000	0.000	0.000	0.000	0.036	0.021	0.000	0.000	0.006	0.002	0.000	0.000	0.000	0.000	0.057
0.005	0.013	0.024	0.000	0.000	0.065	0.006	0.000	0.005	0.074	0.018	0.036	0.000	0.000	0.026	0.076
0.002	0.004	0.023	0.030	0.004	0.002	0.065	0.121	0.008	0.018	0.000	0.077	0.138	0.237	0.085	0.074
0.127	0.207	0.030	0.119	0.180	0.082	0.044	0.044	0.044	0.044	0.044	0.044				

Row 37, column 10, zone 3

0.044	0.044	0.044	0.068	0.045	0.000	0.005	0.065	0.018	0.000	0.128	0.000	0.000	0.000	0.002	0.014
0.016	0.000	0.000	0.000	0.000	0.036	0.021	0.000	0.000	0.006	0.002	0.000	0.000	0.000	0.000	0.057
0.005	0.013	0.024	0.000	0.000	0.065	0.006	0.000	0.005	0.074	0.018	0.036	0.000	0.000	0.026	0.076
0.002	0.004	0.023	0.030	0.004	0.002	0.065	0.121	0.008	0.018	0.000	0.077	0.138	0.237	0.085	0.074
0.127	0.207	0.030	0.119	0.180	0.082	0.044	0.044	0.044	0.044	0.044	0.044				

Table 17.--Specified recharge for the mountains of the Zuni uplift, in cubic feet per second--Continued

Stress period															
1	2	3	4	5	6	7	8	9	10	11	12	13	14	15	16
17	18	19	20	21	22	23	24	25	26	27	28	29	30	31	32
33	34	35	36	37	38	39	40	41	42	43	44	45	46	47	48
49	50	51	52	53	54	55	56	57	58	59	60	61	62	63	64
65	66	67	68	69	70	71	72	73	74	75	76	77			

Specified recharge for the San Andres-Glorieta aquifer in the mountains of the Zuni uplift, represented by layer 2

Row 38, column 10, zone 3

0.109	0.109	0.110	0.170	0.112	0.000	0.013	0.162	0.044	0.001	0.319	0.000	0.000	0.000	0.004	0.034
0.041	0.000	0.000	0.000	0.000	0.090	0.053	0.000	0.000	0.016	0.004	0.000	0.000	0.000	0.000	0.142
0.013	0.033	0.059	0.000	0.000	0.162	0.015	0.001	0.013	0.184	0.045	0.091	0.001	0.000	0.065	0.190
0.005	0.010	0.057	0.074	0.010	0.005	0.163	0.302	0.021	0.046	0.000	0.192	0.346	0.592	0.212	0.185
0.317	0.517	0.076	0.298	0.449	0.206	0.109	0.109	0.109	0.109	0.109	0.109				

Row 38, column 8, zone 4

0.030	0.030	0.031	0.047	0.031	0.000	0.001	0.059	0.003	0.000	0.087	0.000	0.000	0.000	0.000	0.012
0.007	0.000	0.000	0.000	0.000	0.033	0.006	0.000	0.000	0.002	0.000	0.000	0.000	0.000	0.000	0.041
0.000	0.008	0.012	0.000	0.000	0.049	0.000	0.000	0.000	0.064	0.004	0.023	0.000	0.000	0.020	0.054
0.000	0.004	0.015	0.020	0.000	0.001	0.038	0.092	0.007	0.011	0.000	0.058	0.084	0.177	0.060	0.050
0.088	0.156	0.020	0.091	0.135	0.048	0.030	0.030	0.030	0.030	0.030	0.030				

Row 38, column 7, zone 4

0.030	0.030	0.031	0.047	0.031	0.000	0.001	0.059	0.003	0.000	0.087	0.000	0.000	0.000	0.000	0.012
0.007	0.000	0.000	0.000	0.000	0.033	0.006	0.000	0.000	0.002	0.000	0.000	0.000	0.000	0.000	0.041
0.000	0.008	0.012	0.000	0.000	0.049	0.000	0.000	0.000	0.064	0.004	0.023	0.000	0.000	0.020	0.054
0.000	0.004	0.015	0.020	0.000	0.001	0.038	0.092	0.007	0.011	0.000	0.058	0.084	0.177	0.060	0.050
0.088	0.156	0.020	0.091	0.135	0.048	0.030	0.030	0.030	0.030	0.030	0.030				

Table 17.--Specified recharge for the mountains of the Zuni uplift, in cubic feet per second--Continued

Stress period															
1	2	3	4	5	6	7	8	9	10	11	12	13	14	15	16
17	18	19	20	21	22	23	24	25	26	27	28	29	30	31	32
33	34	35	36	37	38	39	40	41	42	43	44	45	46	47	48
49	50	51	52	53	54	55	56	57	58	59	60	61	62	63	64
65	66	67	68	69	70	71	72	73	74	75	76	77			

Specified recharge for the San Andres-Glorieta aquifer in the mountains of the Zuni uplift, represented by layer 2

Row 39, column 6, zone 4

0.030	0.030	0.031	0.047	0.031	0.000	0.001	0.059	0.003	0.000	0.087	0.000	0.000	0.000	0.000	0.012
0.007	0.000	0.000	0.000	0.000	0.033	0.006	0.000	0.000	0.002	0.000	0.000	0.000	0.000	0.000	0.041
0.000	0.008	0.012	0.000	0.000	0.049	0.000	0.000	0.000	0.064	0.004	0.023	0.000	0.000	0.020	0.054
0.000	0.004	0.015	0.020	0.000	0.001	0.038	0.092	0.007	0.011	0.000	0.058	0.084	0.177	0.060	0.050
0.088	0.156	0.020	0.091	0.135	0.048	0.030	0.030	0.030	0.030	0.030	0.030				

Row 41, column 6, zone 4

0.041	0.041	0.041	0.063	0.041	0.000	0.001	0.079	0.004	0.000	0.116	0.000	0.000	0.000	0.000	0.016
0.009	0.000	0.000	0.000	0.000	0.045	0.008	0.000	0.000	0.003	0.000	0.000	0.000	0.000	0.000	0.055
0.000	0.010	0.016	0.000	0.000	0.065	0.000	0.000	0.000	0.085	0.006	0.031	0.000	0.000	0.026	0.072
0.000	0.005	0.019	0.027	0.000	0.002	0.051	0.123	0.009	0.015	0.000	0.077	0.112	0.236	0.080	0.067
0.117	0.207	0.026	0.122	0.180	0.064	0.041	0.041	0.041	0.041	0.041	0.041				

Row 43, column 6, zone 4

0.061	0.061	0.061	0.095	0.062	0.000	0.002	0.118	0.005	0.000	0.174	0.000	0.000	0.000	0.000	0.024
0.014	0.000	0.000	0.000	0.000	0.067	0.012	0.000	0.000	0.004	0.000	0.000	0.000	0.000	0.000	0.082
0.000	0.015	0.023	0.000	0.000	0.097	0.000	0.000	0.000	0.128	0.009	0.047	0.000	0.000	0.039	0.109
0.000	0.007	0.029	0.040	0.001	0.003	0.077	0.184	0.014	0.022	0.000	0.116	0.168	0.354	0.120	0.100
0.176	0.311	0.040	0.183	0.270	0.096	0.061	0.061	0.061	0.061	0.061	0.061				

Table 17.--Specified recharge for the mountains of the Zuni uplift, in cubic feet per second--Continued

Stress period															
1	2	3	4	5	6	7	8	9	10	11	12	13	14	15	16
17	18	19	20	21	22	23	24	25	26	27	28	29	30	31	32
33	34	35	36	37	38	39	40	41	42	43	44	45	46	47	48
49	50	51	52	53	54	55	56	57	58	59	60	61	62	63	64
65	66	67	68	69	70	71	72	73	74	75	76	77			

Specified recharge for the San Andres-Glorieta aquifer in the mountains of the Zuni uplift, represented by layer 2

Row 44, column 6, zone 5

0.051	0.051	0.053	0.082	0.050	0.000	0.001	0.074	0.001	0.000	0.164	0.000	0.000	0.000	0.000	0.013
0.006	0.000	0.000	0.000	0.000	0.040	0.003	0.000	0.000	0.002	0.000	0.000	0.000	0.000	0.000	0.046
0.000	0.006	0.016	0.000	0.000	0.076	0.000	0.000	0.000	0.102	0.002	0.023	0.000	0.000	0.028	0.075
0.000	0.004	0.026	0.023	0.000	0.002	0.100	0.128	0.007	0.012	0.000	0.096	0.194	0.310	0.073	0.115
0.158	0.214	0.043	0.134	0.278	0.033	0.051	0.051	0.051	0.051	0.051	0.051				

Row 45, column 6, zone 5

0.051	0.051	0.053	0.082	0.050	0.000	0.001	0.074	0.001	0.000	0.164	0.000	0.000	0.000	0.000	0.013
0.006	0.000	0.000	0.000	0.000	0.040	0.003	0.000	0.000	0.002	0.000	0.000	0.000	0.000	0.000	0.046
0.000	0.006	0.016	0.000	0.000	0.076	0.000	0.000	0.000	0.102	0.002	0.023	0.000	0.000	0.028	0.075
0.000	0.004	0.026	0.023	0.000	0.002	0.100	0.128	0.007	0.012	0.000	0.096	0.194	0.310	0.073	0.115
0.158	0.214	0.043	0.134	0.278	0.033	0.051	0.051	0.051	0.051	0.051	0.051				

Row 46, column 6, zone 5

0.051	0.051	0.053	0.082	0.050	0.000	0.001	0.074	0.001	0.000	0.164	0.000	0.000	0.000	0.000	0.013
0.006	0.000	0.000	0.000	0.000	0.040	0.003	0.000	0.000	0.002	0.000	0.000	0.000	0.000	0.000	0.046
0.000	0.006	0.016	0.000	0.000	0.076	0.000	0.000	0.000	0.102	0.002	0.023	0.000	0.000	0.028	0.075
0.000	0.004	0.026	0.023	0.000	0.002	0.100	0.128	0.007	0.012	0.000	0.096	0.194	0.310	0.073	0.115
0.158	0.214	0.043	0.134	0.278	0.033	0.051	0.051	0.051	0.051	0.051	0.051				

Table 17.--Specified recharge for the mountains of the Zuni uplift, in cubic feet per second--Continued

Stress period															
1	2	3	4	5	6	7	8	9	10	11	12	13	14	15	16
17	18	19	20	21	22	23	24	25	26	27	28	29	30	31	32
33	34	35	36	37	38	39	40	41	42	43	44	45	46	47	48
49	50	51	52	53	54	55	56	57	58	59	60	61	62	63	64
65	66	67	68	69	70	71	72	73	74	75	76	77			

Specified recharge for the San Andres-Glorieta aquifer in the mountains of the Zuni uplift, represented by layer 2

Row 47, column 6, zone 5

0.051	0.051	0.053	0.082	0.050	0.000	0.001	0.074	0.001	0.000	0.164	0.000	0.000	0.000	0.000	0.013
0.006	0.000	0.000	0.000	0.000	0.040	0.003	0.000	0.000	0.002	0.000	0.000	0.000	0.000	0.000	0.046
0.000	0.006	0.016	0.000	0.000	0.076	0.000	0.000	0.000	0.102	0.002	0.023	0.000	0.000	0.028	0.075
0.000	0.004	0.026	0.023	0.000	0.002	0.100	0.128	0.007	0.012	0.000	0.096	0.194	0.310	0.073	0.115
0.158	0.214	0.043	0.134	0.278	0.033	0.051	0.051	0.051	0.051	0.051	0.051				

Row 48, column 5, zone 5

0.067	0.067	0.070	0.109	0.067	0.001	0.001	0.098	0.002	0.000	0.218	0.000	0.000	0.000	0.000	0.017
0.008	0.000	0.000	0.000	0.000	0.053	0.004	0.000	0.000	0.003	0.000	0.000	0.000	0.000	0.000	0.062
0.000	0.008	0.021	0.000	0.000	0.101	0.000	0.000	0.000	0.135	0.003	0.031	0.000	0.000	0.037	0.100
0.000	0.006	0.035	0.031	0.000	0.002	0.133	0.171	0.009	0.016	0.000	0.128	0.259	0.413	0.097	0.154
0.211	0.286	0.058	0.179	0.370	0.043	0.067	0.067	0.067	0.067	0.067	0.067				

Row 49, column 4, zone 5

0.101	0.101	0.106	0.163	0.101	0.001	0.002	0.148	0.003	0.000	0.327	0.000	0.000	0.000	0.000	0.025
0.011	0.000	0.000	0.000	0.000	0.079	0.006	0.000	0.000	0.004	0.000	0.000	0.000	0.000	0.000	0.092
0.000	0.012	0.032	0.000	0.000	0.152	0.000	0.000	0.000	0.203	0.004	0.047	0.000	0.000	0.055	0.150
0.000	0.008	0.052	0.046	0.000	0.004	0.199	0.257	0.014	0.024	0.000	0.192	0.388	0.620	0.146	0.230
0.317	0.429	0.087	0.269	0.555	0.065	0.101	0.101	0.101	0.101	0.101	0.101				

Table 17.--Specified recharge for the mountains of the Zuni uplift, in cubic feet per second--Continued

Stress period															
1	2	3	4	5	6	7	8	9	10	11	12	13	14	15	16
17	18	19	20	21	22	23	24	25	26	27	28	29	30	31	32
33	34	35	36	37	38	39	40	41	42	43	44	45	46	47	48
49	50	51	52	53	54	55	56	57	58	59	60	61	62	63	64
65	66	67	68	69	70	71	72	73	74	75	76	77			

Specified recharge for the San Andres-Glorieta aquifer in the mountains of the Zuni uplift, represented by layer 2

Row 49, column 3, zone 5

0.135	0.135	0.141	0.218	0.135	0.001	0.003	0.197	0.004	0.000	0.436	0.000	0.000	0.000	0.000	0.034
0.015	0.000	0.000	0.000	0.000	0.105	0.008	0.000	0.000	0.005	0.000	0.000	0.000	0.000	0.000	0.123
0.000	0.016	0.043	0.000	0.000	0.202	0.000	0.000	0.000	0.271	0.006	0.063	0.000	0.000	0.074	0.200
0.000	0.011	0.069	0.061	0.000	0.005	0.265	0.342	0.019	0.032	0.000	0.256	0.518	0.826	0.195	0.307
0.423	0.572	0.116	0.358	0.740	0.087	0.135	0.135	0.135	0.135	0.135	0.135				

Total specified recharge for the San Andres-Glorieta aquifer in the mountains of the Zuni uplift, represented by layer 2

3.52	3.52	3.45	5.31	3.64	0.26	0.62	5.83	1.61	0.14	8.95	0.06	0.15	0.27	0.10	1.52
1.57	0.16	0.00	0.00	0.00	3.41	1.83	0.04	0.00	0.82	0.14	0.00	0.00	0.00	0.00	5.35
0.35	1.53	2.47	0.00	0.00	5.54	0.38	0.08	0.64	6.21	1.73	3.70	0.02	0.10	2.69	6.35
0.14	0.55	1.98	2.41	0.48	0.40	4.23	10.13	0.94	1.58	0.07	6.33	8.66	18.32	7.25	5.71
9.40	17.01	2.54	10.03	13.50	7.24	3.52	3.52	3.52	3.52	3.52	3.52				

Table 17.--Specified recharge for the mountains of the Zuni uplift, in cubic feet per second--Continued

Stress period															
1	2	3	4	5	6	7	8	9	10	11	12	13	14	15	16
17	18	19	20	21	22	23	24	25	26	27	28	29	30	31	32
33	34	35	36	37	38	39	40	41	42	43	44	45	46	47	48
49	50	51	52	53	54	55	56	57	58	59	60	61	62	63	64
65	66	67	68	69	70	71	72	73	74	75	76	77			

Specified recharge for the valley-fill aquifer near the mountains of the Zuni uplift, represented by layer 1

Row 43, column 11, zone 4

0.039	0.039	0.039	0.060	0.039	0.000	0.001	0.075	0.003	0.000	0.110	0.000	0.000	0.000	0.000	0.015
0.009	0.000	0.000	0.000	0.000	0.042	0.007	0.000	0.000	0.002	0.000	0.000	0.000	0.000	0.000	0.052
0.000	0.010	0.015	0.000	0.000	0.062	0.000	0.000	0.000	0.081	0.005	0.029	0.000	0.000	0.025	0.069
0.000	0.004	0.018	0.026	0.000	0.002	0.049	0.117	0.009	0.014	0.000	0.074	0.106	0.224	0.076	0.064
0.111	0.197	0.025	0.116	0.171	0.061	0.039	0.039	0.039	0.039	0.039	0.039				

Row 44, column 10, zone 4

0.039	0.039	0.039	0.060	0.039	0.000	0.001	0.075	0.003	0.000	0.110	0.000	0.000	0.000	0.000	0.015
0.009	0.000	0.000	0.000	0.000	0.042	0.007	0.000	0.000	0.002	0.000	0.000	0.000	0.000	0.000	0.052
0.000	0.010	0.015	0.000	0.000	0.062	0.000	0.000	0.000	0.081	0.005	0.029	0.000	0.000	0.025	0.069
0.000	0.004	0.018	0.026	0.000	0.002	0.049	0.117	0.009	0.014	0.000	0.074	0.106	0.224	0.076	0.064
0.111	0.197	0.025	0.116	0.171	0.061	0.039	0.039	0.039	0.039	0.039	0.039				

Row 44, column 9, zone 4

0.039	0.039	0.039	0.060	0.039	0.000	0.001	0.075	0.003	0.000	0.110	0.000	0.000	0.000	0.000	0.015
0.009	0.000	0.000	0.000	0.000	0.042	0.007	0.000	0.000	0.002	0.000	0.000	0.000	0.000	0.000	0.052
0.000	0.010	0.015	0.000	0.000	0.062	0.000	0.000	0.000	0.081	0.005	0.029	0.000	0.000	0.025	0.069
0.000	0.004	0.018	0.026	0.000	0.002	0.049	0.117	0.009	0.014	0.000	0.074	0.106	0.224	0.076	0.064
0.111	0.197	0.025	0.116	0.171	0.061	0.039	0.039	0.039	0.039	0.039	0.039				

Table 17.--Specified recharge for the mountains of the Zuni uplift, in cubic feet per second--Continued

Stress period															
1	2	3	4	5	6	7	8	9	10	11	12	13	14	15	16
17	18	19	20	21	22	23	24	25	26	27	28	29	30	31	32
33	34	35	36	37	38	39	40	41	42	43	44	45	46	47	48
49	50	51	52	53	54	55	56	57	58	59	60	61	62	63	64
65	66	67	68	69	70	71	72	73	74	75	76	77			

Specified recharge for the valley-fill aquifer near the mountains of the Zuni uplift, represented by layer 1

Row 44, column 8, zone 4

0.039	0.039	0.039	0.060	0.039	0.000	0.001	0.075	0.003	0.000	0.110	0.000	0.000	0.000	0.000	0.015
0.009	0.000	0.000	0.000	0.000	0.042	0.007	0.000	0.000	0.002	0.000	0.000	0.000	0.000	0.000	0.052
0.000	0.010	0.015	0.000	0.000	0.062	0.000	0.000	0.000	0.081	0.005	0.029	0.000	0.000	0.025	0.069
0.000	0.004	0.018	0.026	0.000	0.002	0.049	0.117	0.009	0.014	0.000	0.074	0.106	0.224	0.076	0.064
0.111	0.197	0.025	0.116	0.171	0.061	0.039	0.039	0.039	0.039	0.039	0.039				

Row 45, column 8, zone 4

0.039	0.039	0.039	0.060	0.039	0.000	0.001	0.075	0.003	0.000	0.110	0.000	0.000	0.000	0.000	0.015
0.009	0.000	0.000	0.000	0.000	0.042	0.007	0.000	0.000	0.002	0.000	0.000	0.000	0.000	0.000	0.052
0.000	0.010	0.015	0.000	0.000	0.062	0.000	0.000	0.000	0.081	0.005	0.029	0.000	0.000	0.025	0.069
0.000	0.004	0.018	0.026	0.000	0.002	0.049	0.117	0.009	0.014	0.000	0.074	0.106	0.224	0.076	0.064
0.111	0.197	0.025	0.116	0.171	0.061	0.039	0.039	0.039	0.039	0.039	0.039				

Row 46, column 8, zone 5

0.024	0.024	0.026	0.040	0.024	0.000	0.000	0.036	0.001	0.000	0.079	0.000	0.000	0.000	0.000	0.006
0.003	0.000	0.000	0.000	0.000	0.019	0.001	0.000	0.000	0.001	0.000	0.000	0.000	0.000	0.000	0.022
0.000	0.003	0.008	0.000	0.000	0.037	0.000	0.000	0.000	0.049	0.001	0.011	0.000	0.000	0.013	0.036
0.000	0.002	0.013	0.011	0.000	0.001	0.048	0.062	0.003	0.006	0.000	0.047	0.094	0.150	0.035	0.056
0.077	0.104	0.021	0.065	0.134	0.016	0.024	0.024	0.024	0.024	0.024	0.024				

Table 17.--Specified recharge for the mountains of the Zuni uplift, in cubic feet per second--Continued

Stress period															
1	2	3	4	5	6	7	8	9	10	11	12	13	14	15	16
17	18	19	20	21	22	23	24	25	26	27	28	29	30	31	32
33	34	35	36	37	38	39	40	41	42	43	44	45	46	47	48
49	50	51	52	53	54	55	56	57	58	59	60	61	62	63	64
65	66	67	68	69	70	71	72	73	74	75	76	77			

Specified recharge for the valley-fill aquifer near the mountains of the Zuni uplift, represented by layer 1

Row 47, column 8, zone 5

0.024	0.024	0.026	0.040	0.024	0.000	0.000	0.036	0.001	0.000	0.079	0.000	0.000	0.000	0.000	0.006
0.003	0.000	0.000	0.000	0.000	0.019	0.001	0.000	0.000	0.001	0.000	0.000	0.000	0.000	0.000	0.022
0.000	0.003	0.008	0.000	0.000	0.037	0.000	0.000	0.000	0.049	0.001	0.011	0.000	0.000	0.013	0.036
0.000	0.002	0.013	0.011	0.000	0.001	0.048	0.062	0.003	0.006	0.000	0.047	0.094	0.150	0.035	0.056
0.077	0.104	0.021	0.065	0.134	0.016	0.024	0.024	0.024	0.024	0.024	0.024				

Row 48, column 8, zone 5

0.024	0.024	0.026	0.040	0.024	0.000	0.000	0.036	0.001	0.000	0.079	0.000	0.000	0.000	0.000	0.006
0.003	0.000	0.000	0.000	0.000	0.019	0.001	0.000	0.000	0.001	0.000	0.000	0.000	0.000	0.000	0.022
0.000	0.003	0.008	0.000	0.000	0.037	0.000	0.000	0.000	0.049	0.001	0.011	0.000	0.000	0.013	0.036
0.000	0.002	0.013	0.011	0.000	0.001	0.048	0.062	0.003	0.006	0.000	0.047	0.094	0.150	0.035	0.056
0.077	0.104	0.021	0.065	0.134	0.016	0.024	0.024	0.024	0.024	0.024	0.024				

Row 49, column 7, zone 5

0.033	0.033	0.034	0.053	0.033	0.000	0.001	0.048	0.001	0.000	0.106	0.000	0.000	0.000	0.000	0.008
0.004	0.000	0.000	0.000	0.000	0.026	0.002	0.000	0.000	0.001	0.000	0.000	0.000	0.000	0.000	0.030
0.000	0.004	0.010	0.000	0.000	0.049	0.000	0.000	0.000	0.066	0.001	0.015	0.000	0.000	0.018	0.048
0.000	0.003	0.017	0.015	0.000	0.001	0.064	0.083	0.005	0.008	0.000	0.062	0.125	0.200	0.047	0.074
0.102	0.138	0.028	0.087	0.179	0.021	0.033	0.033	0.033	0.033	0.033	0.033				

Table 17.--Specified recharge for the mountains of the Zuni uplift, in cubic feet per second--Continued

Stress period															
1	2	3	4	5	6	7	8	9	10	11	12	13	14	15	16
17	18	19	20	21	22	23	24	25	26	27	28	29	30	31	32
33	34	35	36	37	38	39	40	41	42	43	44	45	46	47	48
49	50	51	52	53	54	55	56	57	58	59	60	61	62	63	64
65	66	67	68	69	70	71	72	73	74	75	76	77			

Specified recharge for the valley-fill aquifer near the mountains of the Zuni uplift, represented by layer 1

Row 49, column 6, zone 5

0.049	0.049	0.051	0.079	0.049	0.000	0.001	0.071	0.001	0.000	0.158	0.000	0.000	0.000	0.000	0.012
0.005	0.000	0.000	0.000	0.000	0.038	0.003	0.000	0.000	0.002	0.000	0.000	0.000	0.000	0.000	0.045
0.000	0.006	0.015	0.000	0.000	0.073	0.000	0.000	0.000	0.098	0.002	0.023	0.000	0.000	0.027	0.073
0.000	0.004	0.025	0.022	0.000	0.002	0.096	0.124	0.007	0.012	0.000	0.093	0.188	0.300	0.071	0.111
0.153	0.207	0.042	0.130	0.269	0.032	0.049	0.049	0.049	0.049	0.049	0.049				

Row 50, column 5, zone 5

0.065	0.065	0.068	0.105	0.065	0.001	0.001	0.095	0.002	0.000	0.211	0.000	0.000	0.000	0.000	0.016
0.007	0.000	0.000	0.000	0.000	0.051	0.004	0.000	0.000	0.003	0.000	0.000	0.000	0.000	0.000	0.060
0.000	0.008	0.021	0.000	0.000	0.098	0.000	0.000	0.000	0.131	0.003	0.030	0.000	0.000	0.036	0.097
0.000	0.005	0.034	0.030	0.000	0.002	0.128	0.166	0.009	0.016	0.000	0.124	0.251	0.400	0.094	0.149
0.204	0.277	0.056	0.173	0.358	0.042	0.065	0.065	0.065	0.065	0.065	0.065				

Row 50, column 4, zone 5

0.098	0.098	0.102	0.158	0.098	0.001	0.002	0.143	0.003	0.000	0.317	0.000	0.000	0.000	0.000	0.025
0.011	0.000	0.000	0.000	0.000	0.077	0.006	0.000	0.000	0.004	0.000	0.000	0.000	0.000	0.000	0.089
0.000	0.012	0.031	0.000	0.000	0.147	0.000	0.000	0.000	0.197	0.004	0.045	0.000	0.000	0.054	0.145
0.000	0.008	0.050	0.044	0.000	0.004	0.193	0.248	0.014	0.024	0.000	0.186	0.376	0.600	0.141	0.223
0.307	0.415	0.084	0.260	0.537	0.063	0.098	0.098	0.098	0.098	0.098	0.098				

Table 17.--Specified recharge for the mountains of the Zuni uplift, in cubic feet per second--Continued

Stress period															
1	2	3	4	5	6	7	8	9	10	11	12	13	14	15	16
17	18	19	20	21	22	23	24	25	26	27	28	29	30	31	32
33	34	35	36	37	38	39	40	41	42	43	44	45	46	47	48
49	50	51	52	53	54	55	56	57	58	59	60	61	62	63	64
65	66	67	68	69	70	71	72	73	74	75	76	77			

Specified recharge for the valley-fill aquifer near the mountains of the Zuni uplift, represented by layer 1

Row 49, column 3, zone 5

0.033	0.033	0.034	0.053	0.033	0.000	0.001	0.048	0.001	0.000	0.106	0.000	0.000	0.000	0.000	0.008
0.004	0.000	0.000	0.000	0.000	0.026	0.002	0.000	0.000	0.001	0.000	0.000	0.000	0.000	0.000	0.030
0.000	0.004	0.010	0.000	0.000	0.049	0.000	0.000	0.000	0.066	0.001	0.015	0.000	0.000	0.018	0.048
0.000	0.003	0.017	0.015	0.000	0.001	0.064	0.083	0.005	0.008	0.000	0.062	0.125	0.200	0.047	0.074
0.102	0.138	0.028	0.087	0.179	0.021	0.033	0.033	0.033	0.033	0.033	0.033				

Row 48, column 3, zone 5

0.024	0.024	0.026	0.040	0.024	0.000	0.000	0.036	0.001	0.000	0.079	0.000	0.000	0.000	0.000	0.006
0.003	0.000	0.000	0.000	0.000	0.019	0.001	0.000	0.000	0.001	0.000	0.000	0.000	0.000	0.000	0.022
0.000	0.003	0.008	0.000	0.000	0.037	0.000	0.000	0.000	0.049	0.001	0.011	0.000	0.000	0.013	0.036
0.000	0.002	0.013	0.011	0.000	0.001	0.048	0.062	0.003	0.006	0.000	0.047	0.094	0.150	0.035	0.056
0.077	0.104	0.021	0.065	0.134	0.016	0.024	0.024	0.024	0.024	0.024	0.024				

Row 47, column 3, zone 5

0.130	0.130	0.136	0.211	0.130	0.001	0.003	0.191	0.004	0.000	0.422	0.000	0.000	0.000	0.000	0.033
0.015	0.000	0.000	0.000	0.000	0.102	0.007	0.000	0.000	0.005	0.000	0.000	0.000	0.000	0.000	0.119
0.000	0.015	0.041	0.000	0.000	0.196	0.000	0.000	0.000	0.262	0.006	0.061	0.000	0.000	0.071	0.193
0.000	0.011	0.067	0.059	0.000	0.005	0.257	0.331	0.018	0.031	0.000	0.248	0.501	0.799	0.189	0.297
0.409	0.553	0.112	0.347	0.716	0.084	0.130	0.130	0.130	0.130	0.130	0.130				

Table 17.--Specified recharge for the mountains of the Zuni uplift, in cubic feet per second--Concluded

Stress period															
1	2	3	4	5	6	7	8	9	10	11	12	13	14	15	16
17	18	19	20	21	22	23	24	25	26	27	28	29	30	31	32
33	34	35	36	37	38	39	40	41	42	43	44	45	46	47	48
49	50	51	52	53	54	55	56	57	58	59	60	61	62	63	64
65	66	67	68	69	70	71	72	73	74	75	76	77			
Total specified recharge for the valley-fill aquifer near the mountains of the Zuni uplift, represented by layer 1															
0.70	0.70	0.72	1.12	0.70	0.01	0.02	1.11	0.03	0.00	2.19	0.00	0.00	0.00	0.00	0.20
0.10	0.00	0.00	0.00	0.00	0.61	0.07	0.00	0.00	0.03	0.00	0.00	0.00	0.00	0.00	0.72
0.00	0.11	0.23	0.00	0.00	1.07	0.00	0.00	0.00	1.42	0.05	0.38	0.00	0.00	0.40	1.09
0.00	0.06	0.35	0.36	0.00	0.03	1.24	1.87	0.12	0.19	0.00	1.33	2.47	4.22	1.11	1.47
2.14	3.13	0.56	1.92	3.63	0.63	0.70	0.70	0.70	0.70	0.70	0.70				
Total of specified recharge for the mountains of the Zuni uplift and barren basalt, layers 1 and 2															
10.92	10.92	11.65	12.98	12.27	0.27	15.49	6.95	10.96	0.14	26.26	0.06	15.14	0.27	16.70	1.73
13.01	0.16	5.94	0.00	6.62	4.01	14.18	0.04	5.59	3.80	12.62	1.76	9.76	2.97	3.74	9.23
8.22	8.04	9.96	3.44	8.60	13.46	5.83	7.38	9.11	12.34	8.26	8.81	8.91	4.73	9.30	18.36
7.39	8.55	7.64	11.15	5.80	7.61	15.37	17.33	7.68	8.07	5.33	13.68	16.83	30.95	15.83	15.10
18.78	29.23	8.72	20.38	23.95	16.51	10.92	10.92	10.92	10.92	10.92	10.92				

Table 18.--Specified river characteristics that were held constant

[Except for the maximum width of river, these approximate values were used to estimate the river stage and hydraulic conductance for the steady-state and transient simulations. The maximum width of river was used only for the transient]

Model block			River-bed altitude	Length of river in block	Approximate width of river bottom (feet)		Estimated river-bottom thickness	Assumed hydraulic conductivity of river-bottom material	Maximum leakage rate from river
Layer	Row	Column	(feet)	(miles)	Minimum	Maximum	(feet)	(foot per second)	(cubic feet per second)
				Reach 1, Cottonwood Creek					
2	3	6	7,620	1.5	20	20	5	0.0000008	2
2	3	7	7,530	1	20	20	5	0.0000008	2
2	4	8	7,480	1	20	20	100	0.00000000001	2
2	4	9	7,460	1	20	20	200	0.00000000001	2
2	5	10	7,420	1	20	20	200	0.00000000001	2
				Reach 2, Bluewater Lake					
2	6	11	7,400	1	20	400	150	0.00000000001	2
2	7	11	7,390	0.75	20	1,200	135	0.00000000001	2
2	8	11	7,380	0.75	20	2,000	115	0.00000000001	2
2	9	12	7,370	0.75	20	2,100	100	0.00000000001	2
2	10	12	7,365	0.5	20	2,500	50	0.00000000001	4
2	11	12	7,360	0.5	20	2,000	30	0.0000008	4
2	12	12	7,355	0.5	20	2,000	20	0.0000008	4
2	13	12	7,350	0.5	20	1,800	10	0.0000008	4
2	14	12	7,340	0.5	20	2,100	10	0.0000008	4
2	15	12	7,330	0.5	20	3,100	5	0.0000008	4
2	15	13	7,360	0.5	20	2,500	1	0.0000008	4
2	16	11	7,360	0.5	20	2,000	5	0.0000008	4
2	16	12	7,325	0.5	20	1,600	1	0.0000008	4
2	17	11	7,400	0.5	20	1,000	5	0.0000008	4
				Reach 3, Bluewater Creek upstream from Bluewater Lake					
2	19	8	7,520	0.5	20	20	5	0.0000008	2
2	18	9	7,460	1	20	20	5	0.0000008	2
2	18	10	7,420	1	20	20	5	0.0000008	2

Table 18.--Specified river characteristics that were held constant--Continued

Model block			River-bed altitude (feet)	Length of river in block (miles)	Approximate width of river bottom (feet)		Estimated river-bottom thickness (feet)	Assumed hydraulic conductivity of river-bottom material (foot per second)	Maximum leakage rate from river (cubic feet per second)
Layer	Row	Column			Minimum	Maximum			
Reach 4, from Bluewater Lake to station 08342000, "Bluewater Creek near Bluewater"									
2	16	13	7,320	0.75	40	200	2	0.000008	4
2	16	14	7,300	0.75	40	200	2	0.000008	4
2	17	15	7,250	1	40	40	2	0.0000008	4
2	17	16	7,210	0.75	40	40	5	0.0000008	4
2	18	16	7,130	0.75	40	40	5	0.0000008	0
2	19	16	7,050	0.5	40	40	5	0.0000008	0
2	20	16	6,970	0.75	40	40	5	0.0000008	0
2	21	17	6,910	0.5	40	40	5	0.0000008	0
2	21	18	6,860	0.25	40	40	5	0.0000008	4
2	22	18	6,800	1	40	40	5	0.0000008	0
Reach 5, from station 08342000 to station 08343000, "Rio San Jose at Grants"									
2	23	18	6,680	0.75	40	40	10	0.0000012	4
2	24	19	6,640	1	40	40	20	0.0000012	4
1	25	19	6,630	1	40	40	30	0.0000008	4
1	26	19	6,620	1	40	40	40	0.0000008	4
1	27	18	6,610	1.25	40	40	48	0.0000008	2
1	28	18	6,590	1	40	40	45	0.0000008	2
1	29	19	6,570	1.25	40	40	40	0.0000008	2
1	30	20	6,560	1.25	20	20	39	0.0000008	2
1	31	19	6,560	0.5	20	20	36	0.0000008	2
1	31	20	6,550	0.5	20	20	33	0.0000008	2
1	32	20	6,540	0.75	20	20	30	0.0000008	2
1	33	20	6,535	1	20	20	27	0.0000008	2
1	34	19	6,525	0.75	20	20	24	0.0000008	2
1	34	18	6,520	0.75	20	20	21	0.0000008	2
1	35	17	6,510	0.75	20	20	18	0.0000008	2
1	36	16	6,505	0.75	20	20	15	0.0000008	2
1	37	15	6,495	0.5	20	20	12	0.0000008	2
1	38	15	6,490	0.5	20	20	9	0.0000008	2
1	39	16	6,480	0.5	20	20	6	0.0000008	2
1	40	16	6,460	0.5	20	20	5	0.0000008	2
Reach 6, from station 08343000 to first sewage outfall									
1	41	17	6,440	1	20	20	5	0.0000008	2
1	42	18	6,420	0.5	20	20	5	0.0000008	2

Table 18.--Specified river characteristics that were held constant--Concluded

Model block			River-bed altitude (feet)	Length of river in block (miles)	Approximate width of river bottom (feet)		Estimated river-bottom thickness (feet)	Assumed hydraulic conductivity of river-bottom material (foot per second)	Maximum leakage rate from river (cubic feet per second)
Layer	Row	Column			Minimum	Maximum			
Reach 7, from first sewage outfall to second sewage outfall									
1	43	18	6,418	0.5	20	20	5	0.0000008	2
1	44	18	6,415	0.5	20	20	5	0.0000008	2
1	45	17	6,410	0.75	20	20	5	0.0000008	2
Reach 8, from second sewage outfall to confluence of Gallo Creek									
1	46	17	6,40	0.75	20	20	5	0.0000008	2
Reach 9, Ojo del Gallo									
2	41	15	6,453	0.5	1	1	1	0.0005682	4
2	42	14	6,453	0.5	1	1	1	0.0005682	4
2	42	13	6,452	0.5	1	1	1	0.0005682	4
2	42	12	6,452	0.5	1	1	1	0.0005682	4
Reach 10, La Vega and Gallo Creek									
1	43	12	6,445	0.5	200	200	5	0.0000008	4
1	44	12	6,440	0.25	200	200	5	0.0000008	4
1	44	11	6,440	0.5	200	200	5	0.0000008	4
1	45	11	6,435	0.25	200	200	5	0.0000008	4
1	45	12	6,435	0.75	200	200	5	0.0000008	4
1	45	13	6,430	0.5	200	200	5	0.0000008	4
1	46	13	6,428	0.25	200	200	5	0.0000008	4
1	46	14	6,425	1	50	50	5	0.0000008	4
1	47	15	6,410	0.5	20	20	5	0.0000008	2
1	47	16	6,400	0.75	20	20	5	0.0000008	2
Reach 11, Rio San Jose from Gallo Creek to station 08343500, "Rio San Jose near Grants"									
1	48	17	6,380	0.75	20	20	5	0.0000008	2
1	49	17	6,360	1	20	20	5	0.0000008	2
1	50	17	6,320	1.25	20	20	5	0.0000008	2
1	51	18	6,305	1.25	20	20	5	0.0000008	2
1	52	17	6,275	1	20	20	5	0.0000947	2

Table 19.--Specified river characteristics that were varied with time for the standard scenario

[Other scenarios except the null had the same variable river characteristics as the standard. The beginning of a stress period is the same as the end of the previous stress period. Stress period 1 begins in 1900.0 (October 1, 1899)]

Stress period	End of period (semi-water year)	Average lake altitude (feet)	Specified inflow at upper ends of river reaches (cubic feet per second)					
			Reach 1 (Cotton-wood Creek)	Reach 2 (lake)	Reach 3 (Bluewater Creek upstream from lake)	Reach 5 (Bluewater Creek near Bluewater)	Reach 7 (first sewage outfall)	Reach 8 (second sewage outfall)
1	1,928.0	7,325.00	3.90	20.00	9.10	4.51	0.00	0.00
2	1,932.0	7,356.00	2.26	20.00	5.42	3.40	0.00	0.00
3	1,936.0	7,371.00	3.81	20.00	8.82	6.55	0.00	0.00
4	1,940.0	7,379.00	5.57	20.00	12.98	7.55	0.00	0.00
5	1,944.0	7,380.00	4.40	20.00	10.21	14.52	0.00	0.00
6	1,944.5	7,374.00	0.13	20.00	0.71	5.06	0.00	0.00
7	1,945.0	7,359.00	1.41	20.00	3.52	8.23	0.00	0.00
8	1,945.5	7,347.00	4.95	20.00	12.49	0.46	0.00	0.00
9	1,946.0	7,356.00	5.54	20.00	11.94	4.42	0.00	0.00
10	1,946.5	7,346.00	0.22	20.00	0.56	0.37	0.00	0.00
11	1,947.0	7,350.00	5.62	20.00	13.85	0.50	0.00	0.00
12	1,947.5	7,361.00	0.09	20.00	0.21	0.99	0.00	0.00
13	1,948.0	7,362.00	0.12	20.00	0.50	0.85	0.00	0.00
14	1,948.5	7,363.00	0.19	20.00	0.91	1.15	0.14	0.00
15	1,949.0	7,375.00	0.57	20.00	1.17	9.36	0.14	0.00
16	1,949.5	7,370.00	1.13	20.00	3.36	2.29	0.15	0.00
17	1,950.0	7,374.00	3.99	20.00	8.99	9.86	0.15	0.00
18	1,950.5	7,367.00	0.14	20.00	0.52	1.85	0.16	0.00
19	1,951.0	7,366.00	0.00	20.00	0.00	1.15	0.17	0.00
20	1,951.5	7,364.00	0.00	20.00	0.00	0.95	0.17	0.00
21	1,952.0	7,363.00	0.00	20.00	0.00	0.67	0.17	0.00
22	1,952.5	7,362.00	2.34	20.00	6.78	0.74	0.17	0.00
23	1,953.0	7,361.00	6.18	20.00	13.12	6.54	0.17	0.00
24	1,953.5	7,360.00	0.08	20.00	0.14	1.99	0.19	0.00
25	1,954.0	7,358.00	0.00	20.00	0.02	0.99	0.21	0.00
26	1,954.5	7,357.00	1.48	20.00	4.07	0.74	0.22	0.00
27	1,955.0	7,356.00	0.53	20.00	1.17	1.13	0.24	0.00
28	1,955.5	7,354.00	0.01	20.00	0.00	0.77	0.25	0.00
29	1,956.0	7,352.00	0.01	20.00	0.00	0.62	0.25	0.00
30	1,956.5	7,350.00	0.00	20.00	0.00	0.41	0.28	0.00

Table 19.--Specified river characteristics that were varied with time for the standard scenario--Continued

Stress period	End of period (semi-water year)	Average lake altitude (feet)	Specified inflow at upper ends of river reaches (cubic feet per second)					
			Reach 1 (Cotton-wood Creek)	Reach 2 (lake)	Reach 3 (Bluewater Creek upstream from lake)	Reach 5 (Bluewater Creek near Bluewater)	Reach 7 (first sewage outfall)	Reach 8 (second sewage outfall)
31	1,957.0	7,347.00	0.00	20.00	0.00	0.29	0.30	0.00
32	1,957.5	7,359.00	8.59	20.00	18.05	0.21	0.33	0.00
33	1,958.0	7,370.00	0.89	20.00	3.85	0.72	0.00	0.36
34	1,958.5	7,376.00	2.85	20.00	5.95	1.06	0.00	0.39
35	1,959.0	7,378.00	3.79	20.00	10.14	3.03	0.00	0.41
36	1,959.5	7,375.00	0.00	20.00	0.00	2.06	0.00	0.44
37	1,960.0	7,372.00	0.00	20.00	0.00	1.54	0.00	0.46
38	1,960.5	7,372.00	5.38	20.00	12.33	1.61	0.00	0.49
39	1,961.0	7,379.00	1.58	20.00	4.15	3.38	0.00	0.52
40	1,961.5	7,376.00	0.29	20.00	0.50	1.92	0.00	0.55
41	1,962.0	7,375.00	1.66	20.00	4.37	0.89	0.00	0.57
42	1,962.5	7,374.00	3.96	20.00	10.56	1.97	0.00	0.62
43	1,963.0	7,381.00	5.54	20.00	11.82	7.76	0.00	1.51
44	1,963.5	7,374.00	5.76	20.00	13.80	2.06	0.00	0.85
45	1,964.0	7,371.00	0.01	20.00	0.43	4.46	0.00	1.33
46	1,964.5	7,368.00	0.06	20.00	0.24	1.25	0.00	0.68
47	1,965.5	7,371.00	2.66	20.00	7.12	3.91	0.00	0.95
48	1,966.5	7,376.00	9.17	20.00	20.17	3.84	0.00	0.90
49	1,967.5	7,376.00	0.34	20.00	1.47	3.92	0.00	1.01
50	1,968.5	7,367.00	0.20	20.00	0.98	1.58	0.00	0.99
51	1,969.5	7,371.00	2.58	20.00	6.12	1.09	0.00	1.05
52	1,970.5	7,375.00	4.06	20.00	8.99	3.06	0.00	1.04
53	1,971.5	7,371.00	1.36	20.00	3.20	1.44	0.00	1.31
54	1,972.5	7,367.00	0.30	20.00	1.09	1.08	0.00	1.36
55	1,973.5	7,366.00	0.75	20.00	2.57	0.38	0.00	1.06
56	1,974.5	7,397.00	14.62	20.00	32.37	6.83	0.00	1.33
57	1,975.5	7,386.00	0.76	20.00	2.45	7.50	0.00	1.27
58	1,976.5	7,388.00	3.24	20.00	7.19	6.77	0.00	1.38
59	1,977.5	7,370.00	0.06	20.00	0.21	7.09	0.00	1.35
60	1,978.5	7,363.00	6.96	20.00	15.13	2.89	0.00	1.75
61	1,979.5	7,369.00	2.24	20.00	7.51	13.73	0.00	1.74
62	1,980.5	7,391.00	18.26	20.00	41.92	15.19	0.00	3.05
63	1,981.5	7,398.00	12.80	20.00	27.86	11.45	0.00	2.01
64	1,982.5	7,388.00	2.94	20.00	8.07	12.98	0.00	1.77
65	1,983.5	7,390.00	8.71	20.00	20.36	10.30	0.00	1.59

Table 19.--Specified river characteristics that were varied with time for the standard scenario--Concluded

Stress period	End of period (semi-water year)	Average lake altitude (feet)	Specified inflow at upper ends of river reaches (cubic feet per second)					
			Reach 1 (Cotton-wood Creek)	Reach 2 (lake)	Reach 3 (Bluewater Creek upstream from lake)	Reach 5 (Bluewater Creek near Bluewater)	Reach 7 (first sewage outfall)	Reach 8 (second sewage outfall)
66	1,984.0	7,401.00	25.69	20.00	56.52	11.08	0.00	1.93
67	1,984.5	7,397.00	0.51	20.00	2.50	8.22	0.00	1.09
68	1,985.0	7,394.00	14.71	20.00	32.43	38.77	0.00	2.07
69	1,985.5	7,392.00	5.32	20.00	15.13	3.60	0.00	1.10
70	1,986.0	7,400.00	18.74	20.00	39.82	9.26	0.00	1.82
71-76	2,021.0	7,372.00	3.90	20.00	9.10	4.37	0.00	1.93

Table 20.--Specified rates of underflow for the valley-fill aquifer at Mitchell Draw, San Mateo Creek, Grants Canyon, and the Rio San Jose downstream from Horace Springs

[Locations shown in figure 25]

Stress period															
1	2	3	4	5	6	7	8	9	10	11	12	13	14	15	16
17	18	19	20	21	22	23	24	25	26	27	28	29	30	31	32
33	34	35	36	37	38	39	40	41	42	43	44	45	46	47	48
49	50	51	52	53	54	55	56	57	58	59	60	61	62	63	64
65	66	67	68	69	70	71	72	73	74	75	76	77			
Row 18, column 23, layer 1, Mitchell Draw															
0.600	0.600	0.669	0.586	0.709	0.000	1.328	0.000	0.833	0.000	1.352	0.000	1.340	0.000	1.485	0.000
1.014	0.000	0.531	0.000	0.592	0.000	1.099	0.000	0.500	0.263	1.117	0.157	0.873	0.266	0.334	0.282
0.704	0.572	0.648	0.308	0.769	0.613	0.488	0.653	0.758	0.421	0.579	0.423	0.796	0.414	0.555	0.976
0.648	0.710	0.475	0.749	0.475	0.643	0.885	0.477	0.593	0.563	0.471	0.538	0.509	0.752	0.668	0.708
0.647	0.812	0.502	0.753	0.610	0.773	0.600	0.600	0.600	0.600	0.600	0.600				
Row 33, column 24, layer 1, San Mateo Creek															
0.000	0.000	0.000	0.000	0.000	0.000	0.000	0.000	0.000	0.000	0.000	0.000	0.000	0.000	0.000	0.000
0.000	0.000	0.000	0.000	0.000	0.000	0.000	0.000	0.000	0.000	0.000	0.000	0.000	0.000	0.750	0.750
0.750	0.750	0.750	0.750	0.750	0.750	0.750	0.750	0.750	0.750	0.750	0.750	0.750	0.750	0.750	0.750
0.750	0.750	0.750	0.750	0.750	0.750	0.750	0.750	0.750	0.750	0.750	0.750	0.750	0.750	0.750	0.000
0.000	0.000	0.000	0.000	0.000	0.000	0.000	0.000	0.000	0.000	0.000	0.000				
Row 34, column 24, layer 1, San Mateo Creek															
0.699	0.699	0.780	0.683	0.827	0.000	1.549	0.000	0.972	0.000	1.577	0.000	1.563	0.000	1.732	0.000
1.183	0.000	0.620	0.000	0.690	0.000	1.282	0.000	0.583	0.307	1.303	0.183	1.018	0.310	1.140	1.080
1.571	1.418	1.506	1.109	1.647	1.466	1.319	1.512	1.635	1.242	1.426	1.243	1.678	1.233	1.398	1.889
1.506	1.578	1.304	1.624	1.304	1.500	1.782	1.306	1.442	1.407	1.299	1.378	1.344	1.628	1.529	0.826
0.755	0.948	0.586	0.879	0.711	0.901	0.699	0.699	0.699	0.699	0.699	0.699				

Table 20.--Specified rates of underflow for the valley-fill aquifer at Mitchell Draw, San Mateo Creek, Grants Canyon, and the Rio San Jose downstream from Horace Springs--Continued

Stress period															
1	2	3	4	5	6	7	8	9	10	11	12	13	14	15	16
17	18	19	20	21	22	23	24	25	26	27	28	29	30	31	32
33	34	35	36	37	38	39	40	41	42	43	44	45	46	47	48
49	50	51	52	53	54	55	56	57	58	59	60	61	62	63	64
65	66	67	68	69	70	71	72	73	74	75	76	77			
Row 44, column 20, layer 1, Grants Canyon															
0.300	0.300	0.334	0.293	0.355	0.000	0.664	0.000	0.416	0.000	0.676	0.000	0.670	0.000	0.742	0.000
0.507	0.000	0.266	0.000	0.296	0.000	0.549	0.000	0.250	0.132	0.558	0.078	0.436	0.133	0.167	0.141
0.352	0.286	0.324	0.154	0.385	0.307	0.244	0.327	0.379	0.211	0.290	0.211	0.398	0.207	0.278	0.488
0.324	0.355	0.238	0.375	0.238	0.321	0.442	0.238	0.296	0.282	0.235	0.269	0.254	0.376	0.334	0.354
0.324	0.406	0.251	0.377	0.305	0.386	0.300	0.300	0.300	0.300	0.300	0.300				
Row 52, column 17, layer 1, Rio San Jose downstream from Horace Springs															
-2.500	-2.500	-2.500	-2.500	-2.500	-2.500	-2.500	-2.500	-2.500	-2.500	-2.500	-2.500	-2.500	-2.500	-2.500	-2.500
-2.500	-2.500	-2.500	-2.500	-2.500	-2.500	-2.500	-2.500	-2.500	-2.500	-2.500	-2.500	-2.500	-2.500	-2.500	-2.500
-2.500	-2.500	-2.500	-2.500	-2.500	-2.500	-2.500	-2.500	-2.500	-2.500	-2.500	-2.500	-2.500	-2.500	-2.500	-2.500
-2.500	-2.500	-2.500	-2.500	-2.500	-2.500	-2.500	-2.500	-2.500	-2.500	-2.500	-2.500	-2.500	-2.500	-2.500	-2.500
-2.500	-2.500	-2.500	-2.500	-2.500	-2.500	-2.500	-2.500	-2.500	-2.500	-2.500	-2.500				
Total inflow															
1.60	1.60	1.78	1.56	1.89	0.00	3.54	0.00	2.22	0.00	3.61	0.00	3.57	0.00	3.96	0.00
2.70	0.00	1.42	0.00	1.58	0.00	2.93	0.00	1.33	0.70	2.98	0.42	2.33	0.71	2.39	2.25
3.38	3.03	3.23	2.32	3.55	3.14	2.80	3.24	3.52	2.62	3.05	2.63	3.62	2.60	2.98	4.10
3.23	3.39	2.77	3.50	2.77	3.21	3.86	2.77	3.08	3.00	2.76	2.94	2.86	3.51	3.28	1.89
1.73	2.17	1.34	2.01	1.63	2.06	1.60	1.60	1.60	1.60	1.60	1.60				

Table 20.--Specified rates of underflow for the valley-fill aquifer at Mitchell Draw, San Mateo Creek, Grants Canyon, and the Rio San Jose downstream from Horace Springs--Concluded

Stress period															
1	2	3	4	5	6	7	8	9	10	11	12	13	14	15	16
17	18	19	20	21	22	23	24	25	26	27	28	29	30	31	32
33	34	35	36	37	38	39	40	41	42	43	44	45	46	47	48
49	50	51	52	53	54	55	56	57	58	59	60	61	62	63	64
65	66	67	68	69	70	71	72	73	74	75	76	77			
Total outflow															
-2.50	-2.50	-2.50	-2.50	-2.50	-2.50	-2.50	-2.50	-2.50	-2.50	-2.50	-2.50	-2.50	-2.50	-2.50	-2.50
-2.50	-2.50	-2.50	-2.50	-2.50	-2.50	-2.50	-2.50	-2.50	-2.50	-2.50	-2.50	-2.50	-2.50	-2.50	-2.50
-2.50	-2.50	-2.50	-2.50	-2.50	-2.50	-2.50	-2.50	-2.50	-2.50	-2.50	-2.50	-2.50	-2.50	-2.50	-2.50
-2.50	-2.50	-2.50	-2.50	-2.50	-2.50	-2.50	-2.50	-2.50	-2.50	-2.50	-2.50	-2.50	-2.50	-2.50	-2.50
-2.50	-2.50	-2.50	-2.50	-2.50	-2.50	-2.50	-2.50	-2.50	-2.50	-2.50	-2.50				
Total combined flow															
-0.90	-0.90	-0.72	-0.94	-0.61	-2.50	1.04	-2.50	-0.28	-2.50	1.11	-2.50	1.07	-2.50	1.46	-2.50
0.20	-2.50	-1.08	-2.50	-0.92	-2.50	0.43	-2.50	-1.17	-1.80	0.48	-2.08	-0.17	-1.79	-0.11	-0.25
0.88	0.53	0.73	-0.18	1.05	0.64	0.30	0.74	1.02	0.12	0.55	0.13	1.12	0.10	0.48	1.60
0.73	0.89	0.27	1.00	0.27	0.71	1.36	0.27	0.58	0.50	0.26	0.44	0.36	1.01	0.78	-0.61
-0.77	-0.33	-1.16	-0.49	-0.87	-0.44	-0.90	-0.90	-0.90	-0.90	-0.90	-0.90				

Table 21.--Specified hydraulic heads and conductances for the general-head boundary

Model			Specified hydraulic head (feet)	Specified hydraulic conductance (feet squared per second)	Model			Specified hydraulic head (feet)	Specified hydraulic conductance (feet squared per second)
Layer	Row	Column			Layer	Row	Column		
2	76	1	5,400	0.00076810	2	70	41	5,400	0.00029476
2	76	2	5,400	0.00049979	2	69	41	5,400	0.00006741
2	76	3	5,400	0.00039983	2	68	42	5,500	0.00027624
2	76	4	5,400	0.00029987	2	67	42	5,500	0.00004889
2	75	5	5,950	0.00060627	2	66	43	5,600	0.00038992
2	75	6	5,950	0.00045471	2	65	43	5,600	0.00004889
2	75	7	5,950	0.00030314	2	64	43	5,600	0.00004889
2	75	8	5,950	0.00022735	2	63	43	5,700	0.00004889
2	75	9	5,950	0.00022735	2	62	43	5,700	0.00004889
2	75	10	5,950	0.00179175	2	61	43	5,700	0.00004889
2	74	11	5,950	0.00011368	2	60	43	5,700	0.00004889
2	74	12	5,950	0.00007578	2	59	43	5,700	0.00004889
2	74	13	5,950	0.00007578	2	58	43	5,700	0.00004889
2	74	14	5,950	0.00007578	2	57	43	5,700	0.00004889
2	74	15	5,950	0.00007578	2	56	43	5,700	0.00004889
2	74	16	5,950	0.00007578	2	55	43	5,700	0.00004889
2	74	17	5,950	0.00007578	2	54	43	5,700	0.00004889
2	74	18	5,950	0.00011368	2	53	43	5,700	0.00004889
2	74	19	5,950	0.00011368	2	52	43	5,700	0.00004889
2	74	20	5,950	0.00011368	2	51	43	5,700	0.00004889
2	74	21	5,950	0.00011368	2	50	43	5,700	0.00004889
2	74	22	5,950	0.00015157	2	49	43	5,800	0.00004889
2	74	23	5,950	0.00015157	2	48	43	5,800	0.00003667
2	74	24	5,950	0.00093377	2	47	43	5,800	0.00003667
2	73	25	5,100	0.00005684	2	46	43	5,800	0.00003667
2	73	26	5,100	0.00005684	2	45	43	5,800	0.00003667
2	73	27	5,100	0.00005684	2	44	43	5,800	0.00002444
2	73	28	5,100	0.00005684	2	43	43	5,800	0.00002444
2	73	29	5,100	0.00005684	2	42	43	5,800	0.00002444
2	73	30	5,100	0.00005684	2	41	43	5,800	0.00002444
2	73	31	5,100	0.00025239	2	40	43	5,800	0.00002444
2	72	32	5,200	0.00005684	2	39	43	5,900	0.00002444
2	72	33	5,200	0.00005684	2	38	43	5,900	0.00002444
2	72	34	5,200	0.00005684	2	37	43	5,900	0.00002444
2	72	35	5,200	0.00005684	2	36	43	5,900	0.00002444
2	72	36	5,200	0.00005684	2	35	43	5,900	0.00002444
2	72	37	5,200	0.00005684	2	34	43	5,900	0.00003667
2	72	38	5,200	0.00023192	2	33	43	5,900	0.00003667
2	71	39	5,300	0.00011368	2	32	43	5,900	0.00003667
2	71	40	5,300	0.00026829	2	31	43	5,900	0.00003667
2	30	43	5,900	0.00004889					

Table 22.--Specified irrigation ground-water withdrawals and recharge, in cubic feet per second

[Irrigated areas shown in figure 31]

Stress period															
1	2	3	4	5	6	7	8	9	10	11	12	13	14	15	16
17	18	19	20	21	22	23	24	25	26	27	28	29	30	31	32
33	34	35	36	37	38	39	40	41	42	43	44	45	46	47	48
49	50	51	52	53	54	55	56	57	58	59	60	61	62	63	64
65	66	67	68	69	70	71	72	73	74	75	76	77			

Row 26, column 19, layer 2, Bluewater-Toltec

0.000	0.000	0.000	0.000	0.000	0.000	0.000	0.000	-1.274	0.000	-3.276	0.000	-3.750	0.000	-3.386	0.000
-2.512	0.000	-4.296	0.000	-4.478	0.000	-3.786	0.000	-4.368	0.000	-4.587	0.000	-4.186	0.000	-3.349	0.000
-2.439	0.000	-2.512	0.000	-2.548	0.000	-2.548	0.000	-0.692	0.000	-0.692	0.000	-0.692	0.000	-0.346	-0.346
-0.346	-0.546	-0.764	-0.328	-0.764	-0.764	-0.764	0.000	0.000	0.000	0.000	-0.910	-0.364	0.000	0.000	0.000
0.000	0.000	0.000	0.000	0.000	0.000	-0.510	-0.510	-0.510	-0.510	-0.510	-0.510				

Row 27, column 18, layer 2, Bluewater-Toltec

0.000	0.000	0.000	0.000	0.000	0.000	0.000	0.000	-0.425	0.000	-1.092	0.000	-1.250	0.000	-1.128	0.000
-0.837	0.000	-1.432	0.000	-1.492	0.000	-1.262	0.000	-1.456	0.000	-1.529	0.000	-1.395	0.000	-1.116	0.000
-0.813	0.000	-0.837	0.000	-0.849	0.000	-0.849	0.000	-0.231	0.000	-0.231	0.000	-0.231	0.000	-0.115	-0.115
-0.115	-0.182	-0.255	-0.109	-0.255	-0.255	-0.255	0.000	0.000	0.000	0.000	-0.303	-0.121	0.000	0.000	0.000
0.000	0.000	0.000	0.000	0.000	0.000	-0.170	-0.170	-0.170	-0.170	-0.170	-0.170				

Row 27, column 19, layer 2, Bluewater-Toltec

0.000	0.000	0.000	0.000	0.000	0.000	0.000	0.000	-0.425	0.000	-1.092	0.000	-1.250	0.000	-1.128	0.000
-0.837	0.000	-1.432	0.000	-1.492	0.000	-1.262	0.000	-1.456	0.000	-1.529	0.000	-1.395	0.000	-1.116	0.000
-0.813	0.000	-0.837	0.000	-0.849	0.000	-0.849	0.000	-0.231	0.000	-0.231	0.000	-0.231	0.000	-0.115	-0.115
-0.115	-0.182	-0.255	-0.109	-0.255	-0.255	-0.255	0.000	0.000	0.000	0.000	-0.303	-0.121	0.000	0.000	0.000
0.000	0.000	0.000	0.000	0.000	0.000	-0.170	-0.170	-0.170	-0.170	-0.170	-0.170				

Table 22.--Specified irrigation ground-water withdrawals and recharge, in cubic feet per second--Continued

Stress period															
1	2	3	4	5	6	7	8	9	10	11	12	13	14	15	16
17	18	19	20	21	22	23	24	25	26	27	28	29	30	31	32
33	34	35	36	37	38	39	40	41	42	43	44	45	46	47	48
49	50	51	52	53	54	55	56	57	58	59	60	61	62	63	64
65	66	67	68	69	70	71	72	73	74	75	76	77			

Row 28, column 18, layer 2, Bluewater-Toltec

0.000	0.000	0.000	0.000	0.000	0.000	0.000	0.000	-0.425	0.000	-1.092	0.000	-1.250	0.000	-1.128	0.000
-0.837	0.000	-1.432	0.000	-1.492	0.000	-1.262	0.000	-1.456	0.000	-1.529	0.000	-1.395	0.000	-1.116	0.000
-0.813	0.000	-0.837	0.000	-0.849	0.000	-0.849	0.000	-0.231	0.000	-0.231	0.000	-0.231	0.000	-0.115	-0.115
-0.115	-0.182	-0.255	-0.109	-0.255	-0.255	-0.255	0.000	0.000	0.000	0.000	-0.303	-0.121	0.000	0.000	0.000
0.000	0.000	0.000	0.000	0.000	0.000	-0.170	-0.170	-0.170	-0.170	-0.170	-0.170				

Row 29, column 18, layer 2, Bluewater-Toltec

0.000	0.000	0.000	0.000	0.000	0.000	0.000	0.000	-0.425	0.000	-1.092	0.000	-1.250	0.000	-1.128	0.000
-0.837	0.000	-1.432	0.000	-1.492	0.000	-1.262	0.000	-1.456	0.000	-1.529	0.000	-1.395	0.000	-1.116	0.000
-0.813	0.000	-0.837	0.000	-0.849	0.000	-0.849	0.000	-0.231	0.000	-0.231	0.000	-0.231	0.000	-0.115	-0.115
-0.115	-0.182	-0.255	-0.109	-0.255	-0.255	-0.255	0.000	0.000	0.000	0.000	-0.303	-0.121	0.000	0.000	0.000
0.000	0.000	0.000	0.000	0.000	0.000	-0.170	-0.170	-0.170	-0.170	-0.170	-0.170				

Row 29, column 19, layer 2, Bluewater-Toltec

0.000	0.000	0.000	0.000	0.000	0.000	0.000	0.000	-0.849	0.000	-2.184	0.000	-2.500	0.000	-2.257	0.000
-1.675	0.000	-2.864	0.000	-2.985	0.000	-2.524	0.000	-2.912	0.000	-3.058	0.000	-2.791	0.000	-2.233	0.000
-1.626	0.000	-1.675	0.000	-1.699	0.000	-1.699	0.000	-0.461	0.000	-0.461	0.000	-0.461	0.000	-0.231	-0.231
-0.231	-0.364	-0.510	-0.218	-0.510	-0.510	-0.510	0.000	0.000	0.000	0.000	-0.607	-0.243	0.000	0.000	0.000
0.000	0.000	0.000	0.000	0.000	0.000	-0.340	-0.340	-0.340	-0.340	-0.340	-0.340				

Table 22.--Specified irrigation ground-water withdrawals and recharge, in cubic feet per second--Continued

Stress period															
1	2	3	4	5	6	7	8	9	10	11	12	13	14	15	16
17	18	19	20	21	22	23	24	25	26	27	28	29	30	31	32
33	34	35	36	37	38	39	40	41	42	43	44	45	46	47	48
49	50	51	52	53	54	55	56	57	58	59	60	61	62	63	64
65	66	67	68	69	70	71	72	73	74	75	76	77			

Row 30, column 19, layer 2, Bluewater-Toltec

0.000	0.000	0.000	0.000	0.000	0.000	0.000	0.000	-0.849	0.000	-2.184	0.000	-2.500	0.000	-2.257	0.000
-1.675	0.000	-2.864	0.000	-2.985	0.000	-2.524	0.000	-2.912	0.000	-3.058	0.000	-2.791	0.000	-2.233	0.000
-1.626	0.000	-1.675	0.000	-1.699	0.000	-1.699	0.000	-0.461	0.000	-0.461	0.000	-0.461	0.000	-0.231	-0.231
-0.231	-0.364	-0.510	-0.218	-0.510	-0.510	-0.510	0.000	0.000	0.000	0.000	-0.607	-0.243	0.000	0.000	0.000
0.000	0.000	0.000	0.000	0.000	0.000	-0.340	-0.340	-0.340	-0.340	-0.340	-0.340				

Row 30, column 20, layer 2, Bluewater-Toltec

0.000	0.000	0.000	0.000	0.000	0.000	0.000	0.000	-0.425	0.000	-1.092	0.000	-1.250	0.000	-1.128	0.000
-0.837	0.000	-1.432	0.000	-1.492	0.000	-1.262	0.000	-1.456	0.000	-1.529	0.000	-1.395	0.000	-1.116	0.000
-0.813	0.000	-0.837	0.000	-0.849	0.000	-0.849	0.000	-0.231	0.000	-0.231	0.000	-0.231	0.000	-0.115	-0.115
-0.115	-0.182	-0.255	-0.109	-0.255	-0.255	-0.255	0.000	0.000	0.000	0.000	-0.303	-0.121	0.000	0.000	0.000
0.000	0.000	0.000	0.000	0.000	0.000	-0.170	-0.170	-0.170	-0.170	-0.170	-0.170				

Row 31, column 19, layer 2, Bluewater-Toltec

0.000	0.000	0.000	0.000	0.000	0.000	0.000	0.000	-0.319	0.000	-0.819	0.000	-0.938	0.000	-0.846	0.000
-0.628	0.000	-1.074	0.000	-1.120	0.000	-0.947	0.000	-1.092	0.000	-1.147	0.000	-1.047	0.000	-0.837	0.000
-0.610	0.000	-0.628	0.000	-0.637	0.000	-0.637	0.000	-0.173	0.000	-0.173	0.000	-0.173	0.000	-0.086	-0.086
-0.086	-0.137	-0.191	-0.082	-0.191	-0.191	-0.191	0.000	0.000	0.000	0.000	-0.228	-0.091	0.000	0.000	0.000
0.000	0.000	0.000	0.000	0.000	0.000	-0.127	-0.127	-0.127	-0.127	-0.127	-0.127				

Table 22.--Specified irrigation ground-water withdrawals and recharge, in cubic feet per second--Continued

Stress period															
1	2	3	4	5	6	7	8	9	10	11	12	13	14	15	16
17	18	19	20	21	22	23	24	25	26	27	28	29	30	31	32
33	34	35	36	37	38	39	40	41	42	43	44	45	46	47	48
49	50	51	52	53	54	55	56	57	58	59	60	61	62	63	64
65	66	67	68	69	70	71	72	73	74	75	76	77			

Row 31, column 20, layer 2, Bluewater-Toltec

0.000	0.000	0.000	0.000	0.000	0.000	0.000	0.000	-0.319	0.000	-0.819	0.000	-0.938	0.000	-0.846	0.000
-0.628	0.000	-1.074	0.000	-1.120	0.000	-0.947	0.000	-1.092	0.000	-1.147	0.000	-1.047	0.000	-0.837	0.000
-0.610	0.000	-0.628	0.000	-0.637	0.000	-0.637	0.000	-0.173	0.000	-0.173	0.000	-0.173	0.000	-0.086	-0.086
-0.086	-0.137	-0.191	-0.082	-0.191	-0.191	-0.191	0.000	0.000	0.000	0.000	-0.228	-0.091	0.000	0.000	0.000
0.000	0.000	0.000	0.000	0.000	0.000	-0.127	-0.127	-0.127	-0.127	-0.127	-0.127				

Row 32, column 19, layer 2, Bluewater-Toltec

0.000	0.000	0.000	0.000	0.000	0.000	0.000	0.000	-0.637	0.000	-1.638	0.000	-1.875	0.000	-1.693	0.000
-1.256	0.000	-2.148	0.000	-2.239	0.000	-1.893	0.000	-2.184	0.000	-2.293	0.000	-2.093	0.000	-1.675	0.000
-1.220	0.000	-1.256	0.000	-1.274	0.000	-1.274	0.000	-0.346	0.000	-0.346	0.000	-0.346	0.000	-0.173	-0.173
-0.173	-0.273	-0.382	-0.164	-0.382	-0.382	-0.382	0.000	0.000	0.000	0.000	-0.455	-0.182	0.000	0.000	0.000
0.000	0.000	0.000	0.000	0.000	0.000	-0.255	-0.255	-0.255	-0.255	-0.255	-0.255				

Row 32, column 20, layer 2, Bluewater-Toltec

0.000	0.000	0.000	0.000	0.000	0.000	0.000	0.000	-0.319	0.000	-0.819	0.000	-0.938	0.000	-0.846	0.000
-0.628	0.000	-1.074	0.000	-1.120	0.000	-0.947	0.000	-1.092	0.000	-1.147	0.000	-1.047	0.000	-0.837	0.000
-0.610	0.000	-0.628	0.000	-0.637	0.000	-0.637	0.000	-0.173	0.000	-0.173	0.000	-0.173	0.000	-0.086	-0.086
-0.086	-0.137	-0.191	-0.082	-0.191	-0.191	-0.191	0.000	0.000	0.000	0.000	-0.228	-0.091	0.000	0.000	0.000
0.000	0.000	0.000	0.000	0.000	0.000	-0.127	-0.127	-0.127	-0.127	-0.127	-0.127				

Table 22.--Specified irrigation ground-water withdrawals and recharge, in cubic feet per second--Continued

Stress period															
1	2	3	4	5	6	7	8	9	10	11	12	13	14	15	16
17	18	19	20	21	22	23	24	25	26	27	28	29	30	31	32
33	34	35	36	37	38	39	40	41	42	43	44	45	46	47	48
49	50	51	52	53	54	55	56	57	58	59	60	61	62	63	64
65	66	67	68	69	70	71	72	73	74	75	76	77			

Row 33, column 19, layer 2, Bluewater-Toltec

0.000	0.000	0.000	0.000	0.000	0.000	0.000	0.000	-0.637	0.000	-1.638	0.000	-1.875	0.000	-1.693	0.000
-1.256	0.000	-2.148	0.000	-2.239	0.000	-1.893	0.000	-2.184	0.000	-2.293	0.000	-2.093	0.000	-1.675	0.000
-1.220	0.000	-1.256	0.000	-1.274	0.000	-1.274	0.000	-0.346	0.000	-0.346	0.000	-0.346	0.000	-0.173	-0.173
-0.173	-0.273	-0.382	-0.164	-0.382	-0.382	-0.382	0.000	0.000	0.000	0.000	-0.455	-0.182	0.000	0.000	0.000
0.000	0.000	0.000	0.000	0.000	0.000	-0.255	-0.255	-0.255	-0.255	-0.255	-0.255				

Row 33, column 20, layer 2, Bluewater-Toltec

0.000	0.000	0.000	0.000	0.000	0.000	0.000	0.000	-0.319	0.000	-0.819	0.000	-0.938	0.000	-0.846	0.000
-0.628	0.000	-1.074	0.000	-1.120	0.000	-0.947	0.000	-1.092	0.000	-1.147	0.000	-1.047	0.000	-0.837	0.000
-0.610	0.000	-0.628	0.000	-0.637	0.000	-0.637	0.000	-0.173	0.000	-0.173	0.000	-0.173	0.000	-0.086	-0.086
-0.086	-0.137	-0.191	-0.082	-0.191	-0.191	-0.191	0.000	0.000	0.000	0.000	-0.228	-0.091	0.000	0.000	0.000
0.000	0.000	0.000	0.000	0.000	0.000	-0.127	-0.127	-0.127	-0.127	-0.127	-0.127				

Row 33, column 21, layer 2, Bluewater-Toltec

0.000	0.000	0.000	0.000	0.000	0.000	0.000	0.000	-0.637	0.000	-1.638	0.000	-1.875	0.000	-1.693	0.000
-1.256	0.000	-2.148	0.000	-2.239	0.000	-1.893	0.000	-2.184	0.000	-2.293	0.000	-2.093	0.000	-1.675	0.000
-1.220	0.000	-1.256	0.000	-1.274	0.000	-1.274	0.000	-0.346	0.000	-0.346	0.000	-0.346	0.000	-0.173	-0.173
-0.173	-0.273	-0.382	-0.164	-0.382	-0.382	-0.382	0.000	0.000	0.000	0.000	-0.455	-0.182	0.000	0.000	0.000
0.000	0.000	0.000	0.000	0.000	0.000	-0.255	-0.255	-0.255	-0.255	-0.255	-0.255				

Table 22.--Specified irrigation ground-water withdrawals and recharge, in cubic feet per second--Continued

Stress period															
1	2	3	4	5	6	7	8	9	10	11	12	13	14	15	16
17	18	19	20	21	22	23	24	25	26	27	28	29	30	31	32
33	34	35	36	37	38	39	40	41	42	43	44	45	46	47	48
49	50	51	52	53	54	55	56	57	58	59	60	61	62	63	64
65	66	67	68	69	70	71	72	73	74	75	76	77			

Row 34, column 16, layer 2, Bluewater-Toltec

0.000	0.000	0.000	0.000	0.000	0.000	0.000	0.000	-0.425	0.000	-1.092	0.000	-1.250	0.000	-1.128	0.000
-0.837	0.000	-1.432	0.000	-1.492	0.000	-1.262	0.000	-1.456	0.000	-1.529	0.000	-1.395	0.000	-1.116	0.000
-0.813	0.000	-0.837	0.000	-0.849	0.000	-0.849	0.000	-0.231	0.000	-0.231	0.000	-0.231	0.000	-0.115	-0.115
-0.115	-0.182	-0.255	-0.109	-0.255	-0.255	-0.255	0.000	0.000	0.000	0.000	-0.303	-0.121	0.000	0.000	0.000
0.000	0.000	0.000	0.000	0.000	0.000	-0.170	-0.170	-0.170	-0.170	-0.170	-0.170				

Row 34, column 18, layer 2, Bluewater-Toltec

0.000	0.000	0.000	0.000	0.000	0.000	0.000	0.000	-0.319	0.000	-0.819	0.000	-0.938	0.000	-0.846	0.000
-0.628	0.000	-1.074	0.000	-1.120	0.000	-0.947	0.000	-1.092	0.000	-1.147	0.000	-1.047	0.000	-0.837	0.000
-0.610	0.000	-0.628	0.000	-0.637	0.000	-0.637	0.000	-0.173	0.000	-0.173	0.000	-0.173	0.000	-0.086	-0.086
-0.086	-0.137	-0.191	-0.082	-0.191	-0.191	-0.191	0.000	0.000	0.000	0.000	-0.228	-0.091	0.000	0.000	0.000
0.000	0.000	0.000	0.000	0.000	0.000	-0.127	-0.127	-0.127	-0.127	-0.127	-0.127				

Row 34, column 19, layer 2, Bluewater-Toltec

0.000	0.000	0.000	0.000	0.000	0.000	0.000	0.000	-0.637	0.000	-1.638	0.000	-1.875	0.000	-1.693	0.000
-1.256	0.000	-2.148	0.000	-2.239	0.000	-1.893	0.000	-2.184	0.000	-2.293	0.000	-2.093	0.000	-1.675	0.000
-1.220	0.000	-1.256	0.000	-1.274	0.000	-1.274	0.000	-0.346	0.000	-0.346	0.000	-0.346	0.000	-0.173	-0.173
-0.173	-0.273	-0.382	-0.164	-0.382	-0.382	-0.382	0.000	0.000	0.000	0.000	-0.455	-0.182	0.000	0.000	0.000
0.000	0.000	0.000	0.000	0.000	0.000	-0.255	-0.255	-0.255	-0.255	-0.255	-0.255				

Table 22.--Specified irrigation ground-water withdrawals and recharge, in cubic feet per second--Continued

Stress period															
1	2	3	4	5	6	7	8	9	10	11	12	13	14	15	16
17	18	19	20	21	22	23	24	25	26	27	28	29	30	31	32
33	34	35	36	37	38	39	40	41	42	43	44	45	46	47	48
49	50	51	52	53	54	55	56	57	58	59	60	61	62	63	64
65	66	67	68	69	70	71	72	73	74	75	76	77			
Row 26, column 19, layer 1, Bluewater-Toltec															
0.291	0.150	0.291	0.378	0.455	0.000	0.546	0.000	0.728	0.000	1.092	0.000	1.238	0.000	1.675	0.000
1.383	0.000	1.420	0.000	1.493	0.000	1.820	0.000	1.456	0.000	1.529	0.000	1.383	0.000	1.092	0.000
0.801	0.000	0.837	0.000	0.837	0.000	0.837	0.000	0.291	0.000	0.728	0.000	0.546	0.000	0.328	0.328
0.328	0.255	0.255	0.255	0.255	0.255	0.255	0.309	0.309	0.309	0.309	0.309	0.309	0.309	0.309	0.309
0.309	0.619	0.000	0.619	0.000	0.309	0.340	0.340	0.340	0.340	0.340	0.340				
Row 27, column 18, layer 1, Bluewater-Toltec															
0.097	0.050	0.097	0.126	0.152	0.000	0.182	0.000	0.243	0.000	0.364	0.000	0.413	0.000	0.558	0.000
0.461	0.000	0.473	0.000	0.497	0.000	0.607	0.000	0.485	0.000	0.510	0.000	0.461	0.000	0.364	0.000
0.267	0.000	0.279	0.000	0.279	0.000	0.279	0.000	0.097	0.000	0.243	0.000	0.182	0.000	0.109	0.109
0.109	0.085	0.085	0.085	0.085	0.085	0.085	0.103	0.103	0.103	0.103	0.103	0.103	0.103	0.103	0.103
0.103	0.206	0.000	0.206	0.000	0.103	0.113	0.113	0.113	0.113	0.113	0.113				
Row 27, layer 19, layer 1, Bluewater-Toltec															
0.097	0.050	0.097	0.126	0.152	0.000	0.182	0.000	0.243	0.000	0.364	0.000	0.413	0.000	0.558	0.000
0.461	0.000	0.473	0.000	0.497	0.000	0.607	0.000	0.485	0.000	0.510	0.000	0.461	0.000	0.364	0.000
0.267	0.000	0.279	0.000	0.279	0.000	0.279	0.000	0.097	0.000	0.243	0.000	0.182	0.000	0.109	0.109
0.109	0.085	0.085	0.085	0.085	0.085	0.085	0.103	0.103	0.103	0.103	0.103	0.103	0.103	0.103	0.103
0.103	0.206	0.000	0.206	0.000	0.103	0.113	0.113	0.113	0.113	0.113	0.113				

Table 22.--Specified irrigation ground-water withdrawals and recharge, in cubic feet per second--Continued

Stress period															
1	2	3	4	5	6	7	8	9	10	11	12	13	14	15	16
17	18	19	20	21	22	23	24	25	26	27	28	29	30	31	32
33	34	35	36	37	38	39	40	41	42	43	44	45	46	47	48
49	50	51	52	53	54	55	56	57	58	59	60	61	62	63	64
65	66	67	68	69	70	71	72	73	74	75	76	77			

Row 28, column 18, layer 1, Bluewater-Toltec

0.097	0.050	0.097	0.126	0.152	0.000	0.182	0.000	0.243	0.000	0.364	0.000	0.413	0.000	0.558	0.000
0.461	0.000	0.473	0.000	0.497	0.000	0.607	0.000	0.485	0.000	0.510	0.000	0.461	0.000	0.364	0.000
0.267	0.000	0.279	0.000	0.279	0.000	0.279	0.000	0.097	0.000	0.243	0.000	0.182	0.000	0.109	0.109
0.109	0.085	0.085	0.085	0.085	0.085	0.085	0.103	0.103	0.103	0.103	0.103	0.103	0.103	0.103	0.103
0.103	0.206	0.000	0.206	0.000	0.103	0.113	0.113	0.113	0.113	0.113	0.113				

Row 29, column 18, layer 1, Bluewater-Toltec

0.097	0.050	0.097	0.126	0.152	0.000	0.182	0.000	0.243	0.000	0.364	0.000	0.413	0.000	0.558	0.000
0.461	0.000	0.473	0.000	0.497	0.000	0.607	0.000	0.485	0.000	0.510	0.000	0.461	0.000	0.364	0.000
0.267	0.000	0.279	0.000	0.279	0.000	0.279	0.000	0.097	0.000	0.243	0.000	0.182	0.000	0.109	0.109
0.109	0.085	0.085	0.085	0.085	0.085	0.085	0.103	0.103	0.103	0.103	0.103	0.103	0.103	0.103	0.103
0.103	0.206	0.000	0.206	0.000	0.103	0.113	0.113	0.113	0.113	0.113	0.113				

Row 29, column 19, layer 1, Bluewater-Toltec

0.194	0.100	0.194	0.252	0.303	0.000	0.364	0.000	0.485	0.000	0.728	0.000	0.825	0.000	1.116	0.000
0.922	0.000	0.947	0.000	0.995	0.000	1.214	0.000	0.971	0.000	1.019	0.000	0.922	0.000	0.728	0.000
0.534	0.000	0.558	0.000	0.558	0.000	0.558	0.000	0.194	0.000	0.485	0.000	0.364	0.000	0.218	0.218
0.218	0.170	0.170	0.170	0.170	0.170	0.170	0.206	0.206	0.206	0.206	0.206	0.206	0.206	0.206	0.206
0.206	0.413	0.000	0.413	0.000	0.206	0.227	0.227	0.227	0.227	0.227	0.227				

Table 22.--Specified irrigation ground-water withdrawals and recharge, in cubic feet per second--Continued

Stress period															
1	2	3	4	5	6	7	8	9	10	11	12	13	14	15	16
17	18	19	20	21	22	23	24	25	26	27	28	29	30	31	32
33	34	35	36	37	38	39	40	41	42	43	44	45	46	47	48
49	50	51	52	53	54	55	56	57	58	59	60	61	62	63	64
65	66	67	68	69	70	71	72	73	74	75	76	77			
Row 30, column 19, layer 1, Bluewater-Toltec															
0.194	0.100	0.194	0.252	0.303	0.000	0.364	0.000	0.485	0.000	0.728	0.000	0.825	0.000	1.116	0.000
0.922	0.000	0.947	0.000	0.995	0.000	1.214	0.000	0.971	0.000	1.019	0.000	0.922	0.000	0.728	0.000
0.534	0.000	0.558	0.000	0.558	0.000	0.558	0.000	0.194	0.000	0.485	0.000	0.364	0.000	0.218	0.218
0.218	0.170	0.170	0.170	0.170	0.170	0.170	0.206	0.206	0.206	0.206	0.206	0.206	0.206	0.206	0.206
0.206	0.413	0.000	0.413	0.000	0.206	0.227	0.227	0.227	0.227	0.227	0.227				
Row 30, column 20, layer 1, Bluewater-Toltec															
0.097	0.050	0.097	0.126	0.152	0.000	0.182	0.000	0.243	0.000	0.364	0.000	0.413	0.000	0.558	0.000
0.461	0.000	0.473	0.000	0.497	0.000	0.607	0.000	0.485	0.000	0.510	0.000	0.461	0.000	0.364	0.000
0.267	0.000	0.279	0.000	0.279	0.000	0.279	0.000	0.097	0.000	0.243	0.000	0.182	0.000	0.109	0.109
0.109	0.085	0.085	0.085	0.085	0.085	0.085	0.103	0.103	0.103	0.103	0.103	0.103	0.103	0.103	0.103
0.103	0.206	0.000	0.206	0.000	0.103	0.113	0.113	0.113	0.113	0.113	0.113				
Row 31, column 19, layer 1, Bluewater-Toltec															
0.073	0.038	0.073	0.094	0.114	0.000	0.137	0.000	0.182	0.000	0.273	0.000	0.309	0.000	0.419	0.000
0.346	0.000	0.355	0.000	0.373	0.000	0.455	0.000	0.364	0.000	0.382	0.000	0.346	0.000	0.273	0.000
0.200	0.000	0.209	0.000	0.209	0.000	0.209	0.000	0.073	0.000	0.182	0.000	0.137	0.000	0.082	0.082
0.082	0.064	0.064	0.064	0.064	0.064	0.064	0.077	0.077	0.077	0.077	0.077	0.077	0.077	0.077	0.077
0.077	0.155	0.000	0.155	0.000	0.077	0.085	0.085	0.085	0.085	0.085	0.085				

Table 22.--Specified irrigation ground-water withdrawals and recharge, in cubic feet per second--Continued

Stress period															
1	2	3	4	5	6	7	8	9	10	11	12	13	14	15	16
17	18	19	20	21	22	23	24	25	26	27	28	29	30	31	32
33	34	35	36	37	38	39	40	41	42	43	44	45	46	47	48
49	50	51	52	53	54	55	56	57	58	59	60	61	62	63	64
65	66	67	68	69	70	71	72	73	74	75	76	77			
Row 31, column 20, layer 1, Bluewater-Toltec															
0.073	0.038	0.073	0.094	0.114	0.000	0.137	0.000	0.182	0.000	0.273	0.000	0.309	0.000	0.419	0.000
0.346	0.000	0.355	0.000	0.373	0.000	0.455	0.000	0.364	0.000	0.382	0.000	0.346	0.000	0.273	0.000
0.200	0.000	0.209	0.000	0.209	0.000	0.209	0.000	0.073	0.000	0.182	0.000	0.137	0.000	0.082	0.082
0.082	0.064	0.064	0.064	0.064	0.064	0.064	0.077	0.077	0.077	0.077	0.077	0.077	0.077	0.077	0.077
0.077	0.155	0.000	0.155	0.000	0.077	0.085	0.085	0.085	0.085	0.085	0.085				
Row 32, column 19, layer 1, Bluewater-Toltec															
0.146	0.075	0.146	0.189	0.228	0.000	0.273	0.000	0.364	0.000	0.546	0.000	0.619	0.000	0.837	0.000
0.692	0.000	0.710	0.000	0.746	0.000	0.910	0.000	0.728	0.000	0.764	0.000	0.692	0.000	0.546	0.000
0.400	0.000	0.419	0.000	0.419	0.000	0.419	0.000	0.146	0.000	0.364	0.000	0.273	0.000	0.164	0.164
0.164	0.127	0.127	0.127	0.127	0.127	0.127	0.155	0.155	0.155	0.155	0.155	0.155	0.155	0.155	0.155
0.155	0.309	0.000	0.309	0.000	0.155	0.170	0.170	0.170	0.170	0.170	0.170				
Row 32, column 20, layer 1, Bluewater-Toltec															
0.073	0.038	0.073	0.094	0.114	0.000	0.137	0.000	0.182	0.000	0.273	0.000	0.309	0.000	0.419	0.000
0.346	0.000	0.355	0.000	0.373	0.000	0.455	0.000	0.364	0.000	0.382	0.000	0.346	0.000	0.273	0.000
0.200	0.000	0.209	0.000	0.209	0.000	0.209	0.000	0.073	0.000	0.182	0.000	0.137	0.000	0.082	0.082
0.082	0.064	0.064	0.064	0.064	0.064	0.064	0.077	0.077	0.077	0.077	0.077	0.077	0.077	0.077	0.077
0.077	0.155	0.000	0.155	0.000	0.077	0.085	0.085	0.085	0.085	0.085	0.085				

Table 22.--Specified irrigation ground-water withdrawals and recharge, in cubic feet per second--Continued

Stress period															
1	2	3	4	5	6	7	8	9	10	11	12	13	14	15	16
17	18	19	20	21	22	23	24	25	26	27	28	29	30	31	32
33	34	35	36	37	38	39	40	41	42	43	44	45	46	47	48
49	50	51	52	53	54	55	56	57	58	59	60	61	62	63	64
65	66	67	68	69	70	71	72	73	74	75	76	77			

Row 33, column 19, layer 1, Bluewater-Toltec

0.146	0.075	0.146	0.189	0.228	0.000	0.273	0.000	0.364	0.000	0.546	0.000	0.619	0.000	0.837	0.000
0.692	0.000	0.710	0.000	0.746	0.000	0.910	0.000	0.728	0.000	0.764	0.000	0.692	0.000	0.546	0.000
0.400	0.000	0.419	0.000	0.419	0.000	0.419	0.000	0.146	0.000	0.364	0.000	0.273	0.000	0.164	0.164
0.164	0.127	0.127	0.127	0.127	0.127	0.127	0.155	0.155	0.155	0.155	0.155	0.155	0.155	0.155	0.155
0.155	0.309	0.000	0.309	0.000	0.155	0.170	0.170	0.170	0.170	0.170	0.170				

Row 33, column 20, layer 1, Bluewater-Toltec

0.073	0.038	0.073	0.094	0.114	0.000	0.137	0.000	0.182	0.000	0.273	0.000	0.309	0.000	0.419	0.000
0.346	0.000	0.355	0.000	0.373	0.000	0.455	0.000	0.364	0.000	0.382	0.000	0.346	0.000	0.273	0.000
0.200	0.000	0.209	0.000	0.209	0.000	0.209	0.000	0.073	0.000	0.182	0.000	0.137	0.000	0.082	0.082
0.082	0.064	0.064	0.064	0.064	0.064	0.064	0.077	0.077	0.077	0.077	0.077	0.077	0.077	0.077	0.077
0.077	0.155	0.000	0.155	0.000	0.077	0.085	0.085	0.085	0.085	0.085	0.085				

Row 33, column 21, layer 1, Bluewater-Toltec

0.146	0.075	0.146	0.189	0.228	0.000	0.273	0.000	0.364	0.000	0.546	0.000	0.619	0.000	0.837	0.000
0.692	0.000	0.710	0.000	0.746	0.000	0.910	0.000	0.728	0.000	0.764	0.000	0.692	0.000	0.546	0.000
0.400	0.000	0.419	0.000	0.419	0.000	0.419	0.000	0.146	0.000	0.364	0.000	0.273	0.000	0.164	0.164
0.164	0.127	0.127	0.127	0.127	0.127	0.127	0.155	0.155	0.155	0.155	0.155	0.155	0.155	0.155	0.155
0.155	0.309	0.000	0.309	0.000	0.155	0.170	0.170	0.170	0.170	0.170	0.170				

Table 22.--Specified irrigation ground-water withdrawals and recharge, in cubic feet per second--Continued

Stress period															
1	2	3	4	5	6	7	8	9	10	11	12	13	14	15	16
17	18	19	20	21	22	23	24	25	26	27	28	29	30	31	32
33	34	35	36	37	38	39	40	41	42	43	44	45	46	47	48
49	50	51	52	53	54	55	56	57	58	59	60	61	62	63	64
65	66	67	68	69	70	71	72	73	74	75	76	77			

Row 34, column 16, layer 1, Bluewater-Toltec

0.097	0.050	0.097	0.126	0.152	0.000	0.182	0.000	0.243	0.000	0.364	0.000	0.413	0.000	0.558	0.000
0.461	0.000	0.473	0.000	0.497	0.000	0.607	0.000	0.485	0.000	0.510	0.000	0.461	0.000	0.364	0.000
0.267	0.000	0.279	0.000	0.279	0.000	0.279	0.000	0.097	0.000	0.243	0.000	0.182	0.000	0.109	0.109
0.109	0.085	0.085	0.085	0.085	0.085	0.085	0.103	0.103	0.103	0.103	0.103	0.103	0.103	0.103	0.103
0.103	0.206	0.000	0.206	0.000	0.103	0.113	0.113	0.113	0.113	0.113	0.113				

Row 34, column 18, layer 1, Bluewater-Toltec

0.073	0.038	0.073	0.094	0.114	0.000	0.137	0.000	0.182	0.000	0.273	0.000	0.309	0.000	0.419	0.000
0.346	0.000	0.355	0.000	0.373	0.000	0.455	0.000	0.364	0.000	0.382	0.000	0.346	0.000	0.273	0.000
0.200	0.000	0.209	0.000	0.209	0.000	0.209	0.000	0.073	0.000	0.182	0.000	0.137	0.000	0.082	0.082
0.082	0.064	0.064	0.064	0.064	0.064	0.064	0.077	0.077	0.077	0.077	0.077	0.077	0.077	0.077	0.077
0.077	0.155	0.000	0.155	0.000	0.077	0.085	0.085	0.085	0.085	0.085	0.085				

Row 34, column 19, layer 1, Bluewater-Toltec

0.146	0.075	0.146	0.189	0.228	0.000	0.273	0.000	0.364	0.000	0.546	0.000	0.619	0.000	0.837	0.000
0.692	0.000	0.710	0.000	0.746	0.000	0.910	0.000	0.728	0.000	0.764	0.000	0.692	0.000	0.546	0.000
0.400	0.000	0.419	0.000	0.419	0.000	0.419	0.000	0.146	0.000	0.364	0.000	0.273	0.000	0.164	0.164
0.164	0.127	0.127	0.127	0.127	0.127	0.127	0.155	0.155	0.155	0.155	0.155	0.155	0.155	0.155	0.155
0.155	0.309	0.000	0.309	0.000	0.155	0.170	0.170	0.170	0.170	0.170	0.170				

Table 22.--Specified irrigation ground-water withdrawals and recharge, in cubic feet per second--Continued

Stress period															
1	2	3	4	5	6	7	8	9	10	11	12	13	14	15	16
17	18	19	20	21	22	23	24	25	26	27	28	29	30	31	32
33	34	35	36	37	38	39	40	41	42	43	44	45	46	47	48
49	50	51	52	53	54	55	56	57	58	59	60	61	62	63	64
65	66	67	68	69	70	71	72	73	74	75	76	77			
Total specified recharge for Bluewater-Toltec															
2.21	1.14	2.21	2.86	3.45	0.00	4.14	0.00	5.52	0.00	8.28	0.00	9.39	0.00	12.70	0.00
10.49	0.00	10.77	0.00	11.32	0.00	13.80	0.00	11.04	0.00	11.59	0.00	10.49	0.00	8.28	0.00
6.07	0.00	6.35	0.00	6.35	0.00	6.35	0.00	2.21	0.00	5.52	0.00	4.14	0.00	2.48	2.48
2.48	1.93	1.93	1.93	1.93	1.93	1.93	2.35	2.35	2.35	2.35	2.35	2.35	2.35	2.35	2.35
2.35	4.69	0.00	4.69	0.00	2.35	2.58	2.58	2.58	2.58	2.58	2.58				
Total specified ground-water withdrawal for Bluewater-Toltec															
0.00	0.00	0.00	0.00	0.00	0.00	0.00	0.00	-9.66	0.00	-24.85	0.00	-28.43	0.00	-25.67	0.00
-19.05	0.00	-32.58	0.00	-33.96	0.00	-28.71	0.00	-33.13	0.00	-34.78	0.00	-31.75	0.00	-25.40	0.00
-18.50	0.00	-19.05	0.00	-19.32	0.00	-19.32	0.00	-5.25	0.00	-5.25	0.00	-5.25	0.00	-2.62	-2.62
-2.62	-4.14	-5.80	-2.48	-5.80	-5.80	-5.80	0.00	0.00	0.00	0.00	-6.90	-2.76	0.00	0.00	0.00
0.00	0.00	0.00	0.00	0.00	0.00	-3.86	-3.86	-3.86	-3.86	-3.86	-3.86				
Net specified ground-water withdrawal and recharge for Bluewater-Toltec															
2.21	1.14	2.21	2.86	3.45	0.00	4.14	0.00	-4.14	0.00	-16.56	0.00	-19.05	0.00	-12.98	0.00
-8.56	0.00	-21.81	0.00	-22.64	0.00	-14.91	0.00	-22.09	0.00	-23.19	0.00	-21.26	0.00	-17.12	0.00
-12.42	0.00	-12.70	0.00	-12.98	0.00	-12.98	0.00	-3.04	0.00	0.28	0.00	-1.10	0.00	-0.14	-0.14
-0.14	-2.21	-3.86	-0.55	-3.86	-3.86	-3.86	2.35	2.35	2.35	2.35	-4.56	-0.41	2.35	2.35	2.35
2.35	4.69	0.00	4.69	0.00	2.35	-1.29	-1.29	-1.29	-1.29	-1.29	-1.29				

Table 22.--Specified irrigation ground-water withdrawals and recharge, in cubic feet per second--Continued

Stress period															
1	2	3	4	5	6	7	8	9	10	11	12	13	14	15	16
17	18	19	20	21	22	23	24	25	26	27	28	29	30	31	32
33	34	35	36	37	38	39	40	41	42	43	44	45	46	47	48
49	50	51	52	53	54	55	56	57	58	59	60	61	62	63	64
65	66	67	68	69	70	71	72	73	74	75	76	77			

Specified ground-water withdrawal for the Ojo del Gallo, south San Rafael, and Acoma irrigated areas

Row 44, column 12, layer 1, Ojo del Gallo (net withdrawal from valley fill to simulate diversion of springflow)

-3.451	-3.451	-3.451	-3.451	-3.451	0.000	-6.902	0.000	-6.902	0.000	-6.902	0.000	-6.902	0.000	-3.589	0.000
-3.589	0.000	-3.589	0.000	0.000	0.000	0.000	0.000	0.000	0.000	0.000	0.000	0.000	0.000	0.000	0.000
0.000	0.000	0.000	0.000	0.000	0.000	0.000	0.000	0.000	0.000	0.000	0.000	0.000	0.000	0.000	0.000
0.000	0.000	0.000	0.000	0.000	0.000	0.000	0.000	0.000	0.000	0.000	0.000	0.000	0.000	0.000	0.000
0.000	0.000	0.000	0.000	0.000	0.000	0.000	0.000	0.000	0.000	0.000	0.000				

Row 46, column 7, layer 2, south San Rafael

0.000	0.000	0.000	0.000	0.000	0.000	0.000	0.000	0.000	0.000	0.000	0.000	0.000	0.000	0.000	0.000
0.000	0.000	0.000	0.000	0.000	0.000	-0.638	0.000	-0.638	0.000	-0.638	0.000	-0.638	0.000	-0.638	0.000
-0.638	0.000	-0.638	0.000	-0.638	0.000	-0.638	0.000	-0.638	0.000	-0.638	0.000	-0.638	0.000	-0.319	-0.319
0.000	0.000	0.000	0.000	0.000	0.000	0.000	0.000	0.000	0.000	-0.159	-0.159	-0.159	-0.159	-0.159	-0.159
-0.159	0.000	0.000	0.000	0.000	0.000	0.000	0.000	0.000	0.000	0.000	0.000				

Row 47, column 8, layer 2, south San Rafael

0.000	0.000	0.000	0.000	0.000	0.000	0.000	0.000	0.000	0.000	0.000	0.000	0.000	0.000	0.000	0.000
0.000	0.000	0.000	0.000	0.000	0.000	-0.591	0.000	-0.591	0.000	-0.591	0.000	-0.591	0.000	-0.591	0.000
-0.591	0.000	-0.591	0.000	-0.591	0.000	-0.591	0.000	-0.591	0.000	-0.591	0.000	-0.591	0.000	-0.296	-0.296
0.000	0.000	0.000	0.000	0.000	0.000	0.000	0.000	0.000	0.000	-0.148	-0.148	-0.148	-0.148	-0.148	-0.148
-0.148	0.000	0.000	0.000	0.000	0.000	0.000	0.000	0.000	0.000	0.000	0.000				

Table 22.--Specified irrigation ground-water withdrawals and recharge, in cubic feet per second--Continued

Stress period															
1	2	3	4	5	6	7	8	9	10	11	12	13	14	15	16
17	18	19	20	21	22	23	24	25	26	27	28	29	30	31	32
33	34	35	36	37	38	39	40	41	42	43	44	45	46	47	48
49	50	51	52	53	54	55	56	57	58	59	60	61	62	63	64
65	66	67	68	69	70	71	72	73	74	75	76	77			
Row 46, column 8, layer 1, south San Rafael															
0.000	0.000	0.000	0.000	0.000	0.000	0.000	0.000	0.000	0.000	0.000	0.000	0.000	0.000	0.000	0.000
0.000	0.000	0.000	0.000	0.000	0.000	0.212	0.000	0.212	0.000	0.212	0.000	0.212	0.000	0.212	0.000
0.212	0.000	0.212	0.000	0.212	0.000	0.212	0.000	0.212	0.000	0.212	0.000	0.212	0.000	0.106	0.106
0.000	0.000	0.000	0.000	0.000	0.000	0.000	0.000	0.000	0.000	0.053	0.053	0.053	0.053	0.053	0.053
0.053	0.000	0.000	0.000	0.000	0.000	0.000	0.000	0.000	0.000	0.000	0.000				
Row 47, column 9, layer 1, south San Rafael															
0.000	0.000	0.000	0.000	0.000	0.000	0.000	0.000	0.000	0.000	0.000	0.000	0.000	0.000	0.000	0.000
0.000	0.000	0.000	0.000	0.000	0.000	0.197	0.000	0.197	0.000	0.197	0.000	0.197	0.000	0.197	0.000
0.197	0.000	0.197	0.000	0.197	0.000	0.197	0.000	0.197	0.000	0.197	0.000	0.197	0.000	0.099	0.099
0.000	0.000	0.000	0.000	0.000	0.000	0.000	0.000	0.000	0.000	0.049	0.049	0.049	0.049	0.049	0.049
0.049	0.000	0.000	0.000	0.000	0.000	0.000	0.000	0.000	0.000	0.000	0.000				
Row 54, column 6, layer 2, Acoma (projection only)															
0.000	0.000	0.000	0.000	0.000	0.000	0.000	0.000	0.000	0.000	0.000	0.000	0.000	0.000	0.000	0.000
0.000	0.000	0.000	0.000	0.000	0.000	0.000	0.000	0.000	0.000	0.000	0.000	0.000	0.000	0.000	0.000
0.000	0.000	0.000	0.000	0.000	0.000	0.000	0.000	0.000	0.000	0.000	0.000	0.000	0.000	0.000	0.000
0.000	0.000	0.000	0.000	0.000	0.000	0.000	0.000	0.000	0.000	0.000	0.000	0.000	0.000	0.000	0.000
0.000	0.000	0.000	0.000	0.000	0.000	-13.80	-13.80	-13.80	-13.80	-13.80	-13.80				

Table 22.--Specified irrigation ground-water withdrawals and recharge, in cubic feet per second--Continued

Stress period

1	2	3	4	5	6	7	8	9	10	11	12	13	14	15	16
17	18	19	20	21	22	23	24	25	26	27	28	29	30	31	32
33	34	35	36	37	38	39	40	41	42	43	44	45	46	47	48
49	50	51	52	53	54	55	56	57	58	59	60	61	62	63	64
65	66	67	68	69	70	71	72	73	74	75	76	77			

Row 53, column 6, layer 1, Acoma (projection only)

0.000	0.000	0.000	0.000	0.000	0.000	0.000	0.000	0.000	0.000	0.000	0.000	0.000	0.000	0.000	0.000
0.000	0.000	0.000	0.000	0.000	0.000	0.000	0.000	0.000	0.000	0.000	0.000	0.000	0.000	0.000	0.000
0.000	0.000	0.000	0.000	0.000	0.000	0.000	0.000	0.000	0.000	0.000	0.000	0.000	0.000	0.000	0.000
0.000	0.000	0.000	0.000	0.000	0.000	0.000	0.000	0.000	0.000	0.000	0.000	0.000	0.000	0.000	0.000
0.000	0.000	0.000	0.000	0.000	0.000	4.601	4.601	4.601	4.601	4.601	4.601				

Totals for Ojo del Gallo, south San Rafael, and Acoma (projection only) irrigated areas: irrigation was simulated as having occurred at different times for each of the three irrigated areas; Ojo del Gallo was first, south San Rafael was second, and Acoma (projection only) was third. In the following totals the irrigated areas are separated by parentheses.

Total specified recharge for south San Rafael and Acoma (projection only) irrigation areas

0.00	0.00	0.00	0.00	0.00	0.00	0.00	0.00	0.00	0.00	0.00	0.00	0.00	0.00	0.00	0.00
0.00	0.00	0.00	0.00	0.00	0.00	(0.41	0.00	0.41	0.00	0.41	0.00	0.41	0.00	0.41	0.00
0.41	0.00	0.41	0.00	0.41	0.00	0.41	0.00	0.41	0.00	0.41	0.00	0.41	0.00	0.20	0.20
0.00	0.00	0.00	0.00	0.00	0.00	0.00	0.00	0.00	0.00	0.10	0.10	0.10	0.10	0.10	0.10
0.10)	0.00	0.00	0.00	0.00	0.00	(4.60	4.60	4.60	4.60	4.60	4.60)				

Table 22.--Specified irrigation ground-water withdrawals and recharge, in cubic feet per second--Continued

Stress period															
1	2	3	4	5	6	7	8	9	10	11	12	13	14	15	16
17	18	19	20	21	22	23	24	25	26	27	28	29	30	31	32
33	34	35	36	37	38	39	40	41	42	43	44	45	46	47	48
49	50	51	52	53	54	55	56	57	58	59	60	61	62	63	64
65	66	67	68	69	70	71	72	73	74	75	76	77			

Total specified withdrawal for Ojo del Gallo, south San Rafael, and Acoma (projection only) irrigation areas

(-3.45	-3.45	-3.45	-3.45	-3.45	0.00	-6.90	0.00	-6.90	0.00	-6.90	0.00	-6.90	0.00	-3.59	0.00
-3.59	0.00	-3.59)	0.00	0.00	0.00	(-1.23	0.00	-1.23	0.00	-1.23	0.00	-1.23	0.00	-1.23	0.00
-1.23	0.00	-1.23	0.00	-1.23	0.00	-1.23	0.00	-1.23	0.00	-1.23	0.00	-1.23	0.00	-0.61	-0.61
0.00	0.00	0.00	0.00	0.00	0.00	0.00	0.00	0.00	0.00	-0.31	-0.31	-0.31	-0.31	-0.31	-0.31
-0.31)	0.00	0.00	0.00	0.00	0.00	(-13.80	-13.80	-13.80	-13.80	-13.80	-13.80)				

Net specified withdrawal and recharge for Ojo del Gallo, south San Rafael, and Acoma (projection only) irrigation areas

(-3.45	-3.45	-3.45	-3.45	-3.45	0.00	-6.90	0.00	-6.90	0.00	-6.90	0.00	-6.90	0.00	-3.59	0.00
-3.59	0.00	-3.59)	0.00	0.00	0.00	(-0.82	0.00	-0.82	0.00	-0.82	0.00	-0.82	0.00	-0.82	0.00
-0.82	0.00	-0.82	0.00	-0.82	0.00	-0.82	0.00	-0.82	0.00	-0.82	0.00	-0.82	0.00	-0.41	-0.41
0.00	0.00	0.00	0.00	0.00	0.00	0.00	0.00	0.00	0.00	-0.20	-0.20	-0.20	-0.20	-0.20	-0.20
-0.20)	0.00	0.00	0.00	0.00	0.00	(-9.20	-9.20	-9.20	-9.20	-9.20	-9.20)				

Combined totals of specified ground-water withdrawals and recharge for irrigation, all areas

Total specified recharge

2.21	1.14	2.21	2.86	3.45	0.00	4.14	0.00	5.52	0.00	8.28	0.00	9.39	0.00	12.70	0.00
10.49	0.00	10.77	0.00	11.32	0.00	14.21	0.00	11.45	0.00	12.00	0.00	10.90	0.00	8.69	0.00
6.48	0.00	6.76	0.00	6.76	0.00	6.76	0.00	2.62	0.00	5.93	0.00	4.55	0.00	2.69	2.69
2.48	1.93	1.93	1.93	1.93	1.93	1.93	2.35	2.35	2.35	2.45	2.45	2.45	2.45	2.45	2.45
2.45	4.69	0.00	4.69	0.00	2.35	7.18	7.18	7.18	7.18	7.18	7.18				

Table 22.--Specified irrigation ground-water withdrawals and recharge, in cubic feet per second--Concluded

Stress period															
1	2	3	4	5	6	7	8	9	10	11	12	13	14	15	16
17	18	19	20	21	22	23	24	25	26	27	28	29	30	31	32
33	34	35	36	37	38	39	40	41	42	43	44	45	46	47	48
49	50	51	52	53	54	55	56	57	58	59	60	61	62	63	64
65	66	67	68	69	70	71	72	73	74	75	76	77			

Total specified withdrawal

-3.45	-3.45	-3.45	-3.45	-3.45	0.00	-6.90	0.00	-16.56	0.00	-31.75	0.00	-35.34	0.00	-29.26	0.00
-22.64	0.00	-36.16	0.00	-33.96	0.00	-29.94	0.00	-34.36	0.00	-36.01	0.00	-32.98	0.00	-26.63	0.00
-19.73	0.00	-20.28	0.00	-20.55	0.00	-20.55	0.00	-6.47	0.00	-6.47	0.00	-6.47	0.00	-3.24	-3.24
-2.62	-4.14	-5.80	-2.48	-5.80	-5.80	-5.80	0.00	0.00	0.00	-0.31	-7.21	-3.07	-0.31	-0.31	-0.31
-0.31	0.00	0.00	0.00	0.00	0.00	-17.67	-17.67	-17.67	-17.67	-17.67	-17.67				

Net specified ground-water withdrawal and recharge

-1.24	-2.31	-1.24	-0.59	0.00	0.00	-2.76	0.00	-11.04	0.00	-23.47	0.00	-25.95	0.00	-16.56	0.00
-12.15	0.00	-25.39	0.00	-22.64	0.00	-15.73	0.00	-22.91	0.00	-24.01	0.00	-22.08	0.00	-17.94	0.00
-13.25	0.00	-13.52	0.00	-13.79	0.00	-13.79	0.00	-3.85	0.00	-0.54	0.00	-1.92	0.00	-0.55	-0.55
-0.14	-2.21	-3.87	-0.55	-3.87	-3.86	-3.87	2.35	2.35	2.35	2.14	-4.76	-0.62	2.14	2.14	2.14
2.14	4.69	0.00	4.69	0.00	2.35	-10.49	-10.49	-10.49	-10.49	-10.49	-10.49				

Table 23.--Specified municipal and industrial ground-water withdrawals and recharge

[Locations shown in figure 17]

Stress period															
1	2	3	4	5	6	7	8	9	10	11	12	13	14	15	16
17	18	19	20	21	22	23	24	25	26	27	28	29	30	31	32
33	34	35	36	37	38	39	40	41	42	43	44	45	46	47	48
49	50	51	52	53	54	55	56	57	58	59	60	61	62	63	64
65	66	67	68	69	70	71	72	73	74	75	76	77			

Row 41, column 17, layer 1, Railroad at Grants station

-0.120	-0.335	-0.276	-0.276	-0.428	-0.690	-0.784	-0.879	-0.974	-0.974	-0.974	-0.974	-0.974	-0.974	-0.974	0.000
0.000	0.000	0.000	0.000	0.000	0.000	0.000	0.000	0.000	0.000	0.000	0.000	0.000	0.000	0.000	0.000
0.000	0.000	0.000	0.000	0.000	0.000	0.000	0.000	0.000	0.000	0.000	0.000	0.000	0.000	0.000	0.000
0.000	0.000	0.000	0.000	0.000	0.000	0.000	0.000	0.000	0.000	0.000	0.000	0.000	0.000	0.000	0.000
0.000	0.000	0.000	0.000	0.000	0.000	0.000	0.000	0.000	0.000	0.000	0.000				

Row 40, column 16, layer 2, City of Grants

0.000	0.000	0.000	0.000	0.000	0.000	0.000	0.000	-0.276	-0.276	-0.276	-0.276	-0.276	-0.276	-0.276	-0.293
-0.309	-0.329	-0.345	-0.345	-0.345	-0.345	-0.345	-0.378	-0.414	-0.442	-0.483	-0.497	-0.511	-0.538	-0.552	-0.585
-0.621	-0.649	-0.676	-0.704	-0.732	-0.759	-0.787	-0.814	-0.842	-0.872	-2.178	-1.231	-1.952	-1.016	-1.366	-1.355
-1.568	-1.452	-1.694	-1.730	-1.879	-2.148	-1.892	-2.309	-2.207	-2.295	-2.291	-2.600	-2.594	-5.137	-2.991	-2.705
-2.458	-2.854	-1.676	-3.075	-1.582	-2.716	-3.037	-3.037	-3.037	-3.037	-3.037	-3.037				

Row 42, column 17, layer 1, City of Grants

0.000	0.000	0.000	0.000	0.000	0.000	0.000	0.000	0.138	0.138	0.138	0.138	0.138	0.138	0.138	0.000
0.000	0.000	0.000	0.000	0.000	0.000	0.000	0.000	0.000	0.000	0.000	0.000	0.000	0.000	0.000	0.000
0.000	0.000	0.000	0.000	0.000	0.000	0.000	0.000	0.000	0.000	0.000	0.000	0.000	0.000	0.000	0.000
0.000	0.000	0.000	0.000	0.000	0.000	0.000	0.000	0.000	0.000	0.000	0.000	0.000	0.000	0.000	0.000
0.000	0.000	0.000	0.000	0.000	0.000	0.000	0.000	0.000	0.000	0.000	0.000				

Table 23.--Specified municipal and industrial ground-water withdrawals and recharge--Continued

Stress period															
1	2	3	4	5	6	7	8	9	10	11	12	13	14	15	16
17	18	19	20	21	22	23	24	25	26	27	28	29	30	31	32
33	34	35	36	37	38	39	40	41	42	43	44	45	46	47	48
49	50	51	52	53	54	55	56	57	58	59	60	61	62	63	64
65	66	67	68	69	70	71	72	73	74	75	76	77			

Row 43, column 11, layer 2, Village of San Rafael

0.000	0.000	0.000	0.000	0.000	0.000	0.000	0.000	0.000	0.000	0.000	0.000	0.000	0.000	0.000	0.000
0.000	0.000	0.000	0.000	0.000	-0.014	-0.028	-0.028	-0.028	-0.028	-0.028	-0.028	-0.028	-0.028	-0.028	-0.028
-0.028	-0.030	-0.033	-0.036	-0.039	-0.041	-0.044	-0.047	-0.047	-0.047	-0.047	-0.047	-0.047	-0.047	-0.047	-0.047
-0.047	-0.047	-0.048	-0.052	-0.051	-0.066	-0.063	-0.065	-0.068	-0.063	-0.070	-0.094	-0.115	-0.124	-0.109	-0.105
-0.110	-0.110	-0.110	-0.110	-0.110	-0.110	-0.110	-0.110	-0.110	-0.110	-0.110	-0.110				

Row 43, column 11, layer 1, Village of San Rafael

0.000	0.000	0.000	0.000	0.000	0.000	0.000	0.000	0.000	0.000	0.000	0.000	0.000	0.000	0.000	0.000
0.000	0.000	0.000	0.000	0.000	0.007	0.014	0.014	0.014	0.014	0.014	0.014	0.014	0.014	0.014	0.014
0.014	0.015	0.017	0.018	0.019	0.021	0.022	0.023	0.023	0.023	0.023	0.023	0.023	0.023	0.023	0.023
0.023	0.023	0.024	0.026	0.026	0.033	0.032	0.032	0.034	0.032	0.035	0.047	0.057	0.062	0.055	0.052
0.055	0.055	0.055	0.055	0.055	0.055	0.055	0.055	0.055	0.055	0.055	0.055				

Row 29, column 19, layer 2, Anaconda uranium mill

0.000	0.000	0.000	0.000	0.000	0.000	0.000	0.000	0.000	0.000	0.000	0.000	0.000	0.000	0.000	0.000
0.000	0.000	0.000	0.000	0.000	-0.207	-0.414	-0.897	-1.380	-1.449	-1.518	-1.932	-2.347	-4.279	-6.211	-6.902
-5.841	-5.284	-5.414	-4.765	-3.506	-2.987	-3.266	-3.233	-3.200	-3.166	-3.133	-3.100	-3.067	-3.034	-2.984	-2.918
-2.853	-2.788	-2.722	-2.656	-2.628	-2.743	-2.983	-3.183	-3.009	-3.009	-3.046	-3.549	-4.047	-4.366	-4.146	-3.409
-0.740	-0.914	-0.707	-0.500	-0.588	-0.674	-0.674	-0.674	-0.674	-0.674	-0.674	-0.674				

Table 23.--Specified municipal and industrial ground-water withdrawals and recharge--Continued

Stress period															
1	2	3	4	5	6	7	8	9	10	11	12	13	14	15	16
17	18	19	20	21	22	23	24	25	26	27	28	29	30	31	32
33	34	35	36	37	38	39	40	41	42	43	44	45	46	47	48
49	50	51	52	53	54	55	56	57	58	59	60	61	62	63	64
65	66	67	68	69	70	71	72	73	74	75	76	77			

Row 28, column 21, layer 1, Anaconda uranium tailings pond

0.000	0.000	0.000	0.000	0.000	0.000	0.000	0.000	0.000	0.000	0.000	0.000	0.000	0.000	0.000	0.000
0.000	0.000	0.000	0.000	0.000	0.137	0.273	0.592	0.911	0.957	1.002	1.275	1.549	2.824	4.099	4.555
3.855	3.487	3.573	3.145	2.314	0.448	0.490	0.485	0.480	0.475	0.470	0.465	0.460	0.455	0.448	0.438
0.428	0.418	0.408	0.398	0.394	0.412	0.448	0.478	0.451	0.451	0.457	0.532	0.607	0.655	0.622	0.512
0.074	0.091	0.071	0.050	0.059	0.067	0.067	0.067	0.067	0.067	0.067	0.067				

Row 27, column 17, layer 2, Village of Bluewater

0.000	0.000	0.000	0.000	0.000	0.000	0.000	0.000	0.000	0.000	0.000	0.000	0.000	0.000	0.000	0.000
0.000	0.000	0.000	0.000	0.000	0.000	0.000	0.000	0.000	-0.014	-0.014	-0.014	-0.014	-0.014	-0.014	-0.014
-0.014	-0.019	-0.022	-0.025	-0.028	-0.030	-0.033	-0.036	-0.036	-0.036	-0.036	-0.036	-0.036	-0.036	-0.036	-0.036
-0.036	-0.036	-0.036	-0.036	-0.036	-0.036	-0.036	-0.036	-0.036	-0.036	-0.036	-0.036	-0.036	-0.036	-0.036	-0.036
-0.036	-0.036	-0.036	-0.036	-0.036	-0.036	-0.036	-0.036	-0.036	-0.036	-0.036	-0.036				

Row 27, column 18, layer 1, Village of Bluewater

0.000	0.000	0.000	0.000	0.000	0.000	0.000	0.000	0.000	0.000	0.000	0.000	0.000	0.000	0.000	0.000
0.000	0.000	0.000	0.000	0.000	0.000	0.000	0.000	0.000	0.007	0.007	0.007	0.007	0.007	0.007	0.007
0.007	0.010	0.011	0.012	0.014	0.015	0.017	0.018	0.018	0.018	0.018	0.018	0.018	0.018	0.018	0.018
0.018	0.018	0.018	0.018	0.018	0.018	0.018	0.018	0.018	0.018	0.018	0.018	0.018	0.018	0.018	0.018
0.018	0.018	0.018	0.018	0.018	0.018	0.018	0.018	0.018	0.018	0.018	0.018				

Table 23.--Specified municipal and industrial ground-water withdrawals and recharge--Continued

Stress period															
1	2	3	4	5	6	7	8	9	10	11	12	13	14	15	16
17	18	19	20	21	22	23	24	25	26	27	28	29	30	31	32
33	34	35	36	37	38	39	40	41	42	43	44	45	46	47	48
49	50	51	52	53	54	55	56	57	58	59	60	61	62	63	64
65	66	67	68	69	70	71	72	73	74	75	76	77			

Row 36, column 16, layer 2, Village of Milan

0.000	0.000	0.000	0.000	0.000	0.000	0.000	0.000	0.000	0.000	0.000	0.000	0.000	0.000	0.000	0.000
0.000	0.000	0.000	0.000	0.000	0.000	0.000	0.000	0.000	0.000	0.000	0.000	0.000	-0.014	-0.041	-0.069
-0.097	-0.121	-0.149	-0.174	-0.199	-0.224	-0.251	-0.276	-0.301	-0.373	-0.842	-0.464	-0.718	-0.340	-0.544	-0.435
-0.444	-0.525	-0.400	-0.345	-0.738	-0.571	-0.224	-0.341	-0.324	-0.457	-0.409	-0.905	-0.878	-0.961	-1.026	-0.842
-0.726	-1.013	-0.500	-1.063	-0.621	-0.928	-0.828	-0.828	-0.828	-0.828	-0.828	-0.828				

Row 34, column 23, layer 2, Homestake uranium mill

0.000	0.000	0.000	0.000	0.000	0.000	0.000	0.000	0.000	0.000	0.000	0.000	0.000	0.000	0.000	0.000
0.000	0.000	0.000	0.000	0.000	0.000	0.000	0.000	0.000	0.000	0.000	0.000	0.000	0.000	0.000	0.000
0.000	0.000	0.000	-0.828	-0.828	-0.828	-0.828	-0.828	-0.828	-1.027	-1.129	-0.933	-1.706	-1.096	-1.180	-1.055
-1.176	-1.288	-1.169	-1.197	-0.995	-0.867	-0.667	-0.770	-1.111	-0.578	-0.784	-0.796	-0.976	-0.936	-0.959	-0.554
-0.828	-0.972	-1.593	-1.662	-1.311	-1.353	-1.353	-1.353	-1.353	-1.353	-1.353	-1.353				

Row 34, column 23, layer 1, Homestake tailings pond and pumped recharge and discharge

0.000	0.000	0.000	0.000	0.000	0.000	0.000	0.000	0.000	0.000	0.000	0.000	0.000	0.000	0.000	0.000
0.000	0.000	0.000	0.000	0.000	0.000	0.000	0.000	0.000	0.000	0.000	0.000	0.000	0.000	0.000	0.000
0.000	0.000	0.000	0.166	0.166	0.166	0.166	0.166	0.166	0.205	0.226	0.187	0.341	0.219	0.236	0.211
0.235	0.258	0.234	0.239	0.199	0.173	0.133	0.154	0.222	0.116	0.157	0.211	0.147	0.129	0.112	-0.048
0.117	0.133	0.643	0.710	0.618	0.560	0.560	0.560	0.560	0.560	0.560	0.560				

Table 23.--Specified municipal and industrial ground-water withdrawals and recharge--Continued

Stress period															
1	2	3	4	5	6	7	8	9	10	11	12	13	14	15	16
17	18	19	20	21	22	23	24	25	26	27	28	29	30	31	32
33	34	35	36	37	38	39	40	41	42	43	44	45	46	47	48
49	50	51	52	53	54	55	56	57	58	59	60	61	62	63	64
65	66	67	68	69	70	71	72	73	74	75	76	77			

Row 3, column 16, layer 2, Village of Thoreau

0.000	0.000	0.000	0.000	0.000	0.000	0.000	0.000	0.000	0.000	0.000	0.000	0.000	0.000	0.000	0.000
0.000	0.000	0.000	0.000	0.000	0.000	0.000	0.000	0.000	0.000	0.000	0.000	0.000	0.000	0.000	0.000
0.000	0.000	0.000	0.000	0.000	0.000	0.000	-0.047	-0.047	-0.047	-0.047	-0.047	-0.047	-0.047	-0.047	-0.047
-0.047	-0.047	-0.047	-0.047	-0.047	-0.047	-0.050	-0.061	-0.070	-0.086	-0.090	-0.105	-0.094	-0.076	-0.164	-0.203
-0.242	-0.271	-0.290	-0.309	-0.329	-0.351	-0.351	-0.351	-0.351	-0.351	-0.351	-0.351				

Row 15, column 22, layer 2, Community of Prewitt

0.000	0.000	0.000	0.000	0.000	0.000	0.000	0.000	0.000	0.000	0.000	0.000	0.000	0.000	0.000	0.000
0.000	0.000	0.000	0.000	0.000	0.000	0.000	0.000	0.000	0.000	0.000	0.000	0.000	0.000	0.000	0.000
0.000	0.000	0.000	0.000	0.000	0.000	0.000	-0.036	-0.036	-0.036	-0.036	-0.036	-0.036	-0.036	-0.036	-0.036
-0.036	-0.036	-0.036	-0.036	-0.036	-0.036	-0.036	-0.036	-0.036	-0.036	-0.036	-0.036	-0.036	-0.036	-0.036	-0.036
-0.036	-0.036	-0.036	-0.036	-0.036	-0.036	-0.036	-0.036	-0.036	-0.036	-0.036	-0.036				

Row 33, column 18, layer 2, Homestake

0.000	0.000	0.000	0.000	0.000	0.000	0.000	0.000	0.000	0.000	0.000	0.000	0.000	0.000	0.000	0.000
0.000	0.000	0.000	0.000	0.000	0.000	0.000	0.000	0.000	0.000	0.000	0.000	0.000	0.000	0.000	0.000
0.000	0.000	0.000	0.000	0.000	0.000	0.000	0.000	0.000	0.000	0.000	0.000	0.000	0.000	0.000	0.000
0.000	0.000	0.000	0.000	0.000	0.000	0.000	0.000	0.000	-0.004	-0.007	-0.007	-0.014	-0.019	-0.019	-0.012
-0.007	-0.003	-0.006	-0.003	0.000	0.000	0.000	0.000	0.000	0.000	0.000	0.000				

Table 23.--Specified municipal and industrial ground-water withdrawals and recharge--Continued

Stress period															
1	2	3	4	5	6	7	8	9	10	11	12	13	14	15	16
17	18	19	20	21	22	23	24	25	26	27	28	29	30	31	32
33	34	35	36	37	38	39	40	41	42	43	44	45	46	47	48
49	50	51	52	53	54	55	56	57	58	59	60	61	62	63	64
65	66	67	68	69	70	71	72	73	74	75	76	77			
Row 2, column 25, layer 2, Western Nuclear Mine supply well															
0.000	0.000	0.000	0.000	0.000	0.000	0.000	0.000	0.000	0.000	0.000	0.000	0.000	0.000	0.000	0.000
0.000	0.000	0.000	0.000	0.000	0.000	0.000	0.000	0.000	0.000	0.000	0.000	0.000	0.000	0.000	0.000
0.000	0.000	0.000	0.000	0.000	0.000	0.000	0.000	0.000	0.000	0.000	0.000	0.000	0.000	0.000	0.000
0.000	0.000	0.000	0.000	0.000	0.000	0.000	0.000	0.000	0.000	0.000	0.000	0.000	0.000	-0.002	-0.004
-0.001	-0.001	-0.001	-0.003	-0.003	0.000	0.000	0.000	0.000	0.000	0.000	0.000				
Row 8, column 24, layer 2, Plains Electric															
0.000	0.000	0.000	0.000	0.000	0.000	0.000	0.000	0.000	0.000	0.000	0.000	0.000	0.000	0.000	0.000
0.000	0.000	0.000	0.000	0.000	0.000	0.000	0.000	0.000	0.000	0.000	0.000	0.000	0.000	0.000	0.000
0.000	0.000	0.000	0.000	0.000	0.000	0.000	0.000	0.000	0.000	0.000	0.000	0.000	0.000	0.000	0.000
0.000	0.000	0.000	0.000	0.000	0.000	0.000	0.000	0.000	0.000	0.000	0.000	0.000	0.000	-0.138	-0.145
-0.629	-0.759	-0.646	-0.638	-0.439	-0.436	-0.436	-0.436	-0.436	-0.436	-0.436	-0.436				
Row 32, column 20, layer 2, Plains Electric															
0.000	0.000	0.000	0.000	0.000	0.000	0.000	0.000	0.000	0.000	0.000	0.000	0.000	0.000	0.000	0.000
0.000	0.000	0.000	0.000	0.000	0.000	0.000	0.000	0.000	0.000	0.000	0.000	0.000	0.000	0.000	0.000
0.000	0.000	0.000	0.000	0.000	0.000	0.000	0.000	0.000	0.000	0.000	0.000	0.000	0.000	0.000	0.000
0.000	0.000	0.000	0.000	0.000	0.000	0.000	0.000	0.000	0.000	0.000	0.000	0.000	0.000	0.000	0.000
0.000	0.000	0.000	-0.754	-1.383	-1.701	-1.701	-1.701	-1.701	-1.701	-1.701	-1.701				

Table 23.--Specified municipal and industrial ground-water withdrawals and recharge--Concluded

Stress period															
1	2	3	4	5	6	7	8	9	10	11	12	13	14	15	16
17	18	19	20	21	22	23	24	25	26	27	28	29	30	31	32
33	34	35	36	37	38	39	40	41	42	43	44	45	46	47	48
49	50	51	52	53	54	55	56	57	58	59	60	61	62	63	64
65	66	67	68	69	70	71	72	73	74	75	76	77			
Total specified recharge															
0.00	0.00	0.00	0.00	0.00	0.00	0.00	0.00	0.14	0.14	0.14	0.14	0.14	0.14	0.14	0.00
0.00	0.00	0.00	0.00	0.00	0.14	0.29	0.61	0.92	0.98	1.02	1.30	1.57	2.84	4.12	4.58
3.88	3.51	3.60	3.34	2.51	0.65	0.69	0.69	0.69	0.72	0.74	0.69	0.84	0.72	0.73	0.69
0.70	0.72	0.68	0.68	0.64	0.64	0.63	0.68	0.73	0.62	0.67	0.81	0.83	0.86	0.81	0.58
0.26	0.30	0.79	0.83	0.75	0.70	0.70	0.70	0.70	0.70	0.70	0.70				
Total specified ground-water withdrawals															
-0.12	-0.34	-0.28	-0.28	-0.43	-0.69	-0.78	-0.88	-1.25	-1.25	-1.25	-1.25	-1.25	-1.25	-1.25	-0.29
-0.31	-0.33	-0.35	-0.35	-0.35	-0.57	-0.79	-1.30	-1.82	-1.93	-2.04	-2.47	-2.90	-4.87	-6.85	-7.60
-6.60	-6.10	-6.29	-6.53	-5.33	-4.87	-5.21	-5.32	-5.34	-5.60	-7.45	-5.89	-7.61	-5.65	-6.24	-5.93
-6.21	-6.22	-6.15	-6.10	-6.41	-6.51	-5.95	-6.80	-6.86	-6.56	-6.77	-8.13	-8.79	-11.69	-9.63	-8.10
-5.81	-6.97	-5.60	-8.19	-6.44	-8.34	-8.56	-8.56	-8.56	-8.56	-8.56	-8.56				
Net specified municipal and industrial ground-water withdrawals and recharge															
-0.12	-0.34	-0.28	-0.28	-0.43	-0.69	-0.78	-0.88	-1.11	-1.11	-1.11	-1.11	-1.11	-1.11	-1.11	-0.29
-0.31	-0.33	-0.35	-0.35	-0.35	-0.43	-0.50	-0.69	-0.90	-0.95	-1.02	-1.17	-1.33	-2.03	-2.73	-3.02
-2.72	-2.59	-2.69	-3.19	-2.82	-4.22	-4.52	-4.63	-4.65	-4.88	-6.71	-5.20	-6.77	-4.93	-5.51	-5.24
-5.51	-5.50	-5.47	-5.42	-5.77	-5.87	-5.32	-6.12	-6.13	-5.94	-6.10	-7.32	-7.96	-10.83	-8.82	-7.52
-5.55	-6.67	-4.81	-7.36	-5.69	-7.64	-7.86	-7.86	-7.86	-7.86	-7.86	-7.86				

Table 24.--Comparison of measured and model-derived hydraulic heads

[Individual comparisons are shown first; statistical comparisons are shown at end of the table]

Model Row	Model Column	Latitude	Longitude	U.S. Geological Survey identification number	Well number	Date	Measured hydraulic head (feet)	Model-derived hydraulic head (feet)	Model-derived minus measured hydraulic head (feet)	Cross reference to text and figures
		---------- Comparisons for layer 1, stress period 10 (1946.5) ----------								
30	20	351434	1075526	351434107552601	12N.10W.30.242	05/10/1946	6,480.55	6,502.50	21.95	
31	20	351400	1075439	351304107543701	12N.10W.29.434	02/26/1946	6,482.77	6,493.90	11.13	Figure 38A
32	19	351255	1075440	351255107544001	11N.10W.05.214	05/10/1946	6,481.21	6,487.80	6.59	
33	20	351303	1075321	351303107532201	11N.10W.04.222	05/10/1946	6,484.30	6,497.10	12.80	San Mateo
34	19	351213	1075316	351213107531701	11N.10W.10.111	02/26/1946	6,484.08	6,490.40	6.32	
35	17	351107	1075352	351107107535201	11N.10W.16.142	02/26/1946	6,485.50	6,480.00	-5.50	
		---------- Comparisons for layer 1, stress period 34 (1958.5) ----------								
27	20	351627	1075802	351630107572801	12N.11W.14.213	02/04/1958	6,514.27	6,532.80	18.53	Figure 37A
31	20	351400	1075439	351304107543701	12N.10W.29.434	02/04/1958	6,453.23	6,454.70	1.47	Figure 38A
33	20	351303	1075321	351303107532201	11N.10W.04.222	02/04/1958	6,463.71	6,472.30	8.59	San Mateo
34	19	351213	1075316	351213107531701	11N.10W.10.111	02/13/1957	6,453.50	6,463.50	10.00	
40	16	350913	1075154	350910107515401	11N.10W.26.321	02/17/1959	6,443.86	6,440.10	-3.76	
43	19	350937	1074930	350937107493201	11N.09W.30.211	01/01/1956	6,437.00	6,416.40	-20.60	Malpais
47	11	350516	1075027	350514107502701	10N.10W.24.212	02/03/1958	6,411.72	6,405.30	-6.42	Malpais
48	10	350417	1075100	350418107510101	10N.10W.25.114	02/03/1958	6,414.91	6,410.40	-4.51	Malpais
48	14	350603	1074859	350603107485801	10N.09W.17.113	02/10/1960	6,398.62	6,388.60	-10.02	Malpais
49	11	350408	1074854	350408107485401	10N.09W.29.132	02/03/1958	6,392.55	6,402.90	10.35	Malpais
50	9	350300	1074942	350300107491201	10N.09W.31.324	02/18/1959	6,408.46	6,422.50	14.04	Malpais
50	15	350516	1074700	350516107470001	10N.09W.21.222	02/03/1958	6,351.40	6,362.20	10.80	Malpais, figure 40

Table 24.--Comparison of measured and model-derived hydraulic heads--Continued

Model Row	Model Column	Latitude	Longitude	U.S. Geological Survey identification number	Well number	Date	Measured hydraulic head (feet)	Model-derived hydraulic head (feet)	Model-derived minus measured hydraulic head (feet)	Cross reference to text and figures
		---------- Comparisons for layer 1, stress period 69 (1985.5)----------								
27	20	351627	1075802	351630107572801	12N.11W.14.213	08/13/1985	6,519.57	6,519.90	0.33	Figure 37A
31	20	351400	1075439	351304107543701	12N.10W.29.434	08/14/1985	6,477.77	6,480.80	3.03	Figure 38A
32	21	351403	1075318	351403107531801	12N.10W.27.343	01/16/1986	6,511.53	6,494.40	-17.13	
33	21	351343	1075237	351343107523701	12N.10W.34.232	01/30/1985	6,524.86	6,509.00	-15.86	San Mateo
33	24	351640	1074948	351640107494801	12N.09W.07.343	03/29/1984	6,599.79	6,578.60	-21.19	San Mateo
34	19	351213	1075316	351213107531701	11N.10W.10.111	03/30/1984	6,462.62	6,477.10	14.48	
34	19	351236	1075320	351237107532201	11N.10W.04.422	03/30/1984	6,464.28	6,477.10	12.82	
40	15	350851	1075224	350851107522401	11N.10W.27.443	04/04/1983	6,445.39	6,449.90	4.51	
41	15	350839	1075224	350839107522401	11N.10W.34.223	04/04/1984	6,458.93	6,444.90	-14.03	
43	11	350630	1075237	350630107523701	10N.10W.10.414	04/13/1984	6,442.18	6,436.50	-5.68	Malpais
43	11	350631	1075258	350631107525801	10N.10W.10.321	07/11/1984	6,428.17	6,436.50	8.33	Malpais
43	11	350633	1075237	350633107523701	10N.10W.10.412	04/13/1984	6,446.88	6,436.50	-10.38	Malpais
45	9	350523	1075256	350523107525501	10N.10W.15.344	06/29/1984	6,414.43	6,421.00	6.57	Malpais
45	18	350815	1074919	350815107491901	11N.09W.31.423	04/12/1984	6,414.00	6,407.70	-6.30	Malpais
48	14	350603	1074859	350603107485801	10N.09W.17.113	03/13/1984	6,392.91	6,386.40	-6.51	Malpais
49	11	350408	1074854	350408107485401	10N.09W.29.132	03/13/1984	6,389.10	6,400.20	11.10	Malpais
50	15	350516	1074700	350516107470001	10N.09W.21.222	01/31/1984	6,351.44	6,360.20	8.76	Malpais, figure 40A
50	18	350609	1074607	350609107460701	10N.09W.15.221	04/12/1984	6,298.81	6,312.30	13.49	Malpais

Table 24.--Comparison of measured and model-derived hydraulic heads--Continued

Model Row	Model Column	Latitude	Longitude	U.S. Geological Survey identification number	Well number	Date	Measured hydraulic head (feet)	Model-derived hydraulic head (feet)	Model-derived minus measured hydraulic head (feet)	Cross reference to text and figures
				Comparisons for layer 2, stress period 10 (1946.5)						
25	19	351719	1075949	351719107594901	12N.11W.09.221	02/26/1946	6,533.30	6,538.10	4.80	Figures 37B, 45A, 60C
26	19	351645	1075900	351645107590001	12N.11W.10.431	02/27/1946	6,530.30	6,534.50	4.20	
27	18	351505	1075850	351505107585001	12N.11W.22.414	02/27/1946	6,519.41	6,521.90	2.49	
27	18	351516	1075857	351516107585701	12N.11W.22.234	05/10/1946	6,537.90	6,521.90	-16.00	
29	18	351417	1075733	351417107573301	12N.11W.26.244	01/10/1946	6,466.10	6,496.40	30.30	Toltec-Milan
29	19	351438	1075648	351441107552401	12N.11W.25.214	02/27/1946	6,478.02	6,494.00	15.98	Toltec-Milan
30	19	351354	1075525	351354107552401	12N.10W.32.111	02/26/1946	6,487.61	6,492.50	4.89	Toltec-Milan
30	19	351420	1075546	351423107554601	12N.10W.30.412	02/26/1946	6,485.96	6,492.50	6.54	Toltec-Milan
30	19	351421	1075539	351419107553101	12N.10W.30.421	02/26/1946	6,487.62	6,492.50	4.88	Toltec-Milan
33	18	351213	1075428	351213107542701	11N.10W.08.221	02/27/1946	6,480.15	6,482.50	2.35	Toltec-Milan
33	20	351304	1075346	351104107534701	11N.10W.04.211	02/27/1946	6,474.01	6,485.10	11.09	Toltec-Milan
33	23	351519	1075139	351519107513901	12N.10W.23.233	02/26/1946	6,476.41	6,486.00	9.59	Figures 38C, 45B, 55B, 56A, 59B
34	17	351122	1075359	351122107535901	11N.10W.16.121	02/27/1946	6,480.53	6,479.40	-1.13	Toltec-Milan
34	18	351158	1075337	351157107532801	11N.10W.09.241	02/26/1946	6,481.76	6,479.80	-1.96	Toltec-Milan
49	6	350111	1075235	350111107523501	09N.10W.10.414	10/02/1946	6,434.97	6,442.20	7.23	

Table 24.--Comparison of measured and model-derived hydraulic heads--Continued

Model Row	Model Column	Latitude	Longitude	U.S. Geological Survey identification number	Well number	Date	Measured hydraulic head (feet)	Model-derived hydraulic head (feet)	Model-derived minus measured hydraulic head (feet)	Cross reference to text and figures
---------- Comparisons for layer 2, stress period 30 (1956.5) ----------										
23	24	352532	1075249	352532107524901	14N.10W.22.414	11/21/1956	6,460.00	6,480.80	20.80	Figure 41B
24	19	351715	1080030	351715108003001	12N.11W.09.114	02/06/1956	6,494.30	6,493.50	-0.80	
25	19	351719	1075949	351719107594901	12N.11W.09.221	04/20/1956	6,482.18	6,490.60	8.42	Figures 37B, 45A, 60A
27	17	351445	1075842	351445107584201	12N.11W.27.222	02/07/1956	6,456.73	6,480.60	23.87	
30	19	351354	1075525	351354107552401	12N.10W.32.111	02/07/1956	6,458.26	6,452.50	-5.76	Toltec-Milan
33	20	351304	1075346	351104107534701	11N.10W.04.211	02/01/1956	6,447.88	6,455.60	7.72	Toltec-Milan
34	19	351213	1075324	351211107532901	11N.10W.09.221	02/07/1956	6,459.19	6,455.40	-3.79	Toltec-Milan
39	16	350925	1075226	350923107522701	11N.10W.27.241	04/17/1956	6,455.42	6,452.60	-2.82	Toltec-Milan
46	7	350336	1075315	350336107531501	10N.10W.27.333	02/08/1956	6,428.34	6,431.40	3.06	
47	8	350345	1075213	350346107521201	10N.10W.26.331	01/21/1956	6,429.11	6,429.60	0.49	Figures 39, 59A
49	6	350053	1075233	350053107523301	09N.10W.15.212	01/21/1956	6,429.40	6,438.80	9.40	
50	4	345815	1075415	345815107541501	09N.10W.33.110	12/28/1955	6,434.63	6,467.30	32.67	
72	31	350106	1071836	350108107183501	09N.05W.12.442	01/01/1964	6,034.00	6,031.30	-2.70	Mesita, East, figure 36

Table 24.--Comparison of measured and model-derived hydraulic heads--Continued

Model Row	Model Column	Latitude	Longitude	U.S. Geological Survey identification number	Well number	Date	Measured hydraulic head (feet)	Model-derived hydraulic head (feet)	Model-derived minus measured hydraulic head (feet)	Cross reference to text and figures
		---------- Comparisons for layer 2, stress period 61 (1979.5) ----------								
2	25	353016	1081004	353016108100401	15N.13W.25.142	01/01/1979	6,935.00	6,913.70	-21.30	North, figures 41A, 56B, 57B
29	18	351417	1075729	351416107571001	12N.11W.25.313	03/28/1979	6,437.95	6,464.10	26.15	Toltec-Milan
30	20	351452	1075523	351452107552301	12N.10W.20.333	03/28/1979	6,448.30	6,462.00	13.70	Toltec-Milan, figure 38B
33	20	351304	1075346	351104107534701	11N.10W.04.211	03/28/1979	6,444.95	6,459.40	14.45	Toltec-Milan
34	19	351213	1075324	351211107532901	11N.10W.09.221	03/26/1979	6,451.60	6,456.80	5.20	Toltec-Milan
39	16	350925	1075226	350923107522701	11N.10W.27.241	03/07/1979	6,445.78	6,450.90	5.12	Toltec-Milan
47	8	350345	1075213	350346107521201	10N.10W.26.331	03/06/1979	6,424.28	6,420.90	-3.38	Figures 39, 59A
65	39	351105	1071948	351105107194801	11N.05W.14.241	03/ /1975	6,223.00	6,241.20	18.20	East, figure 36
75	2	343158	1072908	343158107290801	04N.06W.32.214	06/05/1981	6,166.00	6,203.30	37.30	East, figure 36
		---------- Comparisons for layer 2, stress period 68 (1985.0) ----------								
2	6	352126	1081938	352126108193801	13N.14W.16.144	07/10/1984	7,587.00	7,593.10	6.10	North, figure 36
2	12	352434	1081642	352434108164201	14N.14W.25.342	06/08/1984	7,176.36	7,276.20	99.84	North
2	25	353016	1081004	353016108100401	15N.13W.25.142	08/23/1984	6,845.96	6,900.10	54.14	North, figures 41A, 56B, 57B
3	13	352324	1081450	352324108145001	13N.13W.06.224	07/10/1984	7,206.51	7,239.00	32.49	North, figure 36
3	14	352315	1081325	352315108132501	13N.13W.04.143	06/12/1984	7,130.82	7,206.00	75.18	North
4	8	352002	1081526	352002108152601	13N.13W.30.122	06/12/1984	7,479.05	7,439.80	-39.25	North, figure 36
5	19	352330	1080934	352330108093402	13N.13W.01.222	06/14/1984	6,987.28	7,061.80	74.52	North
17	22	352135	1080148	352135108014801	13N.11N.17.123	06/06/1984	6,583.84	6,594.00	10.16	North, figure 36
23	31	352532	1075249	352532107524901	14N.10W.22.414	08/22/1984	6,473.70	6,488.00	14.30	North, figures 36, 41B, 57A, 58A, 60D
29	34	352433	1074621	352433107462101	14N.09W.28.441	05/21/1984	6,449.85	6,463.30	13.45	Toltec-Milan, figure 36

Table 24.--Comparison of measured and model-derived hydraulic heads--Continued

Model Row	Model Column	Latitude	Longitude	U.S. Geological Survey identification number	Well number	Date	Measured hydraulic head (feet)	Model-derived hydraulic head (feet)	Model-derived minus measured hydraulic head (feet)	Cross reference to text and figures
---------- Comparisons for layer 2, stress period 70 (1986.0) ----------										
2	25	353016	1081004	353016108100401	15N.13W.25.142	08/29/1985	6,840.95	6,894.70	53.75	North, figures 36, 41A, 56B, 57B
2	12	352434	1081642	352434108164201	14N.14W.25.342	01/14/1986	7,206.50	7,271.30	64.80	North, figure 36
5	19	352330	1080934	352330108093401	13N.13W.01.222	01/14/1986	6,978.59	7,056.20	77.61	North, figure 36
22	24	352115	1075828	352115107582801	13N.11W.14.322	08/14/1985	6,485.14	6,514.70	29.56	Figure 36
24	19	351715	1080030	351715108003001	12N.11W.09.114	08/13/1985	6,545.11	6,544.40	-0.71	
25	19	351719	1075949	351719107594901	12N.11W.09.221	08/13/1985	6,542.32	6,538.70	-3.62	Figures 36, 37B, 45A, 60C
27	17	351445	1075842	351445107584201	12N.11W.27.222	08/14/1985	6,489.68	6,518.10	28.42	
30	20	351452	1075523	351452107552301	12N.10W.20.333	08/14/1985	6,470.16	6,478.40	8.24	Toltec-Milan, figures 36, 38B
33	20	351304	1075346	351104107534701	11N.10W.04.211	08/12/1985	6,466.67	6,471.90	5.23	Toltec-Milan
33	23	351519	1075139	351519107513901	12N.10W.23.233	08/14/1985	6,463.31	6,472.80	9.49	Toltec-Milan, figures 36, 38C, 45B, 55B, 56A, 59B
34	17	351118	1075423	351117107542301	11N.10W.17.222	08/13/1985	6,468.84	6,466.80	-2.04	Toltec-Milan
34	19	351213	1075324	351211107532901	11N.10W.09.221	08/12/1985	6,467.64	6,468.30	0.66	Toltec-Milan, figure 36
38	14	350911	1075353	350911107535301	11N.10W.28.322	08/13/1985	6,458.91	6,458.30	-0.61	Toltec-Milan
39	16	350925	1075226	350923107522701	11N.10W.27.241	08/08/1985	6,458.42	6,459.40	0.98	Toltec-Milan, figure 36
40	14	350829	1075243	350829107524301	11N.10W.34.231	08/13/1985	6,458.67	6,455.20	-3.47	Toltec-Milan
44	10	350613	1075245	350615107524601	10N.10W.10.433	08/13/1985	6,421.60	6,425.70	4.10	Figures 36, 11
46	6	350311	1075421	350311107542101	10N.10W.33.133	08/14/1985	6,414.65	6,445.80	31.15	

Table 24.--Comparison of measured and model-derived hydraulic heads--Continued

Model Row	Model Column	Latitude	Longitude	U.S. Geological Survey identification number	Well number	Date	Measured hydraulic head (feet)	Model-derived hydraulic head (feet)	Model-derived minus measured hydraulic head (feet)	Cross reference to text and figures
47	8	350345	1075213	350346107521201	10N.10W.26.331	08/13/1985	6,425.28	6,427.60	2.32	Figures 36, 39, 59A
49	6	350053	1075233	350053107523301	09N.10W.15.212	01/15/1986	6,422.98	6,434.10	11.12	
50	4	345815	1075415	345815107541501	09N.10W.33.110	01/15/1986	6,429.33	6,465.00	35.67	Figure 36
53	16	350352	1074426	350352107442601	09N.10W.25.324	06/11/1986	6,427.00	6,421.00	-6.00	Figure 36
54	6	345850	1074754	345850107475401	09N.09W.28.1344	1986	6,425.00	6,421.20	-3.80	Figures 36, 11, 45C, 55A, 56C, 57C, 58B, 59C
58	1	344548	1075608	344548107560801	06N.10W.07.141	11/17/1986	6,419.00	6,414.80	-4.20	Figure 36
65	8	345325	1073742	345325107374201	08N.08W.25.414	11/ /1986	6,417.00	6,410.80	-6.20	East, figures 36, 11
66	24	350053	1072901	350053107290101	09N.06W.16.111	07/08/1986	6,358.00	6,358.70	0.70	East, figure 36
70	17	345402	1072957	345402107295701	08N.06W.20.333	05/23/1986	6,390.00	6,368.00	-22.00	East, figure 36
73	2	343714	1073843	343714107384301	05N.08W.35.123	12/14/1986	6,424.00	6,410.60	-13.40	East, figure 36

Table 24.--Comparison of measured and model-derived hydraulic heads--Concluded

Group	Number of points	Differences, in feet: Mean total	Median	Root mean square	Mean absolute
Statistical comparisons					
Comparisons for layer 1, stress period 10 (1946.5)	6	8.88	8.86	12.13	10.72
Comparisons for layer 1, stress period 34 (1958.5)	12	2.37	5.03	11.33	9.92
Comparisons for layer 1, stress period 69 (1985.5)	18	-0.76	1.68	11.33	10.03
Comparisons for layer 2, stress period 10 (1946.5)	15	5.68	4.88	11.09	8.23
Comparisons for layer 2, stress period 30 (1956.5)	13	6.97	3.06	13.48	9.41
Comparisons for layer 2, stress period 61 (1979.5)	9	10.60	13.70	19.21	16.09
Comparisons for layer 2, stress period 68 (1985.0) (Points were all in northern part of modeled area)	10	34.09	23.39	52.18	41.94
Comparisons for layer 2, stress period 70 (1986.0)	27	11.03	0.98	25.94	15.92
Comparisons for points in all groups combined	110	8.89	5.21	22.89	14.58

Table 25.--Water budget for all stress periods of the standard scenario, in cubic feet per second

[All flows in this budget are model-derived except specified flow. Inflows are positive and outflows are negative]

Stress period	Stress-period end date		Specified flows	Evapotranspiration from water table	River boundary	General-head boundary	Ground-water storage	Constant-head boundary	Sum
1	1928.0	Inflow	14.73	0.00	14.67	0.00	0.02	0.44	29.86
		Outflow	-6.07	-4.24	-15.08	-4.08	-0.16	-0.14	-29.77
		Net	8.66	-4.24	-0.41	-4.08	-0.14	0.30	0.09
2	1932.0	Inflow	13.66	0.00	14.68	0.00	1.42	0.44	30.20
		Outflow	-6.29	-4.14	-15.27	-4.08	-0.32	-0.14	-30.24
		Net	7.37	-4.14	-0.59	-4.08	1.10	0.30	-0.04
3	1936.0	Inflow	15.64	0.00	19.26	0.00	0.11	0.44	35.45
		Outflow	-6.23	-4.29	-17.51	-4.08	-3.14	-0.14	-35.38
		Net	9.41	-4.29	1.75	-4.08	-3.03	0.30	0.07
4	1940.0	Inflow	17.40	0.00	19.56	0.00	0.22	0.44	37.63
		Outflow	-6.23	-4.37	-18.51	-4.08	-4.17	-0.14	-37.50
		Net	11.17	-4.37	1.05	-4.08	-3.95	0.30	0.13
5	1944.0	Inflow	17.61	0.00	19.46	0.00	0.08	0.44	37.60
		Outflow	-6.38	-4.34	-18.99	-4.08	-3.56	-0.14	-37.48
		Net	11.23	-4.34	0.47	-4.08	-3.48	0.30	0.12
6	1944.5	Inflow	0.27	0.00	17.69	0.00	16.16	0.44	34.56
		Outflow	-3.19	-4.45	-18.68	-4.08	-3.96	-0.14	-34.51
		Net	-2.92	-4.45	-0.99	-4.08	12.20	0.30	0.05
7	1945.0	Inflow	23.17	0.00	17.16	0.00	7.68	0.44	48.46
		Outflow	-10.18	-4.30	-17.23	-4.08	-12.34	-0.14	-48.28
		Net	12.99	-4.30	-0.07	-4.08	-4.66	0.30	0.18
8	1945.5	Inflow	6.95	0.00	10.61	0.00	16.92	0.44	34.92
		Outflow	-3.38	-4.43	-16.47	-4.08	-6.33	-0.14	-34.82
		Net	3.57	-4.43	-5.86	-4.08	10.59	0.30	0.10
9	1946.0	Inflow	18.84	0.00	15.32	0.00	13.61	0.44	48.22
		Outflow	-20.31	-4.20	-15.44	-4.08	-4.00	-0.14	-48.18
		Net	-1.47	-4.20	-0.12	-4.08	9.61	0.30	0.04
10	1946.5	Inflow	0.27	0.00	10.61	0.00	19.99	0.44	31.32
		Outflow	-3.75	-4.33	-15.42	-4.08	-3.49	-0.14	-31.22
		Net	-3.48	-4.33	-4.81	-4.08	16.50	0.30	0.10

Table 25.--Water budget for all stress periods of the standard scenario, in cubic feet per second--Continued

Stress period	Stress-period end date		Specified flows	Evapotranspiration from water table	River boundary	General-head boundary	Ground-water storage	Constant-head boundary	Sum
11	1947.0	Inflow	38.28	0.00	9.27	0.00	26.06	0.44	74.05
		Outflow	-35.50	-4.00	-12.58	-4.08	-17.69	-0.14	-73.99
		Net	2.78	-4.00	-3.31	-4.08	8.37	0.30	0.06
12	1947.5	Inflow	0.20	0.00	12.23	0.00	19.74	0.44	32.61
		Outflow	-3.75	-4.07	-14.81	-4.08	-5.55	-0.14	-32.40
		Net	-3.55	-4.07	-2.58	-4.08	14.19	0.30	0.21
13	1948.0	Inflow	28.23	0.00	9.17	0.00	31.35	0.44	69.19
		Outflow	-39.09	-3.30	-11.85	-4.08	-10.65	-0.14	-69.11
		Net	-10.85	-3.30	-2.68	-4.08	20.70	0.30	0.08
14	1948.5	Inflow	0.41	0.00	11.67	0.00	20.33	0.44	32.85
		Outflow	-3.75	-3.50	-13.75	-4.08	-7.41	-0.14	-32.64
		Net	-3.34	-3.50	-2.08	-4.08	12.92	0.30	0.21
15	1949.0	Inflow	33.50	0.00	18.93	0.00	15.08	0.44	67.95
		Outflow	-33.01	-3.18	-12.31	-4.08	-15.08	-0.14	-67.80
		Net	0.49	-3.18	6.62	-4.08	0.00	0.30	0.15
16	1949.5	Inflow	1.73	0.00	13.17	0.00	16.76	0.44	32.11
		Outflow	-2.79	-3.31	-13.99	-4.08	-7.62	-0.14	-31.93
		Net	-1.06	-3.31	-0.82	-4.08	9.14	0.30	0.18
17	1950.0	Inflow	26.21	0.00	18.41	0.00	8.97	0.44	54.03
		Outflow	-25.45	-3.25	-12.71	-4.08	-8.31	-0.14	-53.93
		Net	0.76	-3.25	5.70	-4.08	0.66	0.30	0.10
18	1950.5	Inflow	0.16	0.00	12.43	0.00	17.58	0.44	30.61
		Outflow	-2.83	-3.32	-13.92	-4.08	-6.12	-0.14	-30.41
		Net	-2.67	-3.32	-1.49	-4.08	11.46	0.30	0.20
19	1951.0	Inflow	18.12	0.00	8.07	0.00	30.91	0.44	57.55
		Outflow	-39.01	-2.85	-10.25	-4.08	-1.10	-0.14	-57.44
		Net	-20.89	-2.85	-2.18	-4.08	29.81	0.30	0.11
20	1951.5	Inflow	0.00	0.00	9.91	0.00	19.70	0.44	30.05
		Outflow	-2.84	-2.95	-12.32	-4.08	-7.49	-0.14	-29.82
		Net	-2.84	-2.95	-2.41	-4.08	12.21	0.30	0.23
21	1952.0	Inflow	19.51	0.00	6.13	0.00	28.82	0.44	54.91
		Outflow	-36.80	-2.56	-8.81	-4.08	-2.44	-0.14	-54.83
		Net	-17.29	-2.56	-2.68	-4.08	26.38	0.30	0.08

Table 25.--Water budget for all stress periods of the standard scenario, in cubic feet per second--Continued

Stress period	Stress-period end date		Specified flows	Evapotranspiration from water table	River boundary	General-head boundary	Ground-water storage	Constant-head boundary	Sum
22	1952.5	Inflow	4.16	0.00	8.69	0.00	16.04	0.44	29.33
		Outflow	-3.07	-2.87	-10.98	-4.08	-7.98	-0.14	-29.12
		Net	1.09	-2.87	-2.29	-4.08	8.06	0.30	0.21
23	1953.0	Inflow	31.60	0.00	12.03	0.00	15.01	0.44	59.08
		Outflow	-33.23	-2.45	-8.55	-4.08	-10.55	-0.14	-58.99
		Net	-1.63	-2.45	3.48	-4.08	4.46	0.30	0.09
24	1953.5	Inflow	0.65	0.00	8.86	0.00	18.22	0.44	28.17
		Outflow	-3.80	-2.69	-10.13	-4.08	-7.11	-0.14	-27.94
		Net	-3.15	-2.69	-1.27	-4.08	11.11	0.30	0.23
25	1954.0	Inflow	19.30	0.00	4.80	0.00	29.41	0.44	53.95
		Outflow	-38.68	-2.24	-7.15	-4.08	-1.75	-0.14	-54.04
		Net	-19.38	-2.24	-2.35	-4.08	27.66	0.30	-0.09
26	1954.5	Inflow	5.48	0.00	6.66	0.00	14.38	0.44	26.96
		Outflow	-4.43	-2.25	-8.93	-4.08	-6.90	-0.14	-26.73
		Net	1.05	-2.25	-2.27	-4.08	7.48	0.30	0.23
27	1955.0	Inflow	28.63	0.00	5.17	0.00	28.39	0.44	62.63
		Outflow	-40.56	-2.17	-7.06	-4.08	-8.73	-0.14	-62.74
		Net	-11.93	-2.17	-1.89	-4.08	19.66	0.30	-0.11
28	1955.5	Inflow	3.47	0.00	5.27	0.00	17.38	0.44	26.55
		Outflow	-4.97	-2.13	-7.85	-4.08	-7.13	-0.14	-26.30
		Net	-1.50	-2.13	-2.58	-4.08	10.25	0.30	0.25
29	1956.0	Inflow	24.56	0.00	4.17	0.00	27.76	0.44	56.93
		Outflow	-38.38	-2.08	-6.91	-4.08	-5.41	-0.14	-57.00
		Net	-13.82	-2.08	-2.74	-4.08	22.35	0.30	-0.07
30	1956.5	Inflow	6.52	0.00	3.86	0.00	16.58	0.44	27.40
		Outflow	-7.37	-2.03	-6.84	-4.08	-6.54	-0.14	-27.00
		Net	-0.85	-2.03	-2.98	-4.08	10.04	0.30	0.40
31	1957.0	Inflow	18.94	0.00	3.63	0.00	30.40	0.44	53.41
		Outflow	-35.97	-1.98	-6.74	-4.08	-4.53	-0.14	-53.44
		Net	-17.03	-1.98	-3.11	-4.08	25.87	0.30	-0.03
32	1957.5	Inflow	16.06	0.00	4.69	0.00	12.62	0.44	33.81
		Outflow	-10.10	-1.93	-7.11	-4.08	-9.97	-0.14	-33.33
		Net	5.96	-1.93	-2.42	-4.08	2.65	0.30	0.48

Table 25.--Water budget for all stress periods of the standard scenario, in cubic feet per second--Continued

Stress period	Stress-period end date		Specified flows	Evapotranspiration from water table	River boundary	General-head boundary	Ground-water storage	Constant-head boundary	Sum
33	1958.0	Inflow	21.96	0.00	6.72	0.00	20.63	0.44	49.74
		Outflow	-28.83	-1.83	-8.21	-4.07	-6.69	-0.14	-49.77
		Net	-6.87	-1.83	-1.49	-4.07	13.94	0.30	-0.03
34	1958.5	Inflow	14.57	0.00	7.52	0.00	9.86	0.44	32.39
		Outflow	-8.60	-1.76	-8.57	-4.07	-8.85	-0.14	-32.00
		Net	5.97	-1.76	-1.05	-4.07	1.01	0.30	0.39
35	1959.0	Inflow	23.54	0.00	9.48	0.00	15.79	0.44	49.25
		Outflow	-29.07	-1.70	-8.69	-4.07	-5.63	-0.14	-49.30
		Net	-5.53	-1.70	0.79	-4.07	10.16	0.30	-0.05
36	1959.5	Inflow	9.10	0.00	7.88	0.00	14.24	0.44	31.66
		Outflow	-9.03	-1.66	-8.61	-4.07	-7.79	-0.14	-31.30
		Net	0.07	-1.66	-0.73	-4.07	6.45	0.30	0.36
37	1960.0	Inflow	21.42	0.00	7.10	0.00	19.27	0.44	48.23
		Outflow	-28.38	-1.62	-8.47	-4.07	-5.64	-0.14	-48.32
		Net	-6.96	-1.62	-1.37	-4.07	13.63	0.30	-0.09
38	1960.5	Inflow	17.25	0.00	7.54	0.00	7.90	0.44	33.12
		Outflow	-7.37	-1.57	-8.38	-4.07	-11.28	-0.14	-32.81
		Net	9.88	-1.57	-0.84	-4.07	-3.38	0.30	0.31
39	1961.0	Inflow	16.08	0.00	10.01	0.00	18.95	0.44	45.49
		Outflow	-28.26	-1.54	-8.71	-4.07	-2.92	-0.14	-45.65
		Net	-12.18	-1.54	1.30	-4.07	16.03	0.30	-0.16
40	1961.5	Inflow	11.32	0.00	8.08	0.00	11.03	0.44	30.87
		Outflow	-7.82	-1.51	-8.63	-4.07	-8.39	-0.14	-30.56
		Net	3.50	-1.51	-0.55	-4.07	2.64	0.30	0.31
41	1962.0	Inflow	15.94	0.00	6.97	0.00	10.46	0.44	33.81
		Outflow	-14.31	-1.48	-8.54	-4.07	-5.14	-0.14	-33.67
		Net	1.63	-1.48	-1.57	-4.07	5.32	0.30	0.14
42	1962.5	Inflow	15.68	0.00	7.95	0.00	7.97	0.44	32.04
		Outflow	-8.10	-1.45	-8.48	-4.07	-9.51	-0.14	-31.74
		Net	7.58	-1.45	-0.53	-4.07	-1.54	0.30	0.30
43	1963.0	Inflow	17.98	0.00	14.46	0.00	7.94	0.44	40.81
		Outflow	-16.42	-1.43	-8.81	-4.06	-9.60	-0.14	-40.47
		Net	1.56	-1.43	5.65	-4.06	-1.66	0.30	0.34

Table 25.--Water budget for all stress periods of the standard scenario, in cubic feet per second--Continued

Stress period	Stress-period end date		Specified flows	Evapotranspiration from water table	River boundary	General-head boundary	Ground-water storage	Constant-head boundary	Sum
44	1963.5	Inflow	12.13	0.00	8.01	0.00	8.49	0.44	29.06
		Outflow	-8.39	-1.40	-8.65	-4.06	-6.15	-0.14	-28.80
		Net	3.74	-1.40	-0.64	-4.06	2.34	0.30	0.26
45	1964.0	Inflow	17.93	0.00	9.93	0.00	9.30	0.44	37.59
		Outflow	-16.58	-1.38	-8.41	-4.06	-6.85	-0.14	-37.43
		Net	1.35	-1.38	1.52	-4.06	2.45	0.30	0.16
46	1964.5	Inflow	8.05	0.00	6.51	0.00	11.55	0.44	26.55
		Outflow	-8.15	-1.37	-8.23	-4.06	-4.37	-0.14	-26.32
		Net	-0.10	-1.37	-1.72	-4.06	7.18	0.30	0.23
47	1965.5	Inflow	15.70	0.00	9.68	0.00	4.96	0.44	30.79
		Outflow	-11.98	-1.34	-8.23	-4.06	-4.87	-0.14	-30.61
		Net	3.72	-1.34	1.45	-4.06	0.09	0.30	0.18
48	1966.5	Inflow	25.84	0.00	9.98	0.00	2.88	0.44	39.14
		Outflow	-11.67	-1.33	-8.49	-4.05	-13.31	-0.14	-38.99
		Net	14.17	-1.33	1.49	-4.05	-10.43	0.30	0.15
49	1967.5	Inflow	13.81	0.00	10.03	0.00	6.40	0.44	30.68
		Outflow	-11.33	-1.33	-8.51	-4.05	-5.16	-0.14	-30.51
		Net	2.48	-1.33	1.52	-4.05	1.24	0.30	0.17
50	1968.5	Inflow	14.59	0.00	6.88	0.00	7.72	0.44	29.63
		Outflow	-12.86	-1.33	-8.12	-4.05	-3.20	-0.14	-29.70
		Net	1.73	-1.33	-1.24	-4.05	4.52	0.30	-0.07
51	1969.5	Inflow	13.02	0.00	6.81	0.00	9.34	0.44	29.61
		Outflow	-14.45	-1.32	-8.19	-4.05	-1.57	-0.14	-29.71
		Net	-1.43	-1.32	-1.38	-4.05	7.77	0.30	-0.10
52	1970.5	Inflow	17.26	0.00	9.10	0.00	3.43	0.44	30.23
		Outflow	-11.08	-1.31	-8.40	-4.05	-5.09	-0.14	-30.06
		Net	6.18	-1.31	0.70	-4.05	-1.66	0.30	0.17
53	1971.5	Inflow	11.14	0.00	7.14	0.00	10.89	0.44	29.61
		Outflow	-14.71	-1.30	-8.23	-4.04	-1.28	-0.14	-29.70
		Net	-3.57	-1.30	-1.09	-4.04	9.61	0.30	-0.09
54	1972.5	Inflow	13.40	0.00	6.45	0.00	9.64	0.44	29.93
		Outflow	-14.81	-1.28	-8.01	-4.04	-1.78	-0.14	-30.06
		Net	-1.41	-1.28	-1.56	-4.04	7.86	0.30	-0.13

Table 25.--Water budget for all stress periods of the standard scenario, in cubic feet per second--Continued

Stress period	Stress-period end date		Specified flows	Evapotranspiration from water table	River boundary	General-head boundary	Groundwater storage	Constant-head boundary	Sum
55	1973.5	Inflow	21.79	0.00	5.68	0.00	6.68	0.44	34.59
		Outflow	-14.25	-1.26	-7.90	-4.04	-7.12	-0.14	-34.71
		Net	7.54	-1.26	-2.22	-4.04	-0.44	0.30	-0.12
56	1974.5	Inflow	23.13	0.00	14.71	0.00	3.79	0.44	42.07
		Outflow	-9.30	-1.25	-9.65	-4.04	-17.48	-0.13	-41.85
		Net	13.83	-1.25	5.06	-4.04	-13.69	0.31	0.22
57	1975.5	Inflow	13.83	0.00	14.34	0.00	4.70	0.44	33.32
		Outflow	-9.36	-1.23	-9.01	-4.03	-9.27	-0.13	-33.04
		Net	4.47	-1.23	5.33	-4.03	-4.57	0.31	0.28
58	1976.5	Inflow	14.03	0.00	13.78	0.00	4.05	0.44	32.30
		Outflow	-9.06	-1.22	-9.11	-4.03	-8.52	-0.13	-32.08
		Net	4.97	-1.22	4.67	-4.03	-4.47	0.31	0.22
59	1977.5	Inflow	11.20	0.00	12.45	0.00	7.46	0.44	31.56
		Outflow	-9.58	-1.23	-8.34	-4.03	-8.03	-0.13	-31.33
		Net	1.62	-1.23	4.11	-4.03	-0.57	0.31	0.23
60	1978.5	Inflow	19.87	0.00	7.80	0.00	8.22	0.44	36.33
		Outflow	-17.84	-1.23	-7.76	-4.03	-5.37	-0.13	-36.36
		Net	2.03	-1.23	0.04	-4.03	2.85	0.31	-0.03
61	1979.5	Inflow	22.96	0.00	14.33	0.00	2.05	0.44	39.78
		Outflow	-14.36	-1.28	-8.04	-4.03	-11.75	-0.13	-39.59
		Net	8.60	-1.28	6.29	-4.03	-9.70	0.31	0.19
62	1980.5	Inflow	37.76	0.00	15.88	0.00	0.67	0.44	54.75
		Outflow	-14.50	-1.40	-9.31	-4.03	-25.09	-0.13	-54.46
		Net	23.26	-1.40	6.57	-4.03	-24.42	0.31	0.29
63	1981.5	Inflow	22.37	0.00	16.14	0.00	1.25	0.44	40.20
		Outflow	-12.43	-1.35	-9.73	-4.03	-12.32	-0.13	-40.00
		Net	9.94	-1.35	6.41	-4.03	-11.07	0.31	0.20
64	1982.5	Inflow	20.02	0.00	16.02	0.00	1.98	0.44	38.46
		Outflow	-10.91	-1.38	-10.20	-4.02	-11.73	-0.13	-38.37
		Net	9.11	-1.38	5.82	-4.02	-9.75	0.31	0.09
65	1983.5	Inflow	23.22	0.00	17.05	0.00	2.38	0.44	43.09
		Outflow	-8.62	-1.53	-11.47	-4.02	-17.21	-0.13	-42.99
		Net	14.60	-1.53	5.58	-4.02	-14.83	0.31	0.10

Table 25.--Water budget for all stress periods of the standard scenario, in cubic feet per second--Concluded

Stress period	Stress-period end date		Specified flows	Evapotranspiration from water table	River boundary	General-head boundary	Ground-water storage	Constant-head boundary	Sum
66	1984.0	Inflow	36.38	0.00	18.52	0.00	2.11	0.44	57.45
		Outflow	-9.47	-1.83	-12.38	-4.02	-29.35	-0.13	-57.18
		Net	26.91	-1.83	6.14	-4.02	-27.24	0.31	0.27
67	1984.5	Inflow	10.84	0.00	18.47	0.00	5.92	0.44	35.67
		Outflow	-8.10	-2.15	-13.06	-4.02	-8.02	-0.13	-35.48
		Net	2.74	-2.15	5.41	-4.02	-2.10	0.31	0.19
68	1985.0	Inflow	27.92	0.00	17.39	0.00	1.55	0.44	47.30
		Outflow	-10.69	-2.32	-12.23	-4.02	-17.57	-0.13	-46.96
		Net	17.23	-2.32	5.16	-4.02	-16.02	0.31	0.34
69	1985.5	Inflow	26.33	0.00	14.21	0.00	4.59	0.44	45.57
		Outflow	-8.94	-2.46	-12.93	-4.02	-17.01	-0.13	-45.49
		Net	17.39	-2.46	1.28	-4.02	-12.42	0.31	0.08
70	1986.0	Inflow	21.62	0.00	18.23	0.00	2.45	0.44	42.74
		Outflow	-10.84	-2.52	-12.75	-4.02	-12.13	-0.13	-42.40
		Net	10.78	-2.52	5.48	-4.02	-9.68	0.31	0.34
71	1987.0	Inflow	20.40	0.00	11.64	0.00	19.78	0.44	52.26
		Outflow	-28.73	-2.24	-10.38	-4.02	-6.69	-0.13	-52.20
		Net	-8.33	-2.24	1.26	-4.02	13.09	0.31	0.06
72	1990.0	Inflow	20.40	0.00	10.08	0.00	17.43	0.44	48.36
		Outflow	-28.73	-1.80	-8.48	-4.00	-5.18	-0.13	-48.32
		Net	-8.33	-1.80	1.60	-4.00	12.25	0.31	0.04
73	1995.0	Inflow	20.40	0.00	10.08	0.00	16.25	0.44	47.17
		Outflow	-28.73	-1.60	-8.51	-3.90	-4.34	-0.14	-47.21
		Net	-8.33	-1.60	1.57	-3.90	11.91	0.30	-0.04
74	2000.0	Inflow	20.40	0.00	10.09	0.00	15.45	0.44	46.39
		Outflow	-28.73	-1.58	-8.62	-3.78	-3.65	-0.14	-46.50
		Net	-8.33	-1.58	1.47	-3.78	11.80	0.30	-0.11
75	2010.0	Inflow	20.40	0.00	10.10	0.00	13.88	0.44	44.83
		Outflow	-28.73	-1.55	-8.80	-3.55	-2.14	-0.14	-44.91
		Net	-8.33	-1.55	1.30	-3.55	11.74	0.30	-0.08
76	2021.0	Inflow	20.40	0.00	10.13	0.00	12.67	0.44	43.64
		Outflow	-28.73	-1.54	-8.91	-3.35	-1.07	-0.14	-43.74
		Net	-8.33	-1.54	1.22	-3.35	11.60	0.30	-0.10

Table 26.--Specified river characteristics that were varied with time for the null scenario

Stress period	End of period (semi-water year)	Average lake altitude (feet)	Specified inflow at upper ends of river reaches (cubic feet per second)		
			Reach 1 (Cotton-wood Creek)	Reach 3 (Bluewater Creek upstream from lake)	Reach 5 (Bluewater Creek near Bluewater)
1	1928.0	7,325.00	3.90	9.10	11.00
2	1932.0	7,325.00	2.26	5.42	8.24
3	1936.0	7,325.00	3.81	8.82	20.52
4	1940.0	7,325.00	5.57	12.98	17.78
5	1944.0	7,325.00	4.40	10.21	34.83
6	1944.5	7,325.00	0.13	0.71	2.31
7	1945.0	7,325.00	1.41	3.52	2.31
8	1945.5	7,325.00	4.95	12.49	7.13
9	1946.0	7,325.00	5.54	11.94	7.13
10	1946.5	7,325.00	0.22	0.56	3.06
11	1947.0	7,325.00	5.62	13.85	3.06
12	1947.5	7,325.00	0.09	0.21	3.91
13	1948.0	7,325.00	0.12	0.50	3.91
14	1948.5	7,325.00	0.19	0.91	18.23
15	1949.0	7,325.00	0.57	1.17	18.23
16	1949.5	7,325.00	1.13	3.36	14.46
17	1950.0	7,325.00	3.99	8.99	14.46
18	1950.5	7,325.00	0.14	0.52	2.09
19	1951.0	7,325.00	0.00	0.00	2.09
20	1951.5	7,325.00	0.00	0.00	2.09
21	1952.0	7,325.00	0.00	0.00	2.09
22	1952.5	7,325.00	2.34	6.78	13.16
23	1953.0	7,325.00	6.18	13.12	13.16
24	1953.5	7,325.00	0.08	0.14	2.88
25	1954.0	7,325.00	0.00	0.02	2.88
26	1954.5	7,325.00	1.48	4.07	2.07
27	1955.0	7,325.00	0.53	1.17	2.07
28	1955.5	7,325.00	0.01	0.00	1.80
29	1956.0	7,325.00	0.01	0.00	1.80
30	1956.5	7,325.00	0.00	0.00	1.52
31	1957.0	7,325.00	0.00	0.00	1.52
32	1957.5	7,325.00	8.59	18.05	1.33
33	1958.0	7,325.00	0.89	3.85	1.33
34	1958.5	7,325.00	2.85	5.95	3.80
35	1959.0	7,325.00	3.79	10.14	3.80

Table 26.--Specified river characteristics that were varied with time for the null scenario--Concluded

Stress period	End of period (semi-water year)	Average lake altitude (feet)	Specified inflow at upper ends of river reaches (cubic feet per second)		
			Reach 1 (Cotton-wood Creek)	Reach 3 (Bluewater Creek upstream from lake)	Reach 5 (Bluewater Creek near Bluewater)
36	1959.5	7,325.00	0.00	0.00	0.00
37	1960.0	7,325.00	0.00	0.00	0.00
38	1960.5	7,325.00	5.38	12.33	10.18
39	1961.0	7,325.00	1.58	4.15	10.18
40	1961.5	7,325.00	0.29	0.50	1.24
41	1962.0	7,325.00	1.66	4.37	1.24
42	1962.5	7,325.00	3.96	10.56	15.81
43	1963.0	7,325.00	5.54	11.82	15.81
44	1963.5	7,325.00	5.76	13.80	4.42
45	1964.0	7,325.00	0.01	0.43	4.42
46	1964.5	7,325.00	0.06	0.24	11.02
47	1965.5	7,325.00	2.66	7.12	13.47
48	1966.5	7,325.00	9.17	20.17	14.18
49	1967.5	7,325.00	0.34	1.47	6.22
50	1968.5	7,325.00	0.20	0.98	2.88
51	1969.5	7,325.00	2.58	6.12	8.41
52	1970.5	7,325.00	4.06	8.99	5.83
53	1971.5	7,325.00	1.36	3.20	0.32
54	1972.5	7,325.00	0.30	1.09	0.61
55	1973.5	7,325.00	0.75	2.57	20.19
56	1974.5	7,325.00	14.62	32.37	19.84
57	1975.5	7,325.00	0.76	2.45	5.03
58	1976.5	7,325.00	3.24	7.19	4.80
59	1977.5	7,325.00	0.06	0.21	0.09
60	1978.5	7,325.00	6.96	15.13	9.82
61	1979.5	7,325.00	2.24	7.51	33.09
62	1980.5	7,325.00	18.26	41.92	43.13
63	1981.5	7,325.00	12.80	27.86	22.38
64	1982.5	7,325.00	2.94	8.07,	13.95
65	1983.5	7,325.00	8.71	20.36	29.72
66	1984.0	7,325.00	25.69	56.52	36.77
67	1984.5	7,325.00	0.51	2.50	19.63
68	1985.0	7,325.00	14.71	32.43	19.63
69	1985.5	7,325.00	5.32	15.13	31.00
70	1986.0	7,325.00	18.74	39.82	31.00
71-76	2021.0	7,325.00	3.90	9.10	11.00

Table 27.--Water budget for all stress periods of the null scenario, in cubic feet per second

[All flows in this budget are model-derived except specified flow. Inflows are positive and outflows are negative. Apparent discrepancies in the hundredth's place are rounding errors]

Stress period	Stress-period end date		Specified flows	Evapotranspiration from water table	River boundary	General-head boundary	Groundwater storage	Constant-head boundary	Sum
1	1928.0	Recharge	12.52	0.00	14.58	0.00	0.00	0.44	27.54
		Discharge	-2.50	-5.77	-15.05	-4.08	0.00	-0.14	-27.54
		Net	10.02	-5.77	-0.47	-4.08	0.00	0.30	0.00
2	1932.0	Recharge	12.52	0.00	14.58	0.00	0.00	0.44	27.54
		Discharge	-2.50	-5.77	-15.04	-4.08	-0.02	-0.14	-27.55
		Net	10.02	-5.77	-0.46	-4.08	-0.01	0.30	0.00
3	1936.0	Recharge	13.43	0.00	14.57	0.00	0.10	0.44	28.55
		Discharge	-2.50	-5.78	-15.03	-4.08	-0.90	-0.14	-28.43
		Net	10.93	-5.78	-0.45	-4.08	-0.80	0.30	0.12
4	1940.0	Recharge	14.54	0.00	14.57	0.00	0.22	0.44	29.76
		Discharge	-2.50	-5.83	-15.04	-4.08	-2.11	-0.14	-29.70
		Net	12.04	-5.83	-0.48	-4.08	-1.89	0.30	0.06
5	1944.0	Recharge	14.16	0.00	14.56	0.00	0.09	0.44	29.25
		Discharge	-2.50	-5.80	-15.05	-4.08	-1.51	-0.14	-29.09
		Net	11.66	-5.80	-0.49	-4.08	-1.43	0.30	0.16
6	1944.5	Recharge	0.27	0.00	8.86	0.00	17.55	0.44	27.11
		Discharge	-2.50	-5.74	-14.50	-4.08	-0.09	-0.14	-27.05
		Net	-2.23	-5.74	-5.64	-4.08	17.46	0.30	0.07
7	1945.0	Recharge	19.03	0.00	10.38	0.00	7.10	0.44	36.95
		Discharge	-2.50	-5.71	-14.58	-4.08	-10.01	-0.14	-37.02
		Net	16.53	-5.71	-4.20	-4.08	-2.91	0.30	-0.08
8	1945.5	Recharge	6.95	0.00	14.90	0.00	9.09	0.44	31.39
		Discharge	-2.50	-5.78	-14.66	-4.08	-4.00	-0.14	-31.17
		Net	4.45	-5.78	0.24	-4.08	5.09	0.30	0.21
9	1946.0	Recharge	13.18	0.00	14.82	0.00	2.80	0.44	31.24
		Discharge	-2.50	-5.75	-14.70	-4.08	-3.76	-0.14	-30.93
		Net	10.68	-5.75	0.12	-4.08	-0.96	0.30	0.31
10	1946.5	Recharge	0.14	0.00	9.54	0.00	16.63	0.44	26.74
		Discharge	-2.50	-5.70	-14.23	-4.08	-0.03	-0.14	-26.68
		Net	-2.36	-5.70	-4.68	-4.08	16.59	0.30	0.07

Table 27.--Water budget for all stress periods of the null scenario, in cubic feet per second--Continued

Stress period	Stress-period end date		Specified flows	Evapotranspiration from water table	River boundary	General-head boundary	Groundwater storage	Constant-head boundary	Sum
11	1947.0	Recharge	29.86	0.00	11.45	0.00	2.61	0.44	44.37
		Discharge	-2.50	-5.75	-14.42	-4.08	-17.36	-0.14	-44.25
		Net	27.36	-5.75	-2.97	-4.08	-14.74	0.30	0.12
12	1947.5	Recharge	0.62	0.00	9.78	0.00	16.09	0.44	26.93
		Discharge	-2.50	-5.68	-13.85	-4.08	-0.17	-0.14	-26.42
		Net	-1.88	-5.68	-4.07	-4.08	15.92	0.30	0.51
13	1948.0	Recharge	18.71	0.00	10.17	0.00	6.93	0.44	36.25
		Discharge	-2.50	-5.65	-13.83	-4.08	-9.87	-0.14	-36.08
		Net	16.21	-5.65	-3.66	-4.08	-2.95	0.30	0.17
14	1948.5	Recharge	0.27	0.00	13.49	0.00	13.68	0.44	27.89
		Discharge	-2.50	-5.68	-13.92	-4.08	-1.51	-0.14	-27.83
		Net	-2.23	-5.68	-0.43	-4.08	12.17	0.30	0.06
15	1949.0	Recharge	20.66	0.00	14.08	0.00	5.04	0.44	40.22
		Discharge	-2.50	-5.69	-14.01	-4.08	-13.48	-0.14	-39.90
		Net	18.16	-5.69	0.07	-4.08	-8.44	0.30	0.33
16	1949.5	Recharge	1.73	0.00	14.89	0.00	11.35	0.44	28.41
		Discharge	-2.50	-5.71	-14.25	-4.08	-1.65	-0.14	-28.32
		Net	-0.77	-5.71	0.65	-4.08	9.70	0.30	0.09
17	1950.0	Recharge	15.72	0.00	15.24	0.00	2.52	0.44	33.92
		Discharge	-2.50	-5.71	-14.48	-4.08	-6.58	-0.14	-33.49
		Net	13.22	-5.71	0.76	-4.08	-4.06	0.30	0.43
18	1950.5	Recharge	0.16	0.00	8.43	0.00	17.47	0.44	26.50
		Discharge	-2.50	-5.67	-13.99	-4.08	-0.03	-0.14	-26.41
		Net	-2.34	-5.67	-5.56	-4.08	17.44	0.30	0.09
19	1951.0	Recharge	7.36	0.00	7.64	0.00	10.76	0.44	26.20
		Discharge	-2.50	-5.65	-13.70	-4.08	-0.11	-0.14	-26.18
		Net	4.86	-5.65	-6.06	-4.08	10.65	0.30	0.02
20	1951.5	Recharge	0.00	0.00	7.65	0.00	17.61	0.44	25.69
		Discharge	-2.50	-5.63	-13.55	-4.08	-0.01	-0.14	-25.91
		Net	-2.50	-5.63	-5.91	-4.08	17.60	0.30	-0.22
21	1952.0	Recharge	8.19	0.00	7.65	0.00	10.00	0.44	26.28
		Discharge	-2.50	-5.61	-13.42	-4.08	-0.69	-0.14	-26.43
		Net	5.69	-5.61	-5.77	-4.08	9.31	0.30	-0.16

Table 27.--Water budget for all stress periods of the null scenario, in cubic feet per second--Continued

Stress period	Stress-period end date		Specified flows	Evapotranspiration from water table	River boundary	General-head boundary	Ground-water storage	Constant-head boundary	Sum
22	1952.5	Recharge	4.01	0.00	16.42	0.00	9.91	0.44	30.79
		Discharge	-2.50	-5.66	-13.88	-4.08	-4.32	-0.14	-30.58
		Net	1.51	-5.66	2.55	-4.08	5.59	0.30	0.21
23	1953.0	Recharge	17.10	0.00	15.88	0.00	3.30	0.44	36.73
		Discharge	-2.50	-5.65	-14.02	-4.08	-9.97	-0.14	-36.35
		Net	14.61	-5.65	1.87	-4.08	-6.68	0.30	0.37
24	1953.5	Recharge	0.42	0.00	8.66	0.00	16.78	0.44	26.30
		Discharge	-2.50	-5.59	-13.51	-4.08	-0.01	-0.14	-25.83
		Net	-2.08	-5.59	-4.85	-4.08	16.77	0.30	0.47
25	1954.0	Recharge	6.92	0.00	8.47	0.00	9.89	0.44	25.72
		Discharge	-2.50	-5.57	-13.40	-4.08	-0.16	-0.14	-25.85
		Net	4.42	-5.57	-4.93	-4.08	9.73	0.30	-0.13
26	1954.5	Recharge	4.50	0.00	11.00	0.00	11.29	0.44	27.23
		Discharge	-2.50	-5.56	-13.53	-4.08	-1.35	-0.14	-27.16
		Net	2.00	-5.56	-2.53	-4.08	9.94	0.30	0.07
27	1955.0	Recharge	15.60	0.00	9.44	0.00	7.80	0.44	33.28
		Discharge	-2.50	-5.54	-13.24	-4.08	-7.80	-0.14	-33.30
		Net	13.10	-5.54	-3.80	-4.08	0.00	0.30	-0.02
28	1955.5	Recharge	2.17	0.00	7.38	0.00	15.24	0.44	25.23
		Discharge	-2.50	-5.53	-13.02	-4.08	0.00	-0.14	-25.27
		Net	-0.33	-5.53	-5.64	-4.08	15.24	0.30	-0.03
29	1956.0	Recharge	12.09	0.00	7.38	0.00	9.25	0.44	29.17
		Discharge	-2.50	-5.52	-12.91	-4.08	-4.06	-0.14	-29.20
		Net	9.59	-5.52	-5.52	-4.08	5.19	0.30	-0.04
30	1956.5	Recharge	3.68	0.00	7.10	0.00	13.72	0.44	24.93
		Discharge	-2.50	-5.51	-12.80	-4.08	0.00	-0.14	-25.03
		Net	1.18	-5.51	-5.70	-4.08	13.71	0.30	-0.10
31	1957.0	Recharge	4.63	0.00	7.10	0.00	12.59	0.44	24.76
		Discharge	-2.50	-5.50	-12.70	-4.08	0.00	-0.14	-24.92
		Net	2.13	-5.50	-5.60	-4.08	12.59	0.30	-0.15
32	1957.5	Recharge	9.99	0.00	11.36	0.00	8.14	0.44	29.93
		Discharge	-2.50	-5.52	-12.92	-4.08	-4.79	-0.14	-29.95
		Net	7.49	-5.52	-1.56	-4.08	3.36	0.30	-0.02

Table 27.--Water budget for all stress periods of the null scenario, in cubic feet per second--Continued

Stress period	Stress-period end date		Specified flows	Evapotranspiration from water table	River boundary	General-head boundary	Groundwater storage	Constant-head boundary	Sum
33	1958.0	Recharge	10.10	0.00	10.03	0.00	7.56	0.44	28.14
		Discharge	-2.50	-5.49	-12.62	-4.08	-3.33	-0.14	-28.15
		Net	7.60	-5.49	-2.58	-4.08	4.23	0.30	-0.01
34	1958.5	Recharge	9.56	0.00	13.02	0.00	4.96	0.44	27.98
		Discharge	-2.50	-5.48	-12.86	-4.08	-2.74	-0.14	-27.79
		Net	7.06	-5.48	0.17	-4.08	2.22	0.30	0.19
35	1959.0	Recharge	11.69	0.00	12.84	0.00	3.61	0.44	28.58
		Discharge	-2.50	-5.47	-12.87	-4.08	-3.29	-0.14	-28.35
		Net	9.19	-5.47	-0.03	-4.08	0.32	0.30	0.22
36	1959.5	Recharge	4.26	0.00	5.60	0.00	14.33	0.44	24.64
		Discharge	-2.50	-5.46	-12.35	-4.08	0.00	-0.14	-24.52
		Net	1.76	-5.46	-6.75	-4.08	14.33	0.30	0.12
37	1960.0	Recharge	10.65	0.00	5.60	0.00	10.55	0.44	27.25
		Discharge	-2.50	-5.45	-12.22	-4.08	-2.77	-0.14	-27.15
		Net	8.15	-5.45	-6.61	-4.08	7.78	0.30	0.09
38	1960.5	Recharge	15.10	0.00	16.98	0.00	2.00	0.44	34.51
		Discharge	-2.50	-5.53	-12.78	-4.08	-9.28	-0.14	-34.32
		Net	12.60	-5.53	4.19	-4.08	-7.29	0.30	0.20
39	1961.0	Recharge	7.13	0.00	16.02	0.00	6.19	0.44	29.78
		Discharge	-2.50	-5.51	-12.97	-4.08	-4.37	-0.14	-29.57
		Net	4.63	-5.51	3.06	-4.08	1.82	0.30	0.22
40	1961.5	Recharge	9.13	0.00	7.67	0.00	8.84	0.44	26.08
		Discharge	-2.50	-5.47	-12.58	-4.07	-1.21	-0.14	-25.98
		Net	6.63	-5.47	-4.90	-4.07	7.63	0.30	0.11
41	1962.0	Recharge	11.14	0.00	10.08	0.00	6.66	0.44	28.32
		Discharge	-2.50	-5.46	-12.78	-4.07	-3.29	-0.14	-28.24
		Net	8.64	-5.46	-2.70	-4.07	3.37	0.30	0.08
42	1962.5	Recharge	13.46	0.00	16.35	0.00	3.72	0.44	33.98
		Discharge	-2.50	-5.56	-12.99	-4.07	-8.52	-0.14	-33.79
		Net	10.96	-5.56	3.36	-4.07	-4.80	0.30	0.19
43	1963.0	Recharge	9.81	0.00	16.07	0.00	3.34	0.44	29.66
		Discharge	-2.50	-5.53	-13.16	-4.07	-3.98	-0.14	-29.38
		Net	7.31	-5.53	2.90	-4.07	-0.64	0.30	0.27

Table 27.--Water budget for all stress periods of the null scenario, in cubic feet per second--Continued

Stress period	Stress-period end date		Specified flows	Evapotranspiration from water table	River boundary	General-head boundary	Groundwater storage	Constant-head boundary	Sum
44	1963.5	Recharge	9.93	0.00	13.22	0.00	4.41	0.44	28.01
		Discharge	-2.50	-5.50	-13.17	-4.07	-2.50	-0.14	-27.88
		Net	7.43	-5.50	0.06	-4.07	1.91	0.30	0.12
45	1964.0	Recharge	11.03	0.00	10.49	0.00	6.68	0.44	28.65
		Discharge	-2.50	-5.47	-12.75	-4.07	-3.58	-0.14	-28.51
		Net	8.54	-5.47	-2.27	-4.07	3.11	0.30	0.13
46	1964.5	Recharge	5.83	0.00	12.94	0.00	8.57	0.44	27.79
		Discharge	-2.50	-5.50	-12.84	-4.07	-2.51	-0.14	-27.56
		Net	3.33	-5.50	0.10	-4.07	6.06	0.30	0.23
47	1965.5	Recharge	10.78	0.00	15.96	0.00	2.00	0.44	29.18
		Discharge	-2.50	-5.54	-13.49	-4.07	-3.14	-0.14	-28.89
		Net	8.29	-5.54	2.47	-4.07	-1.15	0.30	0.29
48	1966.5	Recharge	20.96	0.00	15.62	0.00	0.72	0.44	37.74
		Discharge	-2.50	-5.61	-13.71	-4.07	-11.34	-0.14	-37.36
		Net	18.46	-5.61	1.91	-4.07	-10.62	0.30	0.38
49	1967.5	Recharge	9.12	0.00	13.71	0.00	4.64	0.44	27.90
		Discharge	-2.50	-5.51	-13.45	-4.07	-2.07	-0.14	-27.74
		Net	6.62	-5.51	0.26	-4.07	2.57	0.30	0.17
50	1968.5	Recharge	10.44	0.00	9.75	0.00	6.31	0.44	26.94
		Discharge	-2.50	-5.50	-13.21	-4.07	-1.53	-0.14	-26.95
		Net	7.95	-5.50	-3.46	-4.07	4.78	0.30	0.00
51	1969.5	Recharge	8.91	0.00	15.66	0.00	3.69	0.44	28.71
		Discharge	-2.50	-5.56	-13.72	-4.07	-2.54	-0.14	-28.53
		Net	6.41	-5.56	1.94	-4.07	1.15	0.31	0.17
52	1970.5	Recharge	13.15	0.00	14.50	0.00	1.57	0.44	29.65
		Discharge	-2.50	-5.53	-13.77	-4.07	-3.45	-0.14	-29.45
		Net	10.65	-5.53	0.73	-4.07	-1.88	0.31	0.20
53	1971.5	Recharge	7.07	0.00	8.54	0.00	9.80	0.44	25.85
		Discharge	-2.50	-5.49	-13.28	-4.07	-0.32	-0.14	-25.80
		Net	4.57	-5.49	-4.73	-4.07	9.48	0.31	0.05
54	1972.5	Recharge	9.33	0.00	7.70	0.00	8.05	0.44	25.52
		Discharge	-2.50	-5.47	-12.70	-4.07	-0.62	-0.14	-25.50
		Net	6.83	-5.47	-5.00	-4.07	7.43	0.31	0.02

Table 27.--Water budget for all stress periods of the null scenario, in cubic feet per second--Continued

Stress period	Stress-period end date		Specified flows	Evapotranspiration from water table	River boundary	General-head boundary	Groundwater storage	Constant-head boundary	Sum
55	1973.5	Recharge	17.73	0.00	15.12	0.00	1.49	0.44	34.78
		Discharge	-2.50	-5.57	-13.05	-4.07	-9.33	-0.14	-34.65
		Net	15.23	-5.57	2.07	-4.07	-7.84	0.31	0.13
56	1974.5	Recharge	18.60	0.00	15.61	0.00	2.39	0.44	37.04
		Discharge	-2.50	-5.66	-13.59	-4.07	-10.91	-0.13	-36.86
		Net	16.10	-5.66	2.02	-4.07	-8.52	0.31	0.18
57	1975.5	Recharge	9.26	0.00	12.94	0.00	3.94	0.44	26.58
		Discharge	-2.50	-5.52	-13.30	-4.07	-0.97	-0.13	-26.51
		Net	6.76	-5.52	-0.37	-4.07	2.96	0.31	0.07
58	1976.5	Recharge	9.57	0.00	13.39	0.00	3.21	0.44	26.61
		Discharge	-2.50	-5.50	-13.51	-4.07	-0.87	-0.13	-26.59
		Net	7.07	-5.50	-0.13	-4.07	2.34	0.31	0.02
59	1977.5	Recharge	6.59	0.00	5.97	0.00	11.94	0.44	24.94
		Discharge	-2.50	-5.48	-12.69	-4.07	-0.02	-0.13	-24.89
		Net	4.09	-5.48	-6.72	-4.07	11.92	0.31	0.05
60	1978.5	Recharge	15.11	0.00	15.96	0.00	1.41	0.44	32.92
		Discharge	-2.50	-5.59	-13.41	-4.07	-7.11	-0.13	-32.81
		Net	12.61	-5.59	2.55	-4.07	-5.70	0.31	0.12
61	1979.5	Recharge	18.19	0.00	15.58	0.00	1.49	0.44	35.69
		Discharge	-2.50	-5.64	-13.64	-4.07	-9.51	-0.13	-35.49
		Net	15.69	-5.64	1.95	-4.07	-8.03	0.31	0.21
62	1980.5	Recharge	32.95	0.00	15.39	0.00	0.29	0.44	49.07
		Discharge	-2.50	-5.91	-13.85	-4.07	-22.20	-0.13	-48.66
		Net	30.45	-5.91	1.54	-4.07	-21.91	0.31	0.41
63	1981.5	Recharge	17.61	0.00	15.27	0.00	0.61	0.44	33.93
		Discharge	-2.50	-5.71	-13.98	-4.07	-6.91	-0.13	-33.31
		Net	15.11	-5.71	1.29	-4.07	-6.30	0.31	0.63
64	1982.5	Recharge	16.99	0.00	15.19	0.00	0.25	0.44	32.87
		Discharge	-2.50	-5.68	-14.08	-4.07	-5.84	-0.13	-32.31
		Net	14.49	-5.68	1.11	-4.07	-5.59	0.31	0.56
65	1983.5	Recharge	20.50	0.00	15.12	0.00	0.19	0.44	36.25
		Discharge	-2.50	-5.78	-14.20	-4.07	-9.24	-0.13	-35.92
		Net	18.00	-5.78	0.91	-4.07	-9.04	0.31	0.33

Table 27.--Water budget for all stress periods of the null scenario, in cubic feet per second--Concluded

Stress period	Stress-period end date		Specified flows	Evapotranspiration from water table	River boundary	General-head boundary	Ground-water storage	Constant-head boundary	Sum
66	1984.0	Recharge	31.39	0.00	15.08	0.00	0.19	0.44	47.11
		Discharge	-2.50	-5.92	-14.28	-4.07	-19.54	-0.13	-46.44
		Net	28.89	-5.92	0.80	-4.07	-19.35	0.31	0.67
67	1984.5	Recharge	10.06	0.00	14.36	0.00	3.92	0.44	28.77
		Discharge	-2.50	-5.72	-14.01	-4.07	-2.19	-0.13	-28.62
		Net	7.56	-5.72	0.35	-4.07	1.73	0.31	0.16
68	1985.0	Recharge	22.39	0.00	15.06	0.00	0.16	0.44	38.06
		Discharge	-2.50	-5.80	-14.35	-4.07	-10.38	-0.13	-37.23
		Net	19.89	-5.80	0.71	-4.07	-10.22	0.31	0.82
69	1985.5	Recharge	25.58	0.00	15.02	0.00	0.32	0.44	41.36
		Discharge	-2.50	-5.90	-14.40	-4.07	-13.73	-0.13	-40.73
		Net	23.08	-5.90	0.62	-4.07	-13.41	0.31	0.63
70	1986.0	Recharge	18.57	0.00	15.00	0.00	1.21	0.44	35.22
		Discharge	-2.50	-5.80	-14.43	-4.07	-7.35	-0.13	-34.28
		Net	16.07	-5.80	0.57	-4.07	-6.14	0.31	0.94
71	1987.0	Recharge	12.52	0.00	14.97	0.00	1.08	0.44	29.01
		Discharge	-2.50	-5.72	-14.47	-4.07	-1.83	-0.13	-28.72
		Net	10.02	-5.72	0.50	-4.07	-0.75	0.31	0.29
72	1990.0	Recharge	12.52	0.00	14.88	0.00	0.69	0.44	28.54
		Discharge	-2.50	-5.73	-14.57	-4.07	-1.38	-0.13	-28.39
		Net	10.02	-5.73	0.31	-4.07	-0.70	0.31	0.15
73	1995.0	Recharge	12.52	0.00	14.81	0.00	0.40	0.44	28.17
		Discharge	-2.50	-5.75	-14.67	-4.07	-0.85	-0.14	-27.97
		Net	10.02	-5.75	0.14	-4.07	-0.46	0.31	0.20
74	2000.0	Recharge	12.52	0.00	14.76	0.00	0.28	0.44	28.01
		Discharge	-2.50	-5.75	-14.73	-4.07	-0.66	-0.14	-27.85
		Net	10.02	-5.75	0.03	-4.07	-0.38	0.30	0.16
75	2010.0	Recharge	12.52	0.00	14.70	0.00	0.18	0.44	27.85
		Discharge	-2.50	-5.76	-14.82	-4.07	-0.49	-0.14	-27.77
		Net	10.02	-5.76	-0.11	-4.07	-0.31	0.30	0.08
76	2021.0	Recharge	12.52	0.00	14.67	0.00	0.11	0.44	27.75
		Discharge	-2.50	-5.76	-14.86	-4.07	-0.32	-0.14	-27.65
		Net	10.02	-5.76	-0.19	-4.07	-0.21	0.30	0.10

Table 28.--Model-derived rates of ground-water evapotranspiration for the steady-state, standard, null, and no-Acoma scenarios

[Locations are shown in figure 28. All blocks are in layer 1. All rates are in cubic feet per second. Because the no-Acoma scenario is different from the Acoma scenario only for projections, only stress periods 71-76 are given]

---------- Steady-state scenario ----------

Location		Evapotranspiration	Location		Evapotranspiration	Location		Evapotranspiration
Row	Column		Row	Column		Row	Column	
41	17	-0.0166	44	12	-0.0562	47	14	-0.0060
42	13	-0.0410	44	17	-0.1384	47	15	-0.0854
42	17	-0.0740	44	18	-0.1279	47	16	-0.2198
42	18	-0.0061	45	11	-0.3091	47	17	-0.1964
43	11	-0.0831	45	12	-0.4570	48	17	-0.2764
43	12	-0.5050	45	13	-0.2041	49	17	-0.1138
43	13	-0.1456	45	17	-0.5352	50	17	-0.1656
43	17	-0.1948	45	18	-0.2162	50	18	-0.4406
43	18	-0.0470	46	16	-0.2735	51	18	-0.1108
44	11	-0.4296	46	17	-0.1646	52	17	-0.1298
						Total for steady-state		-5.7696

Table 28.--Model-derived rates of ground-water evapotranspiration for the steady-state, standard, null, and no-Acoma scenarios--Continued

--- Standard scenario ---

Stress period

1	2	3	4	5	6	7	8	9	10	11	12	13	14	15	16
17	18	19	20	21	22	23	24	25	26	27	28	29	30	31	32
33	34	35	36	37	38	39	40	41	42	43	44	45	46	47	48
49	50	51	52	53	54	55	56	57	58	59	60	61	62	63	64
65	66	67	68	69	70	71	72	73	74	75	76				

Row 42, column 13

-0.033	-0.032	-0.034	-0.035	-0.035	-0.035	-0.035	-0.035	-0.034	-0.034	-0.033	-0.032	-0.031	-0.030	-0.029	-0.029
-0.028	-0.028	-0.027	-0.027	0.000	-0.025	0.000	-0.024	0.000	0.000	0.000	0.000	0.000	0.000	0.000	0.000
0.000	0.000	0.000	0.000	0.000	0.000	0.000	0.000	0.000	0.000	0.000	0.000	0.000	0.000	0.000	0.000
0.000	0.000	0.000	0.000	0.000	0.000	0.000	0.000	0.000	0.000	0.000	0.000	0.000	0.000	0.000	0.000
0.000	-0.017	-0.022	-0.024	-0.026	-0.027	-0.014	0.000	0.000	0.000	0.000	0.000				

Row 42, column 17

-0.039	0.000	-0.028	-0.034	-0.018	-0.003	0.000	0.000	0.000	-0.009	-0.005	0.000	0.000	0.000	0.000	0.000
0.000	0.000	0.000	0.000	0.000	0.000	0.000	0.000	0.000	0.000	0.000	0.000	0.000	0.000	0.000	0.000
0.000	0.000	0.000	0.000	0.000	0.000	0.000	0.000	0.000	0.000	0.000	0.000	0.000	0.000	0.000	0.000
0.000	0.000	0.000	0.000	0.000	0.000	0.000	0.000	0.000	0.000	0.000	0.000	0.000	0.000	0.000	0.000
0.000	0.000	0.000	-0.009	-0.016	-0.022	-0.026	-0.004	0.000	0.000	0.000	0.000				

Row 42, column 18

-0.002	0.000	-0.002	-0.003	-0.002	-0.001	0.000	0.000	0.000	0.000	0.000	0.000	0.000	0.000	0.000	0.000
0.000	0.000	0.000	0.000	0.000	0.000	0.000	0.000	0.000	0.000	0.000	0.000	0.000	0.000	0.000	0.000
0.000	0.000	0.000	0.000	0.000	0.000	0.000	0.000	0.000	0.000	0.000	0.000	0.000	0.000	0.000	0.000
0.000	0.000	0.000	0.000	0.000	0.000	0.000	0.000	0.000	0.000	0.000	0.000	0.000	0.000	0.000	0.000
0.000	0.000	0.000	0.000	0.000	0.000	0.000	0.000	0.000	0.000	0.000	0.000				

Table 28.--Model-derived rates of ground-water evapotranspiration for the steady-state, standard, null, and no-Acoma scenarios--Continued

Standard scenario

Stress period

1	2	3	4	5	6	7	8	9	10	11	12	13	14	15	16
17	18	19	20	21	22	23	24	25	26	27	28	29	30	31	32
33	34	35	36	37	38	39	40	41	42	43	44	45	46	47	48
49	50	51	52	53	54	55	56	57	58	59	60	61	62	63	64
65	66	67	68	69	70	71	72	73	74	75	76				

Row 43, column 11

-0.066	-0.065	-0.066	-0.086	-0.067	-0.042	-0.035	-0.085	-0.047	-0.035	-0.108	-0.050	-0.033	-0.030	-0.026	-0.040
-0.041	-0.036	-0.024	-0.022	-0.010	-0.036	-0.011	0.000	0.000	0.000	0.000	0.000	0.000	0.000	0.000	0.000
0.000	0.000	0.000	0.000	0.000	0.000	0.000	0.000	0.000	0.000	0.000	0.000	0.000	0.000	0.000	0.000
0.000	0.000	0.000	0.000	0.000	0.000	0.000	0.000	0.000	0.000	0.000	0.000	0.000	-0.100	-0.029	-0.016
-0.079	-0.156	-0.073	-0.120	-0.191	-0.140	-0.070	0.000	0.000	0.000	0.000	0.000				

Row 43, column 12

-0.278	-0.276	-0.277	-0.278	-0.278	-0.335	-0.283	-0.324	-0.272	-0.315	-0.265	-0.308	-0.258	-0.300	-0.304	-0.352
-0.347	-0.386	-0.249	-0.389	-0.126	-0.408	-0.112	-0.335	-0.001	-0.019	0.000	0.000	0.000	0.000	0.000	0.000
0.000	0.000	0.000	0.000	0.000	0.000	0.000	0.000	0.000	0.000	0.000	0.000	0.000	0.000	0.000	0.000
0.000	0.000	0.000	0.000	0.000	0.000	0.000	0.000	0.000	0.000	0.000	0.000	0.000	0.000	0.000	0.000
0.000	-0.109	-0.411	-0.438	-0.456	-0.465	-0.215	0.000	0.000	0.000	0.000	0.000				

Row 43, column 13

-0.086	-0.084	-0.087	-0.089	-0.089	-0.095	-0.093	-0.094	-0.091	-0.091	-0.088	-0.087	-0.081	-0.076	-0.074	-0.074
-0.074	-0.077	-0.074	-0.076	-0.039	-0.072	-0.031	-0.064	0.000	-0.023	0.000	0.000	0.000	0.000	0.000	0.000
0.000	0.000	0.000	0.000	0.000	0.000	0.000	0.000	0.000	0.000	0.000	0.000	0.000	0.000	0.000	0.000
0.000	0.000	0.000	0.000	0.000	0.000	0.000	0.000	0.000	0.000	0.000	0.000	0.000	0.000	0.000	0.000
0.000	-0.031	-0.062	-0.076	-0.085	-0.091	-0.083	0.000	0.000	0.000	0.000	0.000				

Table 28.--Model-derived rates of ground-water evapotranspiration for the steady-state, standard, null, and no-Acoma scenarios--Continued

------------------------------ Standard scenario ------------------------------

Stress period															
1	2	3	4	5	6	7	8	9	10	11	12	13	14	15	16
17	18	19	20	21	22	23	24	25	26	27	28	29	30	31	32
33	34	35	36	37	38	39	40	41	42	43	44	45	46	47	48
49	50	51	52	53	54	55	56	57	58	59	60	61	62	63	64
65	66	67	68	69	70	71	72	73	74	75	76				
Row 43, column 17															
-0.157	-0.136	-0.154	-0.160	-0.154	-0.150	-0.145	-0.137	-0.139	-0.145	-0.146	-0.141	-0.132	-0.120	-0.110	-0.096
-0.088	-0.087	-0.087	-0.083	-0.079	-0.078	-0.082	-0.087	-0.091	-0.090	-0.088	-0.081	-0.072	-0.062	-0.051	-0.039
-0.026	-0.013	-0.001	0.000	0.000	0.000	0.000	0.000	0.000	0.000	0.000	0.000	0.000	0.000	0.000	0.000
0.000	0.000	0.000	0.000	0.000	0.000	0.000	0.000	0.000	0.000	0.000	0.000	0.000	0.000	0.000	0.000
-0.024	-0.046	-0.067	-0.085	-0.097	-0.106	-0.115	-0.082	-0.003	0.000	0.000	0.000				
Row 43, column 18															
-0.023	-0.020	-0.041	-0.042	-0.042	-0.030	-0.038	-0.027	-0.023	-0.022	-0.022	-0.021	-0.020	-0.032	-0.034	-0.034
-0.033	-0.032	-0.031	-0.030	-0.029	-0.028	-0.027	-0.027	-0.027	-0.027	-0.027	-0.026	-0.025	-0.024	-0.023	-0.021
-0.006	0.000	0.000	0.000	0.000	0.000	0.000	0.000	0.000	0.000	0.000	0.000	0.000	0.000	0.000	0.000
0.000	0.000	0.000	0.000	0.000	0.000	0.000	0.000	0.000	0.000	0.000	0.000	0.000	0.000	0.000	-0.004
-0.012	-0.015	-0.019	-0.022	-0.011	-0.022	-0.012	-0.008	0.000	0.000	0.000	0.000				
Row 44, column 10															
0.000	0.000	0.000	-0.003	0.000	0.000	0.000	0.000	0.000	0.000	0.000	0.000	0.000	0.000	0.000	0.000
0.000	0.000	0.000	0.000	0.000	0.000	0.000	0.000	0.000	0.000	0.000	0.000	0.000	0.000	0.000	0.000
0.000	0.000	0.000	0.000	0.000	0.000	0.000	0.000	0.000	0.000	0.000	0.000	0.000	0.000	0.000	0.000
0.000	0.000	0.000	0.000	0.000	0.000	0.000	0.000	0.000	0.000	0.000	0.000	0.000	0.000	0.000	0.000
0.000	0.000	0.000	0.000	0.000	0.000	0.000	0.000	0.000	0.000	0.000	0.000				

Table 28.--Model-derived rates of ground-water evapotranspiration for the steady-state, standard, null, and no-Acoma scenarios--Continued

---------- Standard scenario ----------

Stress period

1	2	3	4	5	6	7	8	9	10	11	12	13	14	15	16
17	18	19	20	21	22	23	24	25	26	27	28	29	30	31	32
33	34	35	36	37	38	39	40	41	42	43	44	45	46	47	48
49	50	51	52	53	54	55	56	57	58	59	60	61	62	63	64
65	66	67	68	69	70	71	72	73	74	75	76				

Row 44, column 11

-0.114	-0.113	-0.113	-0.115	-0.114	-0.176	-0.122	-0.164	-0.110	-0.153	-0.102	-0.147	0.000	-0.121	0.000	-0.161
-0.180	-0.231	0.000	-0.001	0.000	0.000	0.000	0.000	0.000	0.000	0.000	0.000	0.000	0.000	0.000	0.000
0.000	0.000	0.000	0.000	0.000	0.000	0.000	0.000	0.000	0.000	0.000	0.000	0.000	0.000	0.000	0.000
0.000	0.000	0.000	0.000	0.000	0.000	0.000	0.000	0.000	0.000	0.000	0.000	0.000	0.000	0.000	0.000
0.000	0.000	0.000	0.000	0.000	0.000	0.000	0.000	0.000	0.000	0.000	0.000				

Row 44, column 17

-0.102	-0.094	-0.104	-0.109	-0.108	-0.106	-0.106	-0.103	-0.101	-0.101	-0.101	-0.097	-0.091	-0.084	-0.075	-0.067
-0.060	-0.057	-0.055	-0.052	-0.048	-0.043	-0.041	-0.039	-0.037	-0.032	-0.029	-0.021	-0.014	-0.005	0.000	0.000
0.000	0.000	0.000	0.000	0.000	0.000	0.000	0.000	0.000	0.000	0.000	0.000	0.000	0.000	0.000	0.000
0.000	0.000	0.000	0.000	0.000	0.000	0.000	0.000	0.000	0.000	0.000	0.000	0.000	0.000	0.000	0.000
0.000	0.000	0.000	-0.012	-0.023	-0.034	-0.042	-0.014	0.000	0.000	0.000	0.000				

Row 44, column 18

-0.105	-0.103	-0.120	-0.121	-0.124	-0.115	-0.120	-0.113	-0.109	-0.107	-0.106	-0.105	-0.104	-0.112	-0.113	-0.112
-0.110	-0.108	-0.105	-0.102	-0.099	-0.096	-0.094	-0.093	-0.091	-0.089	-0.088	-0.087	-0.086	-0.084	-0.082	-0.078
-0.064	-0.057	-0.053	-0.050	-0.046	-0.042	-0.039	-0.035	-0.032	-0.030	-0.027	-0.024	-0.021	-0.019	-0.016	-0.018
-0.021	-0.023	-0.022	-0.022	-0.021	-0.019	-0.018	-0.016	-0.014	-0.013	-0.013	-0.014	-0.034	-0.043	-0.050	-0.057
-0.065	-0.071	-0.076	-0.081	-0.075	-0.086	-0.081	-0.076	-0.055	-0.032	0.000	0.000				

Table 28.--Model-derived rates of ground-water evapotranspiration for the steady-state, standard, null, and no-Acoma scenarios--Continued

-- Standard scenario --

Stress period															
1	2	3	4	5	6	7	8	9	10	11	12	13	14	15	16
17	18	19	20	21	22	23	24	25	26	27	28	29	30	31	32
33	34	35	36	37	38	39	40	41	42	43	44	45	46	47	48
49	50	51	52	53	54	55	56	57	58	59	60	61	62	63	64
65	66	67	68	69	70	71	72	73	74	75	76				
Row 45, column 11															
-0.218	-0.217	-0.217	-0.220	-0.222	-0.232	-0.228	-0.230	-0.225	-0.227	-0.218	-0.219	-0.013	-0.116	0.000	0.000
0.000	-0.036	0.000	0.000	0.000	0.000	0.000	0.000	0.000	0.000	0.000	0.000	0.000	0.000	0.000	0.000
0.000	0.000	0.000	0.000	0.000	0.000	0.000	0.000	0.000	0.000	0.000	0.000	0.000	0.000	0.000	0.000
0.000	0.000	0.000	0.000	0.000	0.000	0.000	0.000	0.000	0.000	0.000	0.000	0.000	0.000	0.000	0.000
0.000	0.000	0.000	0.000	0.000	0.000	0.000	0.000	0.000	0.000	0.000	0.000				
Row 45, column 12															
-0.165	-0.164	-0.164	-0.165	-0.166	-0.220	-0.170	-0.209	-0.160	-0.201	-0.115	-0.182	0.000	0.000	0.000	0.000
0.000	0.000	0.000	0.000	0.000	0.000	0.000	0.000	0.000	0.000	0.000	0.000	0.000	0.000	0.000	0.000
0.000	0.000	0.000	0.000	0.000	0.000	0.000	0.000	0.000	0.000	0.000	0.000	0.000	0.000	0.000	0.000
0.000	0.000	0.000	0.000	0.000	0.000	0.000	0.000	0.000	0.000	0.000	0.000	0.000	0.000	0.000	0.000
0.000	0.000	0.000	0.000	0.000	0.000	0.000	0.000	0.000	0.000	0.000	0.000				
Row 45, column 13															
-0.092	-0.089	-0.091	-0.094	-0.095	-0.105	-0.102	-0.104	-0.099	-0.101	0.000	-0.072	0.000	0.000	0.000	0.000
0.000	0.000	0.000	0.000	0.000	0.000	0.000	0.000	0.000	0.000	0.000	0.000	0.000	0.000	0.000	0.000
0.000	0.000	0.000	0.000	0.000	0.000	0.000	0.000	0.000	0.000	0.000	0.000	0.000	0.000	0.000	0.000
0.000	0.000	0.000	0.000	0.000	0.000	0.000	0.000	0.000	0.000	0.000	0.000	0.000	0.000	0.000	0.000
0.000	0.000	0.000	0.000	0.000	0.000	0.000	0.000	0.000	0.000	0.000	0.000				

Table 28.--Model-derived rates of ground-water evapotranspiration for the steady-state, standard, null, and no-Acoma scenarios--Continued

Standard scenario

Stress period

1	2	3	4	5	6	7	8	9	10	11	12	13	14	15	16
17	18	19	20	21	22	23	24	25	26	27	28	29	30	31	32
33	34	35	36	37	38	39	40	41	42	43	44	45	46	47	48
49	50	51	52	53	54	55	56	57	58	59	60	61	62	63	64
65	66	67	68	69	70	71	72	73	74	75	76				

Row 45, column 17

-0.484	-0.479	-0.495	-0.500	-0.502	-0.495	-0.499	-0.493	-0.490	-0.488	-0.485	-0.476	-0.466	-0.459	-0.445	-0.432
-0.422	-0.415	-0.410	-0.405	-0.399	-0.392	-0.387	-0.382	-0.377	-0.371	-0.366	-0.359	-0.351	-0.342	-0.332	-0.321
-0.298	-0.283	-0.271	-0.259	-0.248	-0.237	-0.226	-0.215	-0.206	-0.198	-0.190	-0.184	-0.179	-0.174	-0.169	-0.168
-0.170	-0.173	-0.175	-0.173	-0.170	-0.165	-0.158	-0.150	-0.146	-0.148	-0.154	-0.162	-0.188	-0.198	-0.207	-0.223
-0.251	-0.271	-0.293	-0.313	-0.319	-0.343	-0.351	-0.331	-0.258	-0.198	-0.096	0.000				

Row 45, column 18

-0.200	-0.199	-0.207	-0.208	-0.212	-0.210	-0.210	-0.208	-0.207	-0.205	-0.203	-0.201	-0.199	-0.199	-0.197	-0.196
-0.194	-0.192	-0.189	-0.186	-0.183	-0.179	-0.176	-0.174	-0.171	-0.169	-0.167	-0.166	-0.164	-0.163	-0.161	-0.158
-0.153	-0.148	-0.145	-0.142	-0.139	-0.136	-0.134	-0.131	-0.129	-0.127	-0.125	-0.123	-0.121	-0.120	-0.117	-0.117
-0.119	-0.121	-0.122	-0.121	-0.120	-0.118	-0.117	-0.116	-0.114	-0.113	-0.112	-0.112	-0.117	-0.121	-0.125	-0.130
-0.137	-0.141	-0.146	-0.151	-0.153	-0.158	-0.162	-0.161	-0.145	-0.130	-0.100	-0.061				

Row 46, column 16

-0.243	-0.241	-0.247	-0.250	-0.251	-0.248	-0.250	-0.248	-0.247	-0.246	-0.228	-0.211	-0.193	-0.173	-0.155	-0.139
-0.127	-0.118	-0.113	-0.108	-0.102	-0.096	-0.090	-0.085	-0.081	-0.076	-0.072	-0.067	-0.062	-0.056	-0.050	-0.043
-0.036	-0.028	-0.021	-0.014	-0.008	-0.001	0.000	0.000	0.000	0.000	0.000	0.000	0.000	0.000	0.000	0.000
0.000	0.000	0.000	0.000	0.000	0.000	0.000	0.000	0.000	0.000	0.000	0.000	0.000	0.000	0.000	0.000
0.000	0.000	0.000	0.000	-0.002	-0.014	-0.032	-0.032	0.000	0.000	0.000	0.000				

Table 28.--Model-derived rates of ground-water evapotranspiration for the steady-state, standard, null, and no-Acoma scenarios--Continued

-- Standard scenario --

Stress period															
1	2	3	4	5	6	7	8	9	10	11	12	13	14	15	16
17	18	19	20	21	22	23	24	25	26	27	28	29	30	31	32
33	34	35	36	37	38	39	40	41	42	43	44	45	46	47	48
49	50	51	52	53	54	55	56	57	58	59	60	61	62	63	64
65	66	67	68	69	70	71	72	73	74	75	76				
Row 46, column 17															
-0.141	-0.140	-0.151	-0.153	-0.154	-0.147	-0.153	-0.146	-0.145	-0.144	-0.139	-0.131	-0.125	-0.125	-0.118	-0.111
-0.106	-0.102	-0.098	-0.096	-0.093	-0.090	-0.087	-0.084	-0.082	-0.080	-0.078	-0.075	-0.073	-0.070	-0.067	-0.064
-0.060	-0.056	-0.052	-0.048	-0.045	-0.041	-0.038	-0.034	-0.030	-0.026	-0.023	-0.020	-0.017	-0.014	-0.010	-0.007
-0.006	-0.005	-0.004	-0.003	-0.001	0.000	0.000	0.000	0.000	0.000	0.000	0.000	0.000	0.000	0.000	-0.003
-0.011	-0.017	-0.024	-0.031	-0.038	-0.045	-0.054	-0.057	-0.041	-0.028	-0.007	0.000				
Row 47, column 14															
-0.001	-0.001	-0.001	-0.002	-0.002	-0.002	-0.002	-0.002	-0.002	-0.002	0.000	0.000	0.000	0.000	0.000	0.000
0.000	0.000	0.000	0.000	0.000	0.000	0.000	0.000	0.000	0.000	0.000	0.000	0.000	0.000	0.000	0.000
0.000	0.000	0.000	0.000	0.000	0.000	0.000	0.000	0.000	0.000	0.000	0.000	0.000	0.000	0.000	0.000
0.000	0.000	0.000	0.000	0.000	0.000	0.000	0.000	0.000	0.000	0.000	0.000	0.000	0.000	0.000	0.000
0.000	0.000	0.000	0.000	0.000	0.000	0.000	0.000	0.000	0.000	0.000	0.000				
Row 47, column 15															
-0.082	-0.081	-0.082	-0.082	-0.082	-0.082	-0.082	-0.082	-0.082	-0.082	-0.075	-0.070	-0.066	-0.062	-0.058	-0.054
-0.051	-0.049	-0.047	-0.046	-0.045	-0.043	-0.042	-0.040	-0.039	-0.038	-0.037	-0.036	-0.035	-0.034	-0.033	-0.032
-0.031	-0.030	-0.029	-0.027	-0.026	-0.025	-0.024	-0.023	-0.021	-0.020	-0.019	-0.018	-0.017	-0.016	-0.014	-0.013
-0.012	-0.011	-0.010	-0.009	-0.008	-0.007	-0.006	-0.005	-0.004	-0.003	-0.003	-0.002	-0.003	-0.003	-0.003	-0.004
-0.006	-0.007	-0.009	-0.011	-0.012	-0.015	-0.018	-0.022	-0.023	-0.026	-0.032	-0.034				

Table 28.--Model-derived rates of ground-water evapotranspiration for the steady-state, standard, null, and no-Acoma scenarios--Continued

---------- Standard scenario ----------

Stress period

1	2	3	4	5	6	7	8	9	10	11	12	13	14	15	16
17	18	19	20	21	22	23	24	25	26	27	28	29	30	31	32
33	34	35	36	37	38	39	40	41	42	43	44	45	46	47	48
49	50	51	52	53	54	55	56	57	58	59	60	61	62	63	64
65	66	67	68	69	70	71	72	73	74	75	76				

Row 47, column 16

-0.206	-0.205	-0.207	-0.208	-0.210	-0.209	-0.209	-0.209	-0.209	-0.208	-0.182	-0.167	-0.155	-0.143	-0.130	-0.120
-0.111	-0.104	-0.098	-0.093	-0.089	-0.084	-0.079	-0.075	-0.071	-0.068	-0.065	-0.062	-0.059	-0.055	-0.052	-0.048
-0.044	-0.040	-0.036	-0.032	-0.028	-0.024	-0.021	-0.016	-0.012	-0.008	-0.003	0.000	0.000	0.000	0.000	0.000
0.000	0.000	0.000	0.000	0.000	0.000	0.000	0.000	0.000	0.000	0.000	0.000	0.000	0.000	0.000	0.000
0.000	0.000	0.000	0.000	0.000	0.000	0.000	-0.014	-0.017	-0.029	-0.047	-0.049				

Row 47, column 17

-0.179	-0.178	-0.182	-0.184	-0.185	-0.184	-0.185	-0.183	-0.183	-0.182	-0.164	-0.148	-0.136	-0.127	-0.116	-0.106
-0.097	-0.089	-0.083	-0.078	-0.073	-0.068	-0.063	-0.059	-0.055	-0.051	-0.048	-0.045	-0.042	-0.038	-0.035	-0.031
-0.026	-0.022	-0.018	-0.013	-0.009	-0.005	-0.001	0.000	0.000	0.000	0.000	0.000	0.000	0.000	0.000	0.000
0.000	0.000	0.000	0.000	0.000	0.000	0.000	0.000	0.000	0.000	0.000	0.000	0.000	0.000	0.000	0.000
0.000	0.000	0.000	0.000	0.000	0.000	0.000	0.000	0.000	-0.006	-0.021	-0.019				

Row 48, column 17

-0.271	-0.271	-0.271	-0.272	-0.273	-0.273	-0.273	-0.273	-0.273	-0.273	-0.264	-0.258	-0.253	-0.255	-0.254	-0.250
-0.247	-0.244	-0.241	-0.238	-0.235	-0.233	-0.231	-0.229	-0.227	-0.225	-0.224	-0.223	-0.222	-0.221	-0.219	-0.218
-0.216	-0.215	-0.213	-0.211	-0.210	-0.208	-0.206	-0.205	-0.203	-0.201	-0.199	-0.197	-0.196	-0.194	-0.191	-0.188
-0.185	-0.183	-0.181	-0.179	-0.178	-0.176	-0.174	-0.171	-0.169	-0.168	-0.167	-0.166	-0.165	-0.165	-0.166	-0.167
-0.168	-0.169	-0.171	-0.173	-0.175	-0.178	-0.183	-0.192	-0.205	-0.221	-0.248	-0.262				

Table 28.--Model-derived rates of ground-water evapotranspiration for the steady-state, standard, null, and no-Acoma scenarios--Continued

---------- Standard scenario ----------

Stress period															
1	2	3	4	5	6	7	8	9	10	11	12	13	14	15	16
17	18	19	20	21	22	23	24	25	26	27	28	29	30	31	32
33	34	35	36	37	38	39	40	41	42	43	44	45	46	47	48
49	50	51	52	53	54	55	56	57	58	59	60	61	62	63	64
65	66	67	68	69	70	71	72	73	74	75	76				

Row 49, column 7

0.000	0.000	0.000	0.000	0.000	0.000	0.000	0.000	0.000	0.000	0.000	0.000	0.000	0.000	0.000	0.000
0.000	0.000	0.000	0.000	0.000	0.000	0.000	0.000	0.000	0.000	0.000	0.000	0.000	0.000	0.000	0.000
0.000	0.000	0.000	0.000	0.000	0.000	0.000	0.000	0.000	0.000	0.000	0.000	0.000	0.000	0.000	0.000
0.000	0.000	0.000	0.000	0.000	0.000	0.000	0.000	0.000	0.000	0.000	0.000	0.000	0.000	0.000	0.000
0.000	0.000	0.000	0.000	0.000	0.000	0.000	0.000	0.000	0.000	0.000	-0.058				

Row 49, column 17

-0.112	-0.111	-0.112	-0.112	-0.113	-0.113	-0.113	-0.113	-0.113	-0.113	-0.109	-0.107	-0.106	-0.104	-0.106	-0.103
-0.104	-0.100	-0.099	-0.097	-0.095	-0.094	-0.092	-0.092	-0.092	-0.092	-0.092	-0.091	-0.091	-0.091	-0.090	-0.089
-0.088	-0.088	-0.087	-0.086	-0.085	-0.084	-0.083	-0.083	-0.082	-0.081	-0.080	-0.079	-0.079	-0.078	-0.076	-0.075
-0.074	-0.073	-0.072	-0.071	-0.069	-0.069	-0.068	-0.067	-0.066	-0.065	-0.064	-0.064	-0.063	-0.063	-0.063	-0.063
-0.064	-0.064	-0.065	-0.065	-0.066	-0.066	-0.068	-0.073	-0.084	-0.097	-0.118	-0.130				

Row 50, column 17

-0.166	-0.166	-0.166	-0.166	-0.166	-0.166	-0.166	-0.166	-0.166	-0.166	-0.166	-0.166	-0.166	-0.166	-0.166	-0.166
-0.166	-0.166	-0.166	-0.166	-0.166	-0.166	-0.166	-0.166	-0.166	-0.166	-0.166	-0.166	-0.166	-0.166	-0.166	-0.166
-0.166	-0.166	-0.166	-0.166	-0.166	-0.166	-0.166	-0.166	-0.166	-0.166	-0.166	-0.166	-0.166	-0.166	-0.166	-0.166
-0.166	-0.166	-0.166	-0.166	-0.166	-0.166	-0.166	-0.166	-0.166	-0.166	-0.166	-0.166	-0.166	-0.166	-0.166	-0.166
-0.166	-0.166	-0.166	-0.166	-0.166	-0.166	-0.166	-0.166	-0.166	-0.166	-0.166	-0.166				

Table 28.--Model-derived rates of ground-water evapotranspiration for the steady-state, standard, null, and no-Acoma scenarios--Continued

Standard scenario

Stress period

1	2	3	4	5	6	7	8	9	10	11	12	13	14	15	16
17	18	19	20	21	22	23	24	25	26	27	28	29	30	31	32
33	34	35	36	37	38	39	40	41	42	43	44	45	46	47	48
49	50	51	52	53	54	55	56	57	58	59	60	61	62	63	64
65	66	67	68	69	70	71	72	73	74	75	76				

Row 50, column 18

-0.438	-0.437	-0.438	-0.438	-0.439	-0.439	-0.439	-0.439	-0.439	-0.439	-0.438	-0.437	-0.436	-0.434	-0.433	-0.432
-0.430	-0.428	-0.426	-0.424	-0.422	-0.419	-0.417	-0.415	-0.414	-0.412	-0.411	-0.410	-0.408	-0.408	-0.407	-0.406
-0.404	-0.403	-0.402	-0.401	-0.399	-0.398	-0.397	-0.396	-0.394	-0.393	-0.392	-0.390	-0.389	-0.388	-0.386	-0.383
-0.381	-0.379	-0.378	-0.376	-0.374	-0.373	-0.371	-0.370	-0.368	-0.367	-0.366	-0.365	-0.364	-0.363	-0.363	-0.363
-0.363	-0.364	-0.364	-0.364	-0.365	-0.366	-0.368	-0.375	-0.396	-0.421	-0.461	-0.486				

Row 51, column 18

-0.109	-0.108	-0.108	-0.109	-0.109	-0.109	-0.109	-0.109	-0.109	-0.109	-0.109	-0.108	-0.107	-0.106	-0.105	-0.104
-0.103	-0.101	-0.100	-0.098	-0.096	-0.094	-0.093	-0.091	-0.089	-0.088	-0.087	-0.086	-0.086	-0.086	-0.085	-0.084
-0.083	-0.083	-0.082	-0.081	-0.080	-0.079	-0.078	-0.077	-0.076	-0.075	-0.074	-0.073	-0.072	-0.071	-0.069	-0.068
-0.066	-0.065	-0.064	-0.062	-0.061	-0.060	-0.059	-0.058	-0.057	-0.056	-0.055	-0.054	-0.053	-0.053	-0.053	-0.053
-0.053	-0.054	-0.054	-0.054	-0.055	-0.055	-0.057	-0.062	-0.078	-0.096	-0.126	-0.144				

Row 52, column 17

-0.130	-0.130	-0.130	-0.130	-0.130	-0.130	-0.130	-0.130	-0.130	-0.130	-0.130	-0.130	-0.130	-0.130	-0.130	-0.130
-0.129	-0.129	-0.129	-0.129	-0.129	-0.129	-0.129	-0.129	-0.129	-0.129	-0.129	-0.129	-0.129	-0.129	-0.129	-0.128
-0.128	-0.128	-0.128	-0.128	-0.128	-0.128	-0.128	-0.128	-0.128	-0.128	-0.128	-0.128	-0.128	-0.128	-0.128	-0.127
-0.127	-0.127	-0.127	-0.127	-0.127	-0.127	-0.127	-0.127	-0.127	-0.127	-0.127	-0.127	-0.127	-0.127	-0.127	-0.127
-0.127	-0.127	-0.127	-0.127	-0.127	-0.127	-0.127	-0.127	-0.128	-0.129	-0.131	-0.132				

Table 28.--Model-derived rates of ground-water evapotranspiration for the steady-state, standard, null, and no-Acoma scenarios--Continued

---------- Standard scenario ----------

Stress period

1	2	3	4	5	6	7	8	9	10	11	12	13	14	15	16
17	18	19	20	21	22	23	24	25	26	27	28	29	30	31	32
33	34	35	36	37	38	39	40	41	42	43	44	45	46	47	48
49	50	51	52	53	54	55	56	57	58	59	60	61	62	63	64
65	66	67	68	69	70	71	72	73	74	75	76				

Total for each stress period of the standard scenario

-4.240	-4.141	-4.292	-4.366	-4.342	-4.451	-4.296	-4.426	-4.202	-4.328	-4.000	-4.070	-3.300	-3.501	-3.178	-3.306
-3.249	-3.316	-2.852	-2.946	-2.556	-2.872	-2.450	-2.688	-2.240	-2.247	-2.171	-2.130	-2.084	-2.033	-1.981	-1.927
-1.830	-1.760	-1.703	-1.658	-1.616	-1.574	-1.540	-1.508	-1.479	-1.452	-1.427	-1.403	-1.385	-1.368	-1.342	-1.330
-1.328	-1.326	-1.320	-1.309	-1.296	-1.279	-1.263	-1.246	-1.231	-1.224	-1.226	-1.231	-1.281	-1.401	-1.351	-1.376
-1.527	-1.825	-2.146	-2.322	-2.457	-2.525	-2.244	-1.796	-1.598	-1.579	-1.551	-1.539				

---------- Null scenario ----------

Row 41, column 17

-0.017	-0.017	-0.017	-0.017	-0.017	-0.016	-0.015	-0.014	-0.014	-0.013	-0.012	-0.011	-0.010	-0.010	-0.010	-0.011
-0.011	-0.011	-0.011	-0.010	-0.009	-0.008	-0.009	-0.009	-0.008	-0.007	-0.007	-0.006	-0.005	-0.004	-0.004	-0.003
-0.002	-0.002	-0.001	-0.001	0.000	-0.001	-0.002	-0.003	-0.003	-0.003	-0.004	-0.004	-0.004	-0.004	-0.006	-0.008
-0.008	-0.006	-0.007	-0.007	-0.006	-0.004	-0.005	-0.007	-0.007	-0.005	-0.004	-0.005	-0.007	-0.009	-0.010	-0.011
-0.012	-0.012	-0.012	-0.013	-0.013	-0.013	-0.013	-0.014	-0.015	-0.015	-0.016	-0.016				

Table 28.--Model-derived rates of ground-water evapotranspiration for the steady-state, standard, null, and no-Acoma scenarios--Continued

Null scenario

Stress period

1	2	3	4	5	6	7	8	9	10	11	12	13	14	15	16
17	18	19	20	21	22	23	24	25	26	27	28	29	30	31	32
33	34	35	36	37	38	39	40	41	42	43	44	45	46	47	48
49	50	51	52	53	54	55	56	57	58	59	60	61	62	63	64
65	66	67	68	69	70	71	72	73	74	75	76				

Row 42, column 13

-0.041	-0.041	-0.041	-0.041	-0.041	-0.041	-0.040	-0.040	-0.040	-0.040	-0.040	-0.040	-0.040	-0.039	-0.039	-0.040
-0.040	-0.040	-0.040	-0.039	-0.039	-0.039	-0.039	-0.039	-0.039	-0.039	-0.039	-0.039	-0.039	-0.038	-0.038	-0.038
-0.038	-0.038	-0.038	-0.038	-0.038	-0.038	-0.038	-0.038	-0.038	-0.038	-0.038	-0.038	-0.038	-0.038	-0.039	-0.039
-0.039	-0.039	-0.039	-0.039	-0.039	-0.038	-0.038	-0.039	-0.039	-0.039	-0.038	-0.038	-0.039	-0.039	-0.039	-0.039
-0.040	-0.040	-0.040	-0.040	-0.040	-0.040	-0.040	-0.040	-0.040	-0.040	-0.041	-0.041				

Row 42, column 17

-0.074	-0.074	-0.074	-0.074	-0.074	-0.074	-0.073	-0.072	-0.072	-0.072	-0.071	-0.070	-0.069	-0.069	-0.069	-0.069
-0.070	-0.070	-0.070	-0.069	-0.068	-0.068	-0.068	-0.068	-0.068	-0.067	-0.066	-0.066	-0.065	-0.065	-0.064	-0.064
-0.063	-0.063	-0.062	-0.062	-0.061	-0.061	-0.062	-0.063	-0.063	-0.063	-0.063	-0.064	-0.064	-0.064	-0.065	-0.067
-0.067	-0.066	-0.066	-0.066	-0.066	-0.065	-0.065	-0.066	-0.066	-0.066	-0.065	-0.065	-0.066	-0.067	-0.068	-0.069
-0.070	-0.070	-0.070	-0.071	-0.071	-0.071	-0.071	-0.072	-0.073	-0.073	-0.073	-0.073				

Row 42, column 18

-0.006	-0.006	-0.006	-0.007	-0.007	-0.006	-0.006	-0.006	-0.006	-0.006	-0.006	-0.006	-0.005	-0.006	-0.006	-0.006
-0.006	-0.006	-0.006	-0.005	-0.005	-0.005	-0.005	-0.005	-0.005	-0.005	-0.005	-0.005	-0.005	-0.005	-0.005	-0.005
-0.004	-0.004	-0.004	-0.004	-0.004	-0.004	-0.005	-0.004	-0.004	-0.005	-0.005	-0.005	-0.005	-0.005	-0.005	-0.005
-0.005	-0.005	-0.005	-0.005	-0.005	-0.005	-0.005	-0.005	-0.005	-0.005	-0.005	-0.005	-0.005	-0.005	-0.006	-0.006
-0.006	-0.006	-0.006	-0.006	-0.006	-0.006	-0.006	-0.006	-0.006	-0.006	-0.006	-0.006				

Table 28.--Model-derived rates of ground-water evapotranspiration for the steady-state, standard, null, and no-Acoma scenarios--Continued

Null scenario

Stress period

1	2	3	4	5	6	7	8	9	10	11	12	13	14	15	16
17	18	19	20	21	22	23	24	25	26	27	28	29	30	31	32
33	34	35	36	37	38	39	40	41	42	43	44	45	46	47	48
49	50	51	52	53	54	55	56	57	58	59	60	61	62	63	64
65	66	67	68	69	70	71	72	73	74	75	76				

Row 43, column 11

-0.083	-0.083	-0.083	-0.105	-0.084	-0.057	-0.050	-0.100	-0.065	-0.051	-0.124	-0.067	-0.052	-0.048	-0.047	-0.057
-0.055	-0.049	-0.047	-0.046	-0.046	-0.076	-0.059	-0.050	-0.047	-0.048	-0.046	-0.046	-0.046	-0.046	-0.045	-0.082
-0.055	-0.055	-0.058	-0.049	-0.046	-0.089	-0.056	-0.048	-0.046	-0.102	-0.064	-0.071	-0.052	-0.047	-0.066	-0.105
-0.051	-0.050	-0.061	-0.068	-0.048	-0.047	-0.087	-0.147	-0.063	-0.058	-0.046	-0.108	-0.141	-0.244	-0.133	-0.109
-0.146	-0.207	-0.106	-0.141	-0.188	-0.134	-0.090	-0.082	-0.083	-0.083	-0.083	-0.083				

Row 43, column 12

-0.505	-0.505	-0.505	-0.505	-0.505	-0.505	-0.505	-0.505	-0.505	-0.505	-0.505	-0.505	-0.504	-0.504	-0.504	-0.504
-0.504	-0.504	-0.504	-0.504	-0.504	-0.504	-0.504	-0.504	-0.504	-0.504	-0.504	-0.504	-0.503	-0.503	-0.503	-0.503
-0.503	-0.503	-0.503	-0.503	-0.503	-0.503	-0.503	-0.503	-0.503	-0.503	-0.503	-0.503	-0.503	-0.503	-0.503	-0.504
-0.504	-0.504	-0.504	-0.504	-0.503	-0.503	-0.503	-0.504	-0.504	-0.503	-0.503	-0.504	-0.504	-0.505	-0.505	-0.505
-0.505	-0.505	-0.505	-0.505	-0.505	-0.505	-0.505	-0.505	-0.505	-0.505	-0.505	-0.505				

Row 43, column 13

-0.146	-0.146	-0.146	-0.146	-0.146	-0.146	-0.145	-0.145	-0.145	-0.145	-0.144	-0.144	-0.144	-0.144	-0.143	-0.144
-0.144	-0.144	-0.144	-0.144	-0.143	-0.143	-0.143	-0.143	-0.143	-0.143	-0.142	-0.142	-0.142	-0.142	-0.141	-0.141
-0.141	-0.141	-0.141	-0.140	-0.140	-0.140	-0.140	-0.141	-0.141	-0.141	-0.141	-0.141	-0.141	-0.141	-0.141	-0.142
-0.142	-0.142	-0.142	-0.142	-0.142	-0.141	-0.141	-0.142	-0.142	-0.142	-0.141	-0.141	-0.142	-0.143	-0.143	-0.143
-0.144	-0.144	-0.144	-0.144	-0.144	-0.144	-0.144	-0.145	-0.145	-0.145	-0.145	-0.145				

Table 28.--Model-derived rates of ground-water evapotranspiration for the steady-state, standard, null, and no-Acoma scenarios--Continued

Null scenario

Stress period															
1	2	3	4	5	6	7	8	9	10	11	12	13	14	15	16
17	18	19	20	21	22	23	24	25	26	27	28	29	30	31	32
33	34	35	36	37	38	39	40	41	42	43	44	45	46	47	48
49	50	51	52	53	54	55	56	57	58	59	60	61	62	63	64
65	66	67	68	69	70	71	72	73	74	75	76				

Row 43, column 17

-0.195	-0.195	-0.195	-0.195	-0.195	-0.195	-0.194	-0.193	-0.192	-0.192	-0.191	-0.190	-0.189	-0.188	-0.188	-0.189
-0.189	-0.189	-0.189	-0.188	-0.187	-0.187	-0.187	-0.186	-0.186	-0.185	-0.185	-0.184	-0.183	-0.182	-0.181	-0.181
-0.180	-0.179	-0.179	-0.178	-0.178	-0.178	-0.179	-0.180	-0.180	-0.180	-0.181	-0.181	-0.181	-0.181	-0.183	-0.185
-0.185	-0.184	-0.185	-0.185	-0.184	-0.182	-0.183	-0.184	-0.185	-0.183	-0.182	-0.183	-0.184	-0.186	-0.187	-0.188
-0.189	-0.190	-0.190	-0.190	-0.190	-0.191	-0.191	-0.192	-0.193	-0.194	-0.194	-0.194				

Row 43, column 18

-0.047	-0.047	-0.047	-0.047	-0.048	-0.042	-0.039	-0.045	-0.046	-0.040	-0.037	-0.036	-0.035	-0.042	-0.045	-0.046
-0.046	-0.039	-0.036	-0.034	-0.033	-0.041	-0.043	-0.035	-0.032	-0.030	-0.029	-0.028	-0.028	-0.027	-0.027	-0.026
-0.026	-0.025	-0.025	-0.025	-0.024	-0.037	-0.041	-0.031	-0.027	-0.038	-0.041	-0.032	-0.029	-0.039	-0.043	-0.044
-0.033	-0.031	-0.044	-0.033	-0.031	-0.030	-0.043	-0.045	-0.034	-0.031	-0.030	-0.043	-0.044	-0.045	-0.045	-0.046
-0.046	-0.046	-0.046	-0.046	-0.047	-0.047	-0.047	-0.047	-0.047	-0.047	-0.047	-0.047				

Row 44, column 10

0.000	0.000	0.000	-0.019	0.000	0.000	0.000	0.000	0.000	0.000	0.000	0.000	0.000	0.000	0.000	0.000
0.000	0.000	0.000	0.000	0.000	0.000	0.000	0.000	0.000	0.000	0.000	0.000	0.000	0.000	0.000	0.000
0.000	0.000	0.000	0.000	0.000	0.000	0.000	0.000	0.000	0.000	0.000	0.000	0.000	0.000	0.000	0.000
0.000	0.000	0.000	0.000	0.000	0.000	0.000	0.000	0.000	0.000	0.000	0.000	0.000	-0.145	-0.043	-0.022
-0.061	-0.124	-0.021	-0.057	-0.106	-0.050	-0.006	0.000	0.000	0.000	0.000	0.000				

Table 28.--Model-derived rates of ground-water evapotranspiration for the steady-state, standard, null, and no-Acoma scenarios--Continued

Null scenario

Stress period

1	2	3	4	5	6	7	8	9	10	11	12	13	14	15	16
17	18	19	20	21	22	23	24	25	26	27	28	29	30	31	32
33	34	35	36	37	38	39	40	41	42	43	44	45	46	47	48
49	50	51	52	53	54	55	56	57	58	59	60	61	62	63	64
65	66	67	68	69	70	71	72	73	74	75	76				

Row 44, column 11

-0.429	-0.429	-0.429	-0.431	-0.430	-0.429	-0.428	-0.429	-0.428	-0.428	-0.429	-0.429	-0.428	-0.427	-0.427	-0.427
-0.426	-0.426	-0.425	-0.425	-0.425	-0.425	-0.425	-0.425	-0.424	-0.424	-0.424	-0.423	-0.423	-0.423	-0.423	-0.424
-0.423	-0.423	-0.423	-0.423	-0.422	-0.423	-0.423	-0.423	-0.422	-0.424	-0.423	-0.423	-0.423	-0.423	-0.423	-0.425
-0.424	-0.423	-0.423	-0.424	-0.423	-0.422	-0.424	-0.427	-0.425	-0.425	-0.424	-0.426	-0.428	-0.433	-0.430	-0.430
-0.431	-0.432	-0.430	-0.431	-0.432	-0.431	-0.430	-0.430	-0.430	-0.429	-0.429	-0.429				

Row 44, column 12

-0.056	-0.056	-0.056	-0.057	-0.056	-0.056	-0.056	-0.056	-0.056	-0.055	-0.055	-0.055	-0.055	-0.055	-0.054	-0.054
-0.055	-0.055	-0.055	-0.054	-0.054	-0.054	-0.054	-0.054	-0.054	-0.054	-0.054	-0.054	-0.053	-0.053	-0.053	-0.053
-0.053	-0.053	-0.053	-0.053	-0.053	-0.053	-0.053	-0.053	-0.053	-0.053	-0.053	-0.053	-0.053	-0.053	-0.053	-0.053
-0.053	-0.053	-0.053	-0.053	-0.053	-0.053	-0.053	-0.053	-0.053	-0.053	-0.053	-0.053	-0.054	-0.055	-0.054	-0.054
-0.055	-0.055	-0.055	-0.055	-0.055	-0.055	-0.055	-0.056	-0.056	-0.056	-0.056	-0.056				

Row 44, column 17

-0.139	-0.139	-0.139	-0.139	-0.139	-0.138	-0.137	-0.137	-0.137	-0.135	-0.134	-0.133	-0.132	-0.133	-0.134	-0.134
-0.134	-0.134	-0.133	-0.132	-0.130	-0.131	-0.131	-0.130	-0.129	-0.128	-0.127	-0.126	-0.126	-0.125	-0.125	-0.124
-0.123	-0.123	-0.123	-0.122	-0.122	-0.123	-0.124	-0.124	-0.123	-0.125	-0.126	-0.125	-0.125	-0.126	-0.128	-0.130
-0.129	-0.128	-0.130	-0.129	-0.128	-0.127	-0.129	-0.130	-0.129	-0.128	-0.127	-0.128	-0.129	-0.131	-0.132	-0.133
-0.134	-0.134	-0.135	-0.135	-0.135	-0.136	-0.136	-0.137	-0.138	-0.138	-0.138	-0.138				

Table 28.--Model-derived rates of ground-water evapotranspiration for the steady-state, standard, null, and no-Acoma scenarios--Continued

Null scenario

Stress period															
1	2	3	4	5	6	7	8	9	10	11	12	13	14	15	16
17	18	19	20	21	22	23	24	25	26	27	28	29	30	31	32
33	34	35	36	37	38	39	40	41	42	43	44	45	46	47	48
49	50	51	52	53	54	55	56	57	58	59	60	61	62	63	64
65	66	67	68	69	70	71	72	73	74	75	76				

Row 44, column 18

-0.128	-0.128	-0.130	-0.130	-0.133	-0.124	-0.121	-0.128	-0.129	-0.120	-0.117	-0.116	-0.116	-0.124	-0.127	-0.129
-0.129	-0.120	-0.117	-0.113	-0.111	-0.117	-0.118	-0.109	-0.106	-0.104	-0.103	-0.104	-0.104	-0.104	-0.103	-0.102
-0.101	-0.101	-0.102	-0.102	-0.102	-0.112	-0.115	-0.107	-0.106	-0.115	-0.117	-0.109	-0.107	-0.116	-0.118	-0.122
-0.115	-0.115	-0.125	-0.116	-0.114	-0.113	-0.125	-0.127	-0.117	-0.114	-0.112	-0.122	-0.122	-0.123	-0.125	-0.127
-0.128	-0.129	-0.129	-0.129	-0.130	-0.130	-0.130	-0.130	-0.129	-0.128	-0.128	-0.128				

Row 45, column 11

-0.309	-0.309	-0.309	-0.312	-0.313	-0.312	-0.312	-0.312	-0.311	-0.311	-0.310	-0.310	-0.310	-0.309	-0.308	-0.308
-0.307	-0.306	-0.305	-0.305	-0.304	-0.303	-0.302	-0.301	-0.300	-0.300	-0.299	-0.298	-0.297	-0.296	-0.295	-0.294
-0.294	-0.293	-0.292	-0.291	-0.291	-0.290	-0.290	-0.289	-0.289	-0.288	-0.288	-0.288	-0.288	-0.287	-0.287	-0.287
-0.287	-0.286	-0.286	-0.285	-0.285	-0.284	-0.283	-0.285	-0.285	-0.286	-0.286	-0.286	-0.288	-0.290	-0.294	-0.296
-0.299	-0.301	-0.302	-0.303	-0.304	-0.305	-0.307	-0.309	-0.309	-0.308	-0.308	-0.307				

Row 45, column 12

-0.457	-0.457	-0.457	-0.458	-0.458	-0.458	-0.458	-0.458	-0.458	-0.458	-0.458	-0.457	-0.457	-0.457	-0.457	-0.457
-0.457	-0.457	-0.457	-0.456	-0.456	-0.456	-0.456	-0.456	-0.456	-0.455	-0.455	-0.455	-0.455	-0.455	-0.454	-0.454
-0.454	-0.454	-0.453	-0.453	-0.453	-0.453	-0.453	-0.453	-0.453	-0.452	-0.452	-0.452	-0.452	-0.452	-0.452	-0.452
-0.452	-0.452	-0.452	-0.452	-0.452	-0.452	-0.452	-0.452	-0.452	-0.452	-0.452	-0.452	-0.452	-0.452	-0.453	-0.453
-0.454	-0.454	-0.455	-0.455	-0.455	-0.455	-0.456	-0.456	-0.457	-0.457	-0.457	-0.457				

Table 28.--Model-derived rates of ground-water evapotranspiration for the steady-state, standard, null, and no-Acoma scenarios--Continued

Null scenario

Stress period

1	2	3	4	5	6	7	8	9	10	11	12	13	14	15	16
17	18	19	20	21	22	23	24	25	26	27	28	29	30	31	32
33	34	35	36	37	38	39	40	41	42	43	44	45	46	47	48
49	50	51	52	53	54	55	56	57	58	59	60	61	62	63	64
65	66	67	68	69	70	71	72	73	74	75	76				

Row 45, column 13

-0.204	-0.204	-0.204	-0.205	-0.205	-0.204	-0.204	-0.204	-0.204	-0.204	-0.203	-0.203	-0.202	-0.202	-0.202	-0.202
-0.202	-0.202	-0.202	-0.202	-0.202	-0.201	-0.201	-0.201	-0.201	-0.201	-0.200	-0.200	-0.199	-0.199	-0.199	-0.199
-0.198	-0.198	-0.197	-0.197	-0.197	-0.197	-0.197	-0.197	-0.197	-0.197	-0.197	-0.197	-0.197	-0.197	-0.197	-0.198
-0.198	-0.198	-0.198	-0.198	-0.198	-0.197	-0.197	-0.197	-0.198	-0.197	-0.197	-0.197	-0.197	-0.198	-0.199	-0.199
-0.200	-0.200	-0.200	-0.201	-0.201	-0.201	-0.201	-0.202	-0.203	-0.204	-0.204	-0.204				

Row 45, column 17

-0.536	-0.536	-0.537	-0.537	-0.538	-0.533	-0.530	-0.534	-0.535	-0.529	-0.527	-0.525	-0.524	-0.529	-0.530	-0.531
-0.532	-0.527	-0.525	-0.524	-0.521	-0.525	-0.525	-0.520	-0.517	-0.516	-0.514	-0.513	-0.513	-0.512	-0.512	-0.510
-0.510	-0.509	-0.508	-0.508	-0.508	-0.513	-0.516	-0.511	-0.510	-0.516	-0.518	-0.513	-0.512	-0.517	-0.520	-0.522
-0.518	-0.518	-0.525	-0.519	-0.518	-0.516	-0.523	-0.526	-0.520	-0.518	-0.516	-0.522	-0.523	-0.525	-0.526	-0.528
-0.530	-0.530	-0.531	-0.531	-0.531	-0.532	-0.533	-0.534	-0.535	-0.535	-0.536	-0.536				

Row 45, column 18

-0.216	-0.216	-0.218	-0.218	-0.221	-0.219	-0.217	-0.218	-0.218	-0.216	-0.214	-0.213	-0.212	-0.213	-0.215	-0.216
-0.217	-0.215	-0.213	-0.211	-0.209	-0.208	-0.207	-0.205	-0.202	-0.201	-0.199	-0.199	-0.199	-0.199	-0.199	-0.198
-0.197	-0.196	-0.196	-0.197	-0.196	-0.199	-0.201	-0.200	-0.200	-0.202	-0.204	-0.203	-0.202	-0.203	-0.205	-0.208
-0.208	-0.210	-0.213	-0.211	-0.210	-0.209	-0.212	-0.215	-0.212	-0.211	-0.209	-0.210	-0.210	-0.210	-0.212	-0.213
-0.215	-0.216	-0.216	-0.217	-0.217	-0.218	-0.218	-0.218	-0.217	-0.217	-0.217	-0.216				

Table 28.--Model-derived rates of ground-water evapotranspiration for the steady-state, standard, null, and no-Acoma scenarios--Continued

Null scenario

Stress period

1	2	3	4	5	6	7	8	9	10	11	12	13	14	15	16
17	18	19	20	21	22	23	24	25	26	27	28	29	30	31	32
33	34	35	36	37	38	39	40	41	42	43	44	45	46	47	48
49	50	51	52	53	54	55	56	57	58	59	60	61	62	63	64
65	66	67	68	69	70	71	72	73	74	75	76				

Row 46, column 16

-0.274	-0.274	-0.274	-0.275	-0.275	-0.273	-0.271	-0.273	-0.273	-0.271	-0.270	-0.270	-0.269	-0.271	-0.271	-0.272
-0.272	-0.270	-0.269	-0.268	-0.268	-0.269	-0.270	-0.267	-0.266	-0.266	-0.265	-0.264	-0.264	-0.263	-0.263	-0.262
-0.262	-0.261	-0.261	-0.260	-0.260	-0.262	-0.263	-0.261	-0.260	-0.262	-0.263	-0.261	-0.260	-0.262	-0.263	-0.264
-0.261	-0.261	-0.264	-0.261	-0.261	-0.260	-0.263	-0.264	-0.261	-0.261	-0.260	-0.263	-0.263	-0.264	-0.265	-0.266
-0.267	-0.267	-0.267	-0.267	-0.268	-0.268	-0.269	-0.271	-0.272	-0.273	-0.273	-0.273				

Row 46, column 17

-0.165	-0.165	-0.165	-0.166	-0.166	-0.159	-0.158	-0.164	-0.165	-0.158	-0.157	-0.156	-0.155	-0.162	-0.163	-0.164
-0.164	-0.157	-0.156	-0.155	-0.155	-0.161	-0.161	-0.155	-0.153	-0.152	-0.151	-0.151	-0.150	-0.150	-0.150	-0.150
-0.149	-0.149	-0.148	-0.148	-0.148	-0.155	-0.157	-0.150	-0.149	-0.156	-0.157	-0.150	-0.149	-0.156	-0.158	-0.158
-0.151	-0.150	-0.159	-0.151	-0.151	-0.150	-0.158	-0.160	-0.152	-0.151	-0.150	-0.158	-0.159	-0.159	-0.160	-0.160
-0.161	-0.161	-0.162	-0.162	-0.162	-0.162	-0.163	-0.164	-0.164	-0.164	-0.165	-0.165				

Row 47, column 14

-0.006	-0.006	-0.006	-0.006	-0.007	-0.007	-0.007	-0.007	-0.007	-0.006	-0.006	-0.006	-0.006	-0.006	-0.006	-0.006
-0.006	-0.006	-0.006	-0.006	-0.006	-0.006	-0.005	-0.005	-0.005	-0.005	-0.005	-0.005	-0.004	-0.004	-0.004	-0.004
-0.004	-0.004	-0.003	-0.003	-0.003	-0.003	-0.003	-0.003	-0.002	-0.002	-0.002	-0.002	-0.002	-0.002	-0.002	-0.002
-0.002	-0.002	-0.002	-0.002	-0.001	-0.001	-0.001	-0.001	-0.001	-0.001	-0.001	-0.001	-0.001	-0.001	-0.002	-0.002
-0.002	-0.002	-0.003	-0.003	-0.003	-0.003	-0.004	-0.004	-0.005	-0.005	-0.005	-0.005				

Table 28.--Model-derived rates of ground-water evapotranspiration for the steady-state, standard, null, and no-Acoma scenarios--Continued

Null scenario

Stress period

1	2	3	4	5	6	7	8	9	10	11	12	13	14	15	16
17	18	19	20	21	22	23	24	25	26	27	28	29	30	31	32
33	34	35	36	37	38	39	40	41	42	43	44	45	46	47	48
49	50	51	52	53	54	55	56	57	58	59	60	61	62	63	64
65	66	67	68	69	70	71	72	73	74	75	76				

Row 47, column 15

-0.085	-0.085	-0.085	-0.086	-0.086	-0.086	-0.086	-0.086	-0.086	-0.086	-0.086	-0.086	-0.086	-0.086	-0.086	-0.086
-0.086	-0.085	-0.085	-0.085	-0.085	-0.085	-0.085	-0.085	-0.085	-0.084	-0.084	-0.084	-0.084	-0.084	-0.084	-0.084
-0.084	-0.083	-0.083	-0.083	-0.083	-0.083	-0.083	-0.083	-0.083	-0.083	-0.083	-0.082	-0.082	-0.082	-0.082	-0.082
-0.082	-0.082	-0.082	-0.082	-0.082	-0.082	-0.082	-0.082	-0.082	-0.082	-0.082	-0.082	-0.082	-0.082	-0.082	-0.082
-0.083	-0.083	-0.083	-0.083	-0.083	-0.083	-0.084	-0.084	-0.085	-0.085	-0.085	-0.085				

Row 47, column 16

-0.220	-0.220	-0.220	-0.221	-0.221	-0.221	-0.220	-0.221	-0.221	-0.220	-0.220	-0.220	-0.219	-0.220	-0.220	-0.220
-0.220	-0.219	-0.219	-0.218	-0.218	-0.218	-0.218	-0.217	-0.217	-0.216	-0.216	-0.215	-0.215	-0.214	-0.214	-0.213
-0.213	-0.212	-0.212	-0.211	-0.211	-0.211	-0.211	-0.210	-0.210	-0.210	-0.210	-0.210	-0.209	-0.209	-0.209	-0.209
-0.209	-0.208	-0.209	-0.208	-0.208	-0.207	-0.208	-0.208	-0.208	-0.207	-0.207	-0.208	-0.208	-0.208	-0.209	-0.210
-0.211	-0.211	-0.211	-0.212	-0.212	-0.213	-0.214	-0.216	-0.218	-0.218	-0.218	-0.218				

Row 47, column 17

-0.197	-0.197	-0.197	-0.198	-0.199	-0.197	-0.196	-0.197	-0.198	-0.196	-0.195	-0.194	-0.194	-0.196	-0.196	-0.197
-0.197	-0.195	-0.194	-0.194	-0.193	-0.194	-0.194	-0.192	-0.191	-0.190	-0.190	-0.189	-0.189	-0.188	-0.188	-0.187
-0.186	-0.186	-0.185	-0.185	-0.184	-0.186	-0.186	-0.185	-0.184	-0.185	-0.185	-0.184	-0.183	-0.184	-0.185	-0.185
-0.183	-0.182	-0.185	-0.182	-0.182	-0.181	-0.183	-0.184	-0.182	-0.181	-0.181	-0.183	-0.184	-0.184	-0.185	-0.186
-0.187	-0.187	-0.188	-0.188	-0.188	-0.189	-0.190	-0.193	-0.194	-0.195	-0.195	-0.195				

Table 28.--Model-derived rates of ground-water evapotranspiration for the steady-state, standard, null, and no-Acoma scenarios--Continued

-- Null scenario --

Stress period															
1	2	3	4	5	6	7	8	9	10	11	12	13	14	15	16
17	18	19	20	21	22	23	24	25	26	27	28	29	30	31	32
33	34	35	36	37	38	39	40	41	42	43	44	45	46	47	48
49	50	51	52	53	54	55	56	57	58	59	60	61	62	63	64
65	66	67	68	69	70	71	72	73	74	75	76				
Row 48, column 17															
-0.276	-0.276	-0.276	-0.277	-0.278	-0.277	-0.277	-0.277	-0.277	-0.277	-0.277	-0.277	-0.277	-0.277	-0.277	-0.277
-0.277	-0.277	-0.276	-0.276	-0.276	-0.276	-0.276	-0.275	-0.275	-0.275	-0.274	-0.274	-0.274	-0.274	-0.273	-0.273
-0.272	-0.272	-0.272	-0.271	-0.271	-0.271	-0.271	-0.271	-0.270	-0.270	-0.270	-0.270	-0.269	-0.269	-0.269	-0.269
-0.269	-0.268	-0.268	-0.268	-0.268	-0.268	-0.268	-0.268	-0.268	-0.268	-0.268	-0.268	-0.268	-0.268	-0.268	-0.269
-0.269	-0.270	-0.270	-0.270	-0.271	-0.271	-0.272	-0.273	-0.275	-0.275	-0.275	-0.275				
Row 49, column 17															
-0.114	-0.114	-0.114	-0.114	-0.115	-0.115	-0.115	-0.115	-0.115	-0.115	-0.114	-0.114	-0.114	-0.114	-0.114	-0.114
-0.114	-0.114	-0.114	-0.114	-0.114	-0.114	-0.113	-0.113	-0.113	-0.113	-0.113	-0.112	-0.112	-0.112	-0.112	-0.112
-0.111	-0.111	-0.111	-0.111	-0.111	-0.110	-0.110	-0.110	-0.110	-0.110	-0.110	-0.110	-0.109	-0.109	-0.109	-0.109
-0.109	-0.109	-0.109	-0.108	-0.108	-0.108	-0.108	-0.108	-0.108	-0.108	-0.108	-0.108	-0.108	-0.108	-0.108	-0.109
-0.109	-0.109	-0.110	-0.110	-0.110	-0.110	-0.111	-0.112	-0.112	-0.113	-0.113	-0.113				
Row 50, column 17															
-0.166	-0.166	-0.166	-0.166	-0.166	-0.166	-0.166	-0.166	-0.166	-0.166	-0.166	-0.166	-0.166	-0.166	-0.166	-0.166
-0.166	-0.166	-0.166	-0.166	-0.166	-0.166	-0.166	-0.166	-0.166	-0.166	-0.166	-0.166	-0.166	-0.166	-0.166	-0.166
-0.166	-0.166	-0.166	-0.166	-0.166	-0.166	-0.166	-0.166	-0.166	-0.166	-0.166	-0.166	-0.166	-0.166	-0.166	-0.166
-0.166	-0.166	-0.166	-0.166	-0.166	-0.166	-0.166	-0.166	-0.166	-0.166	-0.166	-0.166	-0.166	-0.166	-0.166	-0.166
-0.166	-0.166	-0.166	-0.166	-0.166	-0.166	-0.166	-0.166	-0.166	-0.166	-0.166	-0.166				

Table 28.--Model-derived rates of ground-water evapotranspiration for the steady-state, standard, null, and no-Acoma scenarios--Continued

Null scenario

Stress period

1	2	3	4	5	6	7	8	9	10	11	12	13	14	15	16
17	18	19	20	21	22	23	24	25	26	27	28	29	30	31	32
33	34	35	36	37	38	39	40	41	42	43	44	45	46	47	48
49	50	51	52	53	54	55	56	57	58	59	60	61	62	63	64
65	66	67	68	69	70	71	72	73	74	75	76				

Row 50, column 18

-0.441	-0.441	-0.441	-0.441	-0.442	-0.442	-0.442	-0.442	-0.442	-0.442	-0.442	-0.442	-0.442	-0.442	-0.442	-0.442
-0.442	-0.442	-0.441	-0.441	-0.441	-0.441	-0.440	-0.440	-0.440	-0.439	-0.439	-0.439	-0.438	-0.438	-0.438	-0.437
-0.437	-0.436	-0.436	-0.436	-0.435	-0.435	-0.434	-0.434	-0.434	-0.433	-0.433	-0.433	-0.433	-0.433	-0.432	-0.432
-0.432	-0.431	-0.431	-0.431	-0.431	-0.431	-0.430	-0.430	-0.430	-0.430	-0.430	-0.430	-0.430	-0.430	-0.430	-0.431
-0.432	-0.432	-0.433	-0.433	-0.433	-0.434	-0.434	-0.437	-0.438	-0.439	-0.439	-0.439				

Row 51, column 18

-0.111	-0.111	-0.111	-0.111	-0.112	-0.112	-0.112	-0.112	-0.112	-0.112	-0.111	-0.111	-0.111	-0.111	-0.111	-0.111
-0.111	-0.111	-0.111	-0.111	-0.111	-0.110	-0.110	-0.110	-0.110	-0.110	-0.109	-0.109	-0.109	-0.109	-0.108	-0.108
-0.108	-0.107	-0.107	-0.107	-0.106	-0.106	-0.106	-0.106	-0.105	-0.105	-0.105	-0.105	-0.105	-0.104	-0.104	-0.104
-0.104	-0.104	-0.104	-0.103	-0.103	-0.103	-0.103	-0.103	-0.103	-0.103	-0.103	-0.103	-0.103	-0.103	-0.103	-0.103
-0.104	-0.104	-0.105	-0.105	-0.105	-0.105	-0.106	-0.108	-0.109	-0.109	-0.109	-0.109				

Row 52, column 17

-0.130	-0.130	-0.130	-0.130	-0.130	-0.130	-0.130	-0.130	-0.130	-0.130	-0.130	-0.130	-0.130	-0.130	-0.130	-0.130
-0.130	-0.130	-0.130	-0.130	-0.130	-0.130	-0.130	-0.130	-0.130	-0.130	-0.130	-0.130	-0.130	-0.130	-0.130	-0.130
-0.130	-0.130	-0.130	-0.130	-0.130	-0.130	-0.130	-0.130	-0.130	-0.130	-0.130	-0.130	-0.130	-0.130	-0.130	-0.130
-0.130	-0.130	-0.129	-0.129	-0.129	-0.129	-0.129	-0.129	-0.129	-0.129	-0.129	-0.129	-0.129	-0.129	-0.129	-0.129
-0.130	-0.130	-0.130	-0.130	-0.130	-0.130	-0.130	-0.130	-0.130	-0.130	-0.130	-0.130				

Table 28.--Model-derived rates of ground-water evapotranspiration for the steady-state, standard, null, and no-Acoma scenarios--Concluded

Null scenario

Stress period

1	2	3	4	5	6	7	8	9	10	11	12	13	14	15	16
17	18	19	20	21	22	23	24	25	26	27	28	29	30	31	32
33	34	35	36	37	38	39	40	41	42	43	44	45	46	47	48
49	50	51	52	53	54	55	56	57	58	59	60	61	62	63	64
65	66	67	68	69	70	71	72	73	74	75	76				

Total for each stress period of the null scenario

-5.772	-5.771	-5.780	-5.831	-5.803	-5.737	-5.710	-5.783	-5.749	-5.697	-5.753	-5.681	-5.654	-5.679	-5.688	-5.706
-5.708	-5.667	-5.646	-5.627	-5.608	-5.661	-5.645	-5.595	-5.571	-5.555	-5.541	-5.529	-5.519	-5.510	-5.499	-5.525
-5.486	-5.476	-5.472	-5.456	-5.447	-5.532	-5.515	-5.473	-5.459	-5.555	-5.531	-5.504	-5.471	-5.502	-5.545	-5.605
-5.513	-5.503	-5.564	-5.529	-5.492	-5.475	-5.569	-5.655	-5.525	-5.503	-5.476	-5.585	-5.637	-5.909	-5.712	-5.685
-5.783	-5.916	-5.717	-5.796	-5.901	-5.796	-5.720	-5.734	-5.747	-5.751	-5.756	-5.757				

No-Acoma scenario

Model		Stress period						Model		Stress period					
Row	Column	71	72	73	74	75	76	Row	Column	71	72	73	74	75	76
42	13	-0.025	0.000	0.000	0.000	0.000	0.000	45	18	-0.162	-0.165	-0.153	-0.143	-0.127	-0.113
42	17	-0.027	-0.013	0.000	0.000	0.000	0.000	46	16	-0.032	-0.041	-0.010	0.000	0.000	0.000
43	11	-0.089	-0.045	-0.014	-0.003	0.000	0.000	46	17	-0.054	-0.061	-0.046	-0.032	-0.009	0.000
43	12	-0.273	0.000	0.000	0.000	0.000	0.000	47	15	-0.018	-0.022	-0.019	-0.015	-0.008	-0.002
43	13	-0.087	0.000	0.000	0.000	0.000	0.000	47	16	0.000	-0.016	-0.005	0.000	0.000	0.000
43	17	-0.116	-0.097	-0.041	-0.005	0.000	0.000	48	17	-0.183	-0.192	-0.191	-0.186	-0.175	-0.165
43	18	-0.012	-0.010	-0.001	0.000	0.000	0.000	49	17	-0.068	-0.072	-0.073	-0.071	-0.067	-0.063
44	17	-0.043	-0.030	0.000	0.000	0.000	0.000	50	17	-0.166	-0.166	-0.166	-0.166	-0.166	-0.166
44	18	-0.081	-0.079	-0.066	-0.054	-0.033	-0.015	50	18	-0.368	-0.373	-0.376	-0.375	-0.369	-0.363
45	17	-0.352	-0.348	-0.292	-0.253	-0.199	-0.154	51	18	-0.057	-0.061	-0.063	-0.062	-0.057	-0.053
								52	17	-0.127	-0.127	-0.127	-0.127	-0.127	-0.127
Total for each stress period of the no-Acoma scenario										-2.340	-1.917	-1.644	-1.493	-1.339	-1.222

Table 29.--Average differences, in feet, between model-derived and measured hydraulic heads for the standard and each sensitivity test

[K, horizontal hydraulic conductivity, in feet per second; K', vertical hydraulic conductivity, in feet per second; S, storage coefficient]

Short description of test	Number of points	Differences			
		Mean total	Median	Root mean square	Mean absolute
Artesian storage coefficient times 0.5	110	7.56	4.91	20.19	13.48
Streambed K times 0.5	110	2.45	-1.61	20.62	13.52
Standard	110	8.89	5.21	22.89	14.58
Leakage layers, $K' = 1 \times 10^{-13}$	110	8.91	5.26	22.90	14.58
Chinle $K' = 1 \times 10^{-12}$	110	8.91	5.26	22.90	14.59
Steady recharge	110	9.03	5.46	22.94	14.60
Chinle $K' = 1 \times 10^{-10}$	110	9.13	5.36	22.96	14.61
Leakage layers, $K= 1 \times 10^{-11}$	110	9.20	5.46	23.28	14.73
Lengthen San Rafael fault	110	7.88	5.44	22.88	14.87
Large S in layer 2 at arbitrary boundary	110	9.98	5.41	25.11	15.29
Artesian storage coefficient times 2	110	10.30	5.86	25.60	15.56
Constant head in layer 2 at arbitrary boundary	110	11.04	6.38	25.98	15.65
Leakage layers, $K= 1 \times 10^{-9}$	110	11.02	6.47	25.97	15.77
Steady recharge and reach 5 inflow	110	10.71	6.85	24.40	15.82
Shorten San Rafael fault	110	10.82	7.95	24.06	15.88
Streambed K times 2	110	13.74	11.05	26.13	17.81
Null, no underflow	110	17.67	10.37	34.14	22.33

Table 30.--Effect of sensitivity tests on model-derived streamflows

[The first section shows the difference between the outflow of Bluewater Canyon (reach 4) calculated by each sensitivity test minus that of the standard. Stream routing is such that this shows only the difference for the lake and canyon reaches (reaches 2 and 4). The second section is the same difference for the Rio San Jose downstream from Horace Springs. Specified inflows to reach 5 (routed through reach 11) generally do not appear because they are the same in the standard and almost all sensitivity tests. The only exception is the test of steady inflow to reach 5. Leakage from confining beds: leak 9 is sensitivity test in which leakage layers were assigned a vertical hydraulic conductivity of 1×10^{-9} foot per second; similarly, leak 11 and leak 13 refer to an assigned vertical conductivity of 1×10^{-11} and 1×10^{-13} foot per second. The test of steady inflow to reach 5 also included steady recharge. Differences are in cubic feet per second]

Sensitivity of model-derived streamflow from lake and canyon reaches

Stress period	End date	Leakage from confining beds			Riverbed hydraulic conductivity		San Rafael faults		Steady state		Boundaries		Artesian storage	
		Leak 9	Leak 11	Leak 13	x 0.5	x 2	Long	Short	Inflow reach 5	Recharge	Large storage	Constant head	x 0.5	x 2
01	1928.0	0.0	0.0	0.0	0.0	0.0	0.0	0.0	0.0	0.0	0.0	0.0	0.0	0.0
02	1932.0	0.0	0.0	0.0	0.0	0.0	0.0	0.0	0.0	0.0	0.0	0.0	0.0	0.0
03	1936.0	0.0	0.0	0.0	-0.1	0.1	0.0	0.0	0.0	0.0	0.0	0.0	0.0	0.0
04	1940.0	0.0	0.0	0.0	-0.1	0.1	0.0	0.0	0.0	0.0	0.0	0.0	0.0	0.0
05	1944.0	0.0	0.0	0.0	-0.1	0.1	0.0	0.0	0.0	0.0	0.0	0.0	0.0	0.0
06	1944.5	0.0	0.0	0.0	0.0	0.0	0.0	0.0	0.0	0.0	0.0	0.0	0.0	0.0
07	1945.0	0.0	0.0	0.0	0.0	0.1	0.0	0.0	0.0	0.0	0.0	0.0	0.0	0.0
08	1945.5	0.0	0.0	0.0	0.0	0.0	0.0	0.0	0.0	0.0	0.0	0.0	0.0	0.0
09	1946.0	0.0	0.0	0.0	0.0	0.1	0.0	0.0	0.0	0.0	0.0	0.0	0.0	0.0
10	1946.5	0.0	0.0	0.0	0.0	0.0	0.0	0.0	0.0	0.0	0.0	0.0	0.0	0.0
11	1947.0	0.0	0.0	0.0	0.0	0.0	0.0	0.0	0.0	0.0	0.0	0.0	0.0	0.0
12	1947.5	0.0	0.0	0.0	-0.1	0.1	0.0	0.0	0.0	0.0	0.0	0.0	0.0	0.0
13	1948.0	0.0	0.0	0.0	-0.1	0.0	0.0	0.0	0.0	0.0	0.0	0.0	0.0	0.0
14	1948.5	0.0	0.0	0.0	0.0	0.0	0.0	0.0	0.0	0.0	0.0	0.0	0.0	0.0
15	1949.0	0.0	0.0	0.0	-0.1	0.2	0.0	0.0	0.0	0.0	0.0	0.0	0.0	0.0

Table 30.--Effect of sensitivity tests on model-derived streamflows--Continued

Sensitivity of model-derived streamflow from lake and canyon reaches

Stress period	End date	Leakage from confining beds: Leak 9	Leak 11	Leak 13	Riverbed hydraulic conductivity: x 0.5	x 2	San Rafael faults: Long	Short	Steady state: Inflow reach 5	Recharge	Boundaries: Large storage	Constant head	Artesian storage: x 0.5	x 2
16	1949.5	0.0	0.0	0.0	-0.1	0.0	0.0	0.0	0.0	0.0	0.0	0.0	0.0	0.0
17	1950.0	0.0	0.0	0.0	-0.1	0.1	0.0	0.0	0.0	0.0	0.0	0.0	0.0	0.0
18	1950.5	0.0	0.0	0.0	-0.1	0.0	0.0	0.0	0.0	0.0	0.0	0.0	0.0	0.0
19	1951.0	0.0	0.0	0.0	0.0	0.0	0.0	0.0	0.0	0.0	0.0	0.0	0.0	0.0
20	1951.5	0.0	0.0	0.0	0.0	0.0	0.0	0.0	0.0	0.0	0.0	0.0	0.0	0.0
21	1952.0	0.0	0.0	0.0	0.0	0.0	0.0	0.0	0.0	0.0	0.0	0.0	0.0	0.0
22	1952.5	0.0	0.0	0.0	0.0	0.0	0.0	0.0	0.0	0.0	0.0	0.0	0.0	0.0
23	1953.0	0.0	0.0	0.0	0.0	0.0	0.0	0.0	0.0	0.0	0.0	0.0	0.0	0.0
24	1953.5	0.0	0.0	0.0	0.0	0.0	0.0	0.0	0.0	0.0	0.0	0.0	0.0	0.0
25	1954.0	0.0	0.0	0.0	0.0	0.0	0.0	0.0	0.0	0.0	0.0	0.0	0.0	0.0
26	1954.5	0.0	0.0	0.0	0.0	0.0	0.0	0.0	0.0	0.0	0.0	0.0	0.0	0.0
27	1955.0	0.0	0.0	0.0	0.0	0.0	0.0	0.0	0.0	0.0	0.0	0.0	0.0	0.0
28	1955.5	0.0	0.0	0.0	0.1	0.0	0.0	0.0	0.0	0.0	0.0	0.0	0.0	0.0
29	1956.0	0.0	0.0	0.0	0.1	0.0	0.0	0.0	0.0	0.0	0.0	0.0	0.0	0.0
30	1956.5	0.0	0.0	0.0	0.1	0.0	0.0	0.0	0.0	0.0	0.0	0.0	0.0	0.0
31	1957.0	0.0	0.0	0.0	0.1	-0.1	0.0	0.0	0.0	0.0	0.0	0.0	0.0	0.0
32	1957.5	0.0	0.0	0.0	0.0	0.0	0.0	0.0	0.0	0.0	0.0	0.0	0.0	0.0
33	1958.0	0.0	0.0	0.0	-0.1	0.1	0.0	0.0	0.1	0.0	0.0	0.0	0.0	0.0
34	1958.5	0.0	0.0	0.0	-0.1	0.2	0.0	0.0	0.1	0.0	0.0	0.0	0.0	0.0
35	1959.0	0.0	0.0	0.0	-0.1	0.1	0.0	0.0	0.1	0.0	0.0	0.0	0.0	0.0
36	1959.5	0.0	0.0	0.0	0.0	0.0	0.0	0.0	0.1	0.0	0.0	0.0	0.0	0.0
37	1960.0	0.0	0.0	0.0	0.0	0.0	0.0	0.0	0.1	0.0	0.0	0.0	0.0	0.0
38	1960.5	0.0	0.0	0.0	0.0	0.0	0.0	0.0	0.1	0.0	0.0	0.0	0.0	0.0
39	1961.0	0.0	0.0	0.0	-0.1	0.1	0.0	0.0	0.1	0.0	0.0	0.0	0.0	0.0
40	1961.5	0.0	0.0	0.0	0.0	0.0	0.0	0.0	0.1	0.0	0.0	0.0	0.0	0.0

Table 30.--Effect of sensitivity tests on model-derived streamflows--Continued

Stress period	End date	Sensitivity of model-derived streamflow from lake and canyon reaches													
		Leakage from confining beds			Riverbed hydraulic conductivity		San Rafael faults		Steady state		Boundaries		Artesian storage	
		Leak 9	Leak 11	Leak 13	x 0.5	x 2	Long	Short	Inflow reach 5	Recharge	Large storage	Constant head	x 0.5	x 2
41	1962.0	0.0	0.0	0.0	0.0	0.0	0.0	0.0	0.1	0.0	0.0	0.0	0.0	0.0
42	1962.5	0.0	0.0	0.0	0.0	0.0	0.0	0.0	0.1	0.0	0.0	0.0	0.0	0.0
43	1963.0	0.0	0.0	0.0	-0.1	0.1	0.0	0.0	0.1	0.0	0.0	0.0	0.0	0.0
44	1963.5	0.0	0.0	0.0	0.0	-0.1	0.0	0.0	0.1	0.0	0.0	0.0	0.0	0.0
45	1964.0	0.0	0.0	0.0	0.1	0.0	0.0	0.0	0.1	0.0	0.0	0.0	0.0	0.0
46	1964.5	0.0	0.0	0.0	0.0	0.0	0.0	0.0	0.1	0.0	0.0	0.0	0.0	0.0
47	1965.5	0.0	-0.4	0.0	0.0	0.0	0.0	0.0	0.1	0.0	0.0	0.0	0.0	0.0
48	1966.5	0.0	0.0	0.0	0.0	0.1	0.0	0.0	0.1	0.0	0.0	0.0	0.0	0.0
49	1967.5	0.0	0.0	0.0	0.0	0.0	0.0	0.0	0.1	0.0	0.0	0.0	0.0	0.0
50	1968.5	0.0	0.0	0.0	0.0	0.0	0.0	0.0	0.1	0.0	0.0	0.0	0.0	0.0
51	1969.5	0.0	0.0	0.0	0.0	0.0	0.0	0.0	0.1	0.0	0.0	0.0	0.0	0.0
52	1970.5	0.0	0.0	0.0	0.0	0.0	0.0	0.0	0.1	0.0	0.0	0.0	0.0	0.0
53	1971.5	0.0	0.0	0.0	0.0	0.0	0.0	0.0	0.1	0.0	0.0	0.0	0.0	0.0
54	1972.5	0.0	0.0	0.0	0.0	0.0	0.0	0.0	0.1	0.0	0.0	0.0	0.0	0.0
55	1973.5	0.0	0.0	0.0	0.0	0.0	0.0	0.0	0.1	0.0	0.0	0.0	0.0	0.0
56	1974.5	0.0	0.0	0.0	-0.1	0.1	0.0	0.0	0.1	0.0	0.0	0.0	0.0	0.0
57	1975.5	0.0	0.0	0.0	0.1	0.0	0.0	0.0	0.1	0.0	0.0	0.0	0.0	0.0
58	1976.5	0.0	0.0	0.0	0.0	0.0	0.0	0.0	0.1	0.0	0.0	0.0	0.0	0.0
59	1977.5	0.0	0.0	0.0	0.1	-0.1	0.0	0.0	0.1	0.0	0.0	0.0	0.0	0.0
60	1978.5	0.0	0.0	0.0	0.0	0.0	0.0	0.0	0.1	0.0	0.0	0.0	0.0	0.0
61	1979.5	0.0	0.0	0.0	0.0	0.0	0.0	0.0	0.0	0.0	0.0	0.0	0.0	0.0
62	1980.5	0.0	0.0	0.0	-0.1	0.1	0.0	0.0	0.0	0.0	0.0	0.0	0.0	0.0
63	1981.5	0.0	0.0	0.0	-0.1	0.1	0.0	0.0	0.0	0.0	0.0	0.0	0.0	0.0
64	1982.5	0.0	0.0	0.0	0.0	0.0	0.0	0.0	0.0	0.0	0.0	0.0	0.0	0.0
65	1983.5	0.0	0.0	0.0	0.0	0.1	0.0	0.0	0.0	0.0	0.0	0.0	0.0	0.0

Table 30.--Effect of sensitivity tests on model-derived streamflows--Continued

Stress period	End date	Leakage from confining beds: Leak 9	Leak 11	Leak 13	Riverbed hydraulic conductivity: x 0.5	x 2	San Rafael faults: Long	Short	Steady state: Inflow reach 5	Re-charge	Boundaries: Large storage	Constant head	Artesian storage: x 0.5	x 2
Sensitivity of model-derived streamflow from lake and canyon reaches														
66	1984.0	0.0	0.0	0.0	-0.2	0.3	0.0	0.0	0.0	0.0	0.0	0.0	0.0	0.0
67	1984.5	0.0	0.0	0.0	0.0	0.0	0.0	0.0	0.0	0.0	0.0	0.0	0.0	0.0
68	1985.0	0.0	0.0	0.0	0.0	0.1	0.0	0.0	0.0	0.0	0.0	0.0	0.0	0.0
69	1985.5	0.0	0.0	0.0	0.0	0.1	0.0	0.0	0.0	0.0	0.0	0.0	0.0	0.0
70	1986.0	0.0	0.0	0.0	-0.2	0.1	0.0	0.0	0.0	0.0	0.0	0.0	0.0	0.0
71	1987.0	0.0	0.0	0.0	0.2	-0.1	0.0	0.0	0.0	0.0	0.0	0.0	0.0	0.0
72	1990.0	0.0	0.0	0.0	0.0	0.0	0.0	0.0	0.0	0.0	0.0	0.0	0.0	0.0
73	1995.0	0.0	0.0	0.0	0.0	0.0	0.0	0.0	0.0	0.0	0.0	0.0	0.0	0.0
74	2000.0	0.0	0.0	0.0	0.0	0.0	0.0	0.0	0.0	0.0	0.0	0.0	0.0	0.0
75	2010.0	0.0	0.0	0.0	0.0	0.0	0.0	0.0	0.0	0.0	0.0	0.1	0.0	0.0
76	2021.0	0.1	0.0	0.0	0.0	0.0	0.0	-0.1	0.0	0.0	0.0	0.1	0.0	0.0
Sensitivity of model-derived streamflow downstream from Horace Springs														
01	1928.0	0.0	0.0	0.0	0.9	-0.9	0.2	-0.4	-0.1	0.0	0.0	0.0	0.0	0.0
02	1932.0	0.0	0.0	0.0	0.4	-0.6	0.2	-0.4	0.2	0.0	0.0	0.0	0.0	0.0
03	1936.0	0.0	0.0	0.0	2.3	-1.6	0.2	-0.5	-0.8	0.0	0.0	0.0	0.0	0.0
04	1940.0	0.0	0.0	0.0	1.9	-2.3	0.2	-0.5	-2.3	0.0	0.0	0.0	0.0	0.0
05	1944.0	-0.1	0.0	0.0	1.7	-3.4	0.2	-0.5	-9.4	0.0	0.0	0.0	0.0	0.0
06	1944.5	0.0	0.0	0.0	0.6	0.0	0.1	-0.4	-1.0	0.0	0.0	0.0	0.0	0.0
07	1945.0	-0.1	0.0	0.0	1.9	-2.1	0.2	-0.5	-3.0	0.0	0.0	0.0	0.0	0.0
08	1945.5	0.0	0.0	0.0	-0.5	-0.1	0.1	-0.4	-0.7	0.0	0.0	0.0	0.0	0.0
09	1946.0	0.0	0.0	0.0	-0.1	-0.3	0.1	-0.4	-0.6	0.0	0.0	0.0	0.0	0.1
10	1946.5	0.0	0.0	0.0	-0.4	-0.3	0.1	-0.4	-0.4	0.0	0.0	0.0	0.0	0.0

Table 30.--Effect of sensitivity tests on model-derived streamflows--Continued

Stress period	End date	Sensitivity of model-derived streamflow downstream from Horace Springs: Leakage from confining beds: Leak 9	Leak 11	Leak 13	Riverbed hydraulic conductivity: x 0.5	x 2	San Rafael faults: Long	Short	Steady state: Inflow reach 5	Re-charge	Boundaries: Large storage	Constant head	Artesian storage: x 0.5	x 2
11	1947.0	0.0	0.0	0.0	-0.1	0.1	0.0	0.1	0.0	0.0	0.0	0.0	0.0	0.0
12	1947.5	0.0	0.0	0.0	-0.1	0.1	0.0	0.1	0.0	0.0	0.0	0.0	0.0	0.0
13	1948.0	0.0	0.0	0.0	-0.1	0.1	0.0	0.1	0.0	0.0	0.0	0.0	0.0	0.0
14	1948.5	0.0	0.0	0.0	-0.1	0.1	0.0	0.1	0.0	0.0	0.0	0.0	0.0	0.0
15	1949.0	0.0	0.0	0.0	3.8	-0.1	0.0	0.0	-0.3	0.0	0.0	0.0	0.0	0.0
16	1949.5	0.0	0.0	0.0	-0.1	0.1	0.0	0.1	0.0	0.0	0.0	0.0	0.0	0.0
17	1950.0	0.0	0.0	0.0	3.5	-1.3	0.0	0.0	-1.5	0.0	0.0	0.0	0.0	0.0
18	1950.5	0.0	0.0	0.0	-0.1	0.1	0.0	0.1	0.0	0.0	0.0	0.0	0.0	0.0
19	1951.0	0.0	0.0	0.0	-0.1	0.1	0.0	0.1	0.0	0.0	0.0	0.0	0.0	0.0
20	1951.5	0.0	0.0	0.0	-0.1	0.1	0.0	0.1	0.0	0.0	0.0	0.0	0.0	0.0
21	1952.0	0.0	0.0	0.0	-0.1	0.1	0.0	0.1	0.0	0.0	0.0	0.0	0.0	0.0
22	1952.5	0.0	0.0	0.0	-0.1	0.1	0.0	0.1	0.0	0.0	0.0	0.0	0.0	0.0
23	1953.0	0.0	0.0	0.0	1.4	0.1	0.0	0.1	0.0	0.0	0.0	0.0	0.0	0.0
24	1953.5	0.0	0.0	0.0	-0.1	0.1	0.0	0.1	0.0	0.0	0.0	0.0	0.0	0.0
25	1954.0	0.0	0.0	0.0	0.0	0.1	0.0	0.1	0.0	0.0	0.0	0.0	0.0	0.0
26	1954.5	0.0	0.0	0.0	0.0	0.1	0.0	0.1	0.0	0.0	0.0	0.0	0.0	0.0
27	1955.0	0.0	0.0	0.0	0.0	0.1	0.0	0.1	0.0	0.0	0.0	0.0	0.0	0.0
28	1955.5	0.0	0.0	0.0	0.0	0.1	0.0	0.1	0.0	0.0	0.0	0.0	0.0	0.0
29	1956.0	0.0	0.0	0.0	0.0	0.1	0.0	0.1	0.0	0.0	0.0	0.0	0.0	0.0
30	1956.5	0.0	0.0	0.0	0.0	0.0	0.0	0.1	0.0	0.0	0.0	0.0	0.0	0.0

Table 30.--Effect of sensitivity tests on model-derived streamflows--Continued

Sensitivity of model-derived streamflow downstream from Horace Springs

Stress period	End date	Leakage from confining beds			Riverbed hydraulic conductivity		San Rafael faults		Steady state		Boundaries		Artesian storage	
		Leak 9	Leak 11	Leak 13	x 0.5	x 2	Long	Short	Inflow reach 5	Recharge	Large storage	Constant head	x 0.5	x 2
31	1957.0	0.0	0.0	0.0	0.0	0.0	-0.1	0.1	0.0	0.0	0.0	0.0	0.0	0.0
32	1957.5	0.0	0.0	0.0	0.0	0.0	-0.1	0.1	0.0	0.0	0.0	0.0	0.0	0.0
33	1958.0	0.0	0.0	0.0	0.0	-0.1	-0.1	0.1	0.0	0.0	0.0	0.0	0.0	0.0
34	1958.5	0.0	0.0	0.0	0.0	-0.1	-0.1	0.1	0.0	0.0	0.0	0.0	0.0	0.0
35	1959.0	0.0	0.0	0.0	0.0	-0.1	-0.1	0.1	0.0	0.0	0.0	0.0	0.0	0.0
36	1959.5	0.0	0.0	0.0	0.0	-0.1	-0.1	0.1	0.0	0.0	0.0	0.0	0.0	0.0
37	1960.0	0.0	0.0	0.0	0.0	-0.1	-0.1	0.1	0.0	0.0	0.0	0.0	0.0	0.0
38	1960.5	0.0	0.0	0.0	0.0	-0.1	-0.1	0.1	0.0	0.0	0.0	0.0	0.0	0.0
39	1961.0	0.0	0.0	0.0	0.0	-0.1	-0.1	0.1	0.0	0.0	0.0	0.0	0.0	0.0
40	1961.5	0.0	0.0	0.0	0.0	-0.1	-0.1	0.1	0.0	0.0	0.0	0.0	0.0	0.0
41	1962.0	0.0	0.0	0.0	0.0	-0.1	-0.1	0.1	0.0	0.0	0.0	0.0	0.0	0.0
42	1962.5	0.0	0.0	0.0	0.0	-0.1	-0.1	0.1	0.1	0.0	0.0	0.0	0.0	0.0
43	1963.0	0.0	0.0	0.0	2.1	-0.1	-0.1	0.1	0.1	0.0	0.0	0.0	0.0	0.0
44	1963.5	0.0	0.0	0.0	0.0	-0.1	-0.1	0.1	0.1	0.0	0.0	0.0	0.0	0.0
45	1964.0	0.0	0.0	0.0	0.0	-0.1	-0.1	0.1	0.1	0.0	0.0	0.0	0.0	0.0
46	1964.5	0.0	0.0	0.0	0.0	-0.1	-0.1	0.1	0.1	0.0	0.0	0.0	0.0	0.0
47	1965.5	0.0	0.0	0.0	0.0	-0.1	-0.1	0.1	0.1	0.0	0.0	0.0	0.0	0.0
48	1966.5	0.0	0.0	0.0	0.0	-0.1	-0.1	0.1	0.1	0.1	0.0	0.0	0.0	0.0
49	1967.5	0.0	0.0	0.0	0.0	-0.1	-0.1	0.1	0.1	0.1	0.0	0.0	0.0	0.0
50	1968.5	0.0	0.0	0.0	0.0	-0.1	-0.1	0.1	0.1	0.1	0.0	0.0	0.0	0.0
51	1969.5	0.0	0.0	0.0	0.0	-0.1	-0.1	0.1	0.1	0.1	0.0	0.0	0.0	0.0
52	1970.5	0.0	0.0	0.0	0.0	-0.1	-0.1	0.1	0.1	0.1	0.0	0.0	0.0	0.0
53	1971.5	0.0	0.0	0.0	0.0	-0.1	-0.1	0.1	0.1	0.1	0.0	0.0	0.0	0.0
54	1972.5	0.0	0.0	0.0	0.0	-0.1	-0.1	0.1	0.1	0.1	0.0	0.0	0.0	0.0
55	1973.5	0.0	0.0	0.0	0.0	-0.1	-0.1	0.1	0.1	0.1	0.0	0.0	0.0	0.0

Table 30.--Effect of sensitivity tests on model-derived streamflows--Concluded

Sensitivity of model-derived streamflow downstream from Horace Springs

Stress period	End date	Leakage from confining beds			Riverbed hydraulic conductivity		San Rafael faults		Steady state		Boundaries		Artesian storage	
		Leak 9	Leak 11	Leak 13	x 0.5	x 2	Long	Short	Inflow reach 5	Recharge	Large storage	Constant head	x 0.5	x 2
56	1974.5	0.0	0.0	0.0	1.3	-0.1	-0.1	0.1	0.1	0.1	0.0	0.0	0.0	0.0
57	1975.5	0.0	0.0	0.0	2.2	-0.1	-0.1	0.1	0.1	0.1	0.0	0.0	0.0	0.0
58	1976.5	0.0	0.0	0.0	1.6	-0.1	-0.1	0.1	0.1	0.1	0.0	0.0	0.0	0.0
59	1977.5	0.0	0.0	0.0	2.0	-0.1	-0.1	0.1	0.1	0.1	0.0	0.0	0.0	0.0
60	1978.5	0.0	0.0	0.0	0.0	-0.1	-0.1	0.1	0.1	0.1	0.0	0.0	0.0	0.0
61	1979.5	0.2	0.0	0.0	3.6	-5.0	0.0	-0.1	-4.8	0.1	0.0	0.1	-0.1	0.1
62	1980.5	0.2	0.0	0.0	3.4	-4.7	0.0	-0.1	-6.5	0.1	0.0	0.1	-0.1	0.1
63	1981.5	0.2	0.0	0.0	3.2	-3.2	0.1	-0.1	-3.0	0.1	0.0	0.1	-0.1	0.1
64	1982.5	0.2	0.0	0.0	3.0	-4.3	0.0	-0.1	-4.8	0.1	0.0	0.1	0.0	0.1
65	1983.5	0.2	0.0	0.0	2.9	-2.6	0.0	-0.1	-2.4	0.1	0.0	0.1	0.0	0.0
66	1984.0	0.2	0.0	0.0	2.8	-3.5	0.0	-0.1	-3.4	0.1	0.0	0.1	0.0	0.0
67	1984.5	0.2	0.0	0.0	2.8	-0.7	0.0	-0.1	-0.5	0.1	0.0	0.1	0.0	0.0
68	1985.0	0.1	0.0	0.0	2.7	-4.0	0.0	-0.1	-31.2	0.1	0.0	0.1	0.0	0.0
69	1985.5	0.0	0.0	0.0	0.0	0.0	-0.1	0.1	0.1	0.0	0.0	0.0	0.0	0.0
70	1986.0	0.1	0.0	0.0	2.8	-1.8	0.0	-0.1	-1.7	0.1	0.0	0.1	0.0	0.0
71	1987.0	0.0	0.0	0.0	0.0	0.0	-0.1	0.1	0.1	0.0	0.0	0.0	0.0	0.0
72	1990.0	0.0	0.0	0.0	-0.1	0.0	0.0	0.1	0.0	0.0	0.0	0.0	0.0	0.0
73	1995.0	0.0	0.0	0.0	-0.1	0.0	0.0	0.1	0.0	0.0	0.0	0.0	0.0	0.0
74	2000.0	0.0	0.0	0.0	-0.1	0.0	0.0	0.1	0.0	0.0	0.0	0.1	0.0	0.0
75	2010.0	0.1	0.0	0.0	0.0	0.0	0.0	0.0	0.0	0.0	0.0	0.1	0.0	0.0
76	2021.0	0.1	0.0	0.0	0.0	0.0	0.0	-0.1	0.0	0.0	0.0	0.2	0.0	0.1

Table 31.--Model budget for tests of leakage from confining beds for selected stress periods

	Standard	Hydraulic conductivity of leakage layers, in foot per second: 1×10^{-9}	1×10^{-11}	1×10^{-13}
	Stress period 70			
Storage				
Inflow	2.45	2.45	2.55	2.48
Outflow	-12.13	-11.92	-11.99	-12.04
Net	-9.68	-9.47	-9.44	-9.56
Specified				
Inflow	21.62	21.62	21.62	21.62
Outflow	-10.84	-10.84	-10.84	-10.84
Net	10.78	10.78	10.78	10.78
River				
Inflow	18.23	18.44	18.27	18.25
Outflow	-12.75	-13.11	-12.80	-12.75
Net	5.48	5.33	5.47	5.50
Evapotranspiration from water table				
Inflow	0.00	0.00	0.00	0.00
Outflow	-2.52	-3.02	-2.60	-2.53
Net	-2.52	-3.02	-2.60	-2.53
General-head boundary				
Inflow	0.00	0.00	0.00	0.00
Outflow	-4.02	-4.06	-4.03	-4.02
Net	-4.02	-4.06	-4.03	-4.02
Constant-head boundary				
Inflow	0.44	1.02	0.44	0.44
Outflow	-0.13	-0.14	-0.13	-0.13
Net	0.31	0.88	0.31	0.31

Table 31.--Model budget for tests of leakage from confining beds for selected stress periods--Continued

	Standard	Hydraulic conductivity of leakage layers, in foot per second		
		1×10^{-9}	1×10^{-11}	1×10^{-13}
	Stress period 73			
Storage				
Inflow	16.25	15.02	16.26	16.26
Outflow	-4.34	-4.18	-4.28	-4.33
Net	11.91	10.84	11.98	11.93
Specified				
Inflow	20.40	20.40	20.40	20.40
Outflow	-28.73	-28.73	-28.73	-28.73
Net	-8.33	-8.33	-8.33	-8.33
River				
Inflow	10.08	10.02	10.08	10.08
Outflow	-8.51	-8.54	-8.51	-8.50
Net	1.57	1.48	1.57	1.58
Evapotranspiration from water table				
Inflow	0.00	0.00	0.00	0.00
Outflow	-1.60	-1.76	-1.62	-1.60
Net	-1.60	-1.76	-1.62	-1.60
General-head boundary				
Inflow	0.00	0.00	0.00	0.00
Outflow	-3.90	-4.03	-3.92	-3.90
Net	-3.90	-4.03	-3.92	-3.90
Constant-head boundary				
Inflow	0.44	1.92	0.44	0.44
Outflow	-0.14	-0.14	-0.14	-0.14
Net	0.31	1.78	0.31	0.31

Table 31.--Model budget for tests of leakage from confining beds for selected stress periods--Concluded

	Standard	Hydraulic conductivity of leakage layers, in foot per second		
		1×10^{-9}	1×10^{-11}	1×10^{-13}
	Stress period 76			
Storage				
Inflow	12.67	9.57	12.90	12.68
Outflow	-1.07	-1.33	-1.10	-1.07
Net	11.60	8.24	11.80	11.61
Specified flow				
Inflow	20.40	20.40	20.40	20.40
Outflow	-28.73	-28.73	-28.73	-28.73
Net	-8.33	-8.33	-8.33	-8.33
River				
Inflow	10.13	10.01	10.11	10.13
Outflow	-8.91	-8.99	-8.92	-8.91
Net	1.22	1.02	1.19	1.22
Evapotranspiration from water table				
Inflow	0.00	0.00	0.00	0.00
Outflow	-1.54	-2.05	-1.60	-1.54
Net	-1.54	-2.05	-1.60	-1.54
General-head boundary				
Inflow	0.00	0.00	0.00	0.00
Outflow	-3.35	-3.88	-3.45	-3.35
Net	-3.35	-3.88	-3.45	-3.35
Constant-head boundary				
Inflow	0.44	5.12	0.44	0.44
Outflow	-0.14	-0.15	-0.14	-0.14
Net	0.30	4.97	0.30	0.30

Table 32.--Regression relation between mean winter precipitation and mean monthly precipitation during summer months

[Weather stations used in this regression were El Morro, Gallup, Grants, Laguna, McGaffey, and Thoreau. Time span of records was 1949-78]

Month	Regression coefficients: Slope R_p	Regression coefficients: Intercept (inches)	Correlation coefficient	Standard error of the estimate (inches)	Mean monthly precipitation at McGaffey Psm (inches)
May	0.00114	0.416	0.40	0.06	0.71
June	.0190	.433	.45	.09	.51
July	.144	1.173	.94	.12	2.37
August	.120	1.501	.64	.35	2.70
September	.161	.885	.74	.13	1.61

Table 33.--Regression relation between altitude and mean monthly temperature

[Weather stations used were El Morro, Gallup, Grants, Laguna, McGaffey, and Thoreau]

Month	Regression coefficients: Slope, Rt (degree Fahrenheit per foot)	Regression coefficients: Intercept (degree Fahrenheit)	Correlation coefficient (dimensionless)	Standard error of the estimate (degrees Fahrenheit)
January	-0.00379	55.1	-0.85	1.64
February	-.00442	63.3	-.90	1.49
March	-.00464	70.5	-.90	1.59
April	-.00494	80.4	-.95	1.18
May	-.00498	89.4	-.92	1.51
June	-.00525	100.8	-.92	1.55
July	-.00479	102.9	-.94	1.26
August	-.00471	99.8	-.95	1.12
September	-.00448	91.8	-.93	1.25
October	-.00378	76.8	-.87	1.48
November	-.00333	61.7	-.82	1.63
December	-.00327	52.6	-.82	1.62

☆U.S. GOVERNMENT PRINTING OFFICE: 1992-675-258/65091